L'astrocyte un nouvel acteur dans la modulation ocytocinergique : du réseau au comportement

Damien Kerspern

UNIVERSITÉ DE STRASBOURG

ÉCOLE DOCTORALE DES SCIENCES DE LA VIE ET DE LA SANTE

Institut des Neurosciences Cellulaires et Intégrative

THÈSE présentée par :

Damien KERSPERN

soutenue le : **15 Décembre 2020**

Pour obtenir le grade de : **Docteur de l'université de Strasbourg**

Discipline/ Spécialité : Neurosciences

L'astrocyte un nouvel acteur dans la modulation ocytocinergique : du réseau au comportement

THÈSE dirigée par :

M. CHARLET Alexandre	CR, Université de Strasbourg, INCI, CRNS UPR 3212

RAPPORTEURS :

Mme LE MERRER Julie	DR, Université de Tours, iBrain, INSERM U1352
M BAUD Olivier	Pr, Université de Genève, Faculté de médecine

AUTRES MEMBRES DU JURY :

Mme Simonneaux Valérie	DR, Université de Strasbourg, INCI, CRNS UPR 3212
M Dallérac Glenn	CR, Université de Paris-Saclay, NeuroPSI, CNRS, UMR 9197

UNIVERSITÉ DE STRASBOURG

UNIVERSITÉ DE STRASBOURG

École Doctorale des Sciences de la Vie et de la Santé STRASBOURG

Ecole Doctorale des sciences de la vie et de la santé

Institut des Neurosciences Cellulaires et Intégratives

THÈSE présentée par :

Damien Kerspern

Soutenue le **15 Décembre 2020**

Pour obtenir le grade de : **Docteur de l'Université de Strasbourg**
Discipline / Spécialité : **Neurosciences**

L'astrocyte un nouvel acteur dans la modulation ocytocinergique : du réseau au comportement.

Thèse dirigée par :

M. CHARLET Alexandre	CR, Université de Strasbourg, INCI, CRNS UPR 3212

Rapporteur

Mme LE MERRER Julie	DR, Université de Tours, iBrain, INSERM U1352
M BAUD Olivier	Pr, Université de Genève, Faculté de médecine

Autre membre du jury

Mme Simonneaux Valérie	DR, Université de Strasbourg, INCI, CRNS UPR 3212
M Dallérac Glenn	CR, Université de Paris-Saclay, NeuroPSI, CNRS, UMR 9197

REMERCIEMENTS

La réalisation de cette thèse n'est bien entendu pas le travail d'une seule personne et je tiens à remercier de tout cœur tous ceux qui m'ont accompagné au cours de ces dernières années.

Je souhaite dans un premier temps remercier les Dr. Julie Le Merrer, Valérie Simmoneaux, Glenn Dallérac ainsi que le Pr. Oliver Baud pour avoir accepté de faire partie de mon jury de manière à évaluer mes travaux.

Je voudrais tout particulièrement remercier le Dr. Alexandre Charlet. Tu m'as permis de m'épanouir au sein du laboratoire ainsi et m'as donné la possibilité de développer mes compétences techniques et scientifiques. Tu as été l'encadrant idéal, toujours présent en cas de besoin et suffisamment sage pour laisser de la place à la confiance nécessaire au développement de mon autonomie. Je te remercie pour tout cela et te souhaite bon courage pour la suite, et crois-moi avec les petits jeunes déjà présents tu vas en avoir besoin…

Je tiens également à remercier tout le reste de l'équipe, Pascal, Hervé, Yann, Virginie vous avez été super. Merci pour tout aussi bien les discussions sérieuses au laboratoire mais aussi pour tous les bons moments de convivialité partagés à l'extérieur.

Un grand merci également à toute l'équipe Chronobiotron avec une mention spéciale pour vous Sophie et Dominique, merci pour votre temps, vos conseils et tout le travail que vous accomplissez au quotidien sans vous rien n'aurait été possible ! Merci aussi à Edouard et Bruno, je n'oublierais jamais tous ces bons moments passé à discuter lors de nos pauses, elles vont me manquer…

Je voudrais également rermercier toute ma famille pour m'avoir donné l'opportunité et le soutien pour réaliser ces années d'études. Sans vous, je n'aurais jamais pu accomplir tout ceci.

Un grand merci également à tous les amis que j'ai pu rencontrer ces dernières années. Par soucis de temps et de place je n'aurais pas la possibilité de vous remercier individuellement mais le cœur y est et je suis sûr que vous saurez vous reconnaître.

Bon Adélie, Gwenaelle ça y est !!! Après toutes ces années on l'a fait !!! Je crois que je ne trouverais pas les mots pour vous dire l'affection que je vous porte ainsi que la fierté pour ce qu'on a réalisé au cours de ces dix dernières années. Qui aurait pu croire que ce groupe de

travail formé au hasard allait conduire à tout cela que ce soit les travaux durant nos études, nos travaux de groupe, la création de l'association, la réalisation de notre thèse et j'en passe. Nous voilà maintenant prêts à soutenir à quelques jours d'intervalle. Je suis heureux de partager ces moments avec vous et je suis sûr que malgré la distance il y en aura encore beaucoup d'autres. J'en profite également pour te remercier Thibaut ! Pour toutes ces années passées et tous les moments partagés. Merci pour cette belle amitié qui m'a beaucoup apportée et soutenue. Un grand merci à toi aussi Géraldine. Si on m'avait dit qu'une cigarette pouvait changer la vie des gens comme ça, je ne l'aurais jamais cru. Je ne te remercierais jamais assez pour tous ces moments passés en ta compagnie. Merci également à tous, Flo, Zélie, Elina, Clarisse pour ces moments partagés. Mais également à vous Quentin, Ludo, Marjo, Sarah, Lou et Clémence pour toutes ces soirées partagées à dire des conneries à n'en plus finir. C'est avec un grand honneur et avec plaisir que j'inaugure la tradition des citations de soirées qui doivent figurer dans la thèse (ça va, vu ce qu'il y a dans le chapeau j'aurais pu tomber sur pire) :

« Je vais te brancher, t'inquiète »

- Clémence, en soirée,
probablement beaucoup trop d'alcool en jeu

Un grand merci également à tous les amis rencontrés en dehors du labo. Merci Manon et Lola pour votre soutien et ces moments qui m'ont permis de sortir la tête du travail. A partir de maintenant, j'aurai plus de temps et j'espère qu'on se verra plus fréquemment. Un grand merci à toi aussi Mathilde pour toute l'aide que tu m'as apporté et toutes les relectures nécessaires vu mon niveau d'orthographe catastrophique. Merci pour ton soutien quotidien durant cette période d'écriture, tu as été géniale. Merci à toi aussi Angel ! Tu as été un stagiaire parfait et maintenant un excellent thésard. Je pense que tout le monde s'accorde à dire que ta folie n'a d'égale que ta générosité. Merci pour ton aide et ta bonne humeur quotidienne. Je te souhaite une très bonne continuation pour l'avenir.

Bon pour finir, tu t'en doutes, tu as droit à ta partie rien que pour toi. Merci beaucoup Léa ! Pour résumer, je dirais que tu as été la petite sœur que je n'ai jamais eue. Tu as le mérite d'avoir failli me faire perdre mon sang froid plus d'une fois, et crois moi, bon nombre de personnes ont essayé avant toi mais personne ne t'a égalé. Mais malgré tout ça, je ne saurais pas exprimer la gratitude que j'ai pour toi. Que ce soit pour les moments de rire, les fermetures des différents bars malgré les « une bière et on rentre », le soutien durant les moments difficiles,

les engueulades et les moqueries. Je ne saurais pas résumer ici tout ce que je te dois, je dirais juste un grand merci pour tout et je te souhaite le meilleur pour les années à venir. Je pense que tu fais partie des personnes qui méritent le plus de réussir dans la voie que tu as choisie. Tu as tout mon soutien et ma confiance pour la suite.

TABLE DES MATIERES

RERSUME ETENDU EN FRANÇAIS

Introduction du sujet de thèse

En 1906, Sir Henry Dale, un physiologiste et pharmacologiste, a mis en évidence que des extraits de glande pituitaire humaine pouvaient générer des contractions utérines chez des chattes gestantes. Le composé urotonique présent dans ces explants ne sera isolé qu'une vingtaine d'années plus tard et nommé ocytocine, du grec ancien ὠκύς (okus-rapide) τόκος (tokos-accouchement). Ce polypeptide sera par la suite séquencé et synthétisé par le biochimiste américain Du Vigneaud dans les années 50. Il recevra le prix Nobel de chimie pour son travail en 1955.

L'ocytocine (OT) est un neuropeptide composé de 9 acides aminés. Il est synthétisé au sein du système nerveux central par trois noyaux hypothalamiques : les noyaux paraventriculaires (PVN), supraoptiques (SON) et accessoires. Ce neuropeptide, qui agit à la fois comme neurohormone périphérique mais aussi comme un neuromodulateur central, est capable de réguler de nombreuses fonctions physiologiques (contraction cardiaque, lactation, accouchement…) mais également de moduler de nombreux comportements sociaux complexes (choix de partenaire, interaction sociale…) ainsi que la régulation de diverses émotions (peur, anxiété…). La libération de l'ocytocine dans la circulation sanguine s'effectue par les neurones magnocellulaires hypothalamiques via la glande pituitaire, à la suite d'une exocytose des vésicules à cœur dense, alors que dans le système nerveux central la libération d'ocytocine se produit au niveau somatodendritique ou axonale de manière synaptique mais aussi via une transmission volumique. Un élément clé du système ocytocinergique est la prédominance des projections asynaptiques. Des études princeps sur les neurones magnocellulaires ocytocinergiques de l'hypothalamus ont mis en évidence que l'OT est libérée dans l'espace extracellulaire à partir du soma et des dendrites de ces neurones. Cette augmentation de concentration d'OT dans cet espace extracellulaire conduit à des changements fonctionnels et morphologiques à la fois dans les réseaux neuronaux et astrogliaux du SON et du PVN.

De récentes études ont mis en avant la capacité de l'OT à moduler le circuit de l'amygdale et ses comportement associés comme la peur, l'anxiété ou encore la douleur. La

majorité de ces synapses ocytocinergiques est englobée par des astrocytes, faisant d'eux des acteurs indispensables pour la détection de l'environnement synaptique, ainsi que pour la modulation de son activité.

Le but de ma thèse a donc été de caractériser le rôle des astrocytes dans la modulation ocytocinergique de l'amygdale centrale et d'évaluer l'impact de ce réseau sur les comportements associés.

Résultats scientifiques

a. Impact de l'ocytocine sur les astrocytes de l'amygdale centrale

L'amygdale centrale (CeA) est une structure composée principalement de neurones GABAergique inhibiteurs. Elle regroupe deux principales sous-parties : la partie latérale de l'amygdale centrale (CeL) qui projette sur la partie médiane du CeA (CeM), principale voie de sortie de cette structure.

En tout premier lieu, nous avons pu mettre en évidence l'expression de récepteurs ocytocinergiques (OTR) par les astrocytes de la partie latérale de l'amygdale centrale en plus des récepteurs ocytocinergiques neuronaux classiquement décrits dans la littérature. Environ 15% des astrocytes présents dans cette structure expriment l'OTR et sont capables d'être directement modulés par la libération endogène d'ocytocine, en présentant des variations de concentration calcique intracytoplasmique mesurés par imagerie calcique. Nous avons pu par la suite mimer cet effet en utilisant des approches pharmacologiques à l'aide d'un agoniste spécifique (TGOT). De plus, à l'aide d'outils optogénétiques, nous avons pu, en activant spécifiquement les astrocytes du CeL, reproduire ces oscillations calciques observées lors de l'application de TGOT.

Dans un second temps, nous avons validé que ces variations calciques étaient dues à l'activation des OTR astrocytaires et non à un effet dépendant du réseau neuronal. Pour ce faire, nous avons utilisé un modèle de souris transgénique couplé à des injections virales de manière à déléter spécifiquement les OTR astrocytaires, sans léser ceux exprimés par les neurones adjacents (OTR-CKO). La délétion spécifique de ces récepteurs a conduit à l'abolition

des variations calciques observées précédemment dans les astrocytes du CeL lors de l'application de TGOT.

Dans un troisième temps, nous avons mis en évidence la présence d'un syncytium astrocytaire communicant via des jonctions GAP. La présence de ce réseau astrocytaire permettant la distribution et l'amplification du signal ocytocinergique à travers le CeL permet d'activer un grand nombre d'astrocytes n'exprimant pas le récepteur per se.

b. Modulation du réseau neuronal de l'amygdale par les astrocytes du CeL

La suite de l'étude a porté sur la modification de l'activité du réseau neuronal de l'amygdale centrale par les astrocytes du CeL. A l'aide d'une approche électrophysiologique, nous avons pu mettre en évidence que l'activation des OTR conduisait à l'augmentation de la fréquence de potentiel d'action des neurones du CeL ainsi qu'a une augmentation de la fréquence de courant post-synaptique inhibiteur (IPSCs) des neurones du CeM. Cette modulation de l'activité neuronale est sous tendue par le réseau astrocytaire. L'inactivation pharmacologique de ceux-ci inhibe complètement l'effet induit par le TGOT sur la fréquence des potentiels d'action des neurones du CeL et sur les IPSCs des neurones du CeM. De manière à déterminer si l'effet modulatoire de l'ocytocine sur le réseau neuronal du CeA était principalement dû à l'action de l'OT sur les astrocytes, nous avons utilisé notre modèle de souris où les OTR astrocytaires ont été délétés. En absence d'OTR astrocytaire, nous n'observons plus aucune modulation de l'activité neuronale des neurones du CeL et du CeM en présence de TGOT, mettant en avant le rôle primordial des astrocytes et de leur récepteur dans la modulation ocytocinergique des réseaux neuronaux de l'amygdale centrale.

Modulation des comportements émotionnels lié à l'amygdale par l'ocytocine

L'amygdale est une structure clé dans la régulation des troubles associés à la douleur et permet d'assigner une émotion à un stimuli externe. Nous avons testé l'implication de la signalisation ocytocinergique dans le CeA dans la modulation de la sensibilité mécanique (Pince calibrée), l'anxiété (Labyrinthe en croix surélevé) ainsi que sur les comportements de préférence de place (Test de conditionnement de préférence de place) sur des rats et des souris neuropathiques. Des injections bilatérales de TGOT dans le CeA ne semblent pas

présenter d'effet sur la sensibilité mécanique. Cependant, l'infusion de TGOT dans le CeA semble promouvoir un effet anxiolytique chez les animaux neuropathiques. L'activation par optogénétique des astrocytes présente des effets similaires à l'infusion du TGOT. De manière à déterminer la valence émotionnelle sous tenue par le réseau de l'amygdale, nous avons réalisé un test de préférence de place. Nous avons pu révéler un fort effet à la fois du TGOT mais aussi de la stimulation optogénétique des astrocytes : dans les deux cas, les animaux neuropathiques et sains présentaient une claire préférence pour la chambre où ils ont reçu le conditionnement. Cela indique que la seule activation des astrocytes du CeL via la stimulation optogénétique peut parfaitement mimer l'effet de renforcement positif du TGOT.

Nous avons par la suite répété ces tests comportementaux chez la souris présentant la délétion des OTR astrocytaires. Le test de labyrinthe en croix surélevé démontre que l'injection de TGOT réduit le niveau d'anxiété chez les animaux neuropathiques, cependant cet effet anxiolytique est complètement aboli chez les animaux dont les OTR astrocytaires sont délétés. Cela confirme que la présence des OTR astrocytaires est cruciale pour la modulation ocytocinergique sur l'anxiété. Ensuite, le test de préférence de place a clairement démontré que le TGOT dans le CeA conduit à une forte préférence de place chez les animaux contrôles et neuropathiques. Cet effet requiert l'expression des OTR astrocytaires dans le CeA puisqu'ils sont complètement perdus chez les animaux dont le récepteur a été délété.

L'ensemble de ces données démontre que la signalisation ocytocinergique médiée par les OTR astrocytaires agit comme un système de balance qui soutient l'état émotionnel positif à la fois dans les cas de douleur chronique et dans les états sains et régule l'anxiété chez les animaux neuropathiques.

Liste des publications scientifiques

Articles scientifiques en qualité de premier auteur

Titre: Astrocytes mediate oxytocin's effect on local amygdala circuitry that regulates emotional behavior
Auteurs **:** Jérôme Wahis*, Angel Baudon*, Ferdinand Althammer*, Damien Kerspern*, Stéphanie Goyon, Daisuke Hagiwara, Arthur Lefevre, Lara Bartezcko, Benjamin Boury-Jamot, Benjamin Bellanger, Marios Abatis, Miriam Silva da Gouveia, Diego Benusiglio, Marina Eliava, Andrej Rozov, Ivan Weinsanto, Hanna Sophie Knobloch-Bollmann, Matthew K. Kirchner, Ranjan K. Roy, Hong Wang, Marie Pertin, Perrine Inquimbert, Claudia Pitzer, Jan Siemens, Yannick Goumon, Benjamin Boutrel, , Christophe Maurice Lamy, Isabelle Decosterd, Jean-Yves Chatton, Nathalie Rouach, W. Scott Young, Javier E. Stern, Pierrick Poisbeau, Ron Stoop, Pascal Darbon, Valery Grinevich, Alexandre Charlet
(*) représente les premiers auteurs
Journal : Nature neurosciences, en révision.

Titre : **Oxytocin modulates central amygdala microcircuits and related behaviors thought astrocytes, pharmacological evidences**
Auteur : Damien Kerspern, Jérôme Wahis, Angel Baudon, Alexandre Charlet
En préparation

Titre : **Targeting non-opioid neuropeptide systems for the management of pain**
Auteurs : João Covita*, Damien Kerspern*, Sherie Ma, Andrew L. Gundlach, Alexandre Charlet, Marc Landry
Revue En préparation

Articles scientifiques co-signés

Titre **: A Nonpeptide Oxytocin Receptor Agonist for a Durable Relief of Inflammatory Pain**
Auteurs **:** Louis Hilfiger, Qian Zhao, Damien Kerspern, Perrine Inquimbert, Virginie Andry, Yannick Goumon, Pascal Darbon, Marcel Hibert, Alexandre Charlet.
Journal **:** Scientific reports (2020)

Titre **: A Fear Memory Engram and Its Plasticity in the Hypothalamic Oxytocin System**
Auteurs **:** Mazahir T Hasan, Ferdinand Althammer , Miriam Silva da Gouveia, Stephanie Goyon, Marina Eliava , Arthur Lefevre, Damien Kerspern, Jonas Schimmer, Androniki Raftogianni, Jerome Wahis, H Sophie Knobloch-Bollmann, Yan Tang, Xinying Liu, Apar Jain, Virginie Chavant, Yannick Goumon, Jan-Marek Weislogel, René Hurlemann, Sabine C Herpertz, Claudia Pitzer, Pascal Darbon, Godwin K Dogbevia, Ilaria Bertocchi, Matthew E Larkum, Rolf Sprengel, Hilmar Bading, Alexandre Charlet , Valery Grinevich
Journal**:** Neuron (2019)

Titre : **Oxytocin release in periaqueductal induces analgesia through long term suppression of spinal cord neurons activity**
Auteurs : Mai Iwasaki*, Arthur Lefèvre*, Damien Kerspern, Jérôme Wahis, Ferdinand Althammer, Louis Hilfiger, Meggane Melchior, Valery Grinevich, Alexandre Charlet
En preparation

Communications Orales

Poster teaser: A new role of astrocyte in the central amygdala neuronal network modulation by oxytocin – Neural circuit of pain. Heidelberg, Germany- 2017

Neuron-glia interaction in the oxytocinergic modulation of central amygdala - XVIème Symposium National du Réseau Français de Recherche sur la Douleur – Bordeaux 2020

Communications par affiche

- A new role of astrocyte in the central amygdala neuronal network modulation by oxytocin. (2017) – J. Wahis, M. da Silva Gouvenia, S. Goyon, D. Kerspern, J. Siemens, P. Poisbeau, V. Grinevich, A. Charlet – au congrès « neuronal circuit of pain » à Heidelberg, Allemagne

- A new role of astrocyte in the central amygdala neuronal network modulation by oxytocin. (2018)- . Wahis1, D. Kerspern, F. Althammer, S. Goyon, D. Hagiwara, B. Boury-Jamot, B. Bellanger, M. Abatis, M. Silva da Gouveia, D. Benusiglio, M. Eliava, A. Rozov, I. Weinsanto, H.S. Knobloch-Bollmann, H. Wang, M. Pertin, P. Inquimbert, J. Siemens, Y. Goumon1, B. Boutrel, C. M. Lamy, I. Décosterd, JY. Chaton, R. Stoop, P. Poisbeau, V. Grinevich, A. Charlet. Présenté à la FENS à Berlin, Allemagne

- A new role of astrocyte in the central amygdala neuronal network modulation by oxytocin. (2019)- J. Wahis, D. Kerspern, F. Althammer, S. Goyon, V. Grinevich, A. Charlet. Présenté au 13th Goettingen Meeting of the German Neuroscience Society. Gottingen, Allemagne

- A new role of astrocyte in the central amygdala neuronal network modulation by oxytocin. (2019) -)- J. Wahis, D. Kerspern, F. Althammer, S. Goyon, V. Grinevich, A. Charlet. Présenté à Neurofrance, France

- A new role of astrocyte in the central amygdala neuronal network modulation by oxytocin. (2019) - J. Wahis, D. Kerspern, F. Althammer, S. Goyon, V. Grinevich, A. Charlet. Présenté à 13th World Congress on Neurohypophysial Hormones à Ein Gedi, Israel

LISTE DES FIGURES

LISTE DES TABLEAUX

LISTE DES ANNEXES

LISTE DES ABREVIATIONS

- AM : Acetoxyméthyle
- AMPc : Adénosine monophosphate cyclique
- ALDH1L1 : Aldéhyde déshydrogénase 1 de la famille L1
- AN : Noyaux accessoires
- AMP : Adénosine monophosphate
- ATP : Adénosine triphosphate
- AQP4 : Aquaporine 4
- ARNm : Acide ribonucléique messager
- AVP : Arginine-vasopressine
- AVPR : Récepteur de la vasopressine
- BRET : Transfert d'énergie de résonnance magnétique
- CCK : Cholecystokinine
- CeA : Amygdale centrale
- CeL : Partie latérale de l'amygdale centrale
- CeM : Partie médiale de l'amygdale centrale
- DA : Dopamine
- DRG : Ganglion de la racine dorsale
- E_x : Potentiel d'équilibre ionique (x étant l'ion concerné)
- EAAT1/2 : Transporteur d'acide aminé excitateur
- EPM : Labyrinthe en croix surélevé
- FRET : Transfert d'énergie entre molécule fluorescentes
- GABA : Acide ϒ-aminobutyrique
- GFAP : Protéine acide fibrillaire gliale
- GnRH : Hormone de libération des gonadotrophines hypophysaire
- I.c.v. : Intra-cérébro-ventriculaire
- IL-1β : Interleukin 1-β
- Ip : Intra-péritonéale
- IP3 : Inositol 3-phosphate
- IPSC : Courants post-synaptiques inhibiteurs

- Iv : intra-veineuse
- Kd : Constante de dissociation
- Ki : Constante d'inhibition
- K_{ir} : Courant potassique entrant rectifiant
- cKO : Knock Out conditionnel
- LCR : Liquide céphalo-rachidien
- MagnOT : magnocellulaire
- mGluR : Récepteur glutamatergique métabotropique
- OT : Ocytocine
- OTR : Récepteur à l'ocytocine
- P-LAP : Leucine aminopeptidase placentaire
- PAG : Substance grise périaqueducale
- ParvOT : Parvocellulaire
- PKA : Protéine kinase A
- PKC : Protéine Kinase C
- PLC : Phospholipase C
- PVN : Noyaux paraventriculaire
- rAAV : Virus recombinant adéno-associés
- RCPG : Récepteurs aux protéines G
- SNC : Système nerveux central
- SON : Noyaux supraoptiques
- SR101 : Sulforhodamine 101
- TGOT : [Thr4, Gly7]OT
- TNF-α : Facteurs de nécrose tumorale-α
- UTP : Uridine triphosphate
- vGluT2 : Transporteur du glutamate vésiculaire
- VMH : Hypothalamus ventro-médial
- WT : Wild

INTRODUCTION

I- Historique, généralités et phylogénie de l'ocytocine

a. Historique de la découverte de l'ocytocine

La découverte du neuropeptide appelé ocytocine (OT) remonte à 1906, lorsque Sir Henry Dale, un physiologiste et pharmacologiste, a mis en évidence le fait que des extraits de glande pituitaire humaine pouvaient générer des contractions utérines chez les chattes gestantes (Dale, 1906). Le composé urotonique présent dans ces explants ne sera isolé qu'une vingtaine d'année plus tard et nommé ocytocine, du grec ancien ὠκύς (*okus*-rapide) τόκος (*tokos*-accouchement) (Kamm et al., 1928). Dans les années cinquante, le biochimiste américain Vincent du Vigneaud déterminera la séquence polypeptidergique de l'OT et réussira à synthétiser ce peptide sous sa forme active (Du Vigneaud et al., 1953; du Vigneaud et al., 1954). Grâce à l'ensemble de son travail, et plus particulièrement ses recherches sur les composés soufrés nécessaires pour la première synthèse d'une hormone polypeptidique (OT), il obtiendra le prix Nobel de chimie en 1955.

b. Généralité sur le neuropeptide ocytocinergique

L'ocytocine est un peptide composé de neufs acides aminés : Cys-Tyr-Ile-Gln-Asn-Cys-Pro-Leu-GlyNH_2. Les deux composés cystéines forment un pont disulfure n'attribuant pas de terminaison carboxyterminale à cette molécule. De par sa structure et son gène d'origine (OXT), l'ocytocine présente de fortes homologies avec la vasopressine (AVP) (Figure 1). En effet, ces deux neuropeptides diffèrent uniquement de deux acides aminés neutres : les résidus isoleucines en position 3 et la leucine en position 8 de l'OT sont remplacés respectivement par la phénylalanine et par l'arginine, un composé basique (Gimpl and Fahrenholz, 2001a). C'est grâce à cette différence de polarité entre ces deux composés que l'interaction de ces deux peptides avec leurs récepteurs spécifiques est possible (Barberis et al., 1998).

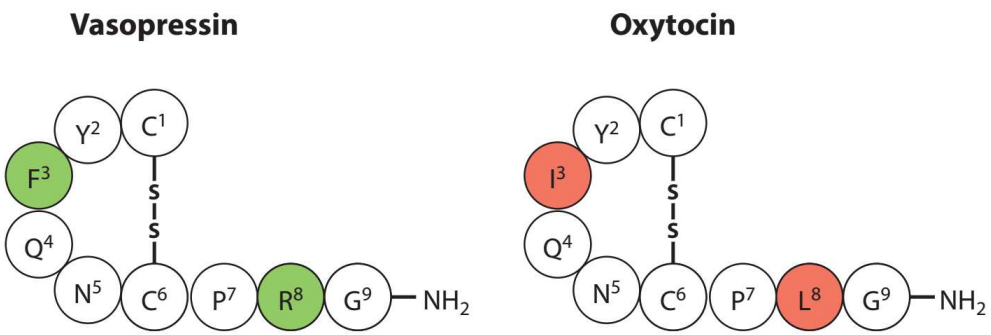

Figure 1 : Comparaison de la structure primaire et secondaire de l'ocytocine et de la vasopressine Les résidus verts et rouges sont ceux qui diffèrent entre les deux peptides. Les lettres indiquent les acides aminés et le chiffre indique leur position dans la séquence peptidique. Adapté de (Stoop et al., 2015)

c. Phylogénie de l'ocytocine et de son analogue au cours de l'évolution

Le peptide ancestral duquel la famille OT/AVP a évolué est estimé avoir émergé avant la séparation entre les protostomiens et les deutérostomiens (Feldman et al., 2016). La séquence similaire et la localisation chromosomique de l'OT et de l'AVP indiquent qu'ils découlent d'une duplication en tandem d'un gène ancestral codant pour la vasotocine chez un ancêtre commun des poissons à mâchoires il y a environ 500 millions d'années (Yamashita and Kitano, 2013). Au cours de l'évolution, l'OT, l'AVP ainsi que leurs récepteurs ont été observés chez de nombreuses espèces incluant de nombreux invertébrés, poissons, amphibiens, reptiles, oiseaux et mammifères, avec pour seule exception le fait que les invertébrés possèdent uniquement un seul homologue à l'OT/AVP, l'isotocine (Beets et al., 2013). Les membres de la famille de l'OT/AVP sont représentés avec leurs listes d'acides aminés dans le tableau 1.

Globalement depuis la duplication du gène ancestral, la famille OT/AVP demeure fortement conservée (Banerjee et al., 2017), particulièrement au sein de la famille des mammifères euthériens (Wallis, 2012). Cette conservation de gène a été notamment démontré par le fait que l'intégration du gène de l'isotocine du poisson Fugu chez le rat et la souris résultait en son expression correcte au sein des neurones ocytocinergiques (Venkatesh et al., 1997). De plus, la réponse du gène de l'OT à la suite d'un stimulus osmotique a été

imitée(Gilligan et al., 2003; Venkatesh et al., 1997), ce qui indique que la région de régulation des gènes de l'OT et de l'isotocine est virtuellement conservée dans sa fonction, du moins depuis la divergence entre les tétrapodes et les poissons.

	1	2	3	4	5	6	7	8	9	
Oxytocin	Cys	Tyr	Ile	Gln	Asn	Cys	Pro	Leu	Gly(NH_2)	Placentals, some marsupials, ratfish (*Hydrolagus colliei*)
Mesotocin	*	*	*	*	*	*	*	Ile	*	Marsupials, nonmammalian tetrapods, lungfishes
Isotocin	*	*	*	Ser	*	*	*	Ile	*	Osteichthyes
Glumitocin	*	*	*	Ser	*	*	*	Gln	*	Skates (Chondrichthyes)
Valitocin	*	*	*	*	*	*	*	Val	*	Sharks (Chondrichthyes)
Aspargtocin	*	*	*	Asn	*	*	*	*	*	Sharks (Chondrichthyes)
Asvatocin	*	*	*	Asn	*	*	*	Val	*	Sharks (Chondrichthyes)
Phasvatocin	*	*	Phe	Asn	*	*	*	Val	*	Sharks (Chondrichthyes)
Cephalotocin	*	*	Phe	Arg	*	*	*	Ile	*	*Octopus vulgaris* (Molluscs)
Annetocin	*	Phe	Val	Arg	*	*	*	Thr	*	*Eisenia foetida* (Annelids)
Vasotocin	*	*	*	*	*	*	*	Arg	*	Nonmammalian vertebrates, cyclostomes
Vasopressin	*	*	Phe	*	*	*	*	Arg	*	Mammals
Lysipressin	*	*	Phe	*	*	*	*	Lys	*	Pig, some marsupials
Phenypressin	*	Phe	Phe	*	*	*	*	Arg	*	Macropodids (Marsupials)
Locupressin	*	Leu	*	Thr	*	*	*	Arg	*	*Locusta migratoria* (Insects)
Arg-conopressin	*	Ile	*	Arg	*	*	*	Arg	*	*Conus geographicus* (Molluscs)
Lys-conopressin	*	Phe	*	Arg	*	*	*	Lys	*	*Lymnaea stagnalis* (Molluscs)

Tableau 2: ***L'OT par rapport aux différents peptides apparentés****. Les * représentent les acides aminés identiques à la séquence de l'OT (Gimpl and Fahrenholz, 2001a)*

Un des points marquants de l'OT et de son analogue est la conservation à travers toutes les espèces de la régulation des fonctions vitales, de la régulation de l'homéostasie à la reproduction. Par exemple, une des fonctions de l'OT est son action myoactive observée des mammifères (e.g. la contraction utérine) jusqu'aux sangsues, où son analogue ocytocinergique induit des mouvements de tremblement, ce qui est couramment associé au comportement lié à la reproduction (Wagenaar et al., 2010). Un autre exemple a été décrit chez *C. elegans*, où les peptides associés à l'OT/AVP possèdent également un rôle dans la reproduction (Garrison et al., 2012). Mais chez les mammifères, l'OT régule également des fonctions plus complexes, comme le comportement social (Donaldson and Young, 2008). Les études de Chang et ses collaborateurs formulent une hypothèse générale intéressante concernant l'attribution des nouvelles fonctions par rapport au « ancien » système évolutif comme l'OT/AVP. Elles proposent que les mécanismes ancestraux soient dupliqués et réaffectés au soutien des

comportements sociaux plus complexes (Chang et al., 2013). Dans le cas de l'OT chez les mammifères, elle soutient notamment les fonctions physiologiques reproductives, e.g. l'initiation de la parturition et de la lactation ; mais l'OT est également capable d'induire le comportement maternel chez les rats (Petersson et al., 1996), et de moduler les comportements complexes entre les humains (Heinrichs et al., 2009), nécessaires pour une éducation viable de la descendance (Feldman et al., 2016). Cela confirme l'idée que le rôle de l'OT (et de ses analogues) dans la régulation des fonctions reproductrices est conservé au cours de l'évolution, et qu'elle est capable de moduler les comportements spécifiques lié à la reproduction des différentes espèces (Lee et al., 2009). Beet et ses collaborateurs ont également proposé une discussion similaire à propos de la conservation des fonctions de la famille des peptides ocytocinergiques dans la régulation des comportements de reproduction des animaux, en comparant l'action du système ocytocinergique et vassopressinergique entre les invertébrés tels que les nématodes et les vertébrés tels que les mammifères (Beets et al., 2013).

En parallèle de la conservation des séquences et des fonctions de l'OT/AVP et de leurs analogues, un certain degré de conservation est présent au niveau des centre cérébraux et des types cellulaire produisant et sécrétant ces peptides. Chez les mammifères, l'OT et l'AVP sont synthétisés dans 3 noyaux principaux : les noyaux paraventriculaires (PVN), supraoptiques (SON) et accessoires (AN) de l'hypothalamus. Ils contiennent, entre autres, des neurones magnocellulaires neurosécréteurs (magnOT) qui libèrent l'OT dans la circulation sanguine par le biais de la glande pituitaire (McEwen, 2004). Chez les invertébrés, l'analogue de l'OT et de l'AVP est synthétisé par des neurones dont les corps cellulaires sont retrouvés dans les ganglions cérébraux et périphériques (Beets et al., 2013). Chez les anamniés, les analogues des magnOT résident dans l'aire pré optique ancestrale (Herget et al., 2014), proche du 3^{e} ventricule, où ils sont distribués de façon aléatoire parmi les autres types cellulaires présents. Chez les amniotes, la distribution des magnOT est mieux définie : elle se trouve limitée entre le PVN, SON et AN. La revue de Knobloch et Grinevich en (2014) en donne une description précise et discute de l'évolution de la distribution anatomique au cours de l'évolution des magnOT parmi les vertébré basaux et supérieurs dont la figure 2 est extraite.

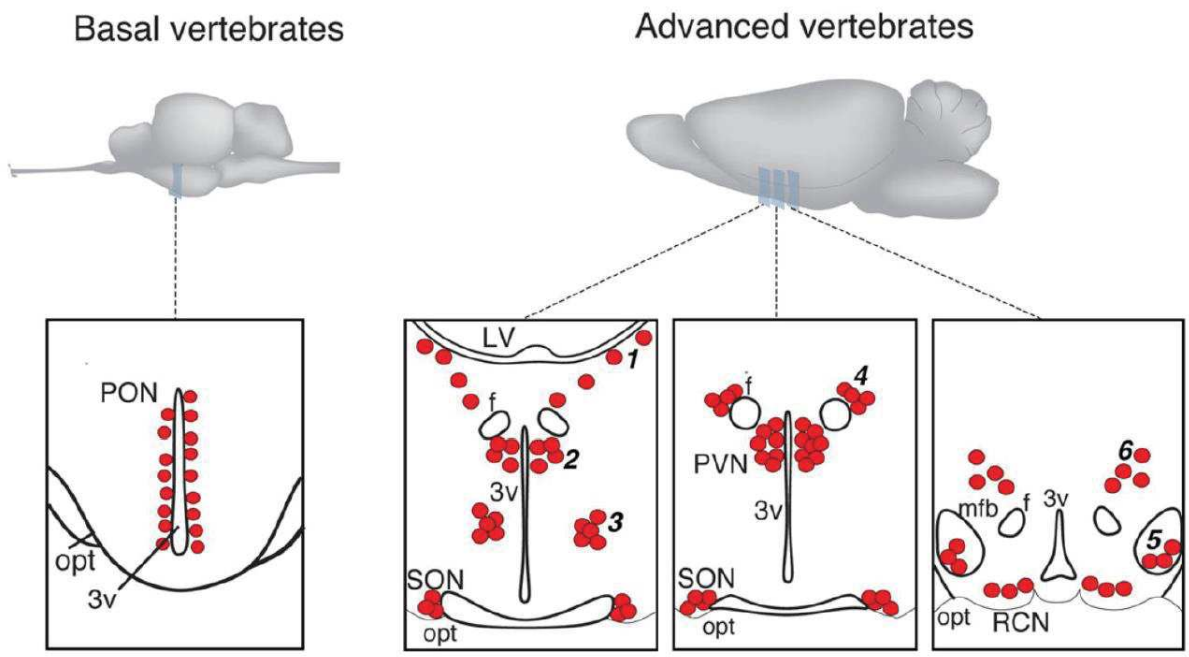

Figure 2 : Distribution anatomique des neurones manOT chez les vertébrés basaux et avancés. Abréviation : 3v, third ventricle; F, columns of fornix; LV, lateral ventricle; MFB, medial forebrain bundle; OC, optic chiasm; OT, optic tract; PON, preoptic nucleus; PVN, paraventricular nucleus; SON, supraoptic nucleus. Accessory nuclei: 1-extrahypothalamic; 2-anterior commissural; 3-circular; 4-fornical; 5-nucleus of the medial forebrain bundle; 6-dorsolateral. Adapté à partir de (Grinevich et al., 2014)

Un autre point intéressant est l'évolution de la morphologie des cellules exprimant l'OT et ses analogues. Chez *C. elegans*, les neurones exprimant la nématocine présentent des process ciliés, à partir desquels sont libérés les granules contenant la nématocine dans le liquide pseudo-cœlomique (Beets et al., 2013). Chez les vertébrés basaux, ces cils sont aussi retrouvés au niveau des dendrites des neurones magnocellulaires et dépassent dans le 3^{e} ventricule où ils peuvent libérer les neuropeptides dans le LCR. Cette caractéristique est toujours présente dans le cerveau des mammifères, bien que peu répandue (Knobloch and Grinevich, 2014). Un autre trait que les magnOT conserve au cours de l'évolution est la neurosecrétion endocrine via la connexion axone- vaisseau sanguin au sein de la glande pituitaire. Cette caractéristique demeure présente chez tous les vertébrés depuis les actinoptérygiens (Egorova et al., 2003). Au cours de l'évolution, il semble qu'il se soit produit une spécialisation neuronale de la synthèse d'ocytocine, ce qui signifie qu'il y a eu une

évolution d'un neurone granulaire primitif uni ou bipolaire en un neurone multipolaire avec une plus grande arborescence dendritique. Elle a permis aux neurones magnocellulaires de libérer les neuropeptides à partir leurs dendrites via exocytose (Pow and Morris, 1989), donnant lieu à la communication paracrine au sein des noyaux hypothalamiques ainsi qu'à une diffusion de l'OT dans le 3e ventricule chez les vertébrés basaux. Au sein des vertébrés supérieurs, on voit apparaître une caractéristique unique : la projection axonale à longue distance de neurones ocytocinergiques (Knobloch et al., 2012). Ces projections seraient capables de réguler avec précision les fonctions complexes de l'OT et de l'AVP, comme la régulation du comportement maternel, la reconnaissance sociale ainsi que le comportement de peur (Knobloch et al., 2012; Marlin et al., 2015; Oettl et al., 2016). Un résumé schématique de la localisation et des changements morphologiques des neurones magnocellulaires au cours de l'évolution des vertébrés est présent en Figure 3.

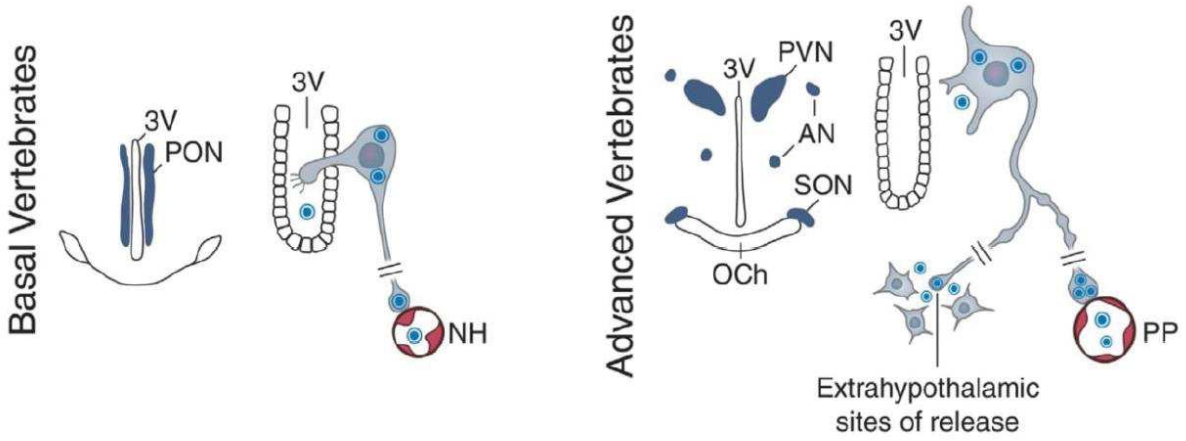

Figure 3 : Evolution phylogénétique des voies de transmission ocytocinergique. Illustration de la complexification du noyau préoptique contenant les neurones magnOT chez les vertébrés primaires en PVN, SON et AN chez les vertébrés supérieurs. De plus, l'évolution de la morphologie des neurones manOT est représentée tout comme que leur distribution autour du 3e ventricule. Au cours de l'évolution, les neurones magnOT ont développé des collatérales projetant vers des région extrahypothalamique. Abréviation : Och, optic chiasma ; NH, neurohypophysis ; PP, posterior pituitary lobe. Adapté à partir de (Grinevich et al., 2016).

d. Evolution du récepteur de l'ocytocine

Tout comme pour la synthèse de l'OT et de l'AVP, leurs récepteurs semblent provenir d'un récepteur ancestral commun, le récepteur à la vasotocine. Au même moment que la duplication des domaines donnant naissance à l'OT et à l'AVP, le récepteur à la vasotocine semble lui aussi avoir subi des duplications provoquant l'apparition de quatre récepteurs différents à la vasotocine. Puis, au cours de l'évolution, ces gènes vont donner, chez les mammifères, trois récepteurs pour la vasopressine (V1a, V1b et V2) ainsi qu'un récepteur OT (OTR) (Figure 4) (Grinevich et al., 2016; Yamashita and Kitano, 2013).

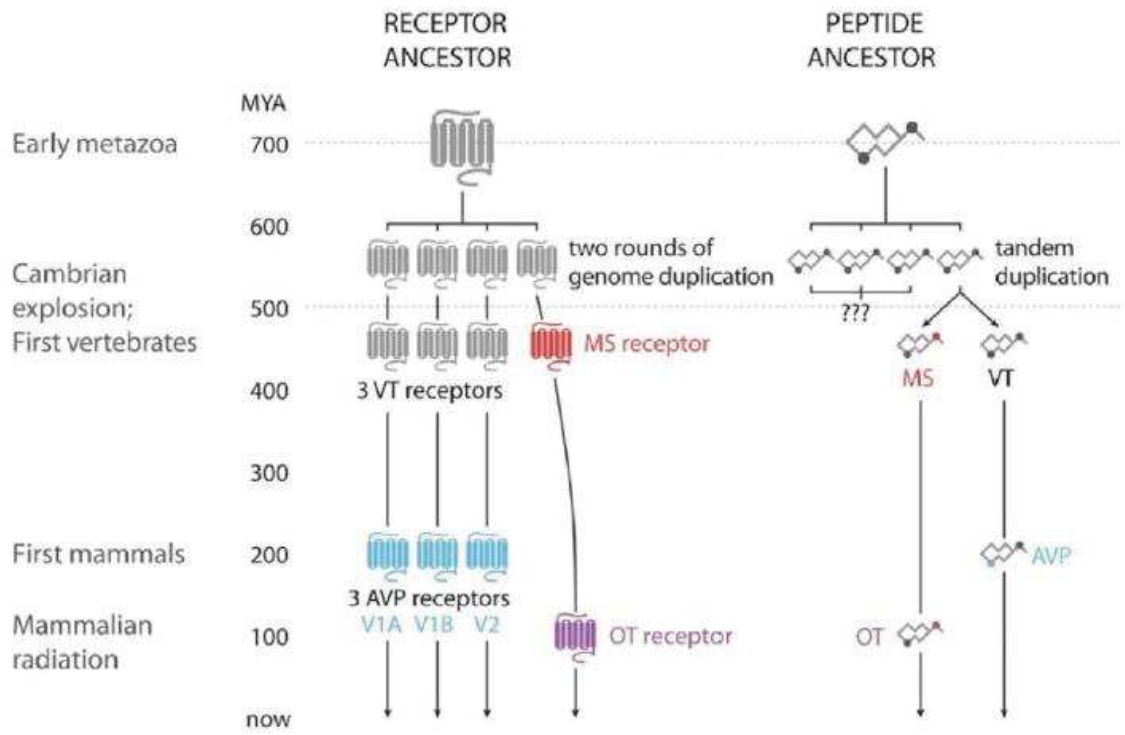

Figure 4 : Evolution des systèmes OT et AVP chez les vertébrés. Abréviation : MS, mésotocine ; VT, vasotocine. Adapté à partir de (Grinevich et al., 2016).

Chez les placentaires, le gène OTR aurait vraisemblablement été soumis à des pressions évolutives à l'inverse de récepteurs à l'AVP (Paré et al., 2016). Pour les singes du nouveau monde, des nouveaux variants génétiques auraient été découverts pour l'OT et son OTR, présentant une évolution conjointe en corrélation avec l'apparition de nouveaux comportements paternels chez ces animaux (Vargas-Pinilla et al., 2015).

II- L'ocytocine et son récepteur

a. Ocytocine synthèse et régulation

Le gène de l'ocytocine (OXT) est fortement conservé dans l'arbre du vivant. Il est composé de 850 paires de base et est localisé entre autres sur le chromosome 20 chez l'humain, le chromosome 3 chez le rat ainsi que sur le chromosome 2 chez la souris. Le gène OXT chez les mammifères est situé sur le même locus chromosomique que le gène codant pour la vasopressine (AVP) et les deux gènes sont fortement liés. Ces deux gènes possèdent une région intergénique dont la distance varie selon les différentes espèces (11kb chez l'humain et le rat et 3.6kb chez la souris) (Hara et al., 1990; Ivell and Richter, 1984; Mohr et al., 1985; Rao et al., 1992; Sausville et al., 1985). Les deux gènes possèdent une structure commune, contenant trois exons et deux introns, mais sont transcrits dans des directions opposées Figure 5. Le premier exon code pour le signal de translocation, l'hormone en tant que telle, le signal de traitement tripeptidique ainsi que pour la neurophysine associée. Le second exon code pour les autres parties de la neurophysine et le troisième exon pour la région carboxy-terminale de la neurophysine (Gimpl and Fahrenholz, 2001a).

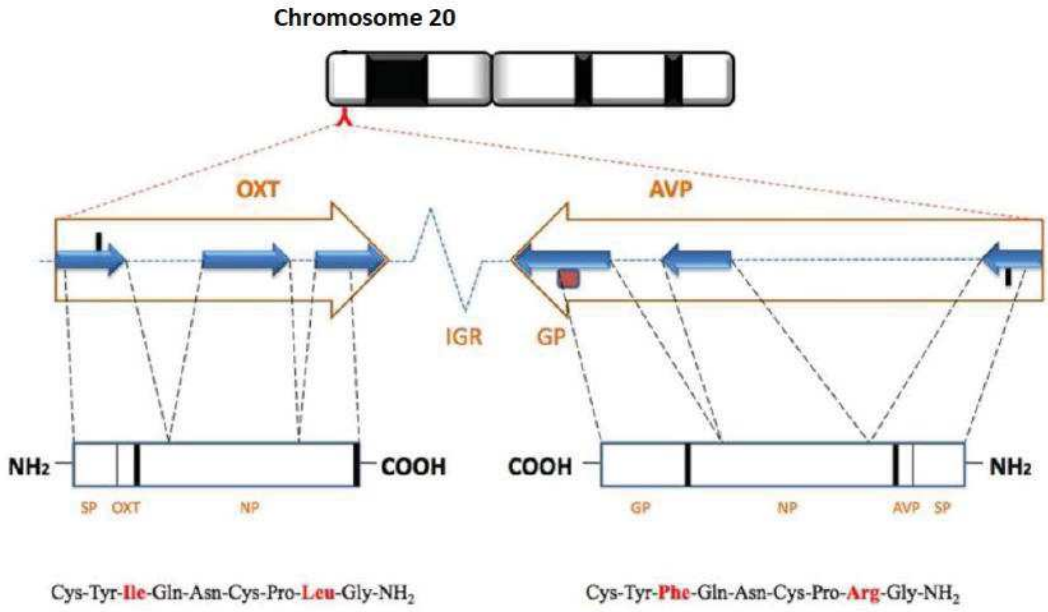

Figure 5 : Représentation schématique des gènes de l'OT et de l'AVP chez l'homme. Localisation du gène de l'OT et de l'AVP sur le chromosome 20. Les gènes de l'OT et de l'AVP sont composés de 3 exons (flèches bleu) séparés par deux introns (traits en pointillé) et en rouge sont représentés les acides aminés qui diffèrent entre l'OT et l'AVP. Abréviation : GP, glucoprotéine ; SP, peptide signal ; NP, neurophysine. Adapté de (Lee et al., 2009)

En termes de biosynthèse, l'OT et l'AVP ne se différencient pas des autres neuropeptides. Le transcrit initial est traduit en un pré-pro-peptide, qui sera par la suite clivé en un pro peptide puis en peptide (Figure 6). Le produit mature de la biosynthèse de l'OXT consiste en un dimère, OT-neurophysine. Ce dimère est produit puis transporté sous cette forme au sein de la cellule. La dissociation du dimère OT-neurophysine a lieu dans des vésicules acides, appelé les granules neurosécrétrices contenant les enzymes pro hormones convertases (type 5 pour les neurones OT et type 1/3 pour les neurones AVP) ainsi que les carboxypeptidases. Une fois l'OT dissociée, elle sera libérée dans le plasma ou le liquide céphalorachidien (LCR) où l'OT pourra ensuite se lier à son récepteur (Blumenstein et al., 1979; Breslow and Burman, 1990). Le rôle des vésicules à cœur dense est un élément fondamental dans la maturation de l'ocytocine, son transport, son stockage et sa sécrétion. Ces vésicules sont appelées comme telles à cause de la grande quantité de protéine et peptide qu'elles contiennent leur conférant cette opacité lors de l'observation au microscope électronique (Castel et al., 1984). Elles présentent un pH acide (ph 5-6) permettant la stabilisation de leur contenu, notamment le complexe OT-neurophysine

1. La libération de ce dimère dans l'environnement extraneuronal facilite sa dissociation en raison du changement de pH vers des valeurs plus basiques altérant la stabilité de la liaison entre les deux éléments. Provenant du système trans golgien, ces vésicules sont transportées de manière antérograde par le réseau microtubulaire où elles seront stockées dans les terminaisons axonales, et seront sécrétées sous l'effet de potentiels d'action. Cependant certaines de ces vésicules ont été observées (au niveau des corps cellulaires et des dendrites où elles peuvent être sécrétées sous l'action de changement de concentration calcique locale, par exemple lors de la lactation (Ludwig, 1998) .

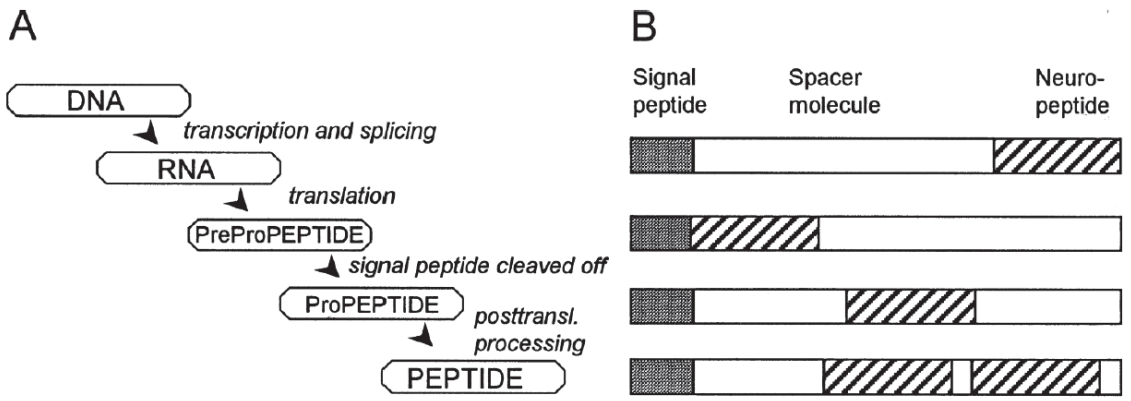

Figure 6 : Schéma représentant la synthèse des neuropeptides. (A) Les processus impliqué depuis la transcription de l'ADN à la formation du neuropeptide actif. (B) Exemple de la disposition de la structure d'un pré-propeptide. Il est composé d'un peptide signal, une ou plusieurs copies d'un neuropeptide et d'une séquence d'espacement. Adapté de (Holmgren and Jensen, 2001)

b. Régulation génétique de l'OT

II.b.i. Régulation en amont

L'expression du gène OXT est fortement régulée, surtout au niveau transcriptionnel. Environ 160 paires de bases en amont du site d'initiation de transcription, une séquence fortement conservée est liée à un motif similaire au « estrogen element response » (ERE) au niveau de la terminaison 5' du gène OXT chez l'humain et le rat. A cause de la forte ressemblance avec le motif ERE, ce motif est nommé « multiple hormone response element »

(Stedronsky et al., 2002). La présence de ce motif en plus du ERE chez le rat impliquerait que de nombreux membres de la famille des récepteurs nucléaires (décrits ou orphelins) pourraient réguler l'expression du gène OXT (Burbach, 2002).

Dans le cas du gène humain codant pour l'OT , il a été démontré que l'œstradiol pouvait en effet induire la synthése de l'OT dans des cellules en cultures (Richard and Zingg, 1990), tout comme une injection unique d'œstrogènes induirait une élévation du taux d'OT circulant chez la femme (Chiodera et al., 1991). Cependant, il n'y a pas d'expression de récepteur α aux œstrogènes dans les neurones ocytocinergiques (Axelson and Leeuwen, 1990; Shughrue et al., 1997), mais les récepteurs β aux œstrogènes sont exprimés par certains neurones ocytocinergiques hypothalamiques (Alves et al., 1998; Hrabovszky et al., 2004). Différentes études proposent que l'œstradiol agirait au niveau du récepteur β de l'œstrogène et induirait l'expression ou l'inhibition du gène OXT dans l'hypothalamus (Nomura et al., 2002; Patisaul et al., 2003; Shughrue et al., 2002). L'hormone thyroïde a été reportée comme étant capable d'induire la transcription du gène OXT dans l'hypothalamus de rat (Adan et al., 1992), alors que l'acide rétinoïque semble à la fois être capable d'induire et d'inhiber l'expression d'OXT dans les cellules non cérébrales (Larcher et al., 1995; Lipkin et al., 1992). En ce qui concerne la régulation d'OXT par les récepteurs nucléaires orphelins, plusieurs études mettent en évidence un double rôle de certains éléments : un contrôle translationnel direct et un contrôle translationnel indirect via la modulation de l'activation hormonale du gène OXT (Burbach, 2002; Koohi et al., 2005; Stedronsky et al., 2002).

II.b.ii. Régulation en aval

La délétion des éléments cis-régulateur du gène OXT à l'aide de souris transgéniques a permis de mettre en avant l'importance des séquences en aval de celui-ci pour la spécificité cellulaire de l'expression de l'OT dans les neurones magnocellulaires hypothalamiques (Murphy and Wells, 2003; Young and Gainer, 2003). L'utilisation de transfection virale dans des neurones magnocellulaires de l'hypothalamus a permis de mettre en évidence que deux « enhancers » en aval de l'OT et de l'AVP présentent des séquences très similaires (Fields et al., 2003). De plus, Gainer démontre que l'inversion de ces deux éléments n'affecte pas les niveaux d'expression de l'OT et de l'AVP. Cela met en évidence que les éléments régulateurs permettant

la spécificité d'expression de l'OT et de l'AVP dans les cellules sont sous tendus par les séquences se trouvant dans la région 5' en amont du gène OXT.

c. Le récepteur de l'ocytocine du gène à la protéine

Le récepteur à l'ocytocine (OTR) est un membre de la famille des récepteurs couplés au protéines G (GPCRs) composé du classique récepteur à sept domaines transmembranaires. Le gène codant pour l'OTR est porté par le chromosome 3 chez l'humain(Kimura et al., 1994), 4 chez le rat (Rozen et al., 1995) et le 6 chez la souris(Kubota et al., 1996). La séquence de l'OTR mesure 17 kb et est composée de quatre exons et trois introns. Les deux premiers exons contiennent la région 5' non codante, alors que l'exon trois et quatre contiennent la séquence pour les 389 amino acides de l'OTR Figure 7.

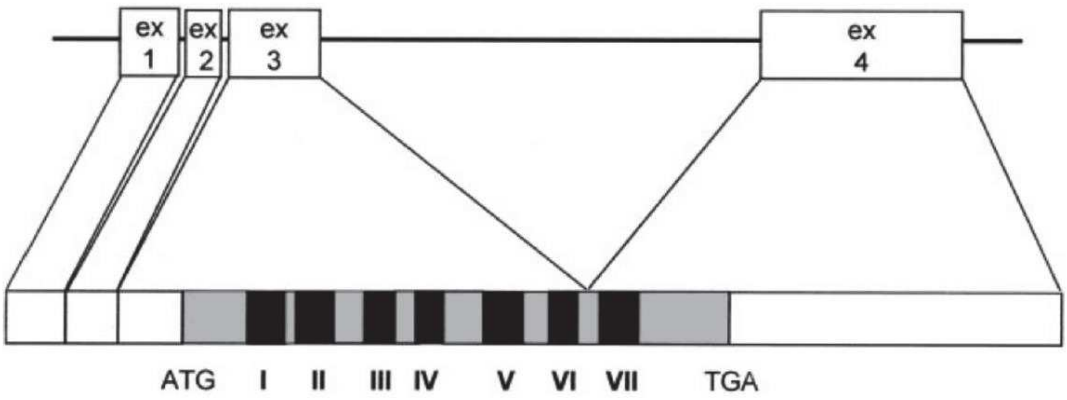

Figure 7 : Structure du gène de l'OTR chez l'Homme. La séquence initiatrice (ATG) et la séquence stop (TGA) sont représentées ainsi que les régions codantes pour les sept régions transmembranaires (rectange noir). Adapté à partir de (Gimpl and Fahrenholz, 2001a)

II.c.i. Régulation génique de l'OTR

Plusieurs séquences régulatrices peuvent être trouvées dans la région 5' du gène OTR. Chez le rat, une région ERE, ERE palindromique, un demi-élément de réponse aux stéroïdes, et un

élément de réponse au AMPc sont présents (Gimpl and Fahrenholz, 2001a). Cela indique que les œstrogènes et les protéines kinases A et C sont impliquées dans la régulation de l'expression des du gène de l'OTR (Bale and Dorsa, 1997). En effet, le traitement à la forskilin pour les cellules de lapin et humaines en culture induisent une up régulation de l'OTR, sous entendant que la voie PKA/PKC peut être potentiellement impliquée dans l'induction de l'expression des OTR(Bale and Dorsa, 1998; Hinko and Soloff, 1993; Jeng et al., 1998).

La régulation du gène OTR par les stéroïdes sexuels est particulière. L'œstrogène est capable d'augmenter la quantité d'ARNm codant pour les OTR ainsi que le nombre de ses sites de liaison, alors que la progestérone a un effet uniquement sur le nombre de sites de liaison disponibles indiquant qu'il agit sur l'OTR en tant que tel (Grazzini et al., 1998; Patchev et al., 1993; Zingg et al., 1998). Cependant, les résultats concernant la régulation de l'OTR par la progestérone sont contradictoires (Ivell et al., 2001).

Bien que le récepteur α, contrairement au β, soit un inducteur de liaison de l'OT à son récepteur dans le cerveau, il a été observé que chez les souris dont le récepteur α oestrogénique a été supprimé, les OTR demeurent toujours présents (Patisaul et al., 2003; Young et al., 1998). Cela suggère que d'autres mécanismes sont capables de réguler l'expression des OTR dans le cerveau (Gimpl and Fahrenholz, 2001a). De plus, des études utilisant la transfection de protéine de fusion contenant la région promotrice du gène d'OTR suivi par un gène rapporteur ont échoué à exprimer le construit à la suite de l'application d'œstrogènes (Ivell et al., 2001; Kimura et al., 2003). L'ensemble de ces études sur la régulation de l'expression de l'OTR par les hormones sexuelles montre un effet clair mais indirect de celles-ci (Fleming et al., 2006; Ivell and Walther, 1999; Ivell et al., 2001). Il semblerait que le gène de l'OTR soit constitutivement actif (Ivell et al., 1998), ce qui suggère que la répression de son promoteur serait un moyen clé dans le contrôle de l'expression de l'OTR. En effet, certaines études démontrent différents états de méthylation pour l'intro 1 et 3 en fonction des tissus, et ainsi proposent que la suppression de la transcription de l'OTR par des mécanismes épigénétiques serait un des moyens de réguler l'expression des récepteurs en fonction des différents tissus (Kimura et al., 2003; Kusui et al., 2001). Cela est prouvé, entre autres, par le fait que différents niveaux de méthylation du promoteur du gène de l'OTR induisent différents niveaux de ARNm pour ce récepteur dans différentes structures cérébrales chez la souris (Harony-Nicolas et al., 2014). De plus, chez l'humain, différents niveaux de méthylation du

gène de l'OTR sont associés à différents modèles d'activité cérébrale dans le traitement des émotions et des perceptions sociales (Puglia et al., 2015), mais également à certains troubles mentaux, comme l'autisme (Kumsta et al., 2013).

II.c.ii. Caractéristiques de l'OTR

II.c.ii.1. Interaction ligand récepteur

L'interaction ligand récepteur pour l'OTR a été fortement étudié à l'aide de diverses techniques et approches. Elles ont, dans un premier temps, identifié la partie N-terminal ainsi que les deux premières boucles extracellulaires comme étant le site de liaison spécifique de l'OT. Il semblerait que la partie N-terminal de l'OTR lie une variété d'agoniste de l'OTR et ne fasse aucune distinction entre eux (Wesley et al., 2002). Le site de liaison spécifique de l'OT réside dans la région E2 et E3 (Fanelli et al., 1999) (Figure 8).

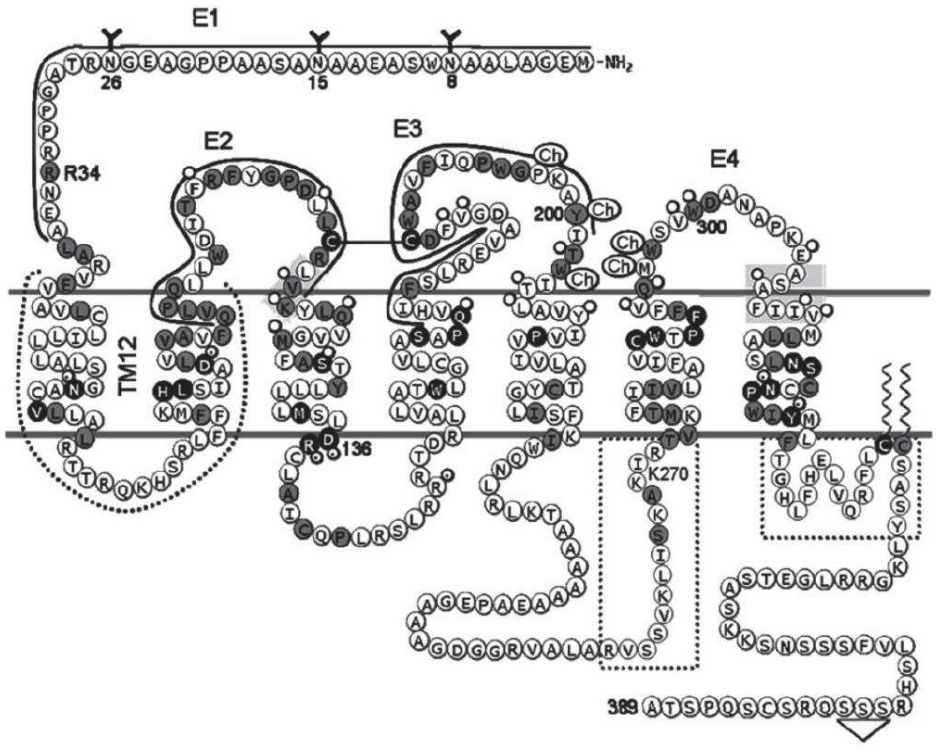

Figure 8 : L'OTR et ses domaines de liaison potentiel. Les lignes continues indiquent les domaines de liaison à l'OT correspondant au domaine extracellulaire E1-3. Les Ch indiquent les sites de liaison potentiel au cholestérol. Les autres détails du schéma sont accessibles dans la revue (Gimpl et al., 2008) d'où le schéma est adapté.

Comme mentionné précédemment, la séquence génique de l'OT est très similaire à l'AVP, ce qui leur permet de se fixer sur leurs propres récepteurs mais également d'interagir avec l'autre. En effet, l'OT et l'AVP présentent tous les deux une forte affinité pour les OTR, mais présentent des valeurs de Ki différentes (OT Ki = 0.79 nM pour l'OTR ; AVP Ki = 1.7nM pour l'OTR). L'AVP peut donc agir comme un agoniste partiel de l'OT (Åkerlund et al., 1999; Chini et al., 1996). Ce profil de sélectivité a conduit au développement de divers agonistes et antagonistes sélectifs de l'OTR. Au cours des dernières décennies, des milliers de peptides synthétiques ont été développé pour leur capacité à se lier et à activer les récepteurs OT et AVP (Busnelli et al., 2013). De plus, il est à préciser que l'OT peut également se lier aux récepteurs de l'AVP mais avec une affinité plus faible que l'AVP lui-même Tableau 2.

	$V_{1a}R$	$V_{1b}R$	V_2R	OTR
OT	120	1782	1544	0.79
AVP	1.1	0.68	1.2	1.7

Tableau 2 : Constance d'affinité de l'AVP et de l'OT pour leurs récepteurs chez l'humain. Les Ki sont exprimés en nM. Adapté de (Chini et al., 1996)

II.c.iii. Implication du cholestérol et des ions divalents

Une autre particularité de l'OTR est sa dépendance fonctionnelle au cholestérol et aux cations divalents. Il y a une relation directe entre la disponibilité du cholestérol et l'affinité de l'OT pour son récepteur, qui peut évoluer d'une constante de dissociation (Kd) de 1 nM en présence de cholestérol à un Kd de 100 nM en cas d'absence (Klein et al., 1995). Cette dépendance au cholestérol est spécifique de l'OTR et n'est pas corrélée aux changements de fluidité membranaire (Gimpl et al., 1997). Des études ont focalisé leur intérêt sur l'identification des sites de liaison spécifique au cholestérol des OTR montré sur la Figure 8. Il a été proposé que

le cholestérol agirait comme un stabilisateur d'un état de haute affinité de l'OTR pour l'OT et faciliterait l'expression de l'OTR. En effet, l'addition de cholestérol dans le milieu de culture de cellules de *Spodoptera frugiperda*, dont la teneur en cholestérol est faible à l'état naturel, augmente l'expression de l'OTR de haute affinité mettant ainsi en évidence l'importance du cholestérol pour la fixation de l'OT sur son récepteur (Gimpl and Fahrenholz, 2002; Gimpl et al., 1995). Une autre théorie est que le cholestérol protégerait l'OTR contre la dégradation protéolytique et thermique. Il a été montré que dans les cellules HEK, les OTR sont plus stables dans les microdomaines plasmatiques riches en cholestérol, retardant ainsi leur inactivation lorsqu'ils sont maintenus en culture à température physiologique (Gimpl and Fahrenholz, 2000). L'adressage des OTR aux radeaux lipidiques est lui aussi capable de modifier les effets de l'activation des OTR. Par exemple, lors de l'adressage des OTR, la présence de cavéoline permet de passer d'un état d'inhibition à un état de prolifération cellulaire (Guzzi et al., 2002). L'ensemble de ces données permet d'expliquer les découvertes des différentes populations d'OTR à haute et faible affinité dans les cellules utérines comme étant des OTR localisés dans des portions de membrane plasmique avec des quantités de cholestérol différentes (Crankshaw et al., 1990).

Les ions divalents tels que le magnésium, le zinc mais aussi le nickel, le manganèse et le cobalt peuvent favoriser la liaison OT/OTR en augmentant l'affinité de liaison entre l'OT et son récepteur et en induisant un changement conformationnel de la structure de l'OT facilitant ainsi sa liaison avec l'OTR (Gimpl and Fahrenholz, 2001a).

II.c.iii.1. Dimérisation du récepteur OTR

La capacité du RCPG à s'associer avec d'autre sous unités pour former des homo- hétéro- ou encore oligo-dimières a été abondamment documentée durant les dernières années notamment à l'aide de techniques biochimiques et biophysiques telles que les co-immunoprécipitations et les études de transfert bioluminescence ou fluorescence (B/FRET) (Bouvier, 2001). Le récepteur à l'ocytocine ne fait pas exception et peut former à la fois des homo- ou des hétéro-dimères (Cottet et al., 2010). Quelques études ont testé l'existence de ces quelques associations pour les OTR. Il a été mis en évidence la capacité de l'OTR et des récepteurs AVP à former des homo et hétéro dimères lors d'étude de biosynthèse *in vitro*

(Terrillon et al., 2003). Dans certains tissus de rat (glande mammaire, cerveau, rein et muscles squelettiques), il a été mis en avant la présence d'homodimères OTR à la surface des cellules (Albizu et al., 2010). De plus, l'OTR est capable d'effectuer un hétérodimère avec le récepteur dopaminergique de type 2 (D2) dans le striatum ventral et dorsal (Romero-Fernandez et al., 2013). Il a également été observé *in vitro* la présence d'hétérodimère entre le récepteur adrénergique β2 et l'OTR (Wrzal et al., 2012a, 2012b).

L'implication physiologique de ces dimères a été testée par le groupe de B. Chini et ses collaborateurs en créant des ligands homobivalents (dOTK2-Cx) (Figure 9). Ils ont, dans un premier temps, en utilisant la technique de BRET, étudié la capacité de ces ligands homobivalents à lier les homodimères OTR. Les OTRs, comme rapporté précédemment, présentent deux états d'affinité différents : faible affinité et affinité élevée. Les récepteurs à faible affinité ne présentent pas de différence d'effet entre la liaison de l'OT et la liaison du ligand homobivalent alors que les récepteurs à haute affinité présentent des réponses de type « super agoniste » lorsqu'ils sont liés avec les ligands homobivalent de longueur appropriée (8 carbones). Le $dOTK_2$-C8 est un ligand homobivalent obtenu suite à la fusion de deux molécules d'OT modifiées (désamination de la terminaison N-ter et remplacement de la leucine en position 8 par la lysine). Ils ont ensuite testé l'effet du ligand le plus efficace parmi ceux synthétisés, le $OTRK_2$-C8, *in vivo* sur des tests comportementaux où l'effet de l'OT a été bien caractérisé : le test des trois chambres chez la souris et le comportement en banc chez le poisson zèbre. Le point commun de ces deux tests est d'évaluer le comportement social chez ces deux modèles d'animaux. Il a été précédemment constaté que l'OT est capable de favoriser le comportement dans ces deux tests. L'injection intra cerebro ventriculaire (i.c.v.) du $OTRK_2$-C8 favorise, elle aussi, le comportement social dans ces deux tests, avec un effet 40 à 100 fois plus important que l'OT (ou l'isotocine chez le poisson). Ces résultats démontrent la dimérisation des OTR au niveau du SNC chez, au moins, deux modèles animaux différents (Busnelli et al., 2016).

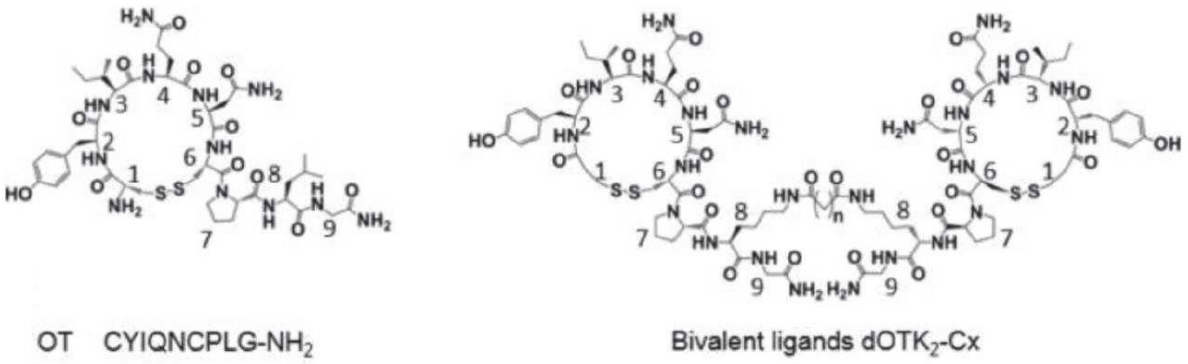

Figure 9 : Représentation 2D de l'OT et d'un ligand bivalent. Cx représente la distance séparant les deux analogues de l'OT modifiés, où le x est le nombre d'atomes de carbone entre les deux groupes lysine. Adapté à partir de (Busnelli et al., 2016).

II.c.iii.2. Signalisation intracellulaire de l'OTR

Les boucles intracellulaires du domaine transmembranaire et du domaine intracellulaire C-Terminal des RCPG sont généralement liées aux complexes hétérotrimériques des protéine G. Ces complexes sont composés de trois sous-unités : α, β et ϒ. Lorsque le ligand se fixe sur le récepteur, celui-ci change de conformation entraînant la phosphorylation d'une guanine diphosphate en guanine triphosphate liée à la protéine G_α. La sous-unité G_α se détache alors du reste du complexe ($G_{\gamma\beta}$) et celui-ci diffuse alors latéralement le long de la membrane plasmique activant divers effecteurs tandis que la sous-unité G_α diffuse pour activer des effecteurs spécifiques dépendant du type de la sous unité G_α. Par la suite, les seconds messagers de la voie de signalisation des RCPG sont activés. Ils permettent l'amplification du signal et modulent de nombreuses fonctions cellulaires. Suite à son activation par le ligand, le récepteur est ensuite recyclé à la membrane ou bien dégradé à la suite de diverses voies cellulaires. Il est important de souligner que le couplage d'un RCPG avec ses différents sous-types de Gα n'est pas fixe, il est soumis à divers facteurs comme le type cellulaire dans lequel il est exprimé. Pour l'OTR, il a été montré que ce récepteur était couplé à différents sous types de Gα comme $G_{q/11}$, G_h, $G_{i/o}$ et G_s (Gimpl and Fahrenholz, 2001a; Reversi et al., 2005a). De plus, ces différents couplages peuvent co-exister au sein d'un même type cellulaire (démontré dans les neurones du bulbe olfactif) (Gravati et al., 2010), ce qui serait favorisé par la localisation des OTR dans différents microdomaines de la membrane plasmique (Rimoldi et al., 2003). Un

point intéressant est que certains agonistes ou antagonistes agissent préférentiellement sur des OTR lié à un certain sous type de Gα, ce qu'on qualifie d'agoniste « biaisé », permettant l'activation sélective des OTR lié au G_q ou G_i (Luttrell et al., 2015).

II.c.iii.3. Couplage ligand-récepteur pour l'OTR

La fonction originelle associée à l'OT, à laquelle elle doit son nom, est la contraction utérine. Au niveau cellulaire, l'activation de l'OTR des cellules myométriales par l'OT conduit à une activation d'une protéine $G_{q/11}$, induisant l'activation de la phospholipase C (PLC) qui induit à son tour la production de l'inositol phosphate (IP3) et diacylglycérol (DAG). L'IP3 va permettre l'ouverture de canaux calciques du réticulum endoplasmique qui finalement conduira à des contractions utérines fines. Pour prévenir les contractions trop précoces de l'utérus durant la grossesse, et éviter le travail prématuré, un antagoniste de l'OTR appelé atosiban a été développé (Thornton et al., 2001). Si l'OTR est lié à la sous unité G_i l'atosiban présente alors un effet agoniste (Reversi et al., 2005a, 2005b).

La carbetocine est également un agoniste biaisé de l'OTR mais spécifique de la voie de signalisation G_q. Cette molécule a initialement été développée comme un analogue de l'OT présentant une plus grande demi-vie dans la circulation périphérique (Barth et al., 1974). Elle présente un effet de contraction utérine post-partum supérieur à l'OT chez la femme (Amsalem et al., 2014), mais chez le rat, la carbetocine et l'ocytocine présentent différents effets, parfois même opposés (Klenerova et al., 2009a, 2009b). Ces différences d'effets pourraient être expliquées par le fait que la carbetocine est en réalité un agoniste biaisé pour l'OTR lié à la signalisation G_q (Passoni et al., 2016).

Les voies de signalisation multiples activées par les différents couplages peuvent dans certain cas être synergiques, comme, par exemple, la stimulation de la protéine G_q et la petite protéine G de la famille des rhos, mais également opposées comme, par exemple, la stimulation conjointe des voies de signalisation G_q et G_i (Gravati et al., 2010). L'utilisation de ces agonistes biaisés permettant de disséquer finement les cascades de signalisation faisant suite à l'activation des RCPGs est de plus en plus populaire en pharmacologie. Elle permet de cibler uniquement une seule fonction des RCPG, permettant des réponses très spécifiques (Busnelli et al., 2012). C'est le cas de l'atosiban, qui, de par sa spécificité à activer les OTR couplés au

protéine G_i, est capable d'inhiber la prolifération des cellules de carcinome mammaire chez le rat et la souris (Cassoni et al., 1996; Reversi et al., 2005b).

II.c.iii.4. Le rôle des GβY dans la signalisation de l'OT

L'implication des sous unités $G_{\beta\gamma}$ suite à l'activation de l'OTR n'a pas été très bien étudiée. Néanmoins, il se peut qu'elles supportent d'importantes fonctions dans la voie de signalisation de l'OTR. Par exemple, il a été montré que, les OTR couplés aux sous unités G_i, sont capables de réguler la libération de calcium des stocks intracellulaires (Hoare et al., 1999). La signalisation intracellulaire pour les OTR couplés aux sous-unités G_q est aussi soutenue par les sous-unités $G_{\beta\gamma}$, au moins dans le myomètre (Zhong et al., 2003). Les sous-unité $G_{\beta\gamma}$ pour les OTR couplés au sous-unités G_q sont impliquées de manière cruciale dans le déclenchement des potentiels d'action en bouffée des neurones ocytocinergiques lors de la lactation (Wang and Hatton, 2007).

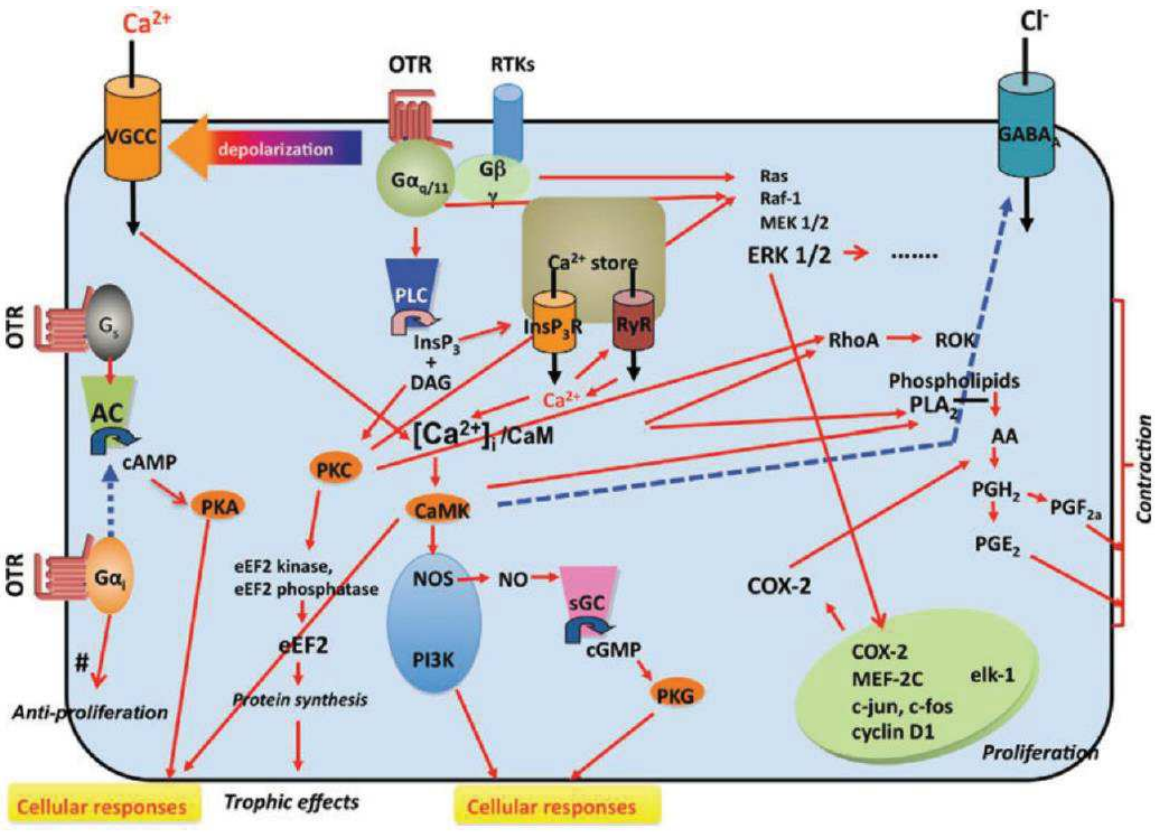

Figure 10 : Voies de signalisation intracellulaire activées par les OTR. Adapté à partir de (Viero et al., 2010)

II.c.iii.5. Les effecteurs secondaires les protéine G couplés aux OTR

Les voies de signalisation intracellulaire activées par les OTR sont variées et nombreuses. Le diagramme Figure 10 a été proposé par Viero et ses collaborateurs ; il résume les voies intracellulaires que l'OTR active (Viero et al., 2010). Pour une vision plus complète de toutes les voies des effecteurs des OTR, il faut se référer à l'ANNEXE 1 et les travaux de (Chatterjee et al., 2016).

II.c.iii.6. Internalisation des récepteurs et leur inactivation.

Suite à une activation persistante des RCPGs, ceux-ci peuvent se désensibiliser. Ce phénomène est présumément médié par la phosphorylation des RCPGs qui inactive les récepteurs, s'en suit la liaison du complexe de β-arrestine (Wolfe and Trejo, 2007). Cela conduit à l'endocytose des récepteurs, leur internalisation ou leur séquestration (Moore et al., 2007). A partir de ce moment-là, le récepteur peut soit être dégradé au sein des lysosomes, soit recyclé et réadressé à la membrane plasmique (Drake et al., 2006). L'OTR ne fait pas exception à cette règle. Les cellules du myomètre exprimant l'OTR après une exposition de 20h à l'OT montrent une réduction de 10% de liaison à l'OT et une diminution de l'expression d'ARNm codant pour l'OTR (Phaneuf et al., 1993; Plested and Bernal, 2001). De plus, les biopsies des myomètres des femme, en culture montrent une diminution de réponse à l'ocytocine, illustrée par une diminution de l'élévation calcique intracellulaire après une exposition à l'OT (Robinson et al., 2003). Cette désensibilisation est probablement due à l'internalisation des récepteurs, et semble se dérouler dans les trente minutes suivant l'application d'agoniste (Guzzi et al., 2002). La désensibilisation des OTR survient par le biais de l'action de la protéine kinase GRK2 (G-protein coupled receptor kinase 2), qui promeut l'action de la β-arrestine et l'endocytose via des puits recouverts de clathrine (Hasbi et al., 2004; Smith et al., 2006). Il a été rapporté que l'OTR appartient à la classe B des récepteurs concernant leur interaction stable avec le complexe de β-arrestine (Oakley et al., 2001). Conti et ses collaborateurs ont démontré que ce n'était pas le cas, que les OTR dans les cellules HEK sont recyclés à la membrane après leur internalisation par ce que l'on nomme « un cycle court » (~quatre heures) (Conti et al., 2009). Il est intéressant de noter que différents agonistes des OTR induisent différents mécanismes et différents types de désensibilisation. L'agoniste sélectif atosiban précédemment décrit ne

semble pas induire l'association des OTR avec le complexe β-arrestine, et l'endocytose des OTR n'a pas été observée même après des expositions soutenues d'atosiban (Busnelli et al., 2012). La carbetocine, quant à elle, induit l'internalisation des OTR, mais par une voie indépendante de celle de la β-arrestine. Par ailleurs, le recyclage des OTR à la membrane n'a pas été observé après l'exposition à cet agoniste (Passoni et al., 2016).

III- Les neurones ocytocinergiques : noyaux et sous type de neurone OT

L'ocytocine est classiquement décrite comme étant synthétisée dans trois noyaux principaux de l'hypothalamus : PVN, SON et AN (Burbach et al., 2001; Sofroniew, 1983; Swanson and Sawchenko, 1983). L'ocytocine est produite par deux type de neurones : les neurones magnocellulaires et les neurones parvocellulaires. Il a été admis que les neurones magnocellulaires projettent à la partie postérieure de la glande pituitaire et soutiennent l'action endocrine de l'OT, tandis que les neurones parvocellulaires ne projettent que centralement et soutiennent (Figure 11).

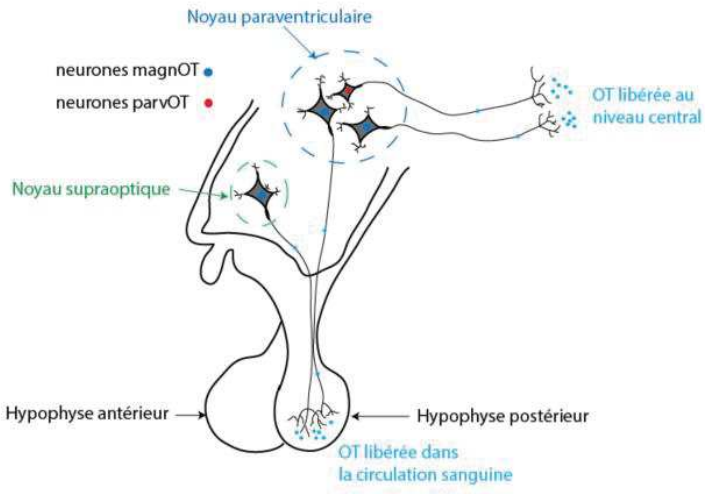

Figure 11 : Schéma représentant le système ocytocinergique

a. Les noyaux ocytocinergiques hypothalamiques

III.a.i. Les noyaux paraventriculaires

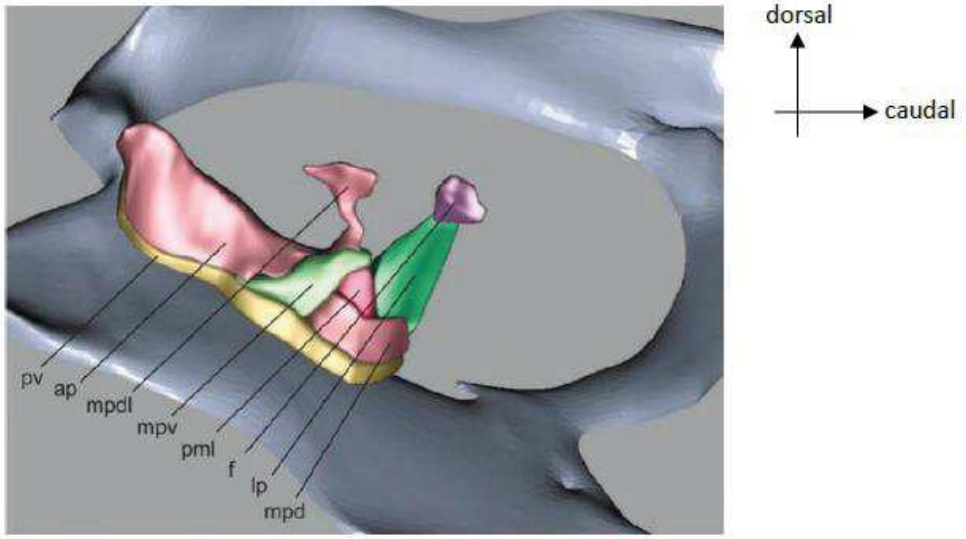

Figure 12 : Reconstruction 3D du PVN et de ses 8 sous-régions. Chaque couleur représente une sous-région du PVN. Abréviation : pv, periventricular part ;ap, anterir parvicellular ; mpdl, lateral wing of mdp ; mpv, ventral zone of medial parvicellular ; pml, lateral zone of posterior magnocellular ; f, forniceal ; lp, lateral parvicellular ; mpd, dorsal zone of medial parvicellular. Adapté à partir de (Simmons and Swanson, 2008)

Le PVN est divisé en huit sous-régions, dont trois contiennent préférentiellement les neurones magnocellulaires, et cinq contiennent les neurones parvocellulaires. Swanson et Kuypers ont décrit l'organisation de ces clusters de cellule dans le PVN de la façon suivante : « Chez le rat, le PVN peut être vu simplement comme étant trois clusters denses de neurones magnocellulaires, intégrés dans une plus grande coquille de neurones parvocellulaires qui se compose de cinq compartiments. » (Swanson and Kuypers, 1980) (Figure 12). D'autre auteurs ont par la suite subdivisé ces clusters pour atteindre un total de onze sous divisions (Simmons and Swanson, 2008). Cependant, tous s'accordent sur le fait que les neurones magnOT et les neurones AVP sont plus ou moins bien séparées comme illustré sur la Figure 13.

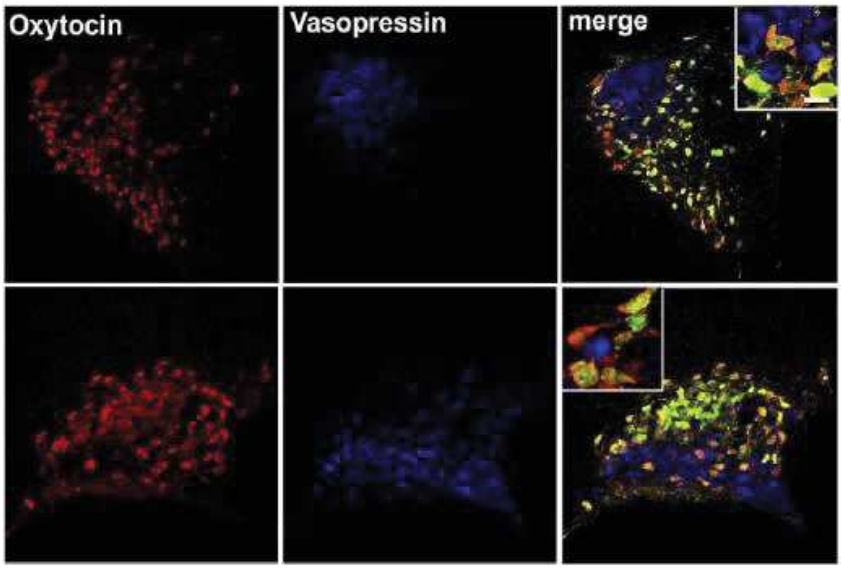

Figure 13 : L'OT et l'AVP sont exprimés par deux populations distinctes dans le PVN (en haut) et dans le SON (en bas). Les images représentées sont des images confocales de coupes coronales. L'OT (rouge) et l'AVP (bleu) ont été révélés par immunohistochimie. Barre d'échelle : 10µm. Adapté à partir de (Knobloch et al., 2012)

III.a.ii. Les noyaux supra optiques

Une différence majeure entre le PVN et le SON est l'absence de neurones parvocellulaires dans le SON, qui est constitué quasi exclusivement de neurones magnocellulaires. Il a été démontré que virtuellement toutes les cellules du SON projettent à la glande pituitaire postérieure. Par exemple, l'absorption d'un marqueur rétrograde injecté dans la neurohypophyse conduit à un marquage présent dans l'intégralité des cellules du SON (Hatton et al., 1984).

III.a.iii. Les noyaux accessoires

Il est estimé que les noyaux accessoires localisés entre le PVN et le SON contiennent ~1/3 de tous les magnOT, et sont une source importante des projections vers d'autres structures cérébrales, dont l'amygdale (Knobloch et al., 2012; Rhodes et al., 1981). A ce jour, six différents noyaux ont été décrits : antérocomissural, circulaire, formique, dorsolatéral, ventrolatérale et extra-hypothalamique (Grinevich and Polenov, 1997; Knobloch and Grinevich, 2014). L'ensemble de ces noyaux forme ce que l'on nomme noyaux accessoires, présenté en Figure 2.

b. Les neurones parvocellulaires

Les neurones parvOT, présents essentiellement au sein du PVN, majoritairement dans la partie caudale, ne projettent pas, à la différence des magnOT, dans l'hypophyse postérieure. Il a été établi que les neurones parvOT projettent dans diverses régions cérébrales (amygdale, locus coeruleus, zona incerta…), le tronc cérébral et la moelle épinière (ME) afin de moduler une multitude de fonctions physiologiques(Atasoy et al., 2012; Baskerville and Douglas, 2008; Eliava et al., 2016; Kita et al., 2006), ainsi qu'un panel d'émotions (peur, anxiété…)(Hasan et al., 2019; Shamay-Tsoory et al., 2009; Tang et al., 2020; Van IJzendoorn and Bakermans-Kranenburg, 2012). Il a été montré que les neurones parvOT sont capables de moduler l'activité des neurones magnOT par leur connexion PVN → SON (Eliava et al., 2016; Tang et al., 2020). Dans la grande majorité des cas, dans le SNC, une fois que l'OT est libérée, elle va se fixer sur son récepteur qui est exprimé dans de nombreuses régions cérébrales. Chez les rongeurs, dans la grande majorité des cas, la distribution des OTR correspond à l'endroit où les neurones OT projettent, tels que la substance périaqueducale grise (PAG) (Nasanbuyan et al., 2018), le tronc cérébral (Blevins et al., 2004; Meddle et al., 2007), en encore la ME (Eliava et al., 2016; Juif and Poisbeau, 2013; Juif et al., 2013). Certains doutes restent présents sur le fait que les neurones parvOT projettent exclusivement dans une seule région cérébrale ; ils pourraient être capables de projeter au sein de plusieurs régions en formant des collatérales(Eliava et al., 2016; Hasan et al., 2019).

c. Les neurones magnocellulaires

En plus de son action de neurotransmetteur, l'OT possède une action hormonale. Ses fonctions neuroendocrines sont médiées par sa neurosécrétion via les neurones magnOT du PVN, SO et AN (Burbach et al., 2001; Sofroniew, 1983; Swanson and Sawchenko, 1983). Les neurones magnocellulaires sont subdivisés en deux populations distinctes en fonction de la nature du peptide qu'ils libèrent (OT et AVP)(Leeuwen and Swaab, 1977; Vandesande and Dierickx, 1975). Ils présentent des propriétés électrophysiologiques différentes (Armstrong, 1995; Renaud and Bourque, 1991). Il existe cependant une petite proportion (1-5%) exprimant les deux. D'autres études ont suggéré que tous les neurones magnocellulaires exprimaient, en réalité, les deux peptides simultanément mais avec de vastes différences dans la quantité synthétisée (Glasgow et al., 1999; Kiyama and Emson, 1990; Xi et al., 1999).

Pour les neurones magnOT, la première étape de la neurosécrétion est la synthèse du pré-propeptide OT dans le réticulum endoplasmique rugueux. S'ensuit le clivage du peptide

signal, la formation des ponts disulfures et son transport dans l'appareil de Golgi. Ce pré-propeptide sera ensuite séquestré dans les vésicules liées à la membrane (granule de sécrétion). Les modifications post-traductionnelles ont lieu au cours de l'adressage vers les terminaisons axonales de l'hypophyse. La libération du complexe OT-neurophysine s'opère via exocytose dans la circulation sanguine suite à l'élévation de la quantité calcique au niveau des terminaison axonales. Une nouvelle dissociation nécessaire à la fixation de l'OT sur son récepteur a alors lieu (Burbach et al., 2001; McEwen, 2004).

Une fois libéré dans la circulation sanguine, l'OT présente une demi-vie estimée entre 3 et 8 minutes chez l'Homme et chez le rat (Morin et al., 2008; Rydén and Sjöholm, 1969), contrairement à la demi-vie dans le liquide céphalo-rachidien chez le rat, qui, elle, est estimée à vingt minutes (Jones and Robinson, 1982; Mens et al., 1983). La dégradation chimique de l'OT dans le sang a lieu suite à l'action du foie et des reins (Claybaugh and Uyehara, 1993). Il existe des peptidases fortement régulées qui permettent l'hydrolyse et le clivage de l'OT, telle que la leucine aminopeptidase placentaire (P-LAP), fortement présente dans le placenta, et également appelée, par abus de langage, « ocytocinase ». Par exemple, la concentration de la P-LAP est régulée positivement au milieu et à la fin de la grossesse, ce qui permet de la mener à terme (Nomura et al., 2005; Yamahara et al., 2000). Une diminution de la concentration de la P-LAP provoque un travail prématuré. En effet, il a été montré que les souris présentant une déficience pour cette peptidase présentent une hypersensibilité à l'OT, ce qui entraîne un déclenchement prématuré de la mise à bas(Ishii et al., 2009). Cependant, la P-LAP est également capable de dégrader l'AVP, l'angiotensine et les endorphines rendant son action non spécifique à l'OT (Tsujimoto and Hattori, 2005). De plus, il semblerait que les P-LAP présentent un rôle particulier dans la modulation de l'effet de l'OT dans la réponse liée au stress au niveau de l'amygdale (Hernández et al., 2009).

En plus de la libération dans la circulation sanguine, des études ont également montré que les magnOT sont capables d'étendre leur axone vers d'autres structures cérébrales, notamment l'amygdale, l'hippocampe, le noyau du lit de la strie terminale ainsi que la zone septale (Buijs et al., 1978; Duque-Wilckens et al., 2017; Knobloch et al., 2012; Sofroniew, 1980). Ces observations, réalisées dans un premier temps chez le rat, ont été retrouvées tant chez les primates non humains (Wang et al., 1997) que chez les humains (Fliers et al., 1986).

d. La libération de l'ocytocine

III.d.i. Libération dendritique de l'OT

Historiquement, une des caractéristiques intéressantes des neurones magnocellulaires décrite, est leur acquisition, au cours de l'évolution, de la capacité de libérer des neuropeptides par exocytose via leurs dendrites (Pow and Morris, 1989). Cette fonction leur permet une communication paracrine au sein des noyaux hypothalamiques, ainsi qu'une diffusion des neuropeptides dans le 3^{e} ventricule. Il a été montré que chez les rongeurs, des neurones OT projettent directement au niveau du 3^{e} ventricule permettant la libération d'ocytocine dans le LCR, en synergie avec la diffusion d'OT dans la matrice extracellulaire environnante (Landgraf and Neumann, 2004). Certaines études ont permis de montrer que la quantité d'OT dans le LCR au niveau du SON est 100 à 1000 fois supérieure à la quantité d'OT mesurée dans le sang, mettant ainsi en évidence une libération dendritique indépendante de la libération axonale (Ludwig and Leng, 2006). De plus, l'activité des neurones OT (synchronisée et en bouffée) serait due à la libération d'OT par ces mêmes neurones au niveau somato-dendritique. L'OT libérée au niveau des dendrites se fixerait au niveau des OTR de ce même neurone ou neurone adjacent activant ainsi ces mêmes cellules, conférant par là même à l'OT une action auto et paracrine (Lambert et al., 1993). La libération d'OT au niveau dendritique permet ainsi l'autorégulation des neurones OT et semble être durable dans le temps. Cependant à ce jour la mise en évidence de la libération axonal de l'ocytocine remet en cause ce mode de libération (Knobloch et al., 2012; Ludwig et al., 2016) et aucune publication depuis ne met en évidence ce mode de communication pour l'ocytocine.

III.d.ii. Libération axonale de l'ocytocine

Les grandes quantités d'OT libérées dans l'hypothalamus (Ludwig and Leng, 2006) ainsi que la répartition différentielle des axones OT au niveau du SNC (Sofroniew, 1980, 1983) laissent fortement penser que l'OT agirait par transmission volumique (Fuxe et al., 2012), diffusion simple à partir des noyaux OT ainsi que par libération dans le LCR au niveau du 3^{e} ventricule. Des études en micro-dialyse ont montré qu'en condition basale, la quantité d'OT avoisinait le 4 pg dans le SON et 2 pg dans le PVN. Au sein des régions cérébrales à proximité tels que l'amygdale, le septum latéral ou encore l'hippocampe dorsale, les concentrations d'OT sont 2 à 4 fois plus faibles qu'au niveau du SON (Wotjak et al., 2008). Ces valeurs sont cohérentes

avec la concentration d'OT dans le milieu extracellulaire (Leng and Ludwig, 2008) et correspondent à l'affinité de l'OT pour son récepteur. Plusieurs études suggèrent que l'OT pourrait agir par le biais de sa diffusion dans le LCR. En effet, environ 80% des régions exprimant les OTR se retrouvent à proximité du LCR, des ventricules ou de l'espace sous-arachnoïdien (Veening et al., 2010). Il est intéressant de noter que les études princeps cherchant à caractériser l'effet de l'OT ont démontré son efficacité en réalisant des injections intracérébrales ventriculaires (i.c.v.). Cependant, les quantités d'OT retrouvées dans le LCR ne sont pas toujours corrélées avec les quantités d'OT plasmatique (Amico et al., 1990), ce qui suggère une modulation différentielle (Veening et al., 2010). La libération somato-dendritique peut avoir lieu sans déclencher la libération axonale et vice-versa. Il y a également des différences au niveau de la demi-vie de l'OT en fonction des différents milieux. La demi-vie de l'OT dans le LCR est beaucoup plus longue que celle de l'OT dans le sang. Cela expliquerait également les différences de concentration observées. De plus, il a été montré chez le rongeur que les neurones OT projetaient directement au 3e ventricule induisant la libération de ce neuropeptide dans le LCR en synergie avec la diffusion d'OT dans la matrice extracellulaire avoisinante (Landgraf and Neumann, 2004) . Cette capacité à libérer l'OT par les dendrites dans le 3e ventricule est un caractère évolutif ancestral des magnOT qui diminue au cours de l'arbre phylogénétique (Figure 14).

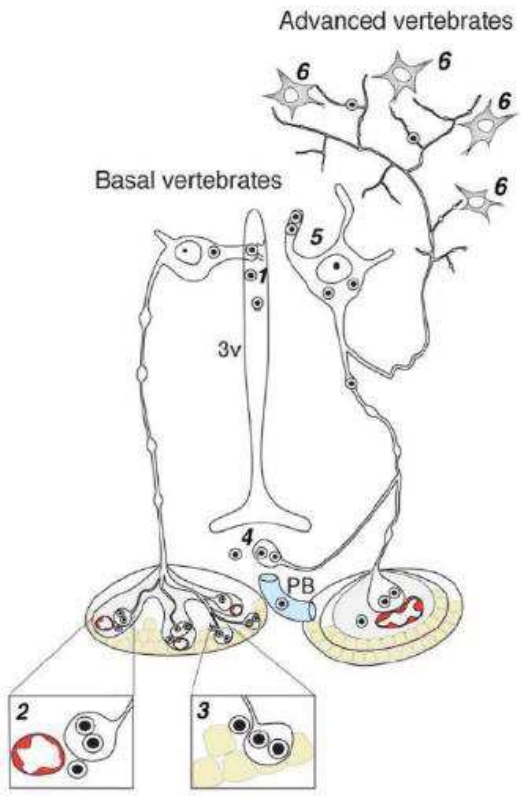

Figure 14 : Voies de libération de l'OT dans le cerveau des vertébrés. 1- voie dendro-ventriculaire ; 2- voies axy-hypophyse postérieur (libération dans la circulation sanguine systémique). 3- voie axo-hypophyse antérieur (action paracrine) 4- contacts axo-hypophyse avec la veine porte ; 5- libération somato-dendritique ; 6- libération axonale. Abréviation : 3v, 3e ventricule ; PB, veine porte. Adapté à partir de (Knobloch and Grinevich, 2014)

Au vu de l'impossibilité de l'OT plasmatique à atteindre le LCR, certains groupes soutiennent l'idée que la quantité importante d'OT retrouvée dans le SNC proviendrait de la libération massive au niveau des dendrites des neurones OT et non de la libération axonale. De telles concentrations d'OT pourraient facilement activer des régions cérébrales proches des ventricules par diffusion à partir du LCR (Veening et al., 2010). Cependant deux récentes études, ont remis en question cette hypothèse en réalisant une nouvelle cartographie des projections des neurone OT renforçant la corrélation entre les projections OT et l'expression des récepteurs dans diverses structures cérébrales (Knobloch et al., 2012; Ross et al., 2009). Une des explications possibles serait que les deux mécanismes soient importants et complémentaires (Landgraf and Neumann, 2004). La diffusion de l'OT agirait sur une période de temps et sur une zone spatiale étendue, tandis que la libération axonale de l'OT permettrait une régulation fine, rapide et plus localisée mais plus contraignante au niveau cellulaire et des microcircuits (Stoop, 2012). En effet, l'effet axonal évoqué n'est pas aussi rapide qu'une libération synaptique. Il a été montré que la stimulation de neurones OT sur des tranches de cerveaux *ex vivo* entraînent des réponses post-synaptiques de l'ordre de la seconde ou dizaine de secondes en comparaison avec la réponse synaptique classique qui est de l'ordre de la milliseconde (Knobloch and Grinevich, 2014). Cela pourrait s'expliquer par le fait que l'OT libérée localement agirait sur des récepteurs localisés à plusieurs micromètres de la terminaison axonale. De plus, pour les neurones OT du SON les vésicules d'OT sont très peu localisées au niveau de la terminaison synaptique mais sont réparties tout le long de l'axone (Knobloch and Grinevich, 2014; Ross et al., 2009) suggérant un mode de libération de l'OT par des synapses « en passant ». Cette notion de libération peptidergique tout du long de l'axone d'un neurone avait été proposée par le passé (Morris and Pow, 1991).

Bien que la concentration en ocytocine dans le SNC soit élevée, de fortes disparités sont observées entre les différentes régions cérébrales (Russell et al., 1992). Cela pourrait s'expliquer dans un premier temps par les différents degrés de régulation des peptidases, mais pas uniquement car cela n'expliquerait pas les différences de concentration d'OT cent fois plus élevée que dans les conditions basales pour certaines régions (Beyer et al., 2010; Ebner et al., 2005). Une autre hypothèse serait que la libération axonale d'OT soit finement régulée et localisée à un noyau donné. Cette théorie est soutenue par diverses études qui montrent que

la stimulation de fibres ocytocinergiques dans diverses structures, ex vivo ou in vitro, induirait des effets cellulaires et comportementaux (Hasan et al., 2019; Knobloch et al., 2012; Mitre et al., 2016; Oettl et al., 2016; Tang et al., 2020). De plus, les différents niveaux de concentration d'OT activeraient des voies de transduction couplées aux différentes protéines G. A forte concentration, le couplage OT avec une $G_{i/o}$ est favorisé, et à l'inverse, à faible concentration, c'est le couplage de l'OT avec une G_q qui est favorisé (Busnelli et al., 2012; Grinevich et al., 2016). Cela signifierait que l'OT peut générer des effets mixtes voire même opposés au niveau des réseaux cellulaires d'une zone donnée.

e. Projection des neurones ocytocinergiques

Dans les années 80, de nombreuses études anatomiques ont commencé à cartographier les projections des neurones OT dans diverses structures cérébrales à l'aide de technique immunohistochimique (De Vries and Buijs, 1983; Sofroniew, 1983). Cependant, avec cette méthode, il a été quasiment impossible de déterminer avec précision de quels noyaux provenaient ces fibres. Plus récemment, grâce à la transfection virale, il a été possible d'exprimer une protéine fluorescente sous le contrôle d'un promoteur génique spécifique permettant un net progrès dans les études anatomiques. Ce fut le cas de l'étude de Knobloch et ses collaborateurs, qui a pu exprimer une protéine fluorescente (Venus) sous le contrôle du promoteur de l'ocytocine et ainsi cartographier les différentes projections de ces neurones dans le cerveau de rats femelles. Les résultats obtenus sont en accord avec les études princeps mais le meilleur marquage des fibres OT a permis de déterminer l'origine de chaque fibre, et donc les noyaux d'origine. (Tableau 3)

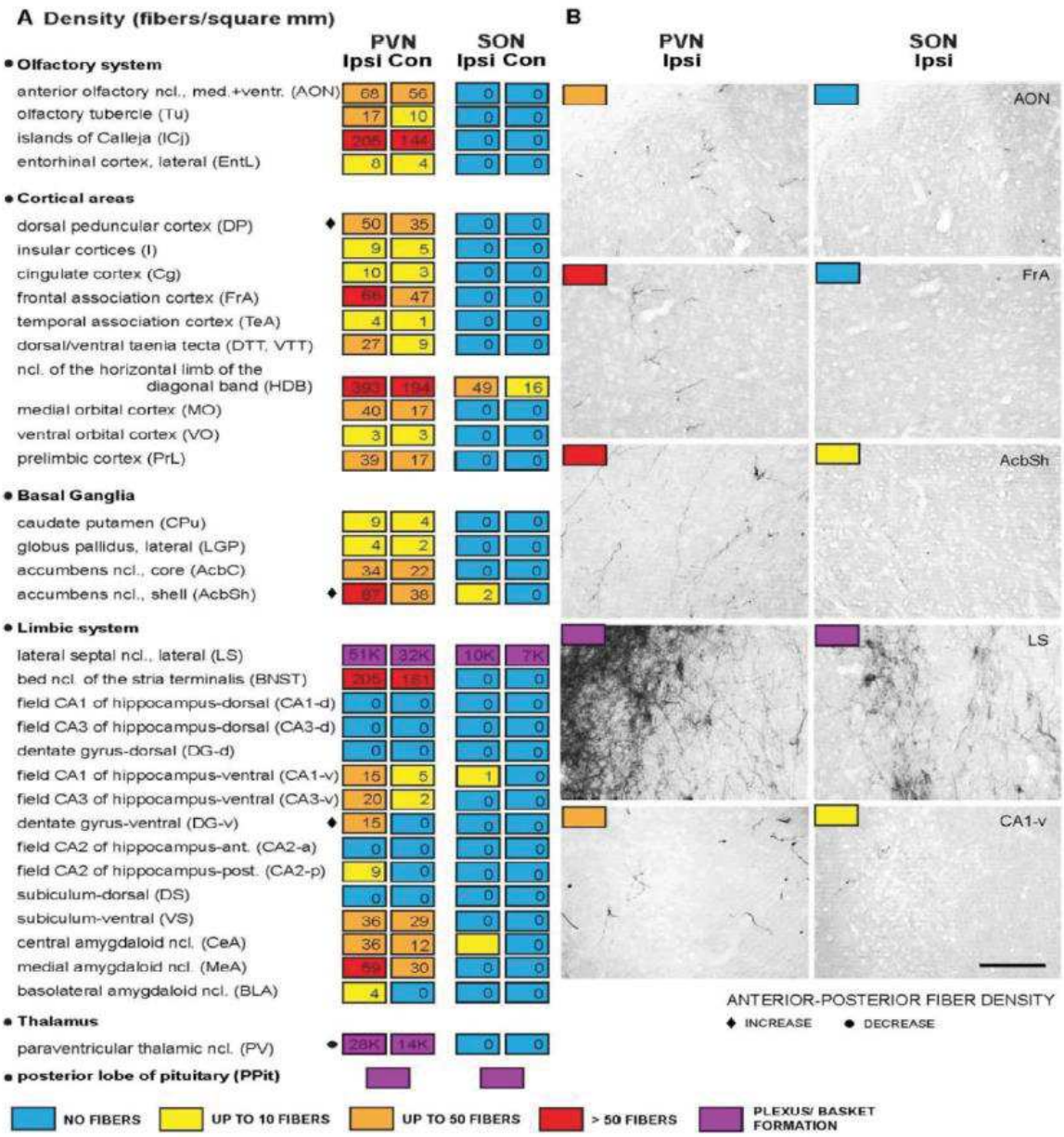

Tableau 3 : Distribution et intensité des fibres OT marquées avec Venus au niveau de diverses régions extra-hypothalamiques. A) Résumé de la distribution et de la densité (nombre de fibre par mm²) des fibres OT exprimant Venus, originaires du PVN ou du SON vers différentes régions extra-hypothalamiques. Abréviation : ipsi, ipsilatéral ; con, controlatéral. Les couleurs, jaune orange, rouge et violette correspondent aux différentes quantifications de fibres OT retrouvées dans les diverses structures analysées. La couleur bleue représente quant à elle les régions dans lesquelles aucune fibre OT n'a été retrouvée ; A l'intérieur de chaque case de couleur est marqué le nombre de fibre OT par mm². A noter, au niveau du CeA, même si la case est colorée en jaune, le nombre de fibres n'est pas indiqué. Ceci est dû au fait que les fibres OT dans le CeA, provenant du SON, étaient marginalement situées sur le bord ventrolatéral du noyau rendant impossible le calcul de la densité de fibres par mm² dans cette structure particulière. Pour les structures avec un gradient prononcé selon l'axe antéro-postérieur, le nombre de fibre OT a été moyennée mais le gradient a été indiqué (•diminution, ◊ augmentation) (B) exemple de fibre OT positive pour Venus dans certaines régions : AON, noyau olfactif antérieur, FrA, cortex préfrontal ; AcbSh, coque du noyau *accumbens* ; LS, septum latéral ; CA1-v, CA1 de l'hippocampe ventral. Les coupes de cerveau ont été colorées avec un anticorps GFP et visualisées par la méthode DAB. Barre d'échelle : 50 µm. Adapté à partir de (Knobloch et al.,2012).

Contrairement à ce qui était classiquement admis, c'est-à-dire que seuls les neurones parvOT projetaient dans le SNC, elle a également montré que des projections ocytocinergiques provenaient du SON, structure décrite comme n'exprimant que des neurones magnOT. Afin de déterminer la nature de ces neurones, elle a prouvé que ces neurones qui projetaient dans l'amygdale centrale (CeA) projetaient également dans l'hypophyse, une caractéristique unique des magnOT. Cette étude se recoupe avec une autre, menée sur un modèle animal différent, le campagnol des prairies, dont le marquage rétrograde des fibres OT innervant les noyaux accumbens provenait du PVN mais également du SON et projetait simultanément au niveau de l'hypophyse (Ross et al., 2009). Knobloch et ses collègues, en plus de la cartographie des projections ocytocinergiques, ont également démontré que la stimulation des fibres OT au niveau du CeA était suffisante pour modifier l'activité électrophysiologique des neurones présents et ce via l'activation des OTR mais également des récepteurs glutamatergiques (AMPA). Ils ont pu démontrer que ces neurones OT projetant au CeA provenaient de l'ensemble des noyaux OT et que ces axones présentaient des varicosités uniquement dans le CeL. Enfin, la stimulation de ces fibres *in vivo* est suffisante pour réduire le comportement d'immobilité induite par la peur (freezing) chez les rats conditionnés (Knobloch et al., 2012).

L'ensemble de ces découvertes a permis de démontrer que les neurones parvOT ne sont pas les seuls neurones ocytocinergiques à projeter au niveau central. L'idée que les neurones magnOT projettent à la fois vers des structures cérébrales et l'hypophyse renforce l'idée du rôle neuromodulateur de l'OT, par sa libération axonale de façon localisée et finement régulée. Une carte schématique présentant les différentes structures innervées est proposée en Figure 15.

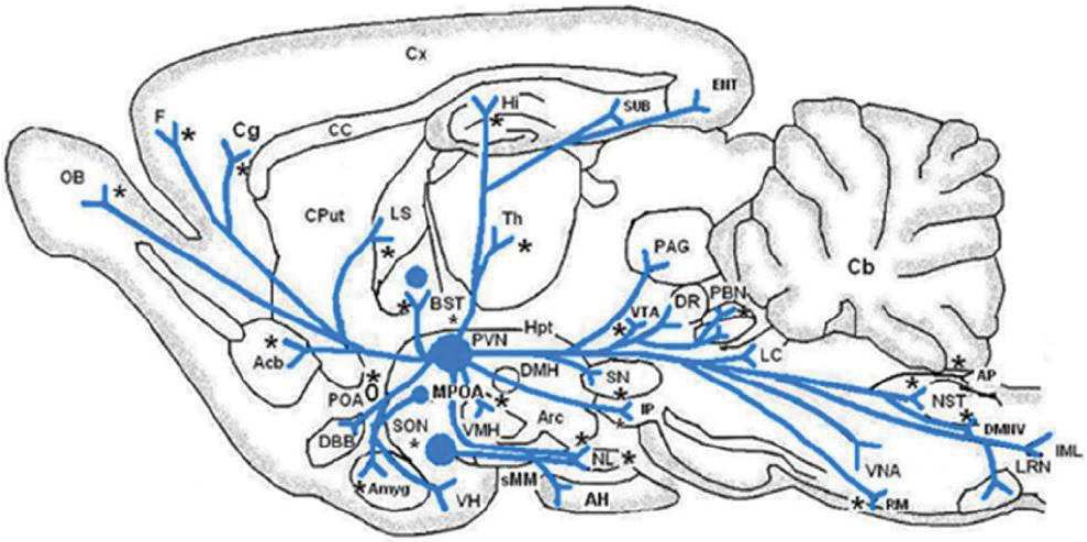

Figure 15 : Projection de neurones OT dans le système nerveux central. Les cercles bleus représentent la localisation des corps cellulaires des neurones OT, les lignes représentent leurs projections, Abréviation : Abbreviations: Acb, accumbens ; Amyg, amygdala ; AP, area postrem a; Arc, arcuate nucleus ; BST, bed nucleus stria terminalis ; Cb, cerebellum ; Cg, cingulated cortex ; Cput, caudate and putamen ; Cx, cortex ; DBB, Broca's diagonal band ; DMH, dorsomedial hypothalamic nucleus ; DMNV ; dorsomedial vagus nucleus ; DR, dorsal raphe nucleus ; ENT, entorhinal cortex ; F, frontal cortex ; Hi, hippocampus ; Hpt, hypothalamus ; IML, intermediolateral column autonomic neurons ; IP, interpeduncular nucleus ; LC, locus coeruleus; LRN, nucleus reticularis lateral ; LS, lateral septum ; sMM, supramammillary nucleus ; NL, neural lobe; NST, nucleus solitary tract ; OB, olfactory bulb; OFC, orbitofrontal cortex ; cPAG, periaqueductal gray ; PBN, parabranquial nucleus ; mPFC, medial prefrontal cortex ; POA, preoptic area ; PVN, hypothalamic paraventricular nucleus ; RM, raphe magnocellularis ; RN, raphe nucleus ; SON, supraoptic nucleus ; SN, substantia nigra ; SU, subiculum ; Th, thalamus ; VMH, ventromedial hypothalamic nucleus ; VMN, ventromedial nucleus of the thalamus ; VP, ventral pallidum ; VTA, ventral tegmental area. Adapté à partir de (Vargas-Martínez et al., 2014)

f. Cartographie du récepteur de l'ocytocine

Dans les années 80, la cartographie de l'expression du récepteur à l'OT a débuté chez le rongeur via l'utilisation de ligand radiomarqué, l'OT tritiée Figure 16 (Freund-Mercier et al.,

1987). Cependant, la limite de cette approche réside dans la capacité de l'OT à se fixer sur les récepteurs à la vasopressine. Il a été dès lors nécessaire de développer de nouveaux ligands radiomarqués. En se basant sur le marquage radioactif à l'iode 125, des chercheurs ont pu développer « ^{125}I-ornithine vasotocin analogue » qui présente un profil hautement sélectif pour l'OTR, permettant ainsi une cartographie efficace des OTR chez les rongeurs (Elands et al., 1988) (Figure 16). Par la suite, plusieurs laboratoires ont cherché à développer de nouveaux agonistes non peptidiques marqués par fluorescence de l'OTR capables de traverser la barrière hémato encéphalique (Karpenko et al., 2015). Il est intéressant de noter que les premières tentatives de cartographier des OTR chez le primate avec les radio-ligands ont échouées dans un premier temps à cause de la perte de spécificité pour les OTR. De manière à pallier ce problème, l'autoradiographie a été optimisée pharmacologiquement en se basant sur une liaison compétitive des molécules radiomarquée avec l'OTR. Le manque de spécificité de la technique a ainsi été surmontée (Freeman and Young, 2016; Freeman et al., 2014a, 2014b). Elle a donc pu être utilisée chez plusieurs espèces de primates non humains. La quantification de l'ARNm des OTR chez le rat et le niveau de liaison de l'OT sur son récepteur chez le rat et l'Homme ont été résumés dans le TABLEAU 4 (Gimpl and Fahrenholz, 2001a).Il est intéressant de noter que les patterns de liaison entre l'OT et la vasopressine ne se chevauchent quasiment jamais (Gimpl and Fahrenholz, 2001a). Lorsque les deux récepteurs sont présents au sein d'une même région cérébrale, ils sont séparés spatialement. C'est par exemple le cas de l'amygdale centrale, où les OTR sont localisés dans la partie latérale (CeL) alors que les récepteurs à la vasopressine sont retrouvés dans la partie médiane (CeM) (Huber et al., 2005; Stoop, 2012).

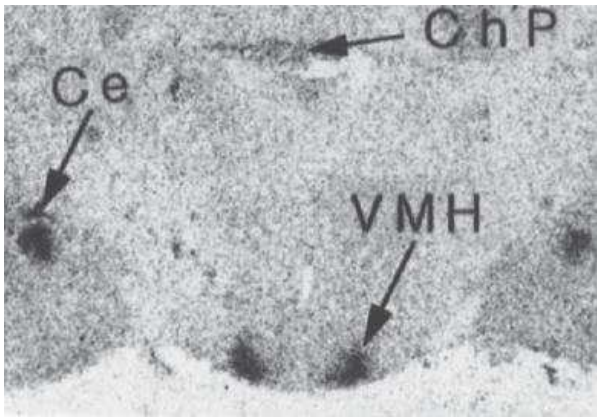

Figure 16 : Photo original d'une autoradiographie à l'aide de [^{3}H]-OT montrant les sites de liaison dans le CeA (Ce) ainsi que dans l'hypothalamus et le plexus choroïde. Adapté à partir de (Freund-Mercier et al., 1987.)

Par la suite, des anticorps dirigés contre les OTR ont été proposés et utilisés pour cartographier l'expression des OTR chez la souris (Mitre et al., 2016). Les résultats sont présentés Figure 17 et concordent avec les précédents résultats cartographiques des OTR obtenus à partir d'une

lignée de souris Knock-in pour la protéine fluorescente Venus dans les OTR (Yoshida et al., 2009).

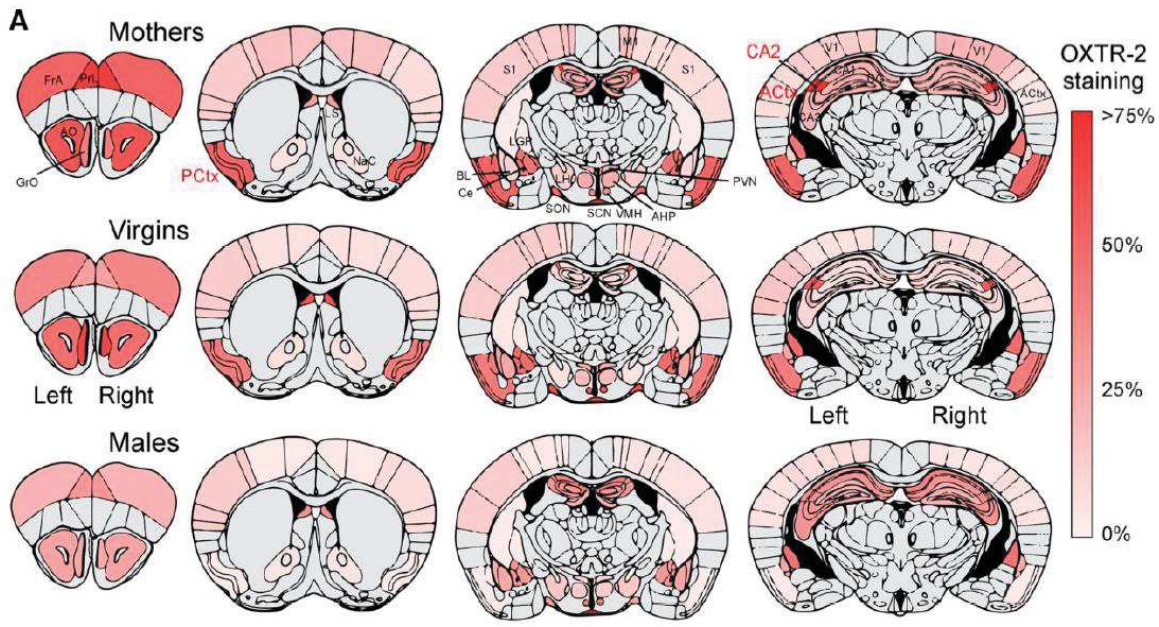

Figure 17 : Profil d'expression des OTR chez la souris femelle (nullipares ou non) et chez le mâle. Les schémas représentent 4 coupes coronales à des coordonnées antéro-postérieures différentes. La couleur rouge représente par région, le pourcentage de cellules exprimant des OTR. Abréviations : auditory cortex (ACtx), anterior hypothalamus (AHP), basolateral amygdaloid nucleus (BL), central amygdaloid nucleus (Ce), anterior olfactory nucleus (AO), bed nucleus of stria terminalis (BST), hippocampal areas CA1-CA3, dentate gyrus (DG), frontal association cortex (FrA), globus pallidus (LGP), granular cell layer of the olfactory bulb (GrO), lateral hypothalamic area (LH), right lateral septum (LS), motor cortex (M1), nucleus accumbens core (NaC), piriform cortex (PCtx), prelimbic cortex (PrL), paraventricular nucleus of hypothalamus (PVN), median raphe (RN), somatosensory cortex (S1), suprachiasmatic nucleus (SCN), supraoptic nucleus of hypothalamus (SON), visual cortex (V1), and ventromedial hypothalamic nucleus (VMH). Les zones grises pourraient exprimer l'OTR mais ils n'ont pas été quantifiées ici. Adapté à partir de (Mitre et al., 2016).

Brain Regions	Rat			Human
	mRNA	OT binding (infant)[a]	OT binding (adult)[a]	OT binding
Olfactory system				
Olfactory bulb	+	?	?	ND
Anterior olfactory nucleus	+++	++	++	?
Olfactory tubercle	+++	?	++	?
Islands of Calleja	ND	ND	+++	+
Piriform cortex	++	?	?	?
Entorhinal/perirhinal area	+	+	+	ND
Cortical areas				
Peduncular cortex	?	++	+++	(+)
Insular cortex	?	+	+	?
Cingulate cortex	+	+++	ND	?
Retrosplenial cortex	?	+++	ND	?
Frontal cortex	++	?	(+)	ND
Temporal cortex	(+)	?	+	ND
Taenia tecta	+++	?	(+)	?
Diagonal band of Broca	+	?	?	+
Basal nucleus of Meynert	ND	ND	ND	+++
Basal ganglia				
Caudoputamen	+++	+++	++	ND
Ventral pallidum cell groups	++	ND	+++	++
Globus pallidus	ND	+++	ND	++
Nucleus accumbens	+	?	+	ND
Limbic system				
Lateral septal nucleus	+	+	+	+++
Bed nucleus of stria terminalis (BNST)	+++	++	+++	ND
Amygdaloid-hippocampal area	+++	+	+	ND
Central amygdaloid nucleus	+++	++	+++	ND
Medial amygdaloid nucleus	++	+	+	ND
Basolateral amygdaloid nucleus	+++	+	+	ND
Parasubiculum and presubiculum	ND	++	++	ND
Dorsal subiculum	+++	+++	(+)	ND
Ventral subiculum	+++	+	+++	ND
Thalamus and hypothalamus				
Anteroventral thalamic nucleus	ND	+	ND	ND
Paraventricular thalamic nucleus	++	++	+	+
Ventromedial hypothalamic nucleus[b]	+++	ND	++	ND
Anterior medial preoptic area	+++	ND	ND	++
Supraoptic nucleus (SON)	+++	ND	(+)	ND
Paraventricular nucleus (PVN)	++	ND	(+)	ND
Medial tuberal nucleus	ND	++	++	+
Posterior hypothalamic area	+	ND	ND	++
Supramammillary nucleus	++	+	+	ND
Lateral mammillary nucleus	ND	+++	+	++
Medial mammillary nucleus	ND	+++	ND	+
Brain stem				
Substantia nigra pars compacta	++	ND	ND	+++
Ventral and dorsal tegmental area	++	ND	ND	ND
Central gray	+	ND	ND	+
Dorsal raphe nucleus	+	ND	ND	+
Reticular nuclei	+	ND	ND	ND
Medial vestibular nucleus	+	ND	ND	ND
Hypoglossus nucleus	++	ND	ND	++
Nucleus of the solitary tract	ND	ND	(+)	+++
Dorsal motor nucleus of the vagus nerve	+++	+	+	+
Inferior olive nucleus	ND	+	+	(+)
Substantia gelatinosa of trigeminal nucleus	+	+++	+	+++
Pituitary gland	ND	+	+	ND

Tableau 4 : Expression de l'ARNm des OTR et les niveaux de liaison avec son ligand dans les structures supraspinales. Les symboles représentent les niveaux d'expression : + faible, ++ modéré, +++ élevé, ND non détecté ; (+) détection limitée et/ou non détecté par tous les scientifiques, ? non enregistré. Adapté à partir de (Gimpl and Fahrenholz, 2001b).

g. Ocytocine et autres neurotransmetteurs

Les neurones ocytocinergiques ont la capacité à sécréter d'autres substances actives en dehors de l'ocytocine telles que :

- Le neuropeptide Y (Larsen et al., 1993)
- La tyrosine hydroxylase (Skutella et al., 1993)
- La Corticotropin releasing hormone (CRH) (Pretel and Piekut, 1990)
- La Thyrotropin-releasing hormone (Tsuruo et al., 1988)
- La Galanine (Landry and Hökfelt, 1998; Landry et al., 1991)
- Et d'autre…

Les neurones OT et AVP peuvent également exprimer les transporteurs du glutamate (Hrabovszky and Liposits, 2008; Ponzio et al., 2006) et libéreraient les deux substances lors de leur stimulation (Knobloch et al., 2012). En se basant sur cette observation, il serait probable que les neurones OT soient capables de libérer diverses molécules bioactives. La découverte de la coexistence entre les neuropeptides et les petits neurotransmetteurs comme le glutamate et le GABA date des années 80. Les deux substances sont stockées dans deux vésicules différentes au niveau des terminaisons axonales et leur libération est nommée : « co-transmission ». Il est classiquement admis que la libération des neuropeptides nécessite des trains de potentiel d'action, alors que pour les petits neurotransmetteurs un potentiel d'action isolé serait suffisant pour générer leur libération (Albers, 2015; Hökfelt, 1991). Cette différence de libération permet alors une régulation fine des circuits neuronaux. Cependant, il a également été montré que des neuropeptides de différentes familles ou différents types de neurotransmetteurs pouvaient être contenus dans les mêmes vésicules, et libérés conjointement lors de l'exocytose. On nomme ce phénomène : la colibération (Vaaga et al., 2014). Une comparaison entre ces deux modes de libération est présentée en Figure 18. Bien que préalablement démontrée pour diverses molécules, de récentes études ont montré la cotransmission ou colibération par les neurones ocytocinergiques de l'OT avec d'autres molécules (Eliava et al., 2016; Hasan et al., 2019; Knobloch et al., 2012). Il a également été prouvé que les neurones OT sont capables de libérer de l'OT tout au long de leurs axones alors

que la libération de glutamate, elle, ne s'effectue qu'au niveau de la terminaison synaptique (Meeker et al., 1991; Navone and Di Gioia, 1988; Ross et al., 2009).

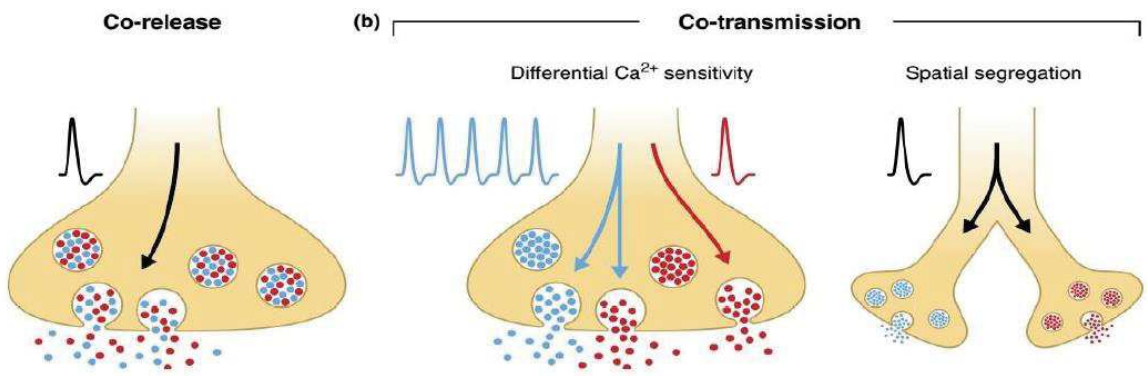

Figure 18 : Illustration de deux modes de libération synaptique : co-libération et co-transmission. La co-libération consiste en la libération de plusieurs molécules neuroactives à partir d'une même vésicule synaptique. Dans le cas de la co-transmission, les molécules neuroactives sont contenues dans des vésicules distinctes, permettant soit une libération différentielle des molécules selon leur sensibilité aux concentrations de calcium soit une libération des molécules neuroactives au niveau de boutons synaptiques différents (ségrégation spatiale). Adapté à partir de (Vaaga et al., 2014).

IV- Fonction de l'ocytocine

a. Généralités

L'ocytocine est une molécule fortement impliquée dans la régulation de nombreuses fonctions physiologiques ainsi que dans la survie et la propagation des espèces : interaction sociale, reconnaissance sociale, choix du partenaire, comportement sexuel, parturition, lactation, comportements parentaux… Elle est également impliquée dans la régulation de la fonction cardiaque, la régulation osmotique ainsi que la modulation des émotions en général. Les études sur les actions diverse de ce neuropeptide nommé « the great facilitator of life » ont fortement augmentées ces dernières années (Lee et al., 2009). (Figure 19).

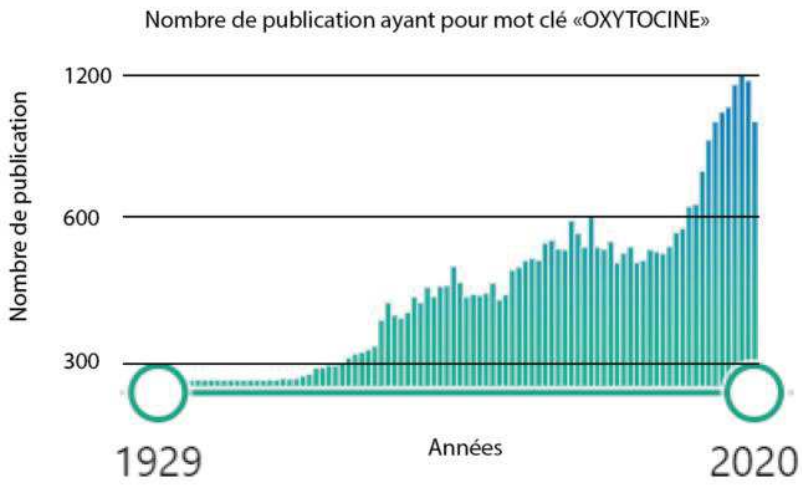

Figure 19 : Augmentation du nombre de publications recensées sur Pubmed ayant pour mot clé « ocytocine ». Depuis les années 2010, les études sur l'OT n'ont cessé d'augmenter

Cette partie se focalisera en détail sur certaines des fonctions de l'OT, mais la liste non exhaustive des autres fonctions est représentée en Tableau 5.

Behavioral classes	Behaviors	Effects of Oxt in rodents	Effects of Oxt in humans
Social behaviors			
Social memory	Social recognition	–⇑ odor processing in olfactory bulb –⇑ social memory –⇓ social recognition in Oxtr KO mice – abnormal Bruce effect in female Oxt KO mice	–⇓ amygdalar activation to social stimuli –⇑ memory for faces
Affiliation	Sexual behavior	–⇑ erections (with T) and ejaculation frequency in males –⇑ receptivity (with E) in females	–⇑ arousal in men and women –⇑ uterine contractions at parturition
	Paternal behavior	–⇓ parental behavior with concomitant Avp/Oxt antagonism –⇓ adult paternal behavior with Oxt antagonist on PND1	no known effect
	Maternal behavior	– ⇑ Oxtr throughout the brain with onset of maternal behavior – necessary for lactation – induces full repertoire of maternal behaviors (in presence of E) – ⇓ pup retrieval and pup survival in Oxtr KO	no known effect
Aggression	Female aggression	–⇑ Oxt levels in CeA correlated with aggression	no known effect
	Male aggression	– may have organizational effect during prenatal period	–⇑ plasma Oxt levels in males with conduct disorder
Non-social behaviors			
Learning and memory	Non-spatial memory	–⇓ memory in passive avoidance tasks	–⇓ episodic memory in men and women –⇓ verbal recall of certain categories of words
	Spatial memory	–⇑ memory when injected into hippocampus – ⇓ memory when injected into NBM	no known effect
Anxiety and depression	Anxiety	–⇓ anxiety following Oxt administration –⇑ anxiety in some Oxtr KO mice; sexually dimorphic	–⇓ amygdalar response to threatening stimuli –⇓ anxiety to social stressors
	Depression	–⇑ active/coping behaviors with i.p. Oxt administration	– ⇓ plasma Oxt associated with major depression

Tableau 5 : Effets comportementaux de l'OT. Ce tableau compile les effets principaux de l'OT dans le comportement des rongeurs mais également chez les humains. Adapté à partir de (Lee et al., 2009)

b. Régulation de la peur par le système ocytocinergique

Selon les études de Barlow dans les années 80, la peur est définie comme étant une émotion primaire éprouvée par un individu lors de la confrontation de celui-ci avec un danger immédiat. Elle est obligatoirement déclenchée par un objet déterminé et limitée dans le temps. La peur peut être classé en deux catégories : spontanée ou apprise. C'est le cas des tests de conditionnement à la peur(Barlow et al., 2003). Antonio Damasio a défini les émotions comme « une modification transitoire de l'état de l'organisme dont les causes sont spécifiques. »

Il ajoute par la suite un exemple basé sur l'expérimentation de la peur : « Quand on est effrayé par quelque chose, notre cœur commence à s'accélérer, notre bouche devient sèche, notre peau pâlit et nos muscles se contractent. C'est la réaction émotionnelle qui se produit de manière automatique et inconsciente. »

La relation entre le système ocytocinergique et la peur a parfaitement été établie au cours des années passées. Il a été montré que l'OT exerce un effet inhibiteur dans le comportement lié à la peur au travers de mécanismes à la fois centraux et périphériques. Une injection i.c.v d'OT ou une stimulation de centre ocytocinergique ont été suffisantes pour diminuer les comportements associés à la peur chez les rongeurs, observable par une diminution du temps de « freezing ». L'administration central d'OT entraîne la fixation de ce peptide sur son récepteur au sein de différentes structures cérébrales, dont le CeL qui présente des projections vers d'autres structures cérébrales impliquées dans la régulation de la peur. Les lésions d'amygdale ont montré une diminution du temps de freezing dans un paradigme de peur. De plus, une étude récente a permis l'identification d'une petite sous population de neurones OT qui, suite à une stimulation optogénétique, diminue fortement le comportement de freezing chez le rat, ainsi que l'implication des neurones OT hypothalamique dans la représentation d'un engramme soutenant la mémoire de la peur. (Hasan et al., 2019; Knobloch et al., 2012).

Une administration périphérique d'OT semble quant à elle diminuer l'anxiété mais ne semble pas spécifiquement moduler la peur en tant que telle (Ayers et al., 2011; Uvnäs-Moberg et al., 1994). Cette différence observée serait en partie due par les propriétés pharmacocinétiques de l'OT, qui varient selon le compartiment.

L'utilisation de lignées de souris transgéniques a également permis d'étudier l'implication des système ocytocinergique dans la modulation de la peur. La délétion après le sevrage des OTR dans la partie cérébrale antérieure induit une diminution du temps de freezing chez les animaux (Pagani et al., 2011). Les OTR mais également les AVPR présenteraient donc une forte implication dans la régulation de la peur (Veinante and Freund-Mercier, 1997). Un point important à soulever est que, bien que l'OT soit impliquée dans la modulation de la peur, cette molécule n'affecte pas l'apprentissage de la peur mais facilite son oubli (Toth et al., 2012).

Des résultats similaires ont été démontrés chez l'humain. L'administration intranasale d'OT semblerait renforcer le phénomène d'oubli de la peur (Acheson et al., 2013; Eckstein et al., 2016) en interagissant avec l'amygdale (Milad and Quirk, 2012; Milad et al., 2007) et en renforçant les connexions entre l'amygdale et le cortex préfrontal, connexion fortement impliquée dans les processus de mémoire (Sripada et al., 2013). Des différences dans les processus de mémorisation des émotions ainsi que dans leur régulation semblent exister entre les mâles et les femelles. Ces différences pourraient être expliquées par l'implication de la progestérone et des œstrogènes dans la modulation des réseaux de l'amygdale activés par la peur (Andreano and Cahill, 2010; Goldstein et al., 2005, 2010).

c. Régulation du stress et de l'anxiété par l'OT

De nombreuses études et observations ont établi un lien entre l'OT et le stress. L'OT serait capable d'agir directement sur l'axe corticotrope, appelé également l'axe du stress. En général, de fortes concentrations plasmatiques d'OT sont retrouvées suite à un stress physiologique ou psychologique. L'injection d'antagonistes de l'OT dans le PVN induirait une augmentation du niveau basal et celui induit par le stress d'adreno-corticotropin hormone (ACTH) (Lee et al., 2009; Neumann et al., 2000). De plus, l'OT serait également un puissant anxiolytique. Il a été montré que la libération d'OT durant l'accouplement réduirait les comportements associés à l'anxiété chez les souris mâles, et cet effet est inhibé en cas d'administration d'un antagoniste aux OTR (Waldherr and Neumann, 2007). Une infusion bilatérale d'OT dans le PVN montre des effets anxiolytiques dans deux tests évaluant l'anxiété, le labyrinthe en croix surélevé et le test de light-dark box, que ce soit chez le mâle ou chez la femelle (Blume et al., 2008). Il a également été montré qu'une injection i.c.v. d'OT induit une diminution dose-dépendante de la concentration de corticostérone circulante chez des animaux préalablement exposés à un stress auditif. Le même effet anxiolytique de l'OT a également été démontré après l'exposition

à un nouvel environnement (Windle et al., 1997). La corrélation entre le système ocytocinergique et le système hormonal a été renforcée par l'étude montrant que l'OT agit comme anxiolytique lors de la réalisation d'un test de labyrinthe en croix surélevé chez des souris ovariectomisées, mais uniquement lorsque l'injection d'OT est couplée avec une administration d'œstradiol (McCarthy et al., 1996). De plus, l'OT semble induire une diminution de l'anxiété induite par la mise basse, car l'injection d'un antagoniste de l'OTR dans la partie ventro-caudale du PAG augmente l'anxiété mesurée chez les femelles allaitantes, mais pas chez les femelles vierges (Figueira et al., 2008).

L'effet anxiolytique de l'OT pourrait être médié par l'amygdale. Lorsque l'OT est injectée au sein de l'amygdale chez des femelles ovariectomisées, elle présente un effet anxiolytique qui n'est pas retrouvé lors d'injection dans l'hypothalamus ventro-médiant (Bale et al., 2001). Cette étude démontre que l'OT joue un rôle clé dans la régulation des émotions négatives par son action sur l'amygdale et plus particulièrement sur le CeA. On notera que les souris OT-KO démontrent un phénotype anxieux lors de la réalisation de test de labyrinthe en croix surélevé, qui se retrouve réduit lors de l'administration i.c.v. d'OT (Mantella et al., 2003). De plus, ces souris OT-KO présentent des taux de corticostérone élevés lorsqu'elles sont soumises à des stress psychogéniques aigus et chroniques, mais pas en condition basale. Ce phénomène n'est pas retrouvé lors de la réalisation de stress physique, comme par exemple lors lors de l'induction d une hypoglycémie par insuline, ce qui indique une régulation de stress spécifique par l'OT (Amico et al., 2008; Ja et al., 2004; Mantella et al., 2003).

d. Nociception et modulation de la douleur par l'ocytocine

La douleur est définie par l'association internationale pour l'étude de la douleur comme : « une expérience sensorielle et émotionnelle désagréable associée avec des dommages tissulaires potentiels ou réels ou décrite dans ces termes ». La douleur est une expérience ubiquitaire chez l'animal, décrite comme une sensation normale déclenchée par le système nerveux alertant d'une blessure potentielle nécessitant un repos et une récupération. Le circuit de la douleur consiste en une voie ascendante qui transmet le signal nociceptif de la périphérie jusqu'au SNC, et d'une voie descendante, qui projettent sur les différents éléments du réseau pouvant soit augmenter ou diminuer le signal de la douleur (Figure 20).

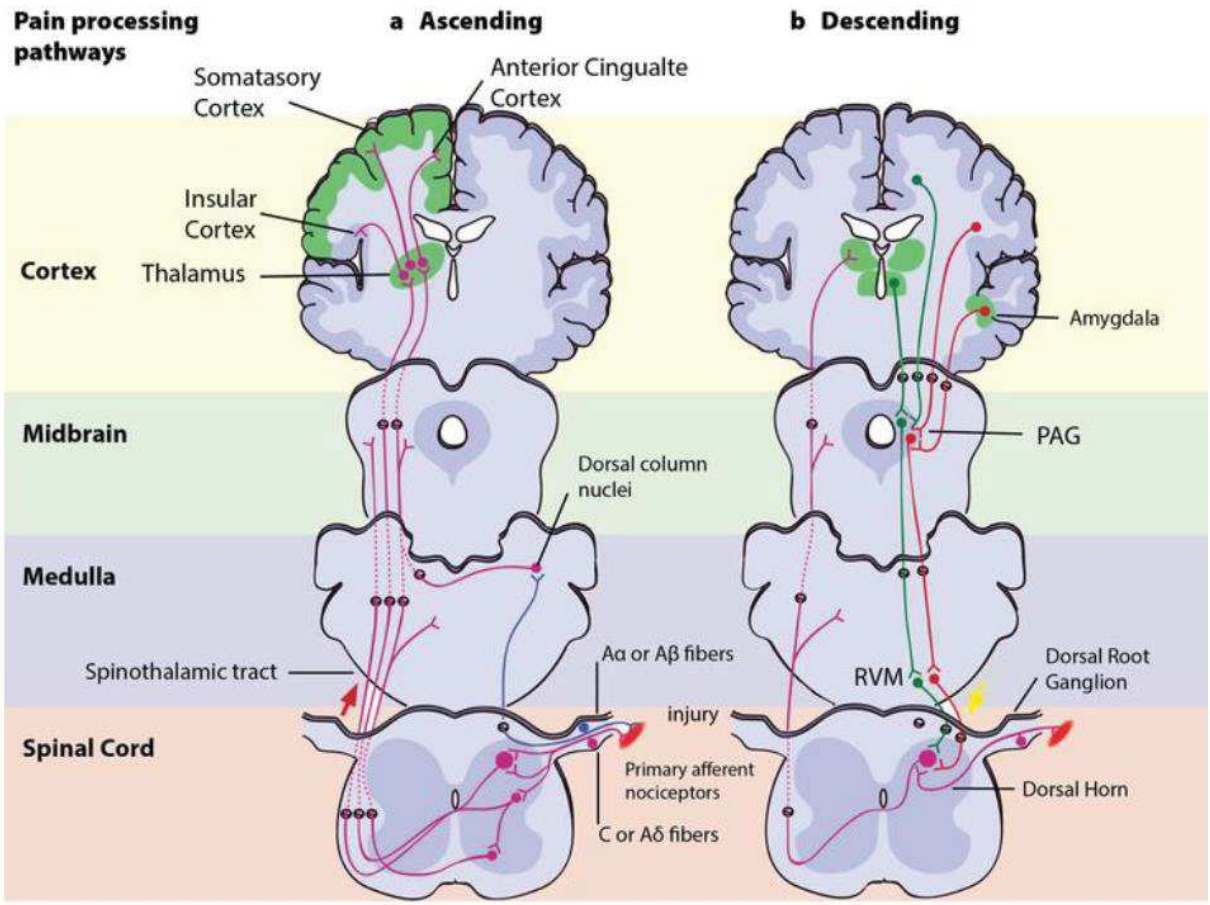

Figure 20 : Voie d'intégration de la douleur. A gauche, la voix ascendante. Une blessure active simultanément les fibres Aα ou Aβ et les fibres C ou Aδ à faible conductance. Le signal codant pour la pression, l'étirement ou les mouvements des tissus remonte par les fibres A rapides jusqu'au cortex via les noyaux de la corne dorsale. Les fibres C et Aδ quant à elles font transiter les informations douloureuses des nocicepteurs présents dans les tissus ou dans la peau jusqu'aux neurones de second ordre dans la corne dorsale de la moelle épinière. Les neurones de second ordre transitent alors de l'autre côté de la moelle épinière, où ils forment le tractus spinothalamique ascendant. Ce tractus transmet alors des signaux au noyaux de la moelle et du mésencéphale jusqu'au thalamus. Le thalamus relaie alors les informations au cortex somatosensoriel et au cortex insulaire ainsi qu'aux régions corticales intégrant les différents aspects de la douleurs, telle que la réponse affective (cortex cingulaire). A droite, la voie descendante. Les informations de l'environnement ainsi que motivationnel peuvent activer ce réseau. Quelques aires dans le système limbique comprenant le cortex cingulaire antérieur, le cortex insulaire, l'amygdale ainsi que l'hypothalamus, projettent au niveau de la PAG (periaqueductal grey), qui est capable de moduler la voix ascendante de la transmission nociceptive de façon indirecte en modulant l'activité du la medulla ventromédiale (RVM). Cette modulation induit une analgésie par la libération d'opioïde endogène ou de substance neuroactive comme l'OT agissant sur des cellules ON et OFF pour exercer soit un contrôle inhibiteur (vert), soit facilitateur (rouge) sur les signaux nociceptifs provenant de la corne dorsale de la ME. Adapté de nobaproject.com.

L'ocytocine est reconnue comme étant un important médiateur de l'analgésie endogène (Tracy et al., 2015). Elle agit à chaque niveau de la nociception et du traitement cognitif de la douleur, du système périphérique en passant par le système spinal jusqu'au système central.

IV.d.i. Effet anti nociceptif de l'OT au niveau spinal

Les neurones parvOT du PVN projettent leurs axones à la lamina I et II de la corne dorsale, autour du canal central (Puder and Papka, 2001; Swanson and McKellar, 1979). Ces axones ocytocinergiques établissent des contacts synaptiques avec les neurones de la lamina I et II de la corne dorsale et également au niveau de la lamina X (Moreno-López et al., 2013; Rousselot et al., 1990).

Les OTR sont fortement exprimés au niveau de la lamina superficielle de la corne dorsale, ce qui concorde avec la présence des fibres ocytocinergiques retrouvées au niveau de cette structure (Reiter et al., 1994). Ces observations anatomiques sont corroborées par les expériences fonctionnelles. Dans le modèle hypersensibilité douloureuse induite par une ligation spinale, les femelles ayant mises bas présentent un seuil à la douleur supérieur aux femelles contrôles si elles sont allaitantes. De plus, ces données sont corrélées avec un taux d'OT circulant élevé dans le LCR. Il est intéressant de noter que, lorsque ces femelles sont séparées de leur progéniture, l'hypersensibilité douloureuse augmente. Cet effet peut être contré par l'administration intrathécale d'OT. A l'inverse, les antagonistes des OTR suppriment cette augmentation du seuil douloureux chez les femelles allaitantes. Cela indique qu'il y a une libération tonique d'OT dans la moelle épinière, ne serait-ce qu'après la mise basse et durant l'allaitement, ce qui permet l'atténuation de l'hypersensibilité douloureuse (Gutierrez et al., 2013). Les enregistrements électrophysiologiques *in vivo* dans les différents niveaux de la moelle épinière chez le rat montrent que l'application d'OT peut susciter soit une activation, soit une inhibition de l'activité électrique des neurones enregistrés. L'ocytocine peut également réduire l'augmentation d'excitabilité provoquée par l'application de glutamate ou les stimulations somatiques douloureuses. Les différences entre l'activation ou l'inhibition des neurones enregistrés suggèrent l'implication d'interneurones inhibiteurs agissant comme neurones de 2nd ordre (Condés-Lara et al., 2003). Par la suite, Breton et ses collègues ont démontré, en enregistrant en patch clamp des neurones de la lamina II, que l'OT activait une sous population d'interneurones glutamatergiques, qui permettent le recrutement d'interneurones Gabaergiques au sein de cette même structure. Cette augmentation de

l'inhibition pourrait potentiellement inhiber le signal nociceptif arrivant via les fibres afférentes Aδ et C (Breton et al., 2008). Ils ont aussi montré qu'au sein de la même lamina, l'activation des OTR diminue les potentiels d'action des neurones présentant une activité en bouffée suite à une dépolarisation préalable (depolarization induced bursting fring pattern), mais que l'activation des OTR n'a pas d'effet sur les neurones présentant une activité électrique « single firing ». Ils ont par la suite prouvé que l'action des OTR sur les changements de type de décharge était médiée par la diminution de l'amplitude et l'inactivation I_A voltage-gated potassium current (Breton et al., 2009). Un point intéressant est que, contrairement à l'effet périphérique de l'OT sur la nociception, le système vassopressinergique ne semble pas être impliqué dans l'effet de l'OT, du moins au niveau spinal (Rojas-Piloni et al., 2010).

Cet effet d'OT exogène peut également être observé lors de la stimulation des projections descendantes des neurones OT du PVN(Eliava et al., 2016). En effet, durant l'enregistrement des décharges évoquées par les fibres Aδ et C, Condès-Lara et ses collègues ont pu diminuer la durée de ces décharges en stimulant électriquement le PVN. L'effet de la stimulation du PVN a également pu être répliqué par l'application d'OT exogène au niveau du site d'enregistrement spinal, et ces deux effets peuvent être supprimés lors de l'application préalable d'antagoniste pour les OTR. Ils ont par la suite montré que, dans le modèle in vivo d'hyperalgésie et d'allodynie, l'injection intrathécale d'OT possède de claires propriétés anti-nociceptives et que la stimulation du PVN démontre des effets similaires (Condés-Lara et al., 2006; Miranda-Cardenas et al., 2006). Ces deux mécanismes sont dépendants de l'activation des OTR. Les mêmes équipes ont par la suite montré, à l'aide d'enregistrement électrophysiologique, une sous-population de cellules dans le PVN répondant au stimulus nociceptif thermique et mécanique. Ces cellules identifiées projettent au niveau de la moelle épinière (Condés-Lara et al., 2009). De plus, la stimulation du PVN antérieur est capable d'élever les taux d'OT circulant au niveau de la moelle épinière alors que la stimulation de la partie postérieure augmente uniquement le taux d'OT au niveau du LCR (Martínez-Lorenzana et al., 2008). Cela peut être expliqué par le fait que, lors de la stimulation dans la partie postérieure du PVN, seuls les neurones magnocellulaires sont activés, et ceux-ci ne projettent pas à la moelle épinière. De plus, la stimulation du PVN génère également des réponses au niveau des neurones de la colonne dorsale projetant au niveau central (Rojas-Piloni et al., 2008).

Les études *in vivo* de DeLaTorre et ses collègues ont par la suite montré que l'OT exogène et la libération endogène d'OT suite à la stimulation du PVN peut réduire ou empêcher la LTP au niveau des « wide dynamic range neurone » (WDR) au niveau spinal. Ces neurones reçoivent des informations sensorielles nociceptives et non nociceptives. Ils projettent à des niveaux supra spinaux. La potentialisation à long terme dans ces cellules facilite les réponses nociceptives évoquées (DeLaTorre et al., 2009). Il a également été montré une activation des cellules du PVN (augmentation de l'expression des gènes précoces) ainsi qu'une augmentation des niveaux d'OT endogènes dans la ME dans le modèle de douleur inflammatoire chez le rat. De plus, l'OT spinal induit une analgésie tonique démontrée par l'augmentation du seuil nociceptif après l'injection d'antagoniste sélectif pour l'OTR. De façon intéressante, l'analgésie à long terme est assurée par l'OT. Elle repose sur la neurosteroidogénèse, qui conduit à une augmentation des inhibitions induite par les neurones $GABA_A$ de la lamina II (Juif et al., 2013). Ces résultats indiquent que l'effet anti-nociceptif prolongé de l'OT pourrait protéger contre une sensibilisation centrale. En effet, ce modèle explique la transition de la douleur aiguë en douleur chronique, induite par la potentialisation des neurones nociceptifs suite à une exposition répétée de stimuli douloureux, qui vont renforcer les prochains signaux nociceptifs. Chez l'humain, il a été montré, chez les patients souffrant de lombalgie, que l'injection intrathécale d'OT induit un effet analgésique de façon dose-dépendante. Il est également montré que l'effet anti nociceptif de l'OT spinale sur les douleurs somatiques, prouvée dans les travaux cités précédemment, agit sur les douleurs viscérales (Engle et al., 2012).

Comme présenté précédemment, les populations d'interneurones GABAergiques répondent de manière directe ou indirecte à l'application d'OT dans la ME (Breton et al., 2008), ou suite à la stimulation du PVN (Rojas-Piloni et al., 2008), et inhibent l'activité des cellules nociceptives projetant au niveau central. Ces résultats ont par la suite été confirmés, et il a été mis en évidence l'implication des récepteurs μ-opioïde. En effet, leur blocage diminue l'effet inhibiteur de l'application d'OT dans la ME ou la stimulation du PVN (Condés-Lara et al., 2009; Miranda-Cardenas et al., 2006). De manière similaire, une autre étude démontre la participation des récepteurs mu et kappa du système opioïde dans la médiation de l'effet anti-nociceptif de l'OT dans les modèles de douleur inflammatoire (Yu et al., 2003). Par la suite, les études in vitro montrent que la libération évoquée d'OT à partir des synaptosomes dérivés de la ME était diminuée par l'effet de la dynorphine, suggérant que la libération d'OT dans la ME

pourrait être sous l'influence des récepteurs opioïdes kappa (Daddona and Haldar, 1994). Le système opioïde constitue un autre système de contrôle descendant de la nociception, il est donc raisonnable de penser que les deux voies pourraient interagir entre elles. Rash et ses collaborateurs ont résumé la littérature sur l'effet de l'OT sur l'intégration nociceptive. Ils rapportent que de nombreuses études démontrant que les antagonistes des récepteurs opioïdes mu ou kappa pourraient partiellement bloquer l'effet anti nociceptif de l'OT, mais surtout par ses actions sur les aires supra spinale (Rash et al., 2014).

IV.d.ii. Les propriétés anti-nociceptive de l'OT dans les structures supra spinales

Les stimulations douloureuses augmentent la concentration de l'OT dans de nombreuses aires supra-spinales, telles que : les noyaux ventro-médian de l'hypothalamus, le noyau réticulé du thalamus, le locus coeruleus, le raphé magnus, le noyau caudé, etc, sans pour autant élever le taux d'OT dans la circulation plasmatique. L'injection i.c.v. d'OT peut augmenter le seuil douloureux, alors qu'un sérum anti-ocytocine le réduit (Yang et al., 2007a). Dans une situation stressante, comme lors de la réalisation d'un test de nage forcé, l'OT est libérée à partir du PVN, à la fois dans le compartiment central et en périphérie (Juif and Poisbeau, 2013; Juif et al., 2016; Robinson et al., 2002). L'injection du sérum anti-OT et non anti AVP inhibe l'augmentation du seul douloureux évoqué par une stimulation chimique dans le SON, une indication que les neurones ocytocinergiques du SON sont également impliqués dans la modulation de la douleur (Yang et al., 2011a). Dans une autre étude, il a été montré qu'une incision cutanée induit une diminution du taux d'OT dans le PVN indiquant une libération de ce peptide et qu'une injection i.c.v. d'OT augmentait le seuil douloureux, alors qu'une injection intrathécale ne semblait pas présenter d'effets (Zhang et al., 2015). Ces résultats démontrent la présence de mécanismes indépendants entre le compartiment spinal et supra spinal dans la modulation ocytocinergique de la douleur. L'effet anti nociceptif de l'OT peut également être observé lors de son injection dans les citernes cérébrales, PAG, noyaux raphé magnus, le ventricule latéral et le noyau accumbens, mais avec l'implication des récepteurs opioïdes mu et kappa, notamment dans la PAG (Ge et al., 2002; Xin et al., 2017). La PAG et la médulla rostro ventro-médiane sont fortement interconnectés, et son des centres clé des voies descendantes (Heinricher and Ingram, 2008). De nombreuses fibres OT et les OTR peuvent être retrouvés dans la PAG (Figueira et al., 2008). Des stimulations douloureuses sont capables d'élever les

niveaux d'OT dans la PAG. De plus, l'injection intra-PAG d'OT augmente le seuil douloureux et stimule la libération d'opioïdes endogènes alors que l'injection d'un antagoniste de l'OT diminue le seuil douloureux. La naloxone (un antagoniste des récepteurs opioïdes) diminue également l'effet anti nociceptif de l'OT, lors de micro injection de ce composé dans la PAG (Yang et al., 2011b, 2011c). Il est intéressant d'ajouter que l'AVP pourrait potentiellement avoir un effet sur la nociception en régulant le système opioïde endogène dans la PAG (Yang et al., 2007b).

Le système sérotoninergique pourrait également être impliqué dans la modulation de la douleur par l'OT. En effet, le noyau raphé montre une augmentation d'expression de *c-fos* à la suite d'une stimulation du PVN connue pour induire un effet anti-nociceptif dans la ME (Condés-Lara et al., 2015). La sérotonine administrée intrathécalement peut mimer l'effet de l'OT, et lors de son administration concomitante avec le neuropeptide, elle est capable de potentialiser l'effet de l'OT anti-nociceptif. De plus, un antagoniste des récepteurs sérotoninergique bloque partiellement l'effet anti-nociceptif retrouvé dans la ME à la suite de la stimulation du PVN (Godínez-Chaparro et al., 2016).

Dans le modèle de douleur inflammatoire, l'effet anti-hyperalgésique de l'injection i.c.v. de l'OT peut être atténué par une co-injection d'un antagoniste des récepteurs endocannabinoïdes CB1 ou un antagoniste des récepteurs opioïdes (Russo et al., 2012). Ces résultats renforcent l'idée selon laquelle plusieurs systèmes neuromodulatoires coopèrent avec l'OT pour induire une analgésie. L'effet anti nociceptif de l'OT dans le CeA, une structure importante dans la modulation des voies ascendantes et descendantes de la douleur, a attiré notre attention. Une étude de Han et ses collaborateurs a montré que l'injection de l'OT dans le CeA a un effet dose dépendant et spécifique des OTR sur le niveau de seuil nociceptif thermique et mécanique (Han and Yu, 2009).

L'OT pourrait également avoir un effet indirect sur la douleur et l'analgésie. Il serait possible que l'OT possède un effet analgésique en améliorant l'humeur. Nous avons vu que l'OT peut interagir avec le système sérotoninergique, et les neurones sérotoninergiques de la souris expriment les OTR. L'injection d'OT dans le noyau raphé médian peut réduire l'anxiété (Yoshida et al., 2009). L'OT est généralement un down-régulateur du stress et de l'anxiété (Neumann and Landgraf, 2012). Chez les humains, le niveau plasmatique d'OT est négativement corrélé avec les scores de dépression et d'anxiété (Anderberg and Uvnäs-Moberg, 2000). Les études

réalisant une administration intranasale d'OT ont montré une diminution de l'activation « dépendante de la peur » de l'amygdale après administration d'OT (Kirsch et al., 2005). Une autre étude montre que l'administration intranasale d'OT augmente le calme et diminue l'anxiété. Elle semble induire une diminution du taux de cortisol durant le test de stress social (Heinrichs et al., 2003). Une étude chez l'humaine corrèle un faible taux d'OT dans le LCR avec un sujet présentant des tendances suicidaires fortes, ce qui indique une implication du niveau central d'OT dans la régulation des troubles d'humeur (Jokinen et al., 2012). Cependant, nous avons vu que, chez l'humain, un faible taux plasmatique d'OT est généralement associé avec une augmentation de la sensation douloureuse. Cependant, comme nous l'avons déjà évoqué, la concentration plasmatique d'OT pourrait ou ne pourrait pas représenter la concentration d'OT centrale (Kagerbauer et al., 2013; Rash et al., 2014; Wotjak et al., 1998). Ainsi, les résultats des études chez l'humain dans lesquelles le niveau d'OT plasmatique est approché comme un reflet du niveau central doivent être considérées précautionneusement. Pour finir, la douleur chronique est liée au développement de symptômes anxiodépressifs (Asmundson and Katz, 2009), ce qui souligne le lien probable entre l'humeur et la douleur. Connaissant les nombreux effets centraux et périphériques de l'OT, des nouvelles thérapies cruciales pourraient émerger grâce à une meilleure compréhension du système ocytocinergique dans le SNC.

V- L'amygdale

L'amygdale est un cluster de neurones en forme d'amande. Elle est localisée profondément dans le cerveau, au niveau des lobes médio-temporaux. Elle fait partie du système limbique et est un élément clé de la circuiterie attribuant une valeur émotionnelle et produisant le comportement approprié en réponse à des stimuli externes (Sah et al., 2003). L'anatomie de l'amygdale est représentée en Figure 21.

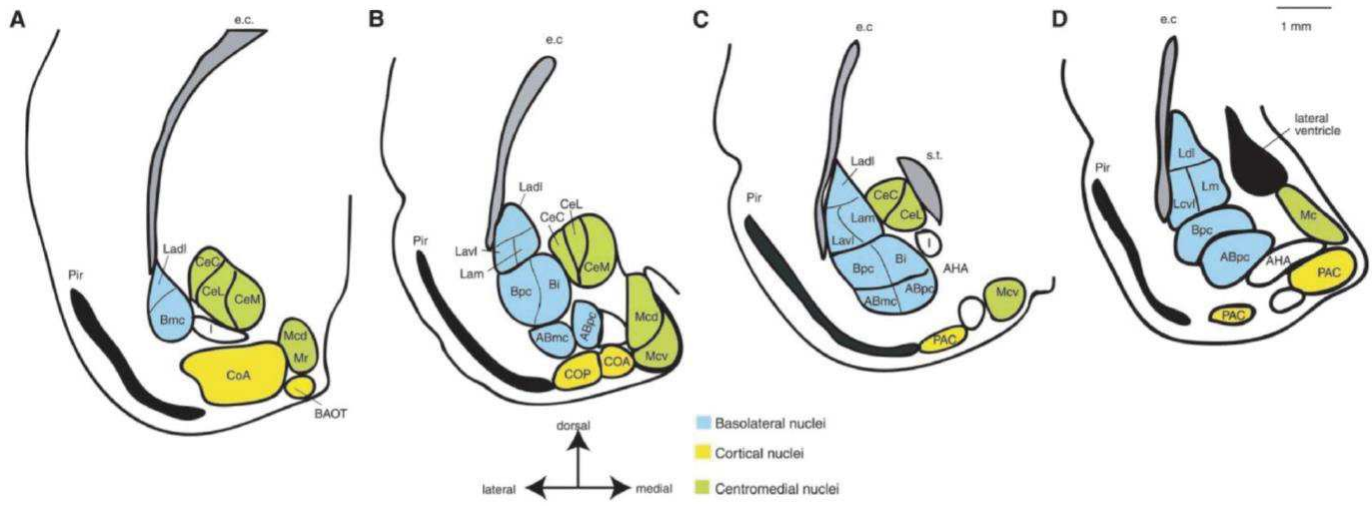

Figure 21 : Cartographie des différents noyaux constituant l'amygdale chez le rat. Les coupes coronales ont été dessinées de la partie rostrale (A) vers la partie caudale (D). L'amygdale est divisée en trois groupes comme décrits dans le texte : En bleu, est représenté le groupe basolatérale de l'amygdale, en jaune, le groupe cortical, en vert, le groupe centromédial. Abréviation : ABmc, accessory basal magnocellular subdivision; ABpc, accessory basal parvicellular subdivision; Bpc, basal nucleus magnocellular subdivision; CeC/L/M, capsular, lateral and medial part of central nucleus; COA(P), anterior and posterior cortical nucleus; e.c., external capsule; Ladl, lateral amygdala medial subdivision; Lam, lateral amygdala medial subdivision; Lavl, lateral amygdala ventrolateral subdivision; Mcd, medial amygdala dorsal subdivision; Mcv, medial amygdala ventral subdivision; Mr, medial amygdala rostral subdivision; PAC periamygdaloid cortex, Pir, piriform cortex; s.t., stria terminalis. Adapté à partire de (Sah et al., 2003)

a. L'amygdale : un centre régulateur de la douleur

La douleur est une expérience multimodale, qui ne se résume pas en un simple stimulus nociceptif mais inclut également des composantes émotionnelles, affectives et cognitives. Nous avons préalablement mentionné que la douleur chronique conduit à l'anxiété et à la dépression, mais l'inverse est également vrai. Les patients souffrants d'anxiété et de dépression sont plus sujets à développer des douleurs chroniques (Neugebauer et al., 2009; Nicholson and Verma, 2004). L'amygdale fait partie du réseau cérébral qui intègre et module les informations relatives à la douleur, révélé notamment par les études de neuroimagerie. Ce réseau est souvent nommé : « pain matrix » ou matrice de la douleur (Neugebauer et al., 2004, 2004, 2009; Tracey and Mantyh, 2007) (Figure 22).

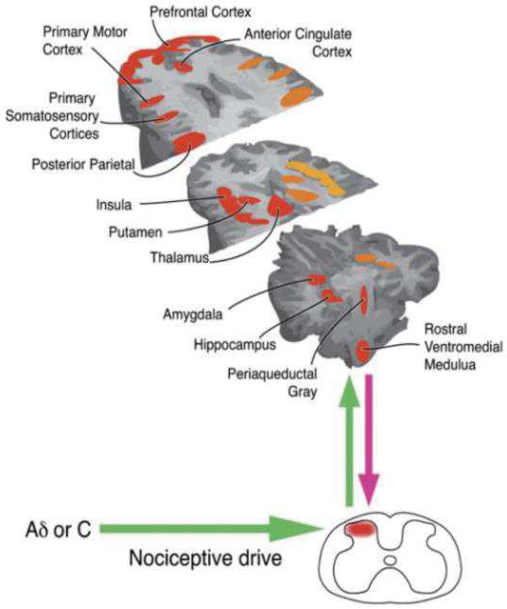

Figure 22 : Neuroanatomie de l'intégration de la douleur. Les régions activées par une expérience douloureuse sont activées de façon bilatérale mais avec une augmentation de l'activité dans l'hémisphère controlatéral au stimuli nociceptif. Adapté de (Tracey and Mantyh, 2007)

.

b. La valence émotionnelle de la douleur

L'amygdale fait partie du soi-disant « secondary affect network of pain ». Dans un sens, elle donne la dimension affective à la nociception *i.e*. la sensation désagréable associée (Neugebauer, 2015). Il y a deux voies afférentes majeures au secondary affect network of pain : les afférences directes provenant de la ME projetant directement au niveau des structures du système limbique et du noyau médian du thalamus, qui fournissent des informations sensorielles directes au réseau émotionnel secondaire, et la voie indirecte via la ME projetant au niveau du thalamus somato-sensoriel et au niveau des aires corticales, qui, à leur tour, projettent via la voie cortico-limbique. Cette voie indirecte intègre les informations contextuelles et mnésiques pour fournir une notion émotionnelle à la douleur (Price, 2000). L'ajout de cette composante affective à la douleur contribue aux conséquences émotionnelles

de la douleur, et inversement : la douleur peut également être modulée par des états émotionnels et cognitifs antérieurs (Rhudy et al., 2008; Seminowicz and Davis, 2007; Seminowicz et al., 2004).

c. L'anatomie de l'amygdale

L'amygdale a longtemps été connue pour son rôle dans le traitement des émotions, des troubles émotionnels (Phelps and LeDoux, 2005) ainsi que dans la dimension émotionnelle et affective de la douleur (Carrasquillo and Gereau, 2007; Neugebauer, 2007). L'amygdale est divisée en plusieurs sous noyaux : l'amygdale basolatérale (BLA), latérale (LA) et l'amygdale centrale (CeA). Ils sont tous fortement impliqués dans l'intégration des informations relative à la douleur. Les informations purement nociceptives en provenance de la ME et du tronc cérébral passant par l'aire para-brachiale atteignent la division latéro-capsulaire de l'amygdale centrale (CeL ou CeLC selon les auteurs). Les informations sensorielles polymodales, incluant la nociception, atteignent la LA, par le biais de l'aire postérieur du thalamus, de l'insula et du cortex associatif. C'est pour cela que la LA est connue pour être le premier site de convergence et d'intégration dans l'amygdale. Le réseau LA-BLA, quant à lui, attribue une signification émotionnelle aux informations sensorielles et transmet ces informations traitées au CeA. Le CeA est, lui, classiquement considéré comme étant le noyau de sortie de l'amygdale, projetant au niveau des noyaux du thalamus impliqués dans la modulation de la voie descendante de la douleur (tel que le PVN) ainsi qu'au niveau du tronc cérébral (incluant la PAG, le RVM, le raphé magnus…) (Price, 2003). Les schémas suivants (Figure 23) de Neugebauer et ses collègues résument les entrées et les sorties de l'amygdale impliqués dans la régulation de la douleur (Neugebauer et al., 2004). Il est intéressant de noter que la BLA est également interconnectée avec les aires corticales, notamment le cortex préfrontal qui est crucial pour la régulation de la douleur et des état affectifs en vue de son implication sur les processus de décision basés sur l'anticipation des risques, l'évitement de la punition… (Ji et al., 2010; Pais-Vieira et al., 2009).

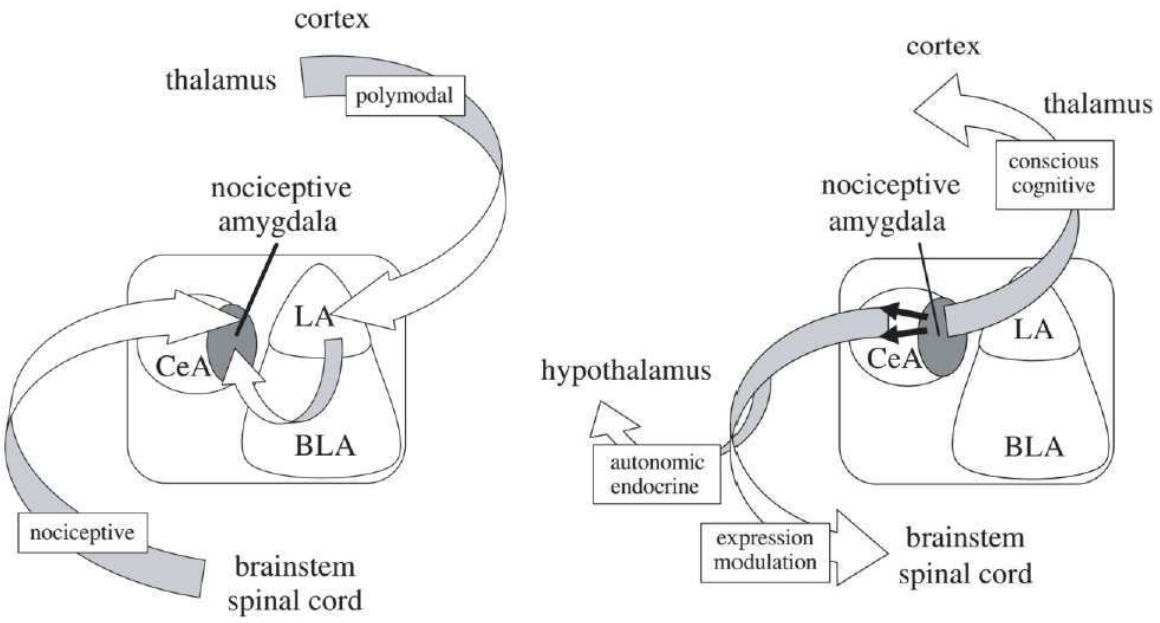

Figure 23 : Principaux Input et Output relatifs à la douleur de l'amygdale. A gauche, les inputs : La partie capsulaire du CeA reçoit les informations purement nociceptives, c'est pour cela qu'elle est classiquement appelée amygdale nociceptive. La partie latérale (LA) reçoit quant à elle les information polymodales déjà traitées qui le seront encore une fois par le réseau LA-BLA (amygdale basolatérale). Ces informations seront ensuite transmises au CeA. A droite, les outputs : Le CeA forme des connexions directes et indirectes avec le mésencéphale et les aires sous-corticales. Adapté de (Neugebauer et al., 2004)

d. La douleur induit de la plasticité au sein de l'amygdale

Les mécanismes de sensibilisation centraux de la douleur chronique observés chez les modèles de douleur chronique induit une augmentation de la neurotransmission au sein de l'amygdale, à la fois au niveau des synapses BLA-CeL et aires para brachial-CeL (Han and Neugebauer, 2004; Ikeda et al., 2007; Neugebauer et al., 2003). Cette observation est corroborée par l'augmentation de l'activité de l'amygdale observée chez l'humain (Simons et al., 2014), par exemple chez les patients souffrant d'arthrite osseuse (Kulkarni et al., 2007). La diminution de l'activité de l'amygdale par des mécanismes de lésion ou par intervention pharmacologique inhibe les comportements associés à la douleur dans de nombreux modèles (Fu et al., 2008; Palazzo et al., 2011). De plus, l'activation de l'amygdale, même en condition non pathologique et sans aucune lésion, peut exacerber voire même générer une réponse à la douleur (Kolber

et al., 2010; Li et al., 2011). Dans un sens, il est possible de considérer l'amygdale comme une structure relais agissant comme un interrupteur ON/OFF de la douleur (Rouwette et al., 2012).

e. L'amygdale centrale n'est pas qu'un noyau de sortie

Toutefois, le CeA n'agit pas uniquement comme un interrupteur de la douleur, il est capable de traiter les informations reçues au niveau du microcircuit interne. Si l'on se concentre uniquement sur le traitement de la douleur, l'amygdale centrale est modulée par de nombreux neurones et acteurs moléculaires présentés par le tableau 6 issue de la revue de Veinante et collaborateurs. Le microcircuit du CeA est composé quasi exclusivement d'interneurones inhibiteurs GABAergiques (Cassell et al., 1999; Sun and Cassell, 1993) qui sont mutuellement connectés et répondent à de nombreux stimuli différents (Figure 24) (Ciocchi et al., 2010; Janak and Tye, 2015; Veinante et al., 2013). Ces microcircuits permettent une intégration et traitement des informations, et régulent l'activité de nombreux autres circuits neuronaux et leurs fonctions (Keifer et al., 2015). Il est important de noter que les neurones du CeL sont extrêmement interconnectés et projettent au CeM où ils régulent l'activité électrique des neurones projetant aux structures distantes. Les neurones du CeL sont aussi capables d'établir des projections à l'extérieur du CeA. Certains neurones du CeM projettent également au CeL, formant un circuit complexe d'inhibition mutuelle (Badrinarayan et al., 2012; Pitkänen et al., 1997).

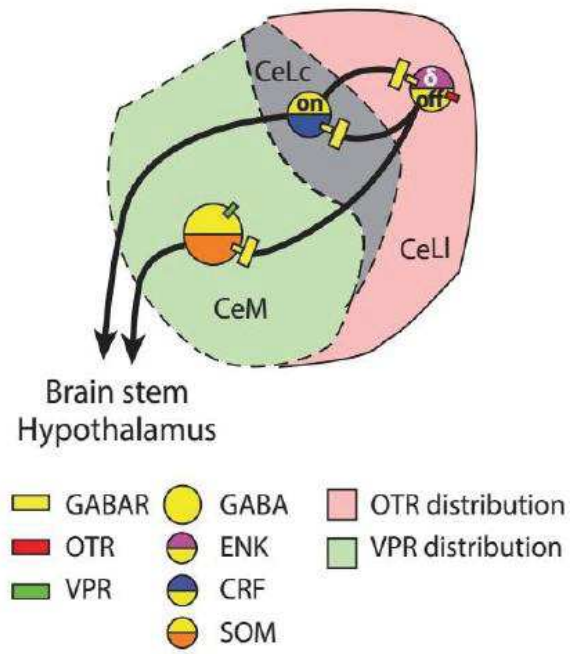

Figure 24 : Le microcircuit du CeA. L'amygdale centrale est constituée d'interneurones et de neurones de projections GABA, exprimant différents marqueurs moléculaires. ENK, encephalin; CRF, corticotropin releasing factor; SOM, somatostatin; CeLl lateral part of CeL; CeLc central part of CeL; VPR, vasopressin receptor V1A. Adapté de (Stoop et al., 2015)

Pain type[a]	Pain related outcome[b]		Reference
	Nociceptive behavior	Affective/emotional	
1. CeA lesion			
Naive	- Reduced morphine-induced, stress-induced and conditioned hypoalgesia		[55,56,69]
Formalin	- Reduced morphine-induced and conditioned hypoalgesia	- Decreased pain-induced CPA	[70-73]
Acetic acid		- Decreased pain-induced CPA	[72]
2. Injection of muscimol			
Neuropathy	- Reduced mechanical hyperalgesia	- Decreased escape/avoidance	[74]
3. Injection of NMDA antagonist			
Neuropathy		- Decreased pain-induced CPA	[75]
4. Injection of group I mGluRs ligands			
Naive	- Agonist induced visceral and mechanical hypersensitivity		[76,77]
	- Antagonist reduced visceral sensitivity		
Formalin	- Antagonist reduced mechanical hypersensitivity		[77]
Arthritis	- Antagonist reduced mechanical hypersensitivity	- Antagonist decreased vocalizations	[78]
Neuropathy		- Agonist increased, and antagonist decreased, pain-induced CPA	[75]
5. Injection of group III mGluRs agonists			
Naive	- Decreased mechanical sensitivity (mGluR7)	- Decreased vocalizations and anxiety	[79]
Arthritis	- Increased mechanical sensitivity (mGluR8)	- Increased vocalizations and anxiety	[79]
6. Injection of cholinergic agonists			
Naive	- Decreased thermal sensitivity, reduced jaw opening reflex	- Decreased vocalizations	[63,65,66]
7. Injection of noradrenergic α_2 ligands			
Naive	- Agonist induced mechanical and thermal hypoalgesia		[64,80]
	- Antagonist reduced stress-induced thermal hypoalgesia		
Acetic acid		- Agonist decreased pain-induced CPA	[81]
8. Injection of noradrenergic β antagonists			
Acetic acid		- Decreased pain-induced CPA	[81]
9. Injection of CGRP receptor ligands			
Naive	- CGRP decreased mechanical and thermal reflexes		[59]
Naive	- CGRP increased mechanical reflexes	- CGRP increased vocalizations	[82]
Arthritis	- CGRP1 antagonist inhibited the enhanced reflex to mechanical stimulus	- CGRP1 antagonist decreased vocalizations	[83]
10. Injection of CRF receptor ligands			
Naive	- CRF decreased mechanical and thermal sensitivity		[58]
Naive	- CRF increases mechanical sensitivity	- CRF increased vocalizations	[84]
Arthritis	- CRF1 antagonist reduced mechanical hypersensitivity	- CRF1 antagonist decreased vocalizations and anxiety	[85,86]
11. Injection of oxytocin, vasopressin, neurotensin, galanin			
Naive	- Decreased mechanical and/or thermal sensitivity		[57,60-62]
12. Injection of opioid receptors ligands			
Naive	- Morphine and β-endorphin induced mechanical and thermal hypoalgesia	- Morphine decreased vocalizations	[47,66]
13. Corticosterone implants			
Naive	- Sensitized visceromotor reflexes to colorectal and urinary bladder distension and to somatic mechanical sensitivity	- Increased anxiety	[87-90]

Tableau 6 : Les différents effet de la modulation de l'amygdale pour les différents modèles de douleur. Le tableau fait la liste des effets multiples de diverses substance neuroactives injectées dans le CeA sur les symptômes de la douleur. Pour les références se référer à (Veinante et al., 2013)

f. L'amygdale centrale et l'ocytocine

Parmi la sous population de neurones GABAergique du CeA, une claire distinction peut être faite regardant l'expression des OTR et de V_{1A}. Huber et ses collègues ont été les premiers à réaliser cette distinction entre les aires exprimant uniquement les OTR et les aires exprimant uniquement V_{1A} dans l'amygdale centrale, jusque-là impossible à discriminer en autoradiographie. Ils ont par la suite démontré que l'expression des neurones exprimant les OTR dans le CeL répondait au TGOT (un agoniste synthétique spécifique de l'OTR) en libérant du GABA, et ce faisant, inhibait les neurones du CeM exprimant les V_{1A}. La réciproque n'étant pas vraie, la vasopressine peut activer les neurones du CeM sans affecter les neurones du CeL, et ses effets ont été inhibés grâce à l'application préalable d'antagonistes. Finalement, ils ont montré que l'activation des neurones GABAergique exprimant l'OTR dans le CeL pouvait réduire de façon efficace le firing des neurones du CeM induits par la stimulation des afférences des neurones du BLA (Huber et al., 2005).

L'inhibition des cellules répondant à l'AVP par les cellules répondantes à l'OT pourrait être un exemple des mécanismes de l'action des neuropeptides sur le comportement (Stoop, 2014; Viviani and Stoop, 2008). Des études supplémentaires chez Viviani et ses collègues ont montré deux populations de neurones dans le CeM, l'une inhibée par l'action de l'OT dans le CeL projetant vers la PAG et l'autre non affectée par l'action de l'OT projetant vers le complexe dorso-vagal (DVG). Puisque le DVG est important pour la régulation cardiovasculaire et que la PAG module le comportement de freezing, les auteurs ont mesuré ces deux paramètres, la variation de la fréquence cardiaque et le comportement de freezing dans un test de conditionnement à la peur. Ils ont montré que le TGOT peut diminuer le comportement de freezing, et que le mucimol, un agoniste gaba, présente le même effet. Bien que le TGOT n'affecte pas le rythme cardiaque, le mucimol, lui, le modifie (Viviani et al., 2011). Cette étude montre que les interneurones du CeL répondant à l'OT peuvent sélectionner spécifiquement différentes réponses, la peur dans ce cas, en agissant sur une sous-population de neurones à projection du CeM. La pertinence physiologique d'une telle régulation du CeA par l'OT a été testée par la suite. A l'aide de la technique d'optogénétique permettant l'activation spécifique des axones des neurones OT, Knobloch et ses collègues ont montré que l'activation de ces axones OT dans le CeL induit la même réponse dans les neurones GABAergiques du CeA que

l'administration de TGOT mais révèle une composante glutamatergique dans ces réponses évoquées par la lumière. Dans le paradigme de conditionnement contextuel à la peur, ils ont pu réduire le temps de freezing suite à l'activation optogénétique des axones des neurones OT dans le CeL, montrant que les quelques fibres ocytocinergiques innervant le CeL sont suffisantes pour induire un changement de comportement drastique chez le rat (Knobloch et al., 2012). L'un des points essentiels à noter est le délai extrêmement variable du début et de fin des réponses comportementales suite à la stimulation lumineuse induisant la libération d'OT qui s'étend dans certain cas à plusieurs secondes voire minutes.

L'étude des mécanismes cellulaires de l'action de l'OT sur le CeA et la façon dont elle régule les émotions, telles que l'anxiété et la douleur, est la partie centrale de mon travail présenté en article 2 et 3.

VI- Les astrocytes

a. Généralité et historique des astrocytes

Les astrocytes constituent une classe de cellules neurales de l'ectoderme, issus du neuroépithélium permettant la régulation de l'homéostasie et participent à la défense du système nerveux central Figure 25. Les astrocytes forment une population très hétérogène au regard de leurs formes et fonctions. Ils présentent une forte plasticité adaptative qui définit le maintien fonctionnel du SNC dans le

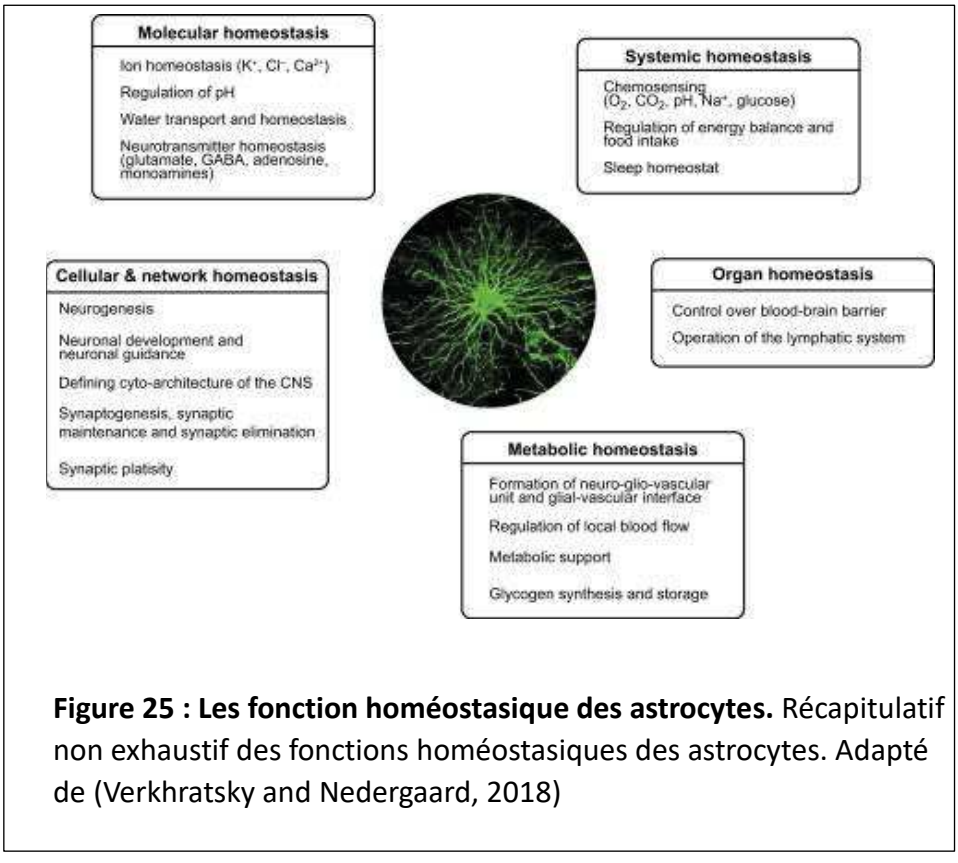

Figure 25 : Les fonction homéostasique des astrocytes. Récapitulatif non exhaustif des fonctions homéostasiques des astrocytes. Adapté de (Verkhratsky and Nedergaard, 2018)

développement et le vieillissement (Burda and Sofroniew, 2014; Burda et al., 2016; Parpura et al., 2012).

Le médecin Rudolf Virchow a été le premier à introduire le concept neuroglial comme étant un véritable tissu du cerveau et en ne considérant que peu sa nature cellulaire. Il qualifie la neuroglie de « Zwischenmasse » signifiant « entre les tissus » (Virchow, 1871). Cependant, la toute première découverte d'une cellule nerveuse qui sera classé en cellule gliale a été découverte quelques temps avant la théorie de Virchow. C'était une « radial-like » cellule gliale de la rétine, la cellule de Müller décrite par Heinrich Müller en 1851. Ces cellules ont par la suite été plus précisément caractérisées par Max Schulze. En 1857, Karl Bergmann découvre des cellules gliales radial-like dans le cervelet connu aujourd'hui sous le nom de cellules gliales de Bergmann. Camillo Golgi fut le premier à démontrer que la glie représentait une population cellulaire distincte des neurones (Golgi, 1885). De plus, il pensait que les cellules gliales et les neurones pouvaient se transformer l'un en l'autre. Golgi a identifié les cellules gliales comme étant ronds avec de nombreux process fins s'étendant dans toutes les directions, et de nombreux process se dirigeant vers les vaisseaux sanguins. A l'aide d'une technique de coloration utilisant l'argent chromé (reazione nera), Golgi a décrit une vaste diversité de cellules gliales dans le cerveau, les réseaux gliaux et identifié les pied gliaux entourant les vaisseaux sanguins (Verkhratsky and Nedergaard, 2018).

Le terme astrocyte (αστρον κψτοσ ; astron, étoile and kytos, un récipient, traduit par la suite en cellule, i.e., cellule étoile) a été introduit en 1895 par Michael von Lenhossék qui avait, dans un premier temps, proposé d'appeler toutes les cellules gliales parenchymateuse spongiocytes, les astrocytes en étant un sous-type (Lenhossék, 1893). Quelques temps auparavant, Albert von Kölliker et William Lloyd Andriezen font la distinction entre la matière grise et la matière blanche gliale. Andriezen nomma par la suite les cellules gliales de la matière grise : protoplasmique et celle de la matière blanche : fibreuse (Andriezen, 1893). A l'époque, Andriezen était persuadé que ces deux types de cellules présentaient une ontogénie différente, les cellules protoplasmiques ayant pour origine le mésoblaste alors que les cellules fibreuses dériveraient de l'ectoderme(Andriezen, 1893). Le terme astrocytes sera surtout popularisé par Santiago Ramón y Cajal, qui a développé une technique de coloration spécifique des astrocytes à l'aide d'or et de mercure chloré (Figure 26) permettant d'identifier la protéine

« glial fibrillary acidic protein » (GFAP) (Ramon y Cajal, 1913, 1917). Cette technique a permis à Cajal de confirmer l'origine des astrocytes comme étant la glie radiaire. La plupart des neuroscientifiques du 19e et du début du 20e siècle attribuent aux astrocytes de nombreuses fonctions. Golgi, par exemple, attribuait à la glie le rôle de distributeur de matériel nutritif pour les neurones(Golgi, 1885, 1903). Lugaro envisageait que les process fins des astrocytes s'infiltraient au niveau des synapses et métabolisaient les substances neuroactives (Lugaro, 1907).

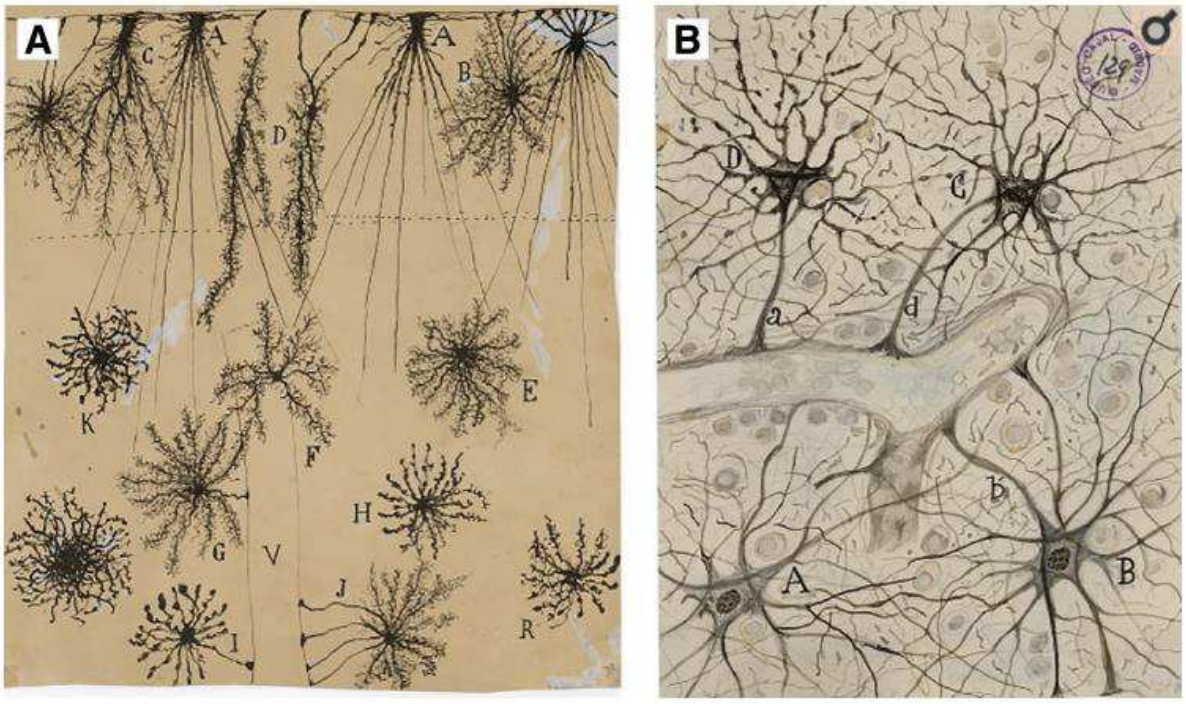

Figure 26 : Image d'astrocyte à la suite d'une coloration d'or et de mercure chloré. (A) Cellule gliale de Müller de la rétine de mouton dessinée par Max Schulze. (B) Astrocytes corticaux dessinés par Albert von Killiker. Adapté de (von Kölliker, 1863; Schultze, 1859)

Le rôle actif des astrocytes dans le contrôle des informations dans le cerveau a été suggéré par Carl Ludwig Schleich, qui postulait que les process astrogliaux pourraient, par gonflement et rétrécissement, contrôler la transmission synaptique (Schleich, 1906). Une idée similaire a été avancée par Ramon y Cajal qui pensait que la rétractation des process astrogliaux permettait le transfert d'information durant les phases d'éveil alors que l'expansion de ces process interrompait la connectivité interneuronale induisant ainsi le sommeil (Ramon y Cajal, 1895).

Fernando De Castro, un élève de Cajal, proposa que les cellules neurogliales pourraient libérer des substances neuroactives participant directement dans la transmission neuronale (De Castro, 1951), alors que Robert Galambos considère la neuroglie comme un élément central pour les fonctions cérébrales supérieures tandis que les neurones « exécutent simplement les instructions données par la glie » (Galambos, 1961). Cette notion de la glie étant l'élément primaire du traitement de l'information, de la mémoire, de la cognition et de la conscience refait surface régulièrement (Bellini-Leite and Pereira, 2013; Caudle, 2006; Pereira et al., 2013; Pereira Jr and Furlan, 2010).

b. Identification des astrocytes, historique

La visualisation et l'identification des astrocytes, surtout dans les préparations in situ et in vivo, sont loin d'être aisées. La difficulté réside dans l'extrême hétérogénéité morphologique et dans l'absence d'un marqueur universel qui permettrait le marquage de tous les cellules astrogliales.

Les techniques existantes comprennent la coloration histologique classique et l'immunocytochimie (effectuée sur des tissus fixés), l'expression génétiquement contrôlée de marqueurs fluorescents spécifiques à l'astroglie, l'incubation avec des sondes fluorescentes avec une affinité gliale préférentielle ou l'injection intra gliale de colorant fluorescents. Les techniques histologiques classiques comprennent : le marquage de Golgi (imprégnation au nitrate d'argent) qui existe sous plusieurs formes, pouvant fournir des images détaillées d'astrocytes avec des process primaires et secondaires fins lorsqu'ils sont couplés à l'utilisation de microscopie électronique (Álvarez et al., 2015; Ogata and Kosaka, 2002; Olude et al., 2015). Elles comprennent également la coloration de l'or-mercure chloré de Cajal qui marque les filament astrocytaires et les pieds astrocytaires (García-Marín et al., 2007; Naoumenko and Feigin, 1961) ainsi que l'imprégnation à l'argent d'Hortega qui, avec quelques modifications, a été occasionnellement utilisée pour marquer les astrocytes pour la microscopie optique et électronique (Kitoh and Matsushita, 1980).

VI.b.i. Identification Immunocytochimique des astrocytes

Il n'existe pas de marqueur universel qui colore et révèle tous les astrocytes dans le SNC. La remarquable hétérogénéité morphologique des astrocytes coïncide avec la diversité de l'expression de différentes molécules. Par conséquent, les anticorps dirigés contre elles ne

marquent que des sous-populations de cellules astrogliales avec des différences régionales substantielles (Tableau 7).

VI.b.i.1. Glial fibrillary acidic protein - GFAP

La GFAP a été découverte dans les années 70 (Eng et al., 1971; Uyeda et al., 1972), et son expression exclusive dans les astrocytes a été très vite identifiée (Bignami et al., 1972; Ludwin et al., 1976) et abondamment documentée depuis (Hol and Pekny, 2015). La GFAP, dont les astrocytes expriment 10 isoformes, appartient à une famille étendue de filaments intermédiaires et, avec la vimentine, la nestine et parfois le synemin, forme le cytosquelette astroglial (Hol and Pekny, 2015; Pekny et al., 2014). La délétion génétique du GFAP produit peu de modifications physiologiques chez la souris KO. Cependant, l'astrogliose réactive est considérablement altérée. Il est intéressant de noter que, si une double suppression est réalisée avec la GFAP et la vimentine, cela perturbe encore plus la réactivité et exacerbe la neuropathologie (Pekny et al., 1999; Wilhelmsson et al., 2004).

L'utilisation d'anticorps anti GFAP ne permet la visualisation que d'une fraction des astrocytes avec une hétérogénéité structurale (et probablement développementale) importante. Un point intéressant est que les astrocytes en culture expriment presque tous la GFAP alors que la proportion de cellules marquées par la GFAP *in situ* ou *in vivo* est beaucoup plus faible (Walz, 2000). La plus grande sous-population de cellules GFAP-positive est retrouvée dans l'hippocampe chez les juvéniles avec ~80% des astrocytes marqués (Bushong et al., 2002; Ogata and Kosaka, 2002). De façon similaire, toutes les cellules gliales de Bergmann dans le cervelet sont GFAP positives (Ango et al., 2008; Nolte et al., 2001). A ce même stade développemental, la majorité des astrocytes dans les autres régions n'est pas marquée par les anticorps anti GFAP (Kimelberg, 2004; Savchenko et al., 2000). La morphologie des profils GFAP-positifs est quelque peu limitée, car l'immunomarquage du cytosquelette ne révèle que des processus majeurs, les parties les plus fines de la cellule restant non colorées. Ainsi, le GFAP ne révèle ni les processus périphériques, ni périsynaptiques, ni les pieds astrocytaires entourant les petits vaisseaux sanguins (<8 µm) (Simard et al., 2003).

Markers of astrocytes

Molecule/Antigen	Detection Agent/Technique	Properties and Functional Relevance	Reference Nos.
Glial fibrillary acidic protein, GFAP	Monoclonal and polyclonal antibodies	Intermediate filament protein, expressed in many cells outside the nervous system; in the CNS expressed in a subpopulation of astrocytes with substantial region variability. Generally, GFAP expression is upregulated in reactive astroglia.	477, 715, 1355, 1880
Vimentin	Monoclonal and polyclonal antibodies	Intermediate filament protein; expressed in immature astrocytes, in subpopulations of protoplasmic and fibrous astrocytes, in Bergmann glia, and in tanycytes. Vimentin expression is upregulated in reactive astrocytes.	394, 597, 1350, 1351, 1568
S100B protein	Monoclonal antibodies	Ca^{2+}-binding proteins, which act as Ca^{2+} buffers as well as Ca^{2+} sensors. Antibodies against S100B stain more astrocytes than GFAP in the grey as well as in the white matter.	444, 1251, 1549
Glutamate transporters: EAAT-1 (GLAST), EAAT-2 (GLT-1)	Monoclonal antibodies	Astroglia-specific glutamate transporters; show regional variability: EAAT1 is predominantly expresed in cerebellum; in other regfions EAAT2 is the main transporter type.	110, 807, 1570, 1606, 1882
Glutamine synthetase	Monoclonal and polyclonal antibodies	Astroglia-specific enzyme converting ammonia and glutamate into glutamine. Expressed in the majority of astrocytes. Immunostaining reveals full structure of the cell due to cytosolic localization of the enzyme.	49, 417, 1237, 1920
Aldehyde dehydrogenase 1 family, member L1 (ALDH1L1)	ALDH1L11-specific polyclonal antibody	ALDH1L1 is a key enzyme in folate metabolism contributing to nucleotide biosynthesis and cell division. Proposed as a specific astroglial markers with a reach substantially broader than GFAP. ALDH1L1 expression however changes with age, and it was also detected in a subpopulation of oligodendrocytes.	275, 1916
Connexins: Cx43, Cx30	Monoclonal and polyclonal antibodies	Both Cx43 and Cx30 are expressed exclusively in astrocytes; the Cx30 is expressed mostly in grey matter (being particularly concentrated in astroglial endfeet) and is absent in astrocytes from white matter.	413, 1189
Aquaporin: AQP4	Monoclonal antibodies	AQP4 in the CNS is expressed exclusively in astrocytes and ependymocytes. In healthy astrocytes, AQP4 is preferentially located in the endfeet and hence stains this structure.	1184
Transcriptional factor SOX9	Polyclonal antibodies	Specifically labels nuclei of astrocytes outside the neurogenic niches.	1701

Tableau 7 : Liste des différents marqueur astrocytaire. Pour les référence de référer à (Verkhratsky and Nedergaard, 2018)

VI.b.i.2. La protéine S100B

La glycoprotéine S100B est une des protéines 24 S100 liant le calcium. Elle est exprimée uniquement chez les vertébrés et agit comme calcium buffer, et calcium senseur pour la signalisation calcique intracellulaire (Donato et al., 2013). Dans le SNC, S100B régule de nombreux aspects de la prolifération et différenciation cellulaire. Elle est également connue comme étant un inhibiteur de l'apoptose (Donato et al., 2013; Hachem et al., 2007; Raponi et al., 2007). Il y a quelques évidences que, dans les astrocytes, S100B contribue à la génération de la signalisation calcique (Xiong et al., 2000). S100B est également lié à la régulation de l'assemblage des filaments intermédiaires en inhibant la polymérisation du GFAP en présence de Ca^{2+}(Bianchi et al., 1994). Les astrocytes produisent et sécrètent la protéine S100B qui, en fonction de la concentration, possède des actions neurotrophiques/neuroprotecteurs ou des effets neurotoxiques. Elle peut stimuler la prolifération astrogliale, contribue à forte concentration à sa réactivité et régule positivement l'activation des microglies (Adami et al., 2001; Bianchi et al., 2010; Van Eldik and Wainwright, 2003). Il existe également des indications selon lesquelles le S100B agirait comme un régulateur de la plasticité synaptique et de la potentialisation à long terme (Nishiyama et al., 2002). Dans l'ensemble, le S100B est engagé dans la signalisation intercellulaire et peut agir comme un messager extracellulaire (Donato et al., 2009). Dans des conditions pathologiques, l'expression de S100B change considérablement. Des niveaux élevés de cette protéine dans le sérum et les liquides céphalo-rachidiens peuvent avoir une certaine pertinence pour les diagnostics (Donato et al., 2013).

A cause de ses hauts niveaux d'expression, S100B est classiquement utilisé comme marqueur astrocytaire, à la fois en condition physiologique et pathologique. La réponse astrocytaire est associée avec la upregulation de S100B. Dans l'hippocampe des rongeurs, S100B est plus exprimé que GFAP. Seuls ~80% des astrocytes marqués exprimant S100B expriment également la GFAP (Ogata and Kosaka, 2002). Dans le cerveau entier, les anticorps dirigés contre S100B marquent approximativement trois fois plus d'astrocytes que GFAP. Cependant, GFAP marque plus de cellules dans la matière blanche que dans la matière grise. Très peu de cellules GFAP positives sont observées dans le cortex et le tronc cérébral (Savchenko et al., 2000). La spécificité cellulaire du S100B est cependant nettement inférieure à celle du GFAP. Dans le SNC, S100B n'est pas exprimé exclusivement par les astrocytes mais également par les

oligodendrocytes, par les cellules épendymaires, dans l'épithélium du plexus choroïde, dans les cellules de l'épithélium vasculaire par les lymphocytes et également quelques neurones, en particulier, les neurones du tronc cérébral, du cervelet, du prosencéphale et du système limbique (Rickmann and Wolff, 1995; Steiner et al., 2007).

VI.b.i.3. Le transporteur du glutamate et la glutamine synthétase.

Le transporteur du glutamate et la glutamine synthétase sont des molécules clé dans le recyclage du glutamate dans le SNC. Les transporteurs au glutamate astrocytaire EAAT-1 (GLAST) et EAAT2 (GLT-1) sont exprimés quasi exclusivement dans les astrocytes (Schmitt et al., 1997). EAAT-1 est plus répandu et ses anticorps permettent son identification dans la glie radiaire, les astrocytes fibreux et protoplasmiques, la glie de Bergmann, la glie de Müller, et la zone sous ventriculaire chez la souris en développement et adulte (Barry and McDermott, 2005; Shibata et al., 1997; Williams et al., 2005). L'anticorps monoclonal spécifique ASCA-1 dirigé contre les épitopes extracellulaires de EAAT-1 marque la plupart des astrocytes protoplasmiques et fibreux mais également la glie de Bergmann et de Müller(Jungblut et al., 2012). Le EAAT2, quant à lui, montre une expression neuronale transitoire au niveau du cortex et des ganglions de la base durant le stade de développement fœtal (Northington et al., 1998).

La glutamine synthétase (GS) marque virtuellement les astrocytes, incluant la glie radiaire, la glie de Bergmann, la glie rétinienne de Müller, les tanycytes, les cellules épendymaires. Il est important de noter que les anticorps anti-GS marquent les astrocytes dans de nombreuses régions où le marquage GFAP est faible (Anlauf and Derouiche, 2013). Dans le cortex entorhinal de la souris, le double marquage GFAP – GS montre que 78% des cellules expriment la GS alors que seulement 12% expriment la GFAP et 10% sont positives pour les deux marqueurs (Yeh et al., 2013). De façon similaire, une population différente de cellules positives à la GS a été identifiée. Le double marquage GS-GFAP montre que seulement 60% de ces cellules sont positives au GFAP. La GS est une enzyme cytosolique : c'est pour cela que le marquage à l'aide d'anticorps révèle l'intégralité du cytoplasme incluant les fins process synaptiques (Derouiche and Frotscher, 1991). Il y a quelques indications montrant que la GS dans les astrocytes en culture peut être associée avec des structures vésiculaires (Anlauf and Derouiche, 2009). Quelques études rapportent toutefois des marquages d'oligodendrocyte (Cammer, 1990)avec la GS et aussi dans certains neurones (Robinson, 2001). Cependant, à l'heure actuelle, la GS est considérée comme le marqueur astrocytaire le plus fiable.

VI.b.i.4. Quelques autres marqueurs astrocytaires

Plusieurs protéines, plus ou moins exprimées exclusivement dans les astrocytes, ont été identifiées et peuvent être utilisées comme marqueurs Tableau 7. La vimentine, similaire à GFAP, est un membre de la famille des filaments intermédiaires présente dans les cellules mésenchymateuses. Elle est impliquée dans de nombreuses fonctions cellulaires et particulièrement dans la régulation de la différentiation cellulaire, l'adhésion, la migration, la régénération et la signalisation cellulaire (Ivaska et al., 2007). Dans le SNC, la vimentine est principalement exprimée dans les astrocytes, particulièrement dans les astrocytes immatures. Après la naissance, l'expression de vimentine décroît. Elle reste cependant toujours détectable dans les astrocytes fibreux et protoplasmiques de l'hippocampe et de corps calleux, mais aussi dans les cellules gliales de Bergmann et les tanycytes où elle est coexprimée avec le GFAP (Pekny et al., 1999; de Vitry et al., 1981). La vimentine semble également être présente dans les cellules souches neurales chez l'adulte présentant un phénotype astroglial-like dans les niches neurogéniques. Son expression est up régulée dans les astrocytes réactifs (Doetsch et al., 1999; Götz et al., 2015).

Un autre marqueur utilisé est l'aquaporine 4 (AQP4) dans le SNC, elle est présente dans les astrocytes et les épendymocytes (Frigeri et al., 1995; Nielsen et al., 1997). Dans les astrocytes, l'expression des AQP4 est fortement polarisée avec de fortes concentrations au niveau des pieds astrocytes (Nagelhus and Ottersen, 2013).

Les astrocytes présents dans le cerveau expriment des connexines, avec une expression prédominante de la Cx43 et également de la Cx30 (Dermietzel et al., 1991). Le marquage des tissus cérébraux avec des anticorps contre les deux connexines montre des motifs ponctués, la Cx30 est exprimée principalement dans les astrocytes de la matière grise (principalement concentrée au niveau des pieds astrocytaires) alors qu'elle est absente des astrocytes de la matière blanche (Nagy et al., 1999).

Une autre enzyme métabolique, l'aldéhyde déshydrogénase 1 de la famille L1 (ALDH1L1), est montrée comme étant exprimée de façon spécifique dans les astrocytes (Neymeyer et al., 1997). Elle a récemment été proposée comme un marqueur antigénique. Les anticorps polyclonaux contre l'ALDH1L1 marquent plus d'astrocytes que la GFAP. Au niveau cellulaire, le marquage ALDH1L1 révèle le soma et le process fin (Cahoy et al., 2008). Cependant, une étude

plus tardive montre que le niveau d'expression d'ALDH1L1 change avec l'âge. De plus, ALDH1L1 peut également se retrouver exprimée dans une sous-population d'oligodendrocytes (Yang et al., 2011d). Toutefois, ALDH1L1 marque principalement les astrocytes corticaux et très peu les astrocytes de la matière blanche (Waller et al., 2016).

Une autre enzyme permettant l'identification des astrocytes est la forme spécifique au cerveau du fructose-1,6-biphosphate aldolase, aussi appelée aldolase C. Elle est connue pour être exprimée préférentiellement dans les astrocytes, bien qu'elle ait également été détectée dans les neurones de Purkinje (Walther et al., 1998).

Les astrocytes chez la souris et l'humain sont enrichies avec le facteur de transcription SOX9. L'immunomarquage de SOX9 a permis de montrer un chevauchement entre le SOX9 nucléaire et EAAT2 indiquant un marquage spécifique aux astrocytes (Sun et al., 2017). Cependant, le marquage SOX9 étant nucléaire, il ne permet pas de déterminer le profil des astrocytes marqués.

Les astrocytes inter laminaires ainsi que les astrocytes fibreux dans le cerveau humain sont facilement marqués avec des anticorps contre CD44, un récepteur pour les molécules de la matrice extracellulaire (Bignami and Dahl, 1986). Les astrocytes protoplasmiques sont, en règle générale, négatifs au CD44, bien qu'ils puissent acquérir cette protéine à des âges plus avancés et dans des cas pathologiques (Sosunov et al., 2014).

VI.b.ii. Les sondes gliophyliques fluorescentes

La capacité des astrocytes à accumuler préférentiellement les sondes calciques fluorescentes sous forme d'acetoxyméthyle (AM) a été montrée dans les premières études réalisées sur les cerveaux en tranche (Kirischuk and Verkhratsky, 1996; Shelton and McCarthy, 2000). Elle a, par la suite, été souvent utilisée pour évaluer l'activité calcique dans les astrocytes (Bernardinelli et al., 2011). La concentration d'indicateurs calciques présente dans les astrocytes est environ 4 à 5 fois supérieure à la concentration retrouvée dans les neurones avoisinants (Hirase et al., 2004). L'accumulation spécifique de ces sondes calciques peut être dûe à la faible expression dans les astrocytes du transporteur cassette ABC qui est impliqué dans l'extrusion de ces sondes (Manzini et al., 2008). (Figure 27).

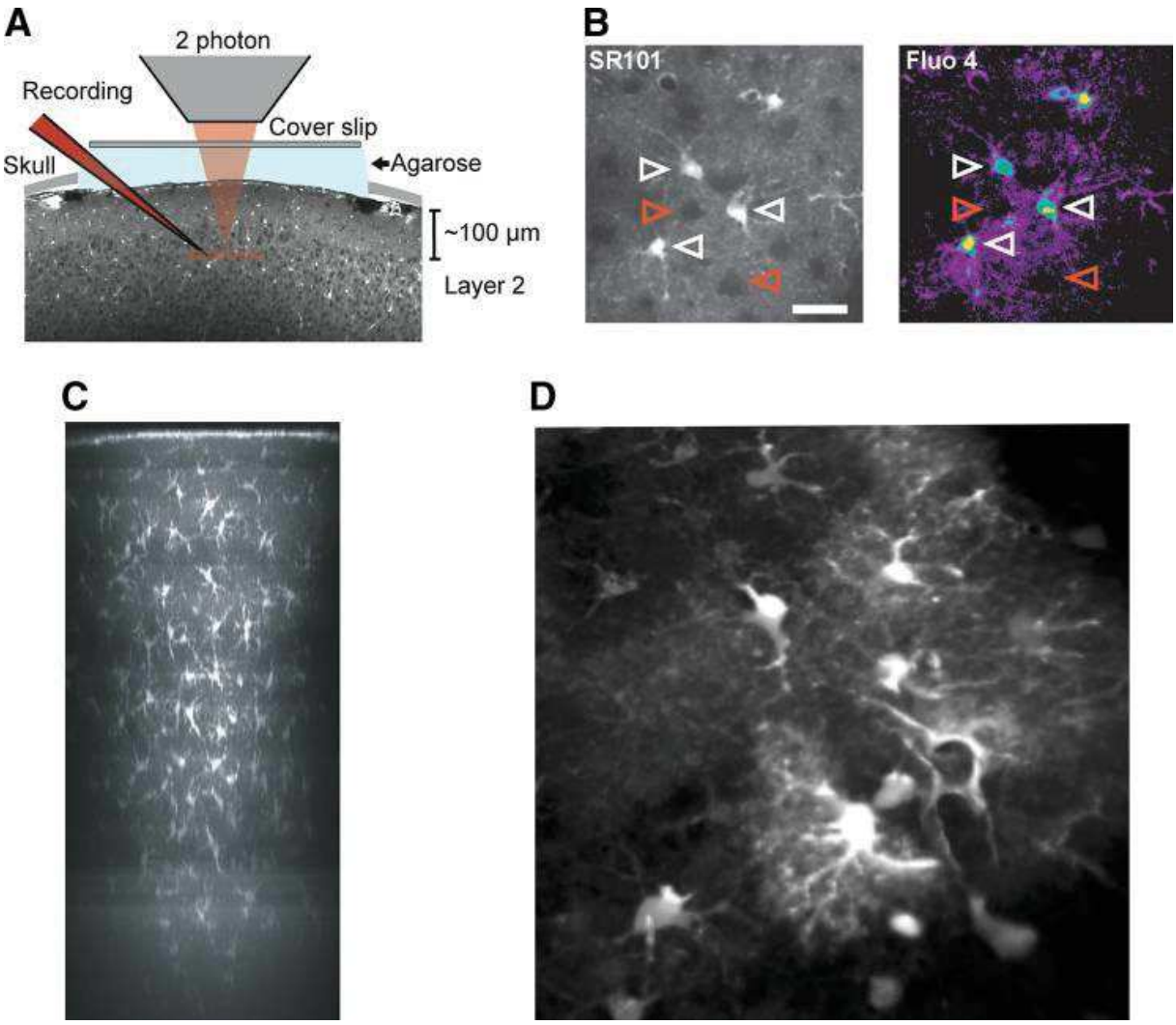

Figure 27 : Imagerie biphotonique des astrocytes *in-vivo*. (A) Schéma représentant le montage expérimental. Les astrocytes du cortex somatosensoriel sont chargés à l'aide d'un marqueur astrocytaire (SR101) ainsi qu'un indicateur calcique (Fluo 4-AM). (B) Exemple d'image obtenu en microscopie biphotonique. A gauche les astrocytes marqués par la SR101 et à droite les astrocytes marqués par la Fluo 4-AM. Les flèches blanches indiquent les astrocytes exprimant les deux sondes. Les flèches rouges montrent les neurones. Barre d'échelle : 30µM. (C) Vue d'ensemble des cellules SR101 positive et leur projection au travers du néocortex de la souris. (D) Astroyctes corticaux chargés en SR101 et imagés avec un système confocal à deux photons chez la souris. Image provenant de (Nimmerjahn et al., 2004; Tian et al., 2006; Verkhratsky and Nedergaard, 2018)

Un autre marqueur fluorescente qui est classiquement utilisée pour imager les astrocytes est la sonde cationique sulforhodamine 101 (SR101) et ses analogues sulforhodamine B ou G (Nimmerjahn et al., 2004). La SR101 est chargée sélectivement par les astrocytes. De par sa

localisation cytoplasmique, elle permet de révéler la structure cellulaire des astrocytes. L'accumulation de SR101 dans les astrocytes semble être médiée par les transporteurs anioniques qui sont exprimés de façon différentielle dépendamment des régions cérébrales. Par exemple, la SR101 marque les astrocytes de l'hippocampe mais ne s'accumule pas dans ceux de la médulla ventro-médiane (Schnell et al., 2012). De plus, la SR101 ne marque qu'une sous-population astrocytaire qui augmente après la naissance et souvent coïncide avec le marquage GFAP présent dans les astrocytes matures (Kafitz et al., 2008). Un des point limites de cette sonde est qu'elle a été montrée comme perturbant l'excitabilité neuronale, et peut provoquer des crises d'épilepsie in vitro et ex vivo (Kang et al., 2010; Rasmussen et al., 2016).

c. Réseau astrocytaire et syncytium

La macroglie (astrocyte et oligodendrocyte) est fortement connectée d'un point de vue intracellulaire et fonctionnel et organisée en syncytium via les jonctions GAP. Ces dernières sont des structures ubiquitaires responsables de l'intégration intercellulaire dans de nombreux tissus reliant, par exemple, les cellules épithéliales du tractus gastro-intestinal et du rein, assurant un couplage métabolique dans le foie, un couplage électrique dans le cœur, la signalisation intercellulaire dans les tissus endocriniens, et définissant la physiologie cochléaire et donc, par extension, le sens de l'ouïe (Bosco et al., 2011; Hanner et al., 2010; Nickel and Forge, 2008; Rohr, 2004). Les jonctions GAP sont des zones spécialisées où deux membranes apposées de cellules adjacentes se rapprochent très étroitement de sorte que la fente intercellulaire est réduite à une largeur d'environ 2 à 3 nm. Dans ces zones, chaque jonction GAP est constituée de plusieurs centaines de canaux intercellulaires ou connexons, qui assurent le transport intercellulaire d'ions, de messagers secondaires ainsi que d'autres molécules biologiquement actives de moins de 1000 Da. Dans la matière grise, des paires d'astrocytes sont connectées grâce à ~ 230 jonctions GAP en moyenne, et l'injection de Lucifer Yellow ou de biocytine dans un seul astrocyte entraîne une coloration d'environ 50 à 100 cellules astrogliales adjacentes (Evans and Martin, 2002).

Le concept qu'un syncytium connecte toutes les macroglies en un réseau fonctionnel, a également été confirmé chez les invertébrés (Mugnaini, 1986), mais ne s'applique pas entièrement au SNC des mammifères. Dans un premier temps, la présence des jonctions GAP

entre les différents oligodendrocytes est plutôt limitée (Rash et al., 2001). Deuxièmement, dans de nombreuses régions du cerveau, les réseaux astrogliaux sont anatomiquement séparés en fonction des structures anatomiques ; par exemple, les syncytium astrogliaux sont confinés à des barrels individuels de cortex somatosensoriel ou dans des glomérules individuels dans le bulbe olfactif (Giaume et al., 2010; Houades et al., 2008; Roux et al., 2011). Le couplage entre astrocytes adjacents n'est pas non plus omniprésent ; certains (probablement jusqu'à 15 à 20%) des astrocytes voisins sont découplés, comme le démontre la diffusion de colorant ou les enregistrements en double patch-clamp des paires de cellules voisines (Houades et al., 2006; Meme et al., 2009).

d. Propriété électrophysiologique de l'astrocyte

VI.d.i. Distribution ionique

Comme pour toutes les cellules vivantes, il y a une différence de concentration ionique entre le milieu cytosolique et le milieu extracellulaire (Figure 28). Le concept de concentration cytosolique en ion est défini par la perméabilité membranaire, par les transporteurs actifs nécessitant de l'énergie et par les tampons cytosoliques. La concentration intra astrocytaire en K+ est retrouvée dans les alentours de 120 et 140 mM, alors que la concentration de K^+ dans le LCR et le liquide interstitielle se retrouve dans les alentours de 3 mM, ce qui est plus faible que la concentration plasmatique (Hansen, 1985; Jones and Keep, 1987). Cette concentration définit le potentiel d'équilibre pour le K^+ (E_K) à -98 mV (37°C). La concentration cytosolique de Na^+ dans les astrocytes (15-20 mM) est généralement plus élevée que dans la majorité des neurones (8-10 mM). De plus, dans certains neurones $[Na^+]_i$ elle peut se retrouver à des concentrations de 15 mM (Rose and Verkhratsky, 2016). Avec la concentration de Na^+ dans le LCR dans les environs de 145-155 mM, le potentiel d'équilibre E_{Na} se retrouve entre +50 et +60 mV. Il a été rapporté que $[Na+]_{LCR}$ présente des variations rhythmiques de 10 à 40 mM (Harrington et al., 2010). La concentration de Ca^{2+} dans le cytoplasme astrocytaire est située entre 50 et 150 mM, valeur plus élevée que dans les neurones (Zheng et al., 2015). En se basant sur le fait que la concentration de Ca^{2+} chez l'adulte est de 1.5 mM le E_{Ca} se situe entre +120 et +140 mV (Jones and Keep, 1988). La distribution astrogliale de Mg^{2+}, le deuxième cation divalent majeur contrôlant plusieurs fonctions cellulaires, a été très peu étudiée. La concentration cytosolique de Mg^{2+} libre dans les astrocytes en culture mesurée avec la sonde fluorescente Mag-fura 2 est d'environ 125 µM (Babu et al., 1999). La $[Mg2+]_{LCR}$ a été

déterminée à ~ 0,9 mM donc E_{Mg} est ~ 25 mV (Sun et al., 2009). Il est généralement admis que les astrocytes contiennent une forte concentration ionique de Cl^- qui varie de 30 à 60 mM (~5 mM dans les neurones) donnant un E_{Cl} de -35 mV ($[Cl^-]_0$ est de 120 mM). La forte concentration de Cl^- intracellulaire a été déduite des enregistrements du potentiel de membrane, dans laquelle l'activation des récepteurs GABAA (essentiellement perméables au Cl-) dépolarise toujours les astrocytes en culture et le E_{Cl} approximatif calculé serait de -35mV (Bekar and Walz, 2002; Kettenmann and Schachner, 1985).

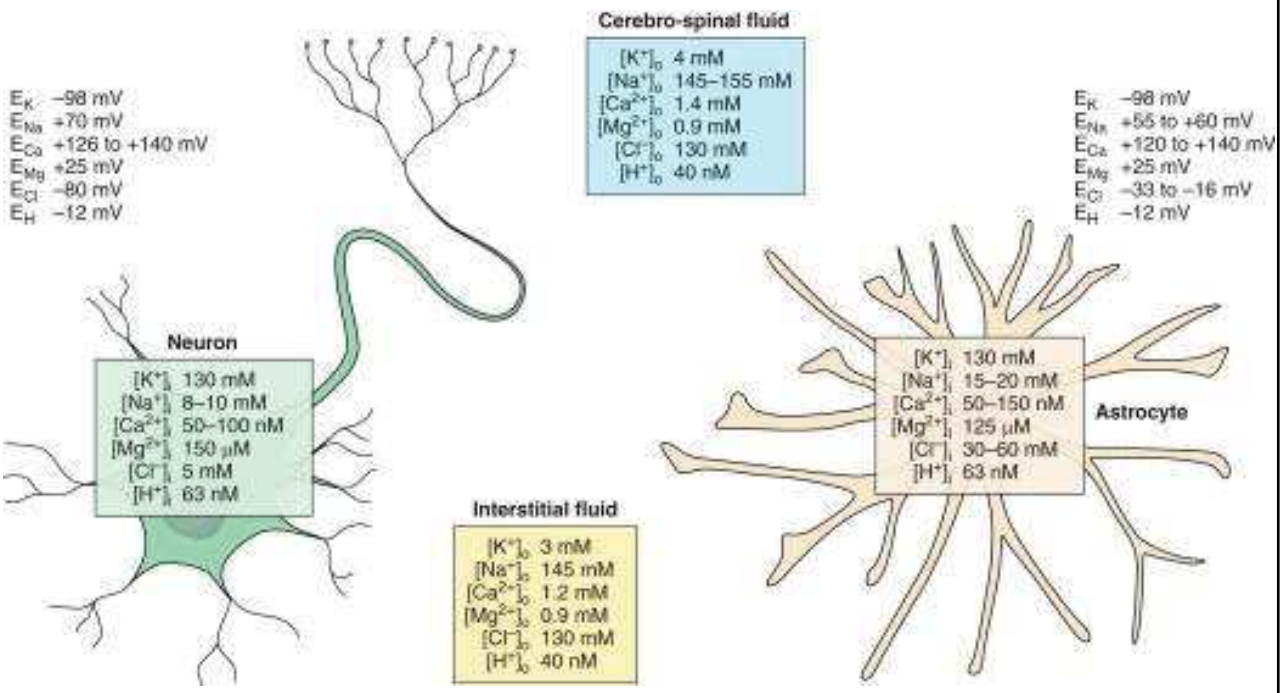

Figure 28 : Distribution ionique et leurs valeurs correspondant au potentiel d'équilibre entre le LCR, le milieu interstitiel ainsi que cytoplasmique. Issus de (Verkhratsky and Nedergaard, 2018)

VI.d.ii. <u>Le potentiel de membrane</u>

La signature électrophysiologique la plus caractéristique des astrocytes matures est son potentiel de repos très hyperpolarisé, très proche du E_K (environ -80mV) et sa faible résistance d'accès (5-20 MΩ), indicateur d'une perméabilité élevée de la membrane au K^+ (Dallérac et al., 2013; Mishima and Hirase, 2010; Mishima et al., 2007). Cela se traduit aussi par une relation courant-tension presque linéaire, qui est également une signature électrophysiologique caractéristique de l'astroglie (Adermark and Lovinger, 2008; Chvátal et al., 1995; Du et al.,

2015; Kafitz et al., 2008; Olsen et al., 2006) (Figure 29) Ces propriétés membranaires sont intrinsèques aux astrocytes car les cellules isolées sont très similaires aux cellules connectées de manière syncytiale dans le tissu nerveux. En temps normal, les astrocytes sont iso potentiels et le V_m reflète généralement les changements de concentration en K^+ extracellulaire (Amzica and Massimini, 2002; Dallérac et al., 2013).

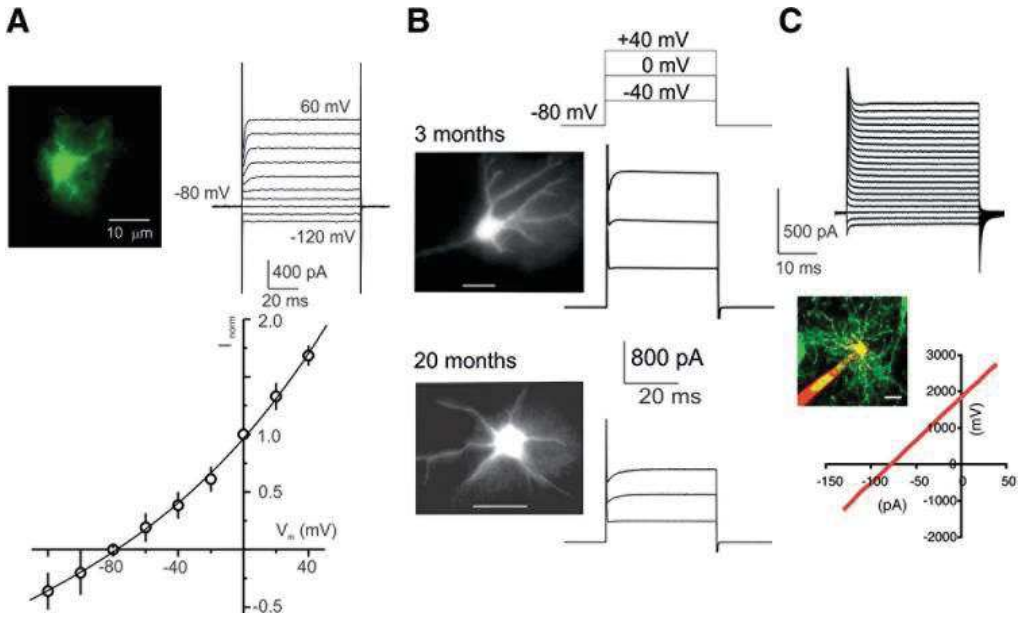

Figure 29 : Propriété membranaire des astrocytes. (A) Enregistrement en voltage clamp d'astrocytes en culture de souris exprimant EGFP sous le contrôle du promoteur GFAP. Les enregistrements en whole cell ont été réalisés en hyperpolarisant et dépolarisant la cellule avec des steps de 20 mV (-120 mV à +60 mV) Pour réaliser la courbe (courant en fonction du voltage) l'amplitude des courants a été normalisée à 0mV. Chaque point représente la moyenne +/- SD pour 20 cellules. (B) Enregistrement en voltage-calmp d'astrocytes sur tranche de cerveau de souris GFAP-EGFP de 3 mois. (C) Enregistrement en voltage clamp d'astrocytes humains greffés dans le cerveau de souris. Adapté de (Han et al., 2013; Lalo et al., 2006, 2011; Verkhratsky and Nedergaard, 2018)

e. Expression de différents types de récepteurs par les astrocytes

Les astrocytes sont capables d'exprimer virtuellement tous les types de récepteurs retrouvés dans le SNC. Les premiers indices montrant l'expression de récepteurs fonctionnels par les astrocytes provenaient d'enregistrements de microélectrodes intracellulaires de cellules corticales de chats anesthésiés. Les cellules ont été enregistrées à l'aveugle, les neurones et la glie se distinguaient par leur excitabilité. Il a été montré que les injections de GABA ou

d'acétylcholine (ACh) provoquaient une dépolarisation gliale, considérée comme reflétant la modulation des pompes ioniques membranaires (Krnjević and Schwartz, 1967). La dépolarisation gliale en réponse aux GABA, glycine, β-alanine et taurine est considérée comme reflétant la libération de K^+ à partir des neurones (Hösli et al., 1981). Les enregistrements électrophysiologiques directs à partir d'astrocytes en culture exempts de contamination neuronale démontrent l'expression fonctionnelle de récepteurs glutamates, GABA, Glycine et également d'OTR (Bowman and Kimelberg, 1984; Kettenmann et al., 1984; Wahis et al., 2020). Des expériences ultérieures sur les astrocytes in vitro ont démontré que ceux-ci expriment en effet plusieurs types de récepteurs (Annexe 2). L'expression des récepteurs par les astrocytes in situ et in vivo est restrictive et dépend de la région cérébrale. La modalité des récepteurs des neurotransmetteurs exprimée par les astrocytes correspond à celle de leurs voisins neuronaux. Elle est très probablement contrôlée par l'environnement local (Verkhratsky et al., 1998). Par exemple, les récepteurs exprimés par les cellules gliales de Bergmann et leurs neurones voisins, les neurones de Purkinje, sont optimisés pour détecter les neurotransmetteurs libérés par les afférences neuronales. De même, les astrocytes expriment des récepteurs de la glycine dans la moelle épinière, où la glycine agit comme un principal médiateur inhibiteur. L'expression astrogliale des récepteurs de la dopamine est quant à elle prédominante dans les noyaux gris centraux, qui utilisent la transmission dopaminergique, tandis que l'expression astrogliale des récepteurs de la sérotonine est limitée aux zones en contact avec les terminaisons sérotoninergiques (Verkhratsky, 2010). Par conséquent, l'expression des récepteurs astrogliaux in vivo est régulée par les afférences et la libération de neurotransmetteur, ce qui rend les astrocytes perceptifs aux signaux spécifiques de chaque région particulière du cerveau.

VI.e.i. Expression des récepteurs purinergiques par les astrocytes

Le système de signalisation purinergique utilisant des purines et des pyrimidines comme molécules de signalisation extracellulaire semblerait être le mode de communication omniprésent dans chaque structure et ce, sans aucune ségrégation anatomique évidente. La plupart des cellules vivantes possède au moins un, et même souvent plusieurs types de

récepteurs purinergiques (Burnstock and Alexei, 2012). Ces derniers sont classifiés de la façon suivante : les récepteurs adénines (P0), les récepteurs adénosines (A ou P1) et les récepteurs nucléotidiques (ATP, ADP, UTP) de la famille des récepteurs P2X (ionotropiques) et P2Y (métabotropiques) (Burnstock and Kennedy, 1985; North, 2002; Verkhratsky and Burnstock, 2014). Dans le SNC, les purines et les pyrimidines sont libérées par les neurones, principalement par leurs terminaisons, et par les astrocytes, grâce à des exocytoses médiées par le calcium, un mécanisme très répandu et certainement l'un des plus étudiés (Abbracchio et al., 2009). Après avoir été libérée, l'ATP est rapidement dégradée par des enzymes extracellulaires spécifiques, les ectonuléotidases (Zimmermann et al., 2012), en ADP, AMP et adénosine, qui agissent tous comme agonistes des récepteurs purinergiques présentant des effets opposés sur les cellules cibles. La majorité absolue des cellules neurogliales étudiées jusqu'à présent exprime certains récepteurs purinergiques. De plus, les cellules gliales sont également capables de libérer de l'ATP et de l'adénosine, ce qui fait d'elles des sources importantes de purine dans le SNC, et place la transmission purinergique au centre de la gliotransmission (Butt, 2011; Verkhratsky et al., 2009). La transmission purinergique contribue également aux neuropathologies, en particulier la libération d'ATP par les cellules endommagées agit comme un signal de « danger » (souvent défini comme : damage-associated molecular pattern, DAMP) qui contrôle les réactions défensives des cellules gliales telles que l'astrogliosis réactive ou l'activation de la microglie (Franke et al., 2012).

VI.e.ii. Expression des récepteurs aux neuropeptides (ocytocine et vasopressine)

Il a été montré que la vasopressine est capable d'induire une augmentation transitoire de la concentration calcique dans des astrocytes en culture, cette action médiée par l'activation de V1 car inhibée suite à l'application de l'antagoniste d(CH2)5[Tyr(Me)2]8-arginine-vasopressin (Jurzak et al., 1995). Il existe une certaine hétérogénéité régionale dans l'expression des récepteurs astrogliaux : les astrocytes hippocampiques *in vitro* expriment principalement les récepteurs V1b, tandis que les astrocytes corticaux expriment principalement le récepteur V1a. L'activation des deux sous types résulte en une élévation de la concentration calcique intracellulaire et stimule la libération de glutamate (Syed et al., 2007). L'activation des récepteurs V1a dans les astrocytes corticaux embryonnaires induit également l'activation de la cascade de signalisation PKC, CaMKII et ERK1/2 (Zhao and Brinton, 2003), tout en diminuant

considérablement l'expression génique des cytokines, comprenant l'IL-1β et le TNF-. Ces effets sont médiés par l'activation de l'élément de réponse liant l'AMPc (CREB) α (Zhao and Brinton, 2004).

Les récepteurs ocytocinergique ont été initialement détectés dans les astrocytes en culture à l'aide d'autoradiographie (Di Scala-Guenot and Strosser, 1992). Par la suite, le lien fonctionnel de ces récepteurs avec la libération de calcium endoplasmique suite à l'activation de la PLC/IP3 a été démontré dans les astrocytes hippocampiques embryonnaires de rat in vitro (Di Scala-Guenot et al., 1994). De façon similaire, la signalisation calcique induite par l'OT a également été démontrée dans des astrocytes hypothalamiques en culture. Cette augmentation transitoire de calcium induite par l'OT est bloquée par les antagonistes mGluR1 et accentuée par les agonistes mGluR1 permettant aux auteurs de supposer que les OTR sont liés à la signalisation calcique au travers des mGluRs (Kuo et al., 2009).

f. Régulation des fonctions physiologique par les astrocytes.

VI.f.i. Régulation de l'homéostasie potassique

L'homéostasie ionique dans le SNC est l'un des points cruciaux pour les fonctions du SNC, car elle régule l'excitabilité et les principaux processus de signalisation. La concentration ionique dans le tissu nerveux n'est cependant pas une composante statique. Les fluctuations ioniques modulent la majeure partie des processus systémiques tels que la mémoire ou encore le sommeil (Ding et al., 2016; Hertz and Chen, 2016). Les astrocytes, grâce à la grande variété de transporteurs ioniques, sont des cellules fondamentales pour la régulation de l'homéostasie.

Par exemple, le contrôle de la concentration interstitielle de K^+ est l'une des grandes fonctions de l'astroglie. L'implication des astrocytes dans le maintien de l'homéostasie potassique du SNC a été proposée dans les années 60. La voie Na/K ATPase ainsi que la diffusion au travers de canaux potassique ont été proposées comme mécanismes soutenant l'homéostasie potassique (Hertz, 1965; Orkand et al., 1966). L'augmentation de la concentration de K^+ extracellulaire durant l'activité neuronale est associée avec l'efflux K^+ repolarisant (Hodgkin and Huxley, 1952). Un potentiel d'action unique est capable d'augmenter la concentration de K^+ locale d'environ 1 mM (Ransom et al., 2000). De plus, la sortie de K^+ est liée à l'activation de récepteurs glutamatergiques postsynaptiques (Rice and Nicholson, 1990). Elle présente de forts efflux de potassium au travers des récepteurs NMDA où la libération de K^+ peut

également intervenir lors du co-transport K^+/ Cl^- activé par la transmission GABAergique (Shih et al., 2013; Viitanen et al., 2010). L'augmentation de K^+ peut également provenir de l'efflux de cet ion par les astrocytes lors du transport du glutamate par EAAT1/2. On peut également supposer que la plupart du K^+ libérés dans l'espace synaptique est due aux arborisations dendritiques, tandis que les potentiels d'action axonaux ne représentent qu'une petite fraction de K^+ libéré dans l'espace interstitiel (Hertz, 2011; Howarth et al., 2012).

Le concept initial de la régulation potassique par les astrocytes postulait que les ions K^+ pénétraient dans les astrocytes par les canaux K^+ membranaires puis étaient redistribués au travers du syncytium glial via les jonctions GAP et relargués à distance. Il a été montré que ce concept fonctionnait également un niveau unicellulaire dans la glie de Müller. Dans ce cas, le K^+ entre par les canaux $K_{ir}4.1$, retrouvés en grande quantité au niveau des process péri synaptique dans la rétine. Le K^+ s'équilibre à travers toute la cellule et est libéré également par les Kir4.1 au niveau des pieds astrocytaires ou par les process périvasculaires. Ce concept de régulation potassique spatiale repose sur la capacité des canaux $K_{ir}4.1$ à accumuler K^+ localement et sur les jonctions GAP, qui assurent la redistribution K^+ (Kofuji and Newman, 2004; Newman et al., 1984). Des expériences in vitro ont démontré que les canaux $K_{ir}4.1$ sont en effet principalement responsables de la perméabilité K^+ au repos des astrocytes et pourraient être considérés comme les principaux acteurs de la régulation K^+ (Ballanyi et al., 1987; Djukic et al., 2007; Kucheryavykh et al., 2007; Neusch et al., 2001). Néanmoins, l'étude menée sur des souris knock-out Kir4.1 spécifique à l'astroglie n'a pu révéler ni le phénotype attendu (hyperexcitabilité neuronale) ni des altérations significatives de la cinétique de $[K^+]_e$ suite à la stimulation neuronale. Les changements de dynamique de $[K^+]_e$ se limitent à une diminution modérée dans la cinétique de récupération et l'apparition d'un undershoot après la récupération (Chever et al., 2010). Dans le même temps, la suppression génétique des canaux $K_{ir}4.1$ induit une dépolarisation significative (~20 mV) au niveau des potentiels de repos membranaire et diminue la perméabilité du K^+ au repos. Ces données plaident donc contre un rôle dominant des canaux $K_{ir}4.1$ dans la régulation de l'homéostasie potassique (Larsen and MacAulay, 2014; Nwaobi et al., 2016). L'expression des canaux $K_{ir}4.1$ varie en fonction des aires cérébrales. C'est pour cela que la contribution de ces canaux dans la régulation de l'homéostasie potassique peut être variable en fonction des régions (Nwaobi et al., 2016).

La régulation potassique faisant intervenir la pompe NA/K a été montrée pour la première fois dans des astrocytes en culture (Hertz, 1979). De nombreuses expériences ultérieures réalisées in situ ont révélé que cette pompe est un des acteurs principaux dans la clairance potassique extracellulaire associée avec l'activité neuronale (D'Ambrosio et al., 2002; Larsen et al., 2014; Ransom et al., 2000; Xiong and Stringer, 2000). Dans ce scénario, le potassium accumulé par les astrocytes est relargué dans l'espace extracellulaire pour être recapté par les neurones, restaurant ainsi leur gradient ionique. Les astrocytes tamponnent donc rapidement l'excès de K^+ libéré durant l'activité neuronale. Quand les neurones arrêtent de générer des potentiels d'action, le K^+ est transporté vers le compartiment neuronal (Hertz and Chen, 2016; Larsen et al., 2016). La libération de K^+ est médiée par les canaux $K_{ir}4.1$ et possiblement par d'autres canaux ou transporteurs SLC (solute carrier familly). Le transporteur NKCC1 ($Na^+/K^+/Cl^-$) a également été proposé comme participant à l'homéostasie potassique suite à une étude menée sur des astrocytes en culture, bien que son rôle in vivo et in situ n'ait pas été confirmé (Larsen et al., 2014). L'activation de la pompe NKCC1 est causée par l'augmentation de K^+ à des valeurs supérieures à 10 mM (Walz and Hertz, 1984) ou par l'hypertonicité (Qusous et al., 2011). Elle peut participer à la clairance du potassium dans des conditions pathologiques.

VI.f.ii. Régulation du calcium extracellulaire

Les astrocytes pourraient également être impliqués dans la régulation de la concentration calcique extracellulaire. Au cours de l'activité neuronale, la concentration calcique avoisine celle du compartiment extracellulaire et en particulier au niveau de la fente périsynaptique qui subit de fortes variations dues à l'influx massif de calcium dans les neurones lors de l'activation des canaux Ca^{2+}. La concentration calcique extracellulaire peut diminuer à des valeurs inférieures à 1 mM, ce qui active la signalisation calcique à la fois dans les compartiments présynaptiques et postsynaptiques, ayant de claires conséquences pour la transmission synaptique (Rusakov and Fine, 2003). Par ailleurs, la diminution de la concentration calcique extracellulaire induit la libération d'ATP par les astrocytes, activant les interneurones de l'hippocampe (Torres et al., 2012). La diminution de la concentration calcique a des valeurs avoisinant 0.5 mM, et déclenche la cascade IP3-induced Ca^{2+} release à partir du réticulum endoplasmique des astrocytes (probablement médiés par une libération autocrine d'ATP) (Zanotti and Charles, 1997). Cela pourrait aider la restauration de la concentration de calcium à des valeurs basales.

VI.f.iii. Homéostasie des neurotransmetteurs

Les astrocytes sont des cellules fondamentales pour le recyclage des neurotransmetteurs dans le cerveau. Ils retirent, inactivent par accumulation et conversion métabolique le glutamate, le GABA, l'adénosine et l'adrénaline Figure 30. De plus, les astrocytes produisent de la glutamine, un précurseur nécessaire pour la synthèse de glutamate et de GABA, deux neurotransmetteurs indispensables à la fois pour l'excitation et l'inhibition.

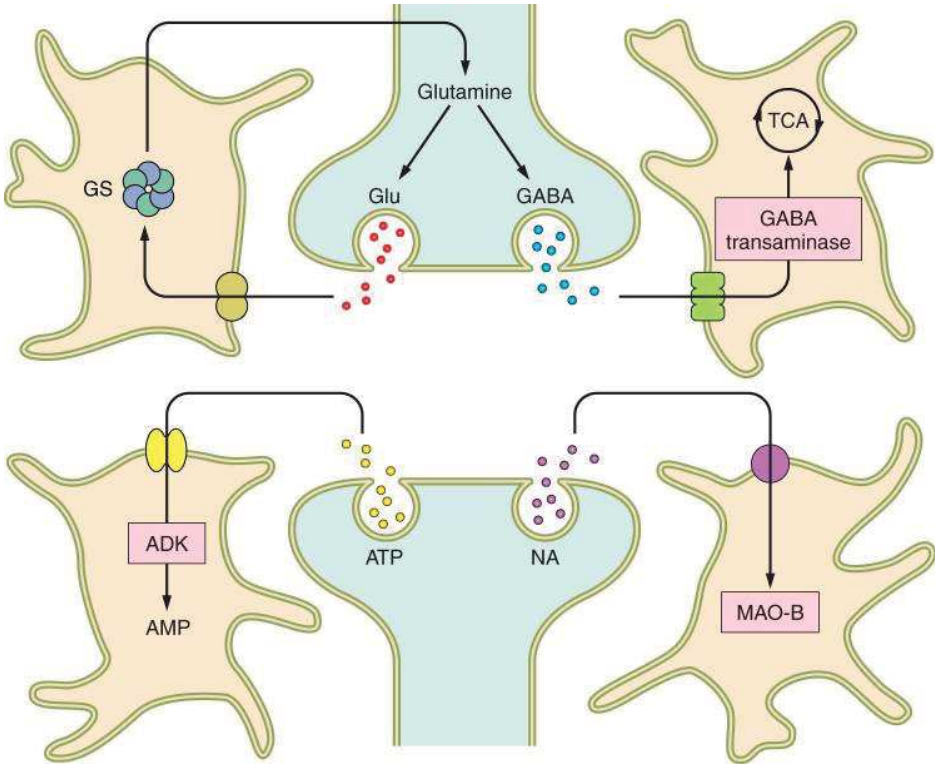

Figure 30 : Homéostasie des astrocytes et des neurotransmetteurs. Les astrocytes récupèrent le glutamate, le GABA, l'Adénosine et les monoamines. Le glutamate est converti en glutamine (par la glutamine synthase, GS), qui est transporté dans les neurones. La glutamine sera par la suite transformée en glutamate ou en GABA. Le GABA accumulé par les astrocytes est principalement dégradé par le cycle de Krebs. L'adénosine est convertie en AMP par l'adénosine kinase (ADK) alors que les monoamines sont dégradées par les monoamines oxydase astrocytaires (MAO-B). Issus de (Verkhratsky and Nedergaard, 2018)

Le glutamate est une molécule ubiquitaire présente dans tous les types de cellules et agit, la majeure partie du temps, comme un neurotransmetteur excitateur dans le SNC. Il est libéré dans la fente synaptique et atteint des valeurs avoisinant le milli molaire (Mayer, 2011). Le système homéostatique du glutamate est responsable de l'élimination rapide du glutamate de

la fente synaptique, du contrôle du débordement du glutamate vers les synapses voisines, et de la reconstitution rapide du pool libérable dans les terminaisons neuronales. De plus, il est important que ce système garde la concentration ambiante de glutamate à de faibles concentrations pour éviter l'excitotoxicité. Ces nombreuses fonctions sont assurées par les astrocytes.

D'abord et avant tout, les astrocytes sont les seuls synthétiseurs de novo du glutamate à partir du glucose dans le SNC (Hertz et al., 1999). Cette synthèse nécessite l'α-cétoglutarate, un intermédiaire du cycle de l'acide Krebs (Schousboe et al., 2014), qui est produit par l'enzyme pyruvate carboxylase exclusivement exprimé par les astrocytes (Shank et al., 1985; Yu et al., 1982). De plus, les astrocytes expriment une autre enzyme fondamentale pour le recyclage du glutamate : la glutamine synthétase (Norenberg and Martinez-Hernandez, 1979). La glutamine synthétase catalyse la conversion du glutamate en glutamine. La glutamine étant un précurseur direct du glutamate, les neurones expriment la phosphate-activated glutaminase qui désamine la glutamine en glutamate. La glutamine synthétase est également une enzyme cytoplasmique nécessaire pour la détoxification de l'ammonium (NH_4^+), qui est converti grâce à cette enzyme en glutamine (Cooper and Plum, 1987). Dans les conditions physiologiques, le NH_4^+ est libéré par les neurones et accumulé par les astrocytes grâce à différents canaux et transporteurs (Marcaggi et al., 2004).

Ensuite, les astrocytes sont les principales cellules recaptant le glutamate durant la neurotransmission, environ 80% du glutamate extracellulaire dans le SNC est recapturé par les astrocytes via les EAAT1/2 (Danbolt, 2001; Marcaggi and Attwell, 2004; Tzingounis and Wadiche, 2007). Il a été montré que la délétion du transporteur du glutamate dans les astrocytes conduit à une excitotoxicité et une paralysie induite par l'augmentation du niveau de glutamate dans les fentes synaptique (Rothstein et al., 1996). De plus, les astrocytes assurent la reconstitution du stock glutamatergique dans les terminaisons axonales. Le glutamate entrant dans les astrocytes subit une conversion en glutamine (une réaction nécessitant de l'énergie, une molécule d'ATP pour une molécule de glutamate), qui est ensuite acheminée vers les neurones. L'entrée de sodium, induite par l'entrée de glutamate médiée par EAAT1/2, stimule l'efflux de glutamine coordonnant ainsi les flux de glutamate/glutamine : l'augmentation de l'absorption de glutamate augmente la libération de glutamine (Todd et al., 2017; Uwechue et al., 2012). Après avoir pénétré dans les terminaisons neuronales, la

glutamine est convertie en glutamate dans les neurones excitateurs ; dans les neurones inhibiteurs, le glutamate est ensuite converti en GABA. Cette séquence d'événements de transport et biochimiques représente la navette glutamine-glutamate (GABA) (Bröer and Brookes, 2001; Hertz, 2013). Une partie du glutamate accumulé dans les astrocytes est métabolisée en α-cétoglutarate par la glutamate-déshydrogénase (GDH) ou l'aspartate-glutamate transférase (AAT). Cette molécule est ensuite utilisée pour la production d'énergie ; on estime qu'environ 85% du glutamate est converti en glutamine et renvoyé aux neurones, alors qu'environ 15% est oxydé (Rothman et al., 2011). Les astrocytes peuvent également réguler dynamiquement la concentration extrasynaptique de glutamate, non pas par son absorption, mais plutôt par sa libération via l'antiporteur cystine / glutamate Sxc^- (Moussawi et al., 2011). Les augmentations du glutamate extrasynaptique peuvent affecter les neurones à la fois par les récepteurs NMDA et également par les récepteurs métabotropiques. La délétion génique de la sous-unité catalytique du Sxc^- conduit à une diminution d'environ 50% du glutamate extracellulaire mesuré par microdialyse (Massie et al., 2011). Une diminution similaire a été observée après l'administration chronique de cocaïne ou de nicotine connue pour réduire l'expression de Sxc^- (Baker et al., 2003; Moussawi et al., 2011).

g. La synapse tripartie et la gliotransmission.

Parmi les nombreuses études abordant le rôle des astrocytes dans le SNC, la plus frappante (bien que débattue) est celle postulant que les astrocytes peuvent affecter directement l'activité neuronale par la modulation dynamique des synapses. Les astrocytes recouvrent à la fois les éléments pré- et post- synaptiques des synapses et interagissent avec eux. Par exemple, plusieurs études ont démontré le rôle actif des astrocytes dans les processus de LTP, au niveau des synapses CA3-CA1 de l'hippocampe (Gómez-Gonzalo et al., 2015; Han et al., 2012; Navarrete and Araque, 2010). Un des mécanismes implique la libération d'acétylcholine des neurones agissant sur les astrocytes, via l'activation des récepteurs muscariniques, induisant une augmentation transitoire de calcium en provenance des stocks intracellulaires. Ces élévations calciques conduisent à la libération de glutamate par les astrocytes au niveau des récepteurs métabotropiques pré-synaptiques, potentialisant alors la libération de glutamate au niveau de la synapse. Une autre étude réalisée sur les mêmes synapses montre que, durant l'induction de LTP, le calcium extracellulaire pénètre dans les astrocytes via TRPA1 (transient

receptor potential cation channel, member A1) conduisant à la libération de la D-sérine, un co-agoniste des récepteurs NMDA, par les astrocytes au niveau de la terminaison post-synaptique (Shigetomi et al., 2013). Ce phénomène conduit à la potentialisation synaptique. Cette influence des astrocytes sur les synapses a donné le nom du modèle de la « synapse tripartite ». Le processus de libération de substances neuroactives par les astrocytes est nommé « gliotransmission » (Volterra et al., 2014). La modulation active des synapses par les astrocytes a par la suite été établie dans d'autres aires cérébrales. Il a été montré que l'activité des astrocytes peut être spécifique aux circuits, c'est-à-dire qu'ils modulent des synapses spécifiques d'une circuiterie donnée et non toutes les synapses avoisinantes.

Cela a été montré dans le striatum en étudiant le rôle des astrocytes dans la modulation des voies directes et indirectes des noyaux gris centraux. Dans le striatum, des récepteurs dopaminergiques D1 ou D2 bien caractérisés exprimés dans les neurones épineux moyens transmettent les informations de chaque voie séparément, bien qu'anatomiquement totalement entremêlés dans le striatum. Dans ce contexte, Martin et ses collègues ont montré que des sous-populations d'astrocytes ont répondu à l'activation d'une voie et non de l'autre, et vice versa. La stimulation unique d'un astrocyte a été suffisante pour potentialiser la synapse spécifique de la voie à laquelle il appartenait, et pas à l'autre (Martín et al., 2015).

In vivo, Poskanzer et ses collaborateurs ont démontré que l'activation spécifique d'astrocytes dans le cortex pouvait déclencher un switch au niveau du réseau cortical en le faisant passer à un état d'oscillation lente, switch qui pourrait être induit par la libération de glutamate au voisinage des neurones. Ces études et concepts ont été sujets à discussion dans de nombreuses revues et chapitres de livres (Poskanzer and Yuste, 2016).

OBJECTIF DE LA THESE

Le but de mon travail de thèse a été de déterminer comment l'ocytocine permet de moduler le micro-réseau de l'amygdale centrale et ses comportement associés ; plus précisément quels sont les acteurs cellulaires impliqués dans cette modulation ocytocinergique aussi bien au niveau réseau cellulaire que du comportemental.

Pour mener à bien ce projet, une collaboration étroite entre le laboratoire du professeur Valery Grinevich du DKFZ à Heidelberg en Allemagne et mon laboratoire d'accueil à Strasbourg a été établie et celle-ci perdure encore à ce jour. Les intérêts à travailler en collaboration avec le Pr. Grinevich sont multiples. Les deux équipes de recherche portent un grand intérêt au système ocytocinergique au sein du système nerveux central et toutes le deux ont une expertise avérée dans le domaine, avec des compétences techniques variées et complémentaires. En effet, le Pr Grinevich et son équipe sont extrêmement compétents dans les techniques de transgénèse et de traçage anatomique tandis que notre équipe présente une expertise focalisée sur les techniques fonctionnelles d'électrophysiologie, d'imagerie calcique et de comportements.

Le fil rouge de mon travail de thèse a été de déterminer le rôle des astrocytes dans la modulation ocytocinergique du circuit de l'amygdale centrale.

a. Caractérisation du système ocytocinergique lors d'un conditionnement à la peur.

Dans un premier temps nous nous sommes intéressés au comportement de peur et sa modulation par le système ocytocinergique. Des études précédentes ont démontré qu'une stimulation des fibres OT était capable d'induire *in vivo* une diminution du comportement de peur chez les rongeurs ainsi qu'une modification de l'activité électrophysiologique du réseau de l'amygdale centrale, démontré en *ex vivo* (Knobloch et al., 2012; Viviani et al., 2011). Cependant les circuits ocytocinergiques impliqués dans la mise en place de ce contrôle restaient à déterminer. Afin de répondre à cette question, nous avons pris avantage d'un nouvel outil viral permettant le marquage ainsi que la manipulation de population de neurones OT spécifique, activé lors du comportement de peur (vGATE). Nous avons ainsi réalisé une étude à la fois *ex vivo* à l'aide d'enregistrements électrophysiologiques, d'analyses neuroanatomiques, et d'approches comportementales (Article 1).

b. Le rôle des astrocytes dans la modulation ocytocinergique du circuit du CeA

Les astrocytes sont des acteurs importants dans le la transmission et la modulation des informations au travers du SNC comme nous l'avons évoqué dans l'introduction. Il a par exemple été décrit qu'ils sont capables de réguler finement l'activité des neurones ocytocinergiques magnocellulaires et peuvent également expriment les OTR dans de nombreuses régions cérébrales. Cependant, plusieurs observations pointent vers une neuromodulation particulière des circuits du CeA par l'ocytocine. Lors de l'application exogène de TGOT ou en stimulant la libération endogène d'OT, nous avons pu observer des délais d'action très longs et variables de ces composés, à la fois *ex vivo* et *in vivo* (données non publiées, (Hasan et al., 2019; Knobloch et al., 2012). Si l'on s'attend à une activation neuronale directe, plusieurs arguments techniques et physiologiques pourraient expliquer ces retards, par exemple dans le cas de la libération évoquée d'OT, le délai pourrait être expliqué par une courte distance de transmission volumique de l'OT des axones au milieu extracellulaire, qui atteindrait par la suite ces cibles neuronales par diffusion passive. Mais il se peut également que le message de l'OT dans le CeA ait été relayé et/ou répercuté et amplifié par des astrocytes. En effet, si un ordre temporel de la transmission neuronale synaptique est la milliseconde, l'excitabilité calcique des astrocytes est quant à elle plus lente et correspond à nos observations des effets de l'OT.

En utilisant des techniques déjà en place au sein du laboratoire tout en dirigeant le développement de nouveaux outils génétiques, nous avons pu démontrer le rôle des astrocytes dans la modulation ocytocinergique de l'amygdale centrale. Ces résultats seront présentés dans l'article 2 et l'article 3.

RESULTATS

Article 1 : A Fear Memory Engram and Its Plasticity in the Hypothalamic Oxytocin System

a. Contexte général

Mémoriser et se remémorer un souvenir met en œuvre la communication entre diverses structures mais également entre différents ensembles de cellules localisées au sein d'une même structure. La mémoire est la faculté à utiliser le passé au service du présent ou du futur (Dudai, 2004 ; Schacter, 2012). La mémoire est essentielle à notre vie quotidienne et définit qui nous sommes. Le fait qu'un souvenir persiste après une expérience vécue suggère une représentation interne de cette expérience. De plus, cela suggère que cette expérience peut être stockée et que cette représentation peut être reconstruite et utilisée. Le zoologiste et évolutionniste Richard Semon, a introduit le terme « d'engramme » pour décrire cette représentation de la mémoire (Schacter, 1982; Schacter et al., 1978). Un engramme équivaut donc à peu près à une « trace mnésique ». Par la suite, le psychologue Donald O. Hebb raffine cette théorie en proposant que l'engramme est défini par un ensemble cellulaire, l'engramme. Il émet l'hypothèse qu'un engramme se forme entre des cellules réciproquement interconnectées qui sont simultanément actives pendant une expérience. Une activité suffisante au sein de cet engramme induit une augmentation et/ou des changements métaboliques qui renforcent les connexions entre ces cellules, un concept qui se résume en une phrase : « neurons that fire together, wire together » (Hebb, 2002; Shaw, 1986).

Les engrammes peuvent également soutenir les représentations mnésiques des émotions, telles que la peur. Cette capacité a été décrite dans différentes régions corticales, dont l'amygdale et l'hippocampe (Kitamura et al., 2017). Chez les rongeurs, ce comportement de peur est classiquement étudié en effectuant un conditionnement pavlovien (stimulus conditionnant suivi d'un choc électrique) et en mesurant le comportement de freezing lors de la réexposition au stimulus. Ce comportement d'immobilité répond à un comportement de survie des rongeurs : en s'immobilisant, ils augmentent leur chance d'échapper aux prédateurs (Blanchard et al., 1986). Ce comportement résulte de l'activité synchrone complexe de différentes régions cérébrales comprenant le cortex, l'hippocampe, l'amygdale et l'hypothalamus. Malgré de nombreuses recherches sur le sujet, les processus neuronaux

soutenant l'acquisition, l'expression et l'extinction de la peur restent peu clairs, tout particulièrement vis-à-vis de l'implication de l'hypothalamus dans ces derniers.

L'hypothalamus est une structure phylogénétiquement très conservée et fortement impliquée dans la coordination des composantes autonomes et somatiques des émotions (Purves et al., 2001). Cette structure permet notamment chez les mammifères l'intégration du comportement de la peur. Il est le lieu principal de production de l'OT. Nous avons émis l'hypothèse que l'hypothalamus serait capable d'encoder des engrammes de façon similaire à ceux classiquement décrits dans les structures plus corticales.

L'amygdale centrale (CeA), est une sous-région du complexe amylagdoïde et est reconnue comme étant essentielle à la génération de l'expression de la peur. Elle entraîne des réponses physiologiques adaptées, comme le comportement de freezing observé chez les rongeurs. Cette structure est composée de plusieurs noyaux, ses sous-divisions latérale (CeL) et médiane (CeM), qui sont principalement composées de neurones inhibiteurs GABA impliqués dans l'acquisition et la réponse à la peur. L'hypothèse émise est qu'en condition basale, les neurones GABA du CeL exercent une inhibition sur les neurones à projection du CeM (également GABAergique) permettant le maintien de la mobilité de l'animal et de son comportement exploratoire. Cependant, lors du conditionnement de peur lié à un contexte, les neurones du CeL sont inhibés ce qui entraîne une élévation de l'activité des neurones du CeM, traduite par un comportement de freezing.

Les neurones ocytocinergiques de l'hypothalamus projettent au niveau du CeA et il a été montré que les neurones du CeL expriment les récepteurs à l'OT (Huber et al., 2005). La libération axonale d'OT permet l'activation des neurones GABA du CeL qui, à leur tour, inhibent les neurones GABA du CeM, entraînant une diminution du temps de freezing chez les rongeurs.

Malgré ces évidences, plusieurs questions persistent vis-à-vis du rôle de l'OT dans le CeA : Parmi tous les neurones OT, quelle proportion soutient l'effet anxiolytique ? Comment sont recrutés ces neurones lors des différents épisodes de peur ? Le circuit amygdale-hypothalamus est-il un système plastique ou figé ? La modulation de ce circuit est-il dépendant d'un contexte ou activé de manière ubiquitaire face à la peur ?

Afin de répondre à l'ensemble de ces questions, nous avons utilisé un « cocktail » viral permettant l'expression d'une protéine d'intérêt dans une population neuronale spécifique

activée pendant une courte fenêtre temporelle. Ce système est appelé vGATE pour Virus-delivered Genetic Activity-induced Tagging of Ensembles. L'utilisation de ces virus nous a ainsi permis de marquer et manipuler spécifiquement les neurones OT recrutés lors d'un épisode de peur.

b. Résultats

Dans un premier temps, il a fallu vérifier la fonctionnalité du système vGATE pour le système OT. L'utilisation de ce système permet l'expression d'un rapporteur fluorescent (Venus dans le cas présent) uniquement dans les neurones OT actifs au moment de l'injection de doxycycline (DOX). Nous avons pu montrer qu'en condition basale, en absence de stimulus, aucun neurone OT n'exprime la Venus et ce, en présence ou en absence de DOX. De plus, l'exposition des animaux à une eau de boisson hypertonique (classiquement utilisée pour induire l'activation des neurones OT et AVP), n'induit pas l'expression de Venus en absence de DOX. Cependant, la combinaison d'une eau de boisson hyperosmotique ainsi que l'administration de DOX induit une expression de Venus dans la quasi-totalité des neurones OT. Ces contrôles permettent de démontrer la fiabilité ainsi que la spécificité de ce système pour la réalisation de notre étude.

À la suite de la validation du système vGATE, nous avons exposé des rats exprimant le vGATE à un conditionnement de peur. Nous avons observé qu'environ ~10% des neurones OT du PVN et du SON ont été marqués. Nous nommerons ces neurones marqués : neurones OT Fear+. Nous avons ensuite induit l'expression de la ChR2 (chanel rhodopsine excitatrice) dans tous les neurones OT, afin de stimuler leurs axones au niveau du CeL et de confirmer que la stimulation des fibres OT au niveau du CeL permet bien de diminuer la réponse de freezing. De manière surprenante, nous avons constaté que la réexposition au contexte de peur induit un effet plus robuste que la première fois. Par ailleurs, si seuls les neurones OT Fear+ sont activés, la latence observée entre la stimulation lumineuse et la diminution du temps de freezing est significativement diminuée. Cela pourrait traduire que la réexposition à un même contexte permet le recrutement d'un plus grand nombre de neurones OT tandis que le système vGATE permet de recruter un ensemble de neurone spécialisés capable d'induire une réponse plus efficace.

Nous nous sommes ensuite intéressés à une plasticité possible du système ocytocinergique à la suite d'un conditionnement de peur. Pour cela, nous avons réalisé des marquages neuroanatomiques de neurones OT et de leurs axones, afin de déterminer l'impact du conditionnement sur la modification de la longueur totale des axones OT au niveau du CeL. Nous avons pu voir que le transporteur vGluT2 semble surexprimé dans les axones OT à la suite du conditionnement de peur. Nous avons alors cherché à déterminer les conséquences fonctionnelles d'un tel changement en réalisant une étude ex vivo combinant des enregistrements électrophysiologiques et optogénétiques. La stimulation des axones OT entraîne une augmentation de la fréquence des courants post-synaptiques inhibiteurs (IPSCs) des neurones du CeM dans l'intégralité des groupes (contrôle et exposé à un conditionnement de peur vGATE). L'utilisation d'un antagoniste spécifique des OTR a permis de mettre en évidence que celui-ci est capable de bloquer la réponse induite par la stimulation optogénétique des fibres OT chez les animaux contrôles mais il présente un effet moindre chez les animaux vGATE. De plus, l'utilisation d'un antagoniste glutamatergique inhibe la réponse chez les animaux vGATE mais l'effet est minime chez les animaux contrôles. De manière à compléter cette observation et à tester la pertinence de ces résultats in vivo, nous avons réalisé l'implantation de fibres optiques de manière à stimuler la libération d'OT, et induire une diminution du freezing. Nous avons pu montrer que cette réponse était bloquée par l'injection intra-CeL d'un antagoniste OTR. Par ailleurs, lors de la réexposition deux semaines plus tard d'un même animal à un deuxième épisode de peur, l'injection de l'antagoniste des OTR ne semble plus présenter d'effet sur le comportement de freezing. L'ensemble de ces résultats neuroanatomiques, fonctionnels et comportementaux semblent supporter l'hypothèse qu'un conditionnement à la peur induit un « switch » entre la libération initiale d'OT et la libération de glutamate.

De manière à fournir une preuve supplémentaire que les neurones OT Fear+ atténuent l'expression de la peur, nous avons émis l'hypothèse que l'inhibition des neurones OT des animaux vGATE inhibe l'extinction de la peur, spécifiquement dans le contexte où ces neurones ont été activés. Pour cela, nous avons fait exprimer le récepteur muscarinique humain modifié hM4D (Gi) sous le contrôle du promoteur OT à des animaux que nous avons par la suite soumis à des paradigmes de conditionnement et d'extinction de la peur contextuelle. Afin d'observer uniquement le rôle potentiel de l'OT dans l'extinction de la peur associé à un contexte, nous

avons introduit un nouveau contexte (contexte B). L'administration de clozapine-N-oxyde (CNO) permettant l'activation des hM4D, et par conséquence une inhibition des neurones OT exprimant ce récepteur, entraîne une augmentation du temps de freezing et cela de manière dépendante au contexte. En utilisant ce système de vGATE modifié, permettant d'exprimer spécifiquement les hM4D dans les neurones Fear nous avons pu montrer que l'inhibition de ces neurones marqués dans le contexte A empêchent l'extinction de la peur dans le même contexte, mais leur activation demeure inefficace lors d'une exposition à un contexte différent (contexte B). Ces résultats démontrent que la modulation effectuée par les neurones OT est dépendante du contexte.

Le marquage neuroanatomique des neurones OT a mis en évidence un très faible nombre de fibres ocytocinergiques au niveau de l'amygdale. Nous avons par conséquence cherché à déterminer si une ou plusieurs populations de neurones OT était recrutée de manière spécifique lors d'un second épisode de peur. Pour ce faire, nous avons exposé les animaux à deux conditionnements, en utilisant soit un contexte identique (A-A), soit un contexte différent (A-B). Nous avons pu démontrer qu'une seconde exposition à un contexte similaire réactive spécifiquement les neurones OT préalablement activés du SON, alors qu'au niveau du PVN, ce sont majoritairement des neurones nouvellement recrutés, quand bien même le nombre total de neurones OT recrutés est identique dans les deux cas. Par ailleurs, un second conditionnement de peur dans un nouveau contexte induit une activation du système ocytocinergique bien plus importante aussi bien au sein du PVN que du SON, traduite par une forte élévation de la concentration d'OT plasmatique. En prenant en considération les deux types de neurones OT, les magnOT et les parvOT, nous avons cherché à déterminer si le recrutement de ces populations de neurones OT diffère au cours de l'exposition répétée à un contexte identique et différent. Pour ce faire, nous avons injecté un traceur rétrograde en systémique de manière à marquer spécifiquement les neurones. Nous avons démontré ainsi qu'environ ~15% des neurones magnOT sont réactivés lors d'un second conditionnement de peur que ce soit au niveau du PVN que du SON, alors que les neurones parvOT sont tous réactivés ~98%.

c. Contribution personnelle

Cette étude a évidemment été un travail collaboratif entre de nombreuses personnes. J'ai pour ma part contribué à l'étude comportementale, depuis les chirurgies jusqu'à l'analyse des résultats.

Article

Neuron

A Fear Memory Engram and Its Plasticity in the Hypothalamic Oxytocin System

Highlights

- A novel method, vGATE, selectively tagged fear-activated oxytocin (OT) neurons
- A subset of tagged OT neurons encodes for context-specific memory engram
- Fear learning induces long-term plasticity in OT neurons
- vGATE-tagged OT neurons predominantly operate by glutamate

Authors

Mazahir T. Hasan, Ferdinand Althammer, Miriam Silva da Gouveia, Stephanie Goyon, ..., Alexandre Charlet, Valery Grinevich

Correspondence

mazahir.t.hasan@gmail.com (M.T.H.), acharlet@unistra.fr (A.C.), v.grinevich@dkfz-heidelberg.de (V.G.)

In Brief

Hasan et al. developed a novel genetic method, vGATE, to tag a context-specific fear memory engram in the hypothalamic oxytocin system that participates in rapid unfreezing, extinction, and enhanced glutamatergic transmission.

Hasan et al., 2019, Neuron *103*, 133–146
July 3, 2019
https://doi.org/10.1016/j.neuron.2019.04.029

CellPress

Neuron
Article

A Fear Memory Engram and Its Plasticity in the Hypothalamic Oxytocin System

Mazahir T. Hasan,[1,2,3,4,14,15,*] Ferdinand Althammer,[5,14] Miriam Silva da Gouveia,[5,14] Stephanie Goyon,[6,14] Marina Eliava,[5] Arthur Lefevre,[5] Damien Kerspern,[6] Jonas Schimmer,[5] Androniki Raftogianni,[5] Jerome Wahis,[6] H. Sophie Knobloch-Bollmann,[5,16] Yan Tang,[5] Xinying Liu,[5] Apar Jain,[5] Virginie Chavant,[6] Yannick Goumon,[6] Jan-Marek Weislogel,[7,17] René Hurlemann,[8] Sabine C. Herpertz,[9] Claudia Pitzer,[10] Pascal Darbon,[6] Godwin K. Dogbevia,[4,18] Ilaria Bertocchi,[4,11,19] Matthew E. Larkum,[3] Rolf Sprengel,[4,11] Hilmar Bading,[7] Alexandre Charlet,[6,12,15,*] and Valery Grinevich[5,13,15,20,*]

[1]Laboratory of Memory Circuits, Achucarro Basque Center for Neuroscience, Science Park of the UPV/EHU, Sede Building, Barrio Sarriena, 48940 Leioa, Spain
[2]Ikerbasque–Basque Foundation for Science, 48013 Bilbao, Spain
[3]Neurocure, Charité-Universitätsmedizin, Virchowweg 6, 10117 Berlin, Germany
[4]Max Planck Institute for Medical Research, Jahnstrasse 29, 69120 Heidelberg, Germany
[5]Schaller Research Group on Neuropeptides, German Cancer Research Center, Im Neuenheimer Feld 307, 69120 Heidelberg, Germany
[6]Centre National de la Recherche Scientifique and University of Strasbourg, Institute of Cellular and Integrative Neurosciences, 8 Allée du Général Rouvillois, 67000 Strasbourg, France
[7]Department of Neurobiology, Heidelberg University, Im Neuenheimer Feld 364, 69120 Heidelberg, Germany
[8]Department of Psychiatry and Division of Medical Psychology, University of Bonn Medical Center, Sigmund-Freud-Strasse 25, 53105 Bonn, Germany
[9]Department of General Psychiatry, Center of Psychosocial Medicine, Heidelberg University, Voßstraße 4, 69115 Heidelberg, Germany
[10]Interdisciplinary Neurobehavioral Core (INBC), Heidelberg University, Im Neuenheimer Feld 515, 69120 Heidelberg, Germany
[11]Max Planck Research Group at the Institute for Anatomy and Cell Biology, Heidelberg University, Im Neuenheimer Feld 307, 69120 Heidelberg, Germany
[12]University of Strasbourg Institute for Advanced Study (USIAS), Strasbourg, France
[13]Department of Neuropeptide Research for Psychiatry, Central Institute of Mental Health, Heidelberg University, J5, 68159 Mannheim, Germany
[14]These authors contributed equally
[15]Senior author
[16]Present address: Institute of Physiology, University of Freiburg, Hermann-Herder-Strasse 7, 79104 Freiburg, Germany
[17]Present address: BioNTech AG, An der Goldgrube 12, 55131 Mainz, Germany
[18]Present address: Division of Cardiac Surgery, University of Ottawa Heart Institute, Ottawa, ON K1Y 4W7, Canada
[19]Present address: Neuroscience Institute Cavalieri-Ottolenghi, University of Turin, Regione Gonzole 10, 10043 Orbassano, Turin, Italy
[20]Lead Contact
*Correspondence: mazahir.t.hasan@gmail.com (M.T.H.), acharlet@unistra.fr (A.C.), v.grinevich@dkfz-heidelberg.de (V.G.)
https://doi.org/10.1016/j.neuron.2019.04.029

SUMMARY

Oxytocin (OT) release by axonal terminals onto the central nucleus of the amygdala exerts anxiolysis. To investigate which subpopulation of OT neurons contributes to this effect, we developed a novel method: virus-delivered genetic activity-induced tagging of cell ensembles (vGATE). With the vGATE method, we identified and permanently tagged a small subpopulation of OT cells, which, by optogenetic stimulation, strongly attenuated contextual fear-induced freezing, and pharmacogenetic silencing of tagged OT neurons impaired context-specific fear extinction, demonstrating that the tagged OT neurons are sufficient and necessary, respectively, to control contextual fear. Intriguingly, OT cell terminals of fear-experienced rats displayed enhanced glutamate release in the amygdala. Furthermore, rats exposed to another round of fear conditioning displayed 5-fold more activated magnocellular OT neurons in a novel environment than a familiar one, possibly for a generalized fear response. Thus, our results provide first evidence that hypothalamic OT neurons represent a fear memory engram.

INTRODUCTION

Emotional memory representations (also called memory engrams), such as for fear, are pivotal for animal survival. Fear-associated behaviors have evolved over millions of years in living systems, from lower to higher animals, so that they can sense, evaluate, respond, and adapt to adequately deal with dangerous situations (Mobbs et al., 2015). Fear-related disorders, such as specific phobias and post-traumatic stress disorder (PTSD), are among the most prevalent human psychiatric conditions and pose debilitating health burdens to affected individuals and immense costs to society (Kessler and Bromet, 2013). Understanding the neural basis of fear learning, expression,

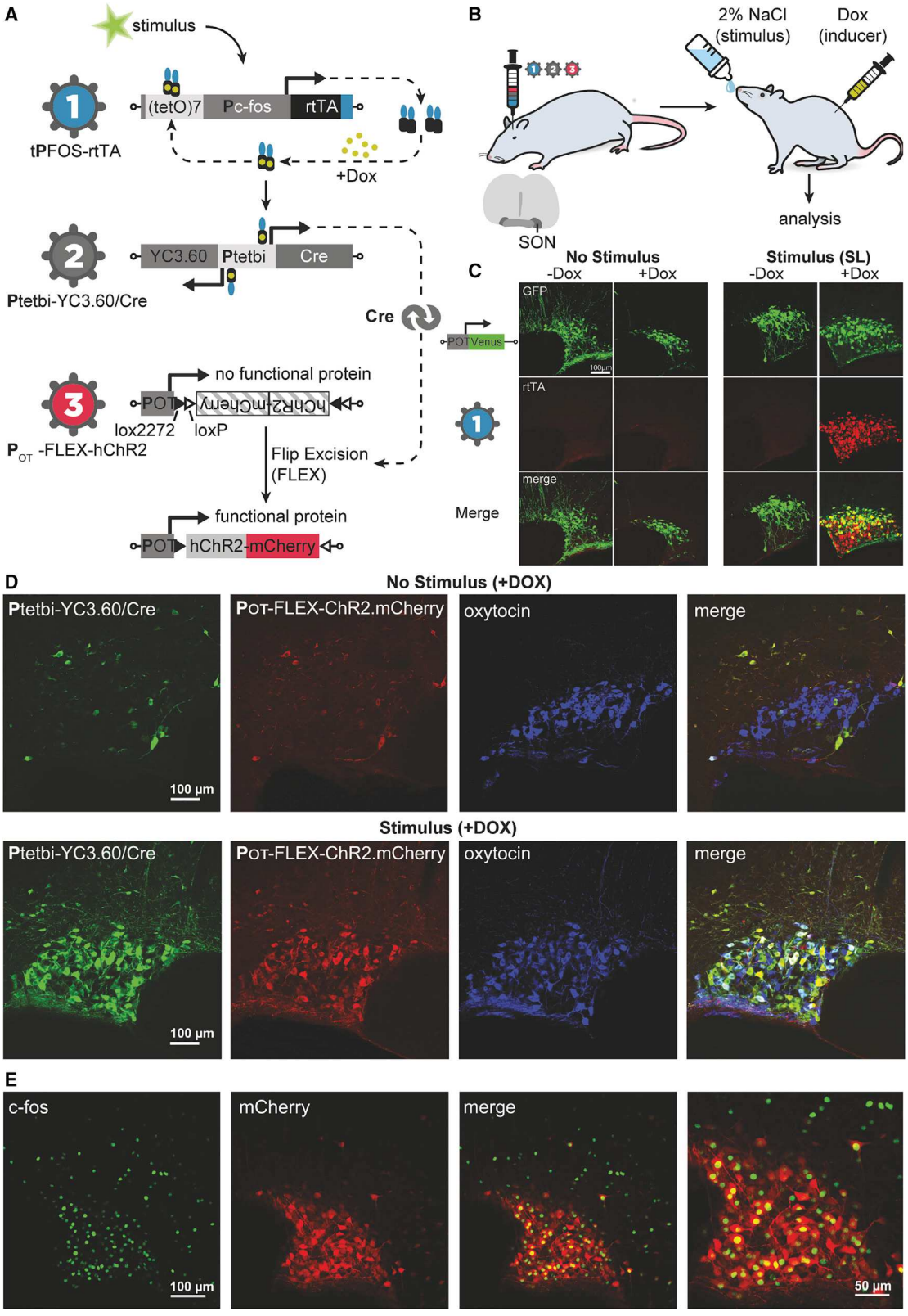

(legend on next page)

and extinction is of paramount importance for PTSD treatment; for example, by targeted circuit-specific therapeutics.

The hypothalamus is an evolutionary old and deeply located brain structure that relays fear-related emotional behavior in mammals. Fear memory engrams are thought to be distributed between the different brain regions in the nervous system; for example, the amygdala, hippocampus, and medial prefrontal cortex (mPFC) (Kitamura et al., 2017). Notably, the hypothalamus is reciprocally connected to different brain regions, including the amygdala (Knobloch et al., 2012) and the mPFC (Heidbreder and Groenewegen, 2003), which, in turn, interact with various other brain regions when organizing fear memories (Tovote et al., 2015). These findings support the view that brain networks, composed of distributed cell assemblies, generate behavior, including the formation of memory representations or engrams. We thus hypothesized that the hypothalamus, being the oldest brain structure, which evolved over time alongside the newer higher brain structures, might be equipped with mechanisms to encode engram-like features and capable of plasticity.

The central nucleus (CeA), a subregion of the amygdala, participates in the acquisition, consolidation, storage, expression, and extinction of fear memories (Ciocchi et al., 2010; Herry et al., 2010; Letzkus et al., 2011) and the subsequent physiological response: freezing behavior (Viviani et al., 2011). Hypothalamic oxytocin (OT) neurons precisely project to the lateral part of the CeA (CeL), where axonal OT release activates CeL neurons (Knobloch et al., 2012), which, in turn, inhibit GABAergic neurons in the medial part of the CeA (CeM), attenuating the fear-related freezing response in rodents. However, the precise role of OT neurons and their projections to the CeA during fear learning is still not well understood. It is unknown which fraction of OT neurons contributes to the anxiolytic effect, how OT neurons are recruited during different fear episodes, and whether the hypothalamus-amygdala circuit is subject to fear-dependent plasticity and contextual specificity.

To tackle these questions, we developed a novel genetic method, virus-delivered genetic activity-induced tagging of cell ensembles (vGATE), to tag fear-experience-activated OT neurons in rats during contextual fear conditioning (FC) (Ehrlich et al., 2009; LeDoux, 2007). Here we provide first evidence that establishes the role of OT neuronal ensembles in fear expression and extinction. We discovered that optogenetic activation of a small subset of fear exposure-activated OT neurons drastically reversed freezing behavior (“unfreezing”) and their silencing impaired context-specific fear extinction. Importantly, fear exposure-tagged OT neurons display an enormous capacity for experience-dependent plasticity by enhancing glutamatergic over OT-ergic transmission in the hypothalamic-amygdalar circuitry. These results clearly demonstrate that fear exposure-tagged OT neurons are both sufficient and necessary for attenuation of fear expression. Altogether, these results satisfy the key criteria of the synaptic plasticity memory hypothesis (Martin et al., 2000) in identifying and validating a fear memory engram in hypothalamic OT circuits. Thus, we conclude that memory engrams are not only restricted to higher brain regions, such as the hippocampus and cortex, but also present in a lower brain region, such as the hypothalamus. This study is a shift in paradigm, revealing the anatomical and functional connectivity organization of fear memory engrams as network-wide distributed cell assemblies that include both higher and lower brain regions.

RESULTS

Activity-Dependent Tagging of OT Neurons

To specifically label activated OT neurons, we developed and describe here a genetic method called vGATE (Figure 1A). In the vGATE system, a c-*fos* promoter ($\mathbf{P}_{fos}$) fragment (Schilling et al., 1991) drives the expression of the reverse tetracycline-sensitive (tet) transactivator (rtTA) (Dogbevia et al., 2015, 2016). In activated neurons, stimulation of the c-*fos* promoter rapidly induces rtTA expression. To obtain sustained rtTA expression for permanent tagging of c-*fos* activated neurons, we designed an autoregulatory expression loop by introducing rtTA-binding DNA sequences (tet operator sequences [$(tetO)_7$]) upstream of $\mathbf{P}_{fos}$ to drive rtTA expression (the full genetic module is $(tetO)_7$-$\mathbf{P}_{fos}$-rtTA). In the presence of doxycycline (Dox), transient $\mathbf{P}_{fos}$ activity drives rtTA expression, which, upon binding to $(tetO)_7$, takes over the transient c-*fos* promoter activity by establishing a Dox-controlled rtTA-dependent and self-sustaining autoregulatory loop (Figure 1A) for persistent rtTA expression. A second virus (virus 2) is equipped with a bidirectional tet promoter ($\mathbf{P}_{tet}$bi) that drives the expression of genes encoding for the Cre recombinase and fluorescent proteins (Figure 1A). Finally, a third virus (virus 3) is equipped with a cell-type-specific promoter (OT in our case) that drives Cre-dependent expression of any gene(s) (Figure 1A).

vGATE-Assisted, Dox-Dependent rtTA Expression *In Vivo*

As a proof of principle, we first validated the vGATE method *in vitro* (Figures S1A–S1D) and, subsequently, *in vivo*. For *in vivo* validation, we injected the vGATE construct rAAV-$(tetO)_7$-$\mathbf{P}_{fos}$-rtTA into the supraoptic nucleus (SON) of the hypothalamus. Three weeks later, rats were treated under four different

Figure 1. Operating Principle of the vGATE System and Activity-Dependent Tagging of OT Neurons

(A) Scheme of the vGATE system: virus 1 (rAAV-$(tetO)_7$-$\mathbf{P}_{fos}$-rtTA), virus 2 (rAAV-$\mathbf{P}_{tet}$bi-Cre/YC3.60), and virus 3 (rAAV-$\mathbf{P}_{OT}$-FLEX-hChR2-mCherry).

(B) Rats were injected with vGATE viral cocktail (3 viruses) into the hypothalamic SON and treated with Dox in combination with osmotic stimulation (salt loading).

(C) Dox-dependent rtTA expression is only detected in the stimulus + Dox group. To verify correct viral targeting of the SON, the rAAV-$(tetO)_7$-$\mathbf{P}_{fos}$-rtTA virus was mixed 1:1 with an rAAV expressing Venus under control of the oxytocin promoter (rAAV-$\mathbf{P}_{OT}$-Venus; Knobloch et al., 2012).

(D) In euhydrated rats (basal, top panel), Dox injection induces rtTA-dependent YC3.60 (via virus 2, green) and Cre-dependent ChR2-mCherry (via virus 3, red) signals in a few scattered neurons. In contrast, both signals were detected in the majority of SON OT neurons (blue) after Dox injection to osmotically challenged, salt-loaded rats (stimulated, bottom panel).

(E) Expression of the endogenous c-*fos* signal (visualized via immunohistochemistry, green) overlays vGATE-assisted the ChR2-mCherry signal (red) in virtually all SON OT neurons of Dox-treated, osmotically challenged rats.

conditions: ± Dox and with or without salt loading (SL), which induced robust c-*fos* expression in OT neurons (Katoh et al., 2010; Figures 1B and 1C; Table S1). Only under the +Dox/+SL condition, robust rtTA expression under a synthetic c-*fos* promoter was detected (red) within 24 h in roughly all of the OT neurons (Hamamura et al., 1991; Figure 1C). This result shows that the vGATE method is compatible with endogenous c-*fos* expression. With rAAV-$\mathbf{P}_{OT}$-Venus as a tracer, it was possible to verify proper virus targeting and spread of infection after injection.

In a different set of experiments, we injected a cocktail of three viruses called OT^{vGATE}: (virus 1, rAAV-$(tetO)_7$-$\mathbf{P}_{fos}$-rtTA; virus 2, rAAV-$\mathbf{P}_{tet}$bi-Cre/YC3.60; virus 3, rAAV-$\mathbf{P}_{OT}$-FLEX-humanized channel rhodopsin (hChR2)-mCherry) and analyzed for YC3.60 (virus 2) and hChR2-mCherry (virus 3). Under +SL/+Dox robust YC3.60 ($\mathbf{P}_{tet}$bi-Cre/YC3.60) and hChR2-mCherry (Cre-dependent, $\mathbf{P}_{OT}$-FLEX-hChR2-mCherry) immunosignals were co-localized in the majority of OT neurons (96.30% ± 1.88% SON, 97.22% ± 2.66% paraventricular nucleus (PVN); Figure 1D). In these animals, we found that 2.4% ± 1.1% (48 of 2,011) of the YC3.60/hChR2-mCherry-expressing cells in the PVN and 5.7% ± 1.4% (132 of 2,320) of cells in the SON were non-OTergic (n = 6 animals). Under the +Dox /−SL (Figure 1D) condition, we found that 7.3% ± 2.2% YC3.60/hChR2-mCherry-positive cells around the SON were non-OTergic (179 of 2,450 neurons) and that 0.8% ± 0.5% YC3.60/hChR2-mCherry-positive cells around the PVN were non-OTergic (22 of 2,450 neurons, n = 6; n = animal number, 6 sections per animal). These unidentified YC3.60/hChR2-mCherry-positive cells were within a radius of 400 μm from the border of the respective nucleus. Under −SL/−Dox conditions (Figure S1E), we observed virtually no YC3.60 and mCherry labeling (0.1% ± 0.03%, 5 of 540 for the PVN; 0.3% ± 0.09%, 22 of 722 for the SON; n = 6, 6 sections per animal), a result of minimal leakiness of the $\mathbf{P}_{tet}$bi. Furthermore, we observed more than 93% (94.74% ± 1.75% for the SON and 93.56% ± 2.46% for the PVN; Table S1) co-localization of endogenous c-*fos* and mCherry in vGATE animals subjected to SL for 5 consecutive days (Figure 1E).

Optogenetic Stimulation of Tagged OT Neurons Reverses Freezing Behavior in Fear-Conditioned Rats

We investigated what fraction of the entire OT population actually contributes to the anxiolytic effect and how OT neurons are recruited during the expression of fear using contextual FC in rats (Figure 2A). We found that only a small number of OT neurons in the SON and PVN expressed c-*fos* during fear exposure (Figures S2A and S2B). Next we generated OT^{vGATE} rats with bilateral injections of the vGATE viral cocktail to permanently tag activated OT neurons in the SON and PVN for activity manipulation by hChR2 (virus 1, rAAV-$(tetO)_7$-$\mathbf{P}_{fos}$-rtTA; virus 2, rAAV-$\mathbf{P}_{tet}$bi-Cre/YC3.60; virus 3, rAAV-$\mathbf{P}_{OT}$-FLEX-hChR2-mCherry) (OT^{vGATE}). We specifically chose day 3 for the Dox injection because we wanted to exclusively label fear-activated OT neurons but not pain-sensitive OT neurons. As a control, we generated rats that constitutively expressed rAAV-delivered hChR2 in all OT neurons ($OT^{Constitutive}$) in the SON and PVN. Although the $OT^{Constitutive}$ group displayed viral expression in virtually all OT neurons (99.4% ± 0.8%, n = 4; Figure 2B1), in the OT^{vGATE} group, only a small fraction of the OT neurons was tagged during fear expression (341 of 2,470, 13.8% ± 0.7% of OT neurons in the SON and 331 of 2,666, 12.4% ± 1.6% of OT neurons in the PVN) of ~6,600 cells comprising the PVN and SON in rats (Althammer and Grinevich, 2017; Figure 2B2; Table S2). We found that only 1.2% of non-OTergic cells were labeled non-specifically (57 cells of 2,051 cells in total labeled via vGATE, PVN/SON combined, n = 4, 6 sections per animal) in the fear-conditioned animals (Figure S2C). To determine whether OT^{vGATE} neurons project axons terminating within the CeA subregion of the amygdala, we analyzed brain slices containing the CeL and found mCherry-positive fibers in the CeL that were also OT-immuno-positive (Figure 2B2). Optogenetic stimulation of these OT axons in the CeL with blue light (BL) induced a prominent decrease in the freezing response (unfreezing) in both groups. Surprisingly, the BL-evoked unfreezing effect in the OT^{vGATE} group was much stronger (freezing time, 6.9 ± 1.1 s versus 38.1 ± 7.6 s, $p < 0.0001$; Figure 2C2) and occurred faster (onset, 3.8 ± 0.7 s versus 25.9 ± 10.8 s, $p < 0.0001$; Figure 2D) than in the $OT^{Constitutive}$ group (Figures 2C1 and 2D). To rule out that the observed behavioral changes were mediated by brain regions other than the CeA, we injected 4 animals with rAAV-$(tetO)_7$-$\mathbf{P}_{fos}$-rtTA, rAAV-$\mathbf{P}_{tet}$bi-Cre/YC3.60, and rAAV-$\mathbf{P}_{OT}$-FLEX-GFP. Four animals injected with rAAV-$\mathbf{P}_{OT}$-Venus served as a control. We analyzed the brains of the vGATE-injected animals and did not find any GFP-positive fibers outside of the CeA, whereas control animals showed prominent labeling of OT fibers in various brain regions, as reported previously (Figure S2D; Knobloch et al., 2012). This indicates that fear-activated, vGATE-labeled OT neurons project exclusively to the CeA. In addition, we did not find a single mCherry-positive fiber in the CeA that was negative for OT immunoreactivity (n = 6 animals, 6 sections per animal, in which more than 15 mm of total axon length was analyzed), indicating that axonal projections from vGATE-labeled axons exclusively represent OT fibers. Conversely, we found no difference between $OT^{Constitutive}$ (98.2% ± 1.4%, n = 6) and OT^{vGATE} (96.9% ± 2.1%, n = 6) groups regarding the labeling of OT-positive fibers in the CeL, indicating that all OT neurons projecting to the CeL are fear-sensitive. Next, to provide additional proof that OT^{vGATE} neurons precisely project to the CeA, we injected green Retrobeads into the CeA of rats with OT^{vGATE} neurons labeled by mCherry. The anatomical analysis revealed that 94.6% ± 3.1% of mCherry-positive OT neurons (1,337 OT^{vGATE} neurons, PVN/SON combined, n = 4) contained green Retrobeads (Figure S2E), indicating that the vast majority of OT^{vGATE} neurons project to the CeA.

Because our FC paradigm comprised an additional shock session (day 14, memory reinforcement) to achieve higher basal freezing rates, we wanted to rule out the possibility that this session leads to recruitment of new OT cells. Therefore, we performed another experiment in which animals were injected with rAAV-$(tetO)_7$-$\mathbf{P}_{fos}$-rtTA and rAAV-$\mathbf{P}_{tet}$bi-Cre/YC3.60 and subjected to our FC paradigm (day 3 Dox injection, day 4 shock; Figure S2F). On day 14, animals received an injection of rAAV-$\mathbf{P}_{OT}$-FLEX-hChr2-mCherry and were subjected to another round of FC 2 weeks later. Then one group received another Dox injection, and the control group was injected with saline one day prior to the additional shock session on day 29 (Figure S2F). Although

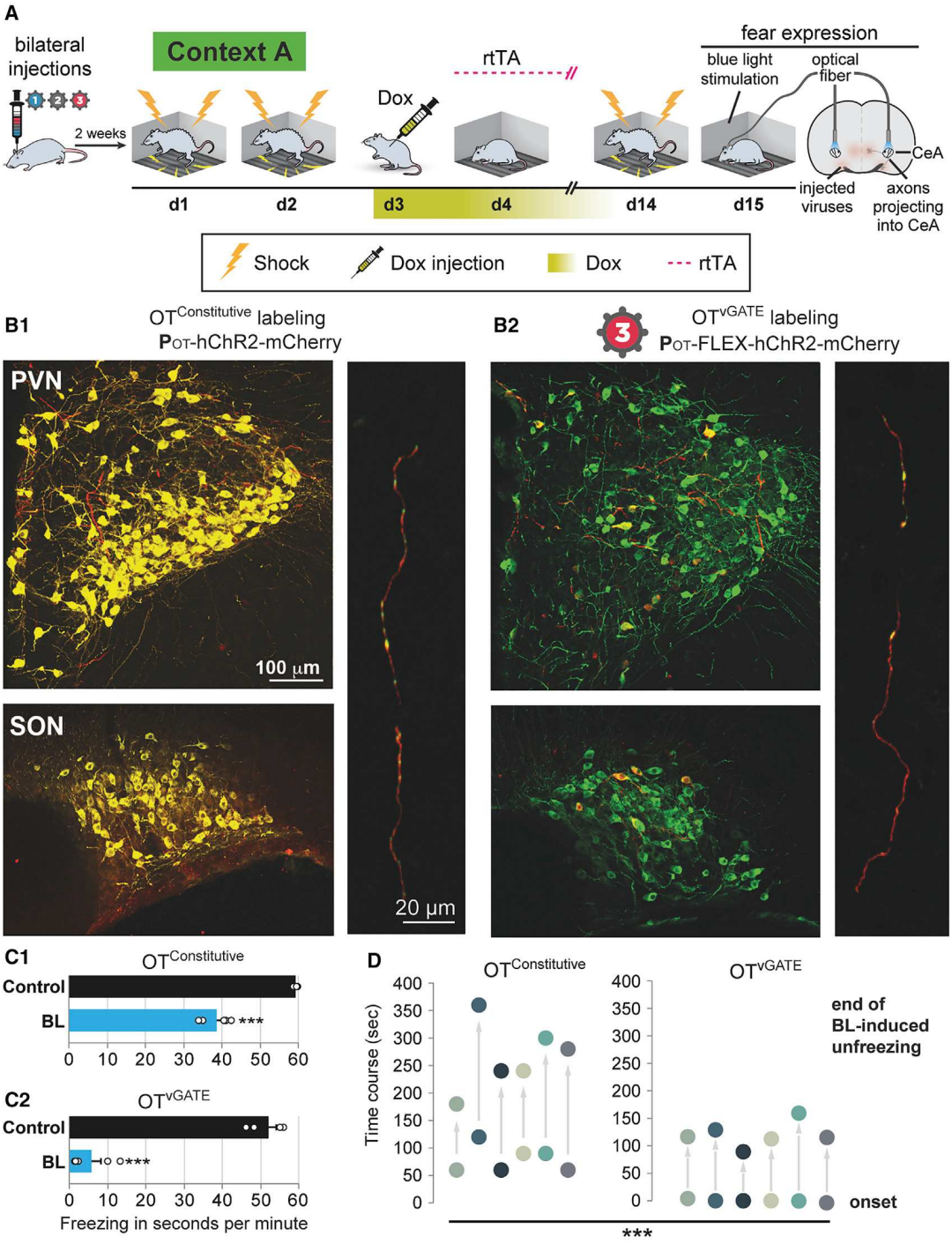

Figure 2. Fear Learning and Optogenetic Control of Fear Behavior

(A) Scheme of the fear condition setup, Dox administration, and blue light stimulation of the CeA.

(B) The vast majority of OT neurons (99.4% ± 0.8%, green) of the PVN and SON were labeled via a constitutive OT promoter driving hChR2-mCherry (B1, red). (B2) Fear expression induced tagging (ChR2-mCherry, red) of a small population of OT neurons (green). (B1 and B2) Vertical panels depict ChR2-mCherry-containing axons (red) with OT-immunopositive puncta (green, appearing in yellow) in the CeL of both groups.

(C) The freezing time before and after blue light illumination of the CeA (C1, top graph: constitutive hChR2 expression, $OT^{Constitutive}$ group; C2, bottom graph: OT^{vGATE} group). The black bars (control) show the freezing time immediately prior to BL stimulation, whereas the blue bars (BL) indicate the freezing time after BL stimulation. ***$p < 0.001$, t test.

(D) The onset and duration of the BL-induced unfreezing effect. Data are presented as mean ± SEM.

the group that was injected with Dox twice displayed normal labeling (224 of 2,033, 11% ± 1.4% for the PVN; 260 of 1,940, 13.4% ± 1.7% for the SON; n = 5; Figure S2G) of OT neurons, we only found a total of 11 mCherry-positive cells in the PVN (11 of 2,020, 0.5%, n = 5) and 17 mCherry-positive cells in the SON (17 of 2,177, 0.8%, n = 5) in the group receiving saline in the first round (Figure S2G). Thus, this experiment demonstrates that, after Dox has been cleared from the brain, only few additional OT cells get labeled. To verify that the comparable labeling of cells also held true on the axonal level, we compared OT-positive fibers within the CeA of animals perfused after 14 days with animals perfused after 43 days (2 weeks after the day 29 shock session; Figure S2F) and found no difference in vGATE-mediated labeling (day 14: 96.9% ± 2.1%, n = 6; day 43: 95.3% ± 3.1%, n = 6).

Because a recent study highlighted the existence of freezing-promoting (somatostatin-ergic) and flight-promoting (corticotropin-releasing hormone-ergic) neurons (Fadok et al., 2017), we sought to find out which cell types within the CeL are activated upon BL stimulation. Therefore, we injected rats with our vGATE viruses (rAAV-$(tetO)_7$-$\mathbf{P}_{fos}$-rtTA and rAAV-$\mathbf{P}_{tet}$bi-Cre/YC3.60) and either rAAV-$\mathbf{P}_{OT}$-FLEX-Venus (n = 4) or rAAV-$\mathbf{P}_{OT}$-FLEX-hChr2-mCherry (n = 4) and subjected them to our FC protocol (Figure 2A). On day 15, we illuminated the CeL for 2 min and sacrificed animals 90 min later. We found that fear exposure itself did not cause c-*fos* expression in the CeL, whereas BL stimulation robustly induced c-*fos* in this structure. In the BL-stimulated animals, we counted 888 corticotropin-releasing hormone (CRH)-positive neurons and 290 SOM-positive neurons, whereas 104 neurons expressed both markers. 84% ± 3.6% of exclusively SOM-positive neurons, 11% ± 0.9% of exclusively CRH-positive neurons, and 58% ± 4.3% of the mixed population expressed c-*fos* (Figure S2H). Thus, these findings suggest that OT release in the CeL predominantly activates SOM-positive interneurons.

Fear-Experience-Dependent Anatomical and Functional Plasticity of Hypothalamic OT Neurons Projecting to the CeA

To investigate potential anatomical and molecular changes following fear experience, we generated OT^{vGATE} rats (virus 3, rAAV-$\mathbf{P}_{OT}$-FLEX-GFP) and quantitatively analyzed OT axons within the CeL. In parallel, we analyzed fear-naive rats expressing $\mathbf{P}_{OT}$-Venus for constitutive labeling of all OT neurons ($OT^{Constitutive}$; Figure 3A1). Although the total length of axonal segments was similar in both groups (Figure 3A3), there was a substantial increase (~3-fold) in the numbers of GFP-positive axonal varicosities containing immunosignals of vesicular glutamate transporter 2 (vGluT2) in the OT^{vGATE} group (Figure 3A3; Table S3). Furthermore, we found that the detectable OT levels in vGATE fibers were at least 3-fold lower compared with the fear-naive animals injected with $\mathbf{P}_{OT}$-Venus, potentially resulting from the enhanced glutamate expression (fear-naïve, 58.0% ± 8.4%; fear-experienced, 15.3% ± 3.1%; signal intensity, n = 4; 6 sections per animal; Figure S3A).

To elucidate the seemingly counter-intuitive observation that activation of a small subset of OT neurons resulted in a stronger behavioral response than activation of axons originating from virtually all OT neurons ($OT^{Constitutive}$ group) in the CeL, we next aimed to investigate the underlying circuitry within the CeA by *ex vivo* electrophysiology in acute brain slices from fear-naive $OT^{Constitutive}$ and fear-experienced OT^{vGATE} groups (Figure 2D). In the naive group, all OT neurons constitutively expressed hChR2 ($OT^{Constitutive}$), whereas in the OT^{vGATE} group, a small fraction of OT neurons was labeled with the vGATE virus cocktail (virus 3, $\mathbf{P}_{OT}$-FLEX-hChr2-mCherry). In both groups, BL stimulation of OT axons in the CeL (Figure 3B) induced an increase in inhibitory postsynaptic current (IPSC) frequencies in neurons of the CeM, which receive direct synaptic input from GABAergic neurons of the CeL (Figure 3C1). Interestingly, the BL-induced increase in CeM IPSC frequencies in the OT^{vGATE} group was almost entirely blocked by the glutamate AMPA receptor antagonist NBQX, whereas it only had a minor effect on the control group (Figure 3C2). On the other hand, the application of the OT receptor antagonist dOVT diminished the BL-induced increase in CeM IPSCs in the OT^{vGATE} group by only 50%, whereas it prevented the increase in CeM IPSCs in the control $OT^{Constitutive}$ group entirely (Figure 3C2).

To rule out that the observed differences were not a result of the fear experience, we injected an additional group of animals with rAAV-$\mathbf{P}_{OT}$-hChR2-mCherry ($OT^{Constitutive}$) and subjected them to the same paradigm as the OT^{vGATE} group (Figure 2A; Figure S3B1). Analysis of the fear-conditioned $OT^{Constitutive}$ group revealed that the BL-induced unfreezing effect, onset, and duration of mobility time (Figures S3B2–S3B4) as well as the effects of NBQX and dOVT on IPSC frequencies in CeM neurons (Figures S3B5–S3B7) were comparable with those observed in the OT^{vGATE} group (Figures 2C, 2D, 3C1, and 3C2). These findings suggest that the initial exposure to FC induced plastic changes in OT neurons, resulting in prevalent release of glutamate from their axonal terminals within the CeL. Because of the similarity of behavioral and amygdala responses to OT axon stimulation in fear-experienced $OT^{Constitutive}$ and OT^{vGATE} groups, the observed effects might stem from the same population of OT neurons naturally activated in both groups of rats during fear expression (Figure 2B).

To test whether the *ex vivo* findings have a functional relevance *in vivo*, we blocked the OT receptor specifically with an antagonist (OTA, L-368,899, 1 mg/kg intraperitoneally [i.p.]) that crosses the blood-brain barrier (Eliava et al., 2016). First, we injected rats bilaterally in the SON and PVN with $\mathbf{P}_{OT}$-hChR2-mCherry ($OT^{Constitutive}$) for optogenetic tagging and implanted optic fibers into the CeA (Figure 3D1). Next we subjected the animals to the FC paradigm. On day 3, treatment of the animals with OTA 40 min prior to BL stimulation (session 1, OTA + BL1) completely prevented the BL-induced unfreezing effect (Figure 3D2). However, 2 weeks later, when we exposed the very same animals to the second session of FC (session 2, OTA + BL2), the animals displayed a rapid BL-induced unfreezing response despite prior application of OTA (Figure 3D3). Interestingly, the onset of BL-induced unfreezing occurred much faster (6 ± 0.8 s versus 25.9 ± 10.8 s, $p < 0.0001$; Figure 3D4) than in the fear-naive $OT^{Constitutive}$ group (Figure 2D). To exclude that the observed unfreezing effects were a result of OTA-induced changes in plasticity originating from the first round of FC, we processed an additional group of animals constitutively

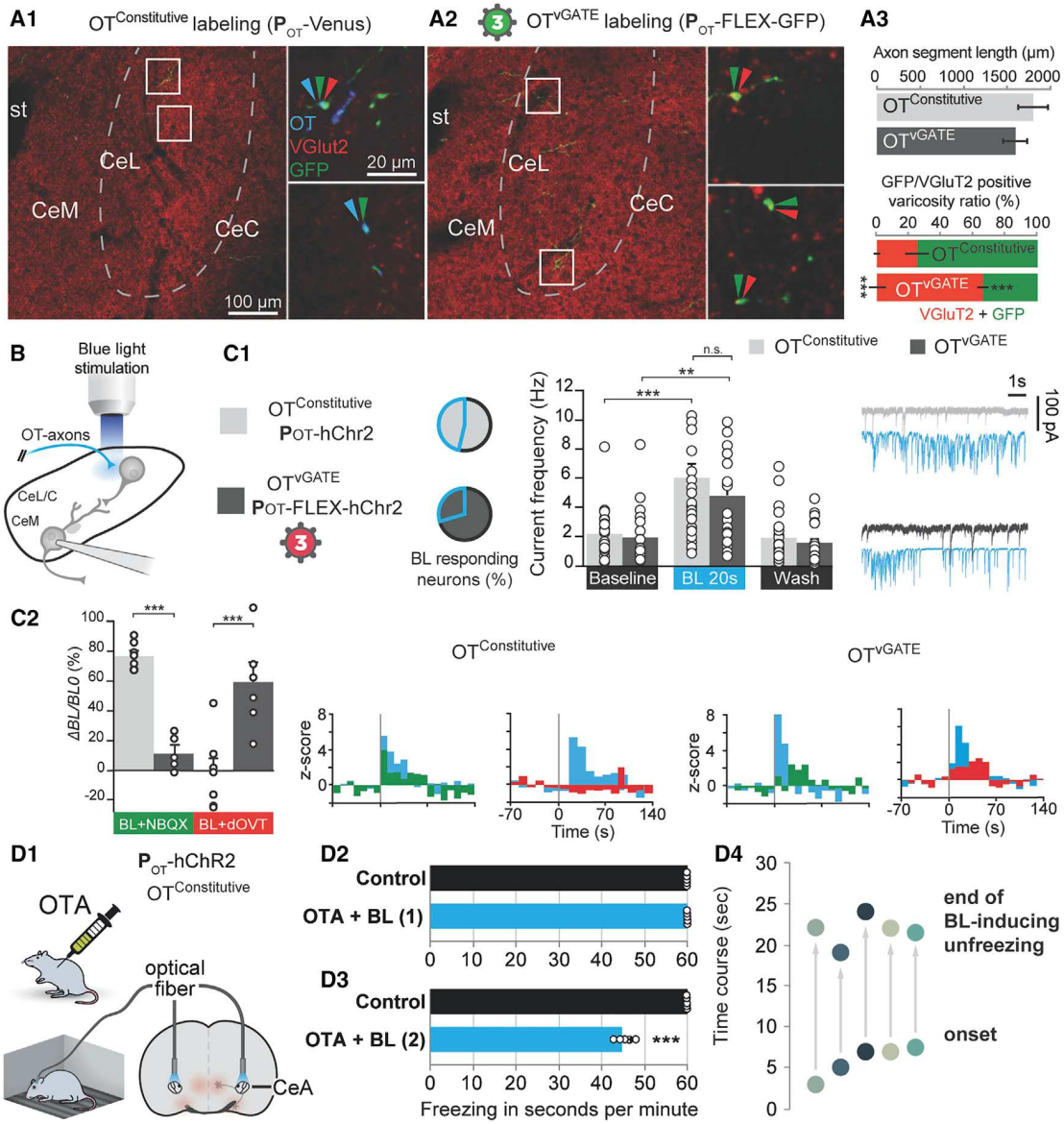

Figure 3. Functional Plasticity of the OT System upon Fear Learning

(A) GFP-labeled axons of OT neurons in the CeL of naive OT^{Constitutive} (A1) and OT^{vGATE} (A2) rats. Shown are an overview and enlarged fragments, showing co-localization of GFP (green) with OT (blue) and vGluT2 (red). (A3) Quantification of total axonal lengths and vGluT2-immunoreactive puncta. Green, OT axons containing no vGluT2; yellow, co-localization of OT and vGluT2; st, *stria terminalis*. *p < 0.05, ***p < 0.001, t test.

(B) Scheme of the *ex vivo* recording setup.

(C) Effect of optical stimulation of OT-ergic axons present in the CeL (BL) on IPSC frequencies recorded in CeM neurons in both fear-naive and fear-experienced vGATE animals (C1). Pie charts depict the proportion of CeM neurons responding to BL (naive OT^{Constitutive}, n = 27 of 56; OT^{vGATE}, n = 23 of 78, not significant).The bar plot shows the change in CeM current frequencies (hertz) in response to BL. Data are expressed as means across slices plus SEM. Individual values are indicated as white circles. **p < 0.01, ***p < 0.001, two-way ANOVA followed by Sidak *post hoc* test. (C2) Pharmacological dissection of BL effects. Left: quantification of the effect of NBQX (green; naive OT^{Constitutive}, n = 7; OT^{vGATE}, n = 5) or dOVT (red; OT^{Constitutive}, n = 7; OT^{vGATE}, n = 6) application on the initial BL effect on IPSC frequencies recorded in the same CeM neurons. Data are expressed as means across slices plus SEM. Individual values are indicated as white circles. ***p < 0.001, Mann-Whitney test. Right: *Z* scores illustrating the time course and modulation of BL effects by NBQX or dOVT.

(D) Scheme of BL stimulation of the CeL in OT^{Consitutive} animals pretreated with OTA (D1). (D2 and D3) The bar charts display the freezing time in the corresponding group and after blue light stimulation of the CeA after OTA administration. Top graph: the first conditioning session (D2, OTA-BL1). Bottom graph: the second conditioning session (D3, OTA-BL2). The black bars (control) show the freezing time immediately prior to BL stimulation, whereas the blue bars (BL) indicate the freezing time after BL stimulation. ***p < 0.001, t test. (D4) Graph displaying the onset and duration of the BL-induced unfreezing effect.

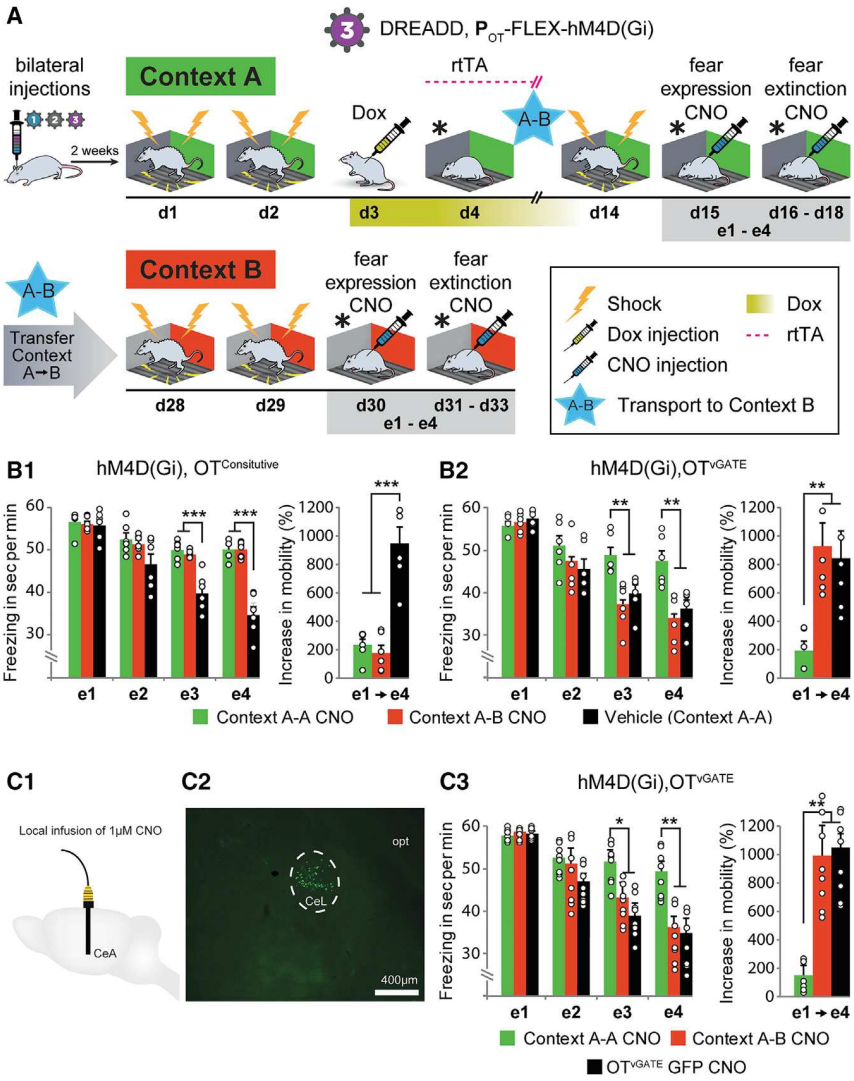

Figure 4. Pharmacogenetic Inhibition of OT Neurons Impairs Fear Extinction

(A) Scheme of the FC setup in contexts A and B (context A, green wall; context B, red wall). Virally injected animals were subjected to contextual FC. After two shock sessions (day 1 and day 2), animals received an i.p. injection of Dox on day 3, followed by another session on day 4 without shocks. Ten days later, animals were subjected to an additional shock day to reinforce the fear memory and then underwent a 4-day fear extinction protocol. During the extinction session, animals received a daily injection of CNO 40 min prior to the experiment. After exposure to context B, animals were subjected to 2 days of shock, followed by another 4-day extinction session, where they again received CNO daily prior to the experiment.

(B) Bar charts showing the average freezing time of animals over the course of a 4-day fear extinction paradigm as well as the total increase in mobility; e1–e4 indicate extinction days. (B1) Although control animals underwent normal fear extinction, CNO-mediated silencing of all OT neurons equally impaired fear extinction in both contexts. **p < 0.01, ***p < 0.0001, t test. (B2) CNO-mediated silencing of vGATE-tagged OT neurons in context A impaired fear extinction in context A but not in context B. **p < 0.01, ***p < 0.0001, one-way ANOVA.

(C) Schematic depiction of the local CNO infusion onto the CeA (C1). (C2) Confocal image showing the site-specific infusion of Retrobeads following CNO infusion to verify proper targeting of the CeA. (C3) Local infusion of CNO into the CeA impaired fear extinction in context A but not context B. *p < 0.05, **p < 0.01.

expressing hChR2 in OT neurons, which received saline (instead of OTA) in the first session and OTA in the second session, and obtained similar results (Figures S3C1–S3C3) as in the initial group, which was treated with OTA in both sessions (Figure 3D). Thus, our data indicate that fear experience drives a shift from OT to glutamate release from OT axons in the CeL of fear-experienced groups. Moreover, the enhanced responsiveness of CeL neurons to glutamate and its correlated effect, which could be abolished by application of NBQX (Figure 3C2), may indicate a transient, fear-experience-induced upregulation of AMPA receptors in these cells.

Inhibition of Fear-Activated OT Neurons Impairs Fear Extinction in a Context-Dependent Manner

To provide further evidence that OT neurons activated by fear exposure attenuate fear expression, we hypothesized that silencing of OT^{vGATE} neurons inhibits fear extinction specifically in the context where these neurons had originally been activated. Therefore, rats (n = 6) were injected with a virus expressing the modified human muscarinic receptor hM4D(Gi) under control of the OT promoter exposed to contextual FC and extinction paradigms (Figure 4A). All four groups of animals (OT^{vGATE} A-A, OT^{vGATE} A-B, OT^{Constitutive} A-A, and OT^{Constitutive} A-B) were subjected to FC in context A (day 1 shock, day 2 shock, day 3 Dox injection, day 4 exposure). To induce fear extinction, the two groups (OT^{vGATE} A-A and OT^{Constitutive} A-A) were exposed to the same context A for four consecutive days (40 min each session) without any electrical shock, receiving a daily i.p. injection of clozapine-N-oxide (CNO) 40 min prior to testing (control groups received saline). In parallel, we processed two additional groups of animals (OT^{vGATE} A-B and OT^{Constitutive} A-B, n = 6) in analogy to the first groups that were submitted to a first round of FC (in context A) and then transferred to a novel context (context B; Figure 4, blue star) prior to being submitted to the extinction protocol. We introduced the novel context (context B) to specifically investigate the potential role of OT in context-dependent fear extinction. This context represented a novel environment that was distinct in terms of visual, tactile, and olfactory cues (Figure S4A). Importantly, rats conditioned in context A did not display contextual FC in context B (Figure S4B), clearly demonstrating that

animals are able to discriminate between the two boxes (the complete dataset on freezing behavior is provided in Table S4). Silencing of all OT neurons by constitutively expressed hM4D(Gi) and application of its agonist CNO resulted in impaired fear extinction in both contexts A and B (Figure 4B1; Table S4). We next applied the vGATE technique to express hM4D(Gi) specifically in OT neurons (virus 3, rAAV-$\mathbf{P}_{OT}$-hM4D-Gi). We discovered that the silencing of OT fear neurons that were tagged in context A impaired fear extinction in context A but not in the novel context B (Figure 4B2). Because CNO has been reported to potentially activate certain neurons (Gomez et al., 2017), we performed control experiments (without virus injection, n = 6), where CNO alone had no effect on context-specific fear extinction (Figure S4C). To further rule out that the observed differences in fear extinction dynamics were a result of the two different contexts, we subjected naive, non-injected animals to fear extinction sessions in both contexts and found comparable freezing times throughout the extinction sessions (n = 6; Figure S4D).

To demonstrate that the observed impairments in fear extinction stem from inhibition of local OT release onto the CeA, we injected rats (n = 8) with the vGATE cocktail (virus 3, rAAV-$\mathbf{P}_{OT}$-hM4D-Gi) and implanted bilateral guide cannulas above the CeA for local infusion of CNO (Figures 4C1–4C2). CeA local infusion of 1 μM CNO (Stachniak et al., 2014) 15 min prior to each session impaired fear extinction in context A but not context B (Figure 4C3), confirming our previous results. To verify proper targeting of the CeA, we infused Retrobeads immediately after the last extinction session and killed the animals 10 min later to avoid spreading of the tracer (Figure 4C2). The control group (n = 8) injected with vGATE-GFP viruses displayed normal fear extinction in both contexts, indicating that local infusion of CNO per se does not impair fear extinction (Figure 4C3).

Activity of OT Neurons in the SON Is Context Dependent

To shed light on the cellular mechanisms underlying the context-dependent effect of neuronal inhibition (Figure 4B2), we labeled the OT^{vGATE} neurons green with the rAAV-$\mathbf{P}_{OT}$-FLEX-GFP (virus 3) and co-stained sections for endogenous c-*fos* red to identify the fraction of OT cells that was active during re-exposure to the same context (Figure 5A). In line with previous results (Figure 2B2), the first round of context A FC induced tagging of 10.8% of OT neurons in the PVN and 11.9% in the SON, visualized by intrinsic GFP (Figure 5A). The second round of context A FC induced c-*fos* signal in 9.5% of OT neurons in the PVN and 16.2% in the SON (Figure 5A). The overlap of virally expressed GFP and c-*fos* was 18% in the PVN and 89% in the SON, suggesting context-dependent activity of OT neurons specifically in the SON as well as a functional difference between the two nuclei. The difference in re-activation of OT cells in context A→A versus context A→B was significant for the SON (context A-A, 89% ± 5.5%; context A-B, 22% ± 3.6%; n = 6, $p < 0.0001$) but not the PVN (context A-A, 18% ± 2.7%; context A-B, 31% ± 3.7%; n = 6, $p = 0.2805$; Table S5). It is important to note that the group of animals that was first exposed to context A displayed ~5 times more activated neurons in both the PVN and SON after further exposure to context B (PVN: context A vGATE-GFP, 9.6%; context B c-*fos*, 47.1%; SON: context A vGATE-GFP, 11.7%; context B c-*fos*, 56.4%; Figure 5B; Table S5). This 5-fold difference in neuronal OT activity in context B correlated with the dramatically increased OT concentration in the blood (27.64% ± 5.4% pmol/mL versus 86.7% ± 12.9% pmol/mL; Figure S5A). However, despite the massive recruitment of new cells, the overlap of GFP-positive and c-*fos*-expressing OT neurons in the SON in context B amounted to only 22%. Taken together, these results indicate that re-exposure to a familiar FC context reactivates the same fraction of OT neurons, whereas exposure to a novel context recruits an entirely different population of cells. Therefore, it is plausible that OT neurons participate in a long-lasting fear memory engram that coordinates the OT-ergic response to different contextual fear episodes.

Finally, to investigate whether OT engram cells display basic electrophysiological properties distinct from non-engram OT cells, we performed an additional experiment where we injected animals (n = 12) with vGATE (virus 3, $\mathbf{P}_{OT}$-FLEX-GFP) and $\mathbf{P}_{OT}$-mCherryChr2 into the SON only. Animals were fear-conditioned, received an injection of Dox on day 3, and were processed for *ex vivo* patch-clamp recordings. In these animals, non-engram OT cells expressed red fluorescence, whereas vGATE-labeled engram cells appeared in yellow (green + red) (Figure 5C1). We analyzed access resistance, membrane capacitance, membrane potential, spontaneous excitatory postsynaptic current (EPSC) amplitudes and frequencies, and discharge profile upon current steps. Interestingly, we found significant differences in membrane capacitance (OT non-engram: 20.81 ± 1.25 pF, n = 16; OT engram: 26.13 ± 1.52 pF, n = 24; $p < 0.05$; Figure 5C2) and frequency of spontaneous EPSCs (OT non-engram, 1.87 ± 0.51; OT engram, 3.18 ± 0.54 Hz; $p < 0.05$; Figure 5C2). All other parameters did not significantly differ between $OT^{Constitutive}$ and OT^{vGATE} cells (Figure S5B). Thus, these findings suggest that vGATE-labeled OT engram cells have a larger membrane surface and receive more excitatory inputs, a feature of engram cells that has already been described for the hippocampus (Kitamura et al., 2017; Ryan et al., 2015).

To investigate whether increased glutamatergic input onto OT^{vGATE} could potentially underlie the observed differences in membrane capacitance and increased spontaneous EPSCs, we stained brain slices of vGATE-injected rats with the vesicular glutamate transporter vGluT2 and compared the number of vGluT2-positive puncta in the immediate surroundings (surface of soma and 5-μm radius around each OT-positive neuron). We found that the number of vGluT2 puncta encompassing the OT engram (OT^{vGATE}) cells (18.6 ± 1.2, 130 cells, n = 3) was significantly higher ($p < 0.001$) compared with non-engram OT neurons (8.3 ± 0.9, 1,044 cells, n = 3) (Figure 5C3). These results suggest that OT engram cells receive more prominent glutamatergic input than OT non-engram cells, potentially explaining the unique electrophysiological properties of engram OT neurons (Figure 5C2).

Parvocellular OT Neurons Activate Magnocellular OT Neurons in a Novel Context

Because the OT system is composed of two types of neurons, magnocellular (magnOT) and parvocellular (parvOT) neurons (Rhodes et al., 1981; Swanson and Kuypers, 1980; Swanson and Sawchenko, 1983), we next aimed to investigate which

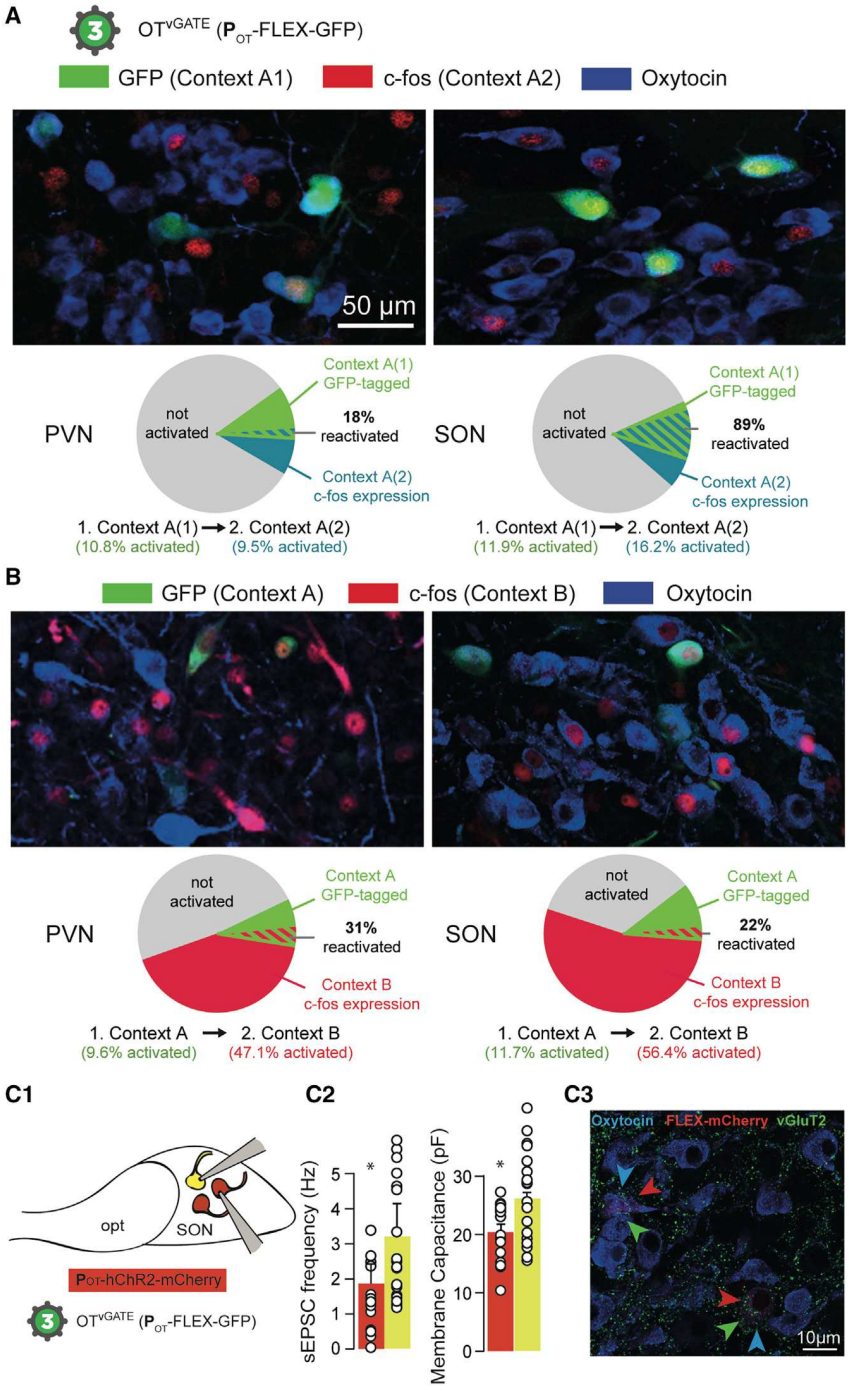

Figure 5. Context-Dependent Tagging of OT Neurons

(A and B) Percentage of OT neurons tagged in context A and reactivated after exposure to a familiar (A) or a novel (B) context. Shown are representative confocal images of the PVN and SON with an intrinsic GFP signal (green, vGATE-based tagged neurons in context A) co-stained for OT (blue) and c-*fos* (red, indicates neurons activated in context B). Pie charts show the relative numbers and percentages of GFP-positive and c-*fos*-expressing OT neurons in each hypothalamic nucleus. In the PVN, the initial exposure to context A resulted in GFP-based tagging of 10.8% of all counted OT neurons (Table S5), whereas re-exposure to the same context led to c-*fos* expression in 9.5% of OT neurons with 18% of reactivated cells (i.e., OT cells expressing GFP and c-*fos*). In the SON, exposure to context A activated 11.9% of OT neurons, and re-exposure to the same context induced c-*fos* in 16.2% of OT cells, displaying an 89% overlap in GFP and c-*fos* signals. For context B, the initial exposure activated 9.6% of OT cells in the PVN, visualized by intrinsic GFP expression, and the second exposure recruited a massive 47.1% of OT cells with a reactivated GFP-expressing fraction of 31%. In the SON, first exposure to novel context B activated 11.7% of OT neurons, whereas re-exposure to the same context resulted in drastically increased activation of 56.4% of cells but reflecting only a 22% overlap of GFP and c-*fos*.

(C) Electrophysiological properties of OT^{vGATE} versus $OT^{Constitutive}$ neurons. (C1) Experimental scheme showing OT^{vGATE} in yellow (co-localization of green and red signals) and $OT^{Constitutive}$ in red in the SON. (C2) Bar plots and individual data (dots) of spontaneous excitatory postsynaptic current (sEPSC) frequency (left) and membrane capacitance (right) recorded in OT^{vGATE} (yellow, n = 24) and $OT^{Constitutive}$ (red, n = 16). *p < 0.05, t test. (C3) VGluT2-immunoreactive puncta (green) in close vicinity of OT neurons (blue) labeled by vGATE viruses (FLEX-mCherry, red) and non-labeled OT cells of the SON. The number of vGLuT2-positive puncta in the vicinity of OT vGATE neurons is significantly higher compared with non-labeled OT neurons (p < 0.001).

hypothalamic OT cell types are reactivated during the two fear episodes. To distinguish between magnOT and parvOT neurons, we used the retrograde marker Fluorogold (FG), which labels magnOT but not parvOT cells (Naumann et al., 2000). Injecting the cocktail of vGATE viruses (virus 3, rAAV-$\mathbf{P}_{OT}$-FLEX-GFP), we found that virtually all FG-negative parvOT neurons of the PVN (parvOT neurons are not present in the SON) were labeled with GFP in context A and contained c-*fos* in context B, whereas only a small fraction (14%–20%) of FG-positive magnOT neurons of the PVN and SON labeled with GFP in context A were c-*fos* positive in context B (Figure 6A; Table S6).

Following previous findings that PVN parvOT neurons provide synaptic inputs onto OT neurons in the SON to activate magnOT neurons (Eliava et al., 2016), we aimed to silence parvOT neurons to elucidate their functional relevance in the novel context B during repeated fear exposure. To achieve this, we expressed hM4D(Gi) in a Cre-dependent manner in the PVN via a CAV2-Cre virus injected into the SON (Figure 6B) to silence parvOT inputs onto magnOT neurons. We found that silencing of parvOT

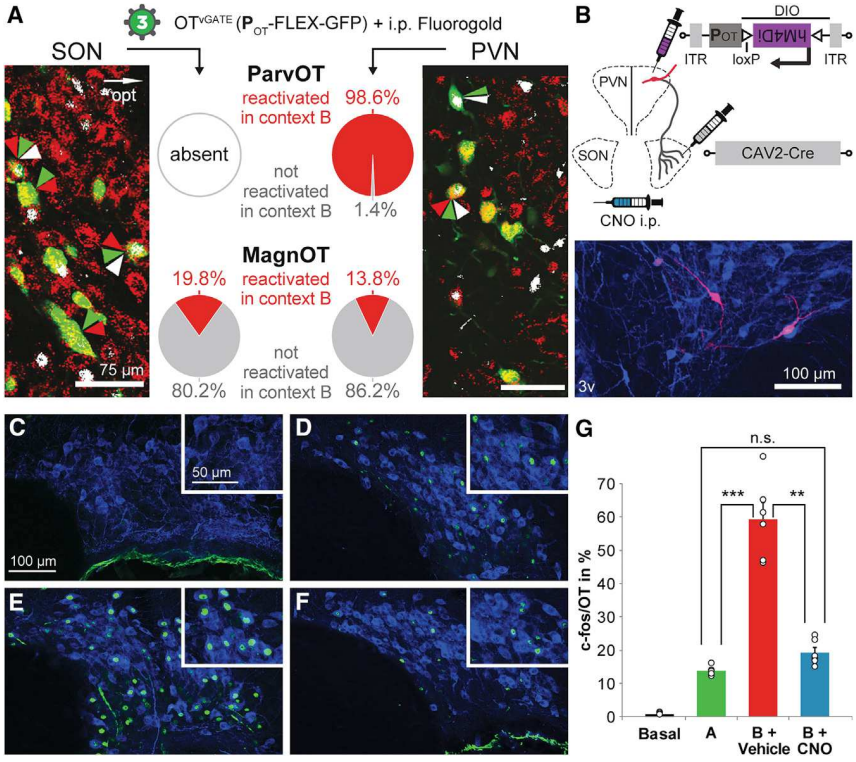

Figure 6. Pharmacogenetic Silencing of Parvocellular OT Neurons

(A) Percentage of parvOT and magnOT, tagged in context A by GFP and reactivated after exposure to context B, and representative confocal images of FG-positive (magnOT neurons, red) and FG-negative (parvOT neurons) containing intrinsic GFP and c-*fos* (white). Green arrows indicate OT neurons activated in context A (GFP), red arrows indicate magnocellular OT neurons, and white arrows indicate OT cells containing c-*fos*. Pie charts between confocal images display the distribution of c-*fos* labeling in parvOT and magnOT neurons.

(B) Experimental setup for exclusive silencing of ParvOT neurons. Animals received an injection of CAV2-Cre into the SON and Cre-dependent rAAV expressing hM4Di-mCherry under the control of the OT promoter into the PVN to specifically label parvocellular OT neurons in the PVN. The confocal image shows parvocellular OT cells (blue) expressing hM4Di-mCherry (red).

(C–F) Images of the SON of naive animals (C), rats conditioned in context A (D), and rats conditioned in context A followed by context B and treated with vehicle (E) or CNO (F).

(G) CNO treatment drastically reduced the number of c-*fos*-expressing OT neurons in the SON of rats exposed to context B. Black, control; green, exposure to context A; red, exposure to context B plus saline injection; blue, exposure to context B plus CNO injection. ***p < 0.0001, one-way ANOVA.

neurons in context B prevented the massive induction of c-*fos* expression in the SON (Figures 6C–6G; Table S6), indicating a critical role of parvOT neurons during repeated fear exposure. Similar results were obtained in the PVN (Figures S6A–S6E), suggesting that parvOT neurons might also directly or indirectly control magnOT activity within PVN neurons. To exclude that the prevented rise in c-*fos* expression was a result of CNO treatment, we subjected animals to the same paradigm, where they received CNO but were not injected with Cre-dependent hM4D(Gi) rAAV, and found no differences in c-*fos* expression in OT neurons of the SON and PVN (Figure S6F).

DISCUSSION

Here we provide first evidence that vGATE-assisted OT-tagged neurons during fear expression are sufficient for controlling fear behavior and necessary for fear extinction. Furthermore, fear experience drives enormous plasticity, mediating a shift from OT to glutamate signaling in the CeL. We propose that repeated fear exposure activates OT-ergic fear engram cells for rapid adaptive behavioral responses.

The Context-Dependent Fear Memory Engram and Its Plasticity in the Hypothalamic OT System

The hypothesis that learning-activated cell ensembles form memory engrams has received substantial attention (Kitamura et al., 2017; Liu et al., 2012; Reijmers et al., 2007). Although memory engrams have been discovered in higher brain regions such as the cortex, hippocampus, or basolateral amygdala (Kitamura et al., 2017; Liu et al., 2012), no study, to our knowledge, has addressed the potential role of the lower brain regions, such as the hypothalamus, in the modulation of fear memory. In a number of studies, the OT system has been highlighted as a key structure modulating various aspects of fear, such as acquisition, expression, and extinction.

To investigate whether OT neurons encode for context-specificity, we applied the vGATE method to identify and manipulate potential OT engram cells and labeled a small fraction (~11%–14%) of hypothalamic OT neurons by contextual FC. Remarkably, the majority of OT^{vGATE} neurons project to the CeA, and optogenetic activation of the OT neuronal axonal fibers in the CeA elicited rapid onset of unfreezing. We further found that, upon fear exposure, OT neurons show enhanced glutamatergic over OT-ergic transmission in the CeM (Figure 3D1) with increased membrane capacitance (Figure 5C2) and elevated vGluT2-levels in OT axons terminating in the CeA (Figure 5C3), consistent with previous studies (Ciocchi et al., 2010; Li et al., 2013; Penzo et al., 2015). Thus, our results provide the first evidence for fear-induced long-term plasticity (15 days) of the OT-CeL circuit. It seems indeed possible that a single episode of fear conditioning permanently alters the OT and glutamate balance, perhaps to strengthen synaptic connections for rapid response and memory maintenance. These findings support the general notion that coordinated release of slow-acting neuromodulator peptides and fast-acting amino acid transmitters could be a likely mechanism to modulate cognitive, emotional, and metabolic processes (van den Pol, 2012).

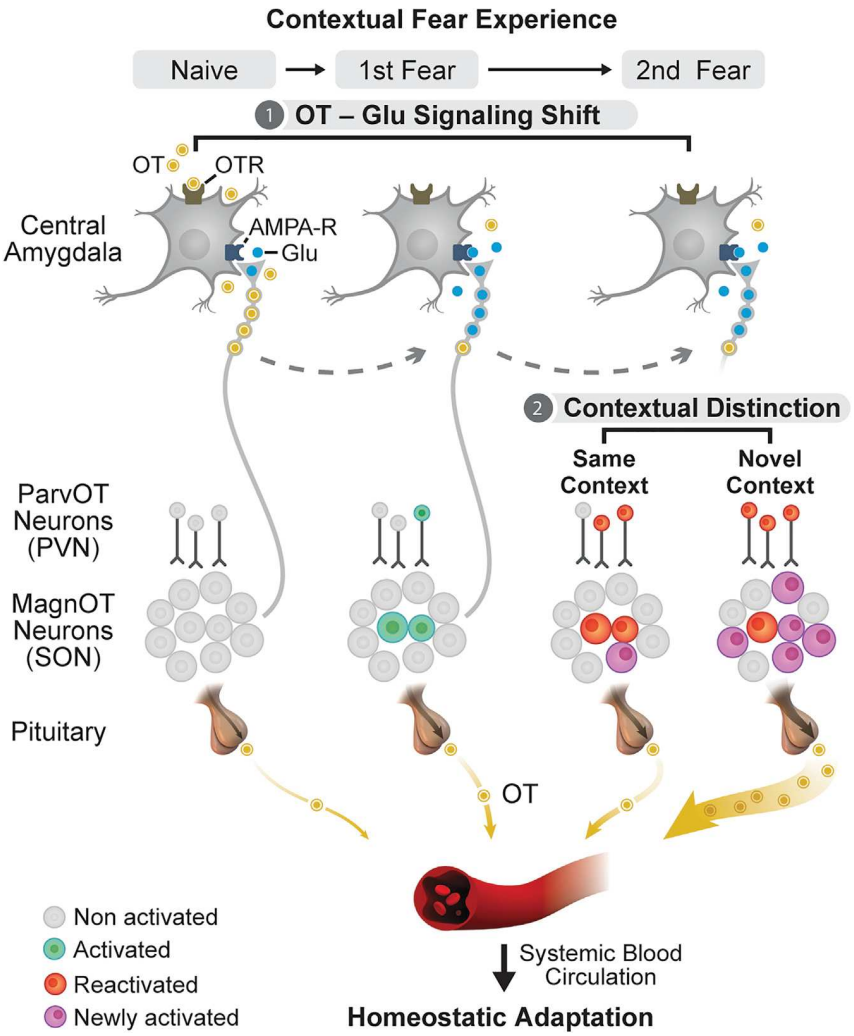

Figure 7. Context-Dependent Changes in OT Neuron Activity Following Contextual Fear Experience

The scheme represents a working hypothesis of plasticity and contextual specificity of the central OT system. At the level of OT terminals in the amygdala (top panel), the fear learning process induces drastic changes in the transmitter and neuromodulator balance: although in naive rats, OT axons predominantly release OT, in fear-experienced rats, the same axons release glutamate instead of OT. At the level of the hypothalamus (center panel), the majority of magnOT neurons in the SON exhibit context specificity and are not reactivated in a novel context. In contrast, parvOT neurons of the PVN, synapsing on SON magnOT neurons, are reactivated in a novel context and drive massive recruitment of new magnOT neurons. The massive activation of new SON OT neurons correlated with OT release to the blood, serving homeostatic adaptation to excessive stress caused by exposure to a novel fearful environment (bottom).

Based on our findings, we hypothesized that OT^{vGATE} engram neurons might also be involved in fear extinction. Given the key role of CeA in fear extinction, we next investigated whether context-specific OT neuronal circuits would control context-specific fear extinction. Although inhibition of virtually all OT neurons resulted in context-independent impairment of fear extinction, inhibition of OT^{vGATE} neurons exclusively affected fear extinction in the context in which the cells had originally been labeled. These OT^{vGATE} neurons might be required for suppression of memory expression, safety cues, and priming for extinction. This could explain the unaffected fear extinction of animals in context B after silencing of OT^{vGATE} neurons that were tagged in context A, where inhibition of these fibers might no longer be relevant, because newly recruited OT neurons in a different context could compensate for the reduced release of OT in the CeA by release of this neuropeptide in other brain regions (Figures 4B2 and 4C3). Therefore, we concluded that silencing of OT^{vGATE} engram cells impaired fear extinction, demonstrating necessity, a likely result of blocking OT and glutamate-mediated neural modulation in the CeA. We propose that OT^{vGATE} cells represent a "neuromodulatory" engram that plays a vital role in controlling simple "contextual memory" representations for context-specific behavioral expression and the extinction phenotype.

Context-Independent Control by Parvocellular OT Neurons of the Hypothalamic OT System

OT neurons are divided into two types: magnOT and parvOT neurons. Despite their relatively low numbers (~70 neurons per rat), parvOT neurons modulate important physiological processes, such as cardiovascular functions, hunger, and pain (Althammer and Grinevich, 2017). The present study highlights the functional relevance of parvOT neurons in contextual FC because virtually all parvOT neurons that were activated in context A were also reactivated in context B, and silencing of parvOT neurons almost entirely blocked the recruitment of novel magnOT neurons in an unfamiliar context. Therefore, we hypothesize that parvOT neurons operate as a class of "master cells," orchestrating magnOT neuron activity and subsequent OT release into the blood. Although the precise role of OT neurons during fear conditioning remains to be determined, it is plausible that the coordinated activity of parvOT neurons may facilitate global priming effects and/or induce plasticity of magnOT neurons in various physiological demands (Theodosis et al., 1986; Tobin et al., 2012). In line with this, global activation of the OT system, driven by parvOT neurons, can be crucial for metabolic, autonomic, and behavioral adaption to exacerbated fear-induced stress. In our current study, the 5-fold increase in c-*fos* expression quite accurately matches the 5-fold elevation of OT levels in the blood (Figure S6A). This indicates that newly activated OT neurons in context B are magnOT cells that release the neuropeptide from the neurohypophysis into the blood.

Thus, the newly recruited OT neurons in both hypothalamic nuclei provide a massive release of OT into the peripheral circulation to regulate various physiological demands to cope with an exacerbated stress response (Yang et al., 2013).

Conclusion

We identified and validated a neuromodulatory engram composed specifically of OT cells that fulfills the key criteria of the synaptic plasticity memory hypothesis (Martin et al., 2000): sufficiency, necessity, and plasticity. We demonstrated that OT neurons of the SON participate in a fear memory engram (Figure 7), whereas parvOT neurons coordinate OT release in a context-independent manner. Our findings will facilitate the investigation of pathophysiological mechanisms underlying emotion-associated mental disorders, especially PTSD symptoms, their potential treatment by exogenous OT (Althammer et al., 2018; Frijling et al., 2014), and virus-delivered genetically based targeted therapeutic agents.

STAR★METHODS

Detailed methods are provided in the online version of this paper and include the following:

- KEY RESOURCES TABLE
- CONTACT FOR REAGENT AND RESOURCE SHARING
- EXPERIMENTAL MODEL AND SUBJECT DETAILS
  - Animals
- METHOD DETAILS
  - The vGATE system
  - Infecting rat hypothalamic neurons *in vivo* with rAAVs
  - Neuroanatomy
  - BEHAVIOR
  - Ex Vivo Electrophysiology
  - Histology
  - Measurement of Plasma ot Concentrations
- QUANTIFICATION AND STATISTICAL ANALYSIS

SUPPLEMENTAL INFORMATION

Supplemental Information can be found online at https://doi.org/10.1016/j.neuron.2019.04.029.

ACKNOWLEDGMENTS

The authors dedicate this manuscript to the memory of Professor Peter H. Seeburg (1944–2016), who generously provided us with enormous support for this 12-year-long project. This work was supported by the Max Planck Society (to M.T.H., R.S., and V.G.); the Fritz Thyssen Stiftung (to M.T.H. and V.G.); the Ministry of Economy and Business (MINECO) under the framework of the ERA-NET Neuron Cofund (to M.T.H.); Ministerio Economia, Industria y Competitividad (Spain) and FEDER (grant RTI2018-101624-B-I00 to M.T.H.); the Chica and Heinz Schaller Research Foundation (to V.G.); German Research Foundation (DFG) grant GR 3619/4-1 (to V.G.); Human Frontier Science Program RGP0019/2015 (to V.G.); the DFG within the Collaborative Research Center (SFB) 1134 (to V.G., R.S., and H.B.) and 1158 (to V.G., S.C.H., R.S., and H.B.); SNSF-DFG grant GR 3619/8-1 (to V.G.); PHC PROCOP program 32975SA (DAAD and Campus France), PICS program 07882 (CNRS), and ANR-DFG grant GR 3619/701 (to V.G. and A.C.); and FP7 career integration grant 334455, University of Strasbourg Institute for Advanced Study (USIAS) fellowship 2014-17, Foundation Fyssen research grant 2015 (to A.C.) and postdoctoral fellowship 2017-2019 (A.L.), and NARSAD young investigator grant 24821 (to A.C.). The authors thank Sadia Oumohand and Jonas Metz for help with behavioral experiments and histology; Judith Müller for cloning Cre-depended rAAVs; Barbara Kurpiers and the Interdisciplinary Neurobehavioral Core Facility of Heidelberg University for behavioral experiments performed there; Diego Benusiglio for help with statistical analysis; Inga Neumann (Regensburg), Ron Stoop (Lausanne), and Mary Lee (Bethesda) for valuable comments on the manuscript; Thomas Splettstoesser (SciStyle) for help with the preparation of figures; and Anne Seller for proofreading the manuscript.

AUTHOR CONTRIBUTIONS

Design and development of the vGATE system, M.T.H.; characterization of vGATE, M.T.H., J.-M.W., G.K.D., and I.B.; project conception, M.T.H., A.C., and V.G.; implementation of other methodologies, M.T.H., J.-M.W., R.H., M.E.L., R.S., and H.B.; *ex vivo* patch-clamp electrophysiology, S.G., J.W., P.D., Y.T., X.L., and A.C.; viral injections, F.A., M.S.d.G., and S.G.; fear behavior, F.A., M.S.d.G., S.G., D.K., A.J., A.R., J.S., and C.P.; immunohistochemistry, F.A., M.S.d.G., A.L., M.E., and H.S.K.-B.; HPLC MS/MS, V.C. and Y.G.; data analysis, F.A., M.S.d.G., S.G., A.R., J.-M.W., and A.C.; confocal microscopy, F.A., M.E.L., M.S.d.G., and A.L.; manuscript preparation, M.T.H., A.C., and V.G.; extended manuscript preparation, F.A., H.S.K.-B., R.H., S.C.H., R.S., H.B., A.C., M.T.H., and V.G.; supervision, M.T.H., A.C., and V.G.; project administration, M.T.H., A.C., and V.G.; funding acquisition, M.T.H., A.C., and V.G.

DECLARATION OF INTERESTS

The authors declare no competing interests.

Received: May 18, 2018
Revised: October 8, 2018
Accepted: April 18, 2019
Published: May 16, 2019

REFERENCES

Althammer, F., and Grinevich, V. (2017). Diversity of oxytocin neurons: beyond magno- and parvocellular cell types? J. Neuroendocrinol. Published online October 12, 2017. https://doi.org/10.1111/jne.12549.

Althammer, F., Jirikowski, G., and Grinevich, V. (2018). The oxytocin system of mice and men-Similarities and discrepancies of oxytocinergic modulation in rodents and primates. Peptides *109*, 1–8.

Bru, T., Salinas, S., and Kremer, E.J. (2010). An update on canine adenovirus type 2 and its vectors. Viruses *2*, 2134–2153.

Cetin, A., Komai, S., Eliava, M., Seeburg, P.H., and Osten, P. (2006). Stereotaxic gene delivery in the rodent brain. Nat. Protoc. *1*, 3166–3173.

Ciocchi, S., Herry, C., Grenier, F., Wolff, S.B., Letzkus, J.J., Vlachos, I., Ehrlich, I., Sprengel, R., Deisseroth, K., Stadler, M.B., et al. (2010). Encoding of conditioned fear in central amygdala inhibitory circuits. Nature *468*, 277–282.

Dogbevia, G.K., Marticorena-Alvarez, R., Bausen, M., Sprengel, R., and Hasan, M.T. (2015). Inducible and combinatorial gene manipulation in mouse brain. Front. Cell. Neurosci. *9*, 142.

Dogbevia, G.K., Roβmanith, M., Sprengel, R., and Hasan, M.T. (2016). Flexible, AAV-equipped Genetic Modules for Inducible Control of Gene Expression in Mammalian Brain. Mol. Ther. Nucleic Acids *5*, e309.

Ehrlich, I., Humeau, Y., Grenier, F., Ciocchi, S., Herry, C., and Lüthi, A. (2009). Amygdala inhibitory circuits and the control of fear memory. Neuron *62*, 757–771.

Eliava, M., Melchior, M., Knobloch-Bollmann, H.S., Wahis, J., da Silva Gouveia, M., Tang, Y., Ciobanu, A.C., Triana Del Rio, R., Roth, L.C., Althammer, F., et al. (2016). A New Population of Parvocellular Oxytocin Neurons Controlling Magnocellular Neuron Activity and Inflammatory Pain Processing. Neuron *89*, 1291–1304.

Fadok, J.P., Krabbe, S., Markovic, M., Courtin, J., Xu, C., Massi, L., Botta, P., Bylund, K., Müller, C., Kovacevic, A., et al. (2017). A competitive inhibitory circuit for selection of active and passive fear responses. Nature *542*, 96–100.

Frijling, J.L., van Zuiden, M., Koch, S.B., Nawijn, L., Goslings, J.C., Luitse, J.S., Biesheuvel, T.H., Honig, A., Bakker, F.C., Denys, D., et al. (2014). Efficacy of oxytocin administration early after psychotrauma in preventing the development of PTSD: study protocol of a randomized controlled trial. BMC Psychiatry *14*, 92.

Gomez, J.L., Bonaventura, J., Lesniak, W., Mathews, W.B., Sysa-Shah, P., Rodriguez, L.A., Ellis, R.J., Richie, C.T., Harvey, B.K., Dannals, R.F., et al. (2017). Chemogenetics revealed: DREADD occupancy and activation via converted clozapine. Science *357*, 503–507.

Grund, T., Goyon, S., Li, Y., Eliava, M., Liu, H., Charlet, A., Grinevich, V., and Neumann, I.D. (2017). Neuropeptide S Activates Paraventricular Oxytocin Neurons to Induce Anxiolysis. J. Neurosci. *37*, 12214–12225.

Guenthner, C.J., Miyamichi, K., Yang, H.H., Heller, H.C., and Luo, L. (2013). Permanent genetic access to transiently active neurons via TRAP: targeted recombination in active populations. Neuron *78*, 773–784.

Hamamura, M., Leng, G., Emson, P.C., and Kiyama, H. (1991). Electrical activation and c-fos mRNA expression in rat neurosecretory neurones after systemic administration of cholecystokinin. J. Physiol. *444*, 51–63.

Heidbreder, C.A., and Groenewegen, H.J. (2003). The medial prefrontal cortex in the rat: evidence for a dorso-ventral distinction based upon functional and anatomical characteristics. Neurosci. Biobehav. Rev. *27*, 555–579.

Herry, C., Ferraguti, F., Singewald, N., Letzkus, J.J., Ehrlich, I., and Lüthi, A. (2010). Neuronal circuits of fear extinction. Eur. J. Neurosci. *31*, 599–612.

Katoh, A., Fujihara, H., Ohbuchi, T., Onaka, T., Young, W.S., 3rd, Dayanithi, G., Yamasaki, Y., Kawata, M., Suzuki, H., Otsubo, H., et al. (2010). Specific expression of an oxytocin-enhanced cyan fluorescent protein fusion transgene in the rat hypothalamus and posterior pituitary. J. Endocrinol. *204*, 275–285.

Kessler, R.C., and Bromet, E.J. (2013). The epidemiology of depression across cultures. Annu. Rev. Public Health *34*, 119–138.

Kitamura, T., Ogawa, S.K., Roy, D.S., Okuyama, T., Morrissey, M.D., Smith, L.M., Redondo, R.L., and Tonegawa, S. (2017). Engrams and circuits crucial for systems consolidation of a memory. Science *356*, 73–78.

Knobloch, H.S., Charlet, A., Hoffmann, L.C., Eliava, M., Khrulev, S., Cetin, A.H., Osten, P., Schwarz, M.K., Seeburg, P.H., Stoop, R., and Grinevich, V. (2012). Evoked axonal oxytocin release in the central amygdala attenuates fear response. Neuron *73*, 553–566.

Koohi, M.K., Ivell, R., and Walther, N. (2005). Transcriptional activation of the oxytocin promoter by oestrogens uses a novel non-classical mechanism of oestrogen receptor action. J. Neuroendocrinol. *17*, 197–207.

LeDoux, J. (2007). The amygdala. Curr. Biol. *17*, R868–R874.

Letzkus, J.J., Wolff, S.B., Meyer, E.M., Tovote, P., Courtin, J., Herry, C., and Lüthi, A. (2011). A disinhibitory microcircuit for associative fear learning in the auditory cortex. Nature *480*, 331–335.

Li, H., Penzo, M.A., Taniguchi, H., Kopec, C.D., Huang, Z.J., and Li, B. (2013). Experience-dependent modification of a central amygdala fear circuit. Nat. Neurosci. *16*, 332–339.

Liu, X., Ramirez, S., Pang, P.T., Puryear, C.B., Govindarajan, A., Deisseroth, K., and Tonegawa, S. (2012). Optogenetic stimulation of a hippocampal engram activates fear memory recall. Nature *484*, 381–385.

Lütcke, H., Murayama, M., Hahn, T., Margolis, D.J., Astori, S., Zum Alten Borgloh, S.M., Göbel, W., Yang, Y., Tang, W., Kügler, S., et al. (2010). Optical recording of neuronal activity with a genetically-encoded calcium indicator in anesthetized and freely moving mice. Front. Neural Circuits *4*, 9.

Martin, S.J., Grimwood, P.D., and Morris, R.G. (2000). Synaptic plasticity and memory: an evaluation of the hypothesis. Annu. Rev. Neurosci. *23*, 649–711.

Mobbs, D., Hagan, C.C., Dalgleish, T., Silston, B., and Prévost, C. (2015). The ecology of human fear: survival optimization and the nervous system. Front. Neurosci. *9*, 55.

Naumann, T., Härtig, W., and Frotscher, M. (2000). Retrograde tracing with Fluoro-Gold: different methods of tracer detection at the ultrastructural level and neurodegenerative changes of back-filled neurons in long-term studies. J. Neurosci. Methods *103*, 11–21.

Penzo, M.A., Robert, V., Tucciarone, J., De Bundel, D., Wang, M., Van Aelst, L., Darvas, M., Parada, L.F., Palmiter, R.D., He, M., et al. (2015). The paraventricular thalamus controls a central amygdala fear circuit. Nature *519*, 455–459.

Reijmers, L.G., Perkins, B.L., Matsuo, N., and Mayford, M. (2007). Localization of a stable neural correlate of associative memory. Science *317*, 1230–1233.

Rhodes, C.H., Morrell, J.I., and Pfaff, D.W. (1981). Immunohistochemical analysis of magnocellular elements in rat hypothalamus: distribution and numbers of cells containing neurophysin, oxytocin, and vasopressin. J. Comp. Neurol. *198*, 45–64.

Ryan, T.J., Roy, D.S., Pignatelli, M., Arons, A., and Tonegawa, S. (2015). Memory. Engram cells retain memory under retrograde amnesia. Science *348*, 1007–1013.

Schilling, K., Luk, D., Morgan, J.I., and Curran, T. (1991). Regulation of a fos-lacZ fusion gene: a paradigm for quantitative analysis of stimulus-transcription coupling. Proc. Natl. Acad. Sci. USA *88*, 5665–5669.

Somponpun, S.J., and Sladek, C.D. (2003). Osmotic regulation of estrogen receptor-beta in rat vasopressin and oxytocin neurons. J. Neurosci. *23*, 4261–4269.

Stachniak, T.J., Ghosh, A., and Sternson, S.M. (2014). Chemogenetic synaptic silencing of neural circuits localizes a hypothalamus→midbrain pathway for feeding behavior. Neuron *82*, 797–808.

Swanson, L.W., and Kuypers, H.G. (1980). The paraventricular nucleus of the hypothalamus: cytoarchitectonic subdivisions and organization of projections to the pituitary, dorsal vagal complex, and spinal cord as demonstrated by retrograde fluorescence double-labeling methods. J. Comp. Neurol. *194*, 555–570.

Swanson, L.W., and Sawchenko, P.E. (1983). Hypothalamic integration: organization of the paraventricular and supraoptic nuclei. Annu. Rev. Neurosci. *6*, 269–324.

Theodosis, D.T., Montagnese, C., Rodriguez, F., Vincent, J.D., and Poulain, D.A. (1986). Oxytocin induces morphological plasticity in the adult hypothalamo-neurohypophysial system. Nature *322*, 738–740.

Tobin, V., Leng, G., and Ludwig, M. (2012). The involvement of actin, calcium channels and exocytosis proteins in somato-dendritic oxytocin and vasopressin release. Front. Physiol. *3*, 261.

Tovote, P., Fadok, J.P., and Lüthi, A. (2015). Neuronal circuits for fear and anxiety. Nat. Rev. Neurosci. *16*, 317–331.

van den Pol, A.N. (2012). Neuropeptide transmission in brain circuits. Neuron *76*, 98–115.

Viviani, D., Charlet, A., van den Burg, E., Robinet, C., Hurni, N., Abatis, M., Magara, F., and Stoop, R. (2011). Oxytocin selectively gates fear responses through distinct outputs from the central amygdala. Science *333*, 104–107.

Yang, H.P., Wang, L., Han, L., and Wang, S.C. (2013). Nonsocial functions of hypothalamic oxytocin. ISRN Neurosci. *2013*, 179272.

STAR★METHODS

KEY RESOURCES TABLE

REAGENT OR RESOURCE	SOURCE	IDENTIFIER
Antibodies		
Chicken anti-GFP primary antibody	Abcam	ab13970
Mouse NeuN primary antibody	Chemicon	A60
Rabbit vGluT2 primary antibody	Synaptic systems	135 103
Rabbit anti-dsRed primary antibody	Clontech	632496
Rabbit anti-Fluorogold primary antibody	Milipore	AB153
Guinea-pig anti-Fluorogold primary antibody	Protos Biotech Corp	NM-101
Rabbit c-fos polyclonal primary antibody	Santa-Cruz	sc-7202
Mouse monoclonal anti-OT primary antibody	Provided by Dr. Harold Gainer	PS 38
Rabbit polyclonal anti-CRH primary antibody	Peninsula Labs	T-4035.0500
Rat monoclonal anti-Somatostatin primary antibody	Chemicon	MAB345
Rabbit polyclonal anti-vGluT2 primary antibody	SYSY	135403
Bacterial and Virus strains		
$(tetO)_7$-$\mathbf{P}_{c\text{-}fos}$-rtTA AAV 1/2	This paper	N/A
YC3.60-$\mathbf{P}_{tet}$bi-Cre AAV 1/2	This paper	N/A
$\mathbf{P}_{OT}$-FLEX-hChr2-mCherry AAV 1/2	Eliava et al., 2016	N/A
CAV2-Cre	Bru et al., 2010	N/A
$\mathbf{P}_{OT}$-Venus AAV 1/2	Knobloch et al., 2012	N/A
$\mathbf{P}_{OT}$-FLEX-GFP AAV 1/2	Eliava et al., 2016	N/A
$\mathbf{P}_{OT}$-FLEX-hM4D(Gi)-mCherry AAV 1/2	Eliava et al., 2016	N/A
Chemicals, Peptides, and Recombinant Proteins		
Fluorogold	Santa-Cruz	sc-358883
Oxytocin Receptor Antagonist	Santa-Cruz	L-368,899
Doxycycline	Cayman Chemical Company	14422
Clozapine-N-Oxide	Tocris Bioscience	4936
NBQX	Abcam	Ab120018
dOVT	Bachem	H2908
Retrobeads	Lumaflour	N/A
Experimental Models: Organisms/Strains		
Rattus Norvegicus (Wistar)	Janvier	N/A
Recombinant DNA		
$(tetO)_7$-$\mathbf{P}_{c\text{-}fos}$-rtTA	This paper	N/A
YC3.60-$\mathbf{P}_{tet}$bi-Cre	This paper	N/A
$\mathbf{P}_{OT}$-FLEX-hChr2-mCherry	Eliava et al., 2016	N/A
$\mathbf{P}_{OT}$-Venus	Knobloch et al., 2012	N/A
$\mathbf{P}_{OT}$-FLEX-GFP	Eliava et al., 2016	N/A
$\mathbf{P}_{OT}$-FLEX-hM4D(Gi)-mCherry	Eliava et al., 2016	N/A
Software and Algorithms		
Graphpad prism 7.0	https://www.graphpad.com/	N/A
Fiji	http://www.imagej.net/Fiji	N/A
Adobe Photoshop CS5	https://www.adobe.com/	N/A
Adobe Illustrator 16.05	https://www.adobe.com/	N/A
Panlab Fear conditioning software	https://www.panlab.com/	N/A

(*Continued on next page*)

Continued

REAGENT OR RESOURCE	SOURCE	IDENTIFIER
Other		
Optic fiber implants	https://www.thorlabs.com/	CFMLC52L02
Laser cables for optogenetics	https://www.thorlabs.com/	M106L01
Guide cannula 5.8mm	http://www.bilaney.com/plastics-one/	C313G/spc
Cannula dummy cap	http://www.bilaney.com/plastics-one/	C313DC/1/spc
Internal cannula	http://www.bilaney.com/plastics-one/	C313I/spc
473nm Blue Laser Generator	http://www.dreamlasers.com	SDL-473-XXXT
Programmable Pulse Stimulator (A.M.P.I.)	http://www.ampi.co.il	Master-9

CONTACT FOR REAGENT AND RESOURCE SHARING

Requests for vGATE tools should be directed to mazahir.t.hasan@gmail.com. For other tools and reagents, contact v.grinevich@dkfz-heidelberg.de.

EXPERIMENTAL MODEL AND SUBJECT DETAILS

Animals

Anatomical, electrophysiological, optogenetic and behavioral studies were performed with female Wistar rats purchased from Janvier, France (8-10 weeks old on arrival at our facility). All rats were housed under standard conditions with *ad libitum* access to food and water. All experiments have been approved by the German Animal Ethics Committee of the Baden Württemberg (licenses numbers 35-9185.81/G-24/12, 35-9185.81/G-26/15 and 35-9185.81G-102/17) and the French Ministry of Research (APAFIS#3668-2016011815445431 v2).

METHOD DETAILS

The vGATE system

Generation and cloning

We engineered a synthetic c-*fos* promoter linked to its first exon (Exon 1; (Schilling et al., 1991) with ATGs in the Exon 1 converted to TTGs by site directed mutagenesis and heptamerized tetracycline (tet) operators, $(tetO)_7$, added upstream of it. These operators drive the expression of a humanized reverse tet transactivator (rtTA) (Dogbevia et al., 2015) named $(tetO)_7$-$\mathbf{P}_{fos}$-rtTA. The entire cassette was subsequently cloned in a plasmid to produce recombinant adeno-associated viruses (rAAVs) packaged with serotype 1 and 2 (Dogbevia et al., 2015) to generate Virus1 (rAAV-$(tetO)_7$-$\mathbf{P}_{fos}$-rtTA). Next, an AAV equipped with bidirectional tet promoter (P_{tet}bi) expressing the Cre-recombinase was linked to a genetically-encoded calcium indicator (YC3.60) (Virus 2, rAAV-$\mathbf{P}_{tet}$bi-Cre/YC3.60, (Lütcke et al., 2010)). As the last component of our viral technique (Virus 3), we generated rAAVs under the OT promoter to drive expression of hChR2-mCherry, GFP or hM4D(Gi)-mCherry (Eliava et al., 2016; Grund et al., 2017) in a Cre-dependent manner. The entire system comprising rAAV-$(tetO)_7$-$\mathbf{P}_{fos}$-rtTA (Virus 1), as the key element of the system, combined with rAAV-$\mathbf{P}_{tet}$bi-Cre/YC3.60 (Virus 2) and the Cre-dependent 'FLEX' viruses (Virus 3, see Key Resources Table) for '**v**irus-delivered, **G**enetic **A**ctivity-dependent **T**agging of cell **E**nsembles' or vGATE. In the vGATE method, the c-*fos* promoter drives rtTA expression only when neurons are activated. The rtTA generated by transient c-*fos* promoter activity binds to the upstream $(tetO)_7$ only in the presence of Dox. This way, the rtTA drives its own expression, thus establishing an autoregulatory loop, even when the induced c-*fos* promoter activity declines to baseline levels as neuronal activity subsides. Therefore, only in the presence of Dox, the rtTA can activate the expression of the bidirectional tet promoter ($\mathbf{P}_{tet}$bi) to express any gene of choice, for example, the Cre recombinase, for permanent tagging of activated cells via a Cre-dependent FLEX cassette.

Validating in cultured neurons

Dissociated rat hippocampal cultured neurons were treated with two viruses (rAAV-$(tetO)_7$-$\mathbf{P}_{fos}$-rtTA + rAAV-$\mathbf{P}_{tet}$bi-Cre/tdTOM) for two weeks. Afterward, cells were treated with bicuculline (bic) for 20 min and replaced with fresh medium supplemented with Dox (1 μg/ml) for 24 h. Only in the presence of bic and Dox, a strong rtTA signal was detected by immunohistochemistry (Figure S1, bottom panel). By live fluorescence imaging of fixed cells, rtTA-dependent tdTOM expression was also clearly detected in +bic/+Dox treated cells. In a few neurons, however, tdTOM expression was also detected under condition of –bic/+Dox. This is likely a result of spontaneous activity in some neurons. Western blot analyses validated tdTOM expression (Figure S1).

Novelty of the method

We describe here a genetic method (vGATE) that uses c-*fos* promoter elements to drive expression of a reverse tetracycline transactivator (rtTA). The key novelty of our method is that the 'recording period' can be rapidly opened within a few hours by a single

intraperitoneal Dox injection before the tagging of activated neurons. In previous methodological studies, we carefully characterized, both *ex vivo* and *in vivo*, the regulation of Dox-controlled gene expression by rtTA expressed under a human synapsin promoter (Dogbevia et al., 2015; Dogbevia et al., 2016). We determined an optimal Dox concentration for *in vivo* application, and the time course of gene activation and inactivation by a single intraperitoneal Dox injection. In our previous studies, we found that the bidirectional Tet promoter ($\mathbf{P}_{tet}$bi) has highly reduced leakiness (Dogbevia et al., 2016) compared to the uni-directional Tet promoter ($\mathbf{P}_{tet}$) (Dogbevia et al., 2015). Indeed, $\mathbf{P}_{tet}$ is very leaky (Dogbevia et al., 2015), due to its close proximity close to an inverted terminal repeat (ITR) of AAV, which appears to have intrinsic enhancer-like activity (Dogbevia et al., 2015). This raises potential concerns that AAVs equipped with a uni-directional tet promoter ($\mathbf{P}_{tet}$) might be leaky enough to non-specifically tag non-engram cells. With these considerations, we characterized the vGATE method both *ex vivo* and *in vivo*. The vGATE method is very tightly controlled and highly flexible; different combination of gene modules in rAAVs can be simultaneously delivered to the targeted brain region(s). With this approach, we performed selective and cell-type-specific tagging of OT neurons activated during contextual fear learning and expressed in the tagged neurons gene(s)-of-interest for pharmacogenetic and optogenetic manipulations, while others might easily target different neuronal populations.

Different methods exist to induce time-dependent conditional protein expression, namely the TetTag (Reijmers et al., 2007) and the TRAP (Guenthner et al., 2013) methods. The TetTag method drives tTA expression under c-*fos* and animals have to be fed Dox to keep the system inactive. However, to open the recording period, TeTag animals have to be switched to diet without Dox for a few days before performing learning-dependent neuronal labeling. However, this non-recording period of a few days is sensitive for non-specific labeling of neurons. In the case of vGATE, the presence of Dox is requested to activate detectable gene expression within a few hours and achieved the maximum expression after 24 h (Dogbevia et al., 2015, 2016) and gene expression is switched-off in 6 days (Dogbevia et al., 2016). In a previous systematic study (Dogbevia et al., 2016), we found similar time course of 6 days to "re-activate" (with the tTA system) by Dox removal and "activate" (with the rtTA system) gene expression by Dox addition. The discrepancy for 3 days for Dox clearance by others using the tTA system is likely due to the sensitivity of the detection method; we used a highly sensitive reporter, the firefly luciferase, for gene expression assay as a proxy for Dox clearance from the brain (Dogbevia et al., 2016), while other labs use GFP (Liu et al., 2012), which are much less sensitive.

In the TRAP method, the inducer, tamoxifen, is needed to facilitate release cytoplasmic ER-Cre for transport to the nucleus to permanently tag neurons by Cre/loxP dependent gene modules. However, TRAP is in itself leaking, since it is known that a fraction of ER-Cre can already move to the nucleus even without tamoxifen treatment. There is even a bigger concern that tamoxifen as a selective estrogen modulator might interfere with various estrogen-sensitive cell types in the brain. The use of tamoxifen is especially critical for OT neurons, which are sensitive for estrogens (Somponpun and Sladek, 2003) and tamoxifen itself triggers the activity of the OT gene promoter (Koohi et al., 2005). Finally, tamoxifen induces c-*fos* expression in OT neurons (F.A. and V.G., unpublished data), thereby precluding the use of the ER-Cre method for this particular neuron type. With our novel vGATE technique, we achieved highly specific labeling of OT neurons and precise temporal control, which we believe to be superior to other comparable, c-*fos* based tagging methods. Therefore, the development of the vGATE method should be able to overcomes the key inherent concerns of the previous two main strategies to induce time-dependent conditional protein expression.

Infecting rat hypothalamic neurons *in vivo* with rAAVs

Cloning of the OT promoter, as well as the production and purification of rAAVs, has been previously described (Knobloch et al., 2012). rAAV genomic titers were determined with QuickTiter AAV Quantitation Kit (Cell Biolabs, San Diego, California, USA) and RT-PCR using the ABI 7700 cycler (Applied Biosystems, California, USA). rAAVs titers were between 10^{10} - 10^{11} genomic copies per 1 μl. Infection of OT neurons was achieved by complementing the two viruses indicated above by an rAAV, driving genes of interest (Venus, hChR2-mCherry, FLEX-GFP, FLEX-hM4D and hM4D(Gi). A cocktail of the three rAAVs (i.e., rAAV-$(tetO)_7$-$\mathbf{P}_{fos}$-rtTA, rAAV-$\mathbf{P}_{tet}$bi-Cre/YC3.60, and rAAV-$\mathbf{P}_{OT}$-Venus) was injected bilaterally into the hypothalamic nuclei, the PVN and SON, using a previously described protocol (Knobloch et al., 2012).

Neuroanatomy

To trace, label and manipulate the hypothalamus-amygdala connections, rAAVs expressing vGATE viruses were injected into the PVN and SON. Alternatively, CAV2-Cre was injected into the SON, while the Cre-dependent "FLEX" $\mathbf{P}_{OT}$-hM4D(Gi) rAAV was injected into the PVN to specifically label and manipulate parvOT neurons. After transcardial perfusion with 4% PFA, brains were sectioned and stained with antibodies against OT, vGluT2, GFP, FG and dsRed. Images for qualitative and quantitative analyses were taken on the confocal microscope Leica SP5.

BEHAVIOR

Salt loading

To validate the vGATE system *in vivo*, we performed salt-loading (SL) as a stimulus to activate c-*fos* expression in OT neurons (Katoh et al., 2010). Here, we used a mixture of two rAAVs (rAAV-$(tetO)_7$-$\mathbf{P}_{fos}$-rtTA and rAAV-$\mathbf{P}_{OT}$-Venus) and co-injected them unilaterally into the SON of rats. The animals were divided into four groups (n = 3/group): Group 1 (Untreated control animals (-Dox/-SL)), Group 2 (-Dox/+SL, 7 days with SL (2% NaCl in drinking water), Group 3 (+Dox/-SL, normally hydrated animals, which received single Dox i.p.

injection) and Group 4 (+Dox/+SL, animals received a single i.p. injection of Dox on the 5th day of SL and were kept under SL for 2 more days before being sacrificed). Expression patterns of the individual groups are depicted in Figure 1D.

Contextual fear conditioning and optogenetics

We used a mixture of three vGATE viruses as depicted (Figure 1A). Two weeks after the viral infection, adult female rats were subjected to either a 3-day (single fear) or 15-day (double fear) contextual fear conditioning protocol, comprising a conditioning session on the first 2 days and a recall session on the 3rd day (Figure 2A). All sessions lasted for 20 min with 7 random foot shocks (1.6mA, 1 s) dispersed between the 10th and 17th min of protocol during the fear conditioning session.

As shown in Figure 2A, animals were treated with Dox (5 mg/kg b.w., i.p.) 24 h after the 2nd day of fear acquisition to tag OT neurons activated during fear expression. The experimental group (animals injected with the vGATE system: rAAV-(tetO)$_7$-**P**$_{fos}$-rtTA + rAAV-**P**$_{tet}$bi-Cre/YC3.60 + rAAV-**P**$_{OT}$-FLEX-hChR2-mCherry) received another re-conditioning session (double fear), two weeks after Dox injection and recovery, for one day, to achieve a higher level of freezing (above 50 s/min) and 24 h later were tested for the recall of fear behavior with blue light (BL) illumination of the CeA. The CeA was illuminated bilaterally with BL (473 nm, 10 ms pulse, 20 s duration, 30 Hz) via 200 μm optical fibers from Thorlabs (BFL37 200) at the 10th min of the recall session. The rats were evaluated for freezing responses and freezing durations were measured through freezing software (Panlab) and manually through an offline video in addition. In Figure 2C, the 2 different graphs display the average freezing time per minute in the corresponding groups (OT^{Constitutive} and OT^{vGATE}) before and after BL illumination. The black bars (control) show the average freezing times in minutes immediately prior to the BL illumination, whereas the gray bars (BL) indicate the average freezing times per minute during the minute in which the BL-induced onset of the unfreezing effect (i.e., where the first signs of mobility appear). All groups of animals were sacrificed 90 min after the start of the optogenetic session.

Estimation of the estrous cycle

To monitor ovarian cycle, we performed vaginal smear collections. Animals in metestus, proestrus and estrus phases were excluded from experiments and reintroduced once they reached diestrus.

Pharmacogenetics (DREADD) and fear extinction in Contexts A and B

In this experiment, animals were subjected to a series of fear conditioning and fear extinction paradigms that we performed in two different contexts (A and B). For this purpose, two visually distinct contextual fear conditioning chambers were used, which were comparable in size, shape of the grid and power of the electrical shocks (1.6 mA). The chambers were located in two different institutes (chamber A, Max Planck Institute of Medical Research (MPI), Heidelberg, Panlab; chamber B, Interdisciplinary Neurobehavioral Core (INBC), Heidelberg, Med Associates) and the animals were exposed to them for the first time in both cases. Animals were injected with **P**$_{OT}$-hM4D(Gi) (OT^{Constitutive}) or rAAV-(tetO)$_7$-**P**$_{fos}$-rtTA, rAAV-**P**$_{tet}$bi-Cre/YC3.60 + rAAV-**P**$_{OT}$-FLEX-hM4D(Gi) (OT^{vGATE}) and subjected to the experimental procedure after recovery and handling. For the contextual fear conditioning, animals were placed in a fear conditioning chamber (Panlab, Harvard Apparatus) with a metal grid for application of electrical foot shocks (1.6 mA). We used a 3-day fear conditioning protocol (2 days shock, 1 day testing, each 20 min) to fear condition the animals. On the first two days, the animals, after a 10 min habituation period, received 7 electrical foot shocks within 7 min (randomly distributed, on average 1 shock per min), followed again by 3 min without shocks. For activation of the viral system, animals received Dox (5 mg/kg b.w., i.p.) on day 3 of the fear conditioning (24 h after the 2nd shock day of the first round of fear conditioning). On the fourth day (24 h after injection), animals were placed in the same box for 20 min without any shocks. The experiment was recorded with a video camera and sensors in the grid measured the total movement of the animals during the procedure. After a 2-week break (Dox clearance and viral expression) animals were exposed to the box in a second session. Here, we used a 5-day fear extinction protocol with one re-conditioning day (in order to maintain a high level of freezing (above 50 s/min) and identical in all groups) and 4 testing days. Due to the 2-week interval in between the two rounds, animals received electrical shocks on the first day (recall session), followed by 4 days on which the animals were placed in the box for 40 min each without any shocks (extinction sessions). Animals expressing the hMD4D(Gi) receptor in all OT neurons (OT^{Constitutive}) or tagged OT neurons (OT^{vGATE}) received a daily injection of Clozapine (3 mg/kg bw i.p., Tocris Bioscience, Bristol, UK, dissolved in 1xPBS) 30 min prior to placing them into the Context A chamber. The control groups (OT^{Constitutive} and OT^{vGATE}) received the same volume of 0.9% NaCl solution. After the first round of fear extinction in Context A, animals were transferred to Context B. Here, an additional round of fear extinction was performed, which comprised two shock sessions followed by 4 consecutive daily extinction sessions, 40 min prior to which the animals received a daily injection of CNO (Figure 4A), whereas the control group received the same volume of 0.9% NaCl solution 40 min prior to the start of the session. All animals were sacrificed and perfused 90 mins after the fear conditioning session in Context B. In the two control groups, the time of freezing in both contexts was almost identical (Figure S4B). Therefore, for the sake of simplicity, only the freezing time of OT^{Constitutive} and OT^{vGATE} control groups in Context A is depicted in Figures 4B1 and 4B2.

Context A versus Context A - mapping of OT neuronal activity via GFP followed by immunostaining for c-fos

Animals were injected in all nuclei with the vGATE system (rAAV-(tetO)$_7$-**P**$_{fos}$-rtTA + rAAV-**P**$_{tet}$bi-Cre/YC3.60 + rAAV-**P**$_{OT}$-FLEX-GFP) and subjected to the 3-day contextual fear conditioning paradigm after recovery and handling. Following the first two shock sessions, animals received Dox (5 mg/kg b.w., i.p.) on the 3rd day of the fear conditioning paradigm. On the 4th day, animals were exposed to the fear conditioning chamber, this time without electrical shocks. Two weeks after the 1st round of fear conditioning in Context A (1), the animals were exposed to Context A(2) for a second time, where they underwent an additional session of fear conditioning. All animals were sacrificed 90 min after the beginning of the test session in Context A (2).

Context A versus Context B - mapping of OT neuronal activity via GFP followed by immunostaining for c-fos

Animals were injected with the vGATE system into all nuclei (rAAV-$(tetO)_7$-$\mathbf{P}_{fos}$-rtTA + rAAV-$\mathbf{P}_{tet}$bi-Cre/YC3.60 + rAAV-$\mathbf{P}_{OT}$-FLEX-GFP) and subjected to the 3-day contextual fear conditioning paradigm after recovery and handling. Following the first two shock sessions, animals received Dox (5 mg/kg b.w., i.p.) on the 3rd day of the fear conditioning paradigm. On the 4th day, animals were exposed to the fear conditioning chamber, this time without electrical shocks. After the 1st round of fear conditioning in Context A, the animals were transferred to Context B, there they underwent an additional session of fear conditioning in analogy to that in Context A, one week later. All animals were sacrificed 90 min after the beginning of the test session in Context B. This point in time was chosen as it is well established that the c-*fos* protein has its peak expression at around 90 min after the initial activation of OT neurons. To label all neuroendocrine cells protruding beyond the blood brain barrier (most importantly, magnOT neurons), animals received a single injection of Fluorogold, Santa Cruz Biotechnology, Dallas, 15 mg/kg bw i.p. dissolved in 1xPBS, 7 days prior to perfusion (Eliava et al., 2016).

DREADD-based inhibition of parvocellular OT neurons of the PVN in Context B

For this experiment, rats were injected with the retrogradely spreading rAAV-CAV2-Cre into the SON and rAAV-$\mathbf{P}_{OT}$-FLEX-hM4D into the PVN to specifically express hM4D in parvOT neurons of the PVN, in analogy to our previous study (Eliava et al., 2016). After one week of recovery, animals were handled 10 min per day for 1 week. In the 3rd week after injection, animals were subjected to fear conditioning in Context A in analogy to Figure 2A. Following the successful fear conditioning in Context A, animals were transferred to Context B, where another round of fear conditioning was performed (see Figure 4A). Thirty minutes prior to the experiment of day 3 (exposure day), the three experimental animals received an i.p. injection of clozapine-N-oxide CNO (3mg/kg bw i.p., Tocris Bioscience, Bristol, UK, dissolved in 1xPBS) to inhibit the activity of parvOT neurons. The control animals received the same volume of vehicle (0.9% NaCl). Ninety minutes after the start of the session, the animals were euthanized with isoflurane and perfused to collect the brains. Brain sections containing SON were used for immunohistochemical staining for OT and c-*fos*. Quantitative analysis of OT versus c-*fos* expressing cells was performed and the results are demonstrated (in Table S4**)**. Naive animals and animals that were only subjected to Context A served as controls.

Stereotaxic injection of viral vectors and implantation of optic fibers

Injection of viral vectors into the rat brain was performed in analogy to Knobloch et al., 2012. If not indicated otherwise, all hypothalamic nuclei were injected bilaterally using the following coordinates: SON (M-L ± 1.6mm, A-P −1.4mm, D-V −9.0mm), PVN (M-L ± 0.3mm, A-P −1.8mm, D-V −8.0mm) and AN (M-L ± 1.2mm, A-P −2.0mm, D-V −8.5mm). Point of origin for the coordinates was Bregma and the Z level difference of Bregma and Bambda did not exceed 0.1mm (Cetin et al., 2006). Injection volume per injection site was 300 nL (either single virus or cocktail), while all viruses used were in the range of 10^{12} −10^{13} genomic copies per ml. For the implantation of optic fibers into the CeA, we used the following coordinates: M-L ± 3.9, A-P −2.5, D-V −8.0 while the optic fibers had a length of 8.5 mm.

Ex Vivo Electrophysiology

Amygdala

Horizontal slices preparation. Animals were anaesthetized with an intraperitoneally administered mixture ketamine/xylazine (Imalgene 90 mg/kg, Rompun, 10 mg/kg). Transcardial perfusion was then performed using one of the following artificial cerebro-spinal fluids (ACSFs) dissection solutions. For rats between 10 and 11 weeks old, an ice-cold NMDG based ACSF was used containing (in mM): NMDG (93), KCl (2.5), NaH_2PO_4 (1.25), $NaHCO_3$ (30), $MgSO_4$ (10), $CaCl_2$ (0.5), HEPES (20), D-Glucose (25), L-ascorbic acid (5), Thiourea (2), Sodium pyruvate (3), N-acetyl-L-cysteine (10), Kynurenic acid (2). The pH was adjusted to 7.4 using HCl 37%, after bubbling in 95% O_2 and 5% CO_2 gas; bubbling was maintained throughout the duration of use of the various ACSFs. Following decapitation, the brain was swiftly transferred into the same ice-cold ACSFs dissection solution as for transcardial perfusion, and 350 μm thick horizontal slices containing the CeA were obtained using a Leica VT1000s vibratome. After slicing, brain slices were hemidissected and placed in a room-temperature holding chamber with normal ACSF, for a minimum of 1 h before the conduction of any experiments. Slices of 10-11 weeks old rats were placed in 35°C NMDG ACSF for 10 min before transferring them to the holding chamber at room temperature. Normal ACSF, also used during experiments, was composed of (in mM): NaCl (124), KCl (2.5), NaH_2PO_4 (1.25), $NaHCO_3$ (26), $MgSO_4$ (2), $CaCl_2$ (2), D-Glucose (15), adjusted for pH values of 7.4 with HCl 37% and continuously bubbled in 95% O_2 and 5% CO_2 gas. All ACSFs were checked for osmolarity and kept for values between 305-312 mOsm/L. For electrophysiology experiments, slices were transferred from the holding chamber to an immersion recording chamber and superfused at a rate of 2 mL/min with normal ACSF unless indicated otherwise.

CeM Neurons recordings. Pipettes were filled with an intracellular solution containing (in mM): KCl (150), HEPES (10), $MgCl_2$ (4), $CaCl_2$ (0.1), BAPTA (0.1), ATP Na salt (2), GTP Na salt (0.3). pH was adjusted to 7.3 with KOH and osmolality checked to be between 290-295 mOsm/L, adjusted with sucrose if needed. All cells were hold at a membrane potential of −70 mV. Series capacitances and resistances were compensated electronically throughout the experiments using the main amplifier. Average IPSC frequencies were calculated in 20 s windows, chosen for light stimulation at maximal effect, as determined by the maximal slope of the cumulative plot of the number of currents using SigmaPlot 11.0. Baselines and recovery IPSC frequencies were measured at the beginning and end of each recording. Z-score values were calculated by subtracting the average baseline IPSC frequency established over 70 s at the recording beginning from individual raw values and by dividing the difference by the baseline standard deviation. Optical BL illumination of CeL OT axons expressing hChR2 was performed using light source X-Cite® 110LED from Excelitas Technologies through a

GFP filter, controlled with a Clampex-driven TTL pulse for 20 s at 30Hz with 10ms pulses. To quantify the pharmacological blockade (NBQX or dOVT) of the BL illumination on the CeM IPSC frequencies, a ratio was first calculated between basal and BL modified IPSC frequencies minus one and that for each recording neuron, in order to obtain the BL effect. Second, the percentage of the remaining BL illumination after pharmacological blockade was obtained by dividing the BL effect after and before drug perfusion. This is reported as ΔBL/BL0 (%) in Figure 3B2.

SON OT neurons recordings. For this experiment, rats received viral injections of 300 nL vGATE with rAAV-$\mathbf{P}_{OT}$-FLEX-GFP as virus 3 or rAAV-$\mathbf{P}_{OT}$-mCherry bilaterally into the SON. Thus, OT engram cells were labeled in green, while OT non-engram cells in red. Recording pipettes were filled with an intracellular solution containing (in mM): $KMeSO_4$ (125), $CaCl_2$ (2), EGTA (1), HEPES (10), $ATPNa_2$ (2), GTPNa (0.3). pH was adjusted to 7.3 with KOH and osmolality checked to be between 290-295 mOsm/L, adjusted with sucrose if needed. After whole-cell patch-clamp of identified OT neuron, the following parameters were recorded: access resistance, membrane capacitance, resting potential, spontaneous EPSC amplitude and frequency, response to current injection (0 to 150 pA for 500ms, with steps of 25 pA).

Optical stimulations. Optical BL illumination of CeL OT-ergic axons expressing hChR2 was performed using light source X-Cite® 110LED from Excelitas Technologies through a GFP filter, controlled with a Clampex-driven TTL pulse for 20 s at 30Hz with 10ms pulses.

Analysis of effect of blue light. Average IPSC frequencies were calculated in 20 s windows, chosen for light stimulation at maximal effect, as determined by the maximal slope of the cumulative plot of the number of currents using SigmaPlot 11.0. Baselines and recovery IPSC frequencies were measured at the beginning and end of each recording. Z-score values were calculated by subtracting the average baseline IPSC frequency established over 70 s at the recording beginning from individual raw values and by dividing the difference by the baseline standard deviation.

Pharmacological assays. To quantify the pharmacological blockade (NBQX or dOVT) of the BL illumination on the CeM IPSC frequencies, a ratio was first calculated between basal and BL modified IPSC frequencies minus one and that for each recording neuron, in order to obtain the BL effect. Second, the percentage of the remaining BL illumination after pharmacological blockade was obtained by dividing the BL effect after and before drug perfusion. This is reported as ΔBL/BL0 (%) in Figure 3B2.

Histology

Animals were perfused through the heart with 1x PBS, followed by 4% paraformaldehyde to fixate the tissue and extracted brains were post-fixed overnight.

The hypothalamus

Brain sections (50 μm) were collected by vibratome slicing and immunohistochemistry was performed with the following antibodies: chicken anti-GFP (Abcam; 1:10000), anti-OT (PS38, 1:1000; mouse; kindly provided by Harold Gainer); anti-c-*fos* (1:1000; rabbit; Santa Cruz Biotechnology), anti-Fluorogold (1:1000, guinea pig, Protos Biotech) and anti-DsRed (1:1000; rabbit; Clontech). GFP signal was enhanced by FITC-conjugated IgGs, hChR2-mCherry signals by CY3-conjugated antibodies and, for different experiments, other markers were visualized by FITC-conjugated; CY3-conjugated or CY5-conjugated antibodies (1:500; Jackson Immuno-Research Laboratories). Nuclei of cells were visualized with DAPI (1:1000; Roche). All images were acquired on a confocal Leica TCS SP5 and Zeiss LSM5 microscopes; digitized images were analyzed using Adobe Photoshop. To quantify vGATE-assisted labeling of cells, we counted all OT-, hChR2-immunoreactive neurons in the SON and PVN (8-150 neurons/section dependent on the anterior-posterior Bregma level) in 5 animals (3 sections for SON and PVN) with the stereotactic rostro-caudal Bregma coordinates (PVN: −1.5, −1.8, and −2.0 mm; SON: −1.1, −1.4, and −1.7 mm). Statistical significance was determined by Student's test for colocalization experiments, OT axon morphology and statistical analysis was performed with Prism 5 (Mac OS X). Results are presented as mean ± SEM.

The amygdala

Staining for the vesicular glutamate transporter vGluT2. Selected sections containing the CeA were then immunolabeled for darkfield and brightfield microscopy. For darkfield fluorescent staining, the cocktail containing different combinations of primary antibodies: anti-vGluT2 (1:2000; rabbit; SySy), anti-OT (1:2000, mouse), anti-DsRed (1:1000; rabbit; Clontech), anti-GFP (1:10,000, chicken, Abcam) were used. The named antigens were detected using appropriate secondary antibodies conjugated with fluoropores of various excitation ranges (Alexa488, Alexa459, Alexa680, Thermofisher). All tissue samples, labeled with fluorescent markers were imaged using Leica SP5 CLSM, and digitized using Adobe Photoshop software. To evaluate the CeL vGluT2 expression level, we processed the tissue for triple GFP, OT and vGluT2 immunolabeling in rats of $OT^{Constitutive}$ and OT^{vGATE} groups. In total, 2000 varicosities per animal group were counted and visually examined to detect the presence of double GFP-vGluT2 signals. The final numbers were computed as a proportion (percentage). For brightfield immunostainings, secondary antibodies conjugated to biotin were used. Final visualization of labeling was carried out with standard ABC HRP Kit (Vector) using DAB as a chromogene. The bright microscopic images were captured using a Nikon Eclipse microscope E200 (Software: Nikon NIS-Elements Version 4.30). We analyzed the number of varicosities and the mean length of OT fiber segments residing in the CeL to trace possible structural changes. Altogether, 72 coronal planes of 6 rats in the OT^{vGATE} group (and 7 in control) were used for this type of analysis. Length of GFP-positive fibers and number of axonal varicosities were measured and counted using free hand tracing and touch-count options in the latest version of ImageJ software (NIH). All statistics were processed in group-specific comparisons between two groups (t-Test, $p < 0,05$, one-tailed), always in one and the same plane of CeL (Bregma: −2,4 to −2,8).

Staining for Somatostatin, Corticotropin-Releasing-Hormone and c-fos. For triple labeling of c-Fos, (Abcam, 1: 1 000), CRH (Peninsula Labs., 1: 10 000), and SOM (Chemicon, 1:500), combination of DAB technique (c-Fos detection) and fluorescent labeling (for CRH and SOM) was applied. First, the sections were incubated with c-Fos antibody and developed using biotinylated secondary antibody, ABC kit (Vector) and conventional DAB detection protocol. Second, the c-Fos DAB-developed tissue was processed for anti-gene retrieval procedure via "boiling" sections in Tris Buffer Saline pH10 at 95°C for 1h for optimal detection of CRH and SOM in the somas of CeA neurons. Afterward all primary and secondary labeling steps for CRF and SOM detection were performed as described. The actual figures represent digital overlays of confocal bright-field scans of DAB-detected c-Fos and florescent-labeled CRH and SOM. All images were obtained using Leica SP5 CLSM (Imaging Facility, DKFZ, Heidelberg).

Fluorogold treatment and visualization. To discriminate between magno- and parvocellular OT neurons, animals received a single injection of Fluorogold (Santa Cruz Biotechnology, Dallas, 15 mg/kg bw i.p.) 7 days prior to the perfusion. Brain sections were stained with a primary antibody for Fluorogold (Guinea pig anti-FG, dilution 1:1000, Protos Biotech Corp, New York) and Fluorogold immunosignal was visualized by secondary antibodies conjugated with CY3 (Donkey anti-rabbit, dilution 1:500, Jackson Immuno Research, Newmarket Suffolk, UK) or Alexa 680 (Alexa 680: Goat anti-guinea-pig, 1:1000, ThermoFisher Scientific, Waltham, Massachusetts). The colocalization of Fluorogold, OT (or c-*fos*) and GFP signals was quantified in the PVN (SON contains only magnOT neurons), (n = 10; 4 sections/brain). Quantitative analyses of parvo- and magnocelluar OT cells expressing GFP are presented in Table S6.

Retrobeads infusion. For the retrograde labeling of vGATE projections terminating in the CeA we used retrobeads from LumaFluor. We used the following coordinates for infusion in accordance with Bregma: (CeA left/right): ML: ± 4.0 mm, AP: 2.5 mm and DV: −8 mm, without angle and an injection volume of 140 nl.

Cannula implantation. Animals were bilaterally implanted with guide cannulas for direct intra-central lateral amygdala infusions. We used the C313G/Spc guide metallic cannulae (Plastics one, VA, USA) cut 5.8 mm below the pedestal. For this purpose, animals were deeply anesthetized with 5% isoflurane and their heads were fixed in a stereotaxic fame. The skull was exposed and two holes were drilled according to coordinates that were adapted from a rat brain atlas (2.3 mm rostro-caudal; 4 mm lateral; 7.5 mm dorso-ventral relative to bregma) by comparing the typical bregma-lambda distance (9 mm) with the one measured in the experimental animal. Two screws were fixed to the caudal part of the skull in order to have an anchor point for the dental cement. Acrylic dental cement was finally used to fix the cannula and the skin was sutured. CNO infusion (1 μm) occurred at 20 nl/s with a final infusion volume of 100nl per CeA.

Measurement of Plasma ot Concentrations

Plasma preparation for LC-MS/MS analysis

50 pmol of D5-oxytocin internal standard was added to 200 μl of lithium heparin plasma. Plasma was acidified with an equal volume of 5% H_3PO_4 (v/v) and was centrifuged (14,000 x g, 5min). The resulting supernatants were collected and adjusted to 1% H_3PO_4 with H_2O prior to solid phase extraction (SPE). The SPE procedure was performed with a positive pressure manifold (Thermo Electron). OASIS HLB SPE-cartridges (1cc, 30mg, Waters, Guyancourt France) were first activated with 1ml of acetonitrile (ACN) and then washed with 1ml of H_2O 99% / H_3PO_4 1% (v/v). The sample was loaded and the SPE-cartridge and the cartridge was washed with 1ml of H_2O 99% / H_3PO_4 1%. After a 1ml wash with H_2O/formic acid 0.1% (v/v) and with 1 mL of ACN 5% / H_2O 94.1% / formic acid 0.1% (v/v/v), elution was performed with 500 μl of acetonitrile 60% / H_2O 40% (v/v). Eluates were collected and dried under vacuum prior to MS analysis (see below).

LC-MS/MS instrumentation and analytical conditions

LC-analyses were used to determine the presence of oxytocin in the selected reaction monitoring mode (SRM). Analyses were performed on a Dionex Ultimate 3000 HPLC system (Thermo Scientific, San Jose, CA, USA) coupled with a triple quadrupole Endura (Thermo Scientific). The system was controlled by Xcalibur v. 2.0 software (Thermo Scientific). Extracted plasma samples were solubilized in 100 μl of H_2O/formic acid 0.1% (v/v) and 20 μl of the solution were loaded into an Accucore RP-MS column (ref 17626-102130; 100 × 2.1 mm 2.6 μm, Thermo Electron) heated at 35°C. Oxytocin and D5-oxytocin elutions were performed by applying a linear gradient of buffers A/B. Buffer A corresponded to H_2O 98.9% / formic acid 0.1% (v/v), whereas buffer B was ACN 99.9%/ formic acid 0.1% (v/v). A linear gradient of 20%–95% of solvent B at 400 μL/min over 2.5min was applied followed by a washing step (0.5min at 95% of solvent B) and an equilibration step (1min of 20% of buffer B). Qualitative analysis and quantification were performed in SRM using an Endura triple quadrupole mass spectrometer and deuterated internal standards. For ionization (positive mode), 3500V of liquid junction voltage and 350°C capillary temperature was applied. The selectivity for both Q1 and Q3 was set to 0.7Da (FWHM). The collision gas pressure of Q2 was set at 2mTorr of argon. For oxytocin and D5-oxytocin, the selection of the monitored transitions and the optimization of the collision energy were preliminarily and manually determined. The transitions and the corresponding collision energies (CE) used for SRM were the following: m/z 504.2 → m/z 285.1 (CE = 15.9 eV), m/z 504.2 → m/z 487.2 (CE = 11.9 eV) and m/z 504.2 → m/z 495.7 (CE = 10.2 eV) for oxytocin with 2 charges; m/z 506.8 → m/z 290.2 (CE = 16.2 eV), m/z 506.8 → m/z 492.9 (CE = 12.9 eV) and m/z 506.8 → m/z 498.3 (CE = 10.7 eV) for D5-oxytocin (with 2 charges). Identification of the compounds was based on precursor ion, selective fragment ions and retention times obtained for oxytocin and D5-oxytocin internal standard. Quantification of oxytocin was done using the ratio of daughter ion response areas of the D5-oxytocin.

Measuring of signal intensity via Fiji (ImageJ)

To compare the signal intensity of neurons or axonal terminals we used the Image Intensity Processing function of ImageJ. Following the detailed description of the analysis (https://imagej.net/Image_Intensity_Processing), we converted the .lif files from the confocal microscope into TIFF images and opened them with ImageJ. For the signal intensity analysis, we used the raw data with no contrast modifications or gamma corrections. The freehand tool was used to delineate the axonal segments and the average signal intensity of the region of interest (ROI) was calculated via the 'Analyze-Measure' function. For the analysis of signal intensity in axons, the entire length per section was used for the quantifications. The numeric values presented in the manuscript represent the output values of ImageJ obtained from the signal intensity measurements. To specifically identify OT-positive varicosities, we first calculated the average signal intensity (via 'Measure-Analyze') and standard deviation of all images included in the data analysis. Next, we used the freehand tool / line to delineate the ROI of the axonal segments and measured the signal intensity. We defined an axon to be 'OT-positive', if the signal intensity within the ROI exceeded the average signal intensity of the included images by at least 4-times the standard deviation. Axonal terminals that could not fulfill this criterion, were considered OT-negative.

QUANTIFICATION AND STATISTICAL ANALYSIS

Quantitative analysis (cell counting, c-*fos* expression and axon length) was performed in a double-blind manner using Fiji or Adobe Photoshop and a superimposed grid feature. Statistical analysis was performed using GraphPad Prism 7. $p < 0.05$ was considered as statistically significant (Tables S1–S6).

Neuron, Volume *103*

Supplemental Information

A Fear Memory Engram and Its Plasticity in the Hypothalamic Oxytocin System

Mazahir T. Hasan, Ferdinand Althammer, Miriam Silva da Gouveia, Stephanie Goyon, Marina Eliava, Arthur Lefevre, Damien Kerspern, Jonas Schimmer, Androniki Raftogianni, Jerome Wahis, H. Sophie Knobloch-Bollmann, Yan Tang, Xinying Liu, Apar Jain, Virginie Chavant, Yannick Goumon, Jan-Marek Weislogel, René Hurlemann, Sabine C. Herpertz, Claudia Pitzer, Pascal Darbon, Godwin K. Dogbevia, Ilaria Bertocchi, Matthew E. Larkum, Rolf Sprengel, Hilmar Bading, Alexandre Charlet, and Valery Grinevich

Supplemental Items

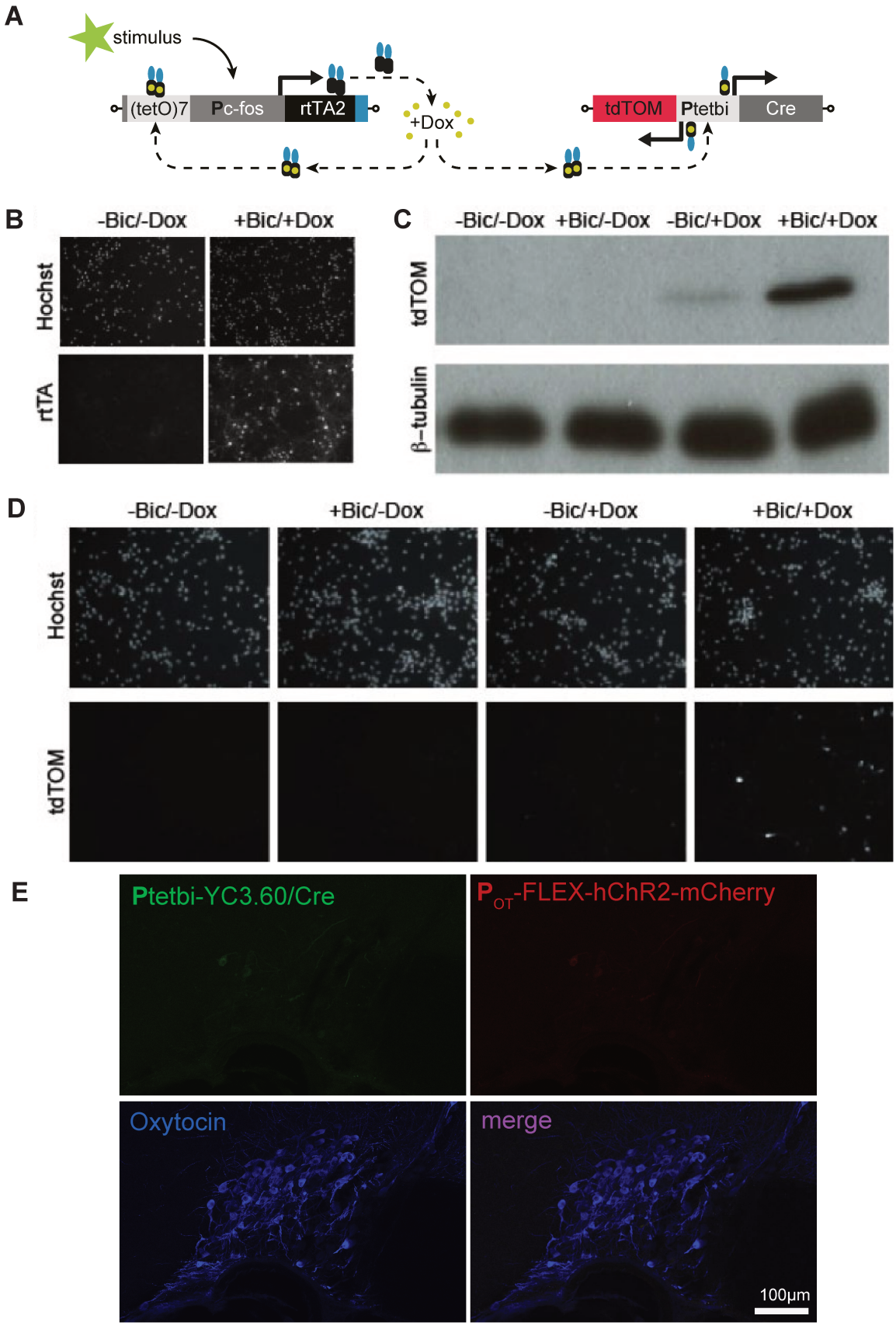

Figure S1

Figure S1 (corresponds to Figure 1). vGATE Validation in Cultured Neurons

In vitro characterization: **(A)** Two rAAVs, carrying a c-fos promoter equipped with an upstream heptamerized tet operators drives rtTA expression and a bidirectional tet promoter (**P**$_{tet}$bi) was used to simultaneously express two different genes; Cre recombinase and a red fluorescent protein tdTomato (tdTOM). As a proof-of-principle *in vitro*, we tested the vGATE method in cultured neurons. We generated two viruses (virus1 = rAAV-(tetO)$_7$-**P**$_{fos}$-rtTA and virus 2 = rAAV-**P**$_{tet}$bi-Cre/tdTOM), infected cultured neurons with the vGATE construct rAAV-(tetO)$_7$-**P**$_{fos}$-rtTA and investigated for activity-dependent c-fos promoter-mediated rtTA-dependent rtTA expression in the presence of Dox. **(B)** *In vivo:* In rat cultured neurons, in the presence of a biccuculine (Bic) and Dox, robust rtTA was expression was detected, but not without bic or Dox. Höchst staining shows all the neurons in the field of view. **(C)** Western blot analyses for tdTOM expression under -/+ Dox & -/+ Bic. **(D)** Similarly, only when both Bic and Dox were added to the culture medium, tdTOM was detected. *In vivo chactarization:* (**E**) Confocal images show the expression of rAAV-**P**$_{tet}$bi-YC3.60/Cre (green), rAAV-**P**$_{OT}$-FLEX-ChR2-mCherry (red) and oxytocin (blue) in the -Dox / - salt-loading (SL) condition.

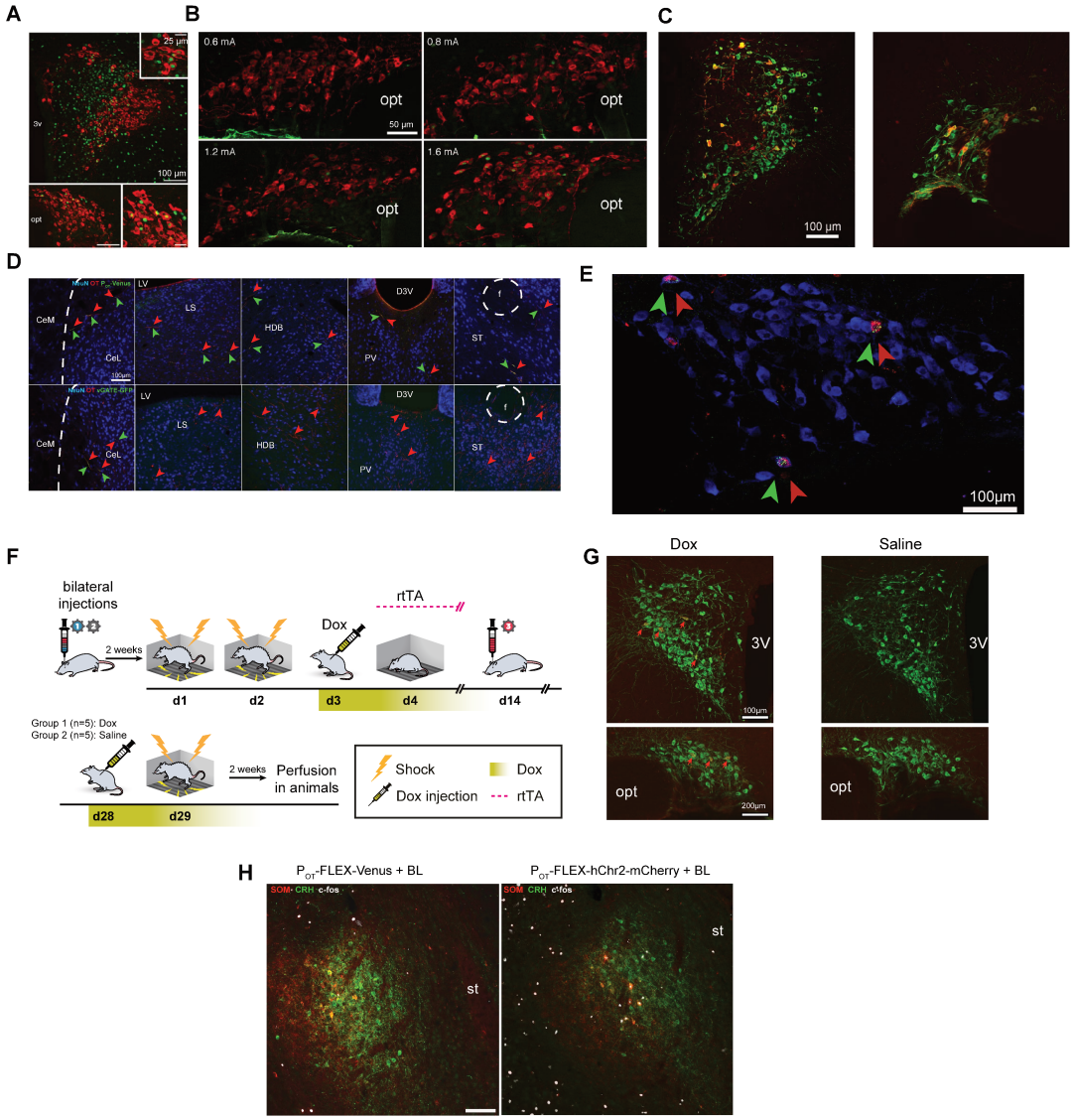

Figure S2

Figure S2 (corresponds to Figure 2). Contextual Fear Conditioning Induces c-fos Expression in OT Neurons.

(A) Representative images of PVN (top) and SON (bottom) of animals, sacrificed 90 mins after exposure to the fear conditioning chamber. Immunohistochemical staining against OT (red) and c-fos (green) revealed colocalization in a small fraction of neurons (see enlarged insets). **(B)** Panel shows the SON of animals exposed to fear conditioning with various shock intensities. Animals were sacrificed 90 mins after exposure (session without any shocks on day 3) to the fear conditioning chamber. Only fear conditioning with 1.6 mA shock reliably induced c-fos expression in OT neurons. OT (red), c-fos (green), asterisks indicate colocalization of c-fos and OT. (**C**) Confocal images show vGATE-labeled OT cells within the PVN and SON. The right image displays a few mCherry-tagged, non-OTergic cells above the SON. (**D**) The panel shows OTergic fibers innervating various brain regions. Top row: Animals injected with P_{OT}-Venus. Bottom row: Animals injected with vGATE-GFP. Animals injected with P_{OT}-Venus displayed prominent labeling of OT neurons in all analyzed brain regions, while vGATE-injected animals displayed co-localization of green and

red immunosignal only in fibers within the CeL. Green arrows depict fibers positive for Venus/GFP; red arrows depict fibers positive for OT. CeM – Central nucleus of amygdala medial part; CeL – Central nucleus of amygdala lateral part; LS – Lateral septum; LV – Lateral ventricle; HDB – Horizontal limb diagonal band of Broca; PV – Paraventricular nucleus of thalamus; D3V – Dorsal third ventricle; ST – Stria terminalis; f – fornix. (**E**) OT^{vGATE} neurons are positive for retrobeads^{TM} following injection into the CeA. OT=blue, mCherry=red, retrobeads=green. (**F**) Experimental scheme for testing the impact of the re-shock day on the tagging of OT neurons. Animals received bilateral injections of rAAV-$(tetO)_7$-FOS-rtTA and rAAV-P_{tet}bi-Cre/YC3.60 into the PVN and SON. After two weeks of recovery and handling, animals were subjected to the fear conditioning paradigm, where they received an i.p. injection of Dox on d3. On d14, animals were injected with rAAV-P_{OT}-Chr2mCherry. Two weeks later, animals received either an i.p. injection of saline or Dox and where subjected to another shock session. After two weeks, all animals were perfused. (**G**) Confocal images show the vGATE-dependent viral expression of mCherry (red arrowheads) in OT neurons after Dox injection (left panel) or saline injection (right panel). (**H**) Confocal images show the CeL of fear conditioned rats killed 90 mins after fear exposure (d3) with and without BL illumination. Brain slices containing the CeL have been stained for SOM, CRH and c-fos. st=stria terminalis.

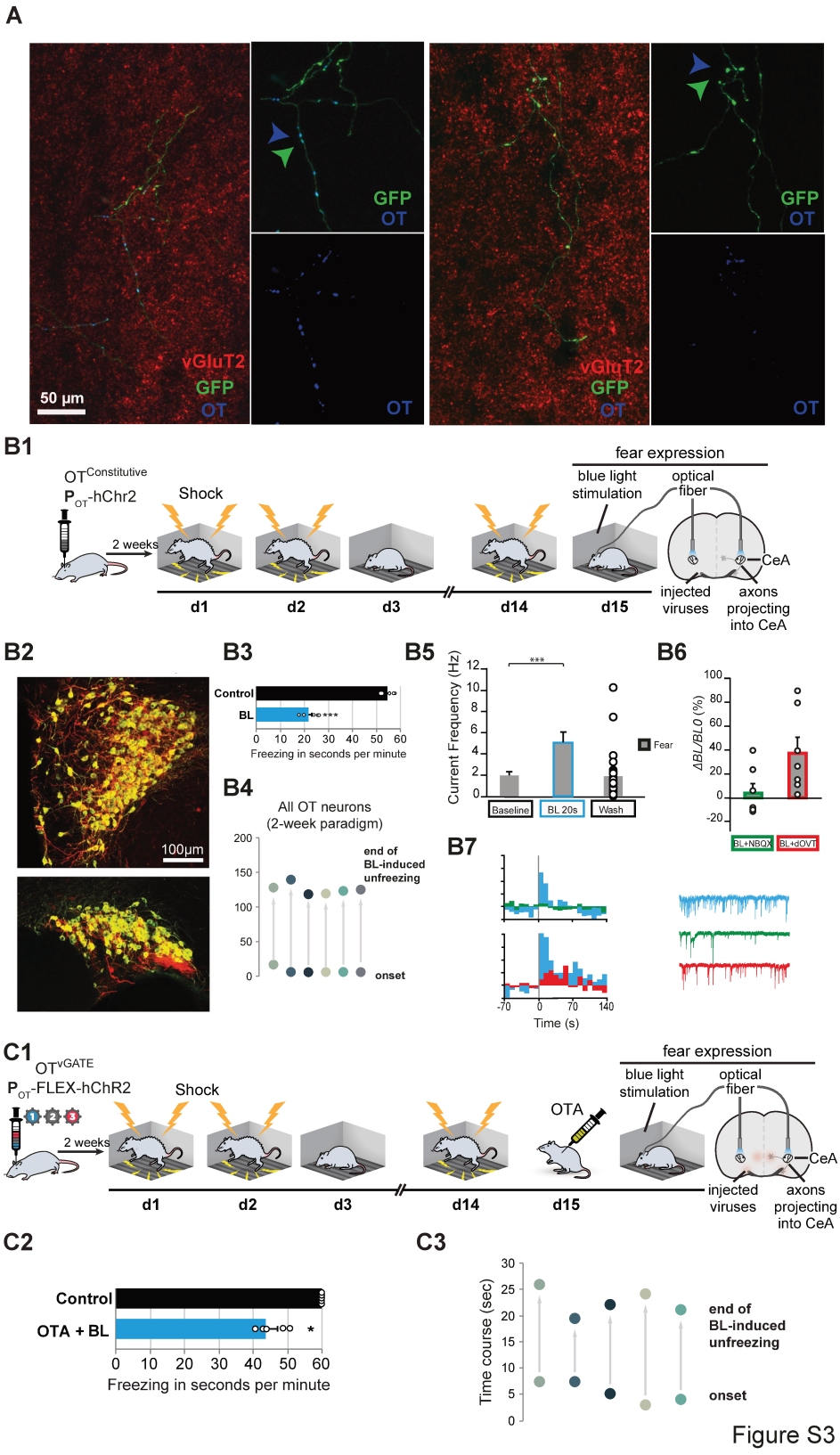

Figure S3

Figure S3 (corresponds to Figure 3). OTA Application in Fear Experienced Rats Does Not Block BL-Induced Unfreezing.

(A) Confocal panel shows OTergic fibers within the CeA of fear-naive (left) and fear-experienced (right) animals. In fear-experienced animals, the immunohistochemical signal for OT is at least 3-fold lower than in the control group (15.3 ± 3.1% vs 58.0 ±

8.4%, signal intensity obtained via ImageJ, n=4, 6 sections per animal). **(B1)** Additional control group injected with $\mathbf{P}_{OT}$-hChR2-mCherry subjected to 2-week paradigm. **(B2)** Immunohistochemical staining against OT (green) and mCherry (red) of sections containing PVN (top) and SON (bottom) **(B3)** BL-induced unfreezing during fear exposure **(B4)** Onset and duration of the BL-induced unfreezing effect. **(B5)** Bar plot shows the change in CeM current frequencies in response to BL (Hz) in Fear animals (n=33/73 recorded neurons). Data are expressed as means across slices plus SEM. Individual values are indicated as white circles. $^{***}p<0.001$, two-way ANOVA followed by Sidak post-hoc test **(B6)** Pharmacological dissection of BL effect. Left, quantification of the effect of NBQX (green; Fear n=7) or dOVT (red; Fear n=7) application on the initial BL effect on IPSCs frequencies recorded in the same CeM neurons. **(B7)** Z-scores illustrating the time course and modulation of BL effects by NBQX or dOVT and example traces. **(C1)** Scheme of the experimental setup. Rats injected with $\mathbf{P}_{OT}$-hChr2-mCherry were subjected to a contextual fear conditioning, where they only received OTA prior to the BL stimulation on d15. **(C2)** Bar charts display the average freezing time per minute in the corresponding group before and after blue light stimulation of the CeA. The black bars (control) show the average freezing times prior to the BL stimulation, whereas the grey bars (BL) indicate the freezing time per minute during the minute in which the BL-induced onset of the unfreezing effect occurred (i.e. where the first signs of mobility appear). *** $p < 0.001$, T-test. **(C3)** Graph displays the onset and duration of the BL-induced unfreezing effect. Data presented as mean ± SEM.

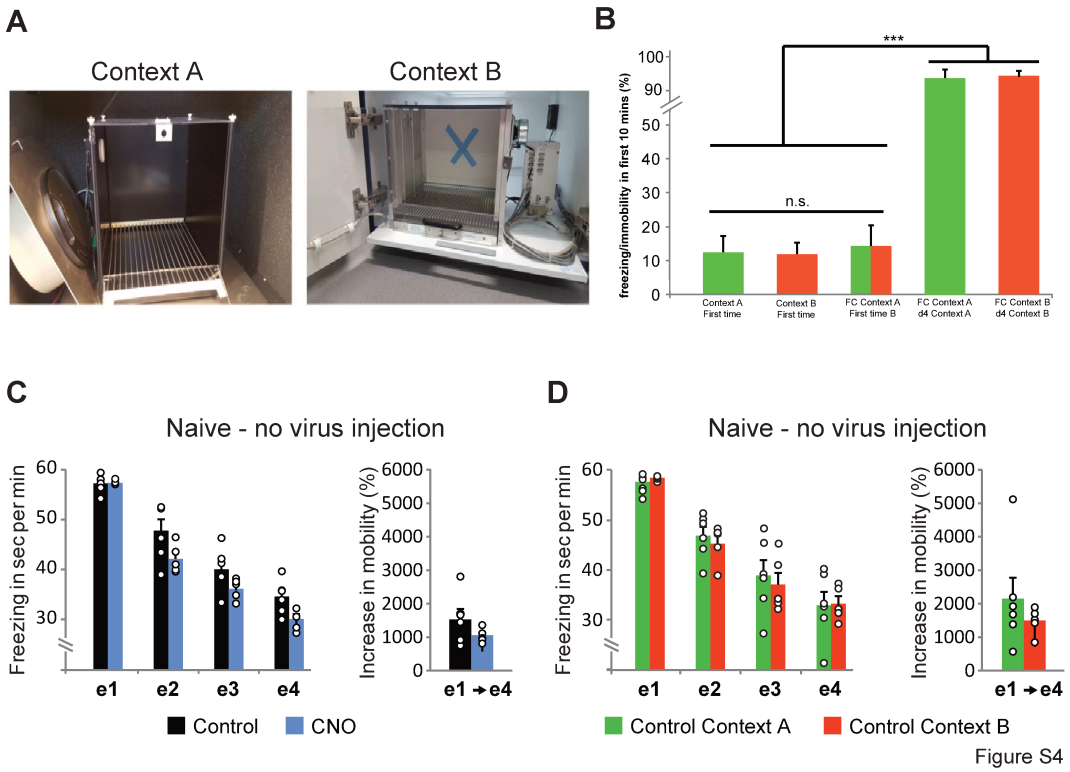

Figure S4

Figure S4 (corresponds to Figure 4). CNO Injection without Expression of DREADD Virus or Nature of Context Does Not Affect Fear Dynamics.

(A) Photos of the two different fear conditioning boxes in Context A and B. (**B**) Graph shows the average freezing rates of rats upon first exposure to Context A (first bar, green), Context B (second bar, red), exposure to Context B after previous fear conditioning in Context A (third bar green/red), as well as the third exposure to both Context A (fourth bar, green) or B (fifth bar, red), after previous fear conditioning in these Contexts. **(C)** Left bar chart shows the amount of freezing displayed by naive animals (without virus injection) that either received saline (control) or CNO during a 4-day fear extinction paradigm. Right bar chart shows the cumulative increase in mobility. **(D)** Left bar chart shows the amount of freezing displayed by naïve (without virus injection) animals after exposure to either context A or B. Right bar chart shows the cumulative increase in mobility. Data presented as mean ± SEM.

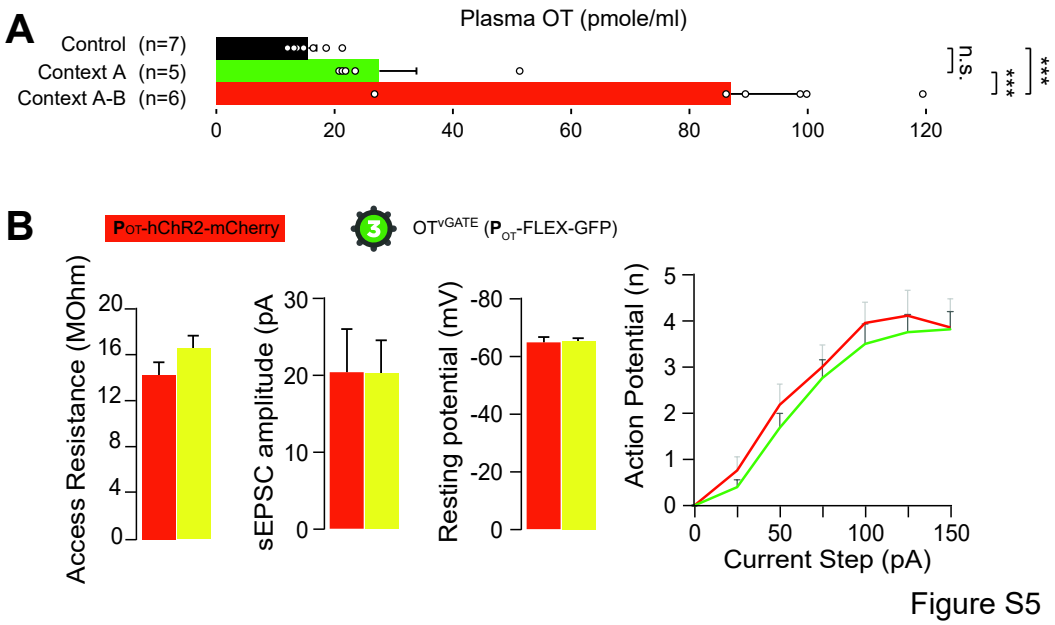

Figure S5 (corresponds to Figure 5). OT Plasma Concentration After Fear Exposure.

(A) Graph shows the OT plasma concentration of naive (control) and fear exposed animals either subjected to context A alone (context A) or context A and B. Animals were sacrificed 10 mins after exposure to the respective fear conditioning chamber. *** $p<0.001$, One Way ANOVA. Data presented as mean ± SEM. (**B**) Bar plots of access resistance, resting potential, sEPSC amplitude and discharge profile recorded in OT^{vGATE} (green; n=24) and $OT^{Constitutive}$ (red; n=16).

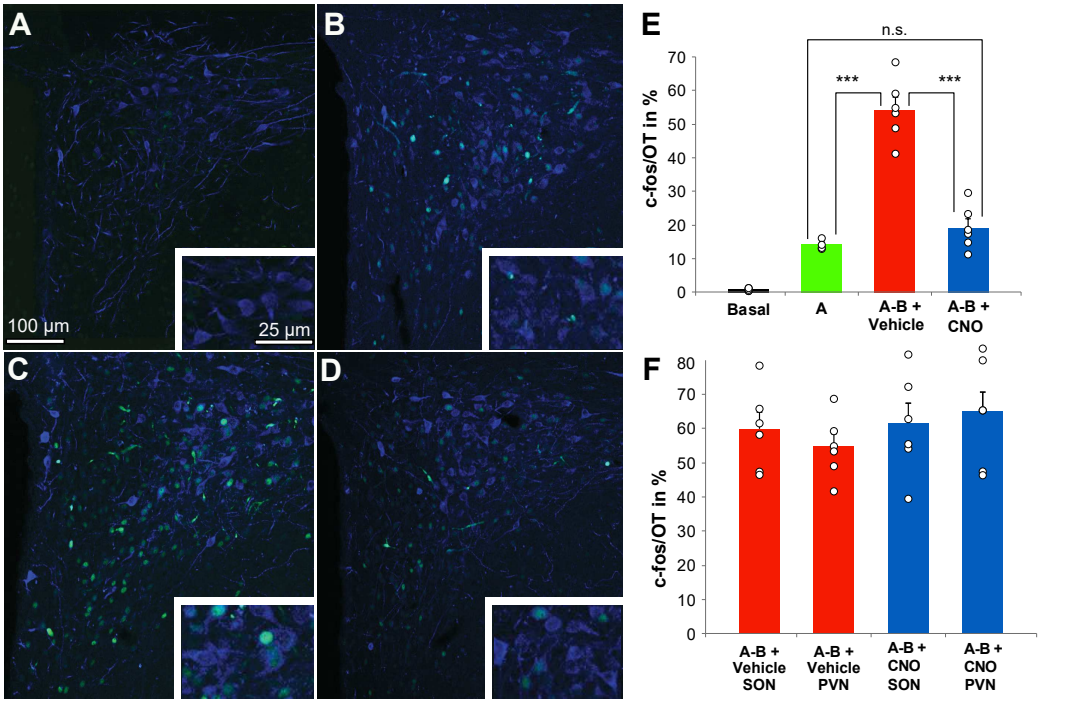

Figure S6

Figure S6 (corresponds to Figure 6). Inhibition of Parvocellular OT Neurons Prevents the c-fos Expression in OT Neurons After Exposure to Context B.

(A-D) Panel shows the immunohistochemical staining against OT (blue) and c-fos (green) in the PVN of naïve animals (**A**), rats conditioned in Context A (**B**), and rats conditioned in Context A followed by Context B and treated with vehicle (**C**) or CNO (**D**). Enlarged insets show the colocalization of c-fos and OT. **(E)** Graph shows the percentage of c-fos expression in OT neurons in the four groups. **(F)** CNO injection alone does not prevent the c-fos expression of OT neurons in animals exposed to context B. One Way ANOVA, ***p<0.0001. Data presented as mean ± SEM.

SUPPLEMENTAL TABLES

Table S1 (corresponds to Figure 1) Quantitative Analysis of ChR2-mCherry Expression and Endogenous c-fos Immunosignal in Rats injected with the vGATE Cocktail after Osmotic Challenge (salt loading)

Experimental Group	Comparison	SON	PVN
OT^{vGATE} Salt loading + Dox	ChR2-mCherry versus endogenous c-fos	94.74%±1.75 n=1496	93.56%±2.46 n=1369
+SL / + Dox	Unspecific expression of mCherry	2.4 ± 1.1% n = 2011	5.7 ± 1.4% n= 2320
-SL / + Dox	Unspecific expression of mCherry	7.3 ± 2.2% n = 2450	0.8 ± 0.5% n = 2450
-SL / - Dox	Unspecific expression of mCherry	0.3 ± 0.09% N = 722	0.1 ± 0.03% n = 540

Experimental procedures	Statistics
Viral injections: $(tetO)_7$-**P**$_{FOS}$-rtTA; P_{tet}bi-YC3.60/Cre; **P**$_{OT}$-FLEX-hChR2 Salt loading with 2% NaCl Immunohistochemical stainings for OT and c-fos Ex vivo optogenetic stimulation of parvOT neurons and recording from magnOT neurons of the PVN	Group difference mCherry/OT in SON vs. PVN: Unpaired, two-tailed t test, p=0.7062, t=0.3907 df=8

Table S2 (corresponds to Figure 2) Quantitative Analysis of ChR2-mCherry Expression and OT Immunosignal in Rats injected with the vGATE Cocktail after Fear Conditioning

Experimental group	Comparison	SON	PVN
OT^{vGATE} Fear conditioning + Dox	OT versus ChR2-mCherry	11.83%±0.9 n=1128	10.16%±0.74 n=1283

Experimental procedures	Statistics
	Group difference mCherry/OT in SON vs. PVN: Unpaired, two-tailed t test, p=0.19, t=1.433 df=8 Group difference control vs. BL ($OT^{Constitutive}$): Unpaired, two-tailed t test, p<0.0001, t=11.91 df=8
Viral injections: t**P**$_{FOS}$-rtTA; P_{tet}bi-YC3.60/Cre; **P**$_{OT}$-FLEX-hChR2 Contextual fear conditioning Context A Doxycycline injection Optogenetic stimulation Immunohistochemical stainings for OT and mCherry	Group difference control vs. BL (OT^{vGATE}): Unpaired, two-tailed t test, p<0.0001, t=14.39 df=8

Shock intensity	OT neurons expressing c-fos
0.6 mA	2.5% ± 0.2 (n=2 animals)
0.8 mA	2.4% ± 0.3 (n=2 animals)
1.2 mA	5.1% ± 0.9 (n=2 animals)
1.6 mA	14.0% ± 1.7 (n=2 animals)

Table S3 (corresponds to Figure 3) Quantitative Analysis of Axonal Length, Number of GFP-positive Varicosities and Number of vGluT2/GFP-positive Puncta in the CeA

Experimental group	Mean axonal length µm	Varicosities GFP (%)	Varicosities vGluT2/GFP (%)

Naive	180±34	65±12	35±6
OT^{vGATE}	162±29	34±8	66±8
n	8	3	3

Experimental procedures	**Statistics**
Viral injections: 1) $\mathbf{P}_{OT}$-hChR2 2) $(tetO)_7$-$\mathbf{P}_{FOS}$-rtTA; $\mathbf{P}_{tet}$bi-YC3.60/Cre; $\mathbf{P}_{OT}$-FLEX-hChr2 3) $(tetO)_7$-$\mathbf{P}_{fos}$-rtTA; $\mathbf{P}_{tet}$bi-YC3.60/Cre; $\mathbf{P}_{OT}$-FLEX-GFP Ex vivo acute slice recordings in the CeM Application of NBQX + dOVT Optogenetic stimulation Contextual fear conditioning Context A Doxycycline injection Immunohistochemical stainings for OT, GFP and vGluT2	Group difference BL (OT^{vGATE} and control): two-way ANOVA and Sidak post-hoc, F(2, 96)=44.34, p<0.0001 Group difference NBQX (OT^{vGATE} vs. control): Unpaired, two-tailed t test, p=0.0025, Mann-Witney U=0.0 Group difference dOVT (OT^{vGATE} vs. control): Unpaired, two-tailed t test, p=0.0022, Mann-Witney U=0.0 Group difference axonal length (Naive vs. OT^{vGATE}): Unpaired, two-tailed t test, p=0.0267, t=2.441 df=16 Group difference control vs. BL (OT^{vGATE} ,OTA1): Unpaired, two-tailed t test, p<0.0001, t=21.53 df=8 Group difference control vs. BL (OT^{vGATE} ,OTA2): Unpaired, two-tailed t test, p<0.0001, t=8.777 df=8

Table S4 (corresponds to Figure 4) Pharmacogenetic Silencing of Fear-activated OT Neurons in Two Different Contexts

Experimental procedures	**Statistics**
Viral injections: t$\mathbf{P}_{FOS}$-rtTA; Ptetbi-YC3.60/Cre; $\mathbf{P}_{OT}$-FLEX-hM4D(Gi) Contextual fear conditioning CNO injection Fear extinction Freezing behavior throughout fear conditioning: d1 – First shock: 12 ± 1.4% d2 – Second shock: 78 ± 3.9% d4 – Exposure without shock: 94 ± 2.1% d14 – Before reinforcement: 69 ± 4.9% d15 – After reinforcement: 91 ± 2.7%	Group difference Freezing Control vs. Context A vs. Context B (e3, OT^{vGATE} CNO): One-way ANOVA, F(2,15)=10.27, p=0.0015 Group difference Increased Mobility Control vs. Context A vs. Context B (e2, $OT^{Constitutive}$ CNO): One-way ANOVA, F(2,15)=32.18, p<0.0001 Group difference Increased Mobility Control vs. Context A vs. Context B (e2, $OT^{Constitutive}$ CNO): One-way ANOVA, F(2,15)=7.224, p=0.0064 Group difference Increased Mobility Control vs CNO: Unpaired, two-tailed t test, p=0.0600, t=2.189 df=8 Group difference Increased Mobility Context A vs. B (Control): Unpaired, two-tailed t test, p=0.4146, t=0.8511 df=10 Group difference Freezing Control vs. Context A vs. Context B (e2, $OT^{Constitutive}$ CNO): One-way ANOVA, F(2,15)=21.75, p<0.0001 Group difference Freezing Control vs. Context A vs. Context B (de3, $OT^{Constitutive}$ CNO): One-way ANOVA, F(2,15)=44.59, p<0.0001 Group difference Freezing Control vs. Context A vs. Context B (e2, OT^{vGATE} CNO): One-way ANOVA, F(2,15)=9.769, p=0,0019 Group difference Freezing OT-GFP Control vs. Context local infusion Context A (e2, OT^{vGATE} CNO): One-way ANOVA, F(2,15)=16.34, p=0.031 Group difference Freezing OT-GFP Control vs. Context local infusior vs. Context A (e3, OT^{vGATE} CNO): One-way ANOVA, F(2,15)=13.37, p=0,0007

Table S5 (corresponds to Figure 5) Quantitative Analysis of Colocalized c-fos and GFP Signals in OT Neurons and Activated Fraction of Magno- and Parvocellular OT Neurons in Contexts A and B

Experimental group	**Comparison**	**SON**	**PVN**
OT^{vGATE}	OT versus c-fos	56.4%±2.9	47.1%±1.9

Context A & Context B	OT versus GFP	11.7%±1.43	9.6%±0.81
	OT versus c-fos/GFP	2.6%±0.62	3.0%±0.32
		n=1206	n=995
OT^{vGATE} Context A(1) & Context A(2)	OT versus c-fos	16.1%±1.7	9.5%±0.8
	OT versus GFP	11.9%±1.2	10.8%±0.81
	OT versus c-fos/GFP	10.3%±0.89	1.9%±0.19
		n=1044	n=1235

Experimental group	**Comparison**	**SON (**OT + GFP)	**SON (**GFP + c-fos)	**SON** (OT + GFP + c-fos)
OT^{vGATE} Context A & Context B	Fluorogold + MagnOT	n=394	n=55	13.8%±1.22

Experimental group	**Comparison**	**PVN (**OT + GFP)	**PVN** (OT + c-fos)	**PVN (**OT + GFP + c-fos)
OT^{vGATE} Context A(1) & Context A(2)	Fluorogold + MagnOT	n=90	n=11	9.9%±1.4
	Fluorogold - ParvOT	n=43	n=27	62.8%±2.5
OT^{vGATE} Context A & Context B	Fluorogold + MagnOT	n=288	n=57	19.80%±2.61
	Fluorogold - ParvOT	n=183	n=180	98.6%±1.4

Experimental procedures	**Statistics**
Viral injections: t**P**$_{FOS}$-rtTA; Ptetbi-YC3.60/Cre; **P**$_{OT}$-FLEX-GFP Immunohistochemical staining for OT and c-fos	Group difference Plasma OT Control vs. Context A vs. Context A-B: One-way ANOVA, $p<0.0001$, $F(2,15)=23.45$

Table S6 (corresponds to Figure 6) Number of c-fos Expressing OT Neurons in the SON and PVN After Pharmacogenetic Silencing of Parvocellular OT Neurons in Context B

Experimental group	**Comparison**	**SON** OT	**SON** c-fos vs. OT	**SON** c-fos vs. OT
Cav2-Cre ParvOT DREADD	Basal control	n=939	n=8	0.85%±0.12
	Context A	n=831	n=114	13.7%±0.56
	Context B	n=855	n=507	59.3%±4.9
	Context B parvOT DREADD	n=901	n=173	19.2%±1.5

Experimental group	**Comparison**	**PVN** OT	**PVN** c-fos vs. OT	**PVN** c-fos vs. OT
Cav2-Cre ParvOT DREADD	Basal control	n=1052	n=8	0.76%±0.15
	Context A	n=890	n=126	14.2%±0.59
	Context B	n=910	n=493	54.2%±3.75
	Context B parvOT DREADD	n=842	n=160	19.0%±2.63

Experimental procedures	**Statistics**
Viral injections: 1) t**P**$_{FOS}$-rtTA; **P**$_{tet}$bi-YC3.60/Cre; **P**$_{OT}$-FLEX-GFP 2) **P**$_{OT}$-FLEX-hM4D(Gi); CAV2-Cre Fluorogold injection CNO injection Fear conditioning Immunohistochemical staining for OT, Fluorogold and c-fos	Group difference c-fos/OT SON (Basal, Context A, Context B vehicle, Context B CNO): One-way ANOVA, $p<0.0001$, $F(3,20)=95.51$ Group difference c-fos/OT PVN (Basal, Context A, Context B vehicle, Context B CNO): One-way ANOVA, $p<0.0001$, $F(3,20)=97.32$

Table S7 (Figures 1-6) Experimental Procedures, Number of Animals, Target Structures, Viral Vectors, and Expression Time

Experiments	**Protocols**	**Figure**	**AAVs**	**Targets**	**n**	**Expression time**
Specificity of the c-fos promoter	No stimulus: -SL	Figure S1	rAAV-**P**$_{OT}$-Venus	SON unilateral	3	2 weeks
	Stimulus: + SL		rAAV-**P**$_{fos}$-tdTomato		3	
Targeting	- SL/ - Dox	2		SON unilateral	3	3 weeks

rtTA expression in OT neurons	+ SL/ - Dox		rAAV-$(tetO)_7$-$\mathbf{P}_{fos}$-rtTA rAAV-$\mathbf{P}_{OT}$-Venus		3	
	- SL/ + Dox				3	
	+ SL/ + Dox				3	
Endogenous c-fos activity induced by fear expression	Fear conditioning	Figure S2	-	-	5	-
Specificity of the vGATE system	- SL/-Dox	1	rAAV-$(tetO)_7$-$\mathbf{P}_{fos}$-rtTA rAAV-$\mathbf{P}_{tet}$bi-Cre/YC3.60 rAAV-$\mathbf{P}_{OT}$-FLEX-ChR2-mCherry	SON and PVN bilateral	4	3 weeks
	+ SL/- Dox				4	
	- SL/+ Dox				4	
	+ SL/+ Dox				4	
Anatomy and count of OT axons	Naive Constitutive OT-labeling	3	rAAV-$\mathbf{P}_{OT}$-Venus	SON and PVN bilateral	8	2-6 weeks
	Fear conditioning Constitutive OT-labeling		rAAV-$\mathbf{P}_{OT}$-Venus		6	6 weeks
	Fear conditioning OT^{vGATE} labeling		rAAV-$(tetO)_7$-$\mathbf{P}_{fos}$-rtTA rAAV-$\mathbf{P}_{tet}$bi-Cre/YC3.60		15	2 weeks
Contextual fear conditioning and optogenetics	Fear conditioning Constitutive OT-labeling	2	rAAV-$\mathbf{P}_{OT}$-hChR2-mCherry	SON and PVN bilateral	13	2-3 weeks
	Fear conditioning OT^{vGATE} labeling		rAAV-$(tetO)_7$-$\mathbf{P}_{fos}$-rtTA rAAV-$\mathbf{P}_{tet}$bi-Cre/YC3.60 rAAV-$\mathbf{P}_{OT}$-FLEX-ChR2-mCherry		10	2 weeks
Contextual fear conditioning and DREADD Fear Extinction Contexts A and B	Fear conditioning Fear extinction Contexts A and B +Dox/+CNO	4	rAAV-$(tetO)_7$-$\mathbf{P}_{fos}$-rtTA rAAV-$\mathbf{P}_{tet}$bi-Cre/YC3.60 rAAV-$\mathbf{P}_{OT}$-FLEX-hM4D(Gi)-mCherry	SON and PVN bilateral	6	3 weeks
	Fear conditioning Fear extinction Contexts A and B Control +Dox/-CNO		rAAV-$(tetO)_7$-$\mathbf{P}_{fos}$-rtTA rAAV-$\mathbf{P}_{tet}$bi-Cre/YC3.60 rAAV-$\mathbf{P}_{OT}$-FLEX-hM4D(Gi)-mCherry		6	3 weeks
	Fear extinction Contexts A and B +CNO/-CNO		rAAV-$\mathbf{P}_{OT}$-hM4D(Gi)-mCherry		12	6-7 weeks
Contexts A-A and A-B	Fear conditioning Contexts A and B	5	rAAV-$(tetO)_7$-$\mathbf{P}_{fos}$-rtTA rAAV-$\mathbf{P}_{tet}$bi-Cre/YC3.60 rAAV-$\mathbf{P}_{OT}$-FLEX-GFP	SON and PVN bilateral	26	2 weeks
	Fluorogold injection					5-7 days prior to perfusion
	Blood OT measures					Animals were killed 10 mins after the fear exposure
Ex vivo electrophysiology	Fear conditioning + Dox	3	rAAV-$(tetO)_7$-$\mathbf{P}_{fos}$-rtTA rAAV-$\mathbf{P}_{tet}$bi-Cre/YC3.60 rAAV-$\mathbf{P}_{OT}$-FLEX-hChR2-mCherry	SON and PVN bilateral	39	3-4 weeks
			rAAV-$\mathbf{P}_{OT}$-Venus		4	3-4 weeks
			CAV2Cre $\mathbf{P}_{OT}$-FLEX-hChR2-mCherry $\mathbf{P}_{OT}$-Venus		2	4 weeks
	No fear conditioning		rAAV-P_{OT}-hChR2-mCherry		7	6-8 weeks
Inhibition of parvocellular OT neurons via DREADD	Fear conditioning Contexts A and B +CNO/-CNO	5	rAAV-CAV2-Cre rAAV-$\mathbf{P}_{OT}$-FLEX-hM4D(Gi)-mCherry	SON and PVN bilateral	12	3 weeks

Optogenetic stimulation and application of OTR antagonist	Fear conditioning Intraperitoneal injection of OTR antagonist	3	rAAV-$\mathbf{P}_{OT}$-hChR2-mCherry	SON and PVN bilateral	10	3 weeks (single fear) or 5 weeks (repeated fear)
SON engram ex vivo electrophysiology	Fear conditioning	5 ,S5	rAAV-$(tetO)_7$-$\mathbf{P}_{fos}$-rtTA rAAV-$\mathbf{P}_{tet}$bi-Cre/YC3.60 rAAV-$\mathbf{P}_{OT}$-FLEX-GFP $\mathbf{P}_{OT}$-hChR2-mCherry	SON	12	3 weeks
Re-shock experiment	Fear conditioning	S2	rAAV-$(tetO)_7$-$\mathbf{P}_{fos}$-rtTA rAAV-$\mathbf{P}_{tet}$bi-Cre/YC3.60 rAAV-$\mathbf{P}_{OT}$-FLEX-hChR2-mCherry	SON and PVN bilateral	10	4 weeks
CRH/Somatostatin Anatomy CeA	Fear conditioning / Optogenetics	S3	-	-	8	-
Retrobeads injections into CeA	Fear conditioning	S2	rAAV-$(tetO)_7$-$\mathbf{P}_{fos}$-rtTA rAAV-$\mathbf{P}_{tet}$bi-Cre/YC3.60 rAAV-$\mathbf{P}_{OT}$-FLEX-hChR2-mCherry	CeA	4	3 weeks
Local infusion of CNO onto CeA	Fear conditioning	4	rAAV-$(tetO)_7$-$\mathbf{P}_{fos}$-rtTA rAAV-$\mathbf{P}_{tet}$bi-Cre/YC3.60 rAAV-$\mathbf{P}_{OT}$-FLEX-hM4D(Gi)-mCherry	PVN SON	16	4 weeks
vGlut2 input onto vGATE neurons	Fear conditioning	5	rAAV-$(tetO)_7$-$\mathbf{P}_{fos}$-rtTA rAAV-$\mathbf{P}_{tet}$bi-Cre/YC3.60 rAAV-$\mathbf{P}_{OT}$-FLEX-hChR2-mCherry	PVN SON	4	4 weeks
				Total number of animals*	**269**	

*The animals used for the preparation of of hippocampal cell cultures (Figure S1) were not included in this table.

Article II : Astrocytes mediate oxytocin's effect on central amygdala circuitry that regulates emotional behavior in rodents

a. Contexte général

Au cours des dernières années il a été largement démontré que les astrocytes sont des acteurs essentiels pour le fonctionnement et la régulation du système nerveux central. Ainsi, de nombreuses publications attribuent un rôle direct de l'astroglie dans le traitement d'information au sein du système nerveux central (SNC), soulignant leur fonction de régulateur homéostatique. De plus, les astrocytes sont capables de participer activement à la transmission synaptique et de la réguler finement au travers de nombreuses actions. Il est notamment montré que les astrocytes régulent l'activité des neurones ocytocinergique magnocellulaire de l'hypothalamus (magnOT), en modifiant l'excitabilité des neurones magnOT, entraînant une régulation de leurs fonctions physiologiques. Les neurones magnOT ne sont pas uniquement des cellules neuroendocrines et projettent vers de nombreuses structures centrales dont le noyau central de l'amygdale (CeA), une structure clé dans les processus associés à la douleur et de l'anxiété. La libération d'OT dans le CeA module le circuit neuronal local et par conséquence l'activité des neurones de la voie de sortie du CeA, retrouvé dans la subdivision médiane (CeM). Le rôle des astrocytes dans la régulation du microcircuit du CeA n'avait à ce jour jamais été étudié et plus particulièrement leur rôle dans l'intégration du signal ocytocinergique au sein de ce circuit. Pourtant, il a été montré que les astrocytes en culture(s) sont capables d'exprimer le récepteur à l'ocytocine. Dans cette étude nous avons ainsi étudié l'implication des astrocytes dans l'intégration du signal ocytocinergique et ses effets sur le microcircuit du CeA au travers d'approches électrophysiologiques, d'imagerie calcique et comportementales.

b. Résultats

Dans un premier temps, nous avons déterminé l'expression des OTR par les différentes populations cellulaires au sein du CeA. En utilisant la technique d'hybridation in situ en

fluorescence (FISH) nous avons montré une co-expression entre l'ARNm codant pour l'OTR et des marqueurs astrocytaires (glutamine synthétase, ALDH1L1). Au sein du CeA l'expression des OTR semble exclusivement localisée au niveau de la sous division latérale du CeA (CeL). Plus particulièrement, ~60% des neurones du CeL expriment le récepteur à l'ocytocine ainsi que ~18% des astrocytes.

De manière à déterminer l'action fonctionnelle de l'OT sur le réseau astrocytaire du CeA nous avons étudié son activité sur des tranches de cerveaux de rats et de souris. En utilisant la technique d'imagerie calcique couplée à l'optogénétique nous avons pu montrer que la libération d'OT endogène induit une élévation calcique oscillatoire au sein des astrocytes du CeL. De plus, l'activation pharmacologique des OTR par un agoniste ocytocinergique spécifique (TGOT) induit des oscillations calciques similaires à celles observées lors de la libération endogène. De manière intéressante, 50-60% des astrocytes du CeL présentent cette élévation calcique en réponse à l'ocytocine et ce malgré la faible proportion d'astrocytes exprimant le récepteur. Ce résultat traduit une communication locale au sein des astrocytes du réseau permettant une amplification du signal ocytocinergique. De plus, cette activation astrocytaire par l'ocytocine est indépendante du réseau neuronal. Le blocage de la transmission synaptique par l'application de TTX dans la préparation n'altère ni la proportion d'astrocytes répondant, ni la dynamique de la réponse calcique. Afin de démontrer la spécificité de l'effet ocytocinergique astrocytaire, nous avons utilisé un modèle de souris permettant la délétion spécifique du récepteur OTR astrocytaire dans l'amygdale (cKO). En absence de l'OTR, l'activité calcique en présence TGOT est complètement inhibée. Ce résultat démontre que la réponse astrocytaire observée est spécifiquement médiée par les récepteurs présents sur les astrocytes.

En utilisant une approche optogénétique, nous avons par la suite caractérisé les interactions astrocytes-neurones au sein du CeA. Nous avons enregistré l'activité électrophysiologique des neurones du CeL et du CeM (principale voie de sortie du CeA) après activation optogénétique des astrocytes du CeL. Dans un premier temps nous avons montré que l'activation optogénétique était efficace pour mimer les oscillations calciques observées après l'activation des OTR (par le TGOT ainsi que par la libération endogène d'OT suite à la stimulation des fibres du PVN). De plus, cette activation astrocytaire est suffisante pour déclencher une augmentation de courants miniatures excitateurs (mEPSCs) ainsi qu'une augmentation de la

fréquence de potentiel d'action dans les neurones du CeL. Pour finir, l'activation optogénétique des astrocytes induit une forte augmentation de la fréquence des courants post-synaptiques inhibiteurs (IPSCs) enregistrés dans les neurones du CeM. Ces données démontrent la capacité des astrocytes à moduler l'activité neuronal au sein de l'intégralité de l'amygdale centrale.

Afin de déterminer si les astrocytes sont des acteurs cellulaires-clés dans la transmission du signal ocytocinergique, nous avons dans un premier temps caractérisé l'effet du TGOT sur les neurones du CeL et du CeM. L'activation des OTR conduit d'une part à une augmentation de la fréquence des mEPSCs et des potentiels d'action au sein des neurones du CeL et d'autre part à une élévation de la fréquence des IPSCs au sein des neurones du CeM. L'inhibition astrocytaire réalisée grâce à un chargement de chélateur calcique (BAPTA) inhibe l'effet observé du TGOT dans les neurones du CeL et du CeM. Ce résultat démontre l'importance des astrocytes dans la médiation du signal ocytocinergique au sein de l'amygdale centrale. Plus précisément, il s'agit de l'activité médiée par les OTR astrocytaires qui semble être au cœur de ce réseau. La délétion spécifique de ce récepteur inhibe totalement les effets du TGOT que ce soit dans les neurones du CeL ou du CeM. Ces données ont donc permis de démontrer que les astrocytes sont les premiers acteurs à répondre au signal ocytocinergique au sein du CeA et sont également des acteurs-clés dans la propagation du signal ocytocinergique au sein de l'amygdale.

Afin de mieux comprendre la communication astrocytes-neurones, nous avons réalisé des enregistrements électrophysiologiques en utilisant des bloqueurs des récepteur NMDA (AP5 et ifenprodil). L'ajout de ces antagonistes dans la préparation inhibe l'effet du TGOT sur la fréquence des mEPSCs ainsi que des potentiels d'action, mettant en évidence l'implication des récepteurs NMDA dans la transmission du signal ocytocinergique. Une des fonctions connues des astrocytes est la gliotransmission, et notamment la libération de co-agonistes NMDA tels que la D-Glycine et la D-Serine. La présence de D-amino acid oxydase (DAAO), une enzyme capable de métaboliser tous les acides aminés de conformation D, inhibe l'effet du TGOT sur l'augmentation de la fréquence de IPSCs des neurones du CeM. En complément, la supplémentation du milieu en D-Serine est quant à elle suffisante pour restaurer l'effet du TGOT. Ces résultats démontrent ainsi que les astrocytes à la suite de leur activation par l'OT, libèrent de la D-serine pour activer le réseau neuronal du CeA. Dans leur ensemble ces

données révèlent que la régulation astrocytaire du réseau neuronal passerait par l'activation des récepteurs NMDA présents sur les neurones du CeA.

Finalement, nous avons voulu étudier l'importance de l'interaction astrocytes-neurones dans la modulation ocytocinergique du CeA dans la réponse comportementale. L'amygdale est une structure fortement impliquée dans de nombreux paradigmes comportementaux, et notamment dans la régulation de l'anxiété. Elle est également appelée amygdale émotionnelle, car c'est un acteur primordial pour la régulation de la valence émotionnelle de la douleur. En réalisant une lésion du nerf sciatique (SNI), induisant l'apparition d'une neuropathie induisant à terme un état anxieux, nous avons pu démontrer que l'activation optogénétique des astrocytes du CeA ainsi que l'infusion de TGOT présentent un effet anxiolytique. De plus, nos résultats montrent que cet effet est directement médié par les OTR présent au niveau des astrocytes du CeA. En effet, cet effet anxiolytique du TGOT n'est plus retrouvé dans le modèle cKO. Enfin, l'activation astrocytaire et l'infusion du TGOT dans le CeA conduisent à une préférence de place conditionnée. L'activation du réseau neuronal par l'OT est donc associée à une valence positive chez les animaux neuropathiques et naïfs. Cet effet semble directement être soutenu par les OTR astrocytaires car absent dans le modèle cKO.

Dans son ensemble cette étude nous a permis de démontrer que les astrocytes sont impliqués de manière cruciale dans l'effet de l'OT sur l'activité du CeA et les comportements régulés par l'activité de cette structure.

c. Contribution personnelle

De façon similaire à la publication précédente, ce travaille a fait l'objet d'une collaboration entre plusieurs laboratoires. J'ai participé à la réalisation et à l'analyse de toutes les parties impliquant, l'électrophysiologie, l'imagerie calcique et le comportement.

Astrocytes mediate oxytocin's effect on central amygdala circuitry that regulates emotional behavior in rodents

Jérôme Wahis[1,†,$], Angel Baudon[1,†], Ferdinand Althammer[2,†], Damien Kerspern[1,†], Stéphanie Goyon[1], Daisuke Hagiwara[3], Arthur Lefevre[1,3], Lara Barteczko[3], Benjamin Boury-Jamot[4], Benjamin Bellanger[1], Marios Abatis[4], Miriam Silva da Gouveia[5], Diego Benusiglio[3], Marina Eliava[3], Andrej Rozov[6], Ivan Weinsanto[1], Hanna Sophie Knobloch-Bollmann[7,$], Matthew K. Kirchner[2], Ranjan K. Roy[2], Hong Wang[8,$], Marie Pertin[9], Perrine Inquimbert[1], Claudia Pitzer[10], Jan Siemens[8], Yannick Goumon[1], Benjamin Boutrel[4], Christophe Maurice Lamy[11], Isabelle Decosterd[9,12], Jean-Yves Chatton[9], Nathalie Rouach[13], Scott W. Young[14], Javier E. Stern[2], Pierrick Poisbeau[1], Ron Stoop[4], Pascal Darbon[1], Valery Grinevich[3,#,*], Alexandre Charlet[1,15,#,*]

[1] Centre National de la Recherche Scientifique and University of Strasbourg, UPR3212 Institute of Cellular and Integrative Neurosciences, Strasbourg, France. [2] Center for Neuroinflammation and Cardiometabolic Diseases, Georgia State University, Atlanta, USA. [3] Department of Neuropeptide Research for Psychiatry, Central Institute of Mental Health, University of Heidelberg, Mannheim, Germany. [4] Center for Psychiatric Neurosciences, Hôpital de Cery, Lausanne University Hospital (CHUV), Lausanne, Switzerland. [5] German Cancer Research Center (DKFZ), Heidelberg, Germany, [6] OpenLab of Neurobiology, Kazan Federal University, Kazan, Russia, Federal Center of Brain Research and Neurotechnologies, Moscow, Russia and Department of Physiology and Pathophysiology, University of Heidelberg, Heidelberg, Germany. [7] Department of Molecular and Cellular Biology, Center for Brain Science, Harvard University, Cambridge, USA[$]. [8] Department of Pharmacology, Heidelberg University, Heidelberg, Germany[$]. [9] Pain center, Department of Anesthesiology, Lausanne University Hospital (CHUV), Lausanne, Switzerland. [10] Interdisciplinary Neurobehavioral Core (INBC), Ruprecht-Karls-Universität, Heidelberg. [11] Division of Anatomy, Faculty of Medicine, University of Geneva, Geneva, Switzerland. [12] Department of Fundamental Neurosciences, Faculty of Biology and Medicine (FBM), University of Lausanne, Lausanne, Switzerland. [13] Neuroglial Interactions in Cerebral Physiopathology, Center for Interdisciplinary Research in Biology, Collège de France, Centre National de la Recherche Scientifique UMR 7241, Institut National de la Santé et de la Recherche Médicale U1050, Labex Memolife, PSL Research University, Paris, France. [14] Section on Neural Gene Expression, National Institute of Mental Health, National Institutes of Health, Bethesda, MD, USA. [15] University of Strasbourg Institute for Advanced Study (USIAS), Strasbourg, France. [$]Present addresses: JW: Laboratory of Glia Biology, VIB-KU Leuven Center for Brain and Disease Research, Department of Neuroscience, KU Leuven Brain Institute, Leuven, Belgium. HSKB: Group of Systemic and Cellular Neuroscience, Institute of Physiology, University of Freiburg, Germany. HW: The Brain Cognition and Brain Disease Institute of Shenzhen Institutes of Advanced Technology, Chinese Academy of Sciences, China.

[†] Equal first author. [#] senior author. * Corresponding author.

Corresponding Authors

Alexandre Charlet, PhD
Institute of Cellular and Integrative Neurosciences,
INCI CNRS UPR3212

8, Allée du Général Rouvillois
67000 Strasbourg
France
Phone: (33) 6070 825 06
E-mail: acharlet@unistra.fr

Valery Grinevich, MD, PhD
Department of Neuropeptide Research in Psychiatry
Central Institute of Mental Health
Medical Faculty Mannheim
University of Heidelberg
J5, Mannheim, 68159
Germany
Phone: (49) 621 1703 2995
E-mail: valery.grinevich@zi-mannheim.de

SUMMARY

Oxytocin (OT) orchestrates social and emotional behaviors through modulation of neural circuits. In the central amygdala (CeA), the release of OT modulates inhibitory circuits and thereby suppresses fear responses and decreases anxiety levels. Using astrocyte-specific gain- and loss-of-function and pharmacological approaches, we demonstrate that a morphologically distinct subpopulation of astrocytes express OT receptors and mediate anxiolytic and positive reinforcement effects of OT in the CeA of mice and rats. The involvement of astrocytes in OT signaling challenges the long-held dogma that OT acts exclusively on neurons and highlight astrocytes as essential components for modulation of emotional states under normal but also chronic pain conditions.

INTRODUCTION

Oxytocin (OT) is a neuropeptide that acts both as a peripheral neurohormone and a central neuromodulator to modulate key physiological functions, from ion homeostasis to complex social behaviors[1,2]. Early studies indicated that locally released OT induces morphological and functional changes in both the astroglial and neuronal networks of the hypothalamic nuclei producing the neuropeptide[3]. Activation of oxytocinergic hypothalamic magnocellular neurons, that project further to virtually all forebrain regions, leads to both synaptic and extra-synaptic OT release in the extra-cellular fluid[4,5]. This last mode of OT release has the potential to activate virtually every cell type expressing OT receptors (OTR) located in close proximity to the sites of axonal OT release[5].

A few studies using either autoradiography on cell cultures derived from rat tissue, immunohistochemistry on CNS sections or knock-in mice models found that not only neurons, but also astrocytes express OTRs[6–9]. Astrocytes are part of the tripartite synapse

and capable to modulate neuronal activity as well as to sense the release of neuromodulators into the neuropil[10]. There is now accumulating evidence which demonstrate that astrocytes express receptors for various neuromodulators and actually mediate their neurophysiological effects[11,12]. Mapping of OTR expression in the rodent brain found it was expressed at high levels in several brain regions[8], and of interest in this study particularly in the lateral and capsular part (CeL) of the central amygdala (CeA)[13], albeit the types of cells expressing the OTR in this brain region was never elucidated.

Functionally, the release of OT in the CeL leads to increased firing of GABA-expressing interneurons[4,13]. These interneurons inhibit projection neurons in the medial CeA (CeM), which serve as CeA output. OT action in this circuit affects amygdala-related functions, including activity of the autonomous nervous system, fear expression and anxious behaviors[4,14,15]. Furthermore, the CeA is involved in the pathophysiology of a number of neurological diseases, including neuropathic pain and anxiety[16,17], in which both astrocytes[18] and the OT system[19] are thought to play a significant role. Therefore, it is crucial to understand how the OT system controls pain and its emotional comorbidities, and if astrocytes are involved in these mechanisms.

Indeed, a role for astrocytes in the regulation of CeA circuits has already been proven in the CeM[20], where astrocyte activity can reduce fear-expression in a fear-conditioning paradigm, a role that is surprisingly similar to the effect of OTR signaling in the CeL[4]. We therefore sought to investigate if CeL astrocytes could also play a role in the OT-mediated regulation of CeA circuits and some of their behavioral correlates.

Our study shows the expression of oxytocin receptors (OTR) in CeL astrocytes and demonstrates that OT directly acts on CeL astrocytes to gate CeL neurons excitability through N-methyl-D-aspartate receptor (NMDAR) (co-)activation. Further, we found that the astrocyte-mediated OTR signaling underlies the anxiolytic and positive reinforcement effects of OT in the CeA. We thus provide the first evidence that OT drives astrocyte activity and that this effect is an essential part of the OTergic modulation of amygdala neuronal circuits and the behaviors they regulate.

RESULTS

CeL astrocytes express functional OTRs in rats and mice

To investigate whether CeA astrocytes express OTRs, we performed fluorescent *in situ* hybridization (FISH) combined with immunohistochemistry on rat CeA sections and found some overlap between OTR mRNA signal and an astrocyte marker, glutamine synthase (GS) (Fig. 1a-b; Extended Data Fig. 1a). Within the rat CeL, 18.6±1.8% of astrocytes and 67.8±3.1% of neurons expressed OTR mRNA (Fig. 1c), with similar results in mice (Extended Data Fig. 1b). Using another astrocyte marker, the aldehyde dehydrogenase 1 family member L1 (ALDH1L1), we found a similar proportion of OTR mRNA positive (OTR+) rat astrocytes (Extended Data Fig. 1c). Combining RNAscope for OTR mRNA with a third astrocyte marker (glial fibrillary acidic protein, GFAP), we again found OTR mRNA to be present in mouse astrocytes (Extended Data Fig. 1d). Next, to unequivocally demonstrate that CeL astrocytes were positive for OTR, we employed IHC-based three-dimensional reconstruction using Imaris technique and combining immunohistochemical staining for GS and GFAP with FISH for OTR mRNA in the rat CeL. Employing glial morphometric profiler, we performed three-dimensional reconstruction of cells through a semi-automated pipeline[21] (Fig. 1d-e). This analysis confirmed the presence of OTR mRNA in astrocytes and revealed that OTR+ astrocytes have on average a significantly larger cell volume, surface area, a higher number and an increased length of processes compared to OTR– astrocytes (Fig. 1e). Subsequent Sholl analysis revealed that OTR+ astrocytes bear more complex morphological features than OTR– astrocytes (Fig. 1f), suggesting that OTR+ astrocytes represent a distinct subpopulation of astrocytes within the CeL.

To test whether CeL astrocytes respond to endogenous OT release, we expressed the ChR1/VChR1 chimaera channel rhodopsin variant[22] (referred here as C1V1) in OTergic neurons to optogenetically control CeA-innervating OT axons (POT-C1V1-mCherry; referred to as OxytOpto). To this end, we employed a previously characterized adeno-associated viral vector (AAV) equipped with the OT promoter[4], which was injected into the paraventricular (PVN), supraoptic, and accessory nuclei of rat hypothalamus (Fig. 2a). First, we validated that red shifted light (λ542 nm light pulses of 10 ms width at 30 Hz) induced activation of C1V1-expressing OT neurons in the PVN (Extended Data Fig. 2a-b). We then identified CeL astrocytes through sulforhodamine 101 (SR101) labeling in acute brain slices and confirmed astrocytes specificity of the labeling by measuring electrophysiological properties of SR101-labelled cells in CeL (Extended Data Fig. 2c-e). We then assessed SR101 labeled astrocytes activity by measuring the relative changes in cytosolic calcium using the small organic dye Oregon Green® 488 BAPTA-1 (OGB1). (Fig. 2b). We found that of recorded astrocytes, 61.9±8.7% responded to the optogenetic OT axons stimulation (Fig. 2c-d). To avoid the possibility that astrocyte activity was increased due to the increased spiking of CeL interneurons caused by optogenetically evoked OT release, tetrodotoxin (TTX) was added to the bath prior the stimulation. Further calcium imaging experiments described below use TTX incubation (if not stated otherwise) for the same reason,. We also compared the frequency of calcium transients as well as the area under the curve before and after optogenetic stimulation, expressing the results as a ratio between post-stimulation and baseline values (referred to as AUC and Ca^{2+} transient frequency normalized to baseline,

analysis method detailed in Extended Data Fig. 2f). As depicted in Fig. 2d, both parameters were increased following stimulation of OT axons. Taken together, these results indicate that optogenetically-evoked OT release from axons present in the CeL elicits an increase in activity of CeL astrocytes.

To ensure that the observed responses are exclusively due to OTR activation, we applied the selective agonist of OTR ([Thr^4Gly^7]-oxytocin, TGOT), which increased calcium transients in 60.1±9.2% of the recorded astrocytes, a result unchanged when replicated with slices pre-incubated with TTX (Fig. 2e-f). Similar pre-incubation of the slices with the OTR antagonist [$d(CH_2)^5$,$Tyr(Me)^2$,Orn^8]-vasotocin (dOVT) reduced the proportion of TGOT-evoked calcium responses in astrocytes and their properties (Fig. 2e-f), confirming that the activation of astrocytes by TGOT is indeed mediated by OTR. However, it cannot be discarded that other OTR-mediated and astrocyte-independent mechanisms may drive CeL astrocyte activity up.

To exclude this possibility, we employed a transgenic mouse line with a LoxP sites flanking the OTR gene[23] (OTR cKO mice). To specifically delete OTRs in astrocytes, we injected an AAV driving expression of Cre recombinase under the control of the GFAP promoter in the CeL (P_{GFAP}-Cre, Fig. 2g). This led to to expression of Cre in 56.0±4.9% of astrocytes within the injection site, with a specificity reaching 96.2±2.1% (Extended Data Fig. 2g). P_{GFAP}-Cre AAV injection in OTR cKO mice resulted in a drastic decrease in OTR mRNA signal in astrocytes (Fig 2h), but not in neurons (Extended Data Fig. 2h). Similarly to results obtained in rats, TGOT application in TTX-treated acute slices of the CeL from control mice led to responses in 43.9±7.2% of astrocytes (Fig. 2i), whereas these responses were largely reduced in CeL astrocytes from P_{GFAP}-Cre AAV injected OTR cKO mice (GFAP OTR KO, Fig. 2i). These results confirm that astrocytes respond directly to OTR activation independently from TGOT effects on CeL neurons.

Activation of OTR+ astrocytes propagates through an astrocyte network

Since astrocytes are known to form extensive intercellular networks, we next studied the spatial connectivity of OTR+ astrocytes in the CeL. (Fig. 3a, Extended Data Fig. 3a). We found that the distance between OTR+ astrocyte pairs (95.8±4.0µm) was larger than the distance between OTR- astrocyte pairs (37.4±0.9µm, Fig. 3a). In addition, we found that OTR+ astrocytes had significantly more contacts with OTR-, than with OTR+ astrocytes (Fig. 3a), whereas OTR- regularly contact other OTR- astrocytes (3.7±1.3 contacts).

These anatomical results suggest a specific distribution pattern of OTR+ astrocytes within the CeL, where OTR+ astrocytes are found distant from their counterparts and exhibit numerous connections with others, OTR- astrocytes. Interestingly, the proportion of rats and mice astrocytes responsive to OTR activation always exceeded 40% of recorded cells (Fig. 2) despite our FISH/Imaris results indicating that less than 20% of astrocytes expressed OTRs mRNA (Fig. 1). This apparent discrepancy led us to test whether the minor population of OTR+ astrocytes could spread their activation following OTR signaling to a much larger population of OTR- astrocytes.

There are two common signaling pathways typical for astrocytes which could facilitate the spread of activation from OTR+ to OTR- astrocytes: (i) paracrine purinergic communication and (ii) gap-junctions mediated spread of activity. To decipher the underlying mechanism, we

first blocked purinergic receptors using pyridoxalphosphate-6-azophenyl-2',4'-disulfonic acid (PPADS) and found that this blocker did not significantly affect the average proportion of astrocytes activated by TGOT (Fig. 3b), nor the properties of these responses (Fig. 3b), a result replicated using a set of purinergic receptors antagonists blocking the majority of known purinergic receptors (Extended Data Fig. 3b-c). Yet, the incubation with the gap-junctions blocker carbenoxolone (CBX) significantly reduced the number of astrocytes responsive to TGOT+TTX application (Fig. 3b). Given that astrocyte gap-junctions are primarily composed of the connexins (Cx) 30 and 43, we further tested their involvement in OTR-induced signal spreading by using a Cx30/Cx43 double KO mice line, previously shown to lack astrocyte gap junctional communication[24] (Fig. 3c). As found with CBX, the number of astrocytes activated by TGOT was significantly reduced in these mice (Fig. 3c). These results indicate that gap junctions play a role in the propagation of responses following OTR activation in the CeL astrocytes network, possibly from OTR+ to OTR- astrocytes. This is corroborated by the anatomical observations that biocytin infused in the cytosol of astrocytes spread from one cell to another within the CeL network at least in part via gap-junctions (Fig. 4e).

CeL astrocyte activity increases CeL neurons excitability

We next wanted to test if this direct astrocyte network response to OTR activation could be relevant to the known effect of OTR signaling on CeA neuronal networks [4,13,14]. To manipulate astrocytic activity, we expressed the opsin C1V1 under the control of the GFAP promoter using rAAV injections (P_{GFAP}-C1V1-mCherry; referred to as AstrOpto, Fig. 4a). After confirmation of vector expression in 62.5±3.1% of all astrocytes in the CeL, with a specificity reaching 98.8±0.7% (Extended Data Fig. 4a), we evaluated the effect of C1V1 stimulation on astrocyte calcium activity (Fig. 4b). We observed responses in 60.8±9.0% of astrocytes (Fig. 4c), a proportion comparable to what we observed following OTR stimulation by TGOT+TTX (AstrOpto vs TGOT+TTX: p = 0.8265, unpaired t-test). The removal of extracellular calcium prevented the C1V1-driven astrocyte activity (Extended Data Fig. 4b). This indicates that influx of extracellular calcium through the plasma membrane is required to generate calcium transient activity in astrocytes following C1V1 activation (Extended Data Fig. 4b).

Next, we measured the effect of evoked astrocyte activity, using AstrOpto or direct OTR stimulation through TGOT application, on CeL neurons excitability measured through patch-clamp techniques. Optical stimulation of C1V1 in astrocytes increased the frequency of miniature excitatory post-synaptic currents (mEPSCs) in CeL neurons (Fig. 4d) while bath-applied TGOT had a similar effect (Fig. 4f). We next infused BAPTA specifically in the astrocyte network (Fig. 4e) to block the increase in calcium transients evoked by TGOT, and found it also blocked TGOT effect on CeL neurons mEPSCs (Fig. 4e-f). This indicates that OTR activation and the ensuing increased in calcium transients in astrocytes is driving up excitatory inputs to CeL neurons.

To identify the intercellular communication pathway involved in astrocytes-neurons communication following OTR-dependent activation of astrocytes, we studied whether N-Methyl-D-Aspartate receptor (NMDAR), a well-known neuronal receptor that can be activated

by astrocytic gliotransmission[12,25,26], was involved. Thus, we applied a NMDAR antagonist (2R)-amino-5-phosphonovaleric acid (AP5) prior to TGOT application and found it inhibited TGOT effect on mEPSCs frequency (Fig. 4f). Importantly, AP5 had no effect on astrocyte responses to TGOT, thereby excluding the involvement of NMDAR in CeL astrocytes responses to TGOT (Extended Data Fig. 3d). Finally, to unambiguously demonstrate that astrocytes underlie the effect of OTR signaling on CeL neuron excitatory synaptic transmission, we repeated the mEPSCs measurements in control and GFAP OTR KO mice. TGOT application increased mEPSCs frequency in control mice, but not in GFAP OTR KO mice (Fig. 4g-h), confirming the role of astrocytic OTR in mediating the effects of OTR signaling on synaptic inputs in CeL neurons.

We then investigated whether the increase in mEPSCs frequency in CeL neurons following OTR activation was able to increase their firing frequency. To address this question, we applied the same stimulation protocols as before, and subsequently recorded spontaneous action potential (AP) firing (Fig. 5a-b). First, AstrOpto increased firing of CeL neurons, an effect that was blocked by previous infusion of BAPTA in the astroglial network, hence proving its dependence on astrocyte calcium signaling (Fig. 5c). Similarly, and in agreement with its effect on CeL neurons mEPSC, TGOT also increased neuronal spiking activity (Fig. 5d), an effect which was abolished following either BAPTA infusion in the astroglial network or pre-incubation of AP5 in the recording bath (Fig. 5d). Crucially, TGOT application increased the firing of CeL neurons in control but not in GFAP OTR KO mice (Fig. 5e-f).

These results unequivocally demonstrate that OTR signaling in the CeL requires the expression and activation of OTR and its associated calcium signaling in astrocytes, which further lead to an increase in the excitability of CeL interneurons through NMDAR-dependent mechanisms.

CeL astrocytes activity increases inhibitory inputs onto CeM projection neurons

Previous work showed that the activation of CeL OTRs leads to an increased activity of GABAergic CeL neurons, a result we replicated here (Fig. 5). A demonstrated direct consequence of this is an increased frequency of $GABA_A$-mediated inhibitory post-synaptic currents (IPSCs) in CeM projection neurons[4,13,14].

In agreement with these findings, we found that optogenetic activation of CeL astrocytes (through AstrOpto) evoked an increase in IPSC frequency in rat CeM neurons (Fig. 6a-c). This effect was also dependent on CeL astrocytic calcium signaling, as BAPTA infusion in CeL astrocytes abolished it (Fig. 6c). Furthermore, the effect of AstrOpto on CeM IPSCs frequency was suppressed by application of AP5, but also by prior degradation of D-serine (an NMDAR co-agonist) with D-amino acid oxidase (DAAO) (Extended Data Fig. 5a). D-Serine is a known gliotransmitters, whose levels have been found to be increased following astrocytic GPCR activation[27]. Altogether, these results indicate that the effect of AstrOpto on IPSCs in CeM neurons is dependent on the activation of NMDARs in CeL neurons. TGOT application produced a similar effect on CeM neurons, also dependent on CeL astrocytic calcium signaling (Fig. 6d) and on NMDARs (Fig. 6d). Initial incubation with DAAO similarly blocked the effect of TGOT on IPSCs frequency (Extended Data Fig. 5b). Crucially, D-serine supplementation in the DAAO-treated slices following the first, effectless, TGOT application rescued the effect of a second TGOT application on IPSCs frequency (Extended Data Fig.

5b-d). This confirms the involvement of neuronal NMDARs and its co-agonist D-Serine in OTR-mediated modulation of CeA neuronal network. To further complement these results, we found that bath application of 5,7-dichlorokynurenic acid (DCKA), a potent antagonist of the NMDAR glycine/D-Serine modulatory site, also abolished TGOT effects on CeM IPSC frequency, while the AMPAR antagonist DNQX had no effect (Extended Data Fig. 5e). In addition, pre-incubation with the purinergic receptors antagonists PPADS, CPT or SCH 58261 had no effects either (Extended Data Fig. 5f). This confirms that the primary mode of astrocyte to neuron communication engaged following OTR signaling in CeA involves NMDARs, but not purinergic signaling in neurons, and is mediated by an increase in D-serine levels.

As in rats, TGOT application also led to an increased IPSC frequency in CeM neurons in brain slices from control mice, but not in slices from GFAP OTR KO mice (Fig. 6e-f). These *ex vivo* results clearly demonstrate that direct of OTR-mediated CeL astrocytes activation leads to an NMDAR-dependent increase in CeL neurons excitability, which further increases inhibitory inputs into CeM projection neurons.

Our data so far demonstrate that when OTR signaling is engaged in astrocytes, these cells increase the excitability of CeL neurons, directly leading to an increase in inhibitory inputs into CeM projection neurons. Altogether, these results demonstrate that the effect of OT on neuronal activity is abolished when astrocyte function is compromised, establishing for the first time that OT signaling in CeA circuitry is locally transduced by astrocytes.

OTR signaling through astrocytes is crucial for emotional balance regulation.

The CeA is a key nucleus for the processing of emotional information, and notably plays an important role in pain-associated disorders[16], for which OT has been demonstrated as a crucial regulator[19]. We therefore chose to first test the involvement of OTR-mediated (or direct) astrocyte activation in modulating mechanical pain hypersensitivity (Fig. 7b,f), levels of anxiety (Fig. 7c,g), and reinforcement behavior (Fig. 7f,h) in rats and mice that developed neuropathic pain and the associated increased anxiety following a spared nerve injury (SNI) surgery[28] (Extended Data Fig. 6a).

Given that there is a proven link between chronic pain etiology and synaptic changes in the CeA[29], we initially tested whether the effect of TGOT on astrocytes calcium signaling and CeM neurons IPSCs frequency was altered in SNI rats, but did not find any differences compared to sham-operated animals (Extended Data Fig. 6b-c). This indicates that OTR signaling in CeA, at least at the levels of the circuit studied here, is unaltered in SNI animals. We further confirmed that D-Serine was still required for TGOT effects in the CeA of SNI animals using DAAO pre-incubation followed by exogenous D-Serine supplementation in the *ex vivo* setting (Extended Data Fig. 6d).

Following our finding that SNI procedure did not alter the effect of TGOT at the circuit level, we next used a nociceptive assay to measure the mechanical threshold for paw withdrawal in both rats and mice. We found that SNI animals displayed a decreased mechanical threshold, but bilateral micro-injections of TGOT in the CeA had no clear effect on it, with only a mild anti-nociceptive effect only in rats (Fig. 7b,f). Moreover, bilateral optogenetic stimulation of

rats CeL astrocytes (AstrOpto) had no noticeable effect on mechanical threshold in rats (Fig. 7b; Extended Data Fig. 7b).

Next we performed an elevated plus maze (EPM) test, and found that SNI animals spent significantly more time in the closed arm compared to sham-operated ones, indicating the SNI procedure induced a state of elevated anxiety (Fig. 7c,g) as expected. When TGOT was injected in CeA, time spent in the closed arm was significantly reduced to levels comparable to those observed in sham animals, indicating an anxiolytic effect of OTR signaling in both rats and mice (Fig. 7c,g). Crucially, AstrOpto in rats had a comparable effect (Fig. 7c), while the deletion of OTR from CeL astrocytes in mice abolished the anxiolytic effects of TGOT (Fig. 7g), highlighting the involvement of astrocytic OTRs also at the behavioral level. Interestingly, sham mice with deletion of OTR in CeL astrocytes displayed an anxious behavior (Fig. 7g), which indicates OTR signaling through astrocytes is involved in emotional balance, even under pain-free conditions.

In order to further investigate the role of the CeA in attributing emotional valence to stimuli, we used the conditioned place preference (CPP) test in rats and mice that underwent an SNI or sham procedures. Here, both SNI and sham animals exhibited a clear preference for the chamber paired with TGOT infusion (Fig. 7d,h). The optogenetic activation of astrocytes in rat CeL also led to a place preference, mimicking TGOT action (Fig. 7d), while TGOT lost its positive conditioning effects in GFAP OTR KO mice (Fig. 7h). Importantly, neither the treatments nor the SNI procedure significantly affected the motor activity of rats and mice in both the EPM or CPP tests (Extended Data Fig. 7).

Collectively, our findings demonstrate from the local circuit to the behavioral levels that OTR signaling through CeL astrocytes is a novel and important mechanism involved in emotional states regulation, this under both normal and chronic pain conditions (Fig. 7i).

DISCUSSION

We here demonstrate that OTR signaling through astrocytes is crucial for the oxytocinergic modulation of the local CeA microcircuit and its behavioral correlates. We further propose that this effect relies on a morphologically defined subpopulation of OTR+ astrocytes (Fig. 1-2), that convey their activation by OT to other astrocytes through gap-junctional communication (Fig. 3), leading to an increase in activity in the majority of CeL astrocytes (Fig. 2-3). In turn, astrocytes increase the excitability of CeL interneurons by gating activation of NMDA receptors (Fig. 4-5), leading to an increase in GABAergic inhibitory inputs in post-synaptic neurons located in the CeM (Fig. 6). At the behavioral level, this OTR-mediated modulation of CeA astro-neuronal network promotes a positive emotional state, measured as clear anxiolytic and positive reinforcement effects (Fig. 7).

Mechanistically, our results reinforce previous demonstrations of a role of astrocytes in transforming neuromodulators signaling into a change in the gain of neuronal circuits, notably by (co-)activating neuronal NMDAR[12,25,26]. Despite the high proportion of OTR+ neurons (up to 70%) compared to the limited number of OTR+ astrocytes (~18%) in the CeL, the activation of OTRs in astrocytes was required to gate CeL neurons responses to OTR activation by allowing a sustained (co)activation of NMDARs. Other mechanisms are probably at play: OTR activation in CeL neurons might inhibit K+ leak current, as has been shown in olfactory neuronal cells[30] and in spinal cord[31]. These mechanisms might act in synergy to induce an elevation in firing rates of CeL neurons by increasing the gain of excitatory inputs in these cells. Furthermore, similar mechanisms of astrocytes to neuron communication through neuronal NMDARs (co)activation have been proposed by other studies to favor a synchronous increase in excitability across an ensemble of neurons[32,33]. This would allow a synchronized and long-lasting switch in the gain of the CeA neuronal circuits, thereby amplifying the effect of OT on CeA outputs in both the spatial and temporal domains. In light of the predominantly non-synaptic mode of OT release from axons *en passant*, which could lead to CeL-restricted micro-volume transmission of the neuropeptide[5], it seems then plausible that astrocytes are required to relay and amplify OT signaling to CeL neurons. Another mechanism that was repeatedly found to be involved in neuromodulators signaling through astrocytes is the activation of purinergic signaling in neurons[34,35]. However, in the case of OT signaling within the CeA, purinergic signaling was not involved (Extended Data Fig. 5). It would then be interesting to test if astrocytes are important to OT signaling in other brain regions, and if they are, if the same mechanisms of astrocytes to neurons communication are at stake.

We found that CeA astrocytes can be divided into two defined populations: OTR+ and OTR- astrocytes. OTR+ astrocytes are morphologically more complex and have more close contacts with neighboring, OTR- astrocytes, while being quite distant from their OTR+ counterparts with whom they have almost no contacts (Fig. 1, 2). Thus, we hypothesize that these morphological peculiarities allow the propagation of OTR evoked calcium transients (Fig. 2) to a much larger number of OTR- astrocytes through, at least partially, gap junctions (Fig. 3b-c). Therefore only a few, strategically positioned OTR+ astrocytes are sufficient to result in a network wide effect of OT release in the CeL, despite the relatively moderate number of OT fibers found in this nucleus[4]. By describing a new population of astrocytes, our

work add to the recent advances in describing molecular, morphological and functional heterogeneity in astrocytes population[36,37] and opens up new perspectives into understanding how astrocytes subpopulations are functionally organized and communicate inside CNS circuits.

OT and its effects on brain circuits, and ultimately behavior, are under intense scrutiny, from fundamental research in animal models to behavioral and physiological studies in humans[38,39]. Among other roles, OT is considered a powerful anxiolytic peptide through its action in the human amygdala[40]. Yet, all studies so far considered as an accomplished fact that OT was acting directly on neurons, despite the controversies regarding the cellular substrates of BOLD fMRI signals often used in human studies, with some results arguing for a major contribution of astrocyte activity to these signals[41,42]. Furthermore, a significant number of studies demonstrated that astrocytes or their invertebrates counterparts are key, if not primary, targets of neuromodulators[12,25,26,34,35,43], and that astrocytes might be the causal elements behind shifts in brain states[11,43,44], a function usually attributed mainly to neuromodulators direct action on neurons[45]. Thus, further research focused on astrocytes-mediated modulation of human brain circuits' activities is particularly promising to develop refined strategies for future therapeutic approaches. Indeed, neuromodulators are the targets of numerous, already available, treatments of psychiatric diseases using either small molecule drugs or electrical stimulation protocols, such as deep brain[46] or transcranial stimulations[47], for which astrocytes also seem particularly involved[46,47]. Taken together, this indicates a need for a more global and systematic consideration of astrocytes roles in brain circuits, notably regarding the effect of neuromodulators, and in particular OT. We believe this is especially relevant for the development of better therapeutics in the field of chronic pain, which imposes a massive burden to society, impacting ~20% of the global population[48].

Indeed, considering that general anxiety and depression are frequent comorbidity of chronic pain[49], our finding that the activation of OT signaling in CeL astrocytes promotes a form of emotional comfort by alleviating anxious behavior and has positive reinforcement properties is promising: it demonstrates that activation of a particular, astrocyte-mediated, OTR pathways affect one of the most impactful aspect of the chronic pain sphere, the emotional one. This further highlights astrocytes as important cellular substrates of emotional regulation, which several studies have also argued for (see[50] and references therein). In this context, targeting the OT system and/or astrocytes specifically, in the amygdala or other CNS regions, might lead to the development of new therapeutic avenues to improve patient's well-being.

ACKNOWLEDGEMENTS

This work was supported by the IASP Early Career Research grant 2012, FP7 Career Integration grant 334455, Initiative of Excellence (IDEX) Attractiveness grant 2013, IDEX Interdisciplinary grant 2015, University of Strasbourg Institute for Advanced Study (USIAS) fellowship 2014-15, Foundation Fyssen research grant 2015, NARSAD Young Investigator Grant 24821, ANR JCJC grant (to AC); ANR-DFG grant GR 3619/701 (to AC and VG); Alexander von Humboldt fellowship (to DH), Seed grant from DFG within the Collaborative center SFB 1158 and Fyssen Foundation fellowship (to AL), DFG grants GR 3619/13-1 and GR 3619/16-1 (to VG), SFB 1158 (to CP, JS, and VG); SNSF-DFG grant GR 3619/8-1 (to RS and VG), Fritz Thyssen foundation (to VG); DFG Postdoc Fellowship AL 2466/1-1 to FA, Alexander von Humboldt Foundation (to DH); Fyssen foundation and PROCOP grant and SFB1158 seed grant for young scientists (to AL); Research Foundation - Flanders, fellowship (12V7519N) (to JW); Russian Science Foundation RSF (17-75-10061) and the Subsidy Allocated to the Kazan Federal University for the State Assignment № 0671-2020-0059 (to AR); the intramural research program of the NIMH (ZIAMH002498) (to WSY); National Institutes of Health grants R01NS094640 and R01HL090948 (to JES). European Research Council (Consolidator grant #683154) and European Union's Horizon 2020 research and innovation program (Marie Sklodowska-Curie Innovative Training Networks, grant #722053, EU-GliaPhD) (to NR). The authors thank Vincent Lelièvre for *in situ* hybridization advices; Romain Goutagny for *in vivo* optogenetics assistance; Fulvio Magara for anxiety behavior advices; Barbara Kurpiers and the Interdisciplinary Neurobehavioral Core Facility of Heidelberg University for experiments performed there; Sophie Reibel and the Chronobiotron UMS 3415 for all animal care; Thomas Splettstoesser (www.scistyle.com) for the help with the preparation of figure 7.

AUTHOR CONTRIBUTIONS

Conceptualization, AC; Methodology, AC, BBo, CML, CP, DK, FA, ID, JES, JW, JYC, NR, PD, PP, RS, VG, WSY, YG; Analysis, AC, BBe, BBJ, CML, DK, FA, HSKB, JW, SG; *In situ* hybridization, DH, FA, HSKB, HW, JS, ME; Immunohistochemistry, AL, DH, FA, JW, ME, MdSG; Imaris analysis: FA, MKK, RKR; *Ex vivo* patch-clamp electrophysiology, AB, AC, JW, SG, DK, IW, BBe, MA; *Ex vivo* calcium imaging, AB, CML, DK, JW; Astrocytes characterization, AB, AR, BBe, DK, IW, ME, SG; Behavior, AC, BBJ, DK, JW; Mice line validation, WSY; Viral vectors validation, MdSG, ME, VG; Spared nerve injuries, PI, MP; Writing, AB, AC, DK, FA, JW, VG; Funding acquisition AC, VG; Supervision, AC, VG; Project administration, AC.

DECLARATION OF INTERESTS

The authors declare no competing interest

REFERENCES

1. Lee, H.-J., Macbeth, A. H., Pagani, J. H. & Young, W. S. Oxytocin: the great facilitator of life. *Prog. Neurobiol.* **88**, 127–51 (2009).
2. Gimpl, G. & Fahrenholz, F. The oxytocin receptor system: structure, function, and regulation. *Physiol. Rev.* **81**, 629–83 (2001).
3. Theodosis, D. T. Oxytocin-secreting neurons: A physiological model of morphological neuronal and glial plasticity in the adult hypothalamus. *Front. Neuroendocrinol.* **23**, 101–35 (2002).
4. Knobloch, H. S. *et al.* Evoked axonal oxytocin release in the central amygdala attenuates fear response. *Neuron* **73**, 553–66 (2012).
5. Chini, B., Verhage, M. & Grinevich, V. The Action Radius of Oxytocin Release in the Mammalian CNS: From Single Vesicles to Behavior. *Trends Pharmacol. Sci.* **38**, 982–991 (2017).
6. Kuo, J., Hariri, O. R. & Micevych, P. An interaction of oxytocin receptors with metabotropic glutamate receptors in hypothalamic astrocytes. *J. Neuroendocrinol.* **21**, 1001–6 (2009).
7. Wang, P., Qin, D. & Wang, Y.-F. Oxytocin Rapidly Changes Astrocytic GFAP Plasticity by Differentially Modulating the Expressions of pERK 1/2 and Protein Kinase A. *Front. Mol. Neurosci.* **10**, 1–14 (2017).
8. Mitre, M. *et al.* A Distributed Network for Social Cognition Enriched for Oxytocin Receptors. *J. Neurosci.* **36**, 2517–2535 (2016).
9. Yoshida, M. *et al.* Evidence that oxytocin exerts anxiolytic effects via oxytocin receptor expressed in serotonergic neurons in mice. *J. Neurosci.* **29**, 2259–71 (2009).
10. Hirase, H., Iwai, Y., Takata, N., Shinohara, Y. & Mishima, T. Volume transmission signalling via astrocytes. *Philos. Trans. R. Soc. B Biol. Sci.* **369**, 20130604–20130604 (2014).
11. Kjaerby, C., Rasmussen, R., Andersen, M. & Nedergaard, M. Does Global Astrocytic Calcium Signaling Participate in Awake Brain State Transitions and Neuronal Circuit Function? *Neurochem. Res.* **42**, 1810–1822 (2017).
12. Papouin, T., Dunphy, J. M., Tolman, M., Dineley, K. T. & Haydon, P. G. Septal Cholinergic Neuromodulation Tunes the Astrocyte-Dependent Gating of Hippocampal NMDA Receptors to Wakefulness. *Neuron* **94**, 840-854.e7 (2017).
13. Huber, D., Veinante, P. & Stoop, R. Vasopressin and oxytocin excite distinct neuronal populations in the central amygdala. *Science* **308**, 245–8 (2005).
14. Viviani, D. *et al.* Oxytocin selectively gates fear responses through distinct outputs from the central amygdala. *Science* **333**, 104–7 (2011).
15. Han, R. T. *et al.* Long-Term Isolation Elicits Depression and Anxiety-Related Behaviors by Reducing Oxytocin-Induced GABAergic Transmission in Central Amygdala. *Front. Mol. Neurosci.* **11**, 246 (2018).
16. Neugebauer, V., Li, W., Bird, G. C. & Han, J. S. The amygdala and persistent pain. *Neuroscientist* **10**, 221–234 (2004).
17. Tye, K. M. *et al.* Amygdala circuitry mediating reversible and bidirectional control of anxiety. *Nature* **471**, 358–62 (2011).
18. Ji, R.-R., Donnelly, C. R. & Nedergaard, M. Astrocytes in chronic pain and itch. *Nat. Rev. Neurosci.* **20**, 667–685 (2019).
19. Poisbeau, P., Grinevich, V. & Charlet, A. Oxytocin Signaling in Pain: Cellular, Circuit, System, and Behavioral Levels. *Curr. Top. Behav. Neurosci.* (2017). doi:10.1007/7854_2017_14
20. Martin-Fernandez, M. *et al.* Synapse-specific astrocyte gating of amygdala-related behavior. *Nat. Neurosci.* **20**, 1540–1548 (2017).
21. Althammer, F. *et al.* Three-dimensional morphometric analysis reveals time-dependent structural changes in microglia and astrocytes in the central amygdala and hypothalamic paraventricular nucleus of heart failure rats. *J. Neuroinflammation* **17**,

221 (2020).
22. Yizhar, O. *et al.* Neocortical excitation/inhibition balance in information processing and social dysfunction. *Nature* **477**, 171–178 (2011).
23. Lee, H. J., Caldwell, H. K., Macbeth, A. H., Tolu, S. G. & Young, W. S. A conditional knockout mouse line of the oxytocin receptor. *Endocrinology* **149**, 3256–3263 (2008).
24. Wallraff, A. *et al.* The impact of astrocytic gap junctional coupling on potassium buffering in the hippocampus. *J. Neurosci.* **26**, 5438–47 (2006).
25. Robin, L. M. *et al.* Astroglial CB1 Receptors Determine Synaptic D-Serine Availability to Enable Recognition Memory. *Neuron* **98**, 935-944.e5 (2018).
26. Corkrum, M., Rothwell, P. E., Thomas, M. J., Kofuji, P. & Araque, A. Opioid-Mediated Astrocyte-Neuron Signaling in the Nucleus Accumbens. *Cells* **8**, 586 (2019).
27. Robin, L. M. *et al.* Astroglial CB1 Receptors Determine Synaptic D-Serine Availability to Enable Recognition Memory. *Neuron* **0**, 1–10 (2018).
28. Decosterd, I. & Woolf, C. J. Spared nerve injury: an animal model of persistent peripheral neuropathic pain. *Pain* **87**, 149–158 (2000).
29. Thompson, J. M. & Neugebauer, V. Amygdala Plasticity and Pain. *Pain Res. Manag.* **2017**, 8296501 (2017).
30. Gravati, M. *et al.* Dual modulation of inward rectifier potassium currents in olfactory neuronal cells by promiscuous G protein coupling of the oxytocin receptor. *J. Neurochem.* **114**, 1424–1435 (2010).
31. Breton, J.-D. *et al.* Oxytocin-induced antinociception in the spinal cord is mediated by a subpopulation of glutamatergic neurons in lamina I-II which amplify GABAergic inhibition. *Mol. Pain* **4**, 19 (2008).
32. Angulo, M. C., Kozlov, A. S., Charpak, S. & Audinat, E. Glutamate released from glial cells synchronizes neuronal activity in the hippocampus. *J. Neurosci.* **24**, 6920–6927 (2004).
33. Fellin, T. *et al.* Neuronal synchrony mediated by astrocytic glutamate through activation of extrasynaptic NMDA receptors. *Neuron* **43**, 729–43 (2004).
34. Corkrum, M. *et al.* Dopamine-Evoked Synaptic Regulation in the Nucleus Accumbens Requires Astrocyte Activity. *Neuron* **105**, 1036-1047.e5 (2020).
35. Ma, Z., Stork, T., Bergles, D. E. & Freeman, M. R. Neuromodulators signal through astrocytes to alter neural circuit activity and behaviour. *Nature* **539**, 428–432 (2016).
36. Pestana, F., Edwards-Faret, G., Belgard, T. G., Martirosyan, A. & Holt, M. G. No longer underappreciated: The emerging concept of astrocyte heterogeneity in neuroscience. *Brain Sci.* **10**, 1–21 (2020).
37. Khakh, B. S. & Deneen, B. The Emerging Nature of Astrocyte Diversity. *Annu. Rev. Neurosci.* **42**, 187–207 (2019).
38. Grinevich, V. & Neumann, I. D. Brain oxytocin: how puzzle stones from animal studies translate into psychiatry. *Mol. Psychiatry* (2020). doi:10.1038/s41380-020-0802-9
39. Quintana, D. S. *et al.* Advances in the field of intranasal oxytocin research: lessons learned and future directions for clinical research. *Mol. Psychiatry* (2020). doi:10.1038/s41380-020-00864-7
40. Neumann, I. D. & Slattery, D. A. Oxytocin in General Anxiety and Social Fear: A Translational Approach. *Biol. Psychiatry* **79**, 213–221 (2016).
41. Takata, N. *et al.* Optogenetic astrocyte activation evokes BOLD fMRI response with oxygen consumption without neuronal activity modulation. *Glia* **66**, (2018).
42. Figley, C. R. & Stroman, P. W. The role(s) of astrocytes and astrocyte activity in neurometabolism, neurovascular coupling, and the production of functional neuroimaging signals. *Eur. J. Neurosci.* **33**, 577–588 (2011).
43. Kastanenka, K. V. *et al.* A roadmap to integrate astrocytes into Systems Neuroscience. *GLIA* (2019). doi:10.1002/glia.23632
44. Poskanzer, K. E. & Yuste, R. Astrocytes regulate cortical state switching in vivo. *Proc. Natl. Acad. Sci. U. S. A.* **2016**, 1–10 (2016).
45. McCormick, D. A., Nestvogel, D. B. & He, B. J. Neuromodulation of Brain State and Behavior. *Annu. Rev. Neurosci.* **43**, 391–415 (2020).

46. Fenoy, A. J., Goetz, L., Chabardès, S. & Xia, Y. Deep brain stimulation: Are astrocytes a key driver behind the scene? *CNS Neurosci. Ther.* **20**, 191–201 (2014).
47. Monai, H. & Hirase, H. Astrocytes as a target of transcranial direct current stimulation (tDCS) to treat depression. *Neurosci. Res.* **126**, 15–21 (2018).
48. Mills, S. E. E., Nicolson, K. P. & Smith, B. H. Chronic pain: a review of its epidemiology and associated factors in population-based studies. *Br. J. Anaesth.* **123**, e273–e283 (2019).
49. Woo, A. K. Depression and Anxiety in Pain. *Rev. pain* **4**, 8–12 (2010).
50. Oliveira, J. F., Sardinha, V. M., Guerra-Gomes, S., Araque, A. & Sousa, N. Do stars govern our actions? Astrocyte involvement in rodent behavior. *Trends Neurosci.* **38**, 535–49 (2015).
51. Rouach, N., Koulakoff, A., Abudara, V., Willecke, K. & Giaume, C. Astroglial metabolic networks sustain hippocampal synaptic transmission. *Science* **322**, 1551–5 (2008).
52. Pannasch, U. *et al.* Astroglial networks scale synaptic activity and plasticity. *Proc. Natl. Acad. Sci. U. S. A.* **108**, 8467–72 (2011).
53. Theis, M. *et al.* Accelerated hippocampal spreading depression and enhanced locomotory activity in mice with astrocyte-directed inactivation of connexin43. *J. Neurosci.* **23**, 766–76 (2003).
54. Teubner, B. *et al.* Connexin30 (Gjb6)-deficiency causes severe hearing impairment and lack of endocochlear potential. *Hum. Mol. Genet.* **12**, 13–21 (2003).
55. Shigetomi, E. *et al.* Imaging calcium microdomains within entire astrocyte territories and endfeet with GCaMPs expressed using adeno-associated viruses. *J. Gen. Physiol.* **141**, 633–647 (2013).
56. Ting, J. T. *et al.* Preparation of Acute Brain Slices Using an Optimized N-Methyl-D-glucamine Protective Recovery Method. *J. Vis. Exp.* 1–13 (2018). doi:10.3791/53825
57. Serrano, A., Haddjeri, N., Lacaille, J., Robitaille, R. & Centre-ville, S. GABAergic Network Activation of Glial Cells Underlies Hippocampal Heterosynaptic Depression. *J. Neurosci.* **26**, 5370–5382 (2006).
58. Jourdain, P. *et al.* Glutamate exocytosis from astrocytes controls synaptic strength. *Nat. Neurosci.* **10**, 331–9 (2007).
59. Ikegaya, Y., Le Bon-Jego, M. & Yuste, R. Large-scale imaging of cortical network activity with calcium indicators. *Neurosci. Res.* **52**, 132–138 (2005).
60. Shigetomi, E., Bowser, D. N., Sofroniew, M. V & Khakh, B. S. Two forms of astrocyte calcium excitability have distinct effects on NMDA receptor-mediated slow inward currents in pyramidal neurons. *J. Neurosci.* **28**, 6659–63 (2008).
61. Anlauf, E. & Derouiche, A. Glutamine synthetase as an astrocytic marker: its cell type and vesicle localization. *Front. Endocrinol. (Lausanne).* **4**, 144 (2013).
62. Luis-Delgado, O. E. *et al.* Calibrated forceps: A sensitive and reliable tool for pain and analgesia studies. *J. Pain* **7**, 32–39 (2006).
63. Walf, A. A. & Frye, C. A. The use of the elevated plus maze as an assay of anxiety-related behavior in rodents. *Nat. Protoc.* **2**, 322–8 (2007).
64. King, T. *et al.* Unmasking the tonic-aversive state in neuropathic pain. *Nat. Neurosci.* **12**, 1364–1366 (2009).
65. Virtanen, P. *et al.* SciPy 1.0: fundamental algorithms for scientific computing in Python. *Nat. Methods* **17**, 261–272 (2020).
66. Zeisel, A. *et al.* Cell types in the mouse cortex and hippocampus revealed by single-cell RNA-seq. *Science (80-.).* **347**, 1138–1142 (2015).
67. Batiuk, M. Y. *et al.* Identification of region-specific astrocyte subtypes at single cell resolution. *Nat Commun* **11**, 1220 (2020).
68. Kofuji, P. & Araque, A. G-Protein-Coupled Receptors in Astrocyte–Neuron Communication. *Neuroscience* (2020). doi:10.1016/j.neuroscience.2020.03.025
69. Octeau, J. C. *et al.* Transient, Consequential Increases in Extracellular Potassium Ions Accompany Channelrhodopsin2 Excitation. *Cell Rep.* **27**, 2249-2261.e7 (2019).
70. Reeves, A. M. B., Shigetomi, E. & Khakh, B. S. Bulk loading of calcium indicator dyes to study astrocyte physiology: Key limitations and improvements using morphological

687 maps. *J. Neurosci.* **31**, 9353–9358 (2011).
688

FIGURE TITLES AND LEGENDS

Figure 1. Specific CeL astrocytes express oxytocin receptors. (**a**) Overview of CeA fluorescent *in situ* hybridization of OTR mRNA (red) and glutamine synthase immunostaining (GS, green). (**b**) High magnification images of cells positive for OTR mRNA and/or GS (double arrows); green arrows point GS positive cells; red arrows point OTR mRNA-positive cells. Scale bars are 100 (a) and 10µm (b). (**c**) Proportion of CeL astrocytes (GS positive cells, left) and neurons (NeuN positive cells, right) positive for OTR mRNA (red) ($n_{astrocytes}$ = 1185, $n_{neurons}$ = 1254, n_{rats} = 4). (**d**) Cells were reconstructed in 3D using Imaris and morphological parameters were evaluated. Scale bar = 20µm (**e**) OTR-expressing astrocytes are bigger and more complex as indicated by several morphological parameters (cell volume, surface, number of processes, process length and domain volume). (**f**) OTR-expressing astrocytes display a more complex morphology as revealed by Sholl analysis. All data are expressed in mean ± SEM except for violin plots where hatched line represent the median and the dot lines are the first and third quartiles. *** $p < 0.0001$, student's *t*-test or two-way ANOVA followed by Tukey post-hoc test. (Statistics in Extended Data Table 1).

Figure 2. Astrocytic OTR activation evokes calcium transients in CeL astrocytes of rats and mice. (**a**) Experimental strategy to express the ChR1/VChR1 chimaera channel rhodopsin variant C1V1 in OTergic neurons (OxytOpto). (**b**) Experimental scheme of the horizontal CeA slice preparation used, showing C1V1 expressing OT axons (yellow) arising from PVN and projecting to the CeL. (**c**) Typical traces of relative changes in intracellular calcium in astrocytes (ΔF) induced by the activation of C1V1 in OT axons located in the CeL through λ542 nm light pulses (10 ms width, 30 Hz, duration 20 s). (**d**) Proportion of responding astrocytes (left), AUC of ΔF traces (middle) and Ca^{2+} transients frequency (right) normalized to baseline values following C1V1 activation in CeL OT axons, n slice (n_s) = 7, n astrocytes (n_a) = 36. (**e**) (left) Images of CeL astrocytes identified through SR101 (red, top) and corresponding pseudo-color images of OGB1 fluorescence during baseline and after drug application (middle, bottom, stacks of 50 images over 25s of recording). Scale bar = 10µm. (right) Typical ΔF traces following TGOT+TTX (Ctrl) application (**f**) Proportion of responding astrocytes (left), AUC of ΔF traces (middle) and Ca^{2+} transients frequency (right) normalized to baseline values following application of TGOT (0.4 µM) with TTX (1 µM) (Ctrl, n_s = 18, n_a = 136), without TTX (No TTX, n_s = 7, n_a = 43), and with an OTR antagonist (dOVT, 1 µM; n_s = 3, n_a = 24). Data are expressed as means across slices plus SEM (**g**) Experimental strategy for the specific deletion of OTRs in mice CeL astrocytes. (**h**) (left) Example pictures of OTR mRNA (red) and GS (green) labelling in mice injected with P_{GFAP}-GFP-IRES-Cre (top) or P_{GFAP}-GFP rAAV vector (bottom) ; (right) Proportion of CeL astrocytes (GS positive cells) also positive for OTR mRNA (left, blue, P_{GFAP}-GFP: $n_{astrocytes}$ = 1340, n_{mice} = 3 ; right, red P_{GFAP}-GFP-IRES-Cre: $n_{astrocytes}$ = 1561, n_{mice} = 4). Scale bar = 50µm. (**i**) Proportion of responding astrocytes (left), AUC of ΔF traces (middle) and Ca^{2+} transients frequency (right) normalized to baseline values following application of TGOT+TTX in control (blue, n_s = 12, n_a = 237) or GFAP OTR KO mice (red, n_s = 5, n_a = 47; red) acute brain slices. Calcium imaging data are expressed as means across slices plus SEM and white circles indicate averages across astrocytes per slices. * $p < 0.05$, ** $p < 0.01$, *** $p<0.001$, Unpaired *t*-test or Mann-Whitney U test. (Statistics in Table Extended Data Table 2).

Figure 3. OTR-expressing CeL astrocytes are positioned to recruit a CeL astrocyte network through gap junction. (**a**) (left) The distance between two OTR+ astrocytes is larger than the distance between two OTR- astrocytes. (right) OTR+ astrocytes predominantly form contacts with OTR- astrocytes, ($n_{astrocytes}$ = 1270, $n_{OTR+\ astrocytes}$ = 236, n_{rats} = 4). Contacts are defined by a proximity of less than 1µm between GFAP-positive fibers/endfeet from two different astrocytes. (**b**) (left) Typical ΔF traces following TGOT+TTX application in presence of CBX (100 µM, top) or PPADS (50 µM, bottom). (right) Proportion of responding astrocytes, AUC of ΔF traces and Ca^{2+} transients frequency normalized to baseline values following application of TGOT+TTX (0.4 µM) in presence of CBX (n_s = 9, n_a = 75) or PPADS (n_s = 7, n_a = 53). (**c**) (left) Typical ΔF traces following TGOT+TTX application in Cx30/Cx43 KO mice brain slices. (right) Proportion of responding astrocytes, AUC of ΔF traces and Ca^{2+} transients frequency normalized to baseline values following TGOT+TTX application in WT mice (n_s = 19, n_a = 78) and in Cx30/Cx43 KO mice acute brain slices (n_s = 17, n_a = 100). Calcium imaging data are expressed as means across slices plus SEM and white circles indicate averages across astrocytes per slices. *p < 0.05, **p < 0.01, ***p < 0.001, unpaired *t*-test or Mann-Whitney U test. (Statistics in Table Extended Data Table 3).

Figure 4. CeL astrocyte activity promotes excitatory transmission into CeL neurons. (**a**) Experimental strategy for the specific expression of C1V1 in mice CeL astrocytes (AstrOpto). (**b**) Experimental scheme of the horizontal CeA slice preparation used, showing a C1V1 expressing astrocytes and a patched CeL neuron, recorded in whole-cell voltage-clamp configuration with bath-applied TTX and bicuculline to isolate mEPSC. (**c**) (left) Proportion of responding astrocytes, AUC of ΔF traces and Ca^{2+} transients frequency following AstrOpto activation (n_s = 12, n_a = 49) (right) Typical ΔF traces following AstrOpto activation. (**d**) Frequency of mEPSCs in CeL neurons before (basal), during (AstrOpto) and after (Wash) AstrOpto activation (λ542 nm, 3 min long, 1 s width pulse at 0,5 Hz; n = 17). (**e**) Example of an astrocyte in CeL patched with a BAPTA-Biocytin filled capillary (white arrow). Biocytin can be seen diffusing in neighboring astrocytes**. f**) Frequency of mEPSCs in CeL neurons before (basal), during (TGOT, 0.4 µM) and after (Wash) TGOT application (left, n=16). This effect can be blocked by loading BAPTA in the CeL astrocyte network (middle, BAPTAstro, n= 11) and by prior incubation of an NMDAR antagonist (right, AP5, 50 µM, n = 9). (**g**) Experimental strategy for the specific deletion of OTRs in mice CeL astrocytes. (**h**) Frequency of mEPSCs in CeL neurons before (basal), during (TGOT, 0.4 µM) and after (Wash) TGOT application in acute brain slice from WT (left, blue, n = 10) and from GFAP OTR KO mice (right, red, n= 8).). Calcium imaging data are expressed as means across slices plus SEM and white circles indicate averages across astrocytes per slices. Patch-clamp data are expressed as averaged frequency plus SEM across cells, linked white circles indicate individual cell values, example traces of the various conditions are displayed on the right. $^{\#}p$ < 0.05, $^{\#\#\#}p$ < 0.001, Friedman and Dunn's Multiple comparisons, *p < 0.05, **p < 0.01, Unpaired *t*-test or Mann-Whitney U test. (Statistics in Table Extended Data Table 4).

Figure 5. CeL astrocyte activity promotes CeL neuron firing. (**a**) Experimental strategy for the specific expression of C1V1 in mice CeL astrocytes (AstrOpto) (**b**) Experimental scheme of the horizontal CeA slice preparation used, showing a C1V1 expressing astrocytes and a patched CeL neuron, recorded in whole-cell current-clamp configuration to record action potentials (APs). (**c**) Frequency of APs in CeL neurons before (basal), during (AstrOpto) and after (Wash) AstrOpto activation (λ542 nm, 3 min long, 1 s width pulse at 0,5 Hz) in control condition (left, n = 10) or following BAPTA loading in the CeL astrocyte network

(right, BAPTAstro, n = 12). (**d**) Frequency of APs in CeL neurons before (basal), during (TGOT, 0.4 µM) and after (Wash) TGOT application (left, n = 9). This effect can be blocked by loading BAPTA in the CeL astrocyte network (middle, BAPTAstro, n = 9) and by prior incubation of the NMDAR antagonist AP5 (right, AP5, 50 µM, n = 7). (**e**) Experimental strategy for the specific deletion of OTRs in mice CeL astrocytes (GFAP OTR KO). (**f**) Frequency of APs in CeL neurons before (basal), during (TGOT, 0.4 µM) and after (Wash) TGOT application in acute brain slices from WT (left, blue, n = 7) and GFAP OTR KO mice (right, red, n = 11). Example traces of the various conditions are displayed on the right. Patch-clamp data are expressed as averaged frequency plus SEM across cells; linked white circles indicate individual cell values. $^{\#}p < 0.05$, $^{\#\#}p < 0.01$, Friedman and Dunn's Multiple comparisons, $^{*}p < 0.05$, $^{***}p < 0.001$, Unpaired *t*-test or Mann-Whitney U test. (Statistics in Table Extended Data Table 5).

Figure 6. Astrocyte-driven CeL neuron activity modifies amygdala output. (**a**) Experimental strategy for the specific expression of C1V1 in mice CeL astrocytes (AstrOpto) (**b**) Experimental scheme of the horizontal CeA slice preparation used, showing a C1V1 expressing astrocytes and a patched CeM neuron, recorded in whole-cell voltage-clamp configuration to record IPSCs. (**c**) Frequency of IPSCs in CeL neurons before (basal), during (AstrOpto) and after (Wash) AstrOpto activation (λ542 nm, 3 min long, 1 s width pulse at 0,5 Hz) in control condition (left, n = 19) or following BAPTA loading in the CeL astrocyte network (right, BAPTAstro, n = 9). (**d**) Frequency of IPSCs in CeL neurons before (basal), during (TGOT, 0.4 µM) and after (Wash) TGOT application (left, n = 17). This effect can be blocked by loading BAPTA in the CeL astrocyte network (middle, BAPTAstro, n = 17) and by prior incubation of the NMDAR antagonist AP5 (right, AP5, 50 µM, n = 5). (**e**) Experimental strategy for the specific deletion of OTRs in mice CeL astrocytes (GFAP OTR KO). (**f**) Frequency of APs in CeL neurons before (basal), during (TGOT, 0.4 µM) and after (Wash) TGOT application in acute brain slices from WT (left, blue, n = 27) and GFAP OTR KO mice (right, red, n = 15). Example traces of the various conditions are displayed on the right. Patch-clamp data are expressed as averaged frequency plus SEM across cells; linked white circles indicate individual cell values. $^{\#}p < 0.05$, $^{\#\#\#}p < 0.001$, Friedman and Dunn's Multiple comparisons, $^{*}p < 0.05$, $^{**}p < 0.01$, $^{***}p < 0.001$, Unpaired *t*-test or Mann-Whitney U test. (Statistics in Table Extended Data Table 6).

Figure 7. CeL astrocytes modulate CeA behavioral correlates of comfort and are required for their OTR-mediated modulation. (**a, e**) Experimental strategy for the specific expression of C1V1 in mice CeL astrocytes (**a,** AstrOpto) or the specific deletion of OTRs in mice CeL astrocytes (**e,** GFAP OTR KO). The treatments applied are color coded as the legend key indicate. Control indicate a vehicle injection. (**b, f**) 4 weeks after the SNI surgery, mechanical pain threshold was assessed on the neuropathic paw before (Ctrl) and at different time points after either TGOT injection or C1V1 activation of CeL astrocytes (gray arrow) for sham (top) and SNI (bottom, gray box) animals (**c, g**) Anxiety levels were assessed through measurements of the time spent in the closed arms of the elevated plus maze after drugs injections or C1V1 light-driven activation of CeL astrocytes for sham (top) and SNI (bottom, gray box). (**d, h**) Conditioned place preference (CPP) was assessed through measurements of the Δ time spent in the paired chamber before and after pairing. Pairing was realized through drugs injections or C1V1 light-evoked activation of CeL astrocytes for sham (top) and SNI (bottom, gray box). Data are expressed as averages across rats or mice plus SEM. n = 4-18 per group (details and statistics in Extended Data

Table 7). $^{\#}$ $P < 0.001$, $^{\#\#}$ $P < 0.01$ Wilcoxon signed rank test; * $P < 0.05$, ** $P < 0.01$, *** $P < 0.001$; ANOVA or mixed-design ANOVA followed by posthoc Bonferroni test (Statistics in Table S7). (**i**) Oxytocin-dependent cellular interactions in the CeA. We hypothesize that OT released from axons of PVN neurons within the CeL activates OTR+ astrocytes (red) which consequently spread their activation to neighboring OTR- astrocytes (green) through, at least partly, gap junctions. Subsequently, the CeL astrocytes release D-serine which gates the activation of NMDAR on CeL interneurons, ultimately increasing their firing rate. This in turn inhibits CeM output projection neurons, resulting in anxiolysis and the promotion of a positive emotional state.

METHODS

Animals

Animals were housed under standard conditions with food and water available *ad libitum* and maintained on a 12-hour light/dark cycle and all experiments were conducted in accordance with EU rules and approbation from French Ministry of Research (01597.05). For *ex vivo* and *in vivo* experiments, Wistar rats or C5BL/6 mice were used. *Ex vivo* experiments used animals between 18 and 25 days old, except in experiments where rAAVs were injected, in which case animals were between 2 and 6 months old at the time of sacrifice. *In vivo* experiments used 2-month-old animals at the time of the first surgery.

Specific deletion of OTRs in CeL astrocytes. To specifically ablate OTRs in CeA astrocytes, transgenic cKO mice, in which *loxP* sites flank the OTR coding sequence[23], received bilateral injections (280 nl) of rAAV-GFAP-GFP-IRES-Cre. Following four weeks of expression of the viral proteins, mice were intracardially perfused with 1x PBS and 4% PFA. Brain sections were used for FISH (OTR mRNA) and IHC (GS) to verify the validity of the approach. Representative images and quantifications are provided in Figure 2H, Extended Data Fig. 2g-h.

Specific deletion of Cx30 and Cx43 in astrocytes. To specifically impaire gap-junctions coupling, we used Cx30-/-Cx43fl/fl:hGFAP-Cre mice (Cx30/Cx43 double KO), which were previously characterized[24,51,52], with conditional deletion of Cx43 in astrocytes[53] and additional deletion of Cx30[54].

Cloning and Production of rAAV Vectors:

The generation of rAAVs allowing for the specific expression of the protein of interest in OT-cells is described in our previous work[4]. Briefly, the conserved promoter region of 2.6 kb was chosen using the software BLAT from UCSC (http://genome.ucsc.edu/cgi-bin/hgBlat), was amplified from BAC clone RP24-388N9 (RPCI-24 Mouse, BACPAC Resources, CHORI, California, USA) and was subcloned into a rAAV2 backbone carrying an Ampicillin-resistance.

To construct the OTp-C1V1(t/t)-TS-mCherry AAV vector we used previously cloned OTp-DIO-GFP-WRE plasmid[2] equipped with the characterized 2.6 kb OT promoter[4]. In this plasmid the DIO-GFP sequence was replaced by C1V1(t/t)-TS-mCherry from the rAAV CaMKIIa-C1V1(t/t)-TS-mCherry (Addgene, plasmid #35500).

To generate GFAP-C1V1(t/t)-TS-mCherry AAV vector, we replaced the CamKIIa promoter from the rAAV CaMKIIa-C1V1(t/t)-TS-mCherry by the Gfa promoter from the pZac2.1 gfaABC1D-tdTomato (Addgene, plasmid: 44332). The cell type specificity of the rAAV carrying the Gfa promoter was confirmed[55]. In analogy, the generation of the GFAP-GFP-IRES-Cre vector was achieved using pZac2.1 gfaABC1D-tdTomato (Addgene, plasmid: 44332). First, the promoter was cloned into a rAAV2 backbone and sticky ends were blunted with EcoR1 and Basrg1. Next, pAAV-CamKIIa-C1V1(t/t)-TS-mCherry was blunted using BamHI and BsrGI. Finally, the pBS-ires cre construct was used and IRES-Cre was inserted into the GFAP-driven vector resulting in the GFAP-GFP-IRES-Cre construct.

Production of chimeric virions (recombinant Adeno-associated virus 1/2; rAAV 1/2) was described in[4]. Briefly, human embryonic kidney cells 293 (HEK293; Agilent #240073) were calcium phosphate-transfected with the recombinant AAV2 plasmid and a 3-helper system. rAAV genomic titers were determined with QuickTiter AAV Quantitation Kit (Cell Biolabs, Inc., San Diego, California, USA) and are ~10^{13} genomic copies per ml for all rAAV vectors used in this study.

Surgeries

Neuropathic Pain Model: Spared Nerve Injury (SNI) Procedure

Animals were randomly separated in two groups to undergo either posterior left hindpaw SNI or sham procedure, with right hindpaw untouched. Animals were anaesthetized using isoflurane at 1.5–2.5%. Incision was made at mid-thigh level using the femur as a landmark and a section was made through the biceps femoris. The three peripheral branches (sural, common peroneal and tibial nerves) of the sciatic nerve were exposed. Both tibial and common peroneal nerves were ligated using a 5.0 silk suture and transected. The sural nerve was carefully preserved by avoiding any nerve stretch or nerve contact[28]. For animals undergoing sham surgery, same procedure was performed but nerves remained untouched. Animals were routinely observed daily for 7 days after surgery and daily tested by the experimenter (Extended Data Fig. 6). Besides observing weight, social and individual behavior, the operated hindpaw was examined for signs of injury or autotomy. In case of autotomy or suffering, the animal was euthanized in respect of the ethical recommendations of the EU. No analgesia was provided after the surgery in order to avoid interference with chronic pain mechanisms and this is in accordance with our veterinary authorization. Suffering was minimized by careful handling and increased bedding.

Stereotaxic Surgery: Injections of rAAV Vectors

Stereotaxic surgery was performed under deep ketamine-xylazine anesthesia, using the KOPF (model 955) stereotaxic system. For specific control of rats CeA astroglial cells, 200 nl of rAAV serotype 1/2 (GFAPp-C1V1(t/t)-mCherry, cloned from plasmids #35500 and 44332, Addgene) were injected bilaterally at the coordinates corresponding to CeL: rostro-caudal: -2.7mm, medio-lateral: 4.2mm, dorso-ventral: -8.0mm (From Paxinos and Watson Atlas). For specific control of OT neurons, 200 nl of rAAV serotype 1/2 (OTp-C1V1(t/t)-mCherry or OTp-ChR2-mCherry) were injected bilaterally at the coordinates corresponding to each hypothalamic OT nuclei. PVN: rostro-caudal: -1.8mm; medio-lateral: +/-0.4mm; dorso-ventral: -8.0mm; SON: rostro-caudal: -1.4mm; medio-lateral: +/-1.6mm; dorso-ventral: -9.0mm; AN: rostro-caudal: -2mm; medio-lateral: +/-1.2mm; dorso-ventral: -8.5mm (From Paxinos and Watson Atlas). For specific deletion of OTR in mice CeL astrocytes, 280 nl of rAAV serotype 1/2 (GFAPp-GFP-IRES-Cre) were injected bilaterally at the coordinates corresponding to CeL: rostro-caudal: -1.4mm, medio-lateral: +/-2.6mm, dorso-ventral: -4.3mm (From Paxinos and Watson Atlas) in OTR cKO mice.

Stereotaxic Surgery: intra-CeL Cannulae

Cannulae Implantation. Animals were bilaterally implanted with guide cannulae for direct intra-CeL infusions. As guide cannulae we used C313G/Spc guide metallic cannulae (Plastics one, VA, USA) cut 5.8 mm below the pedestal. For this purpose, animals were deeply anesthetized with 4% isoflurane and their heads were fixed in a stereotaxic frame. The skull was exposed and two holes were drilled according to coordinates that were adapted from brain atlas (rat, 2.3 mm rostro-caudal; 4 mm lateral; 7.5 mm dorso-ventral relative to bregma; mice, 1.4 mm rostro-caudal; 2.6 mm lateral; 4.3 mm dorso-ventral relative to bregma) by comparing the typical bregma-lambda distance with the one measured in the experimental animal. Two screws were fixed to the caudal part of the skull in order to have an anchor point for the dental cement. Acrylic dental cement was finally used to fix the cannulae and the skin was sutured. In case of long lasting experiments (neuropathy-induced anxiety) with a cannula implantation at distance of the behavioral assay (> 4 weeks), cannulae were sometimes lost or cloaked, and concerned animals therefore excluded from testing.

Drugs Infusions. We used bilateral injections of 0.5 µl containing either vehicle (NaCl 0.9%) or oxytocin receptor agonist TGOT (1 µM) dissolved in NaCl 0.9%. For this procedure two injectors (cut to fit 5.8 mm guide cannulae protruding 2 to 2.5 mm beyond the lower end of the cannula in older animals and 1.8 mm in 3-4 week old rats) were bilaterally lowered into the guide cannula, connected via polythene tubing to two Hamilton syringes that were placed in an infusion pump and 0.5 µl of liquid was injected in each hemisphere over a 2-minute period. After the injection procedure, the injectors were kept in place for an additional minute in order to allow a complete diffusion of liquid throughout the tissue. Rats were subsequently left in the home cage for 15 minutes to recover from the stress of the injection and then handled for mechanical pain threshold or anxiety assessment. Animals that received TGOT injections for the first experiment (mechanical sensitivity assessment) were switched to the vehicle injected groups for the elevated plus maze experiment.

Stereotaxic Surgery: intra-CeL Optical Fiber

Optical Fiber Implantation. Sham and rAAVs injected animals both underwent a single surgical procedure in which after vector injection or no injection for sham, optical fibers designed to target the CeL were implanted and firmly maintained on the skull using dental cement. See "***cannulae implantation***" for the surgical procedure. Implantable optical fibers were homemade using optical fiber cut at appropriate length (FT200EMT, Thorlabs, NJ, USA) inserted and glued using epoxy based glue in ferrules (CFLC230-10, Thorlabs, NJ, USA).

Horizontal and Coronal Slices

Slices Preparations. In all cases, animals were anaesthetized using ketamine (Imalgene 90 mg/kg) and xylazine (Rompun, 10 mg/kg) administered intraperitoneally. Intracardiac perfusion was then performed using one of the following artificial cerebrospinal fluids (aCSFs) dissection solutions. For animals between 18 and 25 days old, an ice-cold sucrose based dissection aCSF was used containing (in mM): Sucrose (170), KCl (2.5), NaH_2PO_4 (1.25), $NaHCO_3$ (15), $MgSO_4$ (10), $CaCl_2$ (0.5), HEPES (20), D-Glucose (20), L-Ascorbic acid (5), Thiourea (2), Sodium pyruvate (3), N-Acetyl-L-cysteine (5), Kynurenic acid (2). For animals between 2 and 6 months old, an ice-cold NMDG based aCSF was used containing

(in mM): NMDG (93), KCl (2.5), NaH_2PO_4 (1.25), $NaHCO_3$ (30), $MgSO_4$ (10), $CaCl_2$ (0.5), HEPES (20), D-Glucose (25), L-Ascorbic acid (5), Thiourea (2), Sodium pyruvate (3), N-Acetyl-L-cysteine (10), Kynurenic acid (2). In both cases, pH was adjusted to 7.4 using either NaOH or HCl, this after bubbling in 95% O_2-5% CO_2 gas, bubbling which was maintained throughout the duration of use of the various aCSFs. Those aCSFs formulae were based on the work of[56]. Following decapitation, brain was swiftly removed in the same ice-cold dissection aCSFs as for intracardiac perfusion, and 350 µm thick horizontal slices containing the CeA was obtained using a Leica VT1000s vibratome. For experiments in Extended Data Fig. 2a-b, coronal slices of the same thickness containing the PVN were used. Upon slicing, brain slices were hemisected and placed, for 1 hour minimum before any experiments were conducted, in a room tempered holding chamber, containing normal aCSFs. For 2 to 6 month old animals, slices were first let for 10 minutes in 35°C NMDG aCSF before placing them in the holding chamber at room temperature. Normal aCSF, also used during all *ex vivo* experiments, is composed of (in mM): NaCl (124), KCl (2.5), NaH_2PO_4 (1.25), $NaHCO_3$ (26), $MgSO_4$ (2), $CaCl_2$ (2), D-Glucose (15), adjusted for pH values of 7.4 with HCL or NaOH and continuously bubbled in 95% O_2-5% CO_2 gas. All aCSFs were checked for osmolality and kept for values between 305-310 mOsm/L. In electrophysiology or calcium imaging experiments, slices were transferred from the holding chamber to an immersion recording chamber and superfused at a rate of 2 ml/min with normal aCSFs unless indicated otherwise.

Drug Application. OTR agonists were bath applied through a 20s long pumping of agonist solution, corresponding to several times the volume of the recording chamber. Other drugs (antagonists, TTX, *etc.*) were applied for at least 20 minutes in the bath before performing any experiments. BAPTA (or BAPTA-free solution for controls) loading of CeL astrocytes was realized following[57] protocol. Two distant CeL astrocytes per slice (label with SR101, 1 µM) were patched in whole cell configuration and voltage steps were applied (2 Hz, Δ40 mV) to help loading the BAPTA contained in the patch pipette (in mM): $MgCl_2$ (1), NaCl (8), $ATPNa_2$ (2) $GTPNa_2$ (0.4) HEPES (10), BAPTA (40) and osmolality checked to be between 275-285 mOsm/l. The whole cell configuration was maintained during 45 min to allow BAPTA diffusion into the astrocyte network[58].

Calcium Imaging and Identification of Astrocytes

To identify astrocytes, SR101 (1 µM) was added to aCSF in a culture well and slices were incubated for 20 minutes at 35°C. The specificity of SR101 labelling to astrocytes of the CeL was verified through patch-clamp experiments, the results of which can be found in Extended Data Fig. 2c-d. The synthetics calcium indicators OGB1 or Rhod-2 was bulk loaded following an adapted version of the method described previously[59] reaching final concentrations of 0.0025 % (~20 µM) for calcium indicators, 0.002% Cremophor EL, 0.01 % Pluronic F- 127 and 0.5% DMSO in aCSF, and incubated for 45 to 60 minutes at 38°C. Upon incubation time, slices were washed in aCSF for at least an hour before any recording was performed. Astrocytes recorded for this study were those co-labeled, in rats for SR101 and OGB1 and in mice for GFP and Rhod2. The spinning disk confocal microscope used to perform astrocyte calcium imaging was composed of a Zeiss Axio examiner microscope with a 40x water immersion objective (numerical aperture of 1.0), mounted with a X-Light Confocal unit – CRESTOPT spinning disk. Images were acquired at 2Hz with either a Rolera em-c² emCCD or an optiMOS sCMOS camera (Qimaging, BC, Canada). Cells within a confocal plane were illuminated for 100 to 150 ms for each wavelength (SR101 and Rhod-2: 575 nm, OGB1 and GFP: 475 nm) using a Spectra 7 LUMENCOR. The different hardware elements were

synchronized through the MetaFluor software (Molecular Devices, LLC, Ca, USA) which was also used for online. Astrocytic calcium levels were measured in hand drawn ROIs comprising the cell body plus, when visible, proximal processes. In all recordings, the Fiji rolling ball algorithm was used to increase signal/noise ratio. Further offline data analysis was performed using a custom written python-based script available on editorial website. Intracellular calcium variation was estimated as changes in fluorescence signals. To take into account micro-movements of the specimen on long duration recordings, the fluorescence values were also calculated for SR101 (or GFP) and subsequently subtracted to the ones of OGB1 (or Rhod2), except in the case of Figure 2a-d, where astrocytes were identified through SR101 fluorescence after the recordings, to avoid unwanted stimulation of the C1V1 opsin. On this last case, recordings in which movements / drifts were visible were discarded. Then, a linear regression and a median filter was applied to each trace. Calcium transients was detected using the find_peaks function of the SciPy library. More precisely, fluorescence variation was identified as a calcium peak if its prominence exceeds the standard deviation (or two times the standard deviation for recordings acquired with the sCMOS camera) and if the maximum peak value surpasses 50 fluorescence units (or 3 units for sCMOS recordings). ROI with zero calcium variations were excluded from the analysis. The remaining ROI were considered as living astrocytes and the number of peaks was quantified before and after the drug application. All data were normalized according to the duration of the recording and astrocytes was labelled as “responsive” when their AUC or their calcium transient frequency was increased by at least 20% after drug application. Because the time post-stimulation is longer than the baseline (10 min vs 5 min), the probability of observing a spontaneous calcium peak is stronger post-stimulation. To avoid this bias, astrocytes with only one calcium peak during the whole recording were not considered as responsive. Finally, all data were averaged across astrocytes per slice, and this results was used as statistical unit. All data were expressed as ratio (baseline/drug effect), a ratio of 1 meaning neither an increase nor a decrease of the measured parameter. For inter-ratio comparison, parametric or non-parametric (depending on data distribution) unpaired statistical tests were used. Fiji software was also used on SR101 / OGB1 pictures to produce illustrative pictures. All calcium imaging experiments was conducted at controlled room temperature (26°C).

Electrophysiology

Whole cell patch-clamp recordings of CeL neurons, CeL astrocytes and CeM neurons were visually guided by infrared oblique light visualization of neurons and completed by SR101 fluorescence observation for astrocytes. Patch-clamp recordings were obtained with an Axon MultiClamp 700B amplifier coupled to a Digidata 1440A Digitizer (Molecular Devices, CA, USA). Borosilicate glass electrodes (R = 3.5 - 7 MΩ) with inner filament (OD 1.5 mm, ID 0.86 mm; Sutter Instrument, CA USA) were pulled using a horizontal flaming/brown micropipette puller (P97; Sutter Instrument, CA, USA). Recordings were filtered at 2 kHz, digitized at 40 kHz and stored with the pClamp 10 software suite (Molecular Devices; CA, USA). Analysis of patch-clamp data were performed using Clampfit 10.7 (Molecular Devices; CA, USA) and Mini analysis 6 software (Synaptosoft, NJ, USA) in a semi-automated fashion (automatic detection of events with chosen parameters followed by a visual validation).

Whole-Cell Recording of CeL Neurons. Recording pipettes were filled with an intracellular solution containing (in mM): $KMeSO_4$ (125), $CaCL_2$ (2), EGTA (1), HEPES (10), $ATPNa_2$ (2), $GTPNa_2$ (0.3). The pH was adjusted to 7.3 with KOH and osmolality checked to be between

290-295 mOsm/l, adjusted with sucrose if needed. For miniature excitatory post synaptic currents (mEPSCs) recordings, neurons were recorded in voltage clamp and hold at a membrane potential of -65 mV. For action potentials (APs) recordings, neurons were recorded in current clamp and hold at I = 0. Series capacitances and resistances were compensated electronically throughout the experiments using the main amplifier. For mEPSCs measurements in CeL neurons (Figure 4), whole cell recordings were conducted in a Mg^{2+} free aCSF, also containing biccuculin (10 µM) and TTX (1 µM) as in[60]. Average events frequencies per cell were calculated on 20s windows, chosen for TGOT or photostimulation during maximal effect, as determined by the visually identified maximal slope of the cumulative plot of the number of events. CeM neurons were classified as TGOT-responsive when the average event frequency was increased by at least 20% during 20s after TGOT application when compared to baseline average frequency. Baseline and recovery frequencies were measured respectively at the beginning and end of each recording. All patch-clamp experiments were conducted at room temperature.

Biocytin Filling of CeL Astrocytes. In the lateral part of the central amygdala slices visualized with infrared-differential contrast optics, astrocytes were identified by their morphological appearance revealed by SR101 and the absence of action potentials in response to depolarizing current injections. Cells were patched with pipettes filled with (in mM) 110 K-Gluconate, 30 KCl, 4 $ATPNa_2$, 10 phosphocreatine, 0.3 $GTPNa_2$, 10 HEPES and 5 biocytin (pH: 7.3; 310 mOsm). After obtaining whole-cell configuration astrocytes were hold at -80 mV and typical filling time was 45 minutes. Then the pipettes were carefully retracted and slices were incubated for additional 20 minutes in the oxygenated aCSF before fixation. Only one cell was filled per slice. Slices with filled cells were immersion-fixed at 4°C for 5 days in 4% PFA-PBS solution. Next, the slices were flat-embedded in 6% Agar-PBS, areas of interest were cut out of, re-embedded onto the Agar block and Vibratome-cut into 80 µm thick free-floating sections. The sections then were incubated with Avidin conjugated to Alexa Fluor488 (1:1000) (Thermo Fisher) in 1% Triton-PBS at 4°C, washed in PBS, mounted and cover-slipped. The tissue was analyzed and images taken at Leica TCS SP5 Confocal Microscope.

Whole-cell Recording of CeM Neurons. Pipettes were filled with an intracellular solution containing (in mM): KCl (150), HEPES (10), $MgCl_2$ (4), $CaCl_2$ (0.1), BAPTA (0.1), $ATPNa_2$ (2), $GTPNa_2$ (0.3). pH was adjusted to 7.3 with KOH and osmolality checked to be between 290-295 mOsm/L, adjusted with sucrose if needed. All cells were hold at a membrane potential of -70 mV. Series capacitances and resistances were compensated electronically throughout the experiments using the main amplifier. Average events frequencies per cell were calculated on 20s windows, chosen for TGOT or photostimulation during maximal effect, as determined by the visually identified maximal slope of the cumulative plot of the number of events. CeM neurons were classified as TGOT-responsive when the average IPSCs frequency was increased by at least 20% during 20s after TGOT application when compared to baseline average frequency. Baseline and recovery frequencies were measured respectively at the beginning and end of each recording. All patch-clamp experiments were conducted at room temperature.

Immunohistochemistry and *in situ* Hybridization

In situ *Hybridization for OTR mRNA in Rat CeL.* The probe for OTR mRNA was *in vitro* transcripted from a 902-bp fragment containing 133-1034 bases of the rat OTR cDNA (NCBI Reference Sequence: NM_012871.3) subcloned into pSP73 Vector (Promega). The digoxigenin (DIG)-labeled antisense and sense RNA probe from the linearized *oxtr* cDNA template was synthesized using DIG RNA Labeling Kit (SP6/T7) (Roche Diagnostics). Sections containing 2 consecutive sections of the CeL (corresponding to Bregma: 2.5) were processed for fluorescent *in situ* hybridization (FISH). Rats were transcardially perfused with PBS followed by 4% PFA. Brains were dissected out and post fixed overnight in 4% PFA at 4°C with gentle agitation. 50 µm vibratome sections were cut, collected and fixed in 4% PFA at 4°C overnight. The free-floating sections were washed in RNase-free PBS, immersed in 0.75% glycine in PBS, treated with 0.5 µg/ml proteinase K for 30 min at 37 °C, acetylated with 0.25% acetic anhydride in 0.1 M triethanolamine, and then hybridized with DIG-labeled RNA probe overnight at 65 °C. After RNase treatment and following intensive wash, the hybridized DIG-labeled probe was detected by incubation with Anti-Digoxigenin-POD (1:200; 11207733910; Roche Diagnostics) for 3 days at 4 °C. Signals were developed with tyramid signal amplification method. Rhodamine-conjugated tyramide was synthesized by coupling NHS-Rhodamine (Pierce Biotechnology, Thermo Fisher Scientific) to Tyramine-HCl (Sigma-Aldrich) in dimethylformamide with triethylamine. For the quantification of OTR mRNA-positive astrocytes, all confocal images were obtained using the same laser intensities and processed with the same brightness / contrast settings in Adobe Photoshop. Since the *in situ* signal for the OTR mRNA in astrocytes was weak, we first calculated the average intensity (signal intensity of all pixels divided by the total number of pixels) of the rhodamine-stained OTR mRNA signal for each individual section containing the CeL. Next, we calculated the standard deviation for each individual confocal image based on the intensity of all pixels comprising the image. We defined the threshold for OTR mRNA-positive astrocytes: If more than 1/4 of all pixels comprising an astrocyte soma displayed a signal intensity exceeding the average background intensity by more than 4-times the standard deviation, the astrocytes were considered as OTR mRNA-positive.

Astrocytes Markers. The aldehyde dehydrogenase 1 antibody is a commonly used marker for glial cells, including astrocytes. Therefore, we used the ALDH1L1 for immunohistochemistry in our initial experimental studies (Extended Data Fig. 1c, S4a). However, due to inconsistencies in staining quality as a result of batch-dependent antibody properties, especially in combination with the OTR mRNA FISH, we decided to employ Glutamine Synthetase (GS, Figure 1). GS is a commonly used glial marker[61], which stains astrocyte cell bodies, faint processes and even astrocytes not expressing GFAP. Using GS, we achieved consistent results in combination with our OTR mRNA FISH.

Glutamine Synthase, ALDH1L1 Colocalization with OTR mRNA in Rat CeL. After development and washing steps the sections were stained with antibodies against GS (mouse monoclonal, 1:500, ref: MAB302, MerckMilipore), ALDH1L1 (rabbit polyclonal, 1:500, ref: ab87117, abcam), in PBS and kept at 4°C on a shaker in a dark room overnight. After intensive washing with PBS, sections were stained with the respective secondary antibodies AlexaFluor488 (goat anti-mouse, 1:1000, ref: A11001, life technologies) and AlexaFluor680 (goat anti-mouse, 1:1000, ref: A27042, ThermoFischer Scientific) for 2 hours at RT. Following intensive washing with PBS, sections were mounted using Mowiol.

Double* in situ *Hybridizations for OTR mRNA and GFAP mRNA in Mice CeL. Fluorescent *in situ* hybridization (FISH) in Extended Data Fig. 1d was performed on 25-µm cryostat-cut coronal sections prepared from fresh-frozen mouse brain (male C57BL/6J, P22). After extraction, brains were immediately frozen in Tissue-Tek O.C.T. compound and stored at -80 degrees Celsius. ISH was performed according to the manufacturer's instructions (Advanced Cell Diagnostics) for Fresh Frozen RNAscope Multiplex Fluorescent Assay. Treatment of amygdala containing sections were adjusted with the 3-plex negative control and then coexpression of OTR and GS examined using ACD designed target probes as well as the nuclear stain DAPI. Single plan images were collected with an upright laser scanning microscope (LSM-710, Carl Zeiss) using a 40x-objective with keeping acquisition parameters constant between control and probe treated sections.

AAV-GFAP-C1V1(t/t)-mCherry Specificity. After 3 weeks of vector expression in the brain, rats were transcardially perfused with 4% paraformaldehyde solution. Tissue blocks, containing CeA were dissected from the fixed brain and Vibratome-cut into 50 µm thick free-floating sections. After several rinse steps sampled sections were blocked with 5% NGS in PBS and incubated for 48 h at 4°C with polyclonal rabbit anti-ALDH1L1 antibody (1:500, Abcam) in 1% Triton-PBS buffer, containing 0,1 % NGS. Appropriate secondary antibody (AlexaFluor488 conjugated goat anti-rabbit (1:1000, LifeTechnologies) was used for further antigen detection. Intrinsic mCherry fluorescence of vector-expressing cells was strong enough to detect them in the tissue without any additional antibody enhancement. The immunolabeled sections were mounted onto Superfrost slides, cover-slipped with Mowiol, analyzed and documented using LEICA SP5 confocal microscope.

Three-dimensional assessment of astrocyte complexity and interaction analysis using Imaris. For the 3D reconstruction of astrocytes, we took Z-stack images (50 µm depth, 1µm steps, 40x magnification) CeL using a Zeiss LSM 780 confocal microscope (1024x1024 pixel, 16-bit depth, pixel size 0.63-micron, zoom 0.7). Raw czi files were used for further analysis using Imaris software (Version 9.31, Oxford Instruments). First, Imaris was used to reconstruct the astrocyte surface using the following custom settings: surfaces Detail 0.700 µm (smooth); thresholding Background subtraction (Local Contrast), diameter of largest Sphere, which fits into the object: 2.00; Color: base, diffusion transparency: 65%. After surface reconstruction, we used the filter function to remove unspecific background signals: Filter: Volume max – 400 µm 3. It is important to note that these settings have to be adjusted for every new batch / IHC staining to guarantee a reliable reconstruction. All astrocytes with incomplete somata (cut by either the x, y or z plane) were manually removed and not included in further analysis Fused astrocytes that were falsely recognized as one entity by the software were manually separated using the cut function, or entirely removed from the sample if a separation was not feasible. The 'filter/area function' was used to remove small astrocytic segments that occurred during manual deletion. After deletion of all background signals the 'mask all' function was used to create the final surface reconstruction. Next, the surface reconstruction was used as the template for the filament reconstruction using the following custom settings: detect new starting points: largest Diameter 7.00 µm, seed points 0.300 µm; remove seed points around starting points: diameter of sphere regions: 15 µm. Seed points were corrected for (either placed in or removed from the center of the somata) manually if the Imaris algorithm placed them incorrectly. All surface and filament parameters were exported into separate Excel files and used for data analysis. All images used for analysis were taken with the same confocal settings (pinhole, laser intensity, digital gain and

digital offset). Sholl analysis was performed using Imaris in the filament reconstruction mode and individual data sets were exported into separate Excel files for further analysis. each individual sphere) per individual astrocyte. For the nearest neighbor and interaction analysis we used the 'Native Distance Measurements' function as depicted in this video: https://imaris.oxinst.com/learning/view/article/imaris-9-5-native-distance-measurements. In brief, we reconstructed astrocytic surfaces based on the GFAP fluorescence and OTR mRNA signal. Next, we manually labelled OTR+ and OTR- astrocytes and performed the native distance measurement allowing us to assess the shortest distance between GFAP-positive processes of different astrocytes. We defined 'astrocytic interaction' when GFAP-positive processes of two different astrocytes were no further than 1µm apart. It is important to note that this method does not allow the discrimination of different astrocytic entities so that several close contacts (contacts being defined as a distance of less than 1µm between GFAP-positive processes or endfeets from two different astrocytes) originating from the same astrocyte result in a higher number of total interactions. For the nearest neighbor analysis, we calculated the distance from the center of the soma to the nearest astrocyte neighbor using GS fluorescence and an artificially created sphere that was placed within the soma and measured the distance accordingly. Distribution plots and correlations as well as all statistics were performed using GraphPad Prism 8.0.

Optogenetics

Ex vivo. We opted for a ChR1/VChR1 chimaera channel rhodopsin displaying a red-shifted absorption spectrum, referred here as C1V1[22]. This choice was made over a classical channelrhodopsin-2 to avoid unwanted stimulation of OT axons while imaging our 488nm light sensitive calcium indicator (OGB1). Optogenetic green light stimulation of C1V1 in *ex vivo* experiments was performed using either the Spectra 7 LUMENCOR (λ542 nm) or light source X-Cite® 110LED from Excelitas Technologies through a Cy3 filter, controlled via MetaFluor or Clampex driven TTL pulses, respectively.

In vivo. Animals were habituated to the fixation of an optical fiber on the ferrule without light stimulation for one week before the experiment. In all cases, optical fibers were attached to the ferrules using an adapter (ADAF2, Thorlabs, NJ, USA) and animals let free to move in a typical home cage for the duration of the stimulation. Implanted optical fibers were connected to two lasers (LRS-0532-GFM-00100-03 LaserGlow 532nm DPSS Laser System) and the output power adjusted to correspond to 20 to 30 mW measured at the tip of 200 µm diameter fibers similar to the one implanted. Stimulation of 500 ms duration at a frequency of 0.5Hz were given for 3 min.

Behavior

Mechanical Sensitivity Assessment. In experiments with rats, we used a calibrated forceps (Bioseb, Chaville, France) previously developed in our laboratory to test the animal mechanical sensitivity[62]. Briefly, the habituated rat was loosely restrained with a towel masking the eyes in order to limit stress by environmental stimulations. The tips of the forceps were placed at each side of the paw and a graduate force applied. The pressure producing a withdrawal of the paw, or in some rare cases vocalization, was considered as the nociceptive threshold value. This manipulation was performed three times for each hind paw and the values were averaged as being the final nociceptive threshold value. In

experiments with mice, we used von Frey filaments tests. Mechanical allodynia (a symptom of neuropathic pain) was tested using von Frey hairs and results were expressed in grams. Tests were performed during the morning starting at least 2 h after lights on. Mice were placed in clear Plexiglas boxes (7 cm x 9 cm x 7 cm) on an elevated mesh floor. Calibrated von Frey filaments (Bioseb) were applied to the plantar surface of each hindpaw until they just bent in a series of ascending forces up to the mechanical threshold. Filaments were tested five times per paw and the paw withdrawal threshold (PWT) was defined as the lower of two consecutive filaments for which three or more withdrawals out of the five trials were observed.

Elevated Plus Maze. Following protocol from[63], the arena is composed of four arms, two open (without walls) and two closed (with walls; rats 30 cm high; mice 15 cm high). Arms are 10 cm wide, 50 cm long and elevated 50 cm off the ground for rats and 5 cm wide, 30 cm long and elevated 40 cm of the ground for mice. Two lamps with intensity adjustable up to 50 watts were positioned on the top of the maze, uniformly illuminating it. Animals were video tracked using a video-tracking systems (Ethovision Pro 3.16 Noldus, Wageningen, Netherlands and Anymaze, Stoelting Europe, Ireland). After each trial, the maze was cleaned with 70% ethanol and dry with paper towel. Twenty minutes after intracerebral injections or directly after optical stimulation, the animal was let free at the center of the plus maze, facing the open arm opposite to where the experimenter is, and was able to freely explore the entire apparatus for six minutes. Total time and time spend in closed and open arms were recorded in seconds and the percentage of time spent in closed arms was calculated as a measure of anxiety-like behavior. As internal control, the total distance travelled during the test period was quantified and compared between all different groups (Extended Data Fig. 7). Animals falling from the apparatus during the test, freezing more than 50% of the total time, or with cannulae/optic fiber issues, were removed from the analysis.

Conditioned Place Preference. The device is composed of two opaque conditioning boxes (rats: 30x32 cm; mice: 22x22 cm) and one clear neutral box (30x20 cm) Animals were video tracked using a video-tracking system (Anymaze, Stoelting Europe, Irland). After each trial, the device was cleaned with a disinfectant (Surfa'Safe, Anios laboratory). Based on[64], all rats underwent a 3 days habituation period during which they were able to freely explore the entire apparatus for 30 min. On the day 3, behavior was record for 15 min to verify the absence of pre-conditioning chamber preference. The time spend in the different compartment were measured and paired compartment was chosen as the compartment in which rat spent the less time during the 3rd day of habituation. On day 4, animals were placed the morning in one compartment for 15 min with no stimulation (unpaired box). Four hours after, the animal were placed 15 min in the opposite box (paired box) and CeL astrocyte expressing C1V1 vector were optogenetically stimulated (3 min – 1 s light pulse at 0.5 Hz - λ542 nm) or TGOT micro-infused through intracerebral cannulae. On day 5, the animals were place in the CPP box and allowed to freely explore the entire apparatus during 15 min. As internal control, the total distance traveled during the test period was quantified and compared between all different groups (Extended Data Fig. 7). Rats falling spending more than 80% of the total time in a single chamber before the conditioning, or with cannulae/optic fiber issues, were removed from the analysis.

QUANTIFICATION AND STATISTICAL ANALYSIS

All parametrical statistical tests presented in figure captions or manuscript were performed following correct verification of the assumptions on the distribution of data, and if not non-parametric tests were used. Statistical test displayed in the text are not shown on figures. Tests were performed using either GraphPad Prism (version 8.0.0 for Windows, GraphPad Software, San Diego, California USA) or the SciPy Python-based library[65]. All values, group compositions and statistical tests for each experiment and figure panel are detailed in Extended Data Tables 1-7.

SUPPLEMENTARY DISCUSSION – TECHNICAL LIMITATIONS

We acknowledged a number of technical limitations in our study, which are discussed in details here:

mRNA detection. It is surprising to find that the loss of OTR expression in astrocytes results in a loss of function of OTR signaling in the CeA-CeM projection, especially considering the high proportion of OTR+ neurons (up to 70%) compared to the lower fraction of OTR+ astrocytes (18%) in the CeL. One methodological limitation here is that we remained limited to measuring mRNA levels through FISH, and could not measure OTR expression at the protein level, notably due to the poor availability of reliable OTR antibodies. It is also possible that a comparison between the astrocytes' and neurons' contents of OTR mRNA is biased, indeed astrocytes have a lower total mRNA contents than neurons, as publicly available databases of single cell RNA sequencing indicate[66,67]. Interestingly, a similar discrepancy between low receptor levels observed in astrocytes compared to neurons and yet a crucial functional relevance of astrocytes' receptors in neuromodulation is also observed for another GPCR, the CB1 receptor[68] (and references therein).

C1V1 red-shifted opsin to activate astrocytes. It has been recently demonstrated that the activation of such depolarizing channel rhodopsins in astrocytes or neurons can lead to a significant leak of potassium ions in the extracellular space, resulting in increased neuronal excitability[69]. Yet, we provide results in which we buffered the astrocytes intracellular calcium using BAPTA infusion before activating astrocytic C1V1, and found that it abolished its effects on CeA neurons (Fig. 4-6). Furthermore, we demonstrate that the AstrOpto effect on CeA neuronal circuit is dependent on NMDARs (Extended Data Fig. 5a). This indicates that consequences of astrocytic C1V1 activation are dependent on the evoked astrocyte calcium signaling rather than potassium leakage.

Bulk loading of organic calcium indicator dyes. It should also be noted that we used bulk loading of organic calcium indicator dyes. This means we could not precisely measure cytosolic calcium changes in fine astrocyte processes[70], which may have revealed more complex activities of astrocytes. We note it has been proven that endogenous or exogenous (designer receptor exclusively activated by designer drugs receptors, DREADD) GPCR signaling in astrocytes produces a global increase in calcium in both the cell body and processes([68] and references therein).

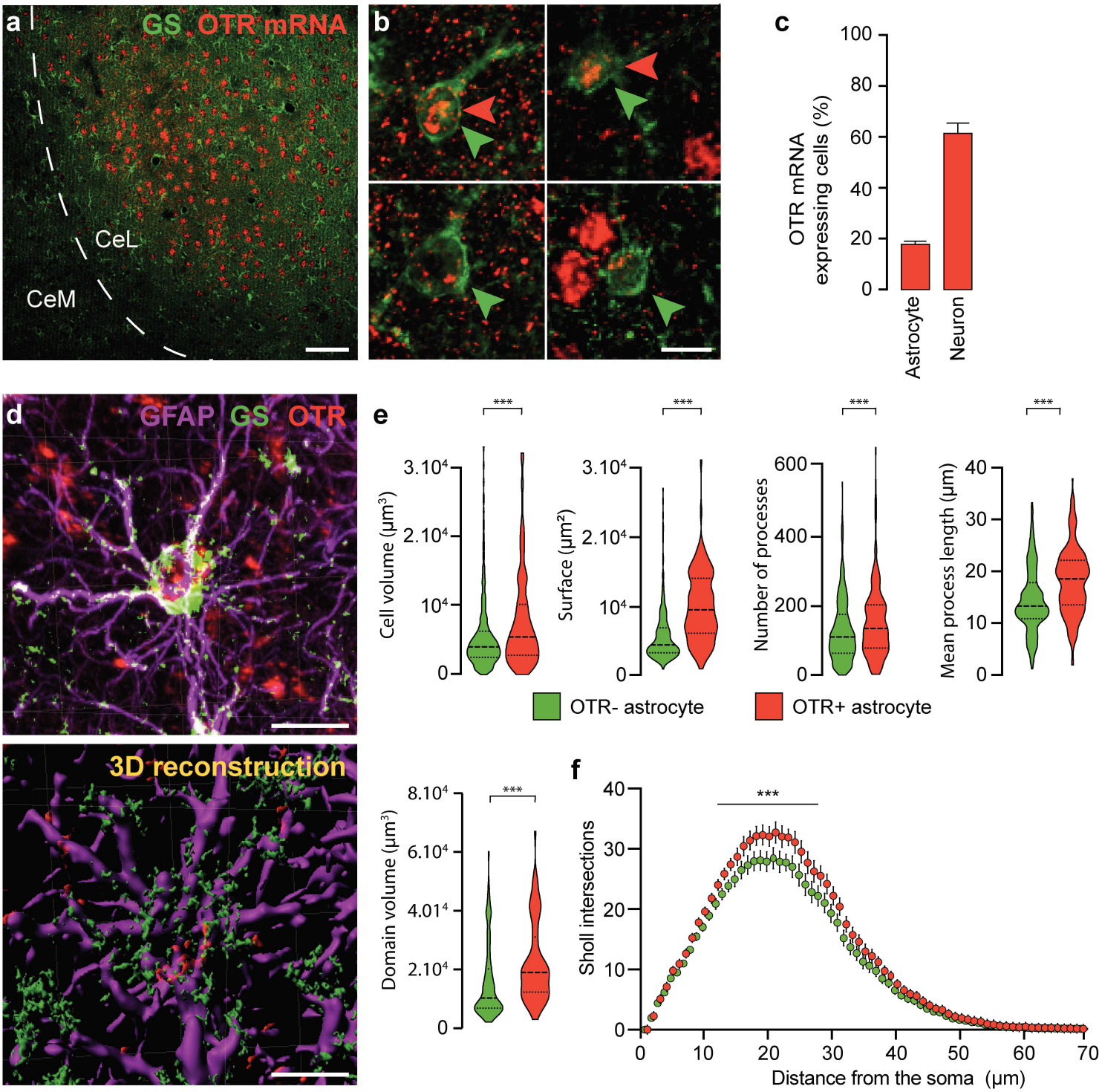
a
GS OTR mRNA
CeL
CeM
b
c
OTR mRNA expressing cells (%)
100
80
60
40
20
0
Astrocyte
Neuron
d
GFAP GS OTR
3D reconstruction
e
***
Cell volume (µm³)
3.10⁴
2.10⁴
10⁴
0
Surface (µm²)
Number of processes
600
400
200
Mean process length (µm)
40
30
20
10
OTR- astrocyte
OTR+ astrocyte
Domain volume (µm³)
8.10⁴
6.10⁴
4.01⁴
2.10⁴
f
Sholl intersections
Distance from the soma (µm)
0
10
20
30
40
50
60
70

Figure 1

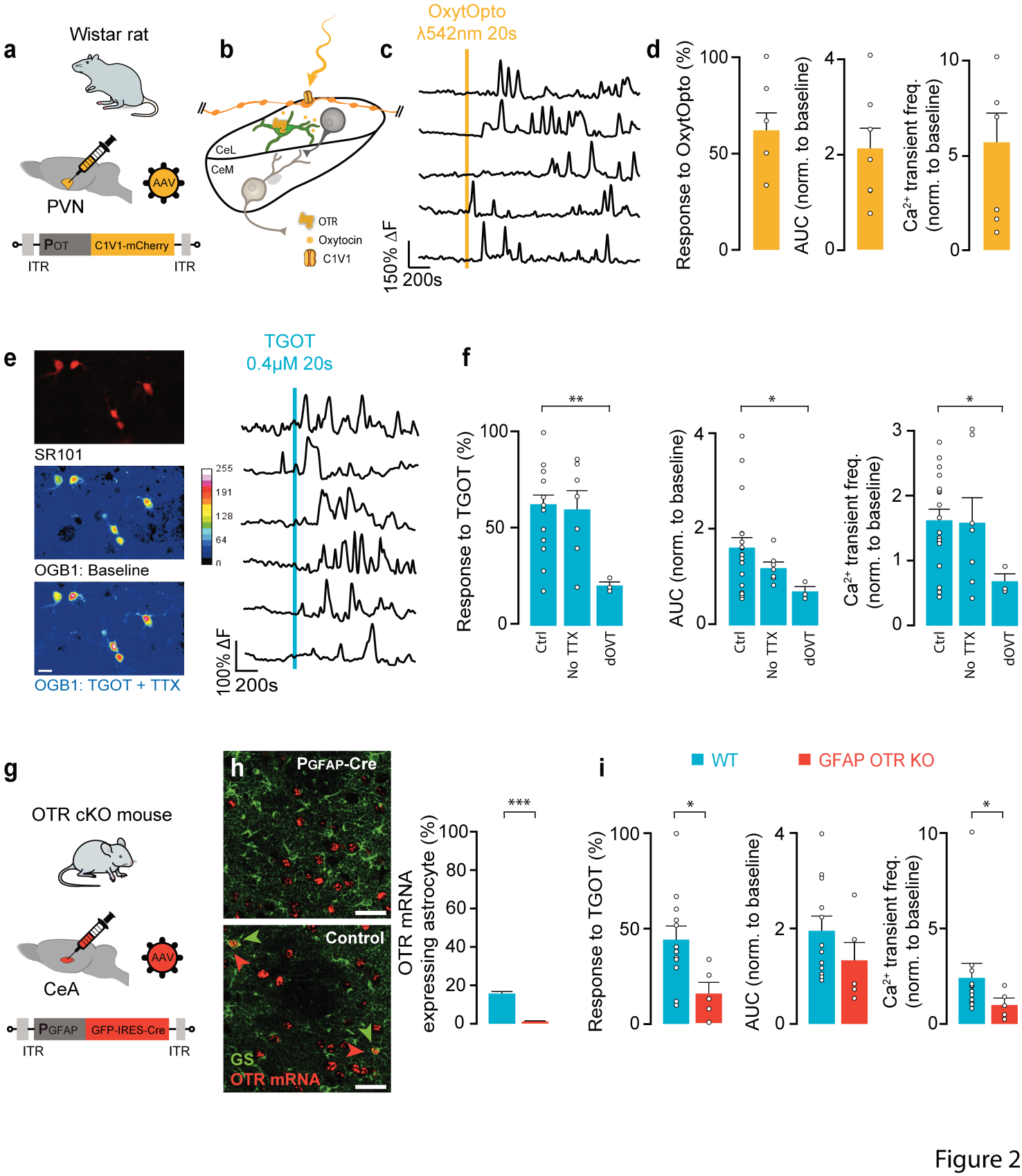
a
Wistar rat
AAV
PVN
POT
C1V1-mCherry
ITR
ITR
b
CeL
CeM
OTR
Oxytocin
C1V1
c
OxytOpto
λ542nm 20s
150% ΔF
200s
d
Response to OxytOpto (%)
AUC (norm. to baseline)
Ca2+ transient freq. (norm. to baseline)
e
SR101
OGB1: Baseline
OGB1: TGOT + TTX
TGOT
0.4μM 20s
255
191
128
64
0
100% ΔF
200s
f
Response to TGOT (%)
AUC (norm. to baseline)
Ca2+ transient freq. (norm. to baseline)
Ctrl
No TTX
dOVT
g
OTR cKO mouse
AAV
CeA
PGFAP
GFP-IRES-Cre
ITR
ITR
h
PGFAP-Cre
Control
GS
OTR mRNA
OTR mRNA expressing astrocyte (%)
i
WT
GFAP OTR KO
Response to TGOT (%)
AUC (norm. to baseline)
Ca2+ transient freq. (norm. to baseline)

Figure 2

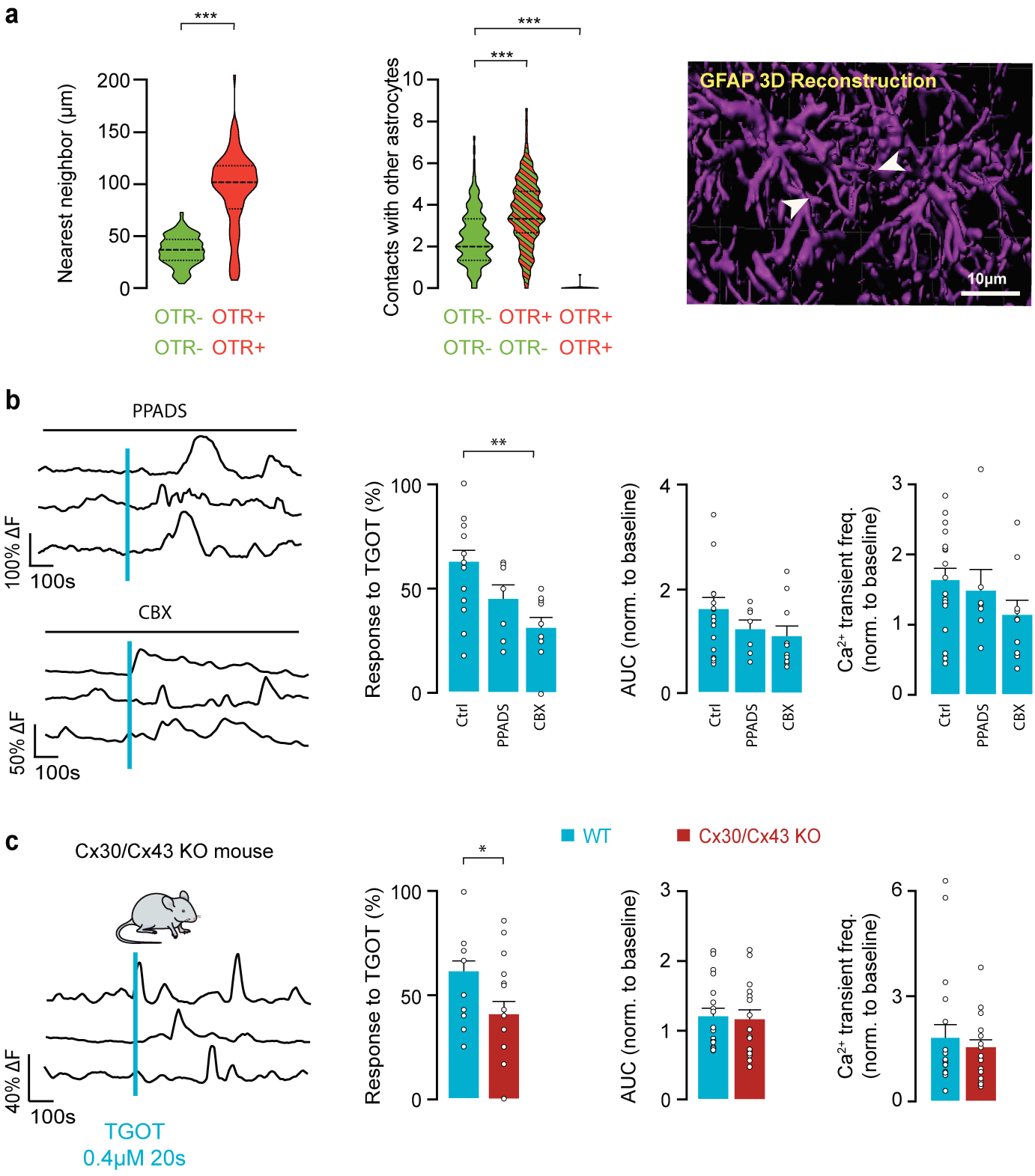
a
***
Nearest neighbor (µm)
200
150
100
50
0
OTR- OTR+
OTR- OTR+
***
***
Contacts with other astrocytes
10
8
6
4
2
0
OTR- OTR+ OTR+
OTR- OTR- OTR+
GFAP 3D Reconstruction
10µm
b
PPADS
100% ΔF
100s
CBX
50% ΔF
100s
**
Response to TGOT (%)
100
50
0
Ctrl
PPADS
CBX
AUC (norm. to baseline)
4
2
0
Ctrl
PPADS
CBX
Ca2+ transient freq. (norm. to baseline)
3
2
1
0
Ctrl
PPADS
CBX
c
Cx30/Cx43 KO mouse
WT
Cx30/Cx43 KO
40% ΔF
100s
TGOT
0.4µM 20s
*
Response to TGOT (%)
100
50
0
AUC (norm. to baseline)
3
2
1
0
Ca2+ transient freq. (norm. to baseline)
6
3
0

Figure 3

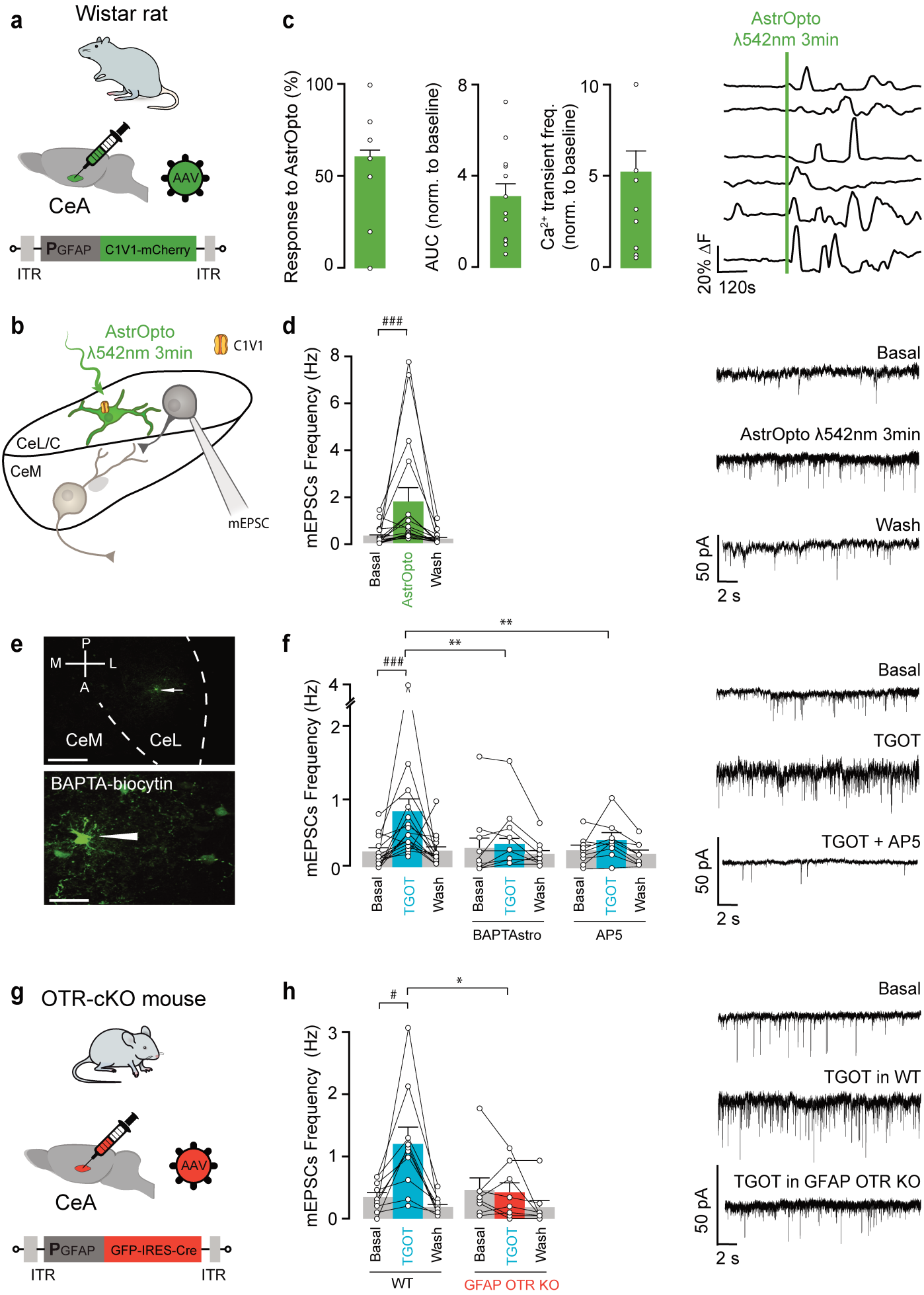
a
Wistar rat
AAV
CeA
PGFAP
C1V1-mCherry
ITR
ITR
b
AstrOpto
λ542nm 3min
C1V1
CeL/C
CeM
mEPSC
c
Response to AstrOpto (%)
100
50
0
AUC (norm. to baseline)
8
4
0
Ca2+ transient freq. (norm. to baseline)
10
5
0
AstrOpto
λ542nm 3min
20% ΔF
120s
d
###
mEPSCs Frequency (Hz)
8
6
4
2
0
Basal
AstrOpto
Wash
Basal
AstrOpto λ542nm 3min
Wash
50 pA
2 s
e
P
M
L
A
CeM
CeL
BAPTA-biocytin
f
**
**
###
mEPSCs Frequency (Hz)
4
2
1
0
Basal
TGOT
Wash
BAPTAstro
AP5
Basal
TGOT
TGOT + AP5
50 pA
2 s
g
OTR-cKO mouse
AAV
CeA
PGFAP
GFP-IRES-Cre
ITR
ITR
h
#
*
mEPSCs Frequency (Hz)
3
2
1
0
Basal
TGOT
Wash
WT
GFAP OTR KO
Basal
TGOT in WT
TGOT in GFAP OTR KO
50 pA
2 s

Figure 4

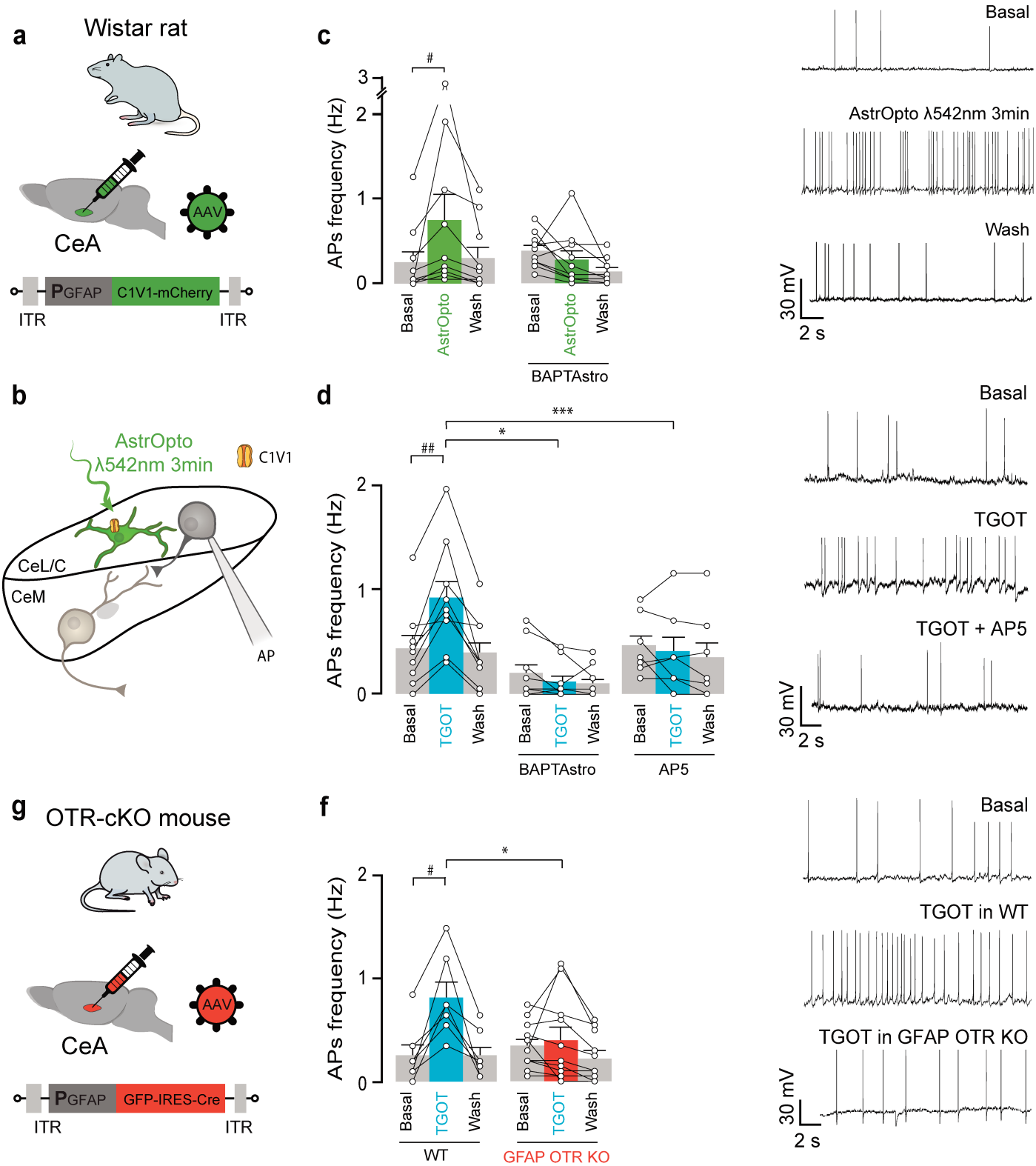
a
Wistar rat
AAV
CeA
PGFAP
C1V1-mCherry
ITR
ITR
b
AstrOpto
λ542nm 3min
C1V1
CeL/C
CeM
AP
c
APs frequency (Hz)
Basal
AstrOpto
Wash
BAPTAstro
Basal
AstrOpto λ542nm 3min
Wash
30 mV
2 s
d
APs frequency (Hz)
Basal
TGOT
Wash
BAPTAstro
AP5
Basal
TGOT
TGOT + AP5
30 mV
2 s
g
OTR-cKO mouse
AAV
CeA
PGFAP
GFP-IRES-Cre
ITR
ITR
f
APs frequency (Hz)
Basal
TGOT
Wash
WT
GFAP OTR KO
Basal
TGOT in WT
TGOT in GFAP OTR KO
30 mV
2 s

Figure 5

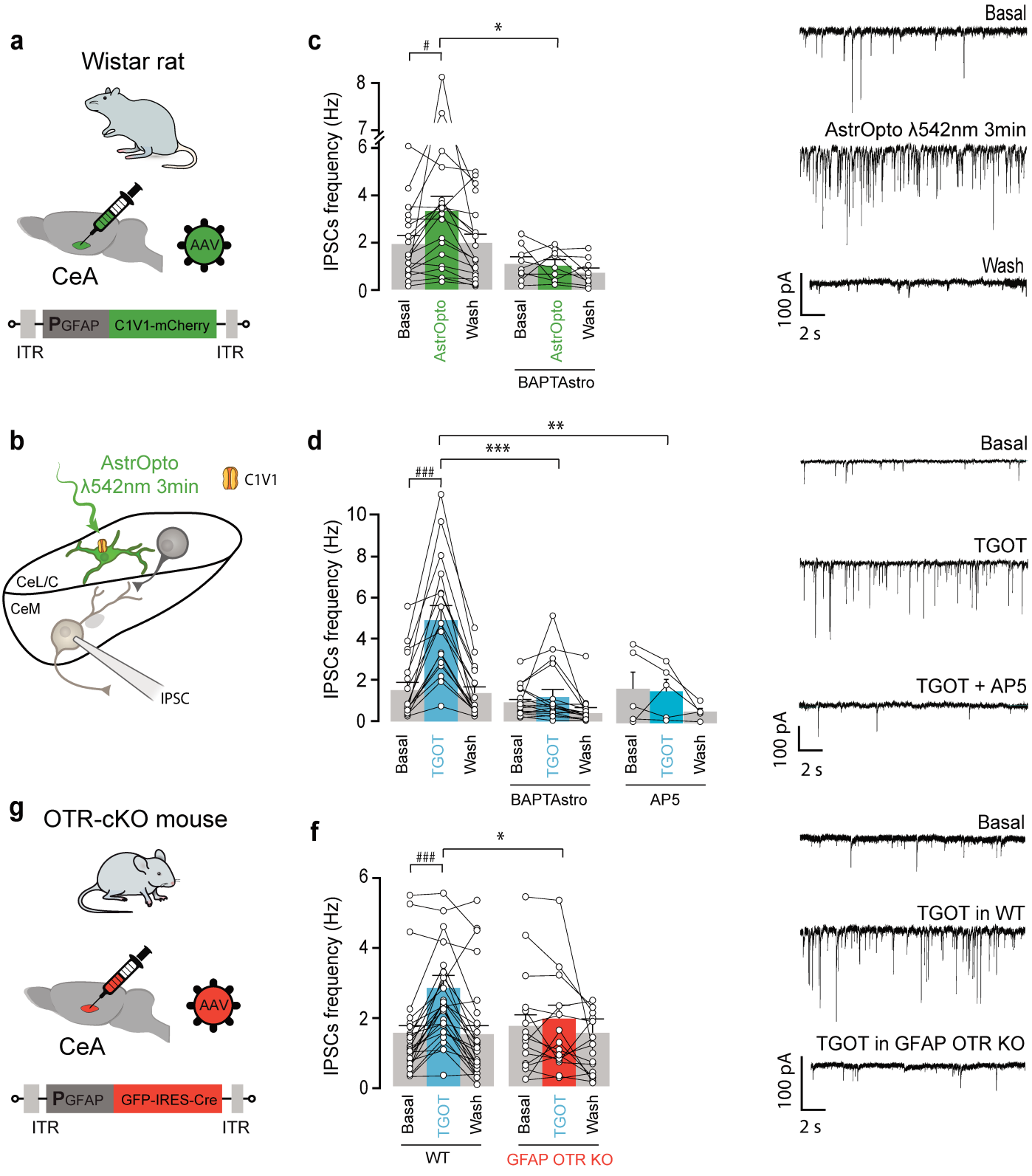
a
Wistar rat
AAV
CeA
PGFAP
C1V1-mCherry
ITR
ITR
b
AstrOpto
λ542nm 3min
C1V1
CeL/C
CeM
IPSC
g
OTR-cKO mouse
AAV
CeA
PGFAP
GFP-IRES-Cre
ITR
ITR
c
IPSCs frequency (Hz)
#
*
Basal
AstrOpto
Wash
Basal
AstrOpto
Wash
BAPTAstro
Basal
AstrOpto λ542nm 3min
Wash
100 pA
2 s
d
IPSCs frequency (Hz)
**
***
###
Basal
TGOT
Wash
Basal
TGOT
Wash
Basal
TGOT
Wash
BAPTAstro
AP5
Basal
TGOT
TGOT + AP5
100 pA
2 s
f
IPSCs frequency (Hz)
*
###
Basal
TGOT
Wash
Basal
TGOT
Wash
WT
GFAP OTR KO
Basal
TGOT in WT
TGOT in GFAP OTR KO
100 pA
2 s

Figure 6

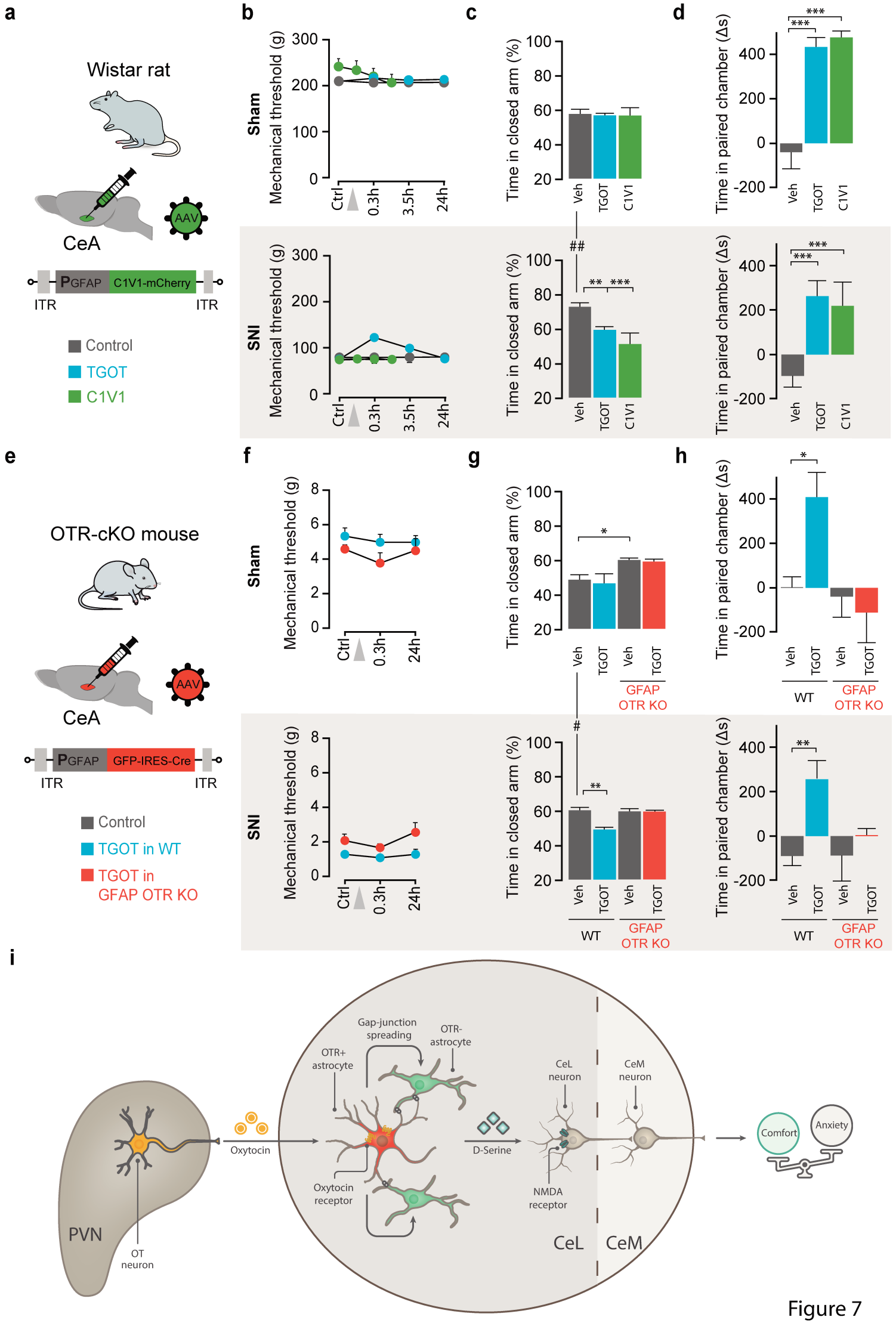
a
Wistar rat
AAV
CeA
PGFAP
C1V1-mCherry
ITR
ITR
Control
TGOT
C1V1
b
Sham
Mechanical threshold (g)
300
200
100
0
Ctrl
0.3h
3.5h
24h
SNI
c
Time in closed arm (%)
100
80
60
40
20
Veh
TGOT
C1V1
##
**
***
d
Time in paired chamber (Δs)
400
200
0
-200
***
e
OTR-cKO mouse
PGFAP
GFP-IRES-Cre
Control
TGOT in WT
TGOT in
GFAP OTR KO
f
8
6
4
2
0
g
WT
GFAP
OTR KO
#
h
i
PVN
OT
neuron
Oxytocin
Gap-junction
spreading
OTR+
astrocyte
OTR-
astrocyte
Oxytocin
receptor
D-Serine
CeL
neuron
CeM
neuron
NMDA
receptor
CeL
CeM
Comfort
Anxiety

Figure 7

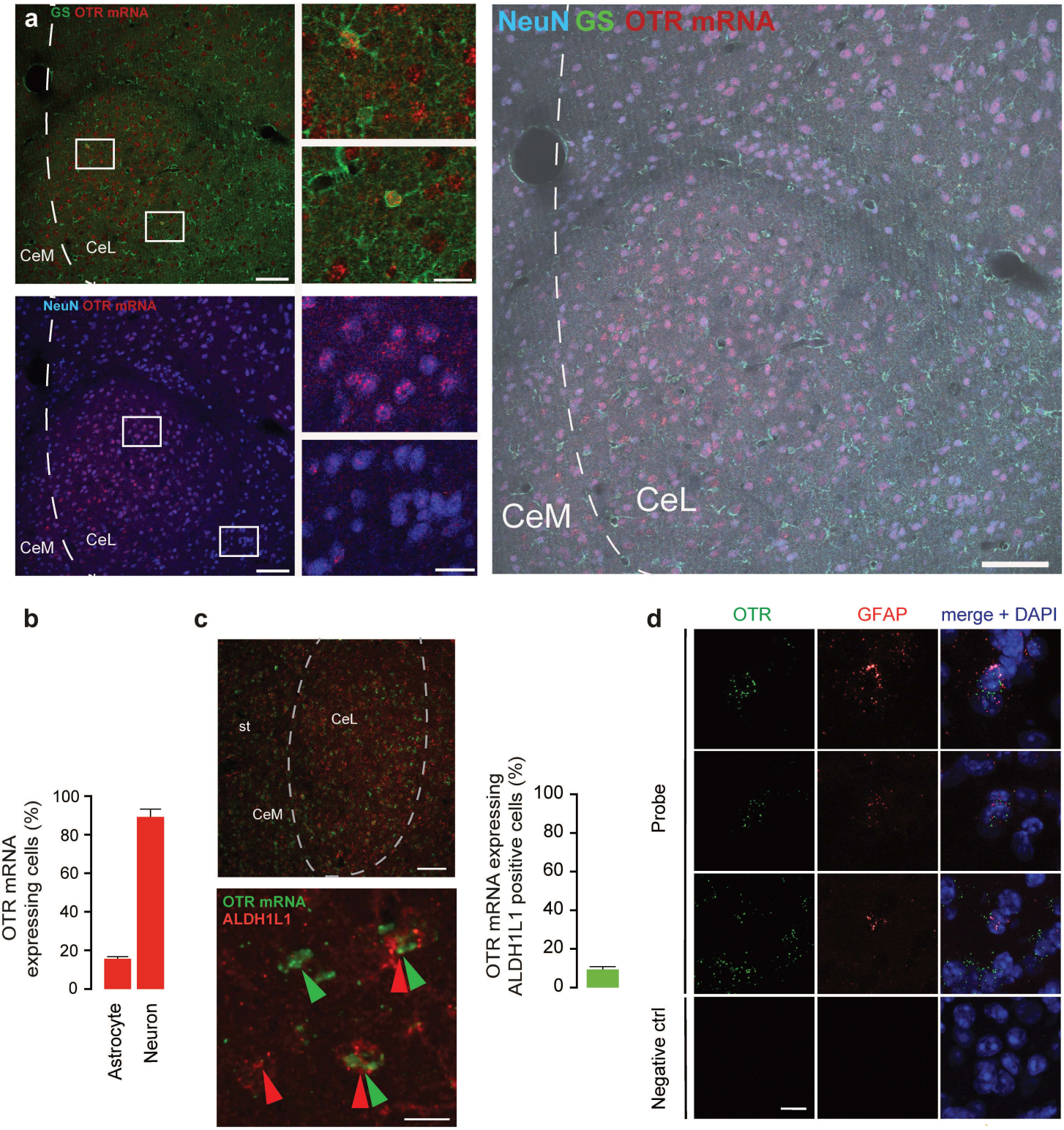

Extended Data Figure 1

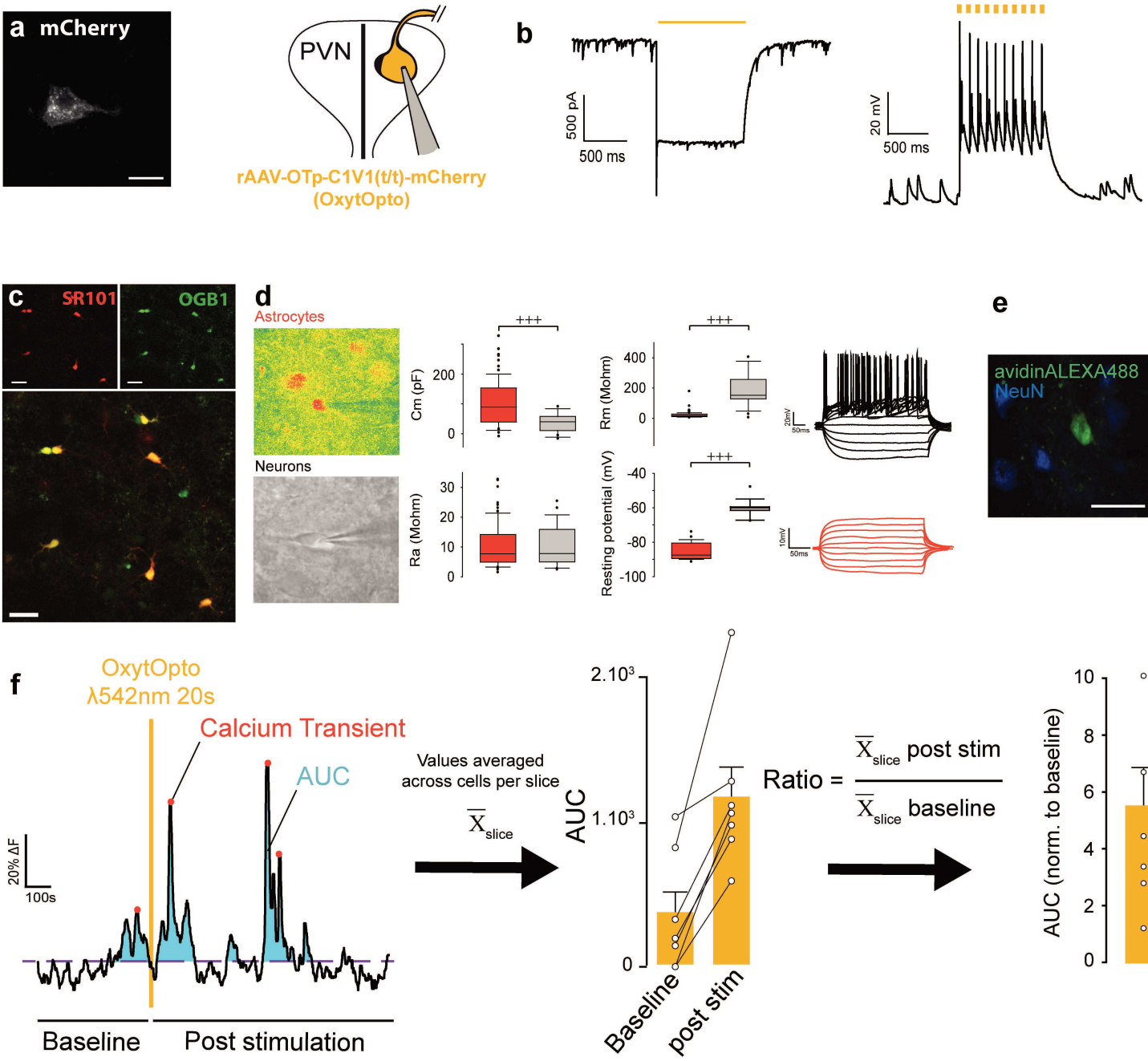

Extended Data Figure 2

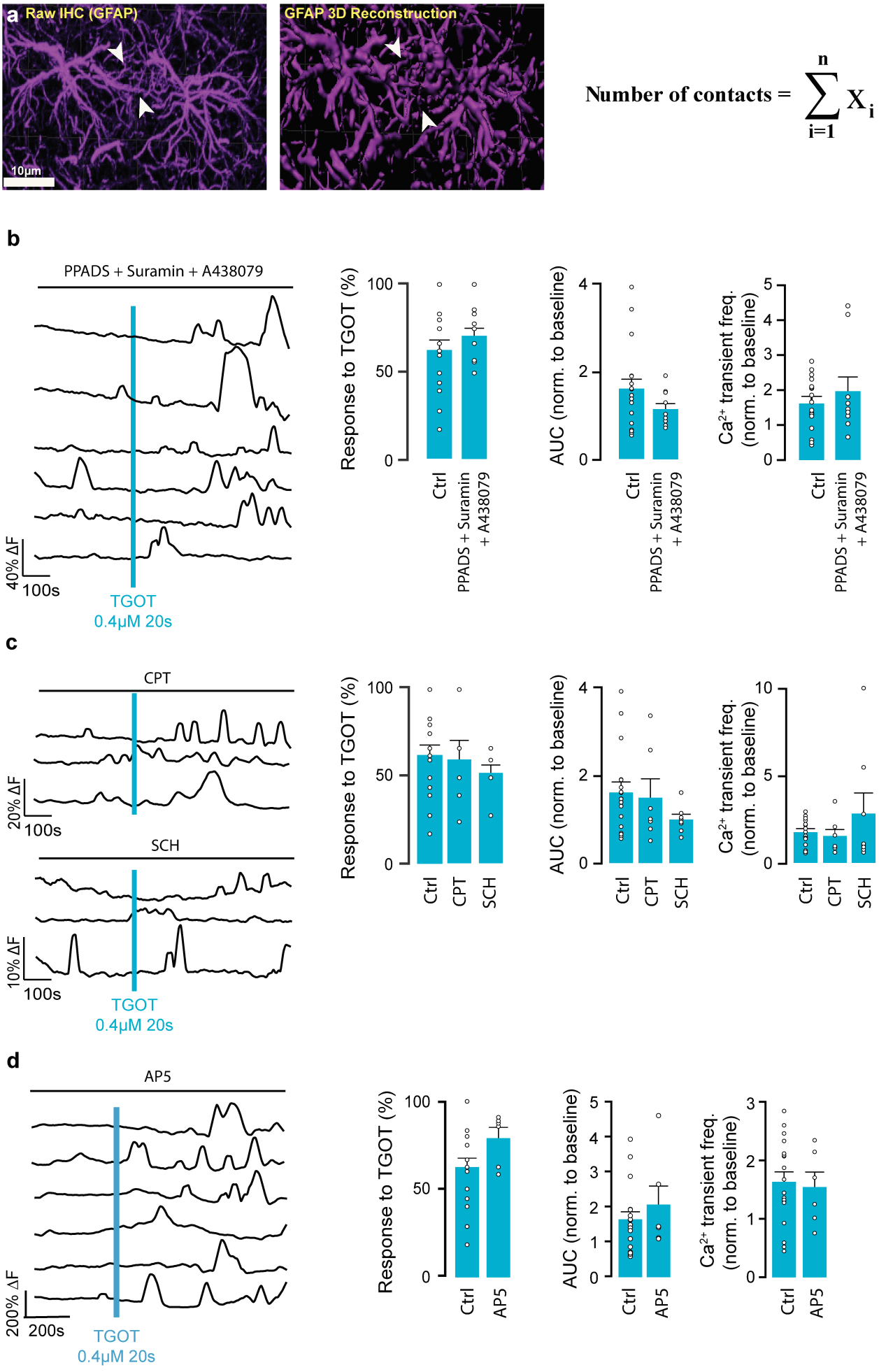

Extended Data Figure 3

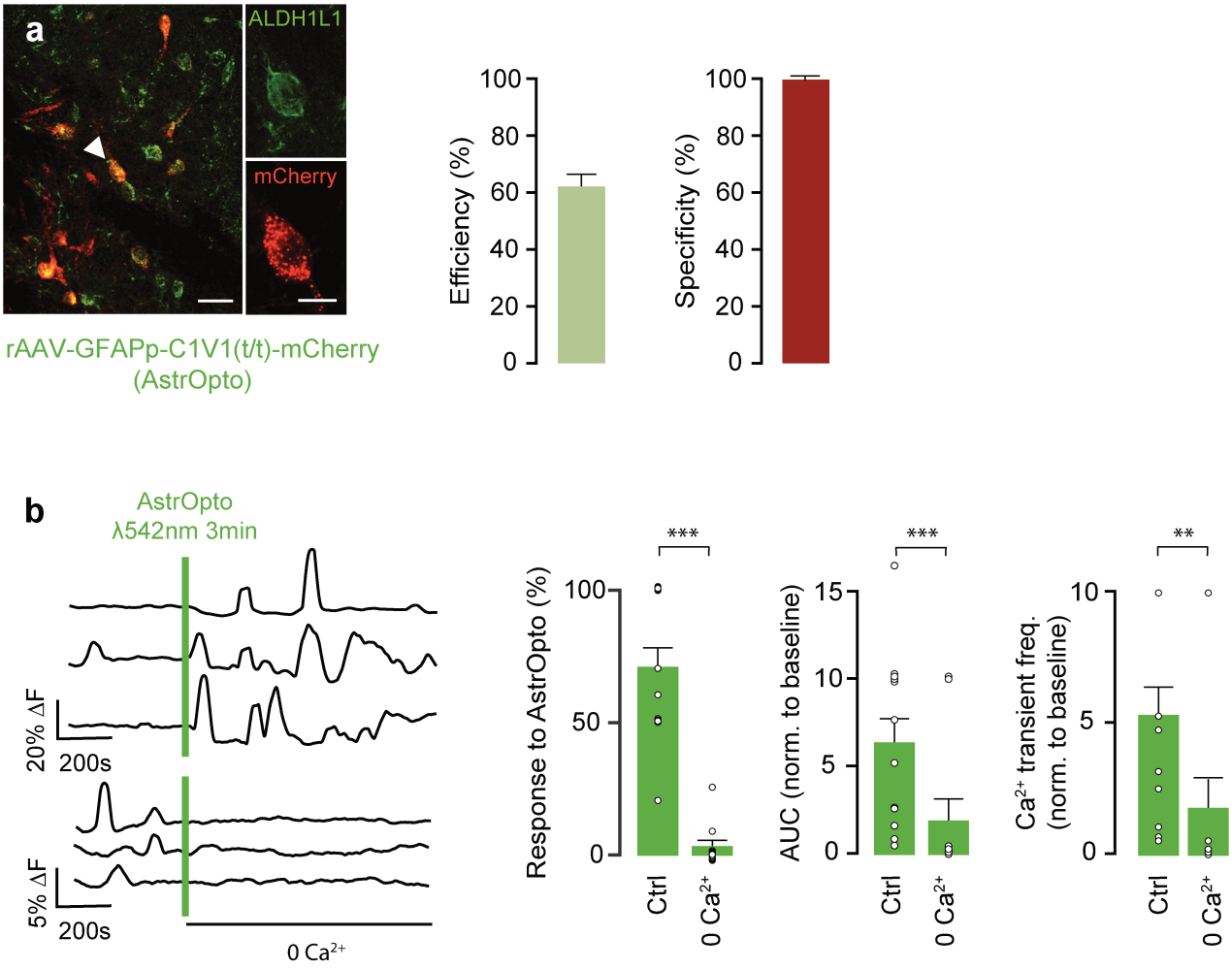

Extended Data Figure 4

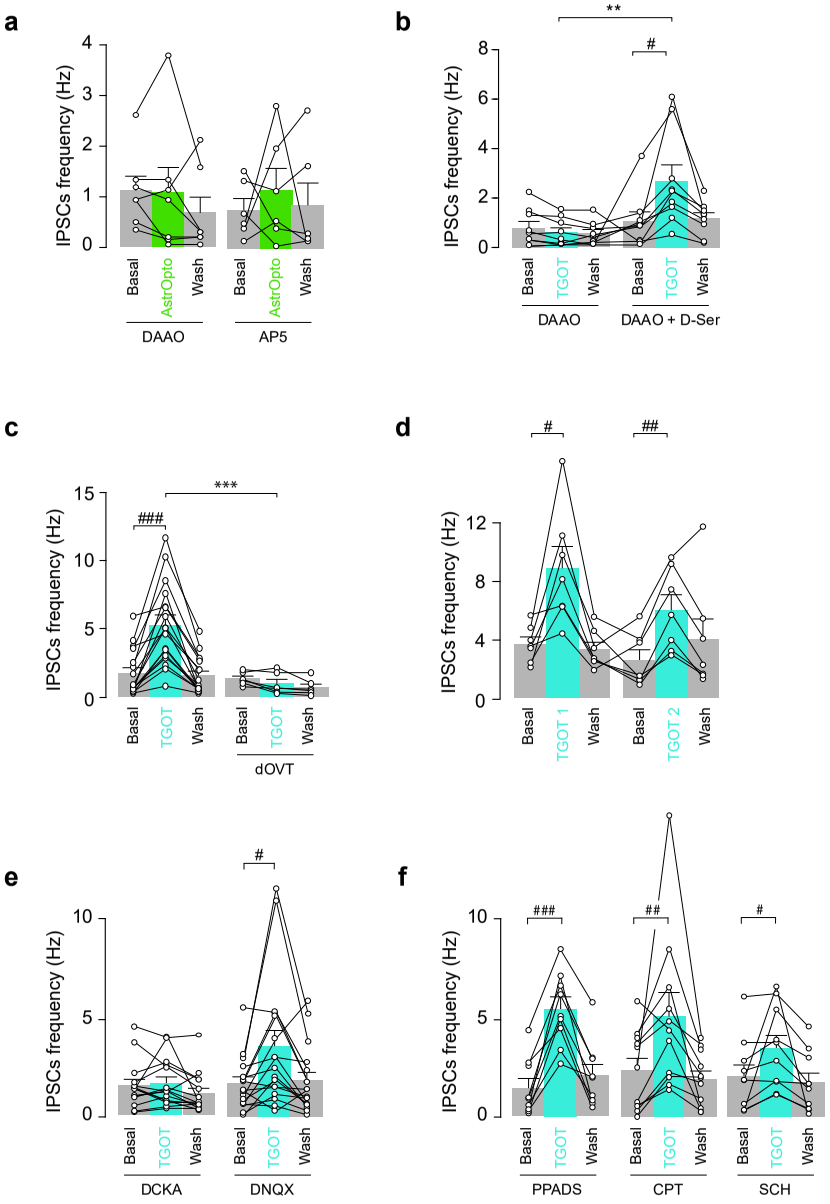

Extended Data Figure 5

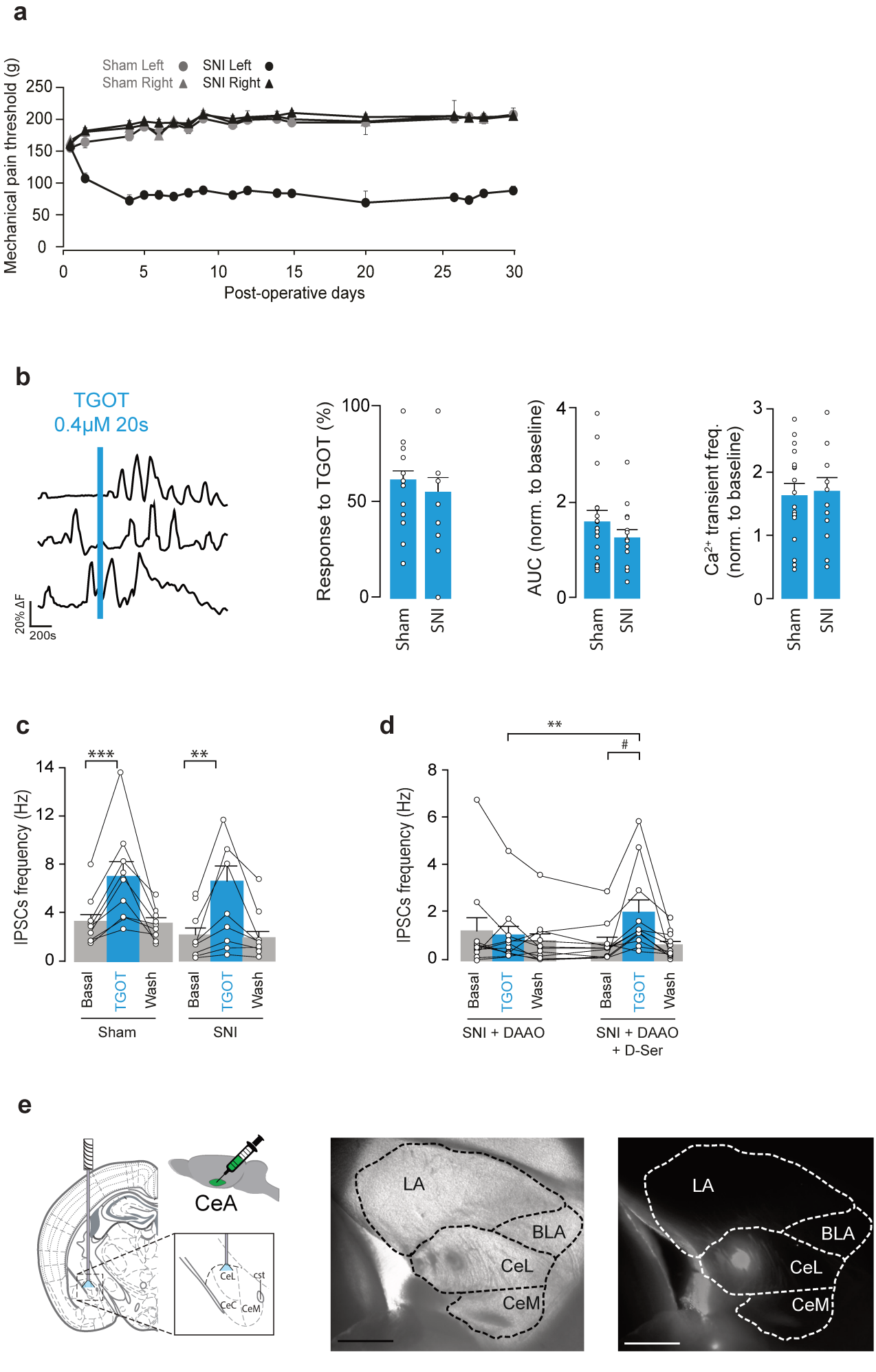

Extended Data Figure 6

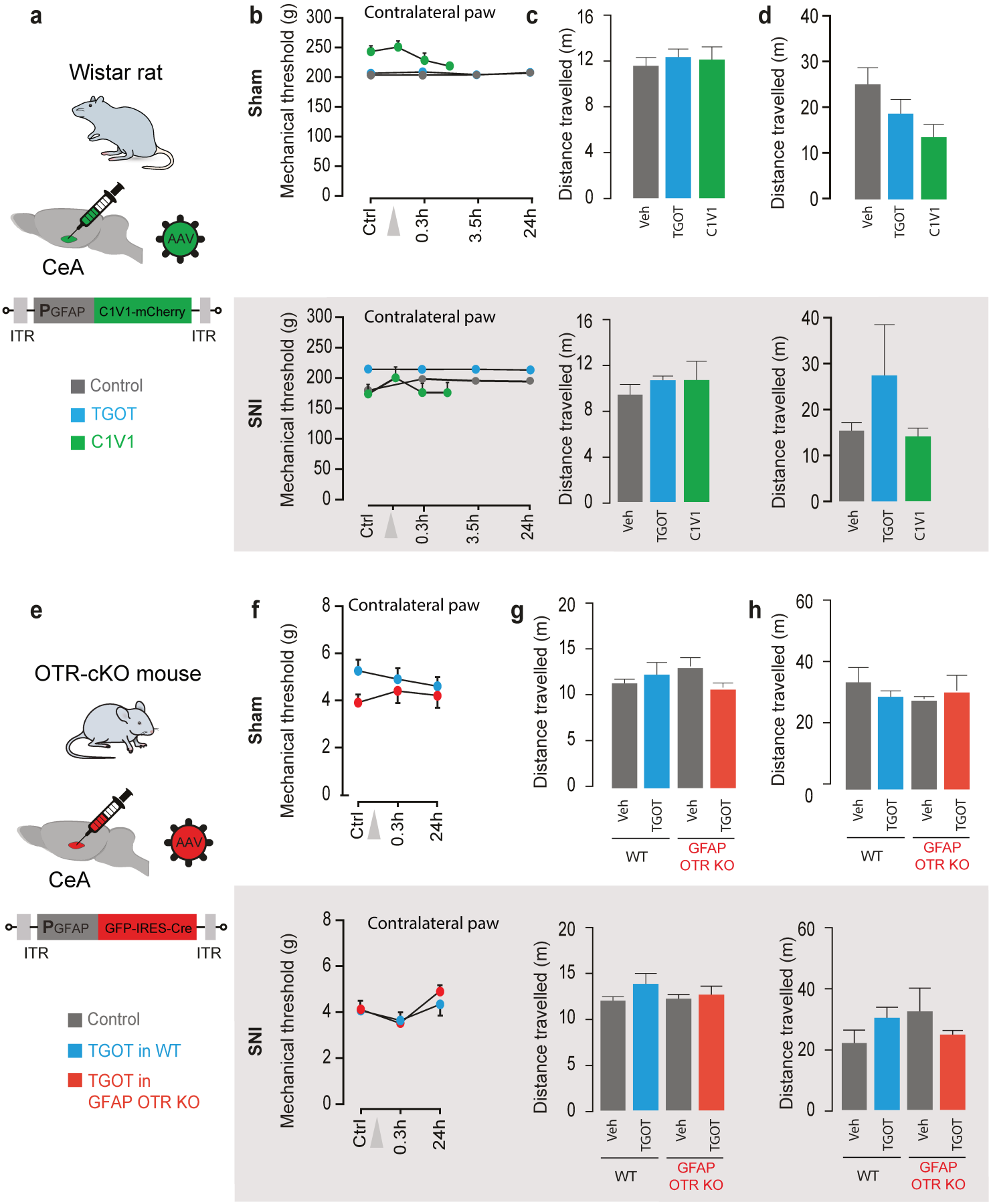

Extended Data Figure 7

Article III : Pharmacologically compromising central amygdala astrocytes prevents the beneficial effects of oxytocin on pain-related behaviors

a. Contexte général

Il a été établi que l'OT est impliquée dans la régulation de nombreuses fonctions neurophysiologiques, comme, la modulation de la douleur ainsi que les comorbidités associées telle que l'anxiété. Cette régulation est notamment supportée par son action sur le microcircuit de l'amygdale centrale (CeA). Il semblerait que les astrocytes soient directement impliqués dans l'étiologie de la douleur chronique tout comme l'est le CeA. Cependant à ce jour, il existe peu d'études montrant le rôle des astrocytes dans la transmission des effets neuromodulateurs de l'OT, et par extension les neuropeptides dans le SNC, bien que de plus en plus d'études mettent en avant le rôle primordial des astrocytes dans la régulation des circuits neuronaux. A ce jour, de nouveaux outils et modèles génétiques chez la souris ou de nouveaux vecteurs viraux ont été mis en place pour étudier la contribution des astrocytes dans la modulation des circuits neuronaux. Cependant l'accès et l'utilisation de ces différents outils restent onéreux et difficiles à mettre en place pour la plupart des laboratoires. Dans l'amygdale centrale, il a été montré que l'OT agit directement sur les astrocytes exprimant l'OTR dans la partie centrale latérale de l'amygdale (CeL), en induisant une augmentation de l'excitabilité des neurones environnants, conduisant à une augmentation des entrées GABAergiques inhibitrices dans les neurones post-synaptiques de la partie centrale médiale de l'amygdale (CeM). Dans cette étude, en se basant sur l'effet de l'OT sur la modulation des astrocytes et des neurones de ce circuit, nous avons validé l'utilisation d'un agent pharmacologique métabolique pour inhiber les astrocytes.

b. Résultat

De manière à valider l'utilisation du fluorocitrate sur l'effet de l'OT sur la modulation du réseau astro-neuronal du CeA, nous avons étudié dans un premier temps son activité en *ex vivo* sur des tranches de cerveau de rats en utilisant les techniques d'imagerie calcique ainsi que d'électrophysiologie. L'ocytocine est capable d'activer directement les astrocytes du CeL, induisant alors une augmentation des oscillations calciques dans ceux-ci et ce de façon indépendante du réseau neuronal. L'application de fluorocitrate en amont s'est révélée être

efficace pour inhiber l'effet du TGOT (un agoniste spécifique des OTR) sur le circuit astrocytaire en supprimant les activités calciques précédemment observées. Par la suite, nous avons pu mettre en évidence que l'application de FC perturbe la communication astro-neuronale. En effet la présence de FC en bloquant l'activité métabolique, prévient de l'augmentation de fréquence de courant post-synaptique inhibiteur (IPSCs) classiquement induit par le TGOT dans les neurones du CeM. De plus, le FC ne semble pas altérer la physiologie du réseau neuronal. En effet, l'administration de KCl est toujours capable de dépolariser les neurones du CeL, induisant alors une augmentation des IPSCs enregistrée dans les neurones du CeM. L'altération du métabolisme astrocytaire semble également bloquer la gliotransmission. Il a été montré que les astrocytes sont capables de libérer des substances de petite taille telle que la D-Serine ou encore la D-Glycine des co-agonistes des récepteurs NMDA. L'application de fluorocitrate semble prévenir de la libération de D-serine, car la supplémentation du bain en D-sérine est capable de rétablir l'augmentation de fréquence des IPSCs induite par le TGOT.

Pour aller plus loin, nous avons réalisé une étude de l'effet du FC *in vivo* en se basant sur les comportements associés au CeA modulés par l'action de l'OT telles que la nociception, l'anxiété ainsi que la promotion d'une sensation de bien-être. L'infusion de FC dans le CeA en est capable d'altérer l'effet anxiolytique induit par l'infusion du TGOT dans le CeA lors de la réalisation d'un test de labyrinthe en croix surélevé ainsi que la promotion de la sensation de confort lors de la réalisation du test de conditionnement de préférence de place.

L'ensemble de ces nouvelles données met en évidence l'efficacité et l'innocuité de l'inhibition astrocytaire par un agent pharmacologique métabolique tel que le fluorocitrate. Un tel composé peut donc se révéler utile en vue d'une alternative ou en complément à l'utilisation d'un modèle génétique.

c. Contribution

J'ai participé à la réalisation et à l'analyse de toutes les parties impliquant l'électrophysiologie, l'imagerie calcique et le comportement.

Pharmacologically compromising central amygdala astrocytes prevents the beneficial effects of oxytocin on pain-related behaviors

Damien Kerspern[1,†], Jérôme Wahis[1,†,$], Angel Baudon[1], Benjamin Boury-Jamot[2], Marie Pertin[3], Perrine Inquimbert[1], Isabelle Decosterd[3,4], Pascal Darbon[1], Alexandre Charlet[1,15,#,*]

[1] Centre National de la Recherche Scientifique and University of Strasbourg, UPR3212 Institute of Cellular and Integrative Neurosciences, Strasbourg, France. [2] Center for Psychiatric Neurosciences, Hôpital de Cery, Lausanne University Hospital (CHUV), Lausanne, Switzerland. [3] Pain center, Department of Anesthesiology, Lausanne University Hospital (CHUV), Lausanne, Switzerland. [4] Department of Fundamental Neurosciences, Faculty of Biology and Medicine (FBM), University of Lausanne, Lausanne, Switzerland. [15] University of Strasbourg Institute for Advanced Study (USIAS), Strasbourg, France.
[$]Present addresses: JW: Laboratory of Glia Biology, VIB-KU Leuven Center for Brain and Disease Research, Department of Neuroscience, KU Leuven Brain Institute, Leuven, Belgium. HSKB: Group of Systemic and Cellular Neuroscience, Institute of Physiology, University of Freiburg, Germany.
[†] Equal first author. [#] senior author. * Corresponding author.

Corresponding Authors
Alexandre Charlet, PhD
Institute of Cellular and Integrative Neurosciences,
INCI CNRS UPR3212
8, Allée du Général Rouvillois
67000 Strasbourg
France
Phone: (33) 6070 825 06
E-mail: acharlet@unistra.fr

Abstract
Over the past decade studies start to focus on the involvement of the astrocytes as key modulator of the neuronal network activity. Importantly, the scientific community have now access to advanced tool to study the astrocyte contribution in the modulation of the neuronal network: genetically modified mice or engineered viral vectors. However, those tools remain expensive and difficult to afford for many labs. Taking advantage of a highly studied circuit, namely the modulation of central amygdala circuit by the neuropeptide oxytocin, in which the crucial involvement of astrocytes has recently been described, we aimed to provide evidence that pharmacological metabolic silencing of astrocyte can be of interest in modern science. Here, we demonstrate that fluorocitrate is an efficient inhibitor of OT-evoked astroglial calcium activity. We further found that metabolic silencing of astrocytes do disturb astro-neuronal communication without impairing the neuronal network basal activity. Finally, we showed that in vivo local infusion of fluorocitrate efficiently and safely impaired the OT-induced modulation of CeA related behavior.

Introduction

The neuropeptide oxytocin (OT) is involved in the regulation of many neurophysiological functions, among which anxiety and pain modulation, notably through its action on central amygdala (CeA) microcircuits (Hasan et al., 2019; Knobloch et al., 2012a; Viviani et al., 2011; Wahis et al., 2020). Further, astrocytes seem to be key players in the etiology of chronic pain pathologies (Ji et al., 2013) as does the CeA (Neugebauer, 2015). However, the role of astrocytes in conveying neuromodulatory effects of oxytocin, and in a greater extend neuropeptides, in the central nervous system has rarely been explored (Di Scala-Guenot et al., 1994; Kuo et al., 2009; Wahis et al., 2020), despite numerous findings of their active involvement in the regulation of neural circuits (Araque et al., 2014; Khakh and Sofroniew, 2015; Ma et al., 2016; Volterra and Meldolesi, 2005) with yet many controversies about the mechanisms involved (Bazargani and Attwell, 2016; Hamilton and Attwell, 2010). While the scientific community have now gained access to advanced tools to study astrocytes contribution in neuronal circuits modulation, mainly through genetically modified mice lines (Davila et al., 2013; Guttenplan et al., 2020; Han et al., 2012; Lee et al., 2008; Suzuki et al., 2003) or engineered viral vectors (Pfrieger and Slezak, 2012), they remain expensive and difficult to manage for most of the labs. In the CeA, OT primarily acts on a specific population of OTR+ astrocytes in the central lateral (CeL) amygdala to induce an increase in excitability of CeL neurons, thereby leading to an increase in GABAergic inhibitory inputs in post-synaptic neurons of the central medial (CeM) amygdala (Wahis et al., 2020). Here, we took advantage of this OT-induced modulation of astrocytes and neuronal circuits to better validate the use of pharmacological metabolic silencing of astrocytes.

Specific metabolic silencing of astrocytes using pharmacological compounds received attention as soon as in the 90's with the characterization of fluorocitrate (FC; (Fonnum et al., 1997)). FC is the product of fluoroacetate, the toxic ingredient of the poison plant *Dichapetalum chymosum* (Peters, 1963). Fluoroacetate and its toxic metabolite fluorocitrate cause inhibition of aconitase. In brain tissue, both substances are preferentially taken up by glial cells and leads to inhibition of the glial tricarboxylic acid cycle (Fonnum et al., 1997). One of the first issues with this compound was its irreversible action. Since fluoride ions are released in the reaction between fluorocitrate and aconitase (Tecle and Casida, 1989), fluorocitrate has been

considered as a suicide substrate (Clarke, 1991). But in the end of the 90's, study demonstrate that fluorocitrate bind closely but not covalently the aconitase (Lauble et al., 1996). Other experiments have shown that the enzyme inhibition is reversed by Sephadex filtration and ammonium sulphate precipitation (Villafranca and Platus, 1973) This is consistent with the recovery of glutamine level or of the glial cell function in the brain 12–24 h after fluorocitrate treatment (Paulsen et al., 1987). The second main concern about fluorocitrate is its putative toxicity. It has been demonstrated that systemic administration may induced cardiac arrhythmia, and central infusion of fluoroacetate or fluorocitrate generate somnolence, and lethargy, followed by the development of convulsions indicating increased neuronal excitability (Bosakowski and Levin, 1986; Goldberg et al., 1966). This primary data put toward the difficulty of using such a compound to inhibit astrocytic activity. Alternative like BAPTA loading into astrocytes exist *ex vivo* (Serrano et al., 2006; Wahis et al., 2020) but remains tricky to perform *in vivo*, moreover in freely behaving animals.

We first test *ex vivo* if metabolic silencing using FC is efficient on CeL astrocytes alter astrocyte-neuron communication through gliotransmission suppression without altering the physiology of the neuronal network. Next, we assess the efficiency of local infusion of FC into the CeA to alter behavior without disturbing the animal physiology. Altogether this new data point toward the efficiency of using pharmacological metabolic silencing through FC as a possible alternative or complement to genetic model.

Material and methods

Surgeries

Neuropathic Pain Model: Spared Nerve Injury (SNI) Procedure

Male Wistar rats were randomly separated in two groups to undergo either posterior left hindpaw SNI or sham procedure, with right hindpaw untouched. Animals were anaesthetized using isoflurane at 1.5–2.5%. Incision was made at mid-thigh level using the femur as a landmark and a section was made through the biceps femoris. The three peripheral branches (sural, common peroneal and tibial nerves) of the sciatic nerve were exposed. Both tibial and common peroneal nerves were ligated using a 5.0 silk suture and transected. The sural nerve was carefully preserved by avoiding any nerve stretch or nerve contact (Decosterd and Woolf, 2000). For animals undergoing sham surgery, same procedure was performed but nerves remained untouched. Animals were routinely observed daily for 7 days after surgery and daily tested by the experimenter. Besides observing weight, social and individual behavior, the operated hindpaw was examined for signs of injury or autotomy. In case of autotomy or suffering, the animal was euthanized in respect of the ethical recommendations of the EU. No analgesia was provided after the surgery in order to avoid interference with chronic pain mechanisms and this is in accordance with our veterinary authorization. Suffering was minimized by careful handling and increased bedding.

Stereotaxic Surgery: intra-CeL Cannulae

Cannulae Implantation. Animals were bilaterally implanted with guide cannulae for direct intra-CeL infusions. As guide cannulae we used C313G/Spc guide metallic cannulae (Plastics one, VA, USA) cut 5.8 mm below the pedestal. For this purpose, animals were deeply anesthetized with 4% isoflurane and their heads were fixed in a stereotaxic frame. The skull was exposed and two holes were drilled according to coordinates that were adapted from brain atlas (rat, 2.7 mm rostro-caudal; 4.2 mm lateral; 8 mm dorso-ventral relative to bregma) by comparing the typical bregma-lambda distance with the one measured in the experimental animal. Two screws were fixed to the caudal part of the skull in order to have an anchor point for the dental cement. Acrylic dental cement was finally used to fix the cannulae and the skin was sutured. In case of long-lasting experiments (neuropathy-induced anxiety) with a cannula implantation at distance of the behavioral assay (> 4 weeks), cannulae were sometimes lost or cloaked, and concerned animals therefore excluded from testing.

Drugs Infusions. We used bilateral injections of 0.5 µl containing either vehicle (NaCl 0.9%) or oxytocin agonist TGOT (1 µM) dissolved in NaCl 0.9%. For this procedure two injectors (cut to fit 5.8 mm guide cannulae protruding 2 to 2.5 mm beyond the lower end of the cannula in older animals and 1.8 mm in 3-4 week old rats) were bilaterally lowered into the guide cannula, connected via polytene tubing to two Hamilton syringes that were placed in an infusion pump and 0.5 µl of liquid was injected in each hemisphere over a 2-minute-period. After the injection procedure, the injectors were kept in place for an additional minute in order to allow a complete diffusion of liquid throughout the tissue. Rats were subsequently left in the home cage for 15 minutes to recover from the stress of the injection and then handled for mechanical pain threshold or anxiety assessment. Animals that received TGOT injections for the first

experiment (mechanical sensitivity assessment) were switched to the vehicle injected groups for the elevated plus maze experiment.

Horizontal and Coronal Slices

Slices Preparations. In all cases, animals were anaesthetized using ketamine (Imalgene 90 mg/kg) and xylazine (Rompun, 10 mg / kg) administered intra-peritoneally. Transcardial perfusion was then performed using one of the following artificial cerebro-spinal fluids (aCSFs) dissection solutions. For animals between 18 and 25 days old, an ice-cold sucrose based dissection aCSFs was used containing (in mM): Sucrose (170), KCl (2.5), NaH_2PO_4 (1.25), $NaHCO_3$ (15), $MgSO_4$ (10), $CaCl_2$ (0.5), HEPES (20), D-Glucose (20), L-ascorbic acid (5), Thiourea (2), Sodium pyruvate (3), N-acetyl-L-cysteine (5), Kynurenic acid (2). For animals between 2 and 6 months old, an ice-cold NMDG based ACSF was used containing (in mM): NMDG (93), KCl (2.5), NaH_2PO_4 (1.25), $NaHCO_3$ (30), $MgSO_4$ (10), $CaCl_2$ (0.5), HEPES (20), D-Glucose (25), L-ascorbic acid (5), Thiourea (2), Sodium pyruvate (3), N-acetyl-L-cysteine (10), Kynurenic acid (2). In both cases, pH was adjusted to 7.4 using either NaOH or HCl, this after bubbling in 95% O_2-5% CO_2 gas, bubbling which was maintained throughout the duration of use of the various ACSFs. Those ACSFs formulae were based on the work of(Ikegaya et al., 2005). Following decapitation, brain was swiftly removed in the same ice-cold dissection aCSFs as for transcardial perfusion, and 350 µm thick horizontal slices containing the CeA obtained using a Leica VT1000s vibratome. Upon slicing, brain slices were hemisected and placed, for 1 hour minimum before any experiments were conducted, in a room tempered holding chamber, containing normal ACSFs. Normal ACSF, also used during all *ex vivo* experiments, is composed of (in mM): NaCl (124), KCl (2.5), NaH_2PO_4 (1.25), $NaHCO_3$ (26), $MgSO_4$ (2), $CaCl_2$ (2), D-Glucose (15), adjusted for pH values of 7.4 with HCL or NaOH and continuously bubbled in 95% O_2-5% CO_2 gas. aCSFs was checked for osmolality and kept for values between 305-310 mOsm/L. In electrophysiology or calcium imaging experiments, slices were transferred from the holding chamber to an immersion recording chamber and superfused at a rate of 2 ml/min with normal aCSFs unless indicated otherwise.

Drug Application. OTR agonist [Thr^4Gly^7]-oxytocin (TGOT) and D-serine were bath applied through a 20s long pumping of agonist solution, corresponding to several times the volume of the recording chamber. Other drugs (fluorocitrate, DAAO) were applied for at least 20 minutes in the bath before performing any experiments.

Calcium Imaging and Identification of Astrocytes

To identify astrocytes, SR101 (1 µM) was added to aCSF in a culture well and slices were incubated for 20 minutes at 35°C. The synthetics calcium indicators OGB1 was bulk loaded following an adapted version of the method described previously (Ikegaya et al., 2005) reaching final concentrations of 0.0025 % (~20 µM) for calcium indicators, 0.002% Cremophor EL, 0.01 % Pluronic F- 127 and 0.5% DMSO in aCSF, and incubated for 45 to 60 minutes at 38°C. Upon incubation time, slices were washed in aCSF for at least an hour before any recording was performed. Astrocytes recorded for this study were those co-labeled, in rats for SR101 and OGB1. The spinning disk confocal microscope used to perform astrocyte calcium imaging was composed of a Zeiss Axio examiner microscope with a 40x water immersion objective (numerical aperture of 1.0), mounted with a X-Light Confocal unit – CRESTOPT spinning disk. Images were acquired at 2Hz with either a Rolera em-c^2 emCCD or an optiMOS

sCMOS camera (Qimaging, BC, Canada). Cells within a confocal plane were illuminated for 100 to 150 ms for each wavelength (SR101: 575 nm, OGB1: 475 nm) using a Spectra 7 LUMENCOR. The different hardware elements were synchronized through the MetaFluor software (Molecular Devices, LLC, Ca, USA) which was also used for online. Astrocytic calcium levels were measured in hand drawn ROIs comprising the cell body plus, when visible, proximal processes. In all recordings, the Fiji rolling ball algorithm was used to increase signal/noise ratio. Further offline data analysis was performed using a custom written python-based script available on editorial website. Intracellular calcium variation was estimated as changes in fluorescence signals. To take into account micro-movements of the specimen on long duration recordings, the fluorescence values were also calculated for SR101 and subsequently subtracted to the ones of OGB1. On this last case, recordings in which movements / drifts were visible were discarded. Then, a linear regression and a median filter was applied to each trace. Calcium transients was detected using the find_peaks function of the SciPy library. More precisely, fluorescence variation was identified as a calcium peak if its prominence exceeds the standard deviation (or two times the standard deviation for recordings acquired with the sCMOS camera) and if the maximum peak value surpasses 50 fluorescence units (or 3 units for sCMOS recordings). The AUC was estimated as the sum of the local area of each peak to avoid biased AUC estimation due to baseline drift. All these data were normalized according to the duration of the recording and astrocytes was labelled as "responsive" when their AUC or their calcium transient frequency was increased by at least 20% after drug application. Because the time post-stimulation is longer than the baseline (10 min vs 5 min), the probability of observing a spontaneous calcium peak is stronger post-stimulation. To avoid this bias, astrocytes with only one calcium peak during the whole recording were not considered as responsive. Finally, all data were averaged across astrocytes per slice, and this result was used as statistical unit. All data were expressed as ratio (baseline/drug effect), a ratio of 1 meaning neither an increase nor a decrease of the measured parameter. For inter-ratio comparison, parametric or non-parametric (depending on data distribution) unpaired statistical tests were used. Fiji software was also used on SR101 / OGB1 pictures to produce illustrative pictures. All calcium imaging experiments was conducted at controlled room temperature (26°C).

Electrophysiology

Whole cell patch-clamp recordings of CeM neurons were visually guided by infrared oblique light visualization of neurons. Patch-clamp recordings were obtained with an Axon MultiClamp 700B amplifier coupled to a Digidata 1440A Digitizer (Molecular Devices, CA, USA). Borosilicate glass electrodes (R = 3.5 - 7 MΩ) with inner filament (OD 1.5 mm, ID 0.86 mm; Sutter Instrument, CA USA) were pulled using a horizontal flaming/brown micropipette puller (P97; Sutter Instrument, CA, USA). Recordings were filtered at 2 kHz, digitized at 40 kHz and stored with the pClamp 10 software suite (Molecular Devices; CA, USA). Analysis of patch-clamp data were performed using Clampfit 10.7 (Molecular Devices; CA, USA) and Mini analysis 6 software (Synaptosoft, NJ, USA) in a semi-automated fashion (automatic detection of events with chosen parameters followed by a visual validation).

Whole-cell Recording of CeM Neurons. Pipettes were filled with an intracellular solution containing (in mM): KCl (150), HEPES (10), $MgCl_2$ (4), $CaCl_2$ (0.1), BAPTA (0.1), ATP Na salt (2), GTP Na salt (0.3). pH was adjusted to 7.3 with KOH and osmolality checked to be between 290-295 mOsm/L, adjusted with sucrose if needed. All cells were hold at a membrane potential

of -70 mV. Series capacitances and resistances were compensated electronically throughout the experiments using the main amplifier. Average events frequencies per cell were calculated on 20s windows, chosen for TGOT or light stimulation during maximal effect, as determined by the visually identified maximal slope of the cumulative plot of the number of events. CeM neurons were classified as TGOT-responsive when the average IPSCs frequency was increased by at least 20% during at least 10s and up to 500s after TGOT application when compared to baseline average frequency. Onset and offset time of the evoked response were defined using respectively the start and end of the increased slope measured on a cumulative plot of the number of events, similarly to the method used in (Wahis et al., 2021). Baseline and recovery frequencies were measured respectively at the beginning and end of each recording. All patch-clamp experiments were conducted at room temperature.

Behavior

***Mechanical Sensitivity Assessment*.** In experiments with rats, we used a calibrated forceps (Bioseb, Chaville, France) previously developed in our laboratory to test the animal mechanical sensitivity(Luis-Delgado et al., 2006). Briefly, the habituated rat was loosely restrained with a towel masking the eyes in order to limit stress by environmental stimulations. The tips of the forceps were placed at each side of the paw and a graduate force applied. The pressure producing a withdrawal of the paw, or in some rare cases vocalization, was considered as the nociceptive threshold value. This manipulation was performed three times for each hind paw and the values were averaged as being the final nociceptive threshold value.

Elevated Plus Maze. Following protocol from (Walf and Frye, 2007), the arena is composed of four arms, two open (without walls) and two closed (with walls; rats 30 cm high; mice 15 cm high). Arms are 10 cm wide, 50 cm long and elevated 50 cm off the ground for rats and 5 cm wide. Two lamps with intensity adjustable up to 50 watts were positioned on the top of the maze, uniformly illuminating it. Animals were video tracked using a video-tracking systems (Ethovision Pro 3.16 Noldus, Wageningen, Netherlands and Anymaze, Stoelting Europe, Ireland). After each trial, the maze was cleaned with 70% ethanol and dry with paper towel. Twenty minutes after intracerebral injections or directly after optical stimulation, the animal was let free at the center of the plus maze, facing the open arm opposite to where the experimenter is, and was able to freely explore the entire apparatus for six minutes. Total time and time spend in closed and open arms were recorded in seconds and the percentage of time spent in closed arms was calculated as a measure of anxiety. As internal control, the total distance traveled during the test period was quantified and compared between all different groups. Animals falling from the apparatus during the test, freezing more than 50% of the total time, or with cannulae/optic fiber issues, were removed from the analysis.

***Conditioned Place Preference*.** The device is composed of two opaque conditioning boxes (rats: 30x32 cm; mice: 22x22 cm) and one clear neutral box (30x20 cm) Animals were video tracked using a video-tracking system (Anymaze, Stoelting Europe, Irland). After each trial, the device was cleaned with a disinfectant (Surfa'Safe, Anios laboratory). Based on (King et al., 2009), all rats underwent a 3 days habituation period during which they were able to freely explore the entire apparatus for 30 min. On the day 3, behavior was record for 15min to verify the absence of pre-conditioning chamber preference. The time spend in the different compartment were measured and paired compartment was chosen as the compartment in which rat spent the less time during the 3rd day of habituation. On day 4, animals were placed

the morning in one compartment for 15 min with no stimulation (unpaired box). Four hours after, the animal were placed 15min in the opposite box (paired box) and CeL astrocyte expressing C1V1 vector were optogenetically stimulated (3 min - 500ms light pulse at 0.5 Hz - λ542nm) or TGOT micro-infused through intracerebral cannulae. On day 5, the animals were place in the CPP box and allowed to freely explore the entire apparatus during 15min. As internal control, the total distance traveled during the test period was quantified and compared between all different groups. Rats falling spending more than 80% of the total time in a single chamber before the conditioning, or with cannulae/optic fiber issues, were removed from the analysis.

Results

Astrocytes metabolic silencing efficiently decrease their passive and OTR-evoked calcium activity

Oxytocin is a neuropeptide able to modulate neurophysiological function such as pain and several associate comorbidities such as anxiety. One of the major structures involved in pain and especially on the modulation of its emotional valence is the amygdala. Recent publications highlight the fact that astrocytes do express functional oxytocin receptor in several structures including the central lateral part of the amygdala, and that oxytocin signaling modulate the network activity of the CeA through its action on CeL astrocytes (Wahis et al.,2021). Base on previous study demonstrating that endogenous oxytocin release or bath application of [Thr^4Gly^7]-oxytocin (TGOT) a specific agonist to oxytocin receptor trigger calcium transient in CeL astrocyte we aim to demonstrate that FC is sufficient to alter this calcium response

We first assessed calcium activity of CeL astrocytes in brain slices of rats using the calcium indicator Oregon Green® 488 BAPTA-1 (OGB1) and identified astrocytes through sulforhodamine 101 labelling (SR101) (Figure 1A). Bath application of TGOT (0.4 µM , 20s) evoked long-lasting calcium transients in astrocytes (Figure 1B) in approximatively 50% of the astrocytes of the CeL network. In presence of TTX, the percentage of responding astrocytes, AUC and calcium transient frequency was not altered (Figure 1C) reinforcing the proof that astrocytes are directly activated by TGOT without neuronal network activity implication. Prior incubation with fluorocitrate (100µM, 1h) does not alter basal calcium activity of CeL astrocytes, and was sufficient to diminish the proportion of responding astrocyte to 10% and those responding astrocyte display reduction in calcium transients magnitude and frequency (Figure 1C).

This experience demonstrates the importance of the astrocytes for the conveyance of the OTR signaling in the CeA, at least for astrocyte activation by oxytocin. The fact basal activity remained unchanged and that still 10% of the astrocytes display calcium elevation prove that fluorocitrate at this concentration do not slew the cells in brain slice.

Astrocytes metabolic silencing prevent the OT-induced modulation of CeA neuronal network activity

The central amygdala is mainly composed of GABAergic neurons. The CeL display inhibitory projection to CeM GABAergique neurons. To access the recruitment of the CeA network, we recorded the post synaptic inhibitory current (IPSCs) in CeM neuron. Bath application of TGOT (0.4µM, 20s) elicits an increase of the IPSCs frequency in CeM neuron up to 4 Hz (0.61 Hz +- 0.18 Hz vs 3.88 Hz+-0.76 Hz, p=0.0156), demonstrating that OTR activation do recruit the CeA network (Figure 2A). Interestingly prior incubation of fluorocitrate (10-100 µM, 20min) does not alter the basal IPSCs frequency and do block the TGOT induced increase IPSCs frequency in CeM neurons (0.87 Hz +- 0.28 Hz vs 1.79 Hz+-0.33 Hz, p= >0.999) (Figure 2A).

To assess the integrity of the neuronal circuit after FC incubation, we performed KCl (50µM, 20s) bath application to depolarize CeL neurons and increase their firing and increase the IPSCs recorded in CeM neurons (0.80 Hz+-0.20 Hz vs 4.12 Hz +-0.90 Hz, p=0.0148, Figure 2B) . Incubation of the highest FC used concentration in a significatively longer time (100µM,

1h) did not alter the KCl effect on IPSCs frequency in CeM neurons (1.75 Hz+-0.56 Hz vs 7.14 Hz+-1.79 Hz, p=0.0117, Figure 2B).

In conclusion, these experiments demonstrate that the neuronal network in still active and mobilizable after FC incubation. This support that the lack of TGOT-induced response after FC incubation is due to the efficient inhibition of astrocytes calcium activity by FC without disturbing neuronal communication.

Astrocytes metabolic silencing do alter NMDAR recruitement .

One known ability of astrocyte is to perform gliotransmission, meaning the release of neuromodulator to modulate surrounding synapse activity. CeL neuron express numerous NMDA receptor sensitive to glutamate release coming from various afference. But to be activate this receptor, the glutamate sole is not enough, it needs a co-agonist: the D-serine or D-Glycine known to be release by the astrocytes. As previously demonstrate application of fluorocitrate prevent the IPSCs increase induced by TGOT (1.18 Hz +-0.23 Hz vs 1.57 Hz+-0.27 Hz, p=0.21). Bath supplementation with the D-serine (100µM) rescue the TGOT signalization allowing the TGOT induced IPSCs frequency increase up to control condition (1.61 Hz+-0.63 Hz vs 4.81 Hz+-1.35 Hz, p=0.0089, Figure 3). This demonstrate that fluorocitrate impaired the gliotransmission of astrocyte and reinforce the idea that the neuronal network basal activity is not impacted by FC incubation.

Astrocytic metabolic silencing prevent the OT-induced behavioral modulations

Previous study has demonstrated that oxytocin modulate the CeA astro-neuronal network to exert an anxiolytic effect and promote positive reinforcement (Wahis et al.,2021). Here we performed local (CeA) infusion of FC to assess the efficiency of metabolic silencing to alter OTR-related behavioral modulation.

Rats were submitted to a spare nerve injury (SNI) on rats, leading to the apparition of a hyperalgesia and an anxious state 4 weeks after the surgery. The SNI rat presented a significant hyperalgesia compared to sham animal (79.19 g+-1.64 g vs 209,72g+-1.91 g, figure 4A). CeA local infusion of TGOT slightly but significantly induced a transitory analgesia (79.19 g+-1.64 g vs 122.63 g +-2.61 g, p=0.023 figure 4A). This analgesic effect was fully abolished with prior CeA local infusion of FC (79.19 g+-1.64 vs 76.25 g +-4.92 g). We further access the involvement of the CeA astrocyte on anxiety. The neuropathic rat spent more time than sham one in the closed arm revealing their anxious state (214.78 s +-12.80s vs 173.90 s +-4.72 s, figure 4B). TGOT infusion directly in the CeA induce a reduction of the time spent in this closed arm to similar level as sham animal (177.77 s +-8.65 s vs 173.90 s +-4.72 s, figure 4B). This anxiolytic effect is however not observed in sham animals, meaning that OT have an effect on anxiety only when the CeA network was altered. Furthermore, the rescue effect of OT on anxiety is totally abolish if the metabolic activity of astrocytes is inhibited by fluorocitrate positioning the astrocytes in the central position for OT signaling (220.82 s+- 21.66 s. vs 177.77 s +-8.65 s Figure 4B).

An interesting fact is metabolic silencing of astrocytes leads to an increase in the time spent in closed arm for both neuropathic and control animal (173.90 s +-4.72 s vs 231.42 s +-20.31s for sham and 214.78 s +-12.80s vs 231.25 +-22.02 s for SNI) . This effect is probably not due

to a sickness effect of fluorocitrate because the distance travelled by the animal do not differ between all the different groups.

The last paradigm we access is the emotional valence of pain with the conditioned place preference test. We compare the time spend in the paired chamber between the day before the conditioning and the day after and express the result as a delta of time spent in the paired chamber (time $_{habituation}$ – time $_{post\ conditioning}$). Rats who received TGOT in a chamber spent significatively more time in it no matter if there are neuropathic or not (-95.47 s +-56.206 vs 267.43 s +- 74.85s for SNI and -35.64 s +-71.39 s vs 435 s +-112.89 s for Sham) . This effect on place preference is clearly altered by the fluorocitrate (267.43 s +- 74.85s vs 0.1s +-118.64 s for SNI and 435 s +-112.89 s vs 76.93 s +-90.15 s for Sham) , showing that the dual infusion of TGOT and FC do not induced a place preference. The locomotion activity of the rat was still not impaired by the FC effect, demonstrating that at this does FC do not trigger sickness on the animal.

Discussion.

Here, we demonstrate that metabolic silencing astrocytes using FC does not impact their basal calcium activity but efficiently decrease the OTR-induced calcium transients (Figure 1). In addition, it does not impact the basal level of CeM neuronal activity, nor their potential recruitment, but significantly preventing the OTR-induced increase in CeM IPSCs frequency (Figure 2). Further, the D-serine gliotransmitters seems to be involved in the astrocyte to neuron gliotransmission (Figure 3). Finally, local pharmacological compromising astrocytes activity does not impact basal behavior, but fully prevent the OTR-induced benefices in pain-related and affective behaviors (Figure 4). In conclusion, using local pharmacological metabolic silencing of CeA astrocytes, we consolidate the idea that OTR signaling through astrocytes is necessary for the modulation of the local CeA microcircuit and its behavioral correlates.

During the past decade interest of the astrocytes as key modulator for the neuronal network emerge (Corkrum et al., 2019; Papouin et al., 2017; Robin et al., 2018). Several studies describe astrocyte as key, if not primary, targets of neuromodulators, and those astrocytes might be the causal elements behind shifts in brain states, a function commonly attributed to neuromodulators direct action on neurons(Lee and Dan, 2012). Neuromodulators are already the target of numerous drugs use for clinical treatment (Monai and Hirase, 2018). Taken together this indicated that we should raise our attention and consideration of astrocytes role in brain circuits, notably regarding the effect of neuromodulators. However, despite the high relevance of such techniques, all laboratory couldn't afford it, highlighting the importance to consider less expensive, but nonetheless effective, methods to encourage further studies in this field.

Using state-of-the-art genetic tools, transgenic mice and rAAV viral vectors, our lab previously demonstrated that astrocytes are critical player in the OT-induced modulation of CeL→CeM neuronal circuits. We found that CeL astrocytes do express functional OTR and convey the OT signal at least through gap junctions coupling. The recruitment of the CeL astrocytes syncytium then leads to a NMDAR mediated tuning of CeA neuronal circuits. Eventually, this oxytocin-modulated astro-neuronal amygdala circuit promotes the behavioral correlates of comfort, and modulate anxiolytic state (Wahis et al., 2021). . Here, we provide evidences that an affordable pharmacological agent allow to reproduce, and extent, the conclusions previously obtained using high-end genetic manipulations with minor side effect, if any. As previously describe, fluorocitrate inhibit the metabolic activity of astrocytes and abolish mainly of its modulatory action on neuronal network. Fluorocitrate is taken up preferentially by glial cell. It has been shown that FC is a suicide inhibitor of the Krebs cycle enzyme aconitase (aconitase hydratase)(Clarke, 1991; Peters, 1957), and might also inhibit mitochondrial transport of citrate (Hertz, 1990). Furthermore, it has been proposed that FC could reduce glytamine synthesis (Balcar et al., 1977; Berg-Johnsen et al., 1993; Cheng et al., 1972), and reduce the K^+ stimulated release of glutamine, glutamate and GABA (Paulsen and Fonnum, 1989; Paulsen et al., 1988; Szerb and Issekutz, 1987). Since glutamine synthesis requires ATP and thid ATP production is mainly due to the Krebs cycle reaction (Geuther, 1977) it has been suggested that the metabolic effects of FC might result from glial energy failure (Berg-Johnsen et al., 1993). Some study also bring the hypothesis that metabolic effect of FC on astrocytes result from impairment of carbon flux through the Krebs cycle, and not from impairment of oxidative APT production (Swanson and Graham, 1994).

Here we demonstrate that metabolic impairment of astrocyte activity with FC efficiently inhibit their intracellular calcium signaling. This suggests that voltage gated calcium channel or reticulum calcium channel depend on the metabolic activity and can be blocked by the inhibition of the tricarboxylic acid cycle (Vance et al., 2015; Wallace, 2014) . In addition, bath applied FC was sufficient to inhibit gliotransmission and communication between the astrocytes and the neuronal network without significantly altering any of the basal neuronal communication or functional connectivity. These are clear arguments pointing toward the pharmacological safety of FC toward neuronal networks, at least in our conditions, allowing further and broader use of such approach.

One of the most debated issues about FC is it specificity to glial cell and side effect. But some studies demonstrate that FC preferentially inhibits the krebs's cycle of astrocytes over neurons, possibly due to its more avid uptake by glial cell. And it has been shown within a certain range of concentration and exposure times, to produce selective damage to glial cells only (Fonnum et al., 1997; Hassel et al., 1992; Volobоueva et al., 2007). FC used in the correct range of concentration is a perfect tool do modulate astrocyte depending calcium activity. Several studies has now demonstrate that FC is efficient to alter calcium activity in astrocyte syncitum (Copeland et al., 2017; Guerra-Gomes et al., 2018; Padmashri et al., 2015; Vance et al., 2015; Wallace, 2014).
Furthermore, even if some alternative technics exist to inhibit astrocytes activity such as loading calcium chelator into astrocytic cytoplasm (Jourdain et al., 2007), it remains difficult to apply for in vivo, and especially freely moving animals, studies. On of the alternative to silencing astrocyte activity is the use of genetic model but they remain expensive and difficult to manage for most laboratory. Genetic tools also could be an issue for silencing astrocyte activity. Molecular engineering of lentiviral vectors has been widely used to express genes of interest specifically in neurons or astrocytes. However, that these strategies are not suitable for astrocyte-specific gene silencing due to the processing of small hairpin RNA (shRNA) in a cell (Merienne et al., 2015). Adeno-associated vectors have been used for astrocyte-specific gene overexpression. This has involved the use of specific serotypes and astrocytic promoters. However, they have not yet been used for cell-type-specific silencing and the small packaging size of adeno-associated vectors limits the integration of complex and large expression cassettes in the astrocytes (Aschauer et al., 2013; Drinkut et al., 2012). Even the DREAD system link to Gi and Gq pathway is not efficient to inhibit astrocyte. Even if the expression of Gq-DREADD and Gi-DREADD under GFAP promoter has been developed (Agulhon et al., 2013; Chen et al.) both pathway has been describe as trigger of calcium elevation in astrocytes and gliotransmission (Di Castro et al., 2011; Durkee et al., 2019; Panatier et al., 2011).
Cell-type specific silencing is critical to understand cell functions in normal and pathological condition, FC remain one of the best candidates to perform astrocytic inhibition. Furthermore, during the past decade glial cell attracted the attention. Glial cell and more especially astrocytes and microglia, have been shown to contribute directly to the modulation of neuronal network and behaviors associate such as pain, anxiety, addiction (Di Benedetto and Rupprecht, 2013; Hutchinson et al., 2008, 2009; Ledeboer et al., 2007; Mika, 2008; Shavit et al., 2005; Song and Zhao, 2001; Wahis et al., 2020). Rising the importance of the validation of the pharmacological tool such as FC, or fluoroacetate for silencing the astrocyte and minocycline for the microglia.

Authors contribution.

Conceptualization, AC; Methodology, AC, JW; Analysis, AB, BBJ, DK, JW; *Ex vivo* patch-clamp electrophysiology, AB, AC, DK, JW; *Ex vivo* calcium imaging, AB, DK, JW; Behavior, AC, BBJ, DK, JW; Spared nerve injuries, PI, MP; Writing, AB, AC, DK, ID, JW, PD; Funding acquisition AC; Supervision, AC; Project administration, AC.

Acknowledgement.

This work was supported by the IASP Early Career Research grant 2012, FP7 Career Integration grant 334455, Initiative of Excellence (IDEX) Attractiveness grant 2013, IDEX Interdisciplinary grant 2015, University of Strasbourg Institute for Advanced Study (USIAS) fellowship 2014-15, Foundation Fyssen research grant 2015, NARSAD Young Investigator Grant 24821, ANR JCJC grant (to AC). The authors thank Fulvio Magara for anxiety behavior advices; Sophie Reibel and the Chronobiotron UMS 3415 for all animal care.

References:

Agulhon, C., Boyt, K.M., Xie, A.X., Friocourt, F., Roth, B.L., and McCarthy, K.D. (2013). Modulation of the autonomic nervous system and behaviour by acute glial cell Gq protein-coupled receptor activation in vivo. J Physiol *591*, 5599–5609.

Araque, A., Carmignoto, G., Haydon, P.G., Oliet, S.H.R., Robitaille, R., and Volterra, A. (2014). Gliotransmitters travel in time and space. Neuron *81*, 728–739.

Aschauer, D.F., Kreuz, S., and Rumpel, S. (2013). Analysis of Transduction Efficiency, Tropism and Axonal Transport of AAV Serotypes 1, 2, 5, 6, 8 and 9 in the Mouse Brain. PLOS ONE *8*, e76310.

Balcar, V.J., Borg, J., and Mandel, P. (1977). High Affinity Uptake of L-Glutamate and L-Aspartate by Glial Cells. Journal of Neurochemistry *28*, 87–93.

Bazargani, N., and Attwell, D. (2016). Astrocyte calcium signaling: the third wave. Nat Neurosci *19*, 182–189.

Berg-Johnsen, J., Paulsen, R.E., Fonnum, F., and Langmoen, I.A. (1993). Changes in evoked potentials and amino acid content during fluorocitrate action studied in rat hippocampal cortex. Exp Brain Res *96*, 241–246.

Bosakowski, T., and Levin, A.A. (1986). Serum citrate as a peripheral indicator of fluoroacetate and fluorocitrate toxicity in rats and dogs. Toxicol Appl Pharmacol *85*, 428–436.

Chen, N., Sugihara, H., Kim, J., Fu, Z., Barak, B., Sur, M., Feng, G., and Han, W. Direct modulation of GFAP-expressing glia in the arcuate nucleus bi-directionally regulates feeding. ELife *5*.

Cheng, S.C., Kumar, S., and Casella, G.A. (1972). Effects of fluoroacetate and fluorocitrate on the metabolic compartmentation of tricarboxylic acid cycle in rat brain slices. Brain Res *42*, 117–128.

Clarke, D.D. (1991). Fluoroacetate and fluorocitrate: Mechanism of action. Neurochem Res *16*, 1055–1058.

Copeland, C.S., Wall, T.M., Sims, R.E., Neale, S.A., Nisenbaum, E., Parri, H.R., and Salt, T.E. (2017). Astrocytes modulate thalamic sensory processing via mGlu2 receptor activation. Neuropharmacology *121*, 100–110.

Corkrum, M., Rothwell, P.E., Thomas, M.J., Kofuji, P., and Araque, A. (2019). Opioid-Mediated Astrocyte-Neuron Signaling in the Nucleus Accumbens. Cells *8*.

Davila, D., Thibault, K., Fiacco, T.A., and Agulhon, C. (2013). Recent molecular approaches to understanding astrocyte function in vivo. Front Cell Neurosci *7*.

Decosterd, I., and Woolf, C.J. (2000). Spared nerve injury: an animal model of persistent peripheral neuropathic pain. Pain *87*, 149–158.

Di Benedetto, B., and Rupprecht, R. (2013). Targeting Glia Cells: Novel Perspectives for the Treatment of Neuropsychiatric Diseases. Curr Neuropharmacol *11*, 171–185.

Di Castro, M.A., Chuquet, J., Liaudet, N., Bhaukaurally, K., Santello, M., Bouvier, D., Tiret, P., and Volterra, A. (2011). Local Ca2+ detection and modulation of synaptic release by astrocytes. Nat Neurosci *14*, 1276–1284.

Di Scala-Guenot, D., Mouginot, D., and Strosser, M.T. (1994). Increase of intracellular calcium induced by oxytocin in hypothalamic cultured astrocytes. Glia *11*, 269–276.

Drinkut, A., Tereshchenko, Y., Schulz, J.B., Bähr, M., and Kügler, S. (2012). Efficient Gene Therapy for Parkinson's Disease Using Astrocytes as Hosts for Localized Neurotrophic Factor Delivery. Molecular Therapy *20*, 534–543.

Durkee, C.A., Covelo, A., Lines, J., Kofuji, P., Aguilar, J., and Araque, A. (2019). Gi/o PROTEIN-COUPLED RECEPTORS INHIBIT NEURONS BUT ACTIVATE ASTROCYTES AND STIMULATE GLIOTRANSMISSION. Glia *67*, 1076–1093.

Fonnum, F., Johnsen, A., and Hassel, B. (1997). Use of fluorocitrate and fluoroacetate in the study of brain metabolism. Glia *21*, 106–113.

Geuther, R. (1977). A. L. LEHNINGER, Biochemistry. The Molecular Basis of Cell Structure and Function (2nd Edition). 1104 S., zahlr. Abb., zahlr. Tab. New York 1975. Worth Publ. Inc. $ 17.50. Zeitschrift Für Allgemeine Mikrobiologie *17*, 86–87.

Goldberg, N.D., Passonneau, J.V., and Lowry, O.H. (1966). Effects of changes in brain metabolism on the levels of citric acid cycle intermediates. J Biol Chem *241*, 3997–4003.

Guerra-Gomes, S., Sousa, N., Pinto, L., and Oliveira, J.F. (2018). Functional Roles of Astrocyte Calcium Elevations: From Synapses to Behavior. Front. Cell. Neurosci. *11*.

Guttenplan, K.A., Weigel, M.K., Adler, D.I., Couthouis, J., Liddelow, S.A., Gitler, A.D., and Barres, B.A. (2020). Knockout of reactive astrocyte activating factors slows disease progression in an ALS mouse model. Nature Communications *11*, 3753.

Hamilton, N.B., and Attwell, D. (2010). Do astrocytes really exocytose neurotransmitters? Nat Rev Neurosci *11*, 227–238.

Han, J., Kesner, P., Metna-Laurent, M., Duan, T., Xu, L., Georges, F., Koehl, M., Abrous, D.N., Mendizabal-Zubiaga, J., Grandes, P., et al. (2012). Acute cannabinoids impair working memory through astroglial CB1 receptor modulation of hippocampal LTD. Cell *148*, 1039–1050.

Hasan, M.T., Althammer, F., Silva da Gouveia, M., Goyon, S., Eliava, M., Lefevre, A., Kerspern, D., Schimmer, J., Raftogianni, A., Wahis, J., et al. (2019). A Fear Memory Engram and Its Plasticity in the Hypothalamic Oxytocin System. Neuron *103*, 133-146.e8.

Hassel, B., Paulsen, R.E., Johnsen, A., and Fonnum, F. (1992). Selective inhibition of glial cell metabolism in vivo by fluorocitrate. Brain Res *576*, 120–124.

Hertz, L. (1990). Dibutyryl cyclic AMP treatment of astrocytes in primary cultures as a substitute for normal morphogenic and "functiogenic" transmitter signals. Adv Exp Med Biol *265*, 227–243.

Hutchinson, M.R., Coats, B.D., Lewis, S.S., Zhang, Y., Sprunger, D.B., Rezvani, N., Baker, E.M., Jekich, B.M., Wieseler, J.L., Somogyi, A.A., et al. (2008). Proinflammatory cytokines oppose opioid induced acute and chronic analgesia. Brain Behav Immun *22*, 1178–1189.

Hutchinson, M.R., Lewis, S.S., Coats, B.D., Skyba, D.A., Crysdale, N.Y., Berkelhammer, D.L., Brzeski, A., Northcutt, A., Vietz, C.M., Judd, C.M., et al. (2009). Reduction of opioid withdrawal and potentiation of acute opioid analgesia by systemic AV411 (ibudilast). Brain Behav Immun *23*, 240–250.

Ikegaya, Y., Le Bon-Jego, M., and Yuste, R. (2005). Large-scale imaging of cortical network activity with calcium indicators. Neuroscience Research *52*, 132–138.

Ji, R.-R., Berta, T., and Nedergaard, M. (2013). Glia and pain: Is chronic pain a gliopathy? PAIN® *154*, S10–S28.

Jourdain, P., Bergersen, L.H., Bhaukaurally, K., Bezzi, P., Santello, M., Domercq, M., Matute, C., Tonello, F., Gundersen, V., and Volterra, A. (2007). Glutamate exocytosis from astrocytes controls synaptic strength. Nat Neurosci *10*, 331–339.

Khakh, B.S., and Sofroniew, M.V. (2015). Diversity of astrocyte functions and phenotypes in neural circuits. Nat Neurosci *18*, 942–952.

King, T., Vera-Portocarrero, L., Gutierrez, T., Vanderah, T.W., Dussor, G., Lai, J., Fields, H.L., and Porreca, F. (2009). Unmasking the tonic-aversive state in neuropathic pain. Nature Neuroscience *12*, 1364–1366.

Knobloch, H.S., Charlet, A., Hoffmann, L.C., Eliava, M., Khrulev, S., Cetin, A.H., Osten, P., Schwarz, M.K., Seeburg, P.H., Stoop, R., et al. (2012a). Evoked Axonal Oxytocin Release in the Central Amygdala Attenuates Fear Response. Neuron *73*, 553–566.

Knobloch, H.S., Charlet, A., Hoffmann, L.C., Eliava, M., Khrulev, S., Cetin, A.H., Osten, P., Schwarz, M.K., Seeburg, P.H., Stoop, R., et al. (2012b). Evoked axonal oxytocin release in the central amygdala attenuates fear response. Neuron *73*, 553–566.

Kuo, J., Hariri, O.R., and Micevych, P. (2009). An interaction of oxytocin receptors with metabotropic glutamate receptors in hypothalamic astrocytes. J Neuroendocrinol *21*, 1001–1006.

Lauble, H., Kennedy, M.C., Emptage, M.H., Beinert, H., and Stout, C.D. (1996). The reaction of fluorocitrate with aconitase and the crystal structure of the enzyme-inhibitor complex. PNAS *93*, 13699–13703.

Ledeboer, A., Hutchinson, M.R., Watkins, L.R., and Johnson, K.W. (2007). Ibudilast (AV-411). A new class therapeutic candidate for neuropathic pain and opioid withdrawal syndromes. Expert Opin Investig Drugs *16*, 935–950.

Lee, S.-H., and Dan, Y. (2012). Neuromodulation of brain states. Neuron *76*, 209–222.

Lee, H.-J., Caldwell, H.K., Macbeth, A.H., Tolu, S.G., and Young, W.S. (2008). A conditional knockout mouse line of the oxytocin receptor. Endocrinology *149*, 3256–3263.

Luis-Delgado, O.E., Barrot, M., Rodeau, J.L., Schott, G., Benbouzid, M., Poisbeau, P., Freund-Mercier, M.J., and Lasbennes, F. (2006). Calibrated forceps: A sensitive and reliable tool for pain and analgesia studies. Journal of Pain *7*, 32–39.

Ma, Z., Stork, T., Bergles, D.E., and Freeman, M.R. (2016). Neuromodulators signal through astrocytes to alter neural circuit activity and behaviour. Nature *539*, 428–432.

Merienne, N., Delzor, A., Viret, A., Dufour, N., Rey, M., Hantraye, P., and Déglon, N. (2015). Gene transfer engineering for astrocyte-specific silencing in the CNS. Gene Therapy *22*, 830–839.

Mika, J. (2008). Modulation of microglia can attenuate neuropathic pain symptoms and enhance morphine effectiveness. Pharmacol Rep *60*, 297–307.

Monai, H., and Hirase, H. (2018). Astrocytes as a target of transcranial direct current stimulation (tDCS) to treat depression. Neurosci Res *126*, 15–21.

Neugebauer, V. (2015). 15. Amygdala pain mechanisms. Handb Exp Pharmacol *227*, 261–284.

Padmashri, R., Suresh, A., Boska, M., and Dunaevsky, A. (2015). Motor-Skill Learning Is Dependent on Astrocytic Activity. Neural Plasticity *2015*, 938023.

Panatier, A., Vallée, J., Haber, M., Murai, K.K., Lacaille, J.-C., and Robitaille, R. (2011). Astrocytes are endogenous regulators of basal transmission at central synapses. Cell *146*, 785–798.

Papouin, T., Dunphy, J.M., Tolman, M., Dineley, K.T., and Haydon, P.G. (2017). Septal Cholinergic Neuromodulation Tunes the Astrocyte-Dependent Gating of Hippocampal NMDA Receptors to Wakefulness. Neuron *94*, 840-854.e7.

Paulsen, R.E., and Fonnum, F. (1989). Role of Glial Cells for the Basal and Ca2+-Dependent K+-Evoked Release of Transmitter Amino Acids Investigated by Microdialysis. Journal of Neurochemistry *52*, 1823–1829.

Paulsen, R.E., Contestabile, A., Villani, L., and Fonnum, F. (1987). An in vivo model for studying function of brain tissue temporarily devoid of glial cell metabolism: the use of fluorocitrate. J Neurochem *48*, 1377–1385.

Paulsen, R.E., Contestabile, A., Villani, L., and Fonnum, F. (1988). The effect of fluorocitrate on transmitter amino acid release from rat striatal slices. Neurochem Res *13*, 637–641.

Peters, R.A. (1957). Mechanism of the toxicity of the active constituent of Dichapetalum cymosum and related compounds. Adv Enzymol Relat Subj Biochem *18*, 113–159.

Peters, R.A. (1963). Biochemical Lesions and Lethal Synthesis (Pergamon Press).

Pfrieger, F.W., and Slezak, M. (2012). Genetic approaches to study glial cells in the rodent brain. Glia *60*, 681–701.

Robin, L.M., Oliveira da Cruz, J.F., Langlais, V.C., Martin-Fernandez, M., Metna-Laurent, M., Busquets-Garcia, A., Bellocchio, L., Soria-Gomez, E., Papouin, T., Varilh, M., et al. (2018). Astroglial CB1 Receptors Determine Synaptic D-Serine Availability to Enable Recognition Memory. Neuron *98*, 935-944.e5.

Serrano, A., Haddjeri, N., Lacaille, J.-C., and Robitaille, R. (2006). GABAergic Network Activation of Glial Cells Underlies Hippocampal Heterosynaptic Depression. J. Neurosci. *26*, 5370–5382.

Shavit, Y., Wolf, G., Goshen, I., Livshits, D., and Yirmiya, R. (2005). Interleukin-1 antagonizes morphine analgesia and underlies morphine tolerance. Pain *115*, 50–59.

Song, P., and Zhao, Z.Q. (2001). The involvement of glial cells in the development of morphine tolerance. Neurosci Res *39*, 281–286.

Suzuki, R., Watanabe, J., Arata, S., Funahashi, H., Kikuyama, S., and Shioda, S. (2003). A transgenic mouse model for the detailed morphological study of astrocytes. Neurosci Res *47*, 451–454.

Swanson, R.A., and Graham, S.H. (1994). Fluorocitrate and fluoroacetate effects on astrocyte metabolism in vitro. Brain Research *664*, 94–100.

Szerb, J.C., and Issekutz, B. (1987). Increase in the stimulation-induced overflow of glutamate by fluoroacetate, a selective inhibitor of the glial tricarboxylic cycle. Brain Research *410*, 116–120.

Tecle, B., and Casida, J.E. (1989). Enzymatic defluorination and metabolism of fluoroacetate, fluoroacetamide, fluoroethanol, and (-)-erythro-fluorocitrate in rats and mice examined by 19F and 13C NMR. Chem Res Toxicol *2*, 429–435.

Vance, K.M., Rogers, R.C., and Hermann, G.E. (2015). PAR1-activated astrocytes in the nucleus of the solitary tract stimulate adjacent neurons via NMDA receptors. J Neurosci *35*, 776–785.

Villafranca, J.J., and Platus, E. (1973). Fluorocitrate inhibition of aconitase. Reversibility of the inactivation. Biochemical and Biophysical Research Communications *55*, 1197–1207.

Viviani, D., Charlet, A., van den Burg, E., Robinet, C., Hurni, N., Abatis, M., Magara, F., and Stoop, R. (2011). Oxytocin selectively gates fear responses through distinct outputs from the central amygdala. Science *333*, 104–107.

Voloboueva, L.A., Suh, S.W., Swanson, R.A., and Giffard, R.G. (2007). Inhibition of mitochondrial function in astrocytes: implications for neuroprotection. Journal of Neurochemistry *102*, 1383–1394.

Volterra, A., and Meldolesi, J. (2005). Astrocytes, from brain glue to communication elements: the revolution continues. Nat Rev Neurosci *6*, 626–640.

Wahis, J., Kerspern, D., Althammer, F., Baudon, A., Goyon, S., Hagiwara, D., Lefèvre, A., Boury-Jamot, B., Bellanger, B., Abatis, M., et al. (2020). Oxytocin Acts on Astrocytes in the Central Amygdala to Promote a Positive Emotional State. BioRxiv 2020.02.25.963884.

Walf, A.A., and Frye, C.A. (2007). The use of the elevated plus maze as an assay of anxiety-related behavior in rodents. Nature Protocols *2*, 322–328.

Wallace, D.R. (2014). Sodium Fluoroacetate. In Encyclopedia of Toxicology (Third Edition), P. Wexler, ed. (Oxford: Academic Press), pp. 331–333.

Figures Legends.

Figure 1: OTR activation evoked calcium transients in CeL astrocytes syncytium are inhibit by fluorocitrate. (A) images of CeL astrocytes identified through SR101 (red) and corresponding pseudo-color images of OGB1 fluorescence during baseline and after drugs application (stacks of 50images/25s of recording). (B) Example trace of astrocytes response after TGOT application (400nM). Left to right: TGOT (light blue), TGOT+TTX (100 µM; dark blue), TGOT + FC (100µM; red). (C) histogram displaying percentage of astrocyte response, relative increase of ΔF/F0 AUCs after drug application and frequency of response. TGOT (400 nM; ns = 4, na = 39; light blue), TGOT+TTX (100µM; ns = 22, na= 182; dark blue), TGOT+FC (100µM; ns= 5, na= 25). ** P < 0.01 Mann-Whitney U test.

Figure 2: Fluorocitrate impaired the transmission of OT signaling through CeA neurons.
(A) Effect of fluorocitrate on KCl (dark grey) increase of IPSCs frequencies (KCl 50mM; fluorocitrate 100µM, 1h; n=6). Patch-clamp data are expressed as averaged currents frequency plus SEM across cells before, during (and after) drug effect; linked white circles indicate individual cell values. * P < 0.05Wilcoxon signed rank test.
(B) (Left)Example trace of CeM neurons IPSCs; under ACSF, TOGT and fluorocitrate. (Right) Effect of TGOT on CeM neurons IPSCs frequency with or without fluorocitrate (TGOT 400 nM; n=7 ; fluorocitrate 100µM, 1h; n=6)

Figure 3: Fluorocitrate impaired gliotransmission.
(Left) Example trace of CeM neuron IPSCs under basal condition (ACSF), Fluorocitrate (TGOT 400nM; FC 100µM, 1h) and D-Serine (TGOT 400 nM; FC 100µM 1h, D-Serine 100µM; 20 min). (Right) Quantification of CeM neurons IPSCs under the previous condition. Patch-clamp data are expressed as averaged currents frequency plus SEM across cells before, during (and after) drug effect; circles indicate individual cell values. * P < 0.05, Wilcoxon signed rank test

Figure 4: Fluorocitrate inhibit oxytocin modulation of amygdala-related behaviors.
FC or vehicle were administered 1h before TGOT or vehicle, which were injected 20min before behavioral tests. (A) On day 30 post SNI surgery, mechanical pain threshold was assessed with a mechanical forceps, on the neuropathic paw and contra lateral paw before (Ctrl) and after drugs for sham and SNI animals. (B) On day 40 post-surgery, anxiety levels were assessed, with an elevated plus maze test through measurements of the time spent in the closed arms of the elevated plus maze after drugs injections for sham and SNI animals(C) Conditioned place preference (CPP) was assessed through measurements of the Δ time spent in the paired chamber before and after pairing. Pairing was realized through drugs injections for SNI and sham animals. Data are expressed as averages across rats plus SEM. Pain threshold measures: **P<0.01, ***P<0.001; mixed-design ANOVA followed by posthoc Bonferroni tests. Elevated plus maze: *P<0.05, **P<0.01, comparisons to respective controls; #P<0.05, Sham control vs SNI control groups post-hoc comparison; 3-ways ANOVA followed by posthoc Fisher tests.

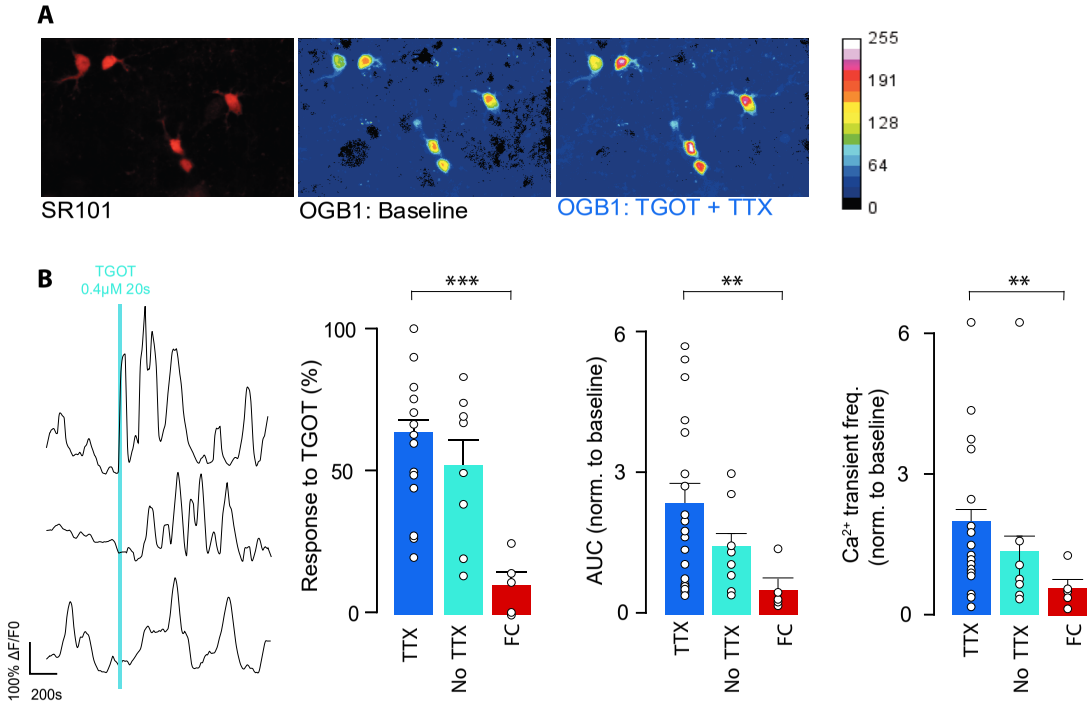
A
SR101
OGB1: Baseline
OGB1: TGOT + TTX
255
191
128
64
0
B
TGOT
0.4μM 20s
100% ΔF/F0
200s
***
**
**
Response to TGOT (%)
AUC (norm. to baseline)
Ca2+ transient freq. (norm. to baseline)
100
50
0
6
3
0
TTX
No TTX
FC

Figure 1

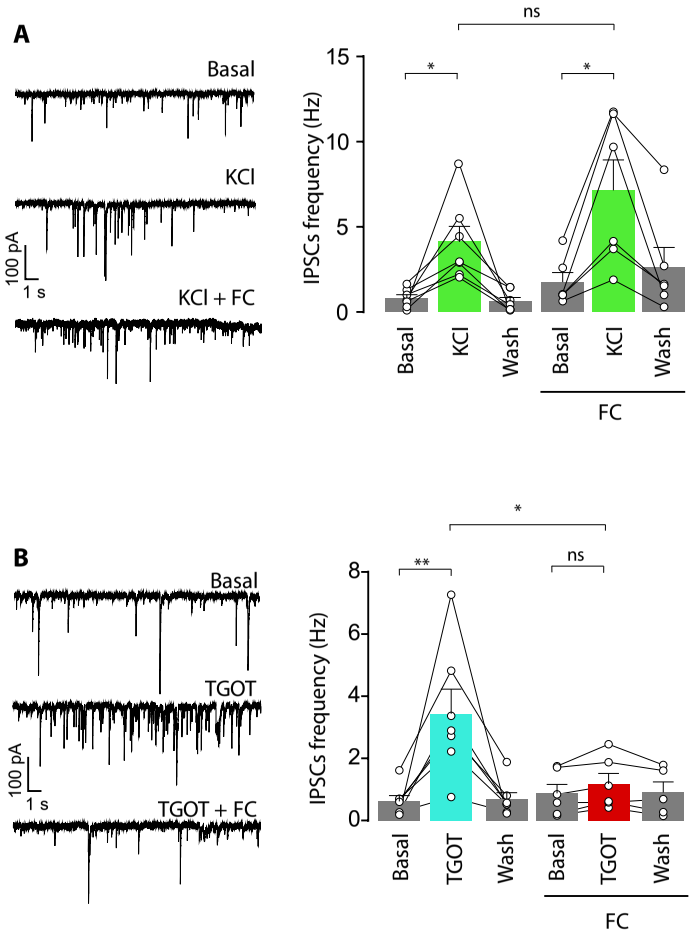
A
Basal
KCl
KCl + FC
100 pA
1 s
IPSCs frequency (Hz)
ns
*
*
Basal
KCl
Wash
Basal
KCl
Wash
FC
B
Basal
TGOT
TGOT + FC
100 pA
1 s
IPSCs frequency (Hz)
*
**
ns
Basal
TGOT
Wash
Basal
TGOT
Wash
FC

Figure 2

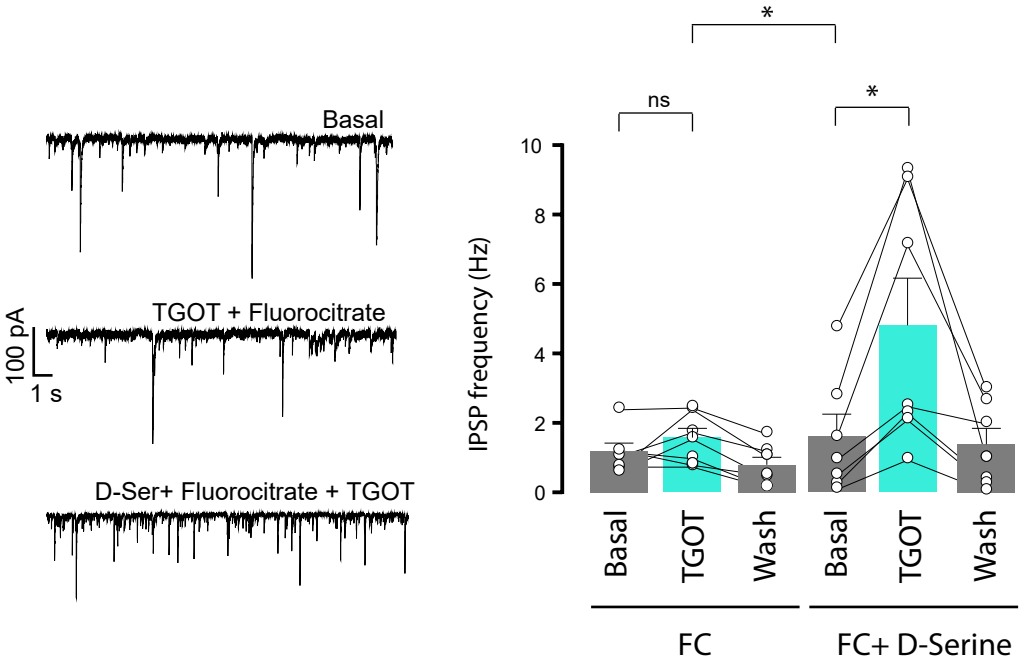
Basal
TGOT + Fluorocitrate
100 pA
1 s
D-Ser+ Fluorocitrate + TGOT
IPSP frequency (Hz)
ns
*
*
0
2
4
6
8
10
Basal
TGOT
Wash
Basal
TGOT
Wash
FC
FC+ D-Serine

Figure 3

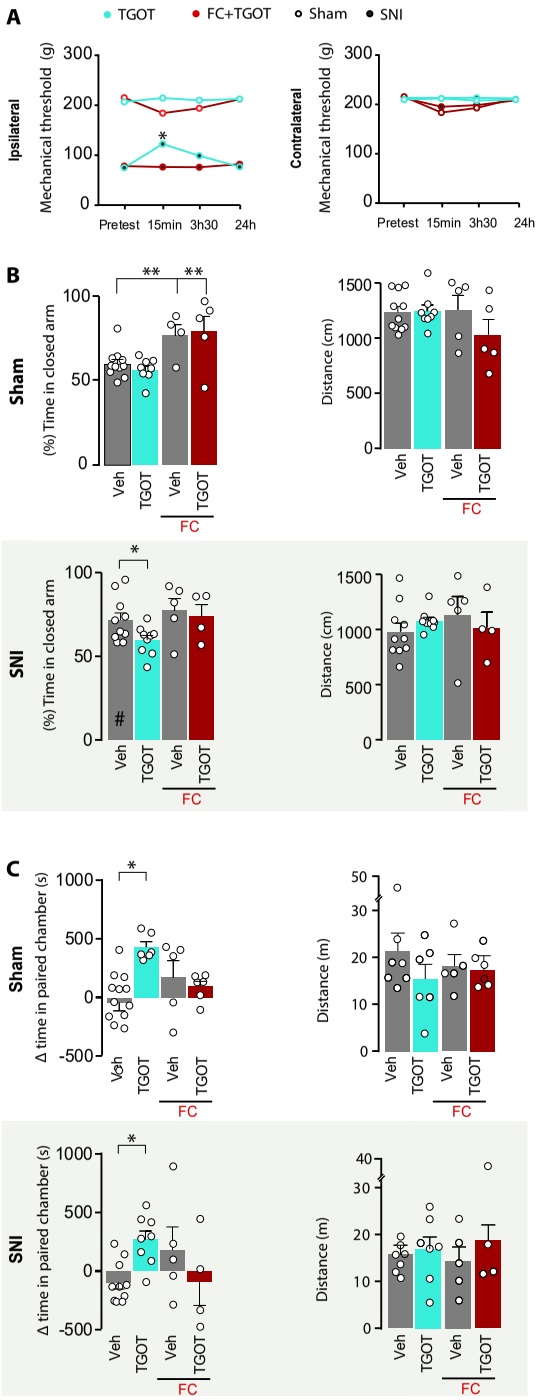
A
TGOT
FC+TGOT
Sham
SNI
Ipsilateral
Mechanical threshold (g)
Contralateral
Pretest 15min 3h30 24h
B
Sham
SNI
(%) Time in closed arm
Distance (cm)
Veh
TGOT
FC
C
Δ time in paired chamber (s)
Distance (m)

Figure 4

DISCUSSION

Durant cette thèse j'ai participé à l'étude de la modulation du circuit de l'amygdale centrale par l'ocytocine et étudié l'implication des astrocytes dans cette modulation. Si ces différents points ont déjà pour la plupart été discutés dans les articles précédents et ce de manière indépendante, il me tient à cœur de les discuter dans l'ensemble. J'aborderai différents arguments pointant les astrocytes comme étant des acteurs clés de la modulation des circuits neuronaux, plus particulièrement dans la modulation du signal ocytocinergique. Plus généralement, je soulignerai l'intérêt d'approfondir les études sur la compréhension de l'intégration des différents types cellulaires lors des études de neurosciences.

La fonction la plus connue du neuropeptide ocytocine est sans doute son rôle dans la régulation hormonale des fonctions de reproduction chez les mammifères, mais également pour son action périphérique lors de la parturition et de l'allaitement. L'ocytocine est également impliquée dans de nombreuses fonctions de régulation des émotions telles que la peur, l'anxiété et la douleur, au niveau strictement central notamment en modulant les circuits de l'amygdale centrale.

I- Une population de neurones ocytocinergique régule la peur en agissant au niveau du CeA : premier indice vers la présence d'un modulateur de réseau.

Lors du début de mon travail de thèse, j'ai eu l'opportunité de participer au projet ayant fait l'objet de la publication « Fear memory engram and its plasticity in the hypothalamic oxytocin system » (Hasan et al., 2019).

Dans un premier temps, elle a permis de confirmer l'implication du système ocytocinergique dans la régulation de la peur par la modulation de l'activité de l'amygdale centrale. Initialement, le système ocytocinergique était décrit comme agissant principalement par libération de l'OT au niveau dendritique dans l'hypothalamus, suivie par sa diffusion aux structures cibles. Il a par la suite été montré à l'aide d'une combinaison d'études anatomique, électrophysiologiques, optogénétiques et comportementales la présence de terminaisons axonales fonctionnelles par lesquelles l'OT synthétisée dans l'hypothalamus est libérée dans le CeA. Cette libération induit à la fois une modification de l'activité au niveau cellulaire mais également comportemental, telle que la diminution du temps de freezing observée chez les

animaux (Knobloch et al., 2012). Cependant, cette première étude ne faisait pas état de l'éventuelle sous-population de neurones ocytocinergiques impliqués, ou de l'éventuelle spécificité de leur activation.

De manière intéressante, l'article 1 a permis de mettre en évidence, grâce à l'utilisation du système vGATE, une sous population de neurones ocytocinergiques recrutée spécifiquement lors de l'exposition à un contexte de peur. Suite à l'exposition des animaux à un conditionnement de peur, seuls ~10% des neurones OT du PVN et du SON ont été activés (OT $Fear^{+}$), et la stimulation de cette faible population neuronale est suffisante pour induire une diminution du temps de freezing. De façon surprenante la stimulation de cette population restreinte induit un effet comportemental majeur, plus important que la stimulation de toute les fibres ocytocinergiques ($Ot_{constitutive}$) projetant au CeA. Bien que contre intuitive, cette efficacité exacerbée d'une petite population de neurones n'est pas invraisemblable : une étude précédente a d'ores et déjà démontrée que la stimulation optogénétique des neurones GABAergiques du CeL ou de l'intégralité de l'amygdale centrale entraînait un effet sur le freezing moins important que lors de la stimulation d'une zone plus ciblée (Ciocchi et al., 2010). Ces données laisseraient à penser que les fibres OT projetant au CeA possèdent une action spécialisée permettant une régulation fine de cette structure. La stimulation de fibre $OT_{constitutive}$ pourrait vraisemblablement activer l'intégralité du CeA alors que la stimulation de fibre spécialisée (OT $Fear^{+}$) activerait probablement une population neuronale particulière ou une zone du CeA plus ciblée permettant la régulation du comportement de peur. Il serait possible que différentes populations de neurones OT régulent différentiellement le CeA afin de moduler différents comportements associés à cette structure et au système ocytocinergique.

De plus, il est étonnant que seulement 10% des neurones ocytocinergiques régulent le comportement de peur. Il a cependant précédemment été montré dans la littérature pour ce même système ocytocinergique, qu'uniquement ~30 neurones OT suffisent pour contrôler la douleur. Ces ~30 neurones parvOT sont capables d'induire une analgésie chez le rat via un mécanisme double : dans un premier temps, par leur action directe sur les centres régulateurs de la douleur de la moelle épinière, mais également par la stimulation de la libération d'OT par les neurones magnOT hypothalamiques (Eliava et al., 2016). Il semblerait qu'une petite population de neurones OT soit suffisante pour moduler significativement une réaction

physiologique. Cela laisserait sous-tendre la présence d'ensembles de cellules spécialisés, amenant l'idée de l'existence d'engrammes hypothalamiques, du moins pour le système ocytocinergique. Un engramme peut être définit par un ensemble de cellules qui se retrouve être simultanément activé durant une expérience (neurons that fire together, wire together) (Hebb, 2002; Shaw, 1986). Si l'on considère que les informations mnésiques et sensorielles sont codées de façon matricielles dans le cerveau, alors une des hypothèses expliquant l'effet de la petite population de neurones OT $Fear^{+}$ est que ces cellules constituent un engramme de la peur au niveau de l'hypothalamus de même qu'une autre population de neurones OT, quant à elle régule la douleur. Il est donc vraisemblable de penser que d'autres sous-populations de neurones OT pourraient également réguler d'autre comportements associés au système OT.

Un autre point à soulever est que l'inhibition des neurones OT Fear+ est capable d'interférer finement avec le souvenir de la peur. A la différence de l'inhibition globale des neurones $Ot_{constitutive}$ qui interfère avec l'extinction de la peur indépendamment du contexte, l'inhibition des neurones OT_{Fear+} interfère avec l'extinction de la peur uniquement dans un contexte familier mais n'a pas dans un nouveau contexte. De façon intéressante depuis quelques années, des études proposent que l'amygdale basolatérale (BLA) et le CeA seraient impliqués dans l'acquisition et la récupération de souvenir associés à la peur (Ciocchi et al., 2010, 2011; Davis and Reijmers, 2018). Les informations sensorielles en provenance du thalamus sont traitées au niveau du BLA, puis relayées au niveau du CeA. Ce dernier noyau projetant a d'autres structures impliquées dans la réponse comportementale associé comme le freezing. Il a été montré que le CeA présentait deux populations de neurones distinctes impliquées dans l'acquisition et l'expression de la peur formant un circuit inhibiteur très organisé permettant l'inhibition du CeM et contrôlant les comportement associés (Figure 31). Lors de la présentation d'un son conditionné, une première population neuronale est activée, il s'agit de neurones CeL_{ON} alors que la deuxième population est inhibée (CeL_{OFF}). Il a été suggéré que les neurones CeL_{ON} pourraient inhiber les neurones CeL_{OFF} lors du conditionnement. De plus, les neurones CeL_{OFF} sont directement connectés avec les neurones du CeM, les inhibant de manière tonique en condition basale. Durant le conditionnement l'inhibition des neurones CeL_{OFF} permet de lever cette inhibition tonique des neurones du CeM, conduisant à l'augmentation des comportements associés à la peur (Ciocchi et al., 2011). De manière intéressante, il a été montré que les neurones CeL_{OFF} expriment la protéine PKCδ et pas la

somatostatine (Haubensak et al., 2010). D'autres études ont également montré qu'au sein du CeL, les neurones exprimant le récepteur à l'ocytocine expriment également la PKCδ mais pas la somatostatine et inversement pour ceux n'exprimant pas l'OTR (Haubensak et al., 2010; Li et al., 2013). Cela laisserait penser que la libération d'OT dans le CeA permettrait l'activation des neurones CeL_{OFF} permettant alors l'inhibition des neurones du CeM et ainsi de réduire les comportements associés à la peur.

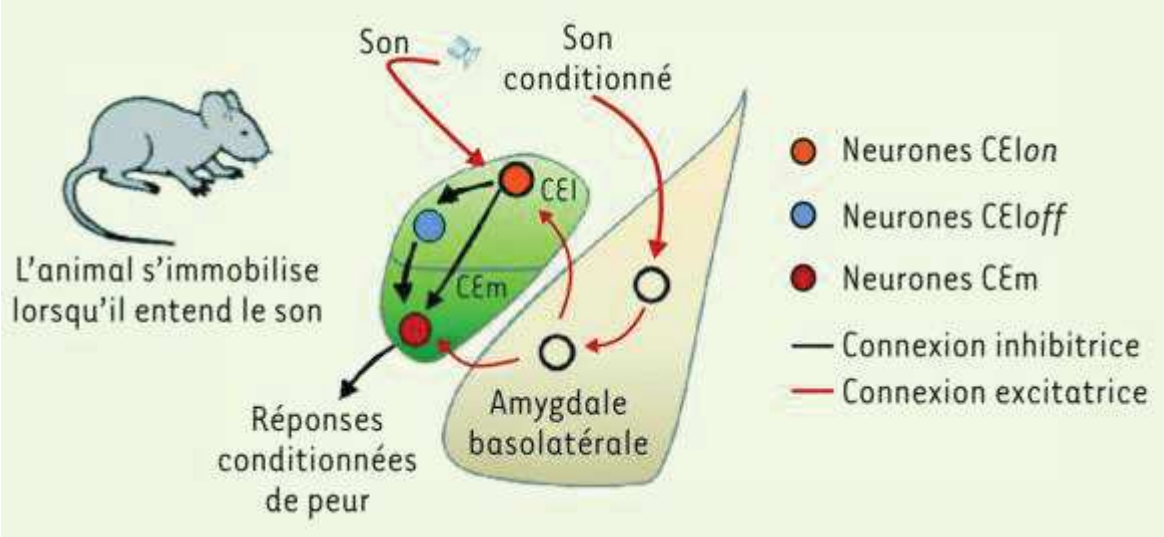

Figure 31 : Modèle des circuits de l'amygdale impliqué dans le conditionnement à la peur. A la suite d'un conditionnement à la peur, **l**a présentation du son conditionné induit l'activation des neurones inhibiteurs CeL_{on}. Ces neurones sont principalement connectés avec les neurones CeL_{off} ce qui a pour conséquence une inhibition de leur activité neuronale lors de la présentation du son. Les neurones CeL_{off} exercent en condition basale une influence inhibitrice tonique sur les neurones CeM du noyau central médian. Lors de la présentation du son, l'inhibition des neurones CeL_{off} induit une levée d'inhibition des neurones CeM ce qui a pour conséquence l'expression des réponses conditionnées de peur. Issus du (Ciocchi et al., 2011)

Il est donc possible de supposer que l'effet de la petite population de neurones OT_{Fear+} constituant l'engramme de la peur hypothalamique agit spécifiquement sur certaines des cellules spécialisées du CeL de manière à réguler finement l'acquisition, l'extinction et l'expression de la peur. La présence de ce type de traitement fin de la peur au niveau de

l'amygdale supposerait également la présence d'un engramme de la peur au sein de l'amygdale. Cette théorie a également été proposée par d'autre études du moins pour le noyau basolatéral de l'amygdale fortement impliqué dans la régulation du noyau du CeA (Bocchio et al., 2017; Davis and Reijmers, 2018; Zaki et al., 2019).

De plus, la régulation de l'amygdale par le système ocytocinergique pourrait également être médiée par un relais cellulaire entre la libération ocytocinergique et l'activation du réseau neuronal du CeA. Au vu de cette faible population de neurones OT régulant la peur ainsi que la quantité limitée de neurones projetant à l'amygdale (Hasan et al., 2019; Knobloch et al., 2012), il serait vraisemblable que les astrocytes soient impliqués dans cette régulation. Le système ocytocinergique a été décrit comme un système n'effectuant pas de synapse classique (élément pré- sur élément post- synaptique), mais effectuant des « synapses en passant ». En effet peu de synapses ocytocinergiques ont été retrouvées au niveau du CeA, de plus les vésicules contenant l'OT sont très peu localisées au niveau de la terminaison synaptique mais sont réparties tout le long de l'axone (Knobloch and Grinevich, 2014; Knobloch et al., 2012; Ross et al., 2009). La libération d'OT dans l'amygdale centrale s'effectue par ce que l'on nomme transmission microvolumique (Chini et al., 2017; Knobloch et al., 2012), permettant d'émettre l'hypothèse que les astrocytes agiraient en temps qu'amplificateur du signal ocytocinergique, et seraient des acteurs principaux pour la régulation à la fois spatiale et temporelle du réseau du CeA, par similitude avec ce qui a été proposé pour d'autres neuromodulateurs (Hirase et al., 2014). Un astrocyte seul peut former des contacts avec plus de 140 000 synapses neuronales (Halassa et al., 2007) faisant d'eux de très bon candidats pour réguler le réseau complexe du CeA lors du paradigme de peur. De plus, de quelques études proposent les astrocytes comme acteurs clé dans la régulation des engrammes mnésiques (Gebicke-Haerter, 2014; Kol et al., 2020; Li et al., 2020).

Une deuxième observation appuyant cette hypothèse d'implication astrocytaire est le temps de latence observé entre la stimulation des fibres ocytocinergiques et l'effet comportementale. Lors de la première stimulation, l'onset de réponse est quasiment de l'ordre de la minute alors que lors de l'activation des fibres OT Fear^{+} le délai de réponse comportementale est de l'ordre de la seconde. Cet effet pourrait dans un premier temps être dû à la transmission microvolumique. L'OT pourrait être libérée par les axones dans le milieu extracellulaire et atteindra sa cible neuronale après une diffusion passive. Mais ces délais de

réponse sont également consistants avec une activation astrocytaire. En effet, la transmission synaptique est de l'ordre de la milliseconde alors que l'excitabilité calcique astrocytaire est de l'ordre de la seconde, cohérant avec les délais observés lors de la réponse comportementale lors de la libération d'OT. De plus nous avons pu démontrer que l'effet modulatoire de l'OT sur le réseau du CeA est soutenu par l'action des astrocytes pour d'autre paradigmes comportementaux laissant sous-entendre que la régulation ocytocinergique de la peur pourrait également être modulée par ceux-ci.

Un troisième résultat surprenant de cette étude est le switch fonctionnel des projections des neurones ocytocinergiques sur le CeL. En effet, à la suite d'un conditionnement à la peur, il semblerait que la physiologie des neurones ocytocinergiques projetant à l'amygdale soit altérée. Les neurones libérant classiquement de l'ocytocine se mettent à libérer majoritairement du glutamate et non de l'ocytocine. En premier lieu, nous avons montré que la stimulation optogénétique ex vivo des fibres OT entraîne une augmentation de la fréquence des IPSCs dans l'ensemble des animaux, ayant subi un conditionnement à la peur ou non. Cette augmentation de fréquence induite par la stimulation de fibres ou par l'application d'un agoniste spécifique des OTR est inhibée par la présence d'un antagoniste des OTR uniquement chez les animaux naïfs mais non pas chez les animaux vGATE. De plus, chez ces animaux conditionnés, l'augmentation de fréquence des IPSCs est quant à elle inhibée par l'administration d'un antagoniste des récepteurs glutamatergiques alors que l'action de cet antagoniste est minime chez les animaux naïfs. De plus, ces résultats sont confirmés par des marquages neuroanatomiques. En effet, l'observation des neurones OT ainsi que de leurs fibres a permis de mettre en évidence que le conditionnement de peur n'entraînait pas de modification de la longueur totale des axones OT au niveau du CeL, mais semblait entraîner une surexpression de vGlut2 dans les axones OT après le conditionnement de peur. Cependant ces données restent corrélatives, nous n'avons pas déterminé si la proportion de libération OT/glutamate a été modifiée par le conditionnement à la peur. Les différences observées peuvent être dues à une modification post-synaptique i.e. une modification des récepteur OTR et glutamatergiques exprimés par les neurones du CeL.

Mais en se basant sur la littérature, la co-libération d'OT et de glutamate par les neurones ocytocinergiques semble très probable (Vaaga et al., 2014). Il a déjà été montré par des marquages immunohistochimiques et des études fonctionnelles que les neurones OT du PVN

contiennent de l'OT mais également du glutamate (Eliava et al., 2016; Knobloch et al., 2012; Meeker et al., 1991). Il est donc intéressant d'essayer de comprendre le bénéfice de ce switch potentiel de libération de neurotransmetteur dans ce comportement. Une des hypothèses pourrait être liée aux types de récepteurs et leur cinétique. En effet, le glutamate peut se lier sur des récepteurs de type ionotropique (récepteur NMDA, AMPA et kaïnate) induisant une ouverture directe de canaux ioniques. L'entrée massive de cations permet la transduction du signal avec un délai très faible, de l'ordre de la milliseconde. Cependant, il a également été montré l'existence de récepteurs glutamatergiques métabotropiques présents sur les neurones qui peuvent également être activés par la libération de glutamate mais avec une temporalité d'effet plus faible que les canaux ionotropiques (Niswender and Conn, 2010). De plus il a également été montré que les astrocytes peuvent également exprimer des récepteurs ionotropiques et métabotropiques au glutamate (Hadzic et al., 2017; Letellier et al., 2016; Skowrońska et al., 2019). Mais à ce jour peu d'études démontrent que l'activation des NMDAR astrocytaires induit une gliotransmission.

L'ocytocine quant à elle se lie uniquement à un RCPG (métabotropique). Ce type de récepteur ne possède pas de canal intégré. La fixation de l'OT sur celui-ci induit un changement de conformation tri-dimensionnelle induisant par la suite une cascade de réactions impliquant des messagers secondaires. Ce type de transmission est relativement lent et peut atteindre l'ordre de la seconde (Byrne et al., 2014). C'est pour cela qu'après un conditionnement de peur, la co-libération de l'OT et du glutamate semble nécessaire : le glutamate induira une réponse rapide afin de fuir face à la situation de peur tandis que l'OT induira une réponse capable de perdurer dans le temps évitant de se retrouver de nouveau dans une situation effrayante.

Une hypothèse liée à ce switch fonctionnel serait l'implication des astrocytes dans cette transmission. En se basant sur les résultats obtenus dans les articles 2 et 3, il semblerait que ces cellules jouent un rôle clef dans la transmission ocytocinergique au sein du CeA. Bien que les neurones du CeL expriment le récepteur ocytocinergique, les astrocytes semblent être les acteurs principaux dans la transmission de ce signal. Il a été montré que les astrocytes sont nécessaires à la modulation de la fréquence des IPSCs des neurones du CeM lors de la stimulation des fibres des neurones ocytocinergiques ou lors de l'application de TGOT. Le délai de réponse discuté précédemment entre les deux expositions au contexte peut être expliqué

par le changement de recrutement du type cellulaire. Lors de la libération d'OT, les cellules principales activées pourraient être les astrocytes dont la cinétique de réponse est lente. Lorsque le switch glutamatergique s'opère le glutamate activerait préférentiellement les neurones du CeL présentant des cinétiques plus courtes se traduisant par une diminution du temps de latence de la réponse comportementale de freezing.

Le changement comportemental pourrait alors être soutenu par la même structure mais par deux réseaux indépendants, expliquant les différences de cinétique de réponse.

Implication des astrocytes dans la modulation ocytocinergique de l'amygdale centrale.

La seconde grande partie de mon travail a porté sur la démonstration du rôle des astrocytes dans la modulation ocytocinergique du circuit de l'amygdale centrale et de ses comportements associés.

La régulation ocytocinergique des circuits neuronaux est extrêmement étudiée depuis ces dernières années tout comme le rôle primordial des astrocytes dans la modulation de la neurotransmission (Figure 32) néanmoins à ce jour aucune étude n'avait encore démontrée l'implication des astrocytes dans la modulation ocytocinergiques du réseau de l'amygdale centrale.

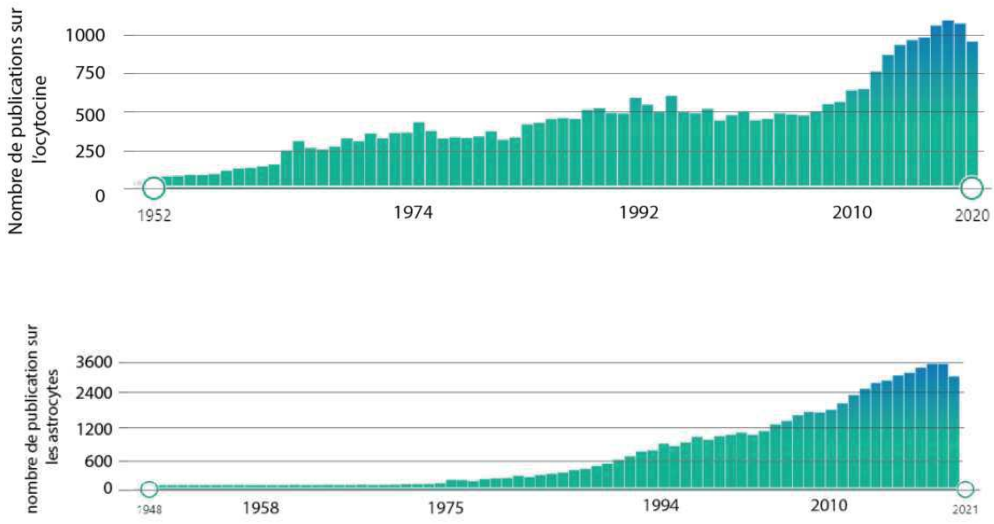

Figure 32 : Evolution du nombre de publication sur l'ocytocine et sur les astrocytes au cours des dernières années.

Dans cette étude, nous avons mis en évidence que ~18% des astrocytes du CeL expriment le récepteur à l'OT, et sont capables de répondre à la libération d'OT endogène et à l'activation directe des OTR de manière indépendante du réseau neuronal en présentant une élévation calcique oscillante et transitoire. Il est intéressant de noter que cette réponse calcique est observée dans ~60% des astrocytes du CeL alors qu'uniquement 18% expriment le récepteur. Ces données mettent en évidence la présence d'un réseau astrocytaire fonctionnel qui pourrait permettre d'amplifier le signal ocytocinergique. En effet il a été montré que le nombre de fibres OT provenant du PVN est très faible au niveau du CeA. De plus, les axones des neurones OT ne semblent pas former de synapse en tant que tel mais des « synapses en passant » (Knobloch et al., 2012) diffusant alors l'OT dans l'espace interstitiel local par un phénomène de transmission microvolumique (Grinevich et al., 2016; Knobloch and Grinevich, 2014). Bien que les OTR soient présents sur ~70% des neurones du CeL, il semblerait que les astrocytes soient primordiaux pour relayer le signal ocytocinergique au sein du CeA. Nous avons pu mettre en évidence que la libération endogène d'OT (par stimulation optogénétique des fibres des neurones OT provenant du PVN) ainsi que l'application d'un agoniste spécifique (TGOT) étaient capables de recruter le réseau astrocytaire du CeL, conduisant à la libération de D-sérine par les astrocytes. Cette activation astrocytaire a pu être mimée artificiellement en activant optogénétiquement les astrocytes du CeL, et est suffisante pour mimer l'action de l'OT, tant sur l'activation des neurones du CeL (augmentation de la fréquence des mEPSCs et des potentiels d'action), que sur l'activation des neurones du CeM (augmentation de la fréquence des IPSCs). Finalement, elle est également suffisante pour mimer les effets comportementaux de l'OT sur les comportements d'anxiété et de valence émotionnelle de la douleur. En plus de la mise en évidence du rôle critique des astrocytes pour l'activation d'un circuit neuronal, nous avons pu démontrer que l'action modulatrice de l'OT dans le CeA nécessitait la participation de ceux-ci. En effet, l'action de l'OT (ex vivo et in vivo) est abolie lors de l'inactivation pharmacologique des astrocytes.

Un point intéressant à soulever est qu'il semble contre intuitif que malgré l'expression à ~60% des OTR au niveau des neurones du CeL, ceux-ci ne soient pas affectés par l'OT. Nous pouvons émettre l'hypothèse que l'activation des OTR astrocytaires est nécessaire pour moduler l'activité des neurones du CeL (via l'activation des NMDA) pour leur permettre à leur tour de

répondre à l'ocytocine/glutamate et probablement à d'autres entrées synaptiques. Il se peut que les OTR neuronaux quant à eux soient liés à une sous-unité Gq. L'activation de OTR neuronaux conduit à l'activation de la PLC et à l'accumulation d'IP3 pouvant inhiber les canaux K_{ir} (Gravati et al., 2010; Hu et al., 2020). L'action de l'OT permettrait ainsi d'augmenter l'excitabilité neuronal en agissant sur les OTR neuronaux et les astrocytes en tant que chef d'orchestre pour réguler spatialement et temporellement l'activité du CeA.

Cependant au sein d'autre structures, différents mécanismes d'actions ont été montrés bien que tous aient pour action d'augmenter l'excitabilité cellulaire des neurones exprimant les OTR. Dans l'hippocampe, l'activation des OTR neuronaux inhibe les canaux potassiques voltage dépendant (Kv7) (Tirko et al., 2018) ou augmente l'activité des canaux calciques de type L (Maniezzi et al., 2019). Dans l'aire tegmentale ventrale, les OTR augmentent l'excitabilité cellulaire en activant un échangeur cationique non sélectif ainsi qu'un échangeur Na^{+}-Ca^{2+} (Tang et al., 2014). Ils ont également été montré que les OTR peuvent activer les canaux TRPC-like au sein des neurones dopaminergiques tubéroinfundibulaires (Briffaud et al., 2015)

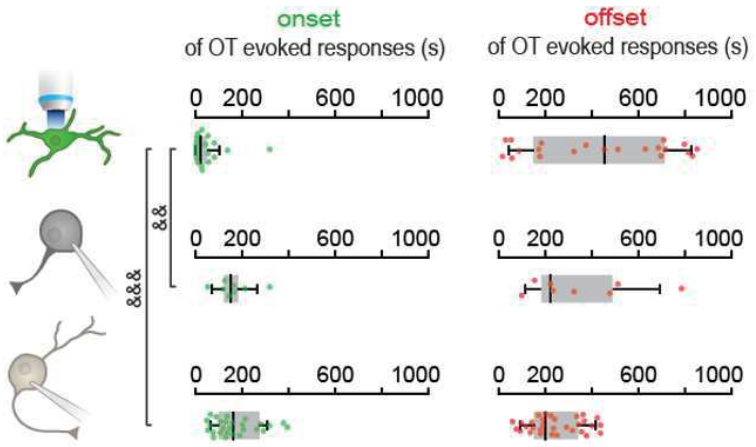

Figure 33 : Représentation des onset et des offset de réponse des astrocytes et des neurones du CeA. De haut en bas, onset et offset de la réponse calcique observée dans les astrocytes du CeL. Onset et offset des potentiels d'actions observés dans les neurones du CeL. Onset et offset de réponse des IPSCs des neurones du CeM.

Le fait que les astrocytes réguleraient l'activité du réseau du CeA d'un point de vue temporel et spatial est renforcé par diverses observations. Dans un premier temps si l'on s'intéresse à l'onset et à l'offset de réponse entre les astrocytes du CeL (oscillation calcique), les neurones du CeL (potentiel d'action) et les neurones du CeM (IPSCs) (Figure 33), on peut remarquer que la réponse neuronale est englobée durant le temps d'activité des astrocytes. De plus, l'application de DAAO dégradant la D-serine libérée par les astrocytes inhibe bien la réponse des neurones du CeM au TGOT. Cependant la supplémentation du bain par la D-Serine n'induit pas d'augmentation *per se* de la fréquence des IPSCs, elle ne restaure que la capacité des neurones à répondre à l'application du TGOT. Ces données mettent en évidence que les astrocytes agissent comme une structure relais, amplifiant l'effet de l'OT envers les neurones comme il l'a été proposé pour d'autres neuromodulateurs (Hirase et al., 2014).

Les régulations comportementales soutenues par l'ocytocine sont nombreuses (Lee et al., 2009) et recoupent pour partie les fonctions de l'amygdale centrale, concernant entre autres la modulation de la peur, de l'anxiété, et de la douleur et de sa valence émotionnelle. Au cours des années, la dynamique et la connectivité différentes des réseaux astro-neuronaux ont fourni de nouvelles informations sur la régulation des fonctions cérébrales et finalement sur le comportement des animaux (Oliveira et al., 2015). Cela a été le cas pour notre étude. Nous avons pu démontrer que le réseau astrocyte-neurone est primordial pour soutenir la modulation ocytocinergique dans la régulation de l'anxiété dans deux modèles de rongeur, rat et souris. Un résultat intéressant à relever est que l'OT ne présente un effet anxiolytique que sur les animaux présentant un phénotype anxieux. Cet état d'anxiété est généré par la présence d'une neuropathie (Yalcin and Barrot, 2014). Bien que l'activité neuronale du CeA ne soit pas modifiée, il est tout à fait probable que la neuropathie soit capable d'induire une modification de la physiologie astrocytaire. En effet, des études récentes suggèrent une forte implication des astrocytes dans l'étiologie de la douleur chronique. Il a été montré par, exemple, que les douleurs chroniques suite à une lésion nerveuse périphérique ou une inflammation sont capables d'activer les astrocytes libérant alors de nombreuse molécule dont l'ATP conduisant à une hyperréactivité neuronale de la moelle épinière. Des corrélations ont également été faites entre l'activité astrocytaire en IRMf ainsi qu'en quantifiant l'expression de la GFAP. Suite à une douleur chronique, il a été montré une augmentation de l'activité

astrocytaire ainsi qu'une surexpression de GFAP dans les structures impliquées dans la régulation de la douleur. (Eto et al., 2018; Hansen and Malcangio, 2013; Ji et al., 2013; Notturno et al., 2009; Robinson et al., 2014). De plus, les astrocytes sembleraient sous tendre une activité basale sur la régulation du réseau de l'amygdale centrale. Effectivement les animaux dont l'activité astrocytaire a été inhibée par le fluorocitrate passent plus de temps dans les bras fermé du labyrinthe en croix surélevé. Cet effet n'est a priori pas dû à une toxicité du composé car aucune différence de distance parcourue par les animaux n'est observée au travers des différents groupes. De plus, cet effet semble être supporté par l'ocytocine. En effet, un phénotype anxieux similaire est retrouvé chez les animaux dont les OTR astrocytaires ont été supprimés bien que les astrocytes en tant que tels restent fonctionnels. Cela mettrait en évidence une libération tonique d'OT agissant comme un frein permanent sur le réseau de l'amygdale centrale, permettant d'abaisser l'état d'anxiété au quotidien.

Un des derniers points mis en évidence est la modulation de la valence émotionnelle de la douleur soutenue par l'amygdale centrale. L'activation astrocytaire ou l'administration de TGOT est capable d'induire une valence positive pour le compartiment associé lors du test de conditionnement de préférence de place. L'effet obtenu à la fois chez des animaux neuropathiques mais également naïfs met en retrait la notion de valence émotionnelle de la douleur au profit d'une valence émotionnelle positive plus générale. Il a été proposé dans la littérature que les astrocytes seraient identifiés comme étant capables de soutenir les modifications issues d'un stress émotionnel, les mettant en avant comme acteurs cérébraux principaux dans la régulation des phénomènes complexes (Bender et al., 2016; Oliveira et al., 2015). De plus, un lien a été montré entre les systèmes dopaminergiques régulant l'intégration des émotions et l'amygdale (Correia and Goosens, 2016; Fudge and Emiliano, 2003; Kim et al., 2018; Murray et al., 2015). De plus, des évidences suggèrent une interaction entre les systèmes ocytocinergiques et dopaminergiques (Baskerville and Douglas, 2010; Love, 2014; de la Mora et al., 2016; Peris et al., 2017). L'implication des astrocytes dans ces cross-talk reste cependant à démontrer, bien que des études commencent déjà à émerger sur le sujet (Corkrum et al., 2020).

A ce jour, un nombre important d'études démontre que les astrocytes sont les cibles clés si ce n'est principales des neuromodulateurs (Corkrum et al., 2020; Kastanenka et al., 2020; Papouin et al., 2017; Robin et al., 2018; Z et al., 2016) et qu'ils pourraient soutenir les modulations

neuronales fines (Kastanenka et al., 2020; Kjaerby et al., 2017; Poskanzer and Yuste, 2016), fonction classiquement attribuée à l'action directe des neuromodulateurs sur les neurones (Lee and Dan, 2012; McCormick et al., 2020). Ainsi il est de tout intérêt d'accentuer les nouvelles recherches sur la capacité des astrocytes à réguler l'activité des circuits neuronaux. Chez l'humain, il serait ainsi intéressant de développer des stratégies affinées ciblant les astrocytes pour de futures approches thérapeutiques. En effet, les neuromodulateurs sont la cible de nombreux traitements déjà disponibles de maladies psychologiques tels que l'utilisation de molécules de petite taille, protocole de stimulation électrique ou encore de stimulation transcrânienne (Monai and Hirase, 2018). Dans l'ensemble, il y a une nécessité de prendre en considération de manière plus globale et systématique le rôle des astrocytes dans les circuits cérébraux, notamment en ce qui concerne l'effet des neuromodulateurs, et en particulier de l'OT. Cela serait hautement pertinent pour le développement de meilleures thérapies dans le domaine de la douleur chronique qui impose un fardeau énorme à la société en touchant environ 20% de la population mondiale (Mills et al., 2019) et dont le traitement actuel est essentiellement basé sur des opioïdes. En plus, en considérant l'anxiété générale (Woo, 2010) et la dépression, comorbidités fréquentes de la douleur chronique, cette découverte selon laquelle l'activation de la signalisation OT dans les astrocytes du CeL favorise une forme de confort émotionnel en atténuant les comportements anxieux est prometteuse.

De manière à encourager la recherche sur ce domaine, il est important de développer de nouveaux outils permettant de disséquer l'implication des astrocytes dans les différents réseaux, tels que des modèles génétiques de plus en plus fiables, de nouveaux vecteurs viraux permettant l'expression conditionnelle de protéines sous certaines conditions tel que le vGATE mais il est tout aussi important de ne pas mettre de côté des techniques moins coûteuses et plus accessibles pour l'ensemble des laboratoires tels que les agents pharmacologiques. Ainsi, le fluorocitrate, bien que son effet soit débattu à cause de sa toxicité avérée dans certaines conditions, n'en demeure pas moins un très bon composé s'il est utilisé avec parcimonie, un point que nous avons voulu aborder dans l'article 3.

CONCLUSION

L'ensemble de ces données obtenues au cours de ce travail de thèse nous a donné l'opportunité de mettre en évidence dans un premier temps qu'une population spécialisée de neurones ocytocinergiques est suffisante pour moduler le comportement de peur. Cette modulation ocytocinergique fait intervenir le noyau central de l'amygdale. Cette structure est capable de moduler un grand nombre de comportements fortement associés à ceux régulés par l'ocytocine. Nous avons eu l'opportunité de montrer que cette modulation ocytocinergique est vraisemblablement sous-tendue par la capacité des astrocytes locaux à moduler finement le réseau de l'amygdale centrale et ses comportements associés. Cependant la compréhension globale de ce réseau et les applications cliniques semblent encore lointaines. Actuellement très débattues, les applications thérapeutiques de l'OT sur l'Homme sont encore très controversées, notamment dû à l'incapacité du composé à traverser la barrière hématoencéphalique. Cependant au vu de la nécessité de lutter contre la crise des opiacés, de la recrudescence des maladies psychiatriques impliquant des dérégulations de neuromodulateurs, ainsi que d'autres pathologies impliquant l'ocytocine (Guastella and Hickie, 2016; Shamay-Tsoory et al., 2009; Zik and Roberts, 2015), il est important de continuer à promouvoir la recherche permettant d'approfondir les connaissances du système nerveux et des acteurs cellulaires participant à son homéostasie.

REFERENCES

A

Abbracchio, M.P., Burnstock, G., Verkhratsky, A., and Zimmermann, H. (2009). Purinergic signalling in the nervous system: an overview. Trends Neurosci *32*, 19–29.

Acheson, D., Feifel, D., de Wilde, S., McKinney, R., Lohr, J., and Risbrough, V. (2013). The effect of intranasal oxytocin treatment on conditioned fear extinction and recall in a healthy human sample. Psychopharmacology (Berl) *229*, 199–208.

Adami, C., Sorci, G., Blasi, E., Agneletti, A.L., Bistoni, F., and Donato, R. (2001). S100B expression in and effects on microglia. Glia *33*, 131–142.

Adan, R., Cox, J.J., Kats, J.P. van, and Burbach, J. (1992). Thyroid hormone regulates the oxytocin gene. The Journal of Biological Chemistry.

Adermark, L., and Lovinger, D.M. (2008). Electrophysiological properties and gap junction coupling of striatal astrocytes. Neurochem Int *52*, 1365–1372.

Åkerlund, M., Bossmar, T., Brouard, R., Kostrzewska, A., Laudanski, T., Lemancewicz, A., Gal, C.S.-L., and Steinwall, M. (1999). Receptor binding of oxytocin and vasopressin antagonists and inhibitory effects on isolated myometrium from preterm and term pregnant women. BJOG: An International Journal of Obstetrics & Gynaecology *106*, 1047–1053.

Albers, H.E. (2015). Species, sex and individual differences in the vasotocin/vasopressin system: Relationship to neurochemical signaling in the social behavior neural network. Frontiers in Neuroendocrinology *36*, 49–71.

Albizu, L., Cottet, M., Kralikova, M., Stoev, S., Seyer, R., Brabet, I., Roux, T., Bazin, H., Bourrier, E., Lamarque, L., et al. (2010). Time-resolved FRET between GPCR ligands reveals oligomers in native tissues. Nat Chem Biol *6*, 587–594.

Álvarez, M.-I., Rivas, L., Lacruz, C., and Toledano, A. (2015). Astroglial cell subtypes in the cerebella of normal adults, elderly adults, and patients with A lzheimer's disease: A histological and immunohistochemical comparison. Glia *63*, 287–312.

Alves, S.E., Lopez, V., McEwen, B.S., and Weiland, N.G. (1998). Differential colocalization of estrogen receptor beta (ERbeta) with oxytocin and vasopressin in the paraventricular and supraoptic nuclei of the female rat brain: an immunocytochemical study. Proc. Natl. Acad. Sci. U.S.A. *95*, 3281–3286.

Amico, J.A., Challinor, S.M., and Cameron, J.L. (1990). Pattern of oxytocin concentrations in the plasma and cerebrospinal fluid of lactating rhesus monkeys (Macaca mulatta): evidence for functionally independent oxytocinergic pathways in primates. J Clin Endocrinol Metab *71*, 1531–1535.

Amico, J.A., Cai, H., and Vollmer, R.R. (2008). Corticosterone release in oxytocin gene deletion mice following exposure to psychogenic versus non-psychogenic stress. Neurosci Lett *442*, 262–266.

Amsalem, H., Aldrich, C.J., Oskamp, M., Windrim, R., and Farine, D. (2014). Postpartum uterine response to oxytocin and carbetocin. J Reprod Med *59*, 167–173.

Amzica, F., and Massimini, M. (2002). Glial and neuronal interactions during slow wave and paroxysmal activities in the neocortex. Cereb Cortex *12*, 1101–1113.

Anderberg, U.M., and Uvnäs-Moberg, K. (2000). Plasma oxytocin levels in female fibromyalgia syndrome patients. Z Rheumatol *59*, 373–379.

Andreano, J.M., and Cahill, L. (2010). Menstrual cycle modulation of medial temporal activity evoked by negative emotion. Neuroimage *53*, 1286–1293.

Andriezen, W.L. (1893). The Neuroglia Elements in the Human Brain. Br Med J *2*, 227–230.

Ango, F., Wu, C., Van der Want, J.J., Wu, P., Schachner, M., and Huang, Z.J. (2008). Bergmann glia and the recognition molecule CHL1 organize GABAergic axons and direct innervation of Purkinje cell dendrites. PLoS Biol *6*, e103.

Anlauf, E., and Derouiche, A. (2009). A practical calibration procedure for fluorescence colocalization at the single organelle level. J Microsc *233*, 225–233.

Anlauf, E., and Derouiche, A. (2013). Glutamine Synthetase as an Astrocytic Marker: Its Cell Type and Vesicle Localization. Front Endocrinol (Lausanne) *4*.

Armstrong, W.E. (1995). Morphological and electrophysiological classification of hypothalamic supraoptic neurons. Prog Neurobiol *47*, 291–339.

Asmundson, G.J.G., and Katz, J. (2009). Understanding the co-occurrence of anxiety disorders and chronic pain: state-of-the-art. Depress Anxiety *26*, 888–901.

Atasoy, D., Betley, J.N., Su, H.H., and Sternson, S.M. (2012). Deconstruction of a neural circuit for hunger. Nature *488*, 172–177.

Axelson, J.F., and Leeuwen, F.W. van (1990). Differential Localization of Estrogen Receptors in Various Vasopressin Synthesizing Nuclei of the Rat Brain. Journal of Neuroendocrinology *2*, 209–216.

Ayers, L.W., Missig, G., Schulkin, J., and Rosen, J.B. (2011). Oxytocin Reduces Background Anxiety in a Fear-Potentiated Startle Paradigm: Peripheral vs Central Administration. Neuropsychopharmacology *36*, 2488–2497.

B

Babu, A.N., Cheng, T.P., Zhang, A., Altura, B.T., and Altura, B.M. (1999). Low concentrations of ethanol deplete type-2 astrocytes of intracellular free magnesium. Brain Res Bull *50*, 59–62.

Badrinarayan, A., Prater, K.E., and Orsini, C.A. (2012). The Role of the Central Amygdala in Selecting Circuits and Responses. J. Neurosci. *32*, 8431–8433.

Baker, D.A., McFarland, K., Lake, R.W., Shen, H., Tang, X.-C., Toda, S., and Kalivas, P.W. (2003). Neuroadaptations in cystine-glutamate exchange underlie cocaine relapse. Nat Neurosci *6*, 743–749.

Bale, T.L., and Dorsa, D.M. (1997). Cloning, Novel Promoter Sequence, and Estrogen Regulation of a Rat Oxytocin Receptor Gene. Endocrinology *138*, 1151–1158.

Bale, T.L., and Dorsa, D.M. (1998). NGF, cyclic AMP, and phorbol esters regulate oxytocin receptor gene transcription in SK-N-SH and MCF7 cells. Molecular Brain Research *53*, 130–137.

Bale, T.L., Davis, A.M., Auger, A.P., Dorsa, D.M., and McCarthy, M.M. (2001). CNS Region-Specific Oxytocin Receptor Expression: Importance in Regulation of Anxiety and Sex Behavior. J Neurosci *21*, 2546–2552.

Ballanyi, K., Grafe, P., and ten Bruggencate, G. (1987). Ion activities and potassium uptake mechanisms of glial cells in guinea-pig olfactory cortex slices. J Physiol *382*, 159–174.

Banerjee, P., Joy, K.P., and Chaube, R. (2017). Structural and functional diversity of nonapeptide hormones from an evolutionary perspective: A review. Gen Comp Endocrinol *241*, 4–23.

Barberis, C., Mouillac, B., and Durroux, T. (1998). Structural bases of vasopressin/oxytocin receptor function. J. Endocrinol. *156*, 223–229.

Barlow, D.H., Pincus, D.B., Heinrichs, N., and Choate, M.L. (2003). Anxiety Disorders. In Handbook of Psychology, (American Cancer Society), pp. 119–147.

Barry, D., and McDermott, K. (2005). Differentiation of radial glia from radial precursor cells and transformation into astrocytes in the developing rat spinal cord. Glia *50*, 187–197.

Barth, T., Krejcí, I., Vaněcková, J., Jost, K., and Rychlík, I. (1974). Prolonged action of deamino-carba analogues of oxytocin on the rat uterus in vivo. Eur J Pharmacol *25*, 67–70.

Baskerville, T.A., and Douglas, A.J. (2008). Interactions between dopamine and oxytocin in the control of sexual behaviour. Prog Brain Res *170*, 277–290.

Baskerville, T.A., and Douglas, A.J. (2010). Dopamine and Oxytocin Interactions Underlying Behaviors: Potential Contributions to Behavioral Disorders. CNS Neuroscience & Therapeutics *16*, e92–e123.

Beets, I., Temmerman, L., Janssen, T., and Schoofs, L. (2013). Ancient neuromodulation by vasopressin/oxytocin-related peptides. Worm *2*.

Bekar, L.K., and Walz, W. (2002). Intracellular chloride modulates A-type potassium currents in astrocytes. Glia *39*, 207–216.

Bellini-Leite, S., and Pereira, A.J. (2013). Is global workspace a cartesian theater? How the neuro-astroglial interaction model solves conceptual issues. Journal of Cognitive Science *14*, 335–360.

Bender, C.L., Calfa, G.D., and Molina, V.A. (2016). Astrocyte plasticity induced by emotional stress: A new partner in psychiatric physiopathology? Prog Neuropsychopharmacol Biol Psychiatry *65*, 68–77.

Bernardinelli, Y., Salmon, C., Jones, E.V., Farmer, W.T., Stellwagen, D., and Murai, K.K. (2011). Astrocytes display complex and localized calcium responses to single-neuron stimulation in the hippocampus. J Neurosci *31*, 8905–8919.

Beyer, C.E., Dwyer, J.M., Platt, B.J., Neal, S., Luo, B., Ling, H.-P., Lin, Q., Mark, R.J., Rosenzweig-Lipson, S., and Schechter, L.E. (2010). Angiotensin IV elevates oxytocin levels in the rat amygdala and produces anxiolytic-like activity through subsequent oxytocin receptor activation. Psychopharmacology (Berl) *209*, 303–311.

Bianchi, R., Verzini, M., Garbuglia, M., Giambanco, I., and Donato, R. (1994). Mechanism of S100 protein-dependent inhibition of glial fibrillary acidic protein (GFAP) polymerization. Biochim Biophys Acta *1223*, 354–360.

Bianchi, R., Giambanco, I., and Donato, R. (2010). S100B/RAGE-dependent activation of microglia via NF-kappaB and AP-1 Co-regulation of COX-2 expression by S100B, IL-1beta and TNF-alpha. Neurobiol Aging *31*, 665–677.

Bignami, A., and Dahl, D. (1986). Brain-specific hyaluronate-binding protein. A product of white matter astrocytes? J Neurocytol *15*, 671–679.

Bignami, A., Eng, L.F., Dahl, D., and Uyeda, C.T. (1972). Localization of the glial fibrillary acidic protein in astrocytes by immunofluorescence. Brain Research *43*, 429–435.

Blanchard, R.J., Flannelly, K.J., and Blanchard, D.C. (1986). Defensive behavior of laboratory and wild Rattus norvegicus. J Comp Psychol *100*, 101–107.

Blevins, J.E., Schwartz, M.W., and Baskin, D.G. (2004). Evidence that paraventricular nucleus oxytocin neurons link hypothalamic leptin action to caudal brain stem nuclei controlling meal size. American Journal of Physiology-Regulatory, Integrative and Comparative Physiology *287*, R87–R96.

Blume, A., Bosch, O.J., Miklos, S., Torner, L., Wales, L., Waldherr, M., and Neumann, I.D. (2008). Oxytocin reduces anxiety via ERK1/2 activation: local effect within the rat hypothalamic paraventricular nucleus. Eur J Neurosci *27*, 1947–1956.

Blumenstein, M., Hruby, V.J., and Viswanatha, V. (1979). Investigation of the interactions of oxytocin with neurophysins at low pH using carbon-13 nuclear magnetic resonance and carbon-13-labeled hormones. Biochemistry *18*, 3552–3557.

Bocchio, M., Nabavi, S., and Capogna, M. (2017). Synaptic Plasticity, Engrams, and Network Oscillations in Amygdala Circuits for Storage and Retrieval of Emotional Memories. Neuron *94*, 731–743.

Bosco, D., Haefliger, J.-A., and Meda, P. (2011). Connexins: key mediators of endocrine function. Physiol Rev *91*, 1393–1445.

Bouvier, M. (2001). Oligomerization of G-protein-coupled transmitter receptors. Nature Reviews Neuroscience *2*, 274–286.

Bowman, C.L., and Kimelberg, H.K. (1984). Excitatory amino acids directly depolarize rat brain astrocytes in primary culture. Nature *311*, 656–659.

Breslow, E., and Burman, S. (1990). Molecular, thermodynamic, and biological aspects of recognition and function in neurophysin-hormone systems: a model system for the analysis of protein-peptide interactions. Adv. Enzymol. Relat. Areas Mol. Biol. *63*, 1–67.

Breton, J.-D., Veinante, P., Uhl-Bronner, S., Vergnano, A.M., Freund-Mercier, M.J., Schlichter, R., and Poisbeau, P. (2008). Oxytocin-induced antinociception in the spinal cord is mediated by a subpopulation of glutamatergic neurons in lamina I-II which amplify GABAergic inhibition. Mol Pain *4*, 19.

Breton, J.D., Poisbeau, P., and Darbon, P. (2009). Antinociceptive action of oxytocin involves inhibition of potassium channel currents in lamina II neurons of the rat spinal cord. Mol Pain *5*, 63.

Briffaud, V., Williams, P., Courty, J., and Broberger, C. (2015). Excitation of Tuberoinfundibular Dopamine Neurons by Oxytocin: Crosstalk in the Control of Lactation. J. Neurosci. *35*, 4229–4237.

Bröer, S., and Brookes, N. (2001). Transfer of glutamine between astrocytes and neurons. J Neurochem *77*, 705–719.

Buijs, R.M., Swaab, D.F., Dogterom, J., and van Leeuwen, F.W. (1978). Intra- and extrahypothalamic vasopressin and oxytocin pathways in the rat. Cell Tissue Res. *186*, 423–433.

Burbach, J.P.H. (2002). Regulation of gene promoters of hypothalamic peptides. Front Neuroendocrinol *23*, 342–369.

Burbach, J.P., Luckman, S.M., Murphy, D., and Gainer, H. (2001). Gene regulation in the magnocellular hypothalamo-neurohypophysial system. Physiol Rev *81*, 1197–1267.

Burda, J.E., and Sofroniew, M.V. (2014). Reactive gliosis and the multicellular response to CNS damage and disease. Neuron *81*, 229–248.

Burda, J.E., Bernstein, A.M., and Sofroniew, M.V. (2016). Astrocyte roles in traumatic brain injury. Exp Neurol *275*, 305–315.

Burnstock, G., and Alexei, V. (2012). Purinergic signalling and the nervous system (Springer Science & Business Media).

Burnstock, G., and Kennedy, C. (1985). Is there a basis for distinguishing two types of P2-purinoceptor? Gen Pharmacol *16*, 433–440.

Bushong, E.A., Martone, M.E., Jones, Y.Z., and Ellisman, M.H. (2002). Protoplasmic Astrocytes in CA1 Stratum Radiatum Occupy Separate Anatomical Domains. J Neurosci *22*, 183–192.

Busnelli, M., Saulière, A., Manning, M., Bouvier, M., Galés, C., and Chini, B. (2012). Functional selective oxytocin-derived agonists discriminate between individual G protein family subtypes. J Biol Chem *287*, 3617–3629.

Busnelli, M., Bulgheroni, E., Manning, M., Kleinau, G., and Chini, B. (2013). Selective and potent agonists and antagonists for investigating the role of mouse oxytocin receptors. J Pharmacol Exp Ther *346*, 318–327.

Busnelli, M., Kleinau, G., Muttenthaler, M., Stoev, S., Manning, M., Bibic, L., Howell, L.A., McCormick, P.J., Di Lascio, S., Braida, D., et al. (2016). Design and Characterization of Superpotent Bivalent Ligands Targeting Oxytocin Receptor Dimers via a Channel-Like Structure. J. Med. Chem. *59*, 7152–7166.

Butt, A.M. (2011). ATP: a ubiquitous gliotransmitter integrating neuron-glial networks. Semin Cell Dev Biol *22*, 205–213.

Byrne, J.H., Heidelberger, R., and Waxham, M.N. (2014). From Molecules to Networks: An Introduction to Cellular and Molecular Neuroscience (Academic Press).

C

Cahoy, J.D., Emery, B., Kaushal, A., Foo, L.C., Zamanian, J.L., Christopherson, K.S., Xing, Y., Lubischer, J.L., Krieg, P.A., Krupenko, S.A., et al. (2008). A transcriptome database for astrocytes, neurons, and oligodendrocytes: a new resource for understanding brain development and function. J Neurosci *28*, 264–278.

y Cajal, S.R. (1913). Un nuevo proceder para la impregnación de la neuroglía.

y Cajal, S.R. (1917). El proceder del oro sublimado para la coloración de la neuroglia (Imp. y lib. de Nicolás Moya).

Cammer, W. (1990). Glutamine synthetase in the central nervous system is not confined to astrocytes. J Neuroimmunol *26*, 173–178.

Carrasquillo, Y., and Gereau, R.W. (2007). Activation of the Extracellular Signal-Regulated Kinase in the Amygdala Modulates Pain Perception. J. Neurosci. *27*, 1543–1551.

Cassell, M.D., Freedman, L.J., and Shi, C. (1999). The intrinsic organization of the central extended amygdala. Ann N Y Acad Sci *877*, 217–241.

Cassoni, P., Sapino, A., Papotti, M., and Bussolati, G. (1996). Oxytocin and oxytocin-analogue F314 inhibit cell proliferation and tumor growth of rat and mouse mammary carcinomas. Int J Cancer *66*, 817–820.

Castel, M., Gainer, H., and Dellmann, H.D. (1984). Neuronal secretory systems. Int Rev Cytol *88*, 303–459.

Caudle, R.M. (2006). Memory in astrocytes: a hypothesis. Theor Biol Med Model *3*, 2.

Chang, S.W.C., Brent, L.J.N., Adams, G.K., Klein, J.T., Pearson, J.M., Watson, K.K., and Platt, M.L. (2013). Neuroethology of primate social behavior. Proc Natl Acad Sci U S A *110 Suppl 2*, 10387–10394.

Chatterjee, O., Patil, K., Sahu, A., Gopalakrishnan, L., Mol, P., Advani, J., Mukherjee, S., Christopher, R., and Prasad, T.S.K. (2016). An overview of the oxytocin-oxytocin receptor signaling network. J Cell Commun Signal *10*, 355–360.

Chever, O., Djukic, B., McCarthy, K.D., and Amzica, F. (2010). Implication of Kir4.1 channel in excess potassium clearance: an in vivo study on anesthetized glial-conditional Kir4.1 knock-out mice. J Neurosci *30*, 15769–15777.

Chini, B., Mouillac, B., Balestre, M.N., Trumpp-Kallmeyer, S., Hoflack, J., Hibert, M., Andriolo, M., Pupier, S., Jard, S., and Barberis, C. (1996). Two aromatic residues regulate the response of the human oxytocin receptor to the partial agonist arginine vasopressin. FEBS Lett *397*, 201–206.

Chini, B., Verhage, M., and Grinevich, V. (2017). The Action Radius of Oxytocin Release in the Mammalian CNS: From Single Vesicles to Behavior. Trends Pharmacol Sci *38*, 982–991.

Chiodera, P., Volpi, R., Capretti, L., Marchesi, C., d'Amato, L., De Ferri, A., Bianconi, L., and Coiro, V. (1991). Effect of estrogen or insulin-induced hypoglycemia on plasma oxytocin levels in bulimia and anorexia nervosa. Metab. Clin. Exp. *40*, 1226–1230.

Chvátal, A., Pastor, A., Mauch, M., Syková, E., and Kettenmann, H. (1995). Distinct populations of identified glial cells in the developing rat spinal cord slice: ion channel properties and cell morphology. Eur J Neurosci *7*, 129–142.

Ciocchi, S., Herry, C., Grenier, F., Wolff, S.B.E., Letzkus, J.J., Vlachos, I., Ehrlich, I., Sprengel, R., Deisseroth, K., Stadler, M.B., et al. (2010). Encoding of conditioned fear in central amygdala inhibitory circuits. Nature *468*, 277–282.

Ciocchi, S., Lüthi, A., and Herry, C. (2011). Nouveaux circuits neuronaux amygdaliens contrôlant le comportement de peur. Med Sci (Paris) *27*, 455–457.

Claybaugh, J.R., and Uyehara, C.F. (1993). Metabolism of neurohypophysial hormones. Ann N Y Acad Sci *689*, 250–268.

Condés-Lara, M., González, N.M., Martínez-Lorenzana, G., Delgado, O.L., and Freund-Mercier, M.J. (2003). Actions of oxytocin and interactions with glutamate on spontaneous and evoked dorsal spinal cord neuronal activities. Brain Res *976*, 75–81.

Condés-Lara, M., Rojas-Piloni, G., Martínez-Lorenzana, G., Rodríguez-Jiménez, J., López Hidalgo, M., and Freund-Mercier, M.J. (2006). Paraventricular hypothalamic influences on spinal nociceptive processing. Brain Res *1081*, 126–137.

Condés-Lara, M., Rojas-Piloni, G., Martínez-Lorenzana, G., and Rodríguez-Jiménez, J. (2009). Paraventricular hypothalamic oxytocinergic cells responding to noxious stimulation and projecting to the spinal dorsal horn represent a homeostatic analgesic mechanism. European Journal of Neuroscience *30*, 1056–1063.

Condés-Lara, M., Rojas-Piloni, G., Martínez-Lorenzana, G., López-Hidalgo, M., and Rodríguez-Jiménez, J. (2009). Hypothalamospinal oxytocinergic antinociception is mediated by GABAergic and opiate neurons that reduce A-delta and C fiber primary afferent excitation of spinal cord cells. Brain Research *1247*, 38–49.

Condés-Lara, M., Martínez-Lorenzana, G., Rubio-Beltrán, E., Rodríguez-Jiménez, J., Rojas-Piloni, G., and González-Hernández, A. (2015). Hypothalamic paraventricular nucleus stimulation enhances c-Fos expression in spinal and supraspinal structures related to pain modulation. Neurosci Res *98*, 59–63.

Conti, F., Sertic, S., Reversi, A., and Chini, B. (2009). Intracellular trafficking of the human oxytocin receptor: evidence of receptor recycling via a Rab4/Rab5 “short cycle.” Am J Physiol Endocrinol Metab *296*, E532-542.

Cooper, A.J., and Plum, F. (1987). Biochemistry and physiology of brain ammonia. Physiol Rev *67*, 440–519.

Corkrum, M., Covelo, A., Lines, J., Bellocchio, L., Pisansky, M., Loke, K., Quintana, R., Rothwell, P.E., Lujan, R., Marsicano, G., et al. (2020). Dopamine-Evoked Synaptic Regulation in the Nucleus Accumbens Requires Astrocyte Activity. Neuron *105*, 1036-1047.e5.

Correia, S.S., and Goosens, K.A. (2016). Input-specific contributions to valence processing in the amygdala. Learn Mem *23*, 534–543.

Cottet, M., Albizu, L., Perkovska, S., Jean-Alphonse, F., Rahmeh, R., Orcel, H., Méjean, C., Granier, S., Mendre, C., Mouillac, B., et al. (2010). Past, present and future of vasopressin and oxytocin receptor oligomers, prototypical GPCR models to study dimerization processes. Current Opinion in Pharmacology *10*, 59–66.

Crankshaw, D., Gaspar, V., and Pliška, V. (1990). Multiple [3H]-Oxytocin Binding Sites in Rat Myometrial Plasma Membranes. Journal of Receptor Research *10*, 269–285.

D

Daddona, M.M., and Haldar, J. (1994). Opioid modulation of oxytocin release from spinal cord synaptosomes. Neuroreport *5*, 1833–1835.

Dallérac, G., Chever, O., and Rouach, N. (2013). How do astrocytes shape synaptic transmission? Insights from electrophysiology. Front Cell Neurosci *7*, 159.

D'Ambrosio, R., Gordon, D.S., and Winn, H.R. (2002). Differential role of KIR channel and Na(+)/K(+)-pump in the regulation of extracellular K(+) in rat hippocampus. J Neurophysiol *87*, 87–102.

Danbolt, N.C. (2001). Glutamate uptake. Prog Neurobiol *65*, 1–105.

Davis, P., and Reijmers, L.G. (2018). The dynamic nature of fear engrams in the basolateral amygdala. Brain Res Bull *141*, 44–49.

De Castro, F. (1951). The anatomical aspects of the ganglionic synaptic transmission in mammals. Archives Internationales de Physiologie *59*, 479.

De Vries, G.J., and Buijs, R.M. (1983). The origin of the vasopressinergic and oxytocinergic innervation of the rat brain with special reference to the lateral septum. Brain Res. *273*, 307–317.

DeLaTorre, S., Rojas-Piloni, G., Martínez-Lorenzana, G., Rodríguez-Jiménez, J., Villanueva, L., and Condés-Lara, M. (2009). Paraventricular oxytocinergic hypothalamic prevention or interruption of long-term potentiation in dorsal horn nociceptive neurons: Electrophysiological and behavioral evidence. PAIN® *144*, 320–328.

Dermietzel, R., Hertberg, E., Kessler, J., and Spray, D. (1991). Gap junctions between cultured astrocytes: immunocytochemical, molecular, and electrophysiological analysis. J Neurosci *11*, 1421–1432.

Derouiche, A., and Frotscher, M. (1991). Astroglial processes around identified glutamatergic synapses contain glutamine synthetase: evidence for transmitter degradation. Brain Res *552*, 346–350.

Di Scala-Guenot, D., and Strosser, M.T. (1992). Oxytocin receptors on cultured astroglial cells. Kinetic and pharmacological characterization of oxytocin-binding sites on intact hypothalamic and hippocampic cells from foetal rat brain. Biochem J *284 (Pt 2)*, 491–497.

Di Scala-Guenot, D., Mouginot, D., and Strosser, M.T. (1994). Increase of intracellular calcium induced by oxytocin in hypothalamic cultured astrocytes. Glia *11*, 269–276.

Ding, F., O'Donnell, J., Xu, Q., Kang, N., Goldman, N., and Nedergaard, M. (2016). Changes in the composition of brain interstitial ions control the sleep-wake cycle. Science *352*, 550–555.

Djukic, B., Casper, K.B., Philpot, B.D., Chin, L.-S., and McCarthy, K.D. (2007). Conditional knock-out of Kir4.1 leads to glial membrane depolarization, inhibition of potassium and glutamate uptake, and enhanced short-term synaptic potentiation. J Neurosci *27*, 11354–11365.

Doetsch, F., Caillé, I., Lim, D.A., García-Verdugo, J.M., and Alvarez-Buylla, A. (1999). Subventricular zone astrocytes are neural stem cells in the adult mammalian brain. Cell *97*, 703–716.

Donaldson, Z.R., and Young, L.J. (2008). Oxytocin, vasopressin, and the neurogenetics of sociality. Science *322*, 900–904.

Donato, R., Sorci, G., Riuzzi, F., Arcuri, C., Bianchi, R., Brozzi, F., Tubaro, C., and Giambanco, I. (2009). S100B's double life: intracellular regulator and extracellular signal. Biochim Biophys Acta *1793*, 1008–1022.

Donato, R., Cannon, B.R., Sorci, G., Riuzzi, F., Hsu, K., Weber, D.J., and Geczy, C.L. (2013). Functions of S100 proteins. Curr Mol Med *13*, 24–57.

Drake, M.T., Shenoy, S.K., and Lefkowitz, R.J. (2006). Trafficking of G protein-coupled receptors. Circ Res *99*, 570–582.

Du, Y., Ma, B., Kiyoshi, C.M., Alford, C.C., Wang, W., and Zhou, M. (2015). Freshly dissociated mature hippocampal astrocytes exhibit passive membrane conductance and low membrane resistance similarly to syncytial coupled astrocytes. J Neurophysiol *113*, 3744–3750.

Du Vigneaud, V., Ressler, C., and Trippett, S. (1953). The sequence of amino acids in oxytocin, with a proposal for the structure of oxytocin. J. Biol. Chem. *205*, 949–957.

Duque-Wilckens, N., Steinman, M., Grinevich, V., and Trainor, B. (2017). The Role of Oxytocin Neurons in the Bed Nucleus of the Stria Terminalis in Mediating Social Withdrawal. Biological Psychiatry *81*, S44–S45.

E

Ebner, K., Bosch, O.J., Krömer, S.A., Singewald, N., and Neumann, I.D. (2005). Release of Oxytocin in the Rat Central Amygdala Modulates Stress-Coping Behavior and the Release of Excitatory Amino Acids. Neuropsychopharmacology *30*, 223–230.

Eckstein, M., Scheele, D., Patin, A., Preckel, K., Becker, B., Walter, A., Domschke, K., Grinevich, V., Maier, W., and Hurlemann, R. (2016). Oxytocin Facilitates Pavlovian Fear Learning in Males. Neuropsychopharmacology *41*, 932–939.

Egorova, A.E., Kuzik, V.V., and Ozirskaya, E.V. (2003). Electron Microscopy Study of Anterior Neuropituitary of the Sterlet Acipenser ruthenus. Journal of Evolutionary Biochemistry and Physiology *39*, 241–248.

Elands, J., Barberis, C., Jard, S., Tribollet, E., Dreifuss, J.J., Bankowski, K., Manning, M., and Sawyer, W.H. (1988). 125I-labelled d(CH2)5[Tyr(Me)2,Thr4,Tyr-NH2(9)]OVT: a selective oxytocin receptor ligand. Eur J Pharmacol *147*, 197–207.

Eliava, M., Melchior, M., Knobloch-Bollmann, H.S., Wahis, J., da Silva Gouveia, M., Tang, Y., Ciobanu, A.C., Triana Del Rio, R., Roth, L.C., Althammer, F., et al. (2016). A New Population of Parvocellular Oxytocin Neurons Controlling Magnocellular Neuron Activity and Inflammatory Pain Processing. Neuron *89*, 1291–1304.

Eng, L., Vanderhaeghen, J.J., Bignami, A., and Gerstl, B. (1971). An acidic protein isolated from fibrous astrocytes. Brain Research *28*, 351–354.

Engle, M.P., Ness, T.J., and Robbins, M.T. (2012). Intrathecal oxytocin inhibits visceromotor reflex and spinal neuronal responses to noxious distention of the rat urinary bladder. Reg Anesth Pain Med *37*, 515–520.

Eto, K., Kim, S.K., Takeda, I., and Nabekura, J. (2018). The roles of cortical astrocytes in chronic pain and other brain pathologies. Neuroscience Research *126*, 3–8.

Evans, W.H., and Martin, P.E.M. (2002). Gap junctions: structure and function (Review). Mol Membr Biol *19*, 121–136.

F

Fanelli, F., Barbier, P., Zanchetta, D., de Benedetti, P.G., and Chini, B. (1999). Activation mechanism of human oxytocin receptor: a combined study of experimental and computer-simulated mutagenesis. Mol Pharmacol *56*, 214–225.

Feldman, R., Monakhov, M., Pratt, M., and Ebstein, R.P. (2016). Oxytocin Pathway Genes: Evolutionary Ancient System Impacting on Human Affiliation, Sociality, and Psychopathology. Biol. Psychiatry *79*, 174–184.

Fields, R.L., House, S.B., and Gainer, H. (2003). Regulatory domains in the intergenic region of the oxytocin and vasopressin genes that control their hypothalamus-specific expression in vitro. J. Neurosci. *23*, 7801–7809.

Figueira, R.J., Peabody, M.F., and Lonstein, J.S. (2008). Oxytocin receptor activity in the ventrocaudal periaqueductal gray modulates anxiety-related behavior in postpartum rats. Behav Neurosci *122*, 618–628.

Fleming, J.G.W., Spencer, T.E., Safe, S.H., and Bazer, F.W. (2006). Estrogen regulates transcription of the ovine oxytocin receptor gene through GC-rich SP1 promoter elements. Endocrinology *147*, 899–911.

Fliers, E., Guldenaar, S.E.F., Wal, N. v. d., and Swaab, D.F. (1986). Extrahypothalamic vasopressin and oxytocin in the human brain; presence of vasopressin cells in the bed nucleus of the stria terminalis. Brain Research *375*, 363–367.

Franke, H., Verkhratsky, A., Burnstock, G., and Illes, P. (2012). Pathophysiology of astroglial purinergic signalling. Purinergic Signal *8*, 629–657.

Freeman, S.M., and Young, L.J. (2016). Comparative Perspectives on Oxytocin and Vasopressin Receptor Research in Rodents and Primates: Translational Implications. J Neuroendocrinol *28*.

Freeman, S.M., Walum, H., Inoue, K., Smith, A.L., Goodman, M.M., Bales, K.L., and Young, L.J. (2014a). Neuroanatomical distribution of oxytocin and vasopressin 1a receptors in the socially monogamous coppery titi monkey (Callicebus cupreus). Neuroscience *273*, 12–23.

Freeman, S.M., Inoue, K., Smith, A.L., Goodman, M.M., and Young, L.J. (2014b). The neuroanatomical distribution of oxytocin receptor binding and mRNA in the male rhesus macaque (Macaca mulatta). Psychoneuroendocrinology *45*, 128–141.

Freund-Mercier, M.J., Stoeckel, M.E., Palacios, J.M., Pazos, A., Reichhart, J.M., Porte, A., and Richard, Ph. (1987). Pharmacological characteristics and anatomical distribution of [3H]oxytocin-binding sites in the wistar rat brain studied by autoradiography. Neuroscience *20*, 599–614.

Frigeri, A., Gropper, M.A., Umenishi, F., Kawashima, M., Brown, D., and Verkman, A.S. (1995). Localization of MIWC and GLIP water channel homologs in neuromuscular, epithelial and glandular tissues. J Cell Sci *108 (Pt 9)*, 2993–3002.

Fu, Y., Han, J., Ishola, T., Scerbo, M., Adwanikar, H., Ramsey, C., and Neugebauer, V. (2008). PKA and ERK, but not PKC, in the amygdala contribute to pain-related synaptic plasticity and behavior. Mol Pain *4*, 26.

Fudge, J.L., and Emiliano, A.B. (2003). The Extended Amygdala and the Dopamine System: Another Piece of the Dopamine Puzzle. J Neuropsychiatry Clin Neurosci *15*, 306–316.

Fuxe, K., Borroto Escuela, D., Romero-Fernandez, W., Ciruela, F., Manger, P., Leo, G., Díaz-Cabiale, Z., and Agnati, L. (2012). On the role of volume transmission and receptor-receptor interactions in social behaviour: Focus on central catecholamine and oxytocin neurons. Brain Research *1476*, 119–131.

G

Galambos, R. (1961). A GLIA-NEURAL THEORY OF BRAIN FUNCTION. Proc Natl Acad Sci U S A *47*, 129–136.

García-Marín, V., García-López, P., and Freire, M. (2007). Cajal's contributions to glia research. Trends in Neurosciences *30*, 479–487.

Garrison, J.L., Macosko, E.Z., Bernstein, S., Pokala, N., Albrecht, D.R., and Bargmann, C.I. (2012). Oxytocin/Vasopressin-Related Peptides Have an Ancient Role in Reproductive Behavior. Science *338*, 540–543.

Ge, Y., Lundeberg, T., and Yu, L.-C. (2002). Blockade effect of mu and kappa opioid antagonists on the anti-nociception induced by intra-periaqueductal grey injection of oxytocin in rats. Brain Res. *927*, 204–207.

Gebicke-Haerter, P.J. (2014). Engram formation in psychiatric disorders. Front Neurosci *8*.

Giaume, C., Koulakoff, A., Roux, L., Holcman, D., and Rouach, N. (2010). Astroglial networks: a step further in neuroglial and gliovascular interactions. Nat Rev Neurosci *11*, 87–99.

Gilligan, P., Brenner, S., and Venkatesh, B. (2003). Neurone-specific expression and regulation of the pufferfish isotocin and vasotocin genes in transgenic mice. J Neuroendocrinol *15*, 1027–1036.

Gimpl, G., and Fahrenholz, F. (2000). Human oxytocin receptors in cholesterol-rich vs. cholesterol-poor microdomains of the plasma membrane. European Journal of Biochemistry *267*, 2483–2497.

Gimpl, G., and Fahrenholz, F. (2001a). The oxytocin receptor system: structure, function, and regulation. Physiol. Rev. *81*, 629–683.

Gimpl, G., and Fahrenholz, F. (2001b). The oxytocin receptor system: structure, function, and regulation. Physiol. Rev. *81*, 629–683.

Gimpl, G., and Fahrenholz, F. (2002). Cholesterol as stabilizer of the oxytocin receptor. Biochimica et Biophysica Acta (BBA) - Biomembranes *1564*, 384–392.

Gimpl, G., Klein, U., Reilaender, H., and Fahrenholz, F. (1995). Expression of the Human Oxytocin Receptor in Baculovirus-Infected Insect Cells: High-Affinity Binding Is Induced by a Cholesterol-Cyclodextrin Complex. Biochemistry *34*, 13794–13801.

Gimpl, G., Burger, K., and Fahrenholz, F. (1997). Cholesterol as Modulator of Receptor Function. Biochemistry *36*, 10959–10974.

Gimpl, G., Reitz, J., Brauer, S., and Trossen, C. (2008). Oxytocin receptors: ligand binding, signalling and cholesterol dependence. Prog Brain Res *170*, 193–204.

Glasgow, E., Kusano, K., Chin, H., Mezey, E., Young, W.S., and Gainer, H. (1999). Single cell reverse transcription-polymerase chain reaction analysis of rat supraoptic magnocellular neurons: neuropeptide phenotypes and high voltage-gated calcium channel subtypes. Endocrinology *140*, 5391–5401.

Godínez-Chaparro, B., Martínez-Lorenzana, G., Rodríguez-Jiménez, J., Manzano-García, A., Rojas-Piloni, G., Condés-Lara, M., and González-Hernández, A. (2016). The potential role of serotonergic mechanisms in the spinal oxytocin-induced antinociception. Neuropeptides *60*, 51–60.

Goldstein, J.M., Jerram, M., Poldrack, R., Ahern, T., Kennedy, D.N., Seidman, L.J., and Makris, N. (2005). Hormonal cycle modulates arousal circuitry in women using functional magnetic resonance imaging. J Neurosci *25*, 9309–9316.

Goldstein, J.M., Jerram, M., Abbs, B., Whitfield-Gabrieli, S., and Makris, N. (2010). Sex differences in stress response circuitry activation dependent on female hormonal cycle. J Neurosci *30*, 431–438.

Golgi, C. (1885). Sulla fina anatomia degli organi centrali del sistema nervoso (S. Calderini).

Golgi, C. (1903). Opera Omnia, Vol. 1. Milano: U. Hoepli 40.

Gómez-Gonzalo, M., Navarrete, M., Perea, G., Covelo, A., Martín-Fernández, M., Shigemoto, R., Luján, R., and Araque, A. (2015). Endocannabinoids Induce Lateral Long-Term Potentiation of Transmitter Release by Stimulation of Gliotransmission. Cereb Cortex *25*, 3699–3712.

Götz, M., Sirko, S., Beckers, J., and Irmler, M. (2015). Reactive astrocytes as neural stem or progenitor cells: In vivo lineage, In vitro potential, and Genome-wide expression analysis. Glia *63*, 1452–1468.

Gravati, M., Busnelli, M., Bulgheroni, E., Reversi, A., Spaiardi, P., Parenti, M., Toselli, M., and Chini, B. (2010). Dual modulation of inward rectifier potassium currents in olfactory neuronal cells by promiscuous G protein coupling of the oxytocin receptor. J Neurochem *114*, 1424–1435.

Grazzini, E., Guillon, G., Mouillac, B., and Zingg, H.H. (1998). Inhibition of oxytocin receptor function by direct binding of progesterone. Nature *392*, 509–512.

Grinevich, V.V., and Polenov, A.L. (1997). [The morphofunctional specialization of the main and accessory magnocellular neuroendocrine nuclei of the hypothalamus]. Morfologiia *112*, 26–29.

Grinevich, V., Desarménien, M.G., Chini, B., Tauber, M., and Muscatelli, F. (2014). Ontogenesis of oxytocin pathways in the mammalian brain: late maturation and psychosocial disorders. Front Neuroanat *8*, 164.

Grinevich, V., Knobloch-Bollmann, H.S., Eliava, M., Busnelli, M., and Chini, B. (2016). Assembling the Puzzle: Pathways of Oxytocin Signaling in the Brain. Biological Psychiatry *79*, 155–164.

Gutierrez, S., Liu, B., Hayashida, K., Houle, T.T., and Eisenach, J.C. (2013). Reversal of peripheral nerve injury-induced hypersensitivity in the postpartum period: role of spinal oxytocin. Anesthesiology *118*, 152–159.

Guzzi, F., Zanchetta, D., Cassoni, P., Guzzi, V., Francolini, M., Parenti, M., and Chini, B. (2002). Localization of the human oxytocin receptor in caveolin-1 enriched domains turns the receptor-mediated inhibition of cell growth into a proliferative response. Oncogene *21*, 1658–1667.

H

Hachem, S., Laurenson, A.-S., Hugnot, J.-P., and Legraverend, C. (2007). Expression of S100B during embryonic development of the mouse cerebellum. BMC Dev Biol *7*, 17.

Hadzic, M., Jack, A., and Wahle, P. (2017). Ionotropic glutamate receptors: Which ones, when, and where in the mammalian neocortex. J Comp Neurol *525*, 976–1033.

Halassa, M.M., Fellin, T., Takano, H., Dong, J.-H., and Haydon, P.G. (2007). Synaptic islands defined by the territory of a single astrocyte. J Neurosci *27*, 6473–6477.

Han, J.S., and Neugebauer, V. (2004). Synaptic plasticity in the amygdala in a visceral pain model in rats. Neurosci. Lett. *361*, 254–257.

Han, Y., and Yu, L.-C. (2009). Involvement of oxytocin and its receptor in nociceptive modulation in the central nucleus of amygdala of rats. Neurosci. Lett. *454*, 101–104.

Han, J., Kesner, P., Metna-Laurent, M., Duan, T., Xu, L., Georges, F., Koehl, M., Abrous, D.N., Mendizabal-Zubiaga, J., Grandes, P., et al. (2012). Acute cannabinoids impair working memory through astroglial CB1 receptor modulation of hippocampal LTD. Cell *148*, 1039–1050.

Han, X., Chen, M., Wang, F., Windrem, M., Wang, S., Shanz, S., Xu, Q., Oberheim, N.A., Bekar, L., Betstadt, S., et al. (2013). Forebrain engraftment by human glial progenitor cells enhances synaptic plasticity and learning in adult mice. Cell Stem Cell *12*, 342–353.

Hanner, F., Sorensen, C.M., Holstein-Rathlou, N.-H., and Peti-Peterdi, J. (2010). Connexins and the kidney. Am J Physiol Regul Integr Comp Physiol *298*, R1143-1155.

Hansen, A.J. (1985). Effect of anoxia on ion distribution in the brain. Physiol Rev *65*, 101–148.

Hansen, R.R., and Malcangio, M. (2013). Astrocytes—Multitaskers in chronic pain. European Journal of Pharmacology *716*, 120–128.

Hara, Y., Battey, J., and Gainer, H. (1990). Structure of mouse vasopressin and oxytocin genes. Brain Res. Mol. Brain Res. *8*, 319–324.

Harony-Nicolas, H., Mamrut, S., Brodsky, L., Shahar-Gold, H., Barki-Harrington, L., and Wagner, S. (2014). Brain region-specific methylation in the promoter of the murine oxytocin receptor gene is involved in its expression regulation. Psychoneuroendocrinology *39*, 121–131.

Harrington, M.G., Salomon, R.M., Pogoda, J.M., Oborina, E., Okey, N., Johnson, B., Schmidt, D., Fonteh, A.N., and Dalleska, N.F. (2010). Cerebrospinal fluid sodium rhythms. Cerebrospinal Fluid Res *7*, 3.

Hasan, M.T., Althammer, F., Silva da Gouveia, M., Goyon, S., Eliava, M., Lefevre, A., Kerspern, D., Schimmer, J., Raftogianni, A., Wahis, J., et al. (2019). A Fear Memory Engram and Its Plasticity in the Hypothalamic Oxytocin System. Neuron *103*, 133-146.e8.

Hasbi, A., Devost, D., Laporte, S.A., and Zingg, H.H. (2004). Real-time detection of interactions between the human oxytocin receptor and G protein-coupled receptor kinase-2. Mol Endocrinol *18*, 1277–1286.

Hatton, G.I., Perlmutter, L.S., Salm, A.K., and Tweedle, C.D. (1984). Dynamic neuronal-glial interactions in hypothalamus and pituitary: Implications for control of hormone synthesis and release. Peptides *5*, 121–138.

Haubensak, W., Kunwar, P., Cai, H., Ciocchi, S., Wall, N., Ponnusamy, R., Biag, J., Dong, H.-W., Deisseroth, K., Callaway, E.M., et al. (2010). Genetic dissection of an amygdala microcircuit that gates conditioned fear. Nature *468*, 270–276.

Hebb, D.O. (2002). The Organization of Behavior: A Neuropsychological Theory (Taylor & Francis).

Heinricher, M., and Ingram, S. (2008). The Brainstem and Nociceptive Modulation. In Science of Pain, pp. 593–626.

Heinrichs, M., Baumgartner, T., Kirschbaum, C., and Ehlert, U. (2003). Social support and oxytocin interact to suppress cortisol and subjective responses to psychosocial stress. Biol Psychiatry *54*, 1389–1398.

Heinrichs, M., von Dawans, B., and Domes, G. (2009). Oxytocin, vasopressin, and human social behavior. Front Neuroendocrinol *30*, 548–557.

Herget, U., Wolf, A., Wullimann, M.F., and Ryu, S. (2014). Molecular neuroanatomy and chemoarchitecture of the neurosecretory preoptic-hypothalamic area in zebrafish larvae. J Comp Neurol *522*, 1542–1564.

Hernández, J., Segarra, A.B., Ramírez, M., Banegas, I., de Gasparo, M., Alba, F., Vives, F., Durán, R., and Prieto, I. (2009). Stress influences brain enkephalinase, oxytocinase and angiotensinase activities: a new hypothesis. Neuropsychobiology *59*, 184–189.

Hertz, L. (1965). Possible role of neuroglia: a potassium-mediated neuronal--neuroglial--neuronal impulse transmission system. Nature *206*, 1091–1094.

Hertz, L. (1979). Inhibition by barbiturates of an intense net uptake of potassium into astrocytes. Neuropharmacology *18*, 629–632.

Hertz, L. (2011). Astrocytic energy metabolism and glutamate formation--relevance for 13C-NMR spectroscopy and importance of cytosolic/mitochondrial trafficking. Magn Reson Imaging *29*, 1319–1329.

Hertz, L. (2013). The Glutamate-Glutamine (GABA) Cycle: Importance of Late Postnatal Development and Potential Reciprocal Interactions between Biosynthesis and Degradation. Front Endocrinol (Lausanne) *4*, 59.

Hertz, L., and Chen, Y. (2016). Importance of astrocytes for potassium ion (K+) homeostasis in brain and glial effects of K+ and its transporters on learning. Neurosci Biobehav Rev *71*, 484–505.

Hertz, L., Dringen, R., Schousboe, A., and Robinson, S.R. (1999). Astrocytes: glutamate producers for neurons. J Neurosci Res *57*, 417–428.

Hinko, A., and Soloff, M.S. (1993). Up-regulation of oxytocin receptors in rabbit amnion by adenosine 3',5'-monophosphate. Endocrinology *132*, 126–132.

Hirase, H., Qian, L., Barthó, P., and Buzsáki, G. (2004). Calcium dynamics of cortical astrocytic networks in vivo. PLoS Biol *2*, E96.

Hirase, H., Iwai, Y., Takata, N., Shinohara, Y., and Mishima, T. (2014). Volume transmission signalling via astrocytes. Philos Trans R Soc Lond B Biol Sci *369*.

Hoare, S., Copland, J.A., Strakova, Z., Ives, K., Jeng, Y.J., Hellmich, M.R., and Soloff, M.S. (1999). The proximal portion of the COOH terminus of the oxytocin receptor is required for coupling to g(q), but not g(i). Independent mechanisms for elevating intracellular calcium concentrations from intracellular stores. J Biol Chem *274*, 28682–28689.

Hodgkin, A.L., and Huxley, A.F. (1952). Currents carried by sodium and potassium ions through the membrane of the giant axon of Loligo. J Physiol *116*, 449–472.

Hökfelt, T. (1991). Neuropeptides in perspective: the last ten years. Neuron *7*, 867–879.

Hol, E.M., and Pekny, M. (2015). Glial fibrillary acidic protein (GFAP) and the astrocyte intermediate filament system in diseases of the central nervous system. Curr Opin Cell Biol *32*, 121–130.

Holmgren, S., and Jensen, J. (2001). Evolution of vertebrate neuropeptides. Brain Research Bulletin *55*, 723–735.

Hösli, L., Hösli, E., Andrès, P.F., and Landolt, H. (1981). Evidence that the depolarization of glial cells by inhibitory amino acids is caused by an efflux of K+ from neurones. Exp Brain Res *42*, 43–48.

Houades, V., Rouach, N., Ezan, P., Kirchhoff, F., Koulakoff, A., and Giaume, C. (2006). Shapes of astrocyte networks in the juvenile brain. Neuron Glia Biol *2*, 3–14.

Houades, V., Koulakoff, A., Ezan, P., Seif, I., and Giaume, C. (2008). Gap junction-mediated astrocytic networks in the mouse barrel cortex. J Neurosci *28*, 5207–5217.

Howarth, C., Gleeson, P., and Attwell, D. (2012). Updated energy budgets for neural computation in the neocortex and cerebellum. J Cereb Blood Flow Metab *32*, 1222–1232.

Hrabovszky, E., and Liposits, Z. (2008). Novel Aspects of Glutamatergic Signalling in the Neuroendocrine System. Journal of Neuroendocrinology *20*, 743–751.

Hrabovszky, E., Kalló, I., Steinhauser, A., Merchenthaler, I., Coen, C.W., Petersen, S.L., and Liposits, Z. (2004). Estrogen receptor-β in oxytocin and vasopressin neurons of the rat and human hypothalamus: Immunocytochemical and in situ hybridization studies. Journal of Comparative Neurology *473*, 315–333.

Hu, B., Boyle, C.A., and Lei, S. (2020). Oxytocin receptors excite lateral nucleus of central amygdala by phospholipase Cβ- and protein kinase C-dependent depression of inwardly rectifying K+ channels. The Journal of Physiology *598*, 3501–3520.

Huber, D., Veinante, P., and Stoop, R. (2005). Vasopressin and Oxytocin Excite Distinct Neuronal Populations in the Central Amygdala. Science *308*, 245–248.

I

Ikeda, R., Takahashi, Y., Inoue, K., and Kato, F. (2007). NMDA receptor-independent synaptic plasticity in the central amygdala in the rat model of neuropathic pain. Pain *127*, 161–172.

Ishii, M., Naruse, K., Hattori, A., Tsujimoto, M., Ishiura, S., Numaguchi, Y., Murohara, T., Kobayashi, H., and Mizutani, S. (2009). Oxytocin hypersensitivity in pregnant P-LAP deficient mice. Life Sci *84*, 668–672.

Ivaska, J., Pallari, H.-M., Nevo, J., and Eriksson, J.E. (2007). Novel functions of vimentin in cell adhesion, migration, and signaling. Exp Cell Res *313*, 2050–2062.

Ivell, R., and Richter, D. (1984). Structure and comparison of the oxytocin and vasopressin genes from rat. Proc. Natl. Acad. Sci. U.S.A. *81*, 2006–2010.

Ivell, R., and Walther, N. (1999). The role of sex steroids in the oxytocin hormone system. Molecular and Cellular Endocrinology *151*, 95–101.

Ivell, R., Bathgate, R.A., Walther, N., and Kimura, T. (1998). The Molecular Basis of Oxytocin and Oxytocin Receptor Gene Expression in Reproductive Tissues. In Vasopressin and Oxytocin: Molecular, Cellular, and Clinical Advances, H.H. Zingg, C.W. Bourque, and D.G. Bichet, eds. (Boston, MA: Springer US), pp. 297–306.

Ivell, R., Kimura, T., Müller, D., Augustin, K., Abend, N., Bathgate, R., Telgmann, R., Balvers, M., Tillmann, G., and Fuchs, A.R. (2001). The structure and regulation of the oxytocin receptor. Exp Physiol *86*, 289–296.

J

Ja, A., Rc, M., Rr, V., and X, L. (2004). Anxiety and stress responses in female oxytocin deficient mice. J Neuroendocrinol *16*, 319–324.

Janak, P.H., and Tye, K.M. (2015). From circuits to behaviour in the amygdala. Nature *517*, 284–292.

Jeng, Y.-J., Lolait, S.J., and Soloff, M.S. (1998). Induction of Oxytocin Receptor Gene Expression in Rabbit Amnion Cells. Endocrinology *139*, 3449–3455.

Ji, G., Sun, H., Fu, Y., Li, Z., Pais-Vieira, M., Galhardo, V., and Neugebauer, V. (2010). Cognitive Impairment in Pain through Amygdala-Driven Prefrontal Cortical Deactivation. J Neurosci *30*, 5451–5464.

Ji, R.-R., Berta, T., and Nedergaard, M. (2013). Glia and pain: Is chronic pain a gliopathy? PAIN® *154*, S10–S28.

Jokinen, J., Chatzittofis, A., Hellström, C., Nordström, P., Uvnäs-Moberg, K., and Åsberg, M. (2012). Low CSF oxytocin reflects high intent in suicide attempters. Psychoneuroendocrinology *37*, 482–490.

Jones, H.C., and Keep, R.F. (1987). The control of potassium concentration in the cerebrospinal fluid and brain interstitial fluid of developing rats. J Physiol *383*, 441–453.

Jones, H.C., and Keep, R.F. (1988). Brain fluid calcium concentration and response to acute hypercalcaemia during development in the rat. J Physiol *402*, 579–593.

Jones, P.M., and Robinson, I.C. (1982). Differential clearance of neurophysin and neurohypophysial peptides from the cerebrospinal fluid in conscious guinea pigs. Neuroendocrinology *34*, 297–302.

Juif, P.-E., and Poisbeau, P. (2013). Neurohormonal effects of oxytocin and vasopressin receptor agonists on spinal pain processing in male rats. Pain *154*, 1449–1456.

Juif, P.-E., Breton, J.-D., Rajalu, M., Charlet, A., Goumon, Y., and Poisbeau, P. (2013). Long-lasting spinal oxytocin analgesia is ensured by the stimulation of allopregnanolone synthesis which potentiates GABA(A) receptor-mediated synaptic inhibition. J. Neurosci. *33*, 16617–16626.

Juif, P.-E., Salio, C., Zell, V., Melchior, M., Lacaud, A., Petit-Demouliere, N., Ferrini, F., Darbon, P., Hanesch, U., Anton, F., et al. (2016). Peripheral and central alterations affecting spinal nociceptive processing and pain at adulthood in rats exposed to neonatal maternal deprivation. Eur J Neurosci *44*, 1952–1962.

Jungblut, M., Tiveron, M.C., Barral, S., Abrahamsen, B., Knöbel, S., Pennartz, S., Schmitz, J., Perraut, M., Pfrieger, F.W., Stoffel, W., et al. (2012). Isolation and characterization of living primary astroglial cells using the new GLAST-specific monoclonal antibody ACSA-1. Glia *60*, 894–907.

Jurzak, M., Müller, A.R., and Gerstberger, R. (1995). Characterization of vasopressin receptors in cultured cells derived from the region of rat brain circumventricular organs. Neuroscience *65*, 1145–1159.

K

Kafitz, K.W., Meier, S.D., Stephan, J., and Rose, C.R. (2008). Developmental profile and properties of sulforhodamine 101--Labeled glial cells in acute brain slices of rat hippocampus. J Neurosci Methods *169*, 84–92.

Kagerbauer, S.M., Martin, J., Schuster, T., Blobner, M., Kochs, E.F., and Landgraf, R. (2013). Plasma oxytocin and vasopressin do not predict neuropeptide concentrations in human cerebrospinal fluid. J Neuroendocrinol *25*, 668–673.

Kamm, O., Aldrich, T.B., Grote, I.W., Rowe, L.W., and Bugbee, E.P. (1928). THE ACTIVE PRINCIPLES OF THE POSTERIOR LOBE OF THE PITUITARY GLAND.1 I. THE DEMONSTRATION OF THE PRESENCE OF TWO ACTIVE PRINCIPLES. II. THE SEPARATION OF THE TWO PRINCIPLES AND THEIR CONCENTRATION IN THE FORM OF POTENT SOLID PREPARATIONS. J. Am. Chem. Soc. *50*, 573–601.

Kang, J., Kang, N., Yu, Y., Zhang, J., Petersen, N., Tian, G.F., and Nedergaard, M. (2010). Sulforhodamine 101 induces long-term potentiation of intrinsic excitability and synaptic efficacy in hippocampal CA1 pyramidal neurons. Neuroscience *169*, 1601–1609.

Karpenko, I.A., Margathe, J.-F., Rodriguez, T., Pflimlin, E., Dupuis, E., Hibert, M., Durroux, T., and Bonnet, D. (2015). Selective Nonpeptidic Fluorescent Ligands for Oxytocin Receptor: Design, Synthesis, and Application to Time-Resolved FRET Binding Assay. J. Med. Chem. *58*, 2547–2552.

Kastanenka, K.V., Moreno-Bote, R., De Pittà, M., Perea, G., Eraso-Pichot, A., Masgrau, R., Poskanzer, K.E., and Galea, E. (2020). A roadmap to integrate astrocytes into Systems Neuroscience. Glia *68*, 5–26.

Keifer, O.P., Hurt, R.C., Ressler, K.J., and Marvar, P.J. (2015). The Physiology of Fear: Reconceptualizing the Role of the Central Amygdala in Fear Learning. Physiology (Bethesda) *30*, 389–401.

Kettenmann, H., and Schachner, M. (1985). Pharmacological properties of gamma-aminobutyric acid-, glutamate-, and aspartate-induced depolarizations in cultured astrocytes. J Neurosci *5*, 3295–3301.

Kettenmann, H., Backus, K.H., and Schachner, M. (1984). Aspartate, glutamate and gamma-aminobutyric acid depolarize cultured astrocytes. Neurosci Lett *52*, 25–29.

Kim, B., Yoon, S., Nakajima, R., Lee, H.J., Lim, H.J., Lee, Y.K., Choi, J.S., Yoon, B.J., Augustine, G.J., and Baik, J.H. (2018). Dopamine D2 receptor-mediated circuit from the central amygdala to the bed nucleus of the stria terminalis regulates impulsive behavior. PROC. NAT. ACAD. OF SCI. (U.S.A.) *115*, E10730–E10739.

Kimelberg, H.K. (2004). The problem of astrocyte identity. Neurochem Int *45*, 191–202.

Kimura, T., Makino, Y., Saji, F., Takemura, M., Inoue, T., Kikuchi, T., Kubota, Y., Azuma, C., Nobunaga, T., and Tokugawa, Y. (1994). Molecular characterization of a cloned human oxytocin receptor. Eur. J. Endocrinol. *131*, 385–390.

Kimura, T., Saji, F., Nishimori, K., Ogita, K., Nakamura, H., Koyama, M., and Murata, Y. (2003). Molecular regulation of the oxytocin receptor in peripheral organs. J Mol Endocrinol *30*, 109–115.

Kirischuk, S., and Verkhratsky, A. (1996). [Ca2+]i recordings from neural cells in acutely isolated cerebellar slices employing differential loading of the membrane-permeant form of the calcium indicator fura-2. Pflugers Arch *431*, 977–983.

Kirsch, P., Esslinger, C., Chen, Q., Mier, D., Lis, S., Siddhanti, S., Gruppe, H., Mattay, V.S., Gallhofer, B., and Meyer-Lindenberg, A. (2005). Oxytocin Modulates Neural Circuitry for Social Cognition and Fear in Humans. J. Neurosci. *25*, 11489–11493.

Kita, I., Yoshida, Y., and Nishino, S. (2006). An activation of parvocellular oxytocinergic neurons in the paraventricular nucleus in oxytocin-induced yawning and penile erection. Neurosci Res *54*, 269–275.

Kitamura, T., Ogawa, S.K., Roy, D.S., Okuyama, T., Morrissey, M.D., Smith, L.M., Redondo, R.L., and Tonegawa, S. (2017). Engrams and circuits crucial for systems consolidation of a memory. Science *356*, 73–78.

Kitoh, T., and Matsushita, M. (1980). A new staining method of astrocytes for paraffin section. Acta Neuropathologica *49*, 67–69.

Kiyama, H., and Emson, P.C. (1990). Evidence for the co-expression of oxytocin and vasopressin messenger ribonucleic acids in magnocellular neurosecretory cells: simultaneous demonstration of two neurohypophysin messenger ribonucleic acids by hybridization histochemistry. J. Neuroendocrinol. *2*, 257–259.

Kjaerby, C., Rasmussen, R., Andersen, M., and Nedergaard, M. (2017). Does Global Astrocytic Calcium Signaling Participate in Awake Brain State Transitions and Neuronal Circuit Function? Neurochem Res *42*, 1810–1822.

Klein, U., Gimpl, G., and Fahrenholz, F. (1995). Alteration of the Myometrial Plasma Membrane Cholesterol Content with .beta.-Cyclodextrin Modulates the Binding Affinity of the Oxytocin Receptor. Biochemistry *34*, 13784–13793.

Klenerova, V., Krejci, I., Sida, P., Hlinak, Z., and Hynie, S. (2009a). Modulary effects of oxytocin and carbetocin on stress-induced changes in rat behavior in the open-field. J Physiol Pharmacol *60*, 57–62.

Klenerova, V., Krejci, I., Sida, P., Hlinak, Z., and Hynie, S. (2009b). Oxytocin and carbetocin effects on spontaneous behavior of male rats: modulation by oxytocin receptor antagonists. Neuro Endocrinol Lett *30*, 335–342.

Knobloch, H.S., and Grinevich, V. (2014). Evolution of oxytocin pathways in the brain of vertebrates. Front Behav Neurosci *8*, 31.

Knobloch, H.S., Charlet, A., Hoffmann, L.C., Eliava, M., Khrulev, S., Cetin, A.H., Osten, P., Schwarz, M.K., Seeburg, P.H., Stoop, R., et al. (2012). Evoked Axonal Oxytocin Release in the Central Amygdala Attenuates Fear Response. Neuron *73*, 553–566.

Kofuji, P., and Newman, E.A. (2004). Potassium buffering in the central nervous system. Neuroscience *129*, 1045–1056.

Kol, A., Adamsky, A., Groysman, M., Kreisel, T., London, M., and Goshen, I. (2020). Astrocytes contribute to remote memory formation by modulating hippocampal–cortical communication during learning. Nature Neuroscience *23*, 1229–1239.

Kolber, B.J., Montana, M.C., Carrasquillo, Y., Xu, J., Heinemann, S.F., Muglia, L.J., and Gereau, R.W. (2010). Activation of Metabotropic Glutamate Receptor 5 in the Amygdala Modulates Pain-Like Behavior. J. Neurosci. *30*, 8203–8213.

von Kölliker, A. (1863). Handbuch der Gewebelehre des menschen für aerzte und studirende (Wilhelm Engelmann).

Koohi, M.K., Ivell, R., and Walther, N. (2005). Transcriptional Activation of the Oxytocin Promoter by Oestrogens Uses a Novel Non-Classical Mechanism of Oestrogen Receptor Action. Journal of Neuroendocrinology *17*, 197–207.

Krnjević, K., and Schwartz, S. (1967). Some properties of unresponsive cells in the cerebral cortex. Exp Brain Res *3*, 306–319.

Kubota, Y., Kimura, T., Hashimoto, K., Tokugawa, Y., Nobunaga, K., Azuma, C., Saji, F., and Murata, Y. (1996). Structure and expression of the mouse oxytocin receptor gene. Mol Cell Endocrinol *124*, 25–32.

Kucheryavykh, Y.V., Kucheryavykh, L.Y., Nichols, C.G., Maldonado, H.M., Baksi, K., Reichenbach, A., Skatchkov, S.N., and Eaton, M.J. (2007). Downregulation of Kir4.1 inward rectifying potassium channel subunits by RNAi impairs potassium transfer and glutamate uptake by cultured cortical astrocytes. Glia *55*, 274–281.

Kulkarni, B., Bentley, D.E., Elliott, R., Julyan, P.J., Boger, E., Watson, A., Boyle, Y., El-Deredy, W., and Jones, A.K.P. (2007). Arthritic pain is processed in brain areas concerned with emotions and fear. Arthritis Rheum *56*, 1345–1354.

Kumsta, R., Hummel, E., Chen, F.S., and Heinrichs, M. (2013). Epigenetic regulation of the oxytocin receptor gene: implications for behavioral neuroscience. Front Neurosci *7*, 83.

Kuo, J., Hariri, O.R., and Micevych, P. (2009). An interaction of oxytocin receptors with metabotropic glutamate receptors in hypothalamic astrocytes. J Neuroendocrinol *21*, 1001–1006.

Kusui, C., Kimura, T., Ogita, K., Nakamura, H., Matsumura, Y., Koyama, M., Azuma, C., and Murata, Y. (2001). DNA methylation of the human oxytocin receptor gene promoter regulates tissue-specific gene suppression. Biochem Biophys Res Commun *289*, 681–686.

L

Lalo, U., Pankratov, Y., Kirchhoff, F., North, R.A., and Verkhratsky, A. (2006). NMDA receptors mediate neuron-to-glia signaling in mouse cortical astrocytes. J Neurosci *26*, 2673–2683.

Lalo, U., Palygin, O., North, R.A., Verkhratsky, A., and Pankratov, Y. (2011). Age-dependent remodelling of ionotropic signalling in cortical astroglia. Aging Cell *10*, 392–402.

Lambert, R.C., Moos, F.C., and Richard, P. (1993). Action of endogenous oxytocin within the paraventricular or supraoptic nuclei: a powerful link in the regulation of the bursting pattern of oxytocin neurons during the milk-ejection reflex in rats. Neuroscience *57*, 1027–1038.

Landgraf, R., and Neumann, I.D. (2004). Vasopressin and oxytocin release within the brain: a dynamic concept of multiple and variable modes of neuropeptide communication. Front Neuroendocrinol *25*, 150–176.

Landry, M., and Hökfelt, T. (1998). Subcellular localization of preprogalanin messenger RNA in perikarya and axons of hypothalamo-posthypophyseal magnocellular neurons: an in situ hybridization study. Neuroscience *84*, 897–912.

Landry, M., Trembleau, A., Arai, R., and Calas, A. (1991). Evidence for a colocalization of oxytocin mRNA and galanin in magnocellular hypothalamic neurons: a study combining in situ hybridization and immunohistochemistry. Molecular Brain Research *10*, 91–95.

Larcher, A., Neculcea, J., Chu, K., and Zingg, H.H. (1995). Effects of retinoic acid and estrogens on oxytocin gene expression in the rat uterus: in vitro and in vivo studies. Mol. Cell. Endocrinol. *114*, 69–76.

Larsen, B.R., and MacAulay, N. (2014). Kir4.1-mediated spatial buffering of K(+): experimental challenges in determination of its temporal and quantitative contribution to K(+) clearance in the brain. Channels (Austin) *8*, 544–550.

Larsen, B.R., Assentoft, M., Cotrina, M.L., Hua, S.Z., Nedergaard, M., Kaila, K., Voipio, J., and MacAulay, N. (2014). Contributions of the Na^+/K^+-ATPase, NKCC1, and Kir4.1 to hippocampal K^+ clearance and volume responses. Glia *62*, 608–622.

Larsen, B.R., Stoica, A., and MacAulay, N. (2016). Managing Brain Extracellular K(+) during Neuronal Activity: The Physiological Role of the Na(+)/K(+)-ATPase Subunit Isoforms. Front Physiol *7*, 141.

Larsen, P., Mikkelsen, J., Jessop, D., Lightman, S., and Chowdrey, H. (1993). Neuropeptide Y mRNA and immunoreactivity in hypothalamic neuroendocrine neurons: effects of adrenalectomy and chronic osmotic stimulation. J Neurosci *13*, 1138–1147.

Lee, S.-H., and Dan, Y. (2012). Neuromodulation of brain states. Neuron *76*, 209–222.

Lee, H.-J., Macbeth, A.H., Pagani, J.H., and Young, W.S. (2009). Oxytocin: the great facilitator of life. Prog. Neurobiol. *88*, 127–151.

Leeuwen, F.W. van (Netherlands C.I. for B.R., and Swaab, D.F. (1977). Specific immunoelectronmicroscopic localization of vasopressin and oxytocin in the rat neurohypophysis. Journal of Endocrinology (UK).

Leng, G., and Ludwig, M. (2008). Neurotransmitters and peptides: whispered secrets and public announcements. J Physiol *586*, 5625–5632.

Lenhossék (1893). Der feinere Bau des Nervensystems im Lichte neuester Forschungen (Fischer).

Letellier, M., Park, Y.K., Chater, T.E., Chipman, P.H., Gautam, S.G., Oshima-Takago, T., and Goda, Y. (2016). Astrocytes regulate heterogeneity of presynaptic strengths in hippocampal networks. Proc Natl Acad Sci U S A *113*, E2685-2694.

Li, H., Penzo, M.A., Taniguchi, H., Kopec, C.D., Huang, Z.J., and Li, B. (2013). Experience-dependent modification of a central amygdala fear circuit. Nat Neurosci *16*, 332–339.

Li, Y., Li, L., Wu, J., Zhu, Z., Feng, X., Qin, L., Zhu, Y., Sun, L., Liu, Y., Qiu, Z., et al. (2020). Activation of astrocytes in hippocampus decreases fear memory through adenosine A1 receptors. ELife *9*, e57155.

Li, Z., Ji, G., and Neugebauer, V. (2011). Mitochondrial reactive oxygen species are activated by mGluR5 through IP3 and activate ERK and PKA to increase excitability of amygdala neurons and pain behavior. J Neurosci *31*, 1114–1127.

Lipkin, S.M., Nelson, C.A., Glass, C.K., and Rosenfeld, M.G. (1992). A negative retinoic acid response element in the rat oxytocin promoter restricts transcriptional stimulation by heterologous transactivation domains. Proc Natl Acad Sci U S A *89*, 1209–1213.

Love, T.M. (2014). Oxytocin, Motivation and the Role of Dopamine. Pharmacol Biochem Behav *0*, 49–60.

Ludwig (1998). Dendritic Release of Vasopressin and Oxytocin. Journal of Neuroendocrinology *10*, 881–895.

Ludwig, M., and Leng, G. (2006). Dendritic peptide release and peptide-dependent behaviours. Nature Reviews Neuroscience *7*, 126–136.

Ludwig, M., Apps, D., Menzies, J., Patel, J.C., and Rice, M.E. (2016). Dendritic release of neurotransmitters. Compr Physiol *7*, 235–252.

Ludwin, S.K., Kosek, J.C., and Eng, L.F. (1976). The topographical distribution of S-100 and GFA proteins in the adult rat brain: an immunohistochemical study using horseradish peroxidase-labelled antibodies. Journal of Comparative Neurology *165*, 197–207.

Lugaro, E. (1907). Sulle funzioni della nevroglia. Riv Patol Nerv Ment *12*, 225–233.

Luttrell, L.M., Maudsley, S., and Bohn, L.M. (2015). Fulfilling the Promise of “Biased” G Protein-Coupled Receptor Agonism. Mol Pharmacol *88*, 579–588.

M

Maniezzi, C., Talpo, F., Spaiardi, P., Toselli, M., and Biella, G. (2019). Oxytocin Increases Phasic and Tonic GABAergic Transmission in CA1 Region of Mouse Hippocampus. Front Cell Neurosci *13*.

Mantella, R.C., Vollmer, R.R., Li, X., and Amico, J.A. (2003). Female Oxytocin-Deficient Mice Display Enhanced Anxiety-Related Behavior. Endocrinology *144*, 2291–2296.

Manzini, I., Schweer, T.-S., and Schild, D. (2008). Improved fluorescent (calcium indicator) dye uptake in brain slices by blocking multidrug resistance transporters. J Neurosci Methods *167*, 140–147.

Marcaggi, P., and Attwell, D. (2004). Role of glial amino acid transporters in synaptic transmission and brain energetics. Glia *47*, 217–225.

Marcaggi, P., Jeanne, M., and Coles, J.A. (2004). Neuron-glial trafficking of NH4+ and K+: separate routes of uptake into glial cells of bee retina. Eur J Neurosci *19*, 966–976.

Marlin, B.J., Mitre, M., D'amour, J.A., Chao, M.V., and Froemke, R.C. (2015). Oxytocin enables maternal behaviour by balancing cortical inhibition. Nature *520*, 499–504.

Martín, R., Bajo-Grañeras, R., Moratalla, R., Perea, G., and Araque, A. (2015). Circuit-specific signaling in astrocyte-neuron networks in basal ganglia pathways. Science *349*, 730–734.

Martínez-Lorenzana, G., Espinosa-López, L., Carranza, M., Aramburo, C., Paz-Tres, C., Rojas-Piloni, G., and Condés-Lara, M. (2008). PVN electrical stimulation prolongs withdrawal latencies and releases oxytocin in cerebrospinal fluid, plasma, and spinal cord tissue in intact and neuropathic rats. Pain *140*, 265–273.

Massie, A., Schallier, A., Kim, S.W., Fernando, R., Kobayashi, S., Beck, H., De Bundel, D., Vermoesen, K., Bannai, S., Smolders, I., et al. (2011). Dopaminergic neurons of system x(c)$^-$-deficient mice are highly protected against 6-hydroxydopamine-induced toxicity. FASEB J *25*, 1359–1369.

Mayer, M.L. (2011). Structure and mechanism of glutamate receptor ion channel assembly, activation and modulation. Curr Opin Neurobiol *21*, 283–290.

McCarthy, M.M., McDonald, C.H., Brooks, P.J., and Goldman, D. (1996). An anxiolytic action of oxytocin is enhanced by estrogen in the mouse. Physiol Behav *60*, 1209–1215.

McCormick, D.A., Nestvogel, D.B., and He, B.J. (2020). Neuromodulation of Brain State and Behavior. Annu. Rev. Neurosci. *43*, 391–415.

McEwen, B.B. (2004). General Introduction to Vasopressin and Oxytocin: Structure ⁄ Metabolism, Evolutionary Aspects, Neural Pathway ⁄ Receptor Distribution, and Functional Aspects Relevant to Memory Processing. In Advances in Pharmacology, (Academic Press), pp. 1–50.

Meddle, S.L., Bishop, V.R., Gkoumassi, E., van Leeuwen, F.W., and Douglas, A.J. (2007). Dynamic changes in oxytocin receptor expression and activation at parturition in the rat brain. Endocrinology *148*, 5095–5104.

Meeker, R.B., Swanson, D.J., Greenwood, R.S., and Hayward, J.N. (1991). Ultrastructural distribution of glutamate immunoreactivity within neurosecretory endings and pituicytes of the rat neurohypophysis. Brain Research *564*, 181–193.

Meme, W., Vandecasteele, M., Giaume, C., and Venance, L. (2009). Electrical coupling between hippocampal astrocytes in rat brain slices. Neurosci Res *63*, 236–243.

Mens, W.B., Witter, A., and van Wimersma Greidanus, T.B. (1983). Penetration of neurohypophyseal hormones from plasma into cerebrospinal fluid (CSF): half-times of disappearance of these neuropeptides from CSF. Brain Res *262*, 143–149.

Milad, M.R., and Quirk, G.J. (2012). Fear Extinction as a Model for Translational Neuroscience: Ten Years of Progress. Annu Rev Psychol *63*, 129–151.

Milad, M.R., Wright, C.I., Orr, S.P., Pitman, R.K., Quirk, G.J., and Rauch, S.L. (2007). Recall of fear extinction in humans activates the ventromedial prefrontal cortex and hippocampus in concert. Biol Psychiatry *62*, 446–454.

Mills, S.E.E., Nicolson, K.P., and Smith, B.H. (2019). Chronic pain: a review of its epidemiology and associated factors in population-based studies. Br J Anaesth *123*, e273–e283.

Miranda-Cardenas, Y., Rojas-Piloni, G., Martínez-Lorenzana, G., Rodríguez-Jiménez, J., López-Hidalgo, M., Freund-Mercier, M.J., and Condés-Lara, M. (2006). Oxytocin and electrical stimulation of the paraventricular hypothalamic nucleus produce antinociceptive effects that are reversed by an oxytocin antagonist. Pain *122*, 182–189.

Mishima, T., and Hirase, H. (2010). In vivo intracellular recording suggests that gray matter astrocytes in mature cerebral cortex and hippocampus are electrophysiologically homogeneous. J Neurosci *30*, 3093–3100.

Mishima, T., Sakatani, S., and Hirase, H. (2007). Intracellular labeling of single cortical astrocytes in vivo. J Neurosci Methods *166*, 32–40.

Mitre, M., Marlin, B.J., Schiavo, J.K., Morina, E., Norden, S.E., Hackett, T.A., Aoki, C.J., Chao, M.V., and Froemke, R.C. (2016). A Distributed Network for Social Cognition Enriched for Oxytocin Receptors. J Neurosci *36*, 2517–2535.

Mohr, E., Hillers, M., Ivell, R., Haulica, I.D., and Richter, D. (1985). Expression of the vasopressin and oxytocin genes in human hypothalami. FEBS Letters *193*, 12–16.

Monai, H., and Hirase, H. (2018). Astrocytes as a target of transcranial direct current stimulation (tDCS) to treat depression. Neurosci Res *126*, 15–21.

Moore, C.A.C., Milano, S.K., and Benovic, J.L. (2007). Regulation of receptor trafficking by GRKs and arrestins. Annu Rev Physiol *69*, 451–482.

de la Mora, M.P., Pérez-Carrera, D., Crespo-Ramírez, M., Tarakanov, A., Fuxe, K., and Borroto-Escuela, D.O. (2016). Signaling in dopamine D2 receptor-oxytocin receptor heterocomplexes and its relevance for the anxiolytic effects of dopamine and oxytocin interactions in the amygdala of the rat. Biochimica et Biophysica Acta (BBA) - Molecular Basis of Disease *1862*, 2075–2085.

Moreno-López, Y., Martínez-Lorenzana, G., Condés-Lara, M., and Rojas-Piloni, G. (2013). Identification of oxytocin receptor in the dorsal horn and nociceptive dorsal root ganglion neurons. Neuropeptides *47*, 117–123.

Morin, V., Del Castillo, J.R.E., Authier, S., Ybarra, N., Otis, C., Gauvin, D., Gutkowska, J., and Troncy, E. (2008). Evidence for non-linear pharmacokinetics of oxytocin in anesthetizetized rat. J Pharm Pharm Sci *11*, 12–24.

Morris, J.F., and Pow, D.V. (1991). Widespread release of peptides in the central nervous system: quantitation of tannic acid-captured exocytoses. Anat Rec *231*, 437–445.

Moussawi, K., Riegel, A., Nair, S., and Kalivas, P.W. (2011). Extracellular glutamate: functional compartments operate in different concentration ranges. Front Syst Neurosci *5*, 94.

Mugnaini, E. (1986). Astrocytes, Vol I (London: Academic Press).

Murphy, D., and Wells, S. (2003). In vivo gene transfer studies on the regulation and function of the vasopressin and oxytocin genes. J. Neuroendocrinol. *15*, 109–125.

Murray, J.E., Belin-Rauscent, A., Simon, M., Giuliano, C., Benoit-Marand, M., Everitt, B.J., and Belin, D. (2015). Basolateral and central amygdala differentially recruit and maintain dorsolateral striatum-dependent cocaine-seeking habits. Nature Communications *6*, 10088.

N

Nagelhus, E.A., and Ottersen, O.P. (2013). Physiological roles of aquaporin-4 in brain. Physiol Rev *93*, 1543–1562.

Nagy, J.I., Patel, D., Ochalski, P.A., and Stelmack, G.L. (1999). Connexin30 in rodent, cat and human brain: selective expression in gray matter astrocytes, co-localization with connexin43 at gap junctions and late developmental appearance. Neuroscience *88*, 447–468.

Naoumenko, J., and Feigin, I. (1961). A modification for paraffin sections of the Cajal gold-sublimate stain for astrocytes. Journal of Neuropathology & Experimental Neurology *20*, 602–604.

Nasanbuyan, N., Yoshida, M., Takayanagi, Y., Inutsuka, A., Nishimori, K., Yamanaka, A., and Onaka, T. (2018). Oxytocin-Oxytocin Receptor Systems Facilitate Social Defeat Posture in Male Mice. Endocrinology *159*, 763–775.

Navarrete, M., and Araque, A. (2010). Endocannabinoids potentiate synaptic transmission through stimulation of astrocytes. Neuron *68*, 113–126.

Navone, F., and Di Gioia, G. (1988). [Microvesicles of secretory nerve endings of the neurohypophysis are biochemically similar to small synaptic vesicles of nerve terminals]. Ann Ist Super Sanita *24*, 507–510.

Neugebauer, V. (2007). The amygdala: different pains, different mechanisms. Pain *127*, 1–2.

Neugebauer, V. (2015). 15. Amygdala pain mechanisms. Handb Exp Pharmacol *227*, 261–284.

Neugebauer, V., Li, W., Bird, G.C., Bhave, G., and Gereau, R.W. (2003). Synaptic plasticity in the amygdala in a model of arthritic pain: differential roles of metabotropic glutamate receptors 1 and 5. J Neurosci *23*, 52–63.

Neugebauer, V., Li, W., Bird, G.C., and Han, J.S. (2004). The amygdala and persistent pain. Neuroscientist *10*, 221–234.

Neugebauer, V., Galhardo, V., Maione, S., and Mackey, S.C. (2009). Forebrain pain mechanisms. Brain Res Rev *60*, 226–242.

Neumann, I.D., and Landgraf, R. (2012). Balance of brain oxytocin and vasopressin: implications for anxiety, depression, and social behaviors. Trends Neurosci *35*, 649–659.

Neumann, I.D., Wigger, A., Torner, L., Holsboer, F., and Landgraf, R. (2000). Brain oxytocin inhibits basal and stress-induced activity of the hypothalamo-pituitary-adrenal axis in male and female rats: partial action within the paraventricular nucleus. J Neuroendocrinol *12*, 235–243.

Neusch, C., Rozengurt, N., Jacobs, R.E., Lester, H.A., and Kofuji, P. (2001). Kir4.1 potassium channel subunit is crucial for oligodendrocyte development and in vivo myelination. J Neurosci *21*, 5429–5438.

Newman, E.A., Frambach, D.A., and Odette, L.L. (1984). Control of extracellular potassium levels by retinal glial cell K+ siphoning. Science *225*, 1174–1175.

Neymeyer, V., Tephly, T.R., and Miller, M.W. (1997). Folate and 10-formyltetrahydrofolate dehydrogenase (FDH) expression in the central nervous system of the mature rat. Brain Res *766*, 195–204.

Nicholson, B., and Verma, S. (2004). Comorbidities in chronic neuropathic pain. Pain Med *5 Suppl 1*, S9–S27.

Nickel, R., and Forge, A. (2008). Gap junctions and connexins in the inner ear: their roles in homeostasis and deafness. Curr Opin Otolaryngol Head Neck Surg *16*, 452–457.

Nielsen, S., Nagelhus, E.A., Amiry-Moghaddam, M., Bourque, C., Agre, P., and Ottersen, O.P. (1997). Specialized membrane domains for water transport in glial cells: high-resolution immunogold cytochemistry of aquaporin-4 in rat brain. J Neurosci *17*, 171–180.

Nimmerjahn, A., Kirchhoff, F., Kerr, J.N.D., and Helmchen, F. (2004). Sulforhodamine 101 as a specific marker of astroglia in the neocortex in vivo. Nat Methods *1*, 31–37.

Nishiyama, H., Knopfel, T., Endo, S., and Itohara, S. (2002). Glial protein S100B modulates long-term neuronal synaptic plasticity. Proc Natl Acad Sci U S A *99*, 4037–4042.

Niswender, C.M., and Conn, P.J. (2010). Metabotropic Glutamate Receptors: Physiology, Pharmacology, and Disease. Annu Rev Pharmacol Toxicol *50*, 295–322.

Nolte, C., Matyash, M., Pivneva, T., Schipke, C.G., Ohlemeyer, C., Hanisch, U.K., Kirchhoff, F., and Kettenmann, H. (2001). GFAP promoter-controlled EGFP-expressing transgenic mice: a tool to visualize astrocytes and astrogliosis in living brain tissue. Glia *33*, 72–86.

Nomura, M., McKenna, E., Korach, K.S., Pfaff, D.W., and Ogawa, S. (2002). Estrogen receptor-beta regulates transcript levels for oxytocin and arginine vasopressin in the hypothalamic paraventricular nucleus of male mice. Brain Res. Mol. Brain Res. *109*, 84–94.

Nomura, S., Ito, T., Yamamoto, E., Sumigama, S., Iwase, A., Okada, M., Shibata, K., Ando, H., Ino, K., Kikkawa, F., et al. (2005). Gene regulation and physiological function of placental leucine aminopeptidase/oxytocinase during pregnancy. Biochim Biophys Acta *1751*, 19–25.

Norenberg, M.D., and Martinez-Hernandez, A. (1979). Fine structural localization of glutamine synthetase in astrocytes of rat brain. Brain Res *161*, 303–310.

North, R.A. (2002). Molecular physiology of P2X receptors. Physiol Rev *82*, 1013–1067.

Northington, F.J., Traystman, R.J., Koehler, R.C., Rothstein, J.D., and Martin, L.J. (1998). Regional and cellular expression of glial (GLT1) and neuronal (EAAC1) glutamate transporter proteins in ovine fetal brain. Neuroscience *85*, 1183–1194.

Notturno, F., Capasso, M., DeLauretis, A., Carpo, M., and Uncini, A. (2009). Glial fibrillary acidic protein as a marker of axonal damage in chronic neuropathies. Muscle Nerve *40*, 50–54.

Nwaobi, S.E., Cuddapah, V.A., Patterson, K.C., Randolph, A.C., and Olsen, M.L. (2016). The role of glial-specific Kir4.1 in normal and pathological states of the CNS. Acta Neuropathol *132*, 1–21.

O

Oakley, R.H., Laporte, S.A., Holt, J.A., Barak, L.S., and Caron, M.G. (2001). Molecular determinants underlying the formation of stable intracellular G protein-coupled receptor-beta-arrestin complexes after receptor endocytosis*. J Biol Chem *276*, 19452–19460.

Oettl, L.-L., Ravi, N., Schneider, M., Scheller, M.F., Schneider, P., Mitre, M., Gouveia, M. da S., Froemke, R.C., Chao, M.V., Young, W.S., et al. (2016). Oxytocin Enhances Social Recognition by Modulating Cortical Control of Early Olfactory Processing. Neuron *90*, 609–621.

Ogata, K., and Kosaka, T. (2002). Structural and quantitative analysis of astrocytes in the mouse hippocampus. Neuroscience *113*, 221–233.

Oliveira, J.F., Sardinha, V.M., Guerra-Gomes, S., Araque, A., and Sousa, N. (2015). Do stars govern our actions? Astrocyte involvement in rodent behavior. Trends Neurosci *38*, 535–549.

Olsen, M.L., Higashimori, H., Campbell, S.L., Hablitz, J.J., and Sontheimer, H. (2006). Functional expression of Kir4.1 channels in spinal cord astrocytes. Glia *53*, 516–528.

Olude, M.A., Mustapha, O.A., Aderounmu, O.A., Olopade, J.O., and Ihunwo, A.O. (2015). Astrocyte morphology, heterogeneity, and density in the developing African giant rat (Cricetomys gambianus). Front Neuroanat *9*.

Orkand, R.K., Nicholls, J.G., and Kuffler, S.W. (1966). Effect of nerve impulses on the membrane potential of glial cells in the central nervous system of amphibia. J Neurophysiol *29*, 788–806.

P

Pagani, J.H., Lee, H.-J., and Young, W.S. (2011). Postweaning, forebrain-specific perturbation of the oxytocin system impairs fear conditioning. Genes Brain Behav *10*, 710–719.

Pais-Vieira, M., Mendes-Pinto, M.M., Lima, D., and Galhardo, V. (2009). Cognitive impairment of prefrontal-dependent decision-making in rats after the onset of chronic pain. Neuroscience *161*, 671–679.

Palazzo, E., Marabese, I., Soukupova, M., Luongo, L., Boccella, S., Giordano, C., de Novellis, V., Rossi, F., and Maione, S. (2011). Metabotropic Glutamate Receptor Subtype 8 in the Amygdala Modulates Thermal Threshold, Neurotransmitter Release, and Rostral Ventromedial Medulla Cell Activity in Inflammatory Pain. J Neurosci *31*, 4687–4697.

Papouin, T., Dunphy, J.M., Tolman, M., Dineley, K.T., and Haydon, P.G. (2017). Septal Cholinergic Neuromodulation Tunes the Astrocyte-Dependent Gating of Hippocampal NMDA Receptors to Wakefulness. Neuron *94*, 840-854.e7.

Paré, P., Paixão-Côrtes, V.R., Tovo-Rodrigues, L., Vargas-Pinilla, P., Viscardi, L.H., Salzano, F.M., Henkes, L.E., Bortolini, M.C., Paré, P., Paixão-Côrtes, V.R., et al. (2016). Oxytocin and arginine vasopressin receptor evolution: implications for adaptive novelties in placental mammals. Genetics and Molecular Biology *39*, 646–657.

Parpura, V., Heneka, M.T., Montana, V., Oliet, S.H.R., Schousboe, A., Haydon, Philip.G., Stout, R.F., Spray, D.C., Reichenbach, A., Pannicke, T., et al. (2012). Glial cells in (patho)physiology. J Neurochem *121*, 4–27.

Passoni, I., Leonzino, M., Gigliucci, V., Chini, B., and Busnelli, M. (2016). Carbetocin is a Functional Selective Gq Agonist That Does Not Promote Oxytocin Receptor Recycling After Inducing β-Arrestin-Independent Internalisation. J Neuroendocrinol *28*.

Patchev, V.K., Schlosser, S.F., Hassan, A.H.S., and Almeida, O.F.X. (1993). Oxytocin binding sites in rat limbic and hypothalamic structures: Site-specific modulation by adrenal and gonadal steroids. Neuroscience *57*, 537–543.

Patisaul, H.B., Scordalakes, E.M., Young, L.J., and Rissman, E.F. (2003). Oxytocin, But Not Oxytocin Receptor, is Regulated by Oestrogen Receptor β in the Female Mouse Hypothalamus. Journal of Neuroendocrinology *15*, 787–793.

Pekny, M., Johansson, C.B., Eliasson, C., Stakeberg, J., Wallén, Å., Perlmann, T., Lendahl, U., Betsholtz, C., Berthold, C.-H., and Frisén, J. (1999). Abnormal Reaction to Central Nervous System Injury in Mice Lacking Glial Fibrillary Acidic Protein and Vimentin. J Cell Biol *145*, 503–514.

Pekny, T., Faiz, M., Wilhelmsson, U., Curtis, M.A., Matej, R., Skalli, O., and Pekny, M. (2014). Synemin is expressed in reactive astrocytes and Rosenthal fibers in Alexander disease. APMIS *122*, 76–80.

Pereira, A., dos Santos, R.P., and Barros, R.F. (2013). The Calcium Wave Model of the Perception-Action Cycle: Evidence from Semantic Relevance in Memory Experiments. Front Psychol *4*.

Pereira Jr, A., and Furlan, F.A. (2010). Astrocytes and human cognition: modeling information integration and modulation of neuronal activity. Progress in Neurobiology *92*, 405–420.

Peris, J., MacFadyen, K., Smith, J.A., de Kloet, A.D., Wang, L., and Krause, E.G. (2017). Oxytocin Receptors Are Expressed on Dopamine and Glutamate Neurons in the Mouse Ventral Tegmental Area That Project to Nucleus Accumbens and Other Mesolimbic Targets. J Comp Neurol *525*, 1094–1108.

Petersson, M., Alster, P., Lundeberg, T., and Uvnäs-Moberg, K. (1996). Oxytocin increases nociceptive thresholds in a long-term perspective in female and male rats. Neurosci. Lett. *212*, 87–90.

Phaneuf, S., Europe-Finner, G.N., Varney, M., MacKenzie, I.Z., Watson, S.P., and Bernal, A.L. (1993). Oxytocin-stimulated phosphoinositide hydrolysis in human myometrial cells: involvement of pertussis toxin-sensitive and -insensitive G-proteins. Journal of Endocrinology *136*, 497-NP.

Phelps, E.A., and LeDoux, J.E. (2005). Contributions of the amygdala to emotion processing: from animal models to human behavior. Neuron *48*, 175–187.

Pitkänen, A., Savander, V., and LeDoux, J.E. (1997). Organization of intra-amygdaloid circuitries in the rat: an emerging framework for understanding functions of the amygdala. Trends Neurosci *20*, 517–523.

Plested, C.P., and Bernal, A.L. (2001). Desensitisation of the Oxytocin Receptor and other G-Protein Coupled Receptors in the Human Myometrium. Experimental Physiology *86*, 303–312.

PliEika, V., Heiniger, J., Muller-Lhotsky, A., and Pliska, P. Binding of Oxytocin to Uterine Cells in Vitro. 6.

Ponzio, T., Ni, Y., Montana, V., Parpura, V., and Hatton, G. (2006). Vesicular Glutamate Transporter Expression in Supraoptic Neurones Suggests a Glutamatergic Phenotype. J Neuroendocrinol *18*, 253–265.

Poskanzer, K.E., and Yuste, R. (2016). Astrocytes regulate cortical state switching in vivo. PNAS *113*, E2675–E2684.

Pow, D.V., and Morris, J.F. (1989). Dendrites of hypothalamic magnocellular neurons release neurohypophysial peptides by exocytosis. Neuroscience *32*, 435–439.

Pretel, S., and Piekut, D.T. (1990). Coexistence of CRF peptide and oxytocin mRNA in the paraventricular nucleus. Peptides *11*, 621–624.

Price, D.D. (2000). Psychological and neural mechanisms of the affective dimension of pain. Science *288*, 1769–1772.

Price, J.L. (2003). Comparative Aspects of Amygdala Connectivity. Annals of the New York Academy of Sciences *985*, 50–58.

Puder, B.A., and Papka, R.E. (2001). Hypothalamic paraventricular axons projecting to the female rat lumbosacral spinal cord contain oxytocin immunoreactivity. Journal of Neuroscience Research *64*, 53–60.

Puglia, M.H., Lillard, T.S., Morris, J.P., and Connelly, J.J. (2015). Epigenetic modification of the oxytocin receptor gene influences the perception of anger and fear in the human brain. PNAS *112*, 3308–3313.

Purves, D., Augustine, G.J., Fitzpatrick, D., Katz, L.C., LaMantia, A.-S., McNamara, J.O., and Williams, S.M. (2001). The Integration of Emotional Behavior. Neuroscience. 2nd Edition.

Q

Qusous, A., Geewan, C.S.V., Greenwell, P., and Kerrigan, M.J.P. (2011). siRNA-mediated inhibition of Na(+)-K(+)-2Cl- cotransporter (NKCC1) and regulatory volume increase in the chondrocyte cell line C-20/A4. J Membr Biol *243*, 25–34.

R

Ramon y Cajal, S. (1895). Algunas conjecturas sobre el mecanismo anatomico de la ideacion. Revista Medica y Cirugia Practicas *36*, 479–508.

Ransom, C.B., Ransom, B.R., and Sontheimer, H. (2000). Activity-dependent extracellular K+ accumulation in rat optic nerve: the role of glial and axonal Na+ pumps. J Physiol *522*, 427–442.

Rao, V.V.N.G., Löffler, C., Battey, J., and Hansmann, I. (1992). The human gene for Oxytocin-neurophysin I (OXT) is physically mapped to chromosome 20p13 by in situ hybridization. CGR *61*, 271–273.

Raponi, E., Agenes, F., Delphin, C., Assard, N., Baudier, J., Legraverend, C., and Deloulme, J.-C. (2007). S100B expression defines a state in which GFAP-expressing cells lose their neural stem cell potential and acquire a more mature developmental stage. Glia *55*, 165–177.

Rash, J.A., Aguirre-Camacho, A., and Campbell, T.S. (2014). Oxytocin and pain: a systematic review and synthesis of findings. Clin J Pain *30*, 453–462.

Rash, J.E., Yasumura, T., Dudek, F.E., and Nagy, J.I. (2001). Cell-specific expression of connexins and evidence of restricted gap junctional coupling between glial cells and between neurons. J Neurosci *21*, 1983–2000.

Rasmussen, R., Nedergaard, M., and Petersen, N.C. (2016). Sulforhodamine 101, a widely used astrocyte marker, can induce cortical seizure-like activity at concentrations commonly used. Sci Rep *6*, 30433.

Reiter, M.K., Kremarik, P., Freund-Mercier, M.J., Stoeckel, M.E., Desaulles, E., and Feltz, P. (1994). Localization of oxytocin binding sites in the thoracic and upper lumbar spinal cord of the adult and postnatal rat: a histoautoradiographic study. Eur J Neurosci *6*, 98–104.

Renaud, L.P., and Bourque, C.W. (1991). Neurophysiology and neuropharmacology of hypothalamic magnocellular neurons secreting vasopressin and oxytocin. Prog Neurobiol *36*, 131–169.

Reversi, A., Cassoni, P., and Chini, B. (2005a). Oxytocin receptor signaling in myoepithelial and cancer cells. J Mammary Gland Biol Neoplasia *10*, 221–229.

Reversi, A., Rimoldi, V., Marrocco, T., Cassoni, P., Bussolati, G., Parenti, M., and Chini, B. (2005b). The oxytocin receptor antagonist atosiban inhibits cell growth via a “biased agonist” mechanism. J Biol Chem *280*, 16311–16318.

Rhodes, C.H., Morrell, J.I., and Pfaff, D.W. (1981). Immunohistochemical analysis of magnocellular elements in rat hypothalamus: distribution and numbers of cells containing neurophysin, oxytocin, and vasopressin. J Comp Neurol *198*, 45–64.

Rhudy, J.L., Williams, A.E., McCabe, K.M., Russell, J.L., and Maynard, L.J. (2008). Emotional control of nociceptive reactions (ECON): do affective valence and arousal play a role? Pain *136*, 250–261.

Rice, M.E., and Nicholson, C. (1990). Glutamate- and aspartate-induced extracellular potassium and calcium shifts and their relation to those of kainate, quisqualate and N-methyl-D-aspartate in the isolated turtle cerebellum. Neuroscience *38*, 295–310.

Richard, S., and Zingg, H.H. (1990). The human oxytocin gene promoter is regulated by estrogens. J. Biol. Chem. *265*, 6098–6103.

Rickmann, M., and Wolff, J.R. (1995). S100 protein expression in subpopulations of neurons of rat brain. Neuroscience *67*, 977–991.

Rimoldi, V., Reversi, A., Taverna, E., Rosa, P., Francolini, M., Cassoni, P., Parenti, M., and Chini, B. (2003). Oxytocin receptor elicits different EGFR/MAPK activation patterns depending on its localization in caveolin-1 enriched domains. Oncogene *22*, 6054–6060.

Robin, L.M., Oliveira da Cruz, J.F., Langlais, V.C., Martin-Fernandez, M., Metna-Laurent, M., Busquets-Garcia, A., Bellocchio, L., Soria-Gomez, E., Papouin, T., Varilh, M., et al. (2018). Astroglial CB1 Receptors Determine Synaptic D-Serine Availability to Enable Recognition Memory. Neuron *98*, 935-944.e5.

Robinson, S.R. (2001). Changes in the cellular distribution of glutamine synthetase in Alzheimer’s disease. J Neurosci Res *66*, 972–980.

Robinson, C., Schumann, R., Zhang, P., and Young, R.C. (2003). Oxytocin-induced desensitization of the oxytocin receptor. Am J Obstet Gynecol *188*, 497–502.

Robinson, C.R., Zhang, H., and Dougherty, P.M. (2014). Astrocytes, but not microglia, are activated in oxaliplatin and bortezomib-induced peripheral neuropathy in the rat. Neuroscience *274*, 308–317.

Robinson, D.A., Wei, F., Wang, G.D., Li, P., Kim, S.J., Vogt, S.K., Muglia, L.J., and Zhuo, M. (2002). Oxytocin mediates stress-induced analgesia in adult mice. J Physiol *540*, 593–606.

Rohr, S. (2004). Role of gap junctions in the propagation of the cardiac action potential. Cardiovasc Res *62*, 309–322.

Rojas-Piloni, G., Martínez-Lorenzana, G., DelaTorre, S., and Condés-Lara, M. (2008). Nociceptive spinothalamic tract and postsynaptic dorsal column neurons are modulated by paraventricular hypothalamic activation. Eur J Neurosci *28*, 546–558.

Rojas-Piloni, G., Gerardo, R.-P., Mejía-Rodríguez, R., Rosalinda, M.-R., Martínez-Lorenzana, G., Guadalupe, M.-L., Condés-Lara, M., and Miguel, C.-L. (2010). Oxytocin, but not vassopressin, modulates nociceptive responses in dorsal horn neurons. Neurosci Lett *476*, 32–35.

Romero-Fernandez, W., Borroto-Escuela, D.O., Agnati, L.F., and Fuxe, K. (2013). Evidence for the existence of dopamine d2-oxytocin receptor heteromers in the ventral and dorsal striatum with facilitatory receptor–receptor interactions. Molecular Psychiatry *18*, 849–850.

Rose, C.R., and Verkhratsky, A. (2016). Principles of sodium homeostasis and sodium signalling in astroglia. Glia *64*, 1611–1627.

Ross, H.E., Cole, C.D., Smith, Y., Neumann, I.D., Landgraf, R., Murphy, A.Z., and Young, L.J. (2009). Characterization of the oxytocin system regulating affiliative behavior in female prairie voles. Neuroscience *162*, 892–903.

Rothman, D.L., De Feyter, H.M., de Graaf, R.A., Mason, G.F., and Behar, K.L. (2011). 13C MRS studies of neuroenergetics and neurotransmitter cycling in humans. NMR Biomed *24*, 943–957.

Rothstein, J.D., Dykes-Hoberg, M., Pardo, C.A., Bristol, L.A., Jin, L., Kuncl, R.W., Kanai, Y., Hediger, M.A., Wang, Y., Schielke, J.P., et al. (1996). Knockout of glutamate transporters reveals a major role for astroglial transport in excitotoxicity and clearance of glutamate. Neuron *16*, 675–686.

Rousselot, P., Papadopoulos, G., Merighi, A., Poulain, D.A., and Theodosis, D.T. (1990). Oxytocinergic innervation of the rat spinal cord. An electron microscopic study. Brain Res *529*, 178–184.

Rouwette, T., Vanelderen, P., Roubos, E.W., Kozicz, T., and Vissers, K. (2012). The amygdala, a relay station for switching on and off pain. European Journal of Pain *16*, 782–792.

Roux, L., Benchenane, K., Rothstein, J.D., Bonvento, G., and Giaume, C. (2011). Plasticity of astroglial networks in olfactory glomeruli. Proc Natl Acad Sci U S A *108*, 18442–18446.

Rozen, F., Russo, C., Banville, D., and Zingg, H.H. (1995). Structure, characterization, and expression of the rat oxytocin receptor gene. Proc Natl Acad Sci U S A *92*, 200–204.

Rusakov, D.A., and Fine, A. (2003). Extracellular Ca2+ depletion contributes to fast activity-dependent modulation of synaptic transmission in the brain. Neuron *37*, 287–297.

Russell, J.A., Neumann, I., and Landgraf, R. (1992). Oxytocin and vasopressin release in discrete brain areas after naloxone in morphine-tolerant and -dependent anesthetized rats: push-pull perfusion study. J. Neurosci. *12*, 1024–1032.

Russo, R., D'Agostino, G., Mattace Raso, G., Avagliano, C., Cristiano, C., Meli, R., and Calignano, A. (2012). Central administration of oxytocin reduces hyperalgesia in mice: implication for cannabinoid and opioid systems. Peptides *38*, 81–88.

Rydén, G., and Sjöholm, I. (1969). Half-life of oxytocin in blood of pregnant and non-pregnant women. Acta Endocrinol (Copenh) *61*, 425–431.

S

Sah, P., Faber, E.S.L., Lopez De Armentia, M., and Power, J. (2003). The amygdaloid complex: anatomy and physiology. Physiol. Rev. *83*, 803–834.

Sausville, E., Carney, D., and Battey, J. (1985). The human vasopressin gene is linked to the oxytocin gene and is selectively expressed in a cultured lung cancer cell line. J. Biol. Chem. *260*, 10236–10241.

Savchenko, V.L., McKanna, J.A., Nikonenko, I.R., and Skibo, G.G. (2000). Microglia and astrocytes in the adult rat brain: comparative immunocytochemical analysis demonstrates the efficacy of lipocortin 1 immunoreactivity. Neuroscience *96*, 195–203.

Schleich, C.L. (1906). Schmerzlose operationen (Рипол Классик).

Schmitt, A., Asan, E., Püschel, B., and Kugler, P. (1997). Cellular and Regional Distribution of the Glutamate Transporter GLAST in the CNS of Rats: Nonradioactive In SituHybridization and Comparative Immunocytochemistry. J Neurosci *17*, 1–10.

Schnell, C., Hagos, Y., and Hülsmann, S. (2012). Active sulforhodamine 101 uptake into hippocampal astrocytes. PLoS One *7*, e49398.

Schousboe, A., Scafidi, S., Bak, L.K., Waagepetersen, H.S., and McKenna, M.C. (2014). Glutamate metabolism in the brain focusing on astrocytes. Adv Neurobiol *11*, 13–30.

Schultze, M. (1859). Observationes de retinae structura penitiori (Apud Adolphum Marcum).

Seminowicz, D.A., and Davis, K.D. (2007). A re-examination of pain-cognition interactions: implications for neuroimaging. Pain *130*, 8–13.

Seminowicz, D.A., Mikulis, D.J., and Davis, K.D. (2004). Cognitive modulation of pain-related brain responses depends on behavioral strategy. Pain *112*, 48–58.

Shamay-Tsoory, S.G., Fischer, M., Dvash, J., Harari, H., Perach-Bloom, N., and Levkovitz, Y. (2009). Intranasal administration of oxytocin increases envy and schadenfreude (gloating). Biol Psychiatry *66*, 864–870.

Shank, R.P., Bennett, G.S., Freytag, S.O., and Campbell, G.L. (1985). Pyruvate carboxylase: an astrocyte-specific enzyme implicated in the replenishment of amino acid neurotransmitter pools. Brain Res *329*, 364–367.

Shaw, G.L. (1986). Donald Hebb: The Organization of Behavior. In Brain Theory, G. Palm, and A. Aertsen, eds. (Berlin, Heidelberg: Springer), pp. 231–233.

Shelton, M.K., and McCarthy, K.D. (2000). Hippocampal astrocytes exhibit Ca2+-elevating muscarinic cholinergic and histaminergic receptors in situ. J Neurochem *74*, 555–563.

Shibata, T., Yamada, K., Watanabe, M., Ikenaka, K., Wada, K., Tanaka, K., and Inoue, Y. (1997). Glutamate transporter GLAST is expressed in the radial glia-astrocyte lineage of developing mouse spinal cord. J Neurosci *17*, 9212–9219.

Shigetomi, E., Jackson-Weaver, O., Huckstepp, R.T., O'Dell, T.J., and Khakh, B.S. (2013). TRPA1 channels are regulators of astrocyte basal calcium levels and long-term potentiation via constitutive D-serine release. J Neurosci *33*, 10143–10153.

Shih, P.-Y., Savtchenko, L.P., Kamasawa, N., Dembitskaya, Y., McHugh, T.J., Rusakov, D.A., Shigemoto, R., and Semyanov, A. (2013). Retrograde synaptic signaling mediated by K+ efflux through postsynaptic NMDA receptors. Cell Rep *5*, 941–951.

Shughrue, P.J., Lane, M.V., and Merchenthaler, I. (1997). Comparative distribution of estrogen receptor-alpha and -beta mRNA in the rat central nervous system. J. Comp. Neurol. *388*, 507–525.

Shughrue, P.J., Dellovade, T.L., and Merchenthaler, I. (2002). Estrogen modulates oxytocin gene expression in regions of the rat supraoptic and paraventricular nuclei that contain estrogen receptor-beta. Prog. Brain Res. *139*, 15–29.

Simard, M., Arcuino, G., Takano, T., Liu, Q.S., and Nedergaard, M. (2003). Signaling at the gliovascular interface. J Neurosci *23*, 9254–9262.

Simmons, D.M., and Swanson, L.W. (2008). High-resolution paraventricular nucleus serial section model constructed within a traditional rat brain atlas. Neuroscience Letters *438*, 85–89.

Simons, L.E., Moulton, E.A., Linnman, C., Carpino, E., Becerra, L., and Borsook, D. (2014). The human amygdala and pain: evidence from neuroimaging. Hum Brain Mapp *35*, 527–538.

Skowrońska, K., Obara-Michlewska, M., Zielińska, M., and Albrecht, J. (2019). NMDA Receptors in Astrocytes: In Search for Roles in Neurotransmission and Astrocytic Homeostasis. Int J Mol Sci *20*.

Skutella, T., Weber, T., and Jirkowski, G.F. (1993). Coexistence of oxytocin and tyrosine hydroxylase in the rat hypothalamus, an immunocytochemical study. J Neural Transm Gen Sect *94*, 55–61.

Smith, M.P., Ayad, V.J., Mundell, S.J., McArdle, C.A., Kelly, E., and López Bernal, A. (2006). Internalization and desensitization of the oxytocin receptor is inhibited by Dynamin and clathrin mutants in human embryonic kidney 293 cells. Mol Endocrinol *20*, 379–388.

Sofroniew, M.V. (1980). Projections from vasopressin, oxytocin, and neurophysin neurons to neural targets in the rat and human. J Histochem Cytochem *28*, 475–478.

Sofroniew, M.V. (1983). Morphology of vasopressin and oxytocin neurones and their central and vascular projections. Prog. Brain Res. *60*, 101–114.

Sosunov, A.A., Wu, X., Tsankova, N.M., Guilfoyle, E., McKhann, G.M., and Goldman, J.E. (2014). Phenotypic heterogeneity and plasticity of isocortical and hippocampal astrocytes in the human brain. J Neurosci *34*, 2285–2298.

Sripada, C.S., Phan, K.L., Labuschagne, I., Welsh, R., Nathan, P.J., and Wood, A.G. (2013). Oxytocin enhances resting-state connectivity between amygdala and medial frontal cortex. Int J Neuropsychopharmacol *16*, 255–260.

Stedronsky, K., Telgmann, R., Tillmann, G., Walther, N., and Ivell, R. (2002). The Affinity and Activity of the Multiple Hormone Response Element in the Proximal Promoter of the Human Oxytocin Gene. Journal of Neuroendocrinology *14*, 472–485.

Steiner, J., Bernstein, H.-G., Bielau, H., Berndt, A., Brisch, R., Mawrin, C., Keilhoff, G., and Bogerts, B. (2007). Evidence for a wide extra-astrocytic distribution of S100B in human brain. BMC Neurosci *8*, 2.

Stoop, R. (2012). Neuromodulation by Oxytocin and Vasopressin. Neuron *76*, 142–159.

Stoop, R. (2014). Neuromodulation by oxytocin and vasopressin in the central nervous system as a basis for their rapid behavioral effects. Curr Opin Neurobiol *29*, 187–193.

Stoop, R., Hegoburu, C., and van den Burg, E. (2015). New opportunities in vasopressin and oxytocin research: a perspective from the amygdala. Annu Rev Neurosci *38*, 369–388.

Sun, N., and Cassell, M.D. (1993). Intrinsic GABAergic neurons in the rat central extended amygdala. J Comp Neurol *330*, 381–404.

Sun, L., Kosugi, Y., Kawakami, E., Piao, Y.-S., Hashimoto, T., and Oyanagi, K. (2009). Magnesium concentration in the cerebrospinal fluid of mice and its response to changes in serum magnesium concentration. Magnes Res *22*, 266–272.

Sun, W., Cornwell, A., Li, J., Peng, S., Osorio, M.J., Aalling, N., Wang, S., Benraiss, A., Lou, N., Goldman, S.A., et al. (2017). SOX9 Is an Astrocyte-Specific Nuclear Marker in the Adult Brain Outside the Neurogenic Regions. J Neurosci *37*, 4493–4507.

Swanson, L.W., and Kuypers, H.G. (1980). The paraventricular nucleus of the hypothalamus: cytoarchitectonic subdivisions and organization of projections to the pituitary, dorsal vagal complex, and spinal cord as demonstrated by retrograde fluorescence double-labeling methods. J Comp Neurol *194*, 555–570.

Swanson, L.W., and McKellar, S. (1979). The distribution of oxytocin- and neurophysin-stained fibers in the spinal cord of the rat and monkey. J Comp Neurol *188*, 87–106.

Swanson, L.W., and Sawchenko, P.E. (1983). Hypothalamic Integration: Organization of the Paraventricular and Supraoptic Nuclei. Annu. Rev. Neurosci. *6*, 269–324.

Syed, N., Martens, C.A., and Hsu, W.H. (2007). Arginine vasopressin increases glutamate release and intracellular Ca2+ concentration in hippocampal and cortical astrocytes through two distinct receptors. J Neurochem *103*, 229–237.

T

Tang, Y., Chen, Z., Tao, H., Li, C., Zhang, X., Tang, A., and Liu, Y. (2014). Oxytocin activation of neurons in ventral tegmental area and interfascicular nucleus of mouse midbrain. Neuropharmacology *77*, 277–284.

Tang, Y., Benusiglio, D., Lefevre, A., Hilfiger, L., Althammer, F., Bludau, A., Hagiwara, D., Baudon, A., Darbon, P., Schimmer, J., et al. (2020). Social touch promotes interfemale communication via activation of parvocellular oxytocin neurons. Nature Neuroscience *23*, 1125–1137.

Terrillon, S., Durroux, T., Mouillac, B., Breit, A., Ayoub, M.A., Taulan, M., Jockers, R., Barberis, C., and Bouvier, M. (2003). Oxytocin and vasopressin V1a and V2 receptors form constitutive homo- and heterodimers during biosynthesis. Mol Endocrinol *17*, 677–691.

Thornton, S., Vatish, M., and Slater, D. (2001). Oxytocin antagonists: clinical and scientific considerations. Exp Physiol *86*, 297–302.

Tian, G.-F., Takano, T., Lin, J.H.-C., Wang, X., Bekar, L., and Nedergaard, M. (2006). Imaging of cortical astrocytes using 2-photon laser scanning microscopy in the intact mouse brain. Adv Drug Deliv Rev *58*, 773–787.

Tirko, N.N., Eyring, K.W., Carcea, I., Mitre, M., Chao, M.V., Froemke, R.C., and Tsien, R.W. (2018). Oxytocin Transforms Firing Mode of CA2 Hippocampal Neurons. Neuron *100*, 593-608.e3.

Todd, A.C., Marx, M.-C., Hulme, S.R., Bröer, S., and Billups, B. (2017). SNAT3-mediated glutamine transport in perisynaptic astrocytes in situ is regulated by intracellular sodium. Glia *65*, 900–916.

Torres, A., Wang, F., Xu, Q., Fujita, T., Dobrowolski, R., Willecke, K., Takano, T., and Nedergaard, M. (2012). Extracellular Ca^{2+} acts as a mediator of communication from neurons to glia. Sci Signal *5*, ra8.

Toth, I., Neumann, I.D., and Slattery, D.A. (2012). Central administration of oxytocin receptor ligands affects cued fear extinction in rats and mice in a timepoint-dependent manner. Psychopharmacology (Berl) *223*, 149–158.

Tracey, I., and Mantyh, P.W. (2007). The Cerebral Signature for Pain Perception and Its Modulation. Neuron *55*, 377–391.

Tracy, L.M., Georgiou-Karistianis, N., Gibson, S.J., and Giummarra, M.J. (2015). Oxytocin and the modulation of pain experience: Implications for chronic pain management. Neurosci Biobehav Rev *55*, 53–67.

Tsujimoto, M., and Hattori, A. (2005). The oxytocinase subfamily of M1 aminopeptidases. Biochim Biophys Acta *1751*, 9–18.

Tsuruo, Y., Ceccatelli, S., Villar, M.J., Hökfelt, T., Visser, T.J., Terenius, L., Goldstein, M., Brown, J.C., Buchan, A., and Walsh, J. (1988). Coexistence of TRH with other neuroactive substances in the rat central nervous system. J Chem Neuroanat *1*, 235–253.

Tzingounis, A.V., and Wadiche, J.I. (2007). Glutamate transporters: confining runaway excitation by shaping synaptic transmission. Nat Rev Neurosci *8*, 935–947.

U

Uvnäs-Moberg, K., Ahlenius, S., Hillegaart, V., and Alster, P. (1994). High doses of oxytocin cause sedation and low doses cause an anxiolytic-like effect in male rats. Pharmacol Biochem Behav *49*, 101–106.

Uwechue, N.M., Marx, M.-C., Chevy, Q., and Billups, B. (2012). Activation of glutamate transport evokes rapid glutamine release from perisynaptic astrocytes. J Physiol *590*, 2317–2331.

Uyeda, C.T., Eng, L.F., and Bignami, A. (1972). Immunological study of the glial fibrillary acidic protein. Brain Research *37*, 81–89.

V

Vaaga, C.E., Borisovska, M., and Westbrook, G.L. (2014). Dual-transmitter neurons: Functional implications of co-release and co-transmission. Current Opinion in Neurobiology *29*, 25–32.

Van Eldik, L.J., and Wainwright, M.S. (2003). The Janus face of glial-derived S100B: beneficial and detrimental functions in the brain. Restor Neurol Neurosci *21*, 97–108.

Van IJzendoorn, M.H., and Bakermans-Kranenburg, M.J. (2012). A sniff of trust: Meta-analysis of the effects of intranasal oxytocin administration on face recognition, trust to in-group, and trust to out-group. Psychoneuroendocrinology *37*, 438–443.

Vandesande, F., and Dierickx, K. (1975). Identification of the vasopressin producing and of the oxytocin producing neurons in the hypothalamic magnocellular neurosecretroy system of the rat. Cell Tissue Res *164*, 153–162.

Vargas-Martínez, F., Uvnäs-Moberg, K., Petersson, M., Olausson, H.A., and Jiménez-Estrada, I. (2014). Neuropeptides as neuroprotective agents: Oxytocin a forefront developmental player in the mammalian brain. Prog Neurobiol *123*, 37–78.

Vargas-Pinilla, P., Paixão-Côrtes, V.R., Paré, P., Tovo-Rodrigues, L., Vieira, C.M. de A.G., Xavier, A., Comas, D., Pissinatti, A., Sinigaglia, M., Rigo, M.M., et al. (2015). Evolutionary pattern in the OXT-OXTR system in primates: Coevolution and positive selection footprints. PNAS *112*, 88–93.

Veening, J.G., de Jong, T., and Barendregt, H.P. (2010). Oxytocin-messages via the cerebrospinal fluid: behavioral effects; a review. Physiol Behav *101*, 193–210.

Veinante, P., and Freund-Mercier, M.J. (1997). Distribution of oxytocin- and vasopressin-binding sites in the rat extended amygdala: a histoautoradiographic study. J Comp Neurol *383*, 305–325.

Veinante, P., Yalcin, I., and Barrot, M. (2013). The amygdala between sensation and affect: a role in pain. J Mol Psychiatry *1*, 9.

Venkatesh, B., Si-Hoe, S.L., Murphy, D., and Brenner, S. (1997). Transgenic rats reveal functional conservation of regulatory controls between the Fugu isotocin and rat oxytocin genes. PNAS *94*, 12462–12466.

Verkhratsky, A. (2010). Physiology of neuronal-glial networking. Neurochem Int *57*, 332–343.

Verkhratsky, A., and Burnstock, G. (2014). Biology of purinergic signalling: its ancient evolutionary roots, its omnipresence and its multiple functional significance. Bioessays *36*, 697–705.

Verkhratsky, A., and Nedergaard, M. (2018). Physiology of Astroglia. Physiol Rev *98*, 239–389.

Verkhratsky, A., Orkand, R.K., and Kettenmann, H. (1998). Glial calcium: homeostasis and signaling function. Physiol Rev *78*, 99–141.

Verkhratsky, A., Verkhrasky, A., Krishtal, O.A., and Burnstock, G. (2009). Purinoceptors on neuroglia. Mol Neurobiol *39*, 190–208.

Viero, C., Shibuya, I., Kitamura, N., Verkhratsky, A., Fujihara, H., Katoh, A., Ueta, Y., Zingg, H.H., Chvatal, A., Sykova, E., et al. (2010). REVIEW: Oxytocin: Crossing the Bridge between Basic Science and Pharmacotherapy. CNS Neurosci Ther *16*, e138–e156.

du Vigneaud, V., Ressler, C., Swan, J.M., Roberts, C.W., and Katsoyannis, P.G. (1954). The Synthesis of Oxytocin1. J. Am. Chem. Soc. *76*, 3115–3121.

Viitanen, T., Ruusuvuori, E., Kaila, K., and Voipio, J. (2010). The K+-Cl cotransporter KCC2 promotes GABAergic excitation in the mature rat hippocampus. J Physiol *588*, 1527–1540.

Virchow, R. (1871). Die Cellularpathologie in ihrer Begründung auf physiologische und pathologische Gewebelehre (Hirschwald).

de Vitry, F., Picart, R., Jacque, C., and Tixier-Vidal, A. (1981). Glial fibrillary acidic protein. A cellular marker of tanycytes in the mouse hypothalamus. Dev Neurosci *4*, 457–460.

Viviani, D., and Stoop, R. (2008). Opposite effects of oxytocin and vasopressin on the emotional expression of the fear response. In Progress in Brain Research, I.D. Neumann, and R. Landgraf, eds. (Elsevier), pp. 207–218.

Viviani, D., Charlet, A., van den Burg, E., Robinet, C., Hurni, N., Abatis, M., Magara, F., and Stoop, R. (2011). Oxytocin selectively gates fear responses through distinct outputs from the central amygdala. Science *333*, 104–107.

Volterra, A., Liaudet, N., and Savtchouk, I. (2014). Astrocyte Ca^{2+} signalling: an unexpected complexity. Nat Rev Neurosci *15*, 327–335.

W

Wagenaar, D.A., Hamilton, M.S., Huang, T., Kristan, W.B., and French, K.A. (2010). A Hormone-Activated Central Pattern Generator For Courtship. Curr Biol *20*, 487–495.

Wahis, J., Kerspern, D., Althammer, F., Baudon, A., Goyon, S., Hagiwara, D., Lefèvre, A., Boury-Jamot, B., Bellanger, B., Abatis, M., et al. (2020). Oxytocin Acts on Astrocytes in the Central Amygdala to Promote a Positive Emotional State. BioRxiv 2020.02.25.963884.

Waldherr, M., and Neumann, I.D. (2007). Centrally released oxytocin mediates mating-induced anxiolysis in male rats. PNAS *104*, 16681–16684.

Waller, R., Woodroofe, M.N., Wharton, S.B., Ince, P.G., Francese, S., Heath, P.R., Cudzich-Madry, A., Thomas, R.H., Rounding, N., Sharrack, B., et al. (2016). Gene expression profiling of the astrocyte transcriptome in multiple sclerosis normal appearing white matter reveals a neuroprotective role. J Neuroimmunol *299*, 139–146.

Wallis, M. (2012). Molecular evolution of the neurohypophysial hormone precursors in mammals: Comparative genomics reveals novel mammalian oxytocin and vasopressin analogues. Gen Comp Endocrinol *179*, 313–318.

Walther, E.U., Dichgans, M., Maricich, S.M., Romito, R.R., Yang, F., Dziennis, S., Zackson, S., Hawkes, R., and Herrup, K. (1998). Genomic sequences of aldolase C (Zebrin II) direct lacZ expression exclusively in non-neuronal cells of transgenic mice. Proc Natl Acad Sci U S A *95*, 2615–2620.

Walz, W. (2000). Controversy surrounding the existence of discrete functional classes of astrocytes in adult gray matter. Glia *31*, 95–103.

Walz, W., and Hertz, L. (1984). Intense furosemide-sensitive potassium accumulation in astrocytes in the presence of pathologically high extracellular potassium levels. J Cereb Blood Flow Metab *4*, 301–304.

Wang, Y.-F., and Hatton, G.I. (2007). Dominant Role of βγ Subunits of G-Proteins in Oxytocin-Evoked Burst Firing. J Neurosci *27*, 1902–1912.

Wang, Z., Moody, K., Newman, J.D., and Insel, T.R. (1997). Vasopressin and oxytocin immunoreactive neurons and fibers in the forebrain of male and female common marmosets (Callithrix jacchus). Synapse *27*, 14–25.

Wesley, V.J., Hawtin, S.R., Howard, H.C., and Wheatley, M. (2002). Agonist-specific, high-affinity binding epitopes are contributed by an arginine in the N-terminus of the human oxytocin receptor. Biochemistry *41*, 5086–5092.

Wilhelmsson, U., Li, L., Pekna, M., Berthold, C.-H., Blom, S., Eliasson, C., Renner, O., Bushong, E., Ellisman, M., Morgan, T.E., et al. (2004). Absence of Glial Fibrillary Acidic Protein and Vimentin Prevents Hypertrophy of Astrocytic Processes and Improves Post-Traumatic Regeneration. J Neurosci *24*, 5016–5021.

Williams, S.M., Sullivan, R.K.P., Scott, H.L., Finkelstein, D.I., Colditz, P.B., Lingwood, B.E., Dodd, P.R., and Pow, D.V. (2005). Glial glutamate transporter expression patterns in brains from multiple mammalian species. Glia *49*, 520–541.

Windle, R.J., Shanks, N., Lightman, S.L., and Ingram, C.D. (1997). Central Oxytocin Administration Reduces Stress-Induced Corticosterone Release and Anxiety Behavior in Rats. Endocrinology *138*, 2829–2834.

Wolfe, B.L., and Trejo, J. (2007). Clathrin-dependent mechanisms of G protein-coupled receptor endocytosis. Traffic *8*, 462–470.

Woo, A.K. (2010). Depression and Anxiety in Pain. Rev Pain *4*, 8–12.

Wotjak, C.T., Ganster, J., Kohl, G., Holsboer, F., Landgraf, R., and Engelmann, M. (1998). Dissociated central and peripheral release of vasopressin, but not oxytocin, in response to repeated swim stress: new insights into the secretory capacities of peptidergic neurons. Neuroscience *85*, 1209–1222.

Wotjak, C.T., Landgraf, R., and Engelmann, M. (2008). Listening to neuropeptides by microdialysis: echoes and new sounds? Pharmacol Biochem Behav *90*, 125–134.

Wrzal, P.K., Devost, D., Pétrin, D., Goupil, E., Iorio-Morin, C., Laporte, S.A., Zingg, H.H., and Hébert, T.E. (2012a). Allosteric interactions between the oxytocin receptor and the β2-adrenergic receptor in the modulation of ERK1/2 activation are mediated by heterodimerization. Cell Signal *24*, 342–350.

Wrzal, P.K., Goupil, E., Laporte, S.A., Hébert, T.E., and Zingg, H.H. (2012b). Functional interactions between the oxytocin receptor and the β2-adrenergic receptor: implications for ERK1/2 activation in human myometrial cells. Cell Signal *24*, 333–341.

X

Xi, D., Kusano, K., and Gainer, H. (1999). Quantitative analysis of oxytocin and vasopressin messenger ribonucleic acids in single magnocellular neurons isolated from supraoptic nucleus of rat hypothalamus. Endocrinology *140*, 4677–4682.

Xin, Q., Bai, B., and Liu, W. (2017). The analgesic effects of oxytocin in the peripheral and central nervous system. Neurochem. Int. *103*, 57–64.

Xiong, Z.Q., and Stringer, J.L. (2000). Sodium pump activity, not glial spatial buffering, clears potassium after epileptiform activity induced in the dentate gyrus. J Neurophysiol *83*, 1443–1451.

Xiong, Z., O'Hanlon, D., Becker, L.E., Roder, J., MacDonald, J.F., and Marks, A. (2000). Enhanced calcium transients in glial cells in neonatal cerebellar cultures derived from S100B null mice. Exp Cell Res *257*, 281–289.

Y

Yalcin, I., and Barrot, M. (2014). The anxiodepressive comorbidity in chronic pain. Curr Opin Anaesthesiol *27*, 520–527.

Yamahara, N., Nomura, S., Suzuki, T., Itakura, A., Ito, M., Okamoto, T., Tsujimoto, M., Nakazato, H., and Mizutani, S. (2000). Placental leucine aminopeptidase/oxytocinase in maternal serum and placenta during normal pregnancy. Life Sci *66*, 1401–1410.

Yamashita, K., and Kitano, T. (2013). Molecular evolution of the oxytocin-oxytocin receptor system in eutherians. Mol Phylogenet Evol *67*, 520–528.

Yang, J., Yang, Y., Chen, J.-M., Liu, W.-Y., Wang, C.-H., and Lin, B.-C. (2007a). Central oxytocin enhances antinociception in the rat. Peptides *28*, 1113–1119.

Yang, J., Yang, Y., Xu, H.-T., Chen, J.-M., Liu, W.-Y., and Lin, B.-C. (2007b). Arginine vasopressin induces periaqueductal gray release of enkephalin and endorphin relating to pain modulation in the rat. Regul. Pept. *142*, 29–36.

Yang, J., Liang, J.-Y., Li, P., Pan, Y.-J., Qiu, P.-Y., Zhang, J., Hao, F., and Wang, D.-X. (2011a). Oxytocin in the periaqueductal gray participates in pain modulation in the rat by influencing endogenous opiate peptides. Peptides *32*, 1255–1261.

Yang, J., Liang, J.-Y., Li, P., Pan, Y.-J., Qiu, P.-Y., Zhang, J., Hao, F., and Wang, D.-X. (2011b). Oxytocin in the periaqueductal gray participates in pain modulation in the rat by influencing endogenous opiate peptides. Peptides *32*, 1255–1261.

Yang, J., Li, P., Liang, J.-Y., Pan, Y.-J., Yan, X.-Q., Yan, F.-L., Hao, F., Zhang, X.-Y., Zhang, J., Qiu, P.-Y., et al. (2011c). Oxytocin in the periaqueductal grey regulates nociception in the rat. Regul Pept *169*, 39–42.

Yang, Y., Vidensky, S., Jin, L., Jie, C., Lorenzini, I., Frankl, M., and Rothstein, J.D. (2011d). Molecular comparison of GLT1+ and ALDH1L1+ astrocytes in vivo in astroglial reporter mice. Glia *59*, 200–207.

Yeh, C.-Y., Verkhratsky, A., Terzieva, S., and Rodríguez, J.J. (2013). Glutamine synthetase in astrocytes from entorhinal cortex of the triple transgenic animal model of Alzheimer's disease is not affected by pathological progression. Biogerontology *14*, 777–787.

Yoshida, M., Takayanagi, Y., Inoue, K., Kimura, T., Young, L.J., Onaka, T., and Nishimori, K. (2009). Evidence that oxytocin exerts anxiolytic effects via oxytocin receptor expressed in serotonergic neurons in mice. J Neurosci *29*, 2259–2271.

Young, W.S., and Gainer, H. (2003). Transgenesis and the study of expression, cellular targeting and function of oxytocin, vasopressin and their receptors. Neuroendocrinology *78*, 185–203.

Young, L.J., Wang, Z., Donaldson, R., and Rissman, E.F. (1998). Estrogen receptor alpha is essential for induction of oxytocin receptor by estrogen. Neuroreport *9*, 933–936.

Yu, A.C., Schousboe, A., and Hertz, L. (1982). Metabolic fate of 14C-labeled glutamate in astrocytes in primary cultures. J Neurochem *39*, 954–960.

Yu, S.Q., Lundeberg, T., and Yu, L.C. (2003). Involvement of oxytocin in spinal antinociception in rats with inflammation. Brain Res *983*, 13–22.

Z

Z, M., T, S., De, B., and Mr, F. (2016). Neuromodulators signal through astrocytes to alter neural circuit activity and behaviour. Nature *539*, 428–432.

Zaki, Y., Mau, W., Cincotta, C., Hamidi, A., Doucette, E., Grella, S.L., Merfeld, E., Murawski, N.J., Shpokayte, M., and Ramirez, S. (2019). Hippocampus and amygdala fear memory engrams re-emerge after contextual fear reinstatement. BioRxiv 2019.12.19.882795.

Zanotti, S., and Charles, A. (1997). Extracellular calcium sensing by glial cells: low extracellular calcium induces intracellular calcium release and intercellular signaling. J Neurochem *69*, 594–602.

Zhang, Y., Yang, Y., Dai, R., Wu, H., Li, C., and Guo, Q. (2015). Oxytocin in the paraventricular nucleus attenuates incision-induced mechanical allodynia. Exp Ther Med *9*, 1351–1356.

Zhao, L., and Brinton, R.D. (2003). Vasopressin-induced cytoplasmic and nuclear calcium signaling in embryonic cortical astrocytes: dynamics of calcium and calcium-dependent kinase translocation. J Neurosci *23*, 4228–4239.

Zhao, L., and Brinton, R.D. (2004). Suppression of proinflammatory cytokines interleukin-1beta and tumor necrosis factor-alpha in astrocytes by a V1 vasopressin receptor agonist: a cAMP response element-binding protein-dependent mechanism. J Neurosci *24*, 2226–2235.

Zheng, K., Bard, L., Reynolds, J.P., King, C., Jensen, T.P., Gourine, A.V., and Rusakov, D.A. (2015). Time-Resolved Imaging Reveals Heterogeneous Landscapes of Nanomolar Ca(2+) in Neurons and Astroglia. Neuron *88*, 277–288.

Zhong, M., Yang, M., and Sanborn, B.M. (2003). Extracellular signal-regulated kinase 1/2 activation by myometrial oxytocin receptor involves Galpha(q)Gbetagamma and epidermal growth factor receptor tyrosine kinase activation. Endocrinology *144*, 2947–2956.

Zimmermann, H., Zebisch, M., and Sträter, N. (2012). Cellular function and molecular structure of ecto-nucleotidases. Purinergic Signal *8*, 437–502.

Zingg, H.H., Grazzini, E., Breton, C., Larcher, A., Rozen, F., Russo, C., Guillon, G., and Mouillac, B. (1998). Genomic and non-genomic mechanisms of oxytocin receptor regulation. Adv Exp Med Biol *449*, 287–295.

ANNEXE 1 : Un aperçu de la signalisation OT-OTR

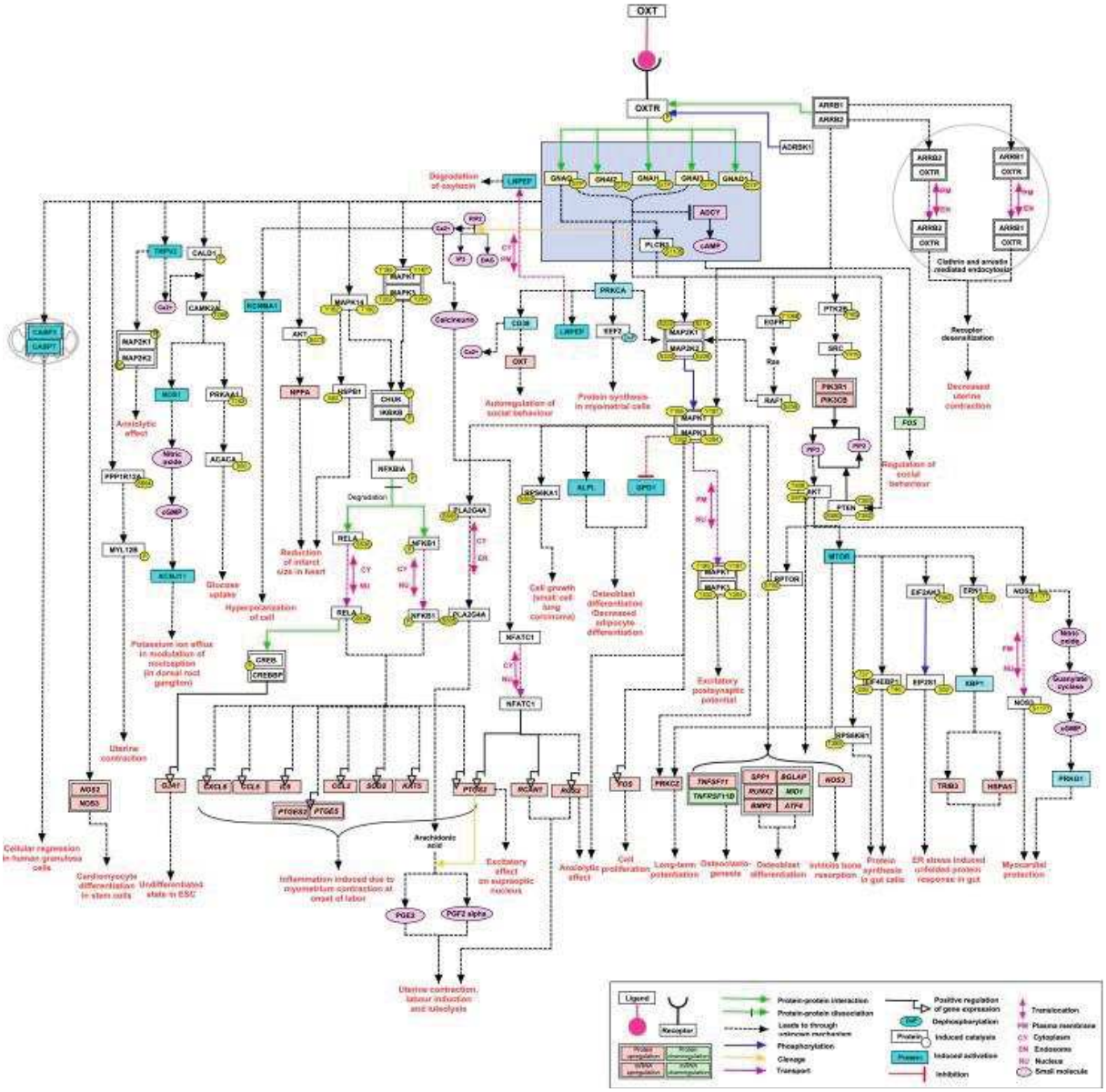

Schéma issus de (Chatterjee et al., 2016).

ANNEXE 2 – Listes récepteurs exprimés par les astrocytes

Issus de (Verkhratsky and Nedergaard, 2018)

Astroglial receptors to neurotransmitters and neuromodulators

Receptor Type/Subunits	Properties, Function, and Localization
Ionotropic receptors	
AMPA glutamate receptors: GluA1, GluA2, GluA3, GluA4	Detected in hippocampus, cortex, cerebellum, white matter, Bergmann glial cells, immature astrocytes. Cationic Na^+/K^+ channels or $Na^+/K^+/Ca^{2+}$ channels. Receptors lacking GluA2 subunit (predominantly localized in Bergmann glial cells) have moderate Ca^{2+} permeability ($P_{Ca}/P_{monovalent}$ ~1). Activation triggers cell depolarization and Ca^{2+} influx.
Glutamate NMDA receptors: GluN1, GluN2C, GluN2D, GluN3	Detected at mRNA and protein level in cortex, hippocampus, spinal cord, amygdala, locus coeruleus, and retinal Müller glia. NMDA receptor-mediated currents were characterized in astrocytes from cortex, spinal cord, and subpopulation of hippocampal astrocytes. $Na^+/K^+/Ca^{2+}$ channels. Astroglial receptors display weak Mg^{2+} block and intermediate Ca^{2+} permeability ($P_{Ca}/P_{monovalent}$ ~3). Activation triggers inward current and Ca^{2+} entry.
P2X purinoceptors: $P2X_{1/5}$, $P2X_7$	At mRNA and protein levels, all seven subunits of P2X receptors were identified (in various combinations) in astrocytes from cortex, hippocampus, cerebellum, spinal cord, brain stem and retina. $P2X_{1/5}$-mediated currents were recorded in cortical astrocytes; functional $P2X_7$ receptors were found in cortex, hippocampus, and retina. $Na^+/K^+/Ca^{2+}$ channels. Ca^{2+} permeability of $P2X_{1/5}$ receptors is: $P_{Ca}/P_{monovalent}$ ~2. Ca^{2+} permeability of $P2X_7$ receptors depends on the pore formation and can be very high ($P_{Ca}/P_{monovalent}$ >10). Activation triggers cationic current and Ca^{2+} entry.
$GABA_A$ receptors: α2, γ1	Detected at mRNA, protein, and functional levels in hippocampus, cortex, cerebellum, optic nerve, spinal cord, and pituitary gland. Cl^- channel. Activation triggers Cl^- efflux and cell depolarization. Possibly play fundamental role in regulation of $[Cl^-]$ in the synaptic cleft to maintain inhibitory transmission.
Glycine receptors: α1, β	Mainly present in the spinal cord, where they were detected at transcript, protein, and functional levels. Cl^- channel. Activation triggers Cl^- efflux and cell depolarization.
Nicotinic cholinoreceptors: α3, α4, α7; β2, β4	Detected in astrocytes in vitro and in hippocampal astrocytes in situ. $Na^+/K^+/Ca^{2+}$ channels. Receptors containing α7 subunit display high Ca^{2+} permeability ($P_{Ca}/P_{monovalent}$ ~6).
Metabotropic receptors	
Glutamate receptors: mGluR3, mGluR5	Detected in astrocytes throughout the CNS. The most abundant is mGluR3 receptor subtype which inhibits adenylyl cyclase; mGluR5 receptors associated with Ca^{2+} signaling are downregulated in first postnatal weeks.
$GABA_B$ receptors: $GABA_{B1a}$, $GABA_{B1b}$, $GABA_{B2}$	Detected in hippocampus, cortex, and spinal cord. Linked to PLC through $G_{i/o}$ proteins; activation of $GABA_B$ receptors triggers Ca^{2+} release from the ER with associated Ca^{2+} signals and $[Ca^{2+}]_i$ oscillations in vitro, in situ and in vivo.
Adenosine receptors: A_1, A_{2A}, A_{2B}, A_3	Detected at mRNA, protein, and functional levels in hippocampus, cortex, cerebellum, and spinal cord. All receptors were found to be linked to Ca^{2+} signaling and to cAMP cascades. A_1 and A_2 receptors regulate expression of glutamate and GABA transporters receptors; A_{2A} receptors regulate Na^+/K^+ pump while A_3 receptors mediate neuroprotection.
P2Y purinoceptors: $P2Y_{1,2,4,6,12,13,14}$	Detected at mRNA, protein, and functional levels throughout the CNS, in hippocampus, cortex, cerebellum, brain stem, retina, and spinal cord; the $P2Y_{1,2,4}$ are being dominating types. Generally are linked to PLC/$InsP_3$/Ca^{2+} signaling cascade. P2Y receptors are also coupled to various signaling pathways, including MAP kinases, extracellular signal-regulated kinase (ERKs), the stress-activated protein kinases (SAPKs), the JNKs, p38/MAPK, glycogen synthase kinase, and the Akt kinase.
Muscarinic cholinoreceptors, mAChR: M_1, M_2, M_3	Detected in hippocampus and amygdala. Control PLC, $InsP_3$ production, and Ca^{2+} release from the ER. M3 receptors are linked to neurogenesis by regulating astroglial expression and release of fibronectin and laminin-1.
Adrenergic receptors: α_1AR, α_2AR; β_1AR, β_2AR, β_3AR	Detected at mRNA, protein, and functional levels in hippocampus, cortex, cerebellum, optic nerve, and spinal cord. α-ARs are mainly linked to PLC/$InsP_3$/Ca^{2+} signaling, whereas β-ARs mainly control cAMP production and glial glucose metabolism.
Serotonin receptors: 5-HT_{1A}, 5-HT_{2A}, 5-HT_{2B}, 5-HT_{5A}, 5-HT_7	Detected at mRNA and protein level throughout the brain. The 5-HT_{2B} is the predominant type; mainly 5-HT receptors are linked to PLC/$InsP_3$/Ca^{2+} signaling. 5-HT_{2B} receptors are also connected to ERK1/2, andcPLA2. 5-HT_7 receptors (found in suprachiasmatic nucleus) stimulate adenylyl cyclase.
Dopamine receptors: D_1, D_2, D_3, D_5	Detected at mRNA and protein levels in basal ganglia and in substantia nigra. Astroglial D_2 receptors are found in neocortex where they account for 30% of all D_2 binding sites; D_2 receptors are also present in fibrous astrocytes of white matter. Mainly linked to PLC/$InsP_3$/Ca^{2+} signaling.
Histamine receptors: H_1, H_2, H_3	Have been detected at mRNA and protein level and functionally characterized in hippocampus and cerebellum. Linked to PLC/$InsP_3$/Ca^{2+} signaling, adenylyl cyclase, glucose metabolism, and regulation of expression of glutamate transporters. Regulate synthesis of cAMP.
Cannabinoid receptors: CB_1	Detected in hippocampus in situ. Linked to Ca^{2+} signaling and to synaptic plasticity.
Oxytocin and vasopressin (V_{1b}) receptors	Detected in hypothalamus. Linked to PLC/$InsP_3$/Ca^{2+} signaling. V_{1b} receptors also control PKC, CaMKII, and ERK1/2 signaling cascades.
PACAP/VIP receptors: PAC_1, $VPAC_1$, $VPAC_2$	Have been detected throughout the brain. All receptors stimulate adenylyl cyclase; PAC_1 receptors are linked to PLC/$InsP_3$/Ca^{2+} signaling. May also regulate energy metabolism and glycogenolysis.
Bradykinin receptors: B_2	Identified in cultured astrocytes; linked to PLC/$InsP_3$/Ca^{2+} signaling and Ca^{2+}-activated Cl^- currents.
Opioid receptors: μ, δ, κ	Mainly detected in astrocytes in vitro. Linked to various signaling cascades, regulate expression of glutamate transporters, and may affect growth and development.

ANNEXE 3- Publications en lien non direct avec ma thèse :

I- A Nonpeptide Oxytocin Receptor Agonist for a Durable Relief of Inflammatory Pain

a. Contexte générale et résultats

L'ocytocine est un neuropeptide possédant de nombreuses fonctions de régulation physiologique et comportementale. Il permet notamment de réguler la douleur. Son effet est principalement médié par l'activation de son récepteur dans le SNC mais également au niveau périphérique où il peut se lier à son récepteur au niveau des terminaisons axonal des fibres nociceptives présentes au niveau la peau. Cependant, malgré son effet analgésique et son utilisation chez l'humain pour faciliter l'accouchement cette molécule n'est actuellement pas utilisée dans le traitement de la douleur. Cela est principalement dû à sa demi-vie très courte dans la circulation sanguine (5 min) et dans le LCR (20 min). De plus, l'ocytocine présente également d'autres limites telles que sa spécificité et sa faible absorption orale. A ce jour une nouvelle molécule non peptidique, agissant comme agoniste spécifique des OTR a été synthétisée : le LIT-001. Il a déjà été montré que ce composé permet de renforcer les interactions sociales à la suite à son administration périphérique. Dans notre étude en utilisant un modèle de rat présentant une douleur inflammatoire induite par l'injection de l'adjuvent complet de Freund, nous avons pu démontrer qu'une injection unique de LIT-001 permet de diminuer l'hyperalgésie mécanique ainsi que thermique sans induire d'effet anti-inflammatoire. De plus cette analgésie est soutenue dans le temps et dure jusqu'à plusieurs heures post-injection. Un autre avantage démontré de ce composé est son absence d'effet secondaire, car il ne semble pas, aux doses utilisées, présenter d'effet anti-nociceptif, une caractéristique importante en vue d'une utilisation clinique, car n'induit pas de perte de sensibilité indésirable. De manière générale en plus de la potentielle perspective d'utilisation du LIT-001 en clinique, cette étude a permis de valider le récepteur à l'ocytocine comme cible pour le traitement de la douleur.

SCIENTIFIC REPORTS
nature research

OPEN

A Nonpeptide Oxytocin Receptor Agonist for a Durable Relief of Inflammatory Pain

Louis Hilfiger[1], Qian Zhao[2], Damien Kerspern[1], Perrine Inquimbert[1], Virginie Andry[1], Yannick Goumon[1], Pascal Darbon[1], Marcel Hibert[2,3] & Alexandre Charlet[1,3*]

Oxytocin possesses several physiological and social functions, among which an important analgesic effect. For this purpose, oxytocin binds mainly to its unique receptor, both in the central nervous system and in the peripheral nociceptive terminal axon in the skin. However, despite its interesting analgesic properties and its current use in clinics to facilitate labor, oxytocin is not used in pain treatment. Indeed, it is rapidly metabolized, with a half-life in the blood circulation estimated at five minutes and in cerebrospinal fluid around twenty minutes in humans and rats. Moreover, oxytocin itself suffers from several additional drawbacks: a lack of specificity, an extremely poor oral absorption and distribution, and finally, a lack of patentability. Recently, a first non-peptide full agonist of oxytocin receptor (LIT-001) of low molecular weight has been synthesized with reported beneficial effect for social interactions after peripheral administration. In the present study, we report that a single intraperitoneal administration of LIT-001 in a rat model induces a long-lasting reduction in inflammatory pain-induced hyperalgesia symptoms, paving the way to an original drug development strategy for pain treatment.

Oxytocin (OT) is a 9–amino acid neuropeptide that plays an important role in several physiological and social functions. It was discovered by Sir Henry Dale for its role in lactation and parturition[1]. In the brain, OT is mainly synthesized in the paraventricular and supraoptic nuclei of the hypothalamus and released into the bloodstream by the neurons of the pituitary gland[2]. OT binds mainly to its unique receptor (OTR), a member of the G-protein coupled receptor (GPCRs) family. Its amino acid sequence was elucidated in 1953[3] and its receptor gene was isolated in 1992[4].

OT has been shown to induce antinociception as well as analgesia[5]. The antinociceptive and analgesic effects after intrathecal or systemic administration of OT are well-documented[6–8]. For instance, OT has a dose dependent analgesic effect in a rat model of inflammatory pain[8], and Petersson *et al*. have shown that OT was also able to reduce the size and volume of the inflammation[7]. In addition, one study proposed that OT can also bind OTR directly in the peripheral nociceptive terminal axon in the skin[9].

Interestingly, in nociception and pain, OT has central and peripheral targets depending on the releasing pathway: plasmatic released OT has *in vivo* antinociceptive action through reduction of C fiber excitability leading to a reduction of activity of wide dynamic range (WDR) spinal sensory neurons[10] whereas OT released by fibers originating from PVN directly on WDR neurons inhibits sensory processing and produces analgesia in inflammatory pain model[11,12]. In these models, direct activation of parvocellular OT neuron by optogenetics, resulting in central and peripheral release of endogenous OT, also produced a significant OTR-dependent analgesia[11].

In clinics, OT is used since many years in patients by the intravenous route for the initiation of labor and the final expulsion of the fetus[13]. It is also administered to women as a nasal spray to stimulate milk ejection. However, despite its interesting analgesic properties, OT is not used in pain treatment because it cannot efficiently penetrate the brain[14] and is rapidly metabolized. OT half-life in the blood circulation is estimated at 5 minutes in humans and rats[15] and around 20 minutes in rat cerebrospinal fluid (CSF)[16]. Moreover, OT suffers from several additional drawbacks: a lack of specificity, since this cyclic nonapeptide has very similar affinities for its receptor OTR, for the V1a vasopressin receptor (V1aR)[17,18] and for the Transient Receptor Potential Vanilloid type-1 (TRPV1) of the capsaicin ($EC_{50} = 0.316\,\mu M$)[19]; an extremely poor oral absorption and distribution since its high

[1]Centre National de la Recherche Scientifique and University of Strasbourg, UPR3212 Institute of Cellular and Integrative Neurosciences, Strasbourg, France. [2]Laboratoire d'Innovation Thérapeutique, Faculté de Pharmacie, UMR7200 CNRS/Université de Strasbourg, Illkirch, France. [3]These authors jointly supervised this work: Marcel Hibert and Alexandre Charlet. *email: acharlet@unistra.fr

molecular weight prevents or strongly limits its absorption from the gastro intestinal tract to the blood or from the blood to the brain; and finally, a lack of patentability.

Recently, a first non-peptide full agonist of oxytocin (LIT-001) has been reported to improve social interactions in a mouse model of autism after peripheral administration[20]. LIT-001 is a pyrazolobenzodiazepine derivative with a non-peptide chemical structure and a low molecular weight (MW) compared to oxytocin (MW = 531 vs. 1007, respectively, Fig. 1a). Frantz *et al*. have shown that LIT-001 is a specific oxytocin receptor agonist with high affinity (EC_{50} = 25 nM and EC_{50} = 18 nM) and efficacy (Emax = 96% and 95%) for human and mouse receptors, respectively. Furthermore, the compound poorly antagonized vasopressin induced calcium release on V1aR (IC_{50} = 5900 nM) and was devoid of agonist or antagonist effect on V1bR.

In the present study, we report that a single intraperitoneal administration of LIT-001 in a rat model induces a long-lasting reduction in inflammatory pain-induced hyperalgesia symptoms, paving the way to an original drug development strategy for pain treatment.

Results

LIT-001, a non-peptidergic oxytocin receptor agonist. The thermodynamic water solubility (S) of LIT-001 was measured in PBS buffer at pH 7.4: S = 0.53 ± 0.03 mM (0.34 mg/mL). Its lipophilicity in the same conditions was experimentally determined: $LogD_{7.4}$ = 2.0 ± 0.3 (Fig. 1a). The selectivity of LIT-001 (at 5 μM) has been tested on classical off-targets: 24 G-protein-coupled receptors (GPCRs), 3 transporters, 10 enzymes and 6 ion channels. No significant agonist or antagonist (Fig. 1b) activity was found at GPCRs levels or at the ionotropic TRPV1 receptor. Similarly, no significant uptake blockade is observed on noradrenaline, dopamine and serotonin transporters from rat brain synaptosomes (Fig. 1c). In addition, no enzyme inhibition activity was found on the human recombinant COX(1), PDE3A, Lck kinase, acetylcholinesterase and MAO-A from human placenta (6.4% to 9.5% inhibition, below significance) (Fig. 1c). Some inhibitory activity of COX(2) and PDE4D2 was however observed (24.6 and 23.1% at 5 μM, respectively) (Fig. 1c). On ion channels, no significant blockade activity was found on human hERG potassium, GABAA (alpha1/beta2/gamma2), Cav1.2 (L-type) calcium, Vav1.5 sodium, nAChR (alpha4/beta2) and KCNQ1/hminK potassium ion channels (Fig. S1). Finally, the lack of hERG inhibition was confirmed at two additional concentrations using patch clamp method (9.50% and 10.63% inhibition at 1 μM and 10 μM concentrations, respectively). *In vitro*, LIT-001 did not interact with CYP 2C9 and 2D6 cytochromes and weakly inhibited CYP 1A2, 2C19 and 3A4 (IC_{50} = 51, 21 and 11 μM, respectively). Interesting, tested at 1 μM, LIT-001 was very stable on human hepatocytes at 37 °C since no degradation was observed after 2 hours.

Altogether, these results indicates that LIT-001 is a very specific agonist for OTR, with limited off-targets and putative side-effects, and a long lasting (>2 h) half-life; all characteristics requested for a clinically-relevant compound.

Ten days' time course of long-term modifications induced by CFA subcutaneous injection. Before testing the putative analgesic action of LIT-001, we started by characterizing the long-term modifications induced by a single subcutaneous injection of complete Freund adjuvant (CFA, 100 μl) in the right hindpaw (Fig. 2a). We first measured the hindpaw diameter and observed that CFA, but not NaCl 0.9%, injection induced a major edema, whose size was maximum 24 h after the injection (CFA: 9.69 ± 0.22 mm, n = 14 vs NaCl: 5.73 ± 0.14 mm, n = 11; $p < 0.01$) and persistent for up to 10 days (Fig. 2b). On the other hand, the mechanical CFA-induced hyperalgesia was maximum 24 h after the injection (threshold pressure CFA: 122 ± 15 g, n = 14 vs NaCl: 520 ± 14 g, n = 18; $p < 0.01$) and, as the edema, was persistent up to 10 days (Fig. 2c1). Similarly, a thermal heat hyperalgesia was detected for up to 10 days and maximum 24 h after the CFA injection (withdrawal latency CFA: 2.5 ± 0.23 s, n = 14 vs NaCl: 10.31 ± 0.38 s, n = 18; $p < 0.01$; Fig. 2c2). Interestingly, the contralateral hindpaw to the CFA-injected one did not present any mechanical nor thermal heat hypersensitivity (Fig. S2). Based on these results, we decided to test the putative analgesic properties of LIT-001 at 24 h (D1) after the CFA injection.

Analgesic properties of LIT-001 on CFA-induced inflammatory pain model. We next aimed to test the putative analgesic properties of LIT-001 in the CFA-induced inflammatory pain model. For this purpose, we first performed a dose-response of the analgesic action of LIT-001 injected intraperitoneally (i.p.) at day 1 (D1) after the CFA injection, when the inflammatory pain symptoms were at their maximum (Fig. 3). We found a first analgesic action of i.p. LIT-001 at 5 mg/kg, an effect rising to reach a plateau at 10 mg/kg, that for both mechanical (Fig. 3a) and thermal heat (Fig. 3b) hypersensitivities. Importantly, none of the doses tested seem to exert an antinociceptive action, as measured on the contralateral hindpaw (Fig. S3).

Therefore, we performed a time-course of the analgesic effect of i.p. LIT-001 (10 mg/kg) injected at day 1 (D1) after the CFA injection (Fig. 4a). For that purpose, we analyzed the hindpaw size as well as the mechanical and thermal heat hypersensitivities for 24 h (Fig. 4b–d).

We first found that i.p. LIT-001, injected alone or with a specific oxytocin receptor antagonist, L-368,699 (L-368), had no effect on the CFA-induced edema size (CFA + Vehicle, 9.44 ± 0.18 mm, n = 7; CFA + LIT-001, 9.49 ± 0.23 mm, n = 8; CFA + LIT-001 + L-368, 10.32 ± 0.17 mm, n = 7; Fig. 4b). This suggests that acute LIT-001 injection, at this stage of the CFA-induced inflammation, may have no or limited anti-inflammatory effect *per se*.

However, we revealed that i.p. LIT-001 exerts an anti-hyperalgesic action on mechanical threshold (Fig. 4c1). This effect was significant from 1 to 5 h after i.p. injection, with a maximal effect at 3 h (CFA + Vehicle, 126 ± 29 g, n = 7 vs CFA + LIT-001, 246 ± 22 g, n = 8; $p < 0.001$), as reflected by an increase of the area under the curve (AUC) of 152 ± 11%. We observed a similar anti-hyperalgesic action on thermal heat latency (Fig. 4c2), significant from 1 to 5 h after i.p. injection, with a maximal effect at 3 h (CFA + Vehicle, 1.94 ± 0.18 s, n = 7 vs CFA + LIT-001, 5.83 ± 0.65 s, n = 8; $p < 0.001$), as reflected by an increase of the AUC of 135 ± 9%. These results indicate that i.p. LIT-001 exerts a strong significant and long-lasting anti-hyperalgesic action on both mechanical and thermal heat sensitivities.

a

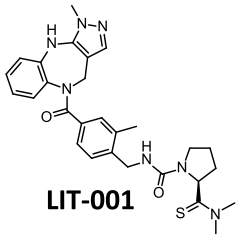

Molecular weight = 531
Thermodynamic solubility = 0.53 mM (PBS, pH 7.4)
$LogD_{7.4}$ = 2.0 (experimental)
EC_{50} (hOTR) = 25 nM; Emax = 96%
EC_{50} (mOTR) = 18 nM; Emax = 95%
EC_{50} ($hV_{1A}R$) = non significant
EC_{50} ($hV_{1B}R$) = non significant

b

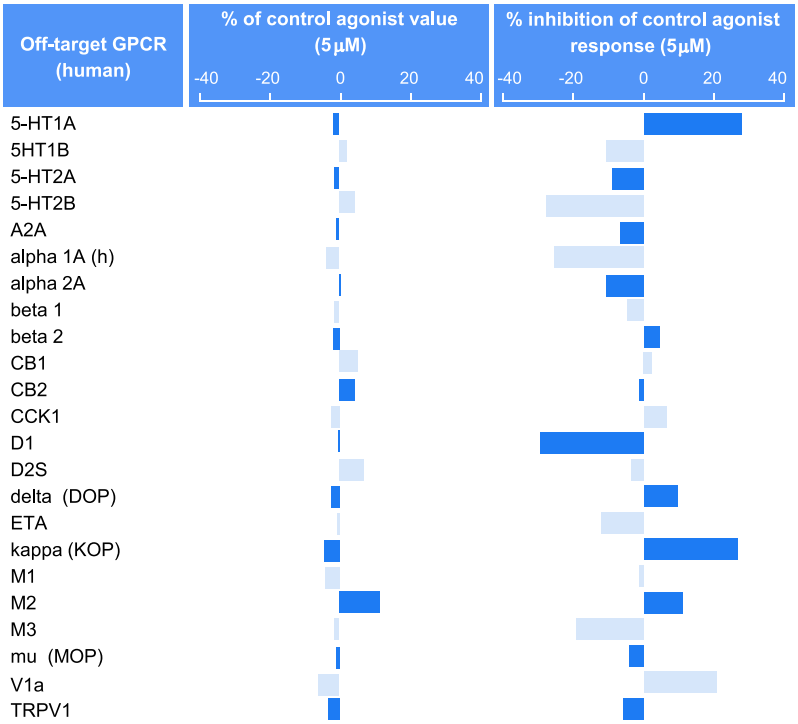

c

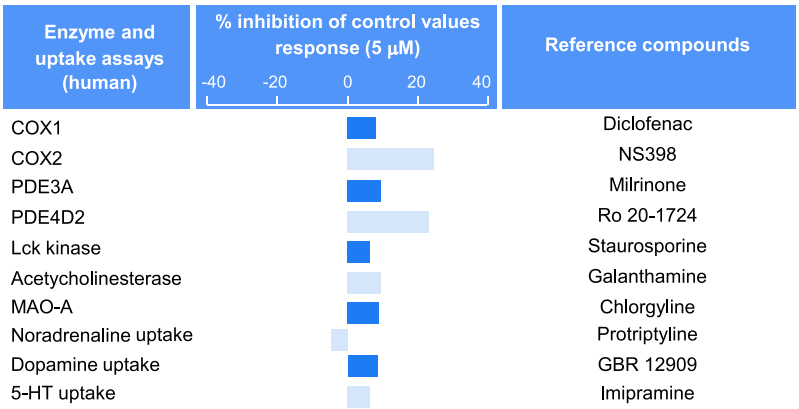

Figure 1. Pharmacological functional profile of LIT-001 on off-targets. (**a**) LIT-001 structure, physico-chemical properties and potency on target receptors. (**b**) *In vitro* agonist and antagonist profiles of LIT-001 on 24 off-target GPCRs. Cellular agonist and antagonist effects of LIT-001 were calculated as a % of control response to a known reference agonist for each target and cellular antagonist. Negative values are non significant in these assay setups. (**c**) Enzyme and transporter inhibition potency of LIT-001 on selected off-targets. Compound enzyme inhibition effect was calculated as a % inhibition of control enzyme activity. Compound uptake inhibition effect was calculated as a % inhibition of control uptake activity. Data are expressed as the mean value of 2 independent tests.

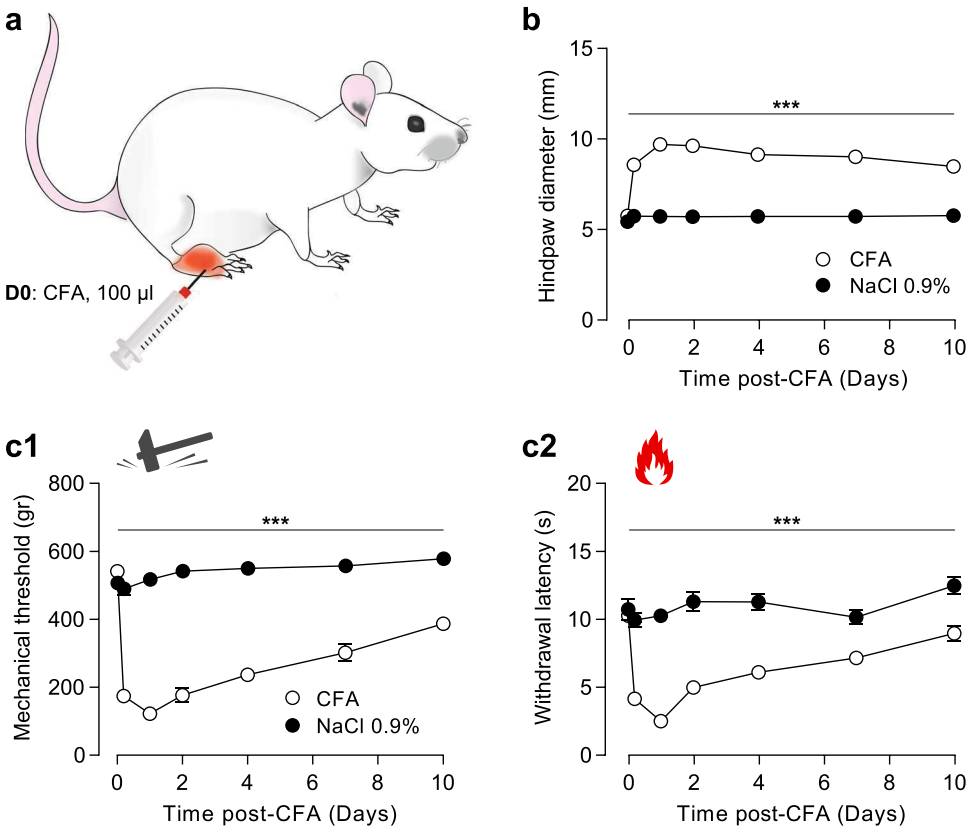

Figure 2. Ten days' time course of long-term modifications induced by CFA subcutaneous injection. (**a**) Scheme of the CFA-induced inflammatory pain model (100 µl). (**b**) Time-course of the CFA-induced edema size (CFA, n = 14; NaCl, n = 18). (**c**) Time-course of the CFA-induced mechanical (**c1**) and thermal heat (**c2**) hyperalgesia (CFA, n = 14; NaCl, n = 18). Data are expressed as mean ± SEM. Asterisks indicate statistical significance (***$p < 0.001$) using two-way ANOVA followed by Tukey multiple comparisons post-hoc test.

Given that LIT-001 was built as a specific agonist for OTR, we thought to validate that these anti-hyperalgesic effects were mediated by OTR activation. For this purpose, we co-injected LIT-001 with a specific OTR antagonist, L-368,699[11]. As expected, the anti-hyperalgesic action of i.p. LIT-001 was fully prevented by L-368,699, as displayed by the mechanical threshold (CFA + LIT-001 + L-368, 119 ± 12 g, n = 7) and thermal heat latency (CFA + LIT-001 + L-368, 3.08 ± 0.29 s, n = 7) and their relative AUC (90 ± 7% and 92 ± 8%, respectively) values 3 h post i.p. (Fig. 4c). These results indicate that i.p. LIT-001 likely exerts its anti-hyperalgesic action through OTR binding.

One important point in the development of a clinically-relevant anti-hyperalgesic compound is the limitation of its side effect, here the absence of anti-nociception. Noteworthy, we did not detect any alteration of contralateral hindpaw sensitivities after i.p. LIT-001, being on mechanical threshold (cCFA + LIT-001, 531 ± 25 g, n = 8; Fig. S4a1) or thermal heat latency (cCFA + LIT-001, 11 ± 0.53 s, n = 8; Fig. S4a2). Interestingly, we made similar observation on control animals, receiving NaCl 0.9% hindpaw injection and thus not presenting inflammatory pain symptoms (Figs. 4d, S4b). Here, i.p. LIT-001, injected alone or co-injected with the specific oxytocin receptor antagonist L-368,699, had no effect on mechanical (NaCl + LIT-001, 526 ± 20 g, n = 7; Figs. 4d1, S4b1) or thermal heat (NaCl + LIT-001, 8.14 ± 0.48 s, n = 7; Figs. 4d2, S4b2) hindpaw sensitivities, as reflected by the absence of increase of the AUC (Figs. 4d, S4b). These results indicate that i.p. LIT-001, as an analgesic, is only effective in case of detectable hypersensitivities.

LIT-001 distribution and clearance in the organism. Because the anti-hyperalgesic effects of i.p. LIT-001 10 mg/kg were long-lasting, up to 5 h, while oxytocin-induced analgesia usually only last for minutes, we analyzed its distribution at key time points in plasma, CSF, brain and urine (n = 5–6, Fig. 5) and performed a quantitative dosage by comparison to a dose-response curve, using Liquid Chromatography Mass Spectrometry (LC-MS/MS; Fig. S5). Interestingly, LIT-001 concentration was found in plasma at its highest 30 min after i.p. injection (650 ± 200 pmole/ml; Fig. 5b) then slowly decreased, but was still significantly present after 300 min (5 h; 95.2 ± 36.5 pmole/ml; Fig. 5b,c). In addition, LIT-001 was found in significant amount in both the brain and CSF 60 min after i.p. injection (1.6 ± 0.8 and 7.4 ± 4.4 pmole/ml, respectively; Fig. 5c) when its analgesic action is significantly observed. As expected according to its chemical structure and previous half-life evaluation, after 5 h most of LIT-001 was found in urine (188951 ± 8475 pmole/ml; Fig. 5c) and was hardly detectable in both CSF (1.5 ± 1.1 pmole/ml) and brain (0.6 ± 0.4 pmole/ml; Fig. 5c). These results indicate that the long-lasting

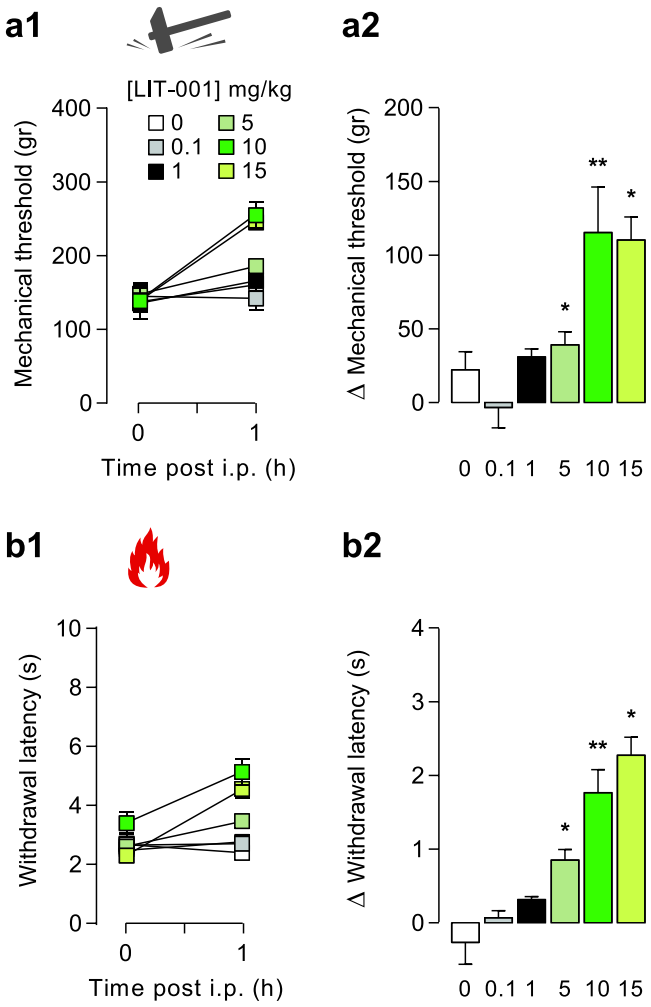

Figure 3. Dose-response of the analgesic properties of LIT-001 on CFA-induced inflammatory pain model. Effects of LIT-001 0.1 (n = 4), 1 (n = 6), 5 (n = 6), 10 (n = 8) and 15 mg/kg (n = 6) or its vehicule (n = 9) measured 1 hour after i.p. injection on mechanical (**a**) and thermal heat (**b**) CFA-induced hyperalgesia. Data are expressed as mean ± SEM. Asterisks indicate statistical significance (**p < 0.01; *p < 0.05) using paired Wilcoxon or T-test, depending on the data's normal distribution.

anti-hyperalgesic effect of i.p. LIT-001 is likely due to its prolonged presence in plasma, with putative central effects.

Discussion

In the present study, we show that LIT-001, a non-peptidergic specific agonist for OTR, exerts a significant long-lasting (>5 h) anti-hyperalgesic effect on both mechanical and thermal heat sensitivity.

Antinociceptive and analgesic action of OT is well documented[21–23]. It has been shown to act at both peripheric and central levels[10] mainly through final reduction of spinal wide dynamic range (WDR) neurons and C fiber excitability[11]. However, the main limitations of OT, or OTR peptidergic agonists, are (i) the short duration of the effect, (ii) the lack of permeability through the blood brain barrier (BBB), and (iii) the lack of specificity, which all are not compatible with clinical use.

Here, we show that a low molecular weight, non-peptidergic agonist, LIT-001, exerts a long lasting antihyperalgesic effect, up to 5 h. Two points may explain the prolonged effect of LIT-001. First, it has a long half-life (>2 h), by comparison to OT or OTR peptidergic agonists, which all have a very short half-life of less than 15 min. Second, it may reach its central and/or peripheral targets and trigger here long lasting mechanisms involving OTR. At this point, it is important to highlight that, for clinical purpose and mainly in case of chronic pain, a strong analgesic candidate should not only focus on nociception but also positively modulate all pain-induced disorders, such as anxiety, depression, loss of social interaction, impaired food intake or stress. Indeed, to attenuate this large variety of pain-relative symptoms may significantly improve the patient quality of life, one of the main goals of modern medicine. In this regard, to target the oxytocinergic system, in particular with specific OTR agonist such as LIT-001, may be particularly relevant. Indeed, activation of OTR is known to induce a variety of molecular cascades[24] resulting in an important modulation of nociception[25], social recognition and interactions[26,27], anxiety[28], feeding behavior[29], and stress[30], all important comorbidity factors in painful patients.

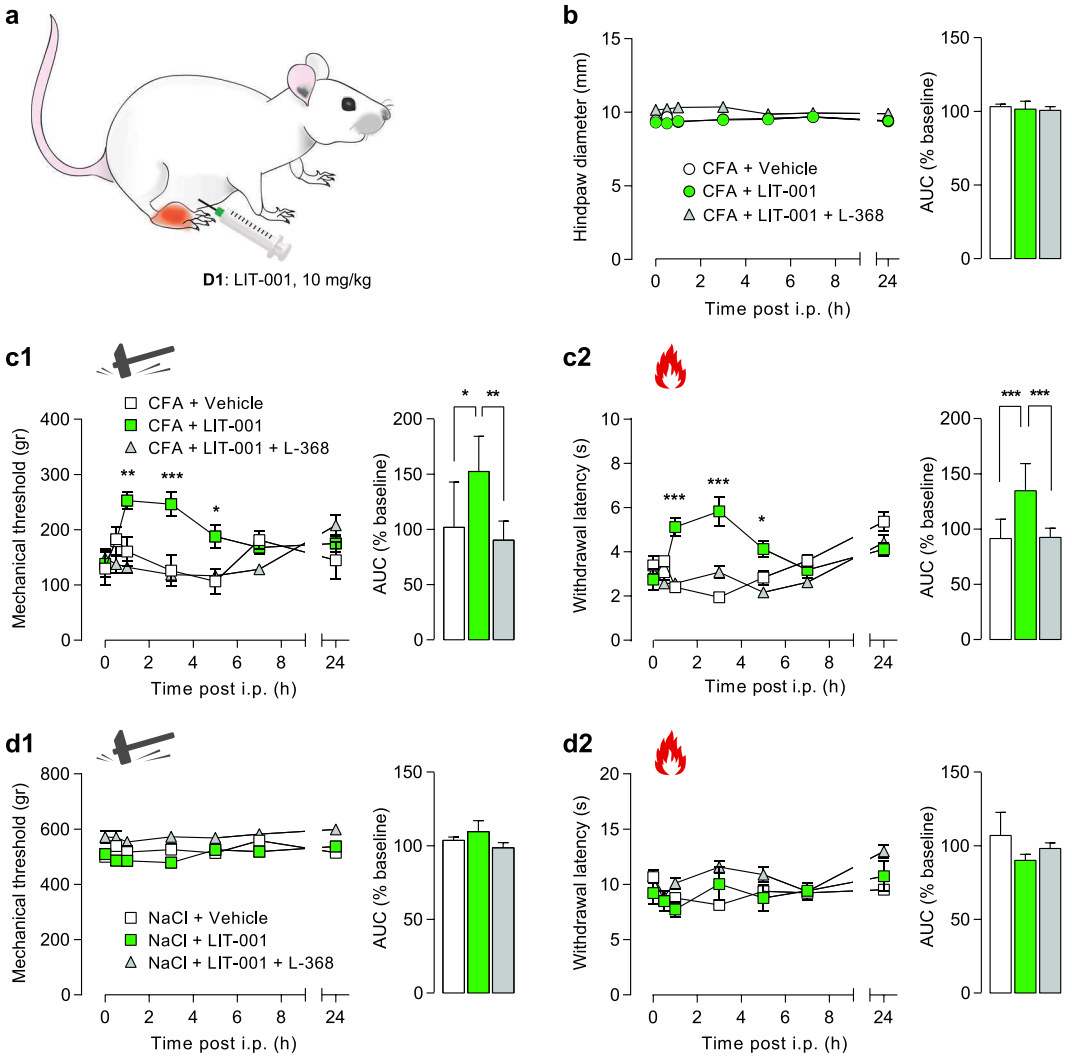

Figure 4. Time-course of the analgesic properties of LIT-001 on CFA-induced inflammatory pain model. (**a**) Scheme of the CFA-induced inflammatory pain model followed by i.p. LIT-001 injection. (**b**) Left, time-course of the effects of i.p. LIT-001 10 mg/kg (n = 8), its vehicule (n = 7) or co-injection with L-368,699 (n = 7), on CFA-induced edema size (CFA, n = 14; NaCl, n = 18). Right, relative-to-baseline AUC (%) of the effects. (**c**) Left, time-course of the effects of i.p. LIT-001 10 mg/kg (n = 7), its vehicule (n = 8) or co-injection with L-368,699 (n = 6) on CFA-induced mechanical (**c1**) and thermal heat (**c2**) hyperalgesia. Right, relative-to-baseline AUC (%) of the effects. (**d**) Left, time-course of the effects of i.p. LIT-001 10 mg/kg (n = 7), its vehicule (n = 8) or co-injection with L-368,699 (n = 6) on mechanical (**d1**) and thermal heat (**d2**) sensitivities of NaCl-injected hindpaw. Right, relative-to-baseline AUC (%) of the effects. Data are expressed as mean ± SEM. Asterisks indicate statistical significance (***$p < 0.001$; **$p < 0.01$; *$p < 0.05$) using two-way ANOVA followed by Tukey's multiple comparisons test.

Interestingly, a previous study has also shown that LIT-001 improved social interaction in a mouse model of autism[20], reinforcing its putative interest as an analgesic molecule.

Besides, we confirm the capability of LIT-001 to cross the blood brain barrier to exert its action in the central nervous system[20] (Fig. 5). In addition, we show that LIT-001 exerts long lasting anti-hyperalgesic effects. Importantly, LIT-001 does not accumulate in the body but is almost entirely excreted as such in the urine. While those data were obtained by intra-peritoneal injection, we hypothesize that similar results may be obtained using an oral administration of LIT-001. If true and transposable to human, it may lead to the development of a drug easy to take every few hours to limit pain symptoms. Those aspects point toward LIT-001, and future non-peptidergic agonists, as key candidates for clinical use. Although it displays a low micromolar affinity for this receptor, LIT-001 is a potent V2R agonist in functional assays[20]. The V2 receptor is peripheral and known to regulate water homeostasis. It is thus likely that LIT-001 will have some antidiuretic effect *in vivo* that will have to be studied and taken into account for a potential development toward clinical studies.

Because of its long half-life and its capability to cross the BBB, one may worried about the putative LIT-001 side effects: to design drugs with limited side-effects is a major challenge in chemical and pharmaceutical industries. Importantly, LIT-001 does not interact significantly with any classical off targets (G protein coupled

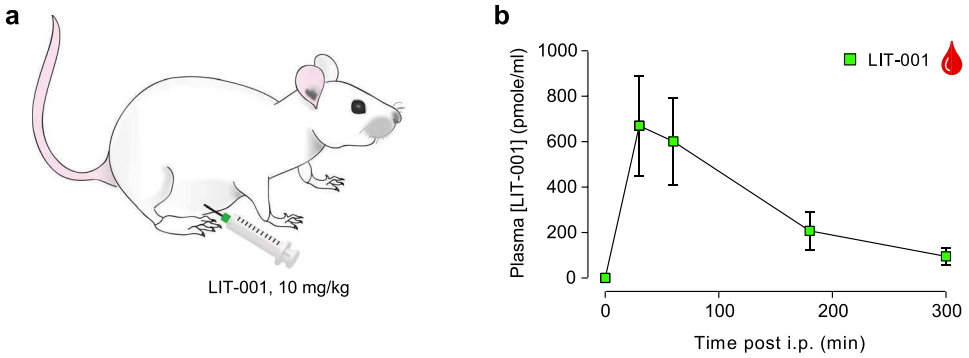

c

Time after i.p. injection (min)	[LIT-001] (pmole/ml +/- sem)			
	Brain	CSF	Plasma	Urine
60	1.6 ± 0.8	7.4 ± 4.4	626.1 ± 112.3	52498 ± 14244
300	0.6 ± 0.4	1.5 ± 1.1	95.2 ± 36.5	188951 ± 8475

Figure 5. LIT-001 distribution and clearance in the organism. (**a**) Scheme displaying the i.p. injection of LIT-001, 10 mg/kg in naïve animal. (**b**) Time course of the concentrations of LIT-001 present in the plasma of rats after an i.p. injection. (**c**) Concentrations of LIT-001 present at 60 and 300 min after i.p. injection, in the brain (60, n = 6; 300, n = 5), CSF (60, n = 4; 300, n = 4), plasma (60, n = 11; 300, n = 5) and urine (60, n = 6; 300, n = 5) 60 min and 300 min after i.p. injection. Data are expressed as mean ± SEM. Data are expressed as mean ± SEM of 5 animals.

receptors, transporters, enzymes, ion channels listed in Figs. 1, S1), neither as an agonist/activator nor an antagonist/inhibitor. Noteworthy, neither LIT-001 nor the OT antagonist L-368,699 displayed any significant agonist or antagonist activity at the TRPV1 receptor at 5 μM (Fig. 1b). Therefore, LIT-001 is a relatively specific OTR agonist likely exerting its analgesic effect via this receptor. This conclusion is strengthened by our results showing that the LIT-001 antihyperalgesic action is fully prevented in presence of L-368,699, a specific OTR antagonist that is also devoid of significant activity at TRPV1 receptor at 5 μM. In addition, an interesting aspect of LIT-001 seems to be its specific action on nociception and pain. Indeed, while LIT-001 shows limited inhibitory activity of COX2, which in a model of inflammatory pain could be relevant, we observed no modification of the size of the edema induced by CFA injection (Fig. 4), indicating that the LIT-001-induced reduction of pain symptoms is not based on a reduction of inflammation. However, we did not rule specific protocols to tests its anti-inflammatory action *per se*, and this should be done before any clinical trial. In addition, it is important to note that LIT-001 did not modify the mechanical/thermal heat sensitivities in control animals or contralateral paws, indicating that LIT-001 does not have antinociceptive effect, which, in a clinical perspective, is an important characteristic in order to limit undesired loss of sensitivities. At this stage, the only known drawback of LIT-001 is its action at the V2 vasopressin receptor (V2R).

In conclusion, we found that LIT-001 is a very useful probe to validate the oxytocin receptor as a target for the treatment of pain and represents a promising drug-like lead compound for the development of novel treatments.

Methods

All the protocols, tests and use and living animals were performed in accordance with European committee council Direction, authorization from French Department of Agriculture and from the regional ethic committee (Comité Régional d'Ethique en Matière d'Expérimentation Animale de Strasbourg, CREMEAS).

Drugs. LIT-001 was prepared as described in Frantz *et al.*[20]. For *in vivo* biological assays, it was dissolved in carboxymethyl cellulose (CMC, 1%) - NaCl (0.9%) and administered at the dose of 10 mg/kg. LIT-001 or vehicle were injected intraperitoneally (i.p.), in a volume of 10 ml/kg[20], 24 h after the induction of the CFA-induced painful inflammatory sensitization. To confirm the implication of the OTR we injected (i.p.) also L-368,899 (Sigma, St. Louis, MO) (1 mg/kg), an OTR antagonist, in combination with LIT-001 in another group of rats[11].

In vitro* physicochemical and pharmacological characterization.** ***Solubility of LIT-001 was determined from solution of about 1 mg of compound in 500 μl of PBS at pH 7.4. (Figs. 1, S1) The solution was stirred at room temperature for 24 h and centrifuged at 15.000 × *g* for 5 min. The supernatant was diluted with a mixture of acetonitrile and water and analyzed by HPLC with a diode detector (Gilson; Kinetex 2.6 μm C18 100 A 50 × 4.6 mm column). No degradation of LIT-001 was observed after 24 h. The lipophilicity ($LogD_{7.4}$) of LIT-001 was measured using 10 ml of a stock solution diluted with different concentrations of octanol and PBS to cover a LogP range from −2 to + 4.5 in a final volume of 1 ml. After stirring for 1 h at room temperature (≈ 20 °C), the

samples were centrifuged and the different phases were analyzed by HPLC (Gilson; diode detector, Kinetex 2.6 µ C18 100 A 50 × 4.6 mm column).

Stability of LIT-001 was determined in human hepatocytes. Cells were unfrozen and their viability measured (Tryptan blue). Cells are suspended (2 × 106 cells/ml) and dispensed in 96 well microtiterplates (50 µl/well). LIT-001 (50 µl of a 2 µM in the incubation media) was added. The final concentration of the compound was 1 µM in 1×10^6 cells/ml. The incubation volume was 100 µl/well. Incubations were stopped after 0, 4, 20, 40, 80 and 120 min in mixing the well content with 100 µl acetonitrile at 0 °C. A positive control (testosterone) was prepared in same conditions. All samples were analyzed by LC-MS/MS (UHPLC coupled to a triple quadripole Shimadzu LC-MS 8030). Each measurement was performed in triplicate.

In vitro profiling of LIT-001 was performed by Eurofins as described in the Eurofins SafetyScreen-Functional panel, 2018[31]. The hepatotoxicity of LIT-001 was studied with cryo-preserved mouse hepatocytes. After unfreezing (optiTHAW and optiINCUBATE media, Xenotech) and cell viability control, cells (2×10^6 cells/ml) were dispatched in 96 well microtiterplates. LIT-001 was added to reach a concentration 1 µM in the presence of 1 × 106 cells/mL in a volume of 100 µl/well. The incubation was stopped at 4, 20, 40, 80 and 120 min in adding 100 µl of acetonitrile at 0 °C. A positive control was treated in the same conditions. All samples were analyzed by UHPLC coupled to a mass spectrometer (Shimadzu LC-MS 8030).

Cytochrome inhibition by LIT-001 was studied as follows. A stock solution of LIT-001 at 10 mM in DMSO was prepared and stored at 4 °C. Solutions containing the cytochrome substrates and control inhibitors or LIT-001 were prepared. 2 µl of substrate-inhibitor solutions were mixed with 176 µl of phosphate buffer containing human liver microsomes (0.2 mg/ml), 1 mM of NADPH and 3 mM of $MgCl_2$. Height concentrations were tested: 0.03; 0.1; 0.3; 1; 3; 10; 30 and 100 µM. The reaction was initiated by addition of the co-factor after 5 min of incubation at 37 °C. After one hour of incubation, 200 µl of acetonitrile were added to stop enzymatic reactions and solubilize the products. Different control inhibitors were used and supernatants were analyzed by LC-MS/MS (UHPLC separation; Shimadzu LC-MS 8030).

- Furafylline (CYP 1A2 inhibitor): 0.03; 0.1; 0.3; 1; 3; 10; 30 and 100 µM
- Sulfaphenazole (CYP 2C9 inhibitor): 0.03; 0.1; 0.3; 1; 3; 10; 30 and 100 µM
- Tranylcypromine (CYP 2C19 inhibitor): 0.03; 0.1; 0.3; 1; 3; 10; 30 and 100 µM
- Quinidine (CYP 2C19 inhibitor): 0.003; 0.01; 0.1; 0.5; 1; 5; 10 and 50 µM
- Kétoconazole (CYP 3A4 inhibitor): 0.003; 0.01; 0.1; 0.5; 1; 5; 10 and 50 µM

Animals. Male Wistar rats (300 g; JANVIER LABS, Le Genest St. Isle, France) were used for this study. They were housed by groups of 3 or 4 under standard conditions (room temperature, 22 °C; 12/12 h light/dark cycle) with *ad libitum* access to food and water and behavioral enrichment. All animals were manipulated and habituated to the tests and to the room for at least 2 weeks. All behavioral tests were done during the light period (i.e., between 7:00 and 19:00). All the procedures were performed in accordance with European committee council Direction, authorization from French Department of Agriculture and from the regional ethic committee.

Behavioral testing. *Mechanical allodynia.* In all experimentations, to test the animal mechanical sensitivity, we used a calibrated forceps (Bioseb, Chaville, France) previously developed in our laboratory (Figs. 2, 3 and S2, S3)[32]. Briefly, the habituated rat is loosely restrained with a towel masking the eyes in order to limit stress by environmental stimulations. The tips of the forceps are placed at each side of the paw and a graduate force is applied. The pressure producing a withdrawal of the paw, or in some rare cases a vocalization of the animal, corresponded to the nociceptive threshold value. This manipulation was performed three times for each hindpaw and the values were averaged averaged.

Thermal allodynia/hyperalgesia. To test the animal heat sensitivity, we used the Plantar test with Hargreaves method (Ugo Basile, Comerio, Italy) to compare the response of each hindpaw[33] when we tested healthy animals (unilateral intraplantar NaCl injection) and animals having received unilateral intraplantar CFA (Freund's Complete Adjuvant) injection. The habituated rat is placed in a small box and we wait until the animal is calmed then we exposed the hindpaw to a radiant heat, the latency time of paw withdrawal was measured.

CFA model of inflammatory pain. In order to induce a peripheral inflammation, 100 µl of complete Freund adjuvant (CFA; Sigma, St. Louis, MO), was injected in the right hindpaw of the rat. All CFA injections were performed under light isoflurane anesthesia (3%). Animals were tested daily for 10 days after the paw injection, a period during which animals exhibited a clear mechanical allodynia and thermal heat hyperalgesia.

Pharmacokinetics of LIT-001. *Preparation of brain, cerebrospinal fluid, plasma and urine extracts.* Brains from rat injected with 10 mg/kg (18.8 µmol/kg) i.p. of LIT-001 were homogenized with an Ultra Turrax instrument (Ika, Staufen, Germany) in 2 ml of H_2O (Figs. 4, S4). The homogenates were then sonicated (3 times 10 s, 100 W) with a Vibra Cell apparatus (Sonics, Newtown, U.S.A.). Protein concentrations were determined using the Bradford method (Protein Assay, Bio-Rad, Marne-la-Coquette, France). 400 µl was mixed with 4 ml of ice cold acetonitrile (ACN) and let 30 min on ice. Samples were then centrifuged (20,000 × *g*, 30 min) at 4 °C. Supernatants were dried under vacuum and resuspended in 400 µl ACN 10%/H_2O 89.9%/formic acid 0.1% (v/v/v) and a volume of 5 µl was injected on the LC-MS/MS. For CSF, plasma and urine, 200 µl of fluids were mixed with 1 ml of ice cold acetonitrile (ACN) and let 30 min on ice. Samples were then centrifuged (20,000 × *g*, 30 min) at 4 °C.

Supernatants were dried under vacuum and suspended in 200 µl ACN 10%/H_2O 89.9%/formic acid 0.1% (v/v/v) and a volume of 5 µl was injected on the LC-MS/MS.

LC-MS/MS instrumentation and analytical conditions. Analyses were performed on a Dionex Ultimate 3000 HPLC system (Thermo Scientific, San Jose, USA) coupled with a triple quadrupole Endura mass spectrometer (Thermo Scientific). The system was controlled by Xcalibur v.2.0 software (Thermo Electron). Samples were loaded onto an Accucore C18 RP-MS column (ref 17126–151030; 150 × 1 mm 2.6 µm, Thermo Scientific) heated at 40 °C. The presence of LIT-001 was studied using the multiple reaction monitoring mode (MRM). Elution was performed at a flow rate of 150 µl/min by applying a linear gradient of mobile phases A/B. Mobile phase A corresponded to ACN 1%/H_2O 98.9%/formic acid 0.1% (v/v/v), whereas mobile phase B was ACN 99.9%/formic acid 0.1% (v/v). The gradient used is detailed in Fig. S4. Electrospray ionization was achieved in the positive mode with the spray voltage set at 3,500 V. Nitrogen was used as the nebulizer gas and the ionization source was heated to 210 °C. Desolvation (nitrogen) sheath gas was set to 27 Arb and Aux gas was set to 9 Arb. The ion transfer tube was heated at 312 °C. Q1 and Q2 resolutions were set at 0.7 FWHM, whereas collision gas (CID, argon) was set to 2 mTorr. Identification of the compounds was based on precursor ion, selective fragment ions and retention times obtained for LIT-001. Selection of the monitored transitions and optimization of collision energy and RF Lens parameters were manually determined (see Fig. S4 for details). Qualification and quantification were performed in MRM mode. Quantification was obtained using Quan Browser software (Thermo Scientific). For tissues and fluids, LIT-001 was quantified using calibration curves of external standards of LIT-001 (125 fmol to 100 pmol/injection; Fig. S4) added to urine, plasma or brain extracts of naive rat and submitted to the same procedure described for respective fluids and tissue recovery. The amounts of LIT-001 measured in samples fit within the standard curve limits, with typical analytical ranges (the range of amounts that can be accurately quantified) from 150 fmol to 120 pmol.

Statistical analysis. Data are expressed as mean ± standard error of the mean (SEM). Statistical tests were performed with GraphPad Prism 7.05 (GraphPas Software, San Diego, California, USA) using repeated-measures two-way ANOVA, with the following factors: treatment (between), and time (within); when the ANOVA test was significant, the Tukey test was used for *post-hoc* multiple comparisons between individual groups. Results were considered to be statistically significant if p values were below 0.05 (*), 0.01 (**), and 0.001 (***). For the area under the curve (AUC) comparisons, we used the one-way ANOVA (factors: treatment); when the ANOVA test was significant, the Tukey test was used for post hoc multiple comparisons.

Received: 7 October 2019; Accepted: 2 February 2020;
Published online: 20 February 2020

References

1. Dale, H. H. The action of extracts of pituitary body. *Biochem J.* **4**, 427–447 (1906).
2. Sawchenko, P. E., Swanson, L. W., Steinbusch, H. W. M. & Verhofstad, A. A. J. The distribution and cells of origin of serotonergic inputs to the paraventricular and supraoptic nuclei of the rat. *Brain Research* **277**, 355–360 (1983).
3. Du Vigneaud, V., Ressler, C. & Trippett, S. The sequence of aminoacids in oxytocin, with a proposal for the structure of oxytocin. *J. Biol. Chem.* **205**, 949–957 (1953).
4. Kimura, T., Tanizawa, O., Mori, K., Brownstein, M. J. & Okayama, H. Structure and expression of a human oxytocin receptor. *Nature* **356**, 526–529 (1992).
5. Grinevich, V. & Charlet, A. Oxytocin: pain relief in skin. *Pain* **158**, 2061–2063 (2017).
6. Lundeberg, T., Uvnäs-Moberg, K., Agren, G. & Bruzelius, G. Anti-nociceptive effects of oxytocin in rats and mice. *Neuroscience Letters* **170**, 153–157 (1994).
7. Petersson, M., Wiberg, U., Lundeberg, T. & Uvnäs-Moberg, K. Oxytocin decreases carrageenan induced inflammation in rats. *Peptides* **22**, 1479–1484 (2001).
8. Yu, S. Q., Lundeberg, T. & Yu, L. C. Involvement of oxytocin in spinal antinociception in rats with inflammation. *Brain Research* **983**, 13–22 (2003).
9. Gonzalez-Hernandez, A. *et al*. Peripheral oxytocin receptors inhibit the nociceptive input signal to spinal dorsal horn wide-dynamic-range neurons. *Pain* **158**, 2117–2128 (2017).
10. Juif, P. E. & Poisbeau, P. Neurohormonal effects of oxytocin and vasopressin receptor agonists on spinal pain processing in male rats. *Pain* **154**, 1449–1456 (2013).
11. Eliava, M. *et al*. A new population of parvocellular oxytocin neurons controlling magnocellular neuron activity and inflammatory pain processing. *Neuron* **89**, 1291–1304 (2016).
12. Jiang, C. Y., Fujita, T. & Kumamoto, E. Synaptic modulation and inward current produced by oxytocin in substantia gelatinosa neurons of adult rat spinal cord slices. *J. Neurophysiol.* **111**, 991–1007 (2013).
13. Heesen, M. *et al*. International consensus statement on the use of uterotonic agents during caesarean section. *Anaesthesia* **74**, 1219–1241 (2019).
14. Gimpl, G. & Fahrenholz, F. The oxytocin receptor system: structure, function, and regulation. *Physiological Reviews* **81**, 629–683 (2001).
15. Morin, V. *et al*. Evidence for non-linear pharmacokinetics of oxytocin in anesthetized rat. *J. Pharm. Pharm. Sci.* **11**, 12–24 (2008).
16. Mens, W., Witter, A. & Van Wimersma Greidanus, T. B. Penetration of neurohypophyseal hormones from plasma into cerebrospinalfluid (CSF): half-times of disappearance of these neuropeptidesfrom CSF. *Brain Res.* **262**, 143–152 (1983).
17. Chini, B. *et al*. Two aromatic residues regulate the response of the human oxytocin receptor to the partial agonist arginine vasopressin. *FEBS Letters* **397**, 201–206 (1996).
18. Kubo, A. *et al*. Oxytocin alleviates orofacial mechanical hypersensitivity associated with infraorbital nerve injury through vasopressin-1A receptors of the rat trigeminal ganglia. *Pain* **158**, 649–659 (2017).
19. Nersesyan, Y. *et al*. Oxytocin modulates nociception as an agonist of pain-sensing TRPV1. *Cell Rep.* **21**, 1681–1691 (2017).
20. Frantz, M. C. *et al*. LIT-001, the first nonpeptide oxytocin receptor agonist that improves social interaction in a mouse model of autism. *J. Med. Chem.* **61**, 8670–8692 (2018).
21. Boll, S., Almeida de Minas, A. C., Raftogianni, A., Herpertz, S. C. & Grinevich, V. Oxytocin and pain perception: from animal models to human research. *Neuroscience* **387**, 149–161 (2017).

22. Gonzalez-Hernandez, A. & Charlet, A. Oxytocin, GABA, and TRPV1, the analgesic triad? *Frontiers in Molecular Neuroscience*, https://doi.org/10.3389/fnmol.2018.00398 (2018).
23. Poisbeau, P., Grinevich, V. & Charlet, A. Oxytocin signaling in pain: cellular, circuit, system, and behavioral levels. *Current Topics in Behavioral Neurosciences* **35**, 193–221 *Behavioral Pharmacology of Neuropeptides: Oxytocin*, (2017).
24. Busnelli, M. & Chini, B. Molecular Basis of Oxytocin Receptor Signalling in the Brain: What we know and what we need to know. *Current Topics in Behavioral Neurosciences* **35**, 3–29 *Behavioral Pharmacology of Neuropeptides: Oxytocin*, (2017).
25. Juif, P. E. *et al*. Long-lasting spinal oxytocin analgesia is ensured by the stimulation of allopregnanolone synthesis which potentiates GABA(A) receptor-mediated synaptic inhibition. *J. Neurosci.* **33**, 16617–16626 (2013).
26. Andari, E. *et al*. Promoting social behavior with oxytocin in high-functioning autism spectrum disorders. *PNAS* **107**, 4389–4394 (2010).
27. Kosfeld, M., Heinrichs, M., Zak, P. J., Fischbacher, U. & Fehr, E. Oxytocin increases trust in humans. *Nature* **435**, 673–676 (2005).
28. Grund, T. *et al*. Neuropeptide S activates paraventricular oxytocin neurons to induce anxiolysis. *J. Neurosci.* **37**, 12214–12225 (2017).
29. Arletti, R., Benelli, A. & Bertolini, A. Influence of oxytocin on feeding behavior in the rat. *Peptides* **10**, 89–93 (1989).
30. Neumann, I. D. Involvement of the brain oxytocin system in stress coping: interactions with the hypothalamo-pituitary-adrenal axis. *Prog. Brain Res.* **139**, 147–162 (2002).
31. Eurofins SafetyScreen - Functional panel. https://www.eurofinsdiscoveryservices.com/ (2018)
32. Charlet, A., Lasbennes, F., Darbon, P. & Poisbeau, P. Fast non-genomic effects of progesterone-derived neurosteroids on nociceptive thresholds and pain symptoms. *Pain* **139**, 603–609 (2008).
33. Hargreaves, K., Dubner, R., Brown, F., Flores, C. & Joris, J. A new and sensitive method for measuring thermal nociception in cutaneous hyperalgesia. *Pain* **32**, 77–88 (1988).

Acknowledgements

This work was supported by the NARSAD Young Investigator Grant 24821 (to AC); the IDEX Interdisciplinary grant 2015 (to AC and MH); the French government under the specific ANR-14-CE-16-0005-01 project (OT-ism; to MH). The authors thank the Chronobiotron (UMS 3512 for assistance in animal cares, experimentations and surgeries), the PCBIS platform (UMS 3286 for physicochemical and pharmacokinetic studies) and the PACSI platform (GDS3670 for analytical chemistry).

Author contributions

Conceptualization, A.C., M.H.; Methodology, A.C., D.K., L.H., M.H., Q.Z., Y.G.; Chemical analysis, Q.Z.; Behavior, L.H.; Samples extracts, L.H., P.I.; H.P.L.C. dosages, V.A., Y.G.; Writing, A.C., L.H., M.H., P.D.; Funding acquisition, M.H., A.C.; Supervision, M.H., A.C.; Project administration, A.C.

Competing interests

The authors declare no competing interests.

Additional information

Supplementary information is available for this paper at https://doi.org/10.1038/s41598-020-59929-w.

Correspondence and requests for materials should be addressed to A.C.

Reprints and permissions information is available at www.nature.com/reprints.

Publisher's note Springer Nature remains neutral with regard to jurisdictional claims in published maps and institutional affiliations.

II- Neuropeptide signaling systems in the control of pain and co-morbid symptoms

a. Résumé

La douleur chronique est actuellement un important fardeau dans la vie des patients touchées par cette pathologie, mais également pour la société. On estime qu'environ 20% de la population européenne et 15% de la population américaine souffre de douleur chronique modérée à sévère. Actuellement la prise en charge de ces douleurs repose presque exclusivement sur la modulation des récepteurs opioïdes. Cependant ce type de traitement est généralement associé à des charges sociales et sanitaires majeures, telles que la dépendance aux opioïdes, ainsi qu'un grand nombre de décès induit par le surdosage. Il s'agit alors d'un enjeu scientifique, économique et social de développer d'autres alternatives thérapeutiques. La nociception est modulée à différents niveaux par une large gamme de composés neurochimiques, dont un large éventail est composé de neuropeptides, comprenant les opioïdes et les peptides non-opioïdes. La plupart de ces peptides agissent via des récepteurs spécifiques couplés aux protéines G. Plusieurs de ces neuropeptides non-opioïdes et leurs récepteurs s'avèrent être des cibles intéressantes pour des recherches plus poussées concernant la modulation du signal nociceptif, présentant ainsi de nouvelles options thérapeutiques pour la gestion de la douleur. Dans cette revue, nous avons voulu résumer les principales avancées historiques et plus récentes dans ce domaine en mettant l'accent sur les données relatives aux systèmes de signalisations neuropeptidiques non-opioïdes. De plus nous avons voulu mettre en évidence certaines caractéristiques clés des études précliniques qui démontrent les progrès de la recherche fondamentale sur les neuropeptides jouant un rôle dans la nociception. Dans le contexte de cette analyse, nous discutons de la relation entre la douleur chronique et les symptômes physiopathologiques et émotionnels, ainsi que les relations entre les systèmes opioïdes et non- opioïdes, les différences de sexe et les différences d'espèces dans la nociception. Une meilleure compréhension de ces systèmes complexes devrait conduire à de meilleurs résultats en ciblant les systèmes peptidiques non- opioïdes pour la gestion de la douleur chronique.

Review article

Neuropeptide signaling systems in the control of pain and co-morbid symptoms

João Covita[a-d], Alexandre Charlet[e-g], Damien Kerspern[e-g], Sherie Ma[c,d,†], Andrew L. Gundlach[c,d,*], Marc Landry[a,b,*]

[a]Interdisciplinary Institute for Neuroscience, University of Bordeaux, Bordeaux, France

[b]UMR 5297, Centre National de la Recherche Scientifique (CNRS), Interdisciplinary Institute for Neuroscience, University of Bordeaux, Bordeaux, France

[c]The Florey Institute of Neuroscience and Mental Health, Parkville, Victoria, Australia

[d]Florey Department of Neuroscience and Mental Health, The University of Melbourne, Victoria, Australia

[e]Institute of Cellular and Integrative Neurosciences (INCI) Strasbourg, France

[f]UPR3212, Centre National de la Recherche Scientifique (CNRS), University of Strasbourg, Strasbourg, France

[g]University of Strasbourg Institute for Advanced Study (USIAS), Strasbourg, France

* Corresponding authors

Email addresses: andrew.gundlach@florey.edu.au (A.L. Gundlach), marc.landry@u-bordeaux.fr (M. Landry)

† Current Address: Servier Program in Drug Discovery, Monash Institute of Pharmacological Sciences, Monash University, Parkville, Victoria, Australia

Key words: Anxiety, Co-morbidity; Depression, GPCR, Neuropeptides; Opioids; Oxytocin; Pain

Word count: 8350 text, 14100 total

Number of tables: 1

Number of figures: 0

Abbreviations

5-HT	5-hydroxytryptamine
AgRP	Agouti-related peptide
AN	Accessory nucleus of the hypothalamus
An2	Angiopep-2
ARC	Arcuate nucleus
BBB	Blood-brain barrier
BK	Bradykinin
BLA	Basolateral amygdala
BNST	Bed nucleus of stria terminals
cAMP	Cyclic adenosine monophosphate
CCI	Chronic constriction injury
CCK	Cholecystokinin
CFA	Complete Freund's adjuvant
CGRP	Calcitonin gene-related peptide
CNS	Central nervous system
CPA	Conditioned place aversion
CPP	Conditioned place preference
CRF	Corticotropin-releasing factor
CSF	Cerebrospinal fluid
dlBNST	Dorsolateral part of bed nucleus of stria terminalis
DOR	δ-Opioid receptor
DORA	Dual orexin receptor antagonist
DRG	Dorsal root ganglion
ERK	Extracellular signal-regulated kinase
GHSR1a	Growth hormone secretagogue receptor-1a
GPCR	G-protein-coupled receptor
i.p.	Intraperitoneal
IBS	Irritable bowel syndrome
icv	Intracerebroventricular
IL-1β	Interleukin-1β
IL-6	Interleukin-6
KOR	κ-Opioid receptor
Kp-10	Kisspeptin-10
MOR	μ-Opioid receptor
MS	Maternal separation
N/OFQ	Nociceptin/orphanin FQ
NK1R	Neurokinin-1 receptor
NPFF	Neuropeptide FF
NPS	Neuropeptide S
NPY	Neuropeptide Y
NT	Neurotensin
NTS1	Neurotensin receptor-1
NTS2	Neurotensin receptor-2
OIH	Opioid-induced hyperalgesia
OR	Opioid receptor
PBN	Parabrachial nucleus

pERK	Phosphorylated extracellular signal-regulated kinase
PKA	Protein kinase A
PNS	Peripheral nervous system
PVN	Paraventricular nucleus of hypothalamus
REM	Rapid eye movement
RFRP-1	RF-amide related peptide-1
RFRP-3	RF-amide related peptide-3
SON	Supraoptic nucleus of the hypothalamus
SORA	Single orexin receptor antagonist
SP	Substance P
Span	Spantide I
SST	Somatostatin
TNFα	Tumor necrosis factor-α
VIP	Vasoactive intestinal polypeptide

Abstract

Chronic pain is a significant burden for the lives of sufferers, and it is currently estimated that ~20% of the European population and ~15% of the United States population suffers from moderate-to-severe chronic pain. Chronic pain and its current therapeutic management strategies that rely heavily on opioid receptor modulation are also associated with major social and health-cost burdens, including opioid addiction and a large number of opioid overdose deaths, making ongoing research in this field a global scientific, economic and social necessity. Nociceptive signaling is modulated at multiple stages by a large range of neurochemicals, one of which is a broad array of neuropeptides, including opioids and non-opioids, most of which signal via specific G-protein-coupled receptors (GPCRs). Several non-opioid neuropeptides and their receptors represent attractive targets for further investigation in regard to nociceptive signal modulation and new therapeutic options for pain management. In this review, we summarize key past and more recent advances in this field, with a focus on data pertaining to non-opioid neuropeptide signalling systems; and highlight some key features of preclinical studies that influence progress in basic research on neuropeptides that play a role in nociception. In the context of this analysis, we discuss the relationship between chronic pain and co-morbid pathophysiological and emotional symptoms, the relationships between non-opioid and opioid systems, and species and gender differences in nociception; as a better understanding of these complex issues should lead to improved outcomes from targeting non-opioid peptide systems for the management of chronic pain.

1. Introduction

Pain is a complex biological phenomenon that is necessary for survival of animals. It serves beneficial purposes, warning about changes in the environment that could compromise proper functioning, and is thus a highly controlled process. However, continuous activation of this integrated signaling system results in maladaptive changes characterized by altered activity and architecture. Pain lasting more than three months is termed 'chronic pain' and it is under these conditions that pain becomes a significant burden for the lives of individuals. It is estimated that ~20% of the European population suffers from moderate-to-severe chronic pain (Reid et al., 2011), whereas ~15% of the United States population suffers from some form of chronic pain (Hardt et al., 2008). Chronic pain is also accompanied by serious social and economic burdens (Smith and Torrance, 2012), making research in this field a prominent and ongoing necessity.

When considering nociceptive signal transmission, the peripheral nervous system (PNS) can be viewed as both the messenger and effector, as it is responsible for receiving the nociceptive message, which it communicates to the spinal cord via low-myelin Aβ and C fibers, and executing actions necessary for survival, such as avoidance. In turn, the spinal cord acts as a second-order messenger, by transmitting information to the brain, and as a signal modulator, by processing the received information and filtering what is transmitted to the brain. The brain then acts as a control center, decoding pain for its sensory-discriminative and aversive components, i.e., deciphering the type of pain (pinch, burn, etc.) and its location in the body, and its associated hedonic value (pleasure *vs* displeasure), respectively. Once the information is decrypted, the brain, via the spinal cord, enables the PNS to act in accordance to the provided stimulus, based on current and past experiences, and stores any new information it has received.

The nociceptive signal is modulated at every step of this process by a large range of neurochemicals, including neuropeptides. Neuropeptides consist of chains of amino acids that are expressed in neurons and signal to other neurons. They are usually expressed in *prepro*-forms and undergo processing (e.g. enzymatic cleavage) to produce their mature form.

The majority of currently known *active* neuropeptides were first described in the second half of the 20th century, as suitable biochemical and cellular assays were developed, and other neuropeptides have been discovered using modern techniques. Most neuropeptides signal with high specificity through G-protein-coupled receptors (GPCRs) linked to different types of G-proteins. The presence of various peptides and/or their receptors in the central nervous system (CNS) areas linked to nociceptive processing and transmission suggests putative roles for multiple neuropeptide systems in the control of nociception.

One family of neuropeptides, the opioids, and drugs that activate opioid receptors, are widely known by both researchers and the broader community to affect pain transmission. This class of neuropeptides has been thoroughly investigated in the past for its potent anti-nociceptive properties. However, opioid receptor drugs are not ideal options for long-term use, given their addictive properties, the development of tolerance, gastrointestinal discomfort, and other side-effects (Schuckit, 2016). Thus, signaling molecules that use similar or distinct mechanisms to produce analgesia, such as non-opioid neuropeptides, present attractive targets for basic research when investigating nociceptive signal modulation and seeking better therapeutic options for pain management.

In this review, we briefly summarize key past findings and explore more recent advances in this field, with a focus on data pertaining to neuropeptide signalling systems. We also highlight some key features of preclinical studies that contribute to, or hinder, progress in basic research, in relation to non-opioid neuropeptides that play a role in nociception, with a focus on the effective assessment and development of pharmacological tools for the management of chronic pain. Given their aetiological importance, and the increased awareness of their existence, we also discuss the relevant co-morbid symptoms associated with different chronic pain conditions.

2. Effects of neuropeptide systems on nociception

The mechanisms by which different neuropeptide systems affect nociception, be it the sensory-discriminative or aversive components of pain, remain relatively elusive, but have been the focus of extensive research and have been reviewed earlier (Table 1). Therefore, a

major goal of this article was to review some recent technical advances and scientific discoveries that have contributed to progress in the field.

When investigating the role of neuropeptides in nociceptive transmission, most studies focus on either spinal or supraspinal modulation of pain. At the spinal level, the pro-nociceptive neuropeptides, substance P (SP) and calcitonin gene-related peptide (CGRP), are commonly used as predictive measures of pain outcomes, whether measured directly through immunohistochemistry (Chiba et al., 2016; Santos et al., 2018), or indirectly in the case of SP by measuring the amount of internalization of its cognate receptor, neurokinin 1 receptor (NK_1) [see e.g. (Li et al., 2018; Nazarian et al., 2014)]. The role of SP as a pain-promoting neuropeptide in the spinal cord is well-accepted within the field, and strategies that seek to dampen SP signaling have been explored as potential pain treatments. This is supported by considerable past and newly emerging evidence. For example, a recent study found that deletion of NK_1-expressing neurons in the dorsal horn increased pain thresholds in rats under normal and inflammatory pain conditions (Iadarola et al., 2017).

In contrast, the mechanisms underlying peripheral oxytocin (OT)-mediated analgesia are only now becoming clear. The nonapeptides oxytocin (OT) and arginine-vasopressin (AVP) display a strong structural homology and differ in two amino acids (Gimpl and Fahrenholz, 2001). In mammals, central OT and AVP are mainly synthetized in the paraventricular (PVN), supraoptic (SON) and accessory nuclei (AN) of hypothalamus (Burbach et al., 2001). Neurons synthetizing OT are parvocellular (parvOT) neurons, which release oxytocin exclusively within the CNS, and magnocellular (magnoOT) neurons, which release oxytocin in the CNS, and influence the pituitary gland (Knobloch et al., 2012), and release OT (and AVP) into the bloodstream. Importantly, parvOT neurons are only present in PVN, while magnoOT neurons are present in both PVN and SON (Knobloch et al., 2014). Recent studies have reported that afferent neurons of the dorsal root ganglia (DRG) express OT receptors (OTR), predominantly non-peptidergic C-fiber cell bodies (González-Hernández et al., 2017; Moreno-López et al., 2013; Wrobel et al., 2011). ParvOT neurons send putative axonal projections to spinal cord laminae processing nociceptive and non-nociceptive somatic and visceral information (laminae

I, II, V, X, spinal lateral nucleus). In addition, this innervation is particularly abundant around the thoracic and lumbar segments, in line with the high OT content in these particular spinal segments (Juif et al., 2013). A recent study demonstrated that activation of a small population of parvOT neurons induced anti-allodynia by controlling magnoOT neuron release of OT into the blood, and through direct OT release in deep laminae of the spinal cord (Eliava et al., 2016).

Electrophysiological recordings of spinal dorsal horn neurons are also a method commonly used for predicting pain outcomes, whereby decreased activity of nociceptive neurons correlates with decreased pain sensitivity. Oral co-administration of a 5-hydroxytryptamine receptor-3 ($5\text{-}HT_3$) antagonist and NK_1 antagonist (palonosetron and netupitant, respectively) provides evidence of a synergistic effect of these receptors in the control of mechanical pain thresholds and action potential firing of lamina V/VI dorsal horn neurons in rats (Greenwood-Van Meerveld et al., 2014). Similarly, intraperitoneal (i.p.) administration of a somatostatin (SST) receptor-4 (SST_4) agonist, J-2156, was shown to produce anti-nociception, and decrease the firing rate of primary afferent nerve fibers and mechanosensitive spinal dorsal horn neurons (Schuelert et al., 2015).

Using behavioral assays and combined immunohistochemistry for the cellular activation protein marker, Fos, Fan and colleagues (2015) demonstrated that intraspinal injection of a corticotropin-releasing factor (CRF) receptor antagonist acting on CRF_1 and CRF_2 receptors alleviated thermal and mechanical pain in a rat model of bone cancer pain by suppressing neuronal activation in the dorsal horn of the spinal cord.

Furthermore, intrathecal injection of the peptide, ghrelin, dose-dependently decreased mechanical and thermal allodynia, and expression of inflammatory markers [interleukin-1β (IL-1β), IL-6, and tumor-necrosis factor-α (TNFα)] in the dorsal horn of mice with a chronic constriction injury (CCI) of the sciatic nerve (Zhou et al., 2014). Similarly, activation of the neuropeptide Y (NPY) receptor Y_1 by intrathecal injection of [Leu^{31},Pro^{34}]- NPY, alleviated mechanical and cold allodynia in the CCI model (Malet et al., 2017), and decreased SP release

from primary afferents onto lamina I neurons, in the carrageenan and complete Freund's adjuvant (CFA) models of inflammatory pain (Taylor et al., 2014).

Brain processing of nociceptive transmission is a complex phenomenon. A multitude of brain areas/circuits collectively evaluate various aspects of the perceived stimulus, including its location in the body, the type of pain, and the level of discomfort it produces. As such, when studying the role of a particular neuropeptide system on nociception, preclinical studies often target a single brain area to dissect the functions that area and the neuropeptide system of interest have in pain processing.

For example, galanin-induced antinociception is observed in neuropathic (Duan et al., 2015; Li et al., 2017) and inflammatory (Yang et al., 2015; Zhang et al., 2017) pain models, with distinct contributions of galanin receptors 1-3 ($GAL_{1/2/3}$). GAL_1 contributes to anti-nociceptive processes in the nucleus accumbens (NAc) and the central amygdala (CeA) (Duan et al., 2015; Li et al., 2017; Zhang et al., 2019b), by inhibiting protein kinase A (PKA) activation (Zhang et al., 2019a), whereas GAL_2 is involved in the nociceptive effects mediated by the anterior cingulate cortex (ACC) (Zhang et al., 2019a, 2019b).

Notably, while the source of peripheral oxytocin-mediated analgesia is currently thought to be the CNS (Eliava et al., 2016), it might be of interest to explore putative peripheral sources such as keratinocytes (Denda et al., 2012; Grinevich and Charlet, 2017).

A test commonly used to distinguish between acute or more persistent actions of a given pain treatment is the formalin test. In this paradigm, an experimental animal is given an injection of the inflammatory compound, formalin, which will produce an initial ("acute") phase of nociception, due to direct activation of peripheral nociceptors. After 5-10 min, pain thresholds will rise again, during what is called the "interphase", which lasts between 5-10 min. Following this, central sensitization of nociceptive cells will trigger the last phase, termed the "tonic" phase, which can last for several hours. This test allows researchers to discern whether treatments that seek to alter pain thresholds act at a peripheral (acute phase) or central (tonic phase) level, by measuring the number of nocifensive behaviors (biting, licking) displayed by the animal.

In the rat striatum, SP release and NK_1 internalization are increased after unilateral injection of formalin in the contralateral hind paw (Nakamura et al., 2013). In the same study, a continuous, but not an acute (single), injection of SP into the contralateral striatum decreased nocifensive behaviors in the tonic phase of the formalin test, increased paw withdrawal thresholds, and induced NK_1 internalization, without affecting hindpaw edema.

Similarly, intracerebroventricular (icv) injection of neuropeptide S (NPS) decreased formalin-induced licking and increased Fos-like immunoreactivity in the PAG (Peng et al., 2010). Furthermore, injection of orexin-A into the *nucleus paragigantocellularis lateralis* induced anti-nociception in the acute and tonic phases of the formalin test (Erami et al., 2012); and McDonald and colleagues (2016) administered a series of single and dual orexin receptor antagonists (SORAs/DORAs) orally to mice, and found that DORAs produce antinociception in both phases of the formalin test.

To investigate the hedonic value of a given stimuli, researchers often employ the condition place avoidance/preference (CPA/CPP) behavioral paradigm. In this test animals are repeatedly exposed to a specific context (compartment) while simultaneously being exposed to a stimulus (drug, footshock, etc.). In a test session, the animal will have the ability to move between the compartment where it received the stimulus and another compartment where no stimulation occurred. The choice to avoid or move to the compartment where the stimulus was provided is taken to mean that the stimulus produces negative or positive emotional effects, respectively. Separate studies by the Minami group provide an example of the use of this test to study the role neuropeptide signaling in the brain and negative emotional effects. Initially, Ide and colleagues (2013) reported that injection of CRF into the dorsolateral part of the *bed nucleus of the stria terminalis* (dlBNST) exacerbated formalin-induced CPA. Subsequently, they reported that pain- and CRF-induced CPA were abolished by intra-dlBNST injection of a PKA inhibitor (Kaneko et al., 2016), suggesting both forms of CPA require activation of PKA signaling pathways and likely involve the same mechanisms in the dlBNST.

The trigeminal ganglion (TG) provides sensory innervation of the face and mouth, and this specific bundle of nerve fibers is targeted in experimental models of orofacial pain. It was

recently reported that after infraorbital nerve injury, NPY expression was upregulated in the trigeminal ganglia (Lynds et al., 2017), and the same was observed after CCI of the mental nerve (Magnussen et al., 2015). Moreover, TG dysfunction is a key feature of headache syndromes, including migraine and cluster headache (Vollesen et al., 2018). CGRP modulates trigeminal pain, which is an important component of migraine (Edvinsson et al., 2018; Holland et al., 2018; Iyengar et al., 2016), and is likely involved in modulation of inflammatory and neuropathic pain (Iyengar et al., 2016). Indeed, intravenous administration of CGRP-scavenging RNA, NOX-C89, decreased spontaneous firing and heat-induced spiking in the trigeminal *nucleus caudalis* (TNC, a brainstem area that receives sensory input from the TG) of rats in a dose-dependent manner (Fischer et al., 2018). Additionally, systemic administration of lacosamide reduced CGRP production and release in TG explants of rats that were pre-sensitized by injection of nitroglycerin in the TG (a model of migraine pain) (Greco et al., 2016); and i.p. injection of MK-8825, a CGRP receptor antagonist, decreased nitroglycerin-induced flinching and shaking in the tonic phase of the formalin test (Greco et al., 2014). With regard to inflammatory pain, CGRP knockout (KO) mice displayed decreased nocifensive behaviors in the tonic phase of the formalin test and impaired excitatory synaptic potentiation of parabrachial nucleus (PBN)-laterocapsular central amygdala (CeLC) synapses 6 h after formalin injection (Shinohara et al., 2017). Another recent study observed increased levels of extracellular CGRP in the dorsal horn of the lumbar spinal cord in a model of cancer-induced bone pain (Hansen et al., 2016). In this model, intrathecal injection of the CGRP antagonist, $\alpha CGRP_{8-37}$, alleviated mechanical allodynia and improved weight bearing (Hansen et al., 2016).

Many recent studies have focused on phenomena resulting from the manipulation of entire circuits, and/or employed transgenic mouse models to produce systemic changes in signaling within neuropeptide-expressing neurons. An example is studies examining the role of SST-expressing interneurons. Ablation of SST-expressing excitatory interneurons in the dorsal horn of the spinal cord specifically abolished the expression of static and dynamic mechanical allodynia in inflammatory and neuropathic pain conditions (Duan et al., 2014). In addition,

Cichon and colleagues (2017) reported that daily chemogenetic activation of SST-expressing inhibitory interneurons of the primary sensory cortex (S1) prevented expression of mechanical allodynia in a model of neuropathic pain; whereas others had earlier reported that optogenetic activation of these interneurons in the ACC did not alter mechanical pain thresholds (Kang et al., 2015). However, while these studies provide important insights into the hodological composition of circuits that influence pain transmission, they generally fail to identify the specific neurochemicals mediating such effects.

An example of the use of a transgenic mouse model involving large-scale changes in neuropeptide signaling is a recent investigation of the role of the neurotensin (NTS) receptor 3 (NTS3) on NTS-mediated analgesia. These authors used a NTS3-deficient mouse ($NTS3^{-/-}$) to investigate the role of the receptor in NTS-elicited analgesia, and found that expression of NTS3 is required for NTS2-mediated analgesia in normal mice (Devader et al., 2016). Another study using *in vivo* recordings of CGRP-expressing neurons in the PBN discovered that these neurons are activated by noxious heat, pinching and itching, as well as exposure to novel foods and recall of conditioned fear memories (Campos et al., 2018), which provides evidence for the interrelationship between pain and other behaviors such as stress responsiveness (see Section 3.1 – Stress – anxiety, depression, fear and PTSD for more details).

In addition to the studies summarized, the reader is referred to reviews of the role of other less-studied, non-opioid neuropeptides in nociception, and articles on neuropeptides that have not been the focus of recent studies, including neuropeptides-B and -W (Dvorakova, 2018), and neuromedins-U, -B and -N (Gajjar and Patel, 2017).

The rapid progress in the development of technical tools and methods for investigating cellular, molecular and hodological underpinnings of nociception has driven the advancement of our understanding of how various neuropeptides and their receptors influence the perception of sensory-discriminative and aversive aspects of pain. This topic remains at the core of the identification of therapeutic targets for pain management.

3. Effects of neuropeptide systems on pain-related behaviors

A major predicament concerning pain therapy is the long-term management of a painful disease/syndrome. Long-term pain leads to maladaptive changes in neural architecture and synaptic plasticity, which in turn contribute to the expression of comorbid disorders, such as anxiety, depression, and sleep disorders, as well as alterations in the reward system. Since the turn of the century, interest has been growing in identifying the mechanisms by which altered pain sensation leads to the development of comorbidities, and how the progression of these comorbid states can be halted (Nicholson and Verma, 2004; Park and Moon, 2010; Reid et al., 2011). Furthermore, currently available treatments prescribed to patients suffering from chronic pain target nociceptive signaling, and often disregard comorbid states that accompany long-lasting pain. These treatments *per se* also have significant side-effects (see Section 4 – Relation of non-opioid neuropeptide systems to opioid signaling), making them inadvisable for continuous use. There is, therefore, a need to investigate how new candidate therapies affect both nociceptive transmission and behaviors commonly associated with painful syndromes.

3.1 Stress – anxiety, depression, fear and PTSD

The most widely studied pain comorbidity is probably neurogenic stress, which can be classified according to its acute or chronic duration. Acute stress comprises the activation of the paraventricular nucleus of the hypothalamus (PVN) and the release of CRF onto the pituitary gland, which in turn releases adrenocorticotropic hormone (ACTH) onto the adrenal glands, which release cortisol (in humans) or corticosterone (CORT, in rodents) (Lariviere and Melzack, 2000). CORT then acts as a negative feedback modulator of this circuit, known as the hypothalamic-pituitary-adrenal (HPA) axis. Several neuropeptides have been reported to affect HPA axis activity at different levels to influence stress responsiveness, including CRF, galanin, OT, AVP, NPS, NPY, pituitary adenylate cyclase-activating peptide (PACAP), substance P, orexin, SST and NPFF [for reviews see (Kormos and Gaszner, 2013; Sargin, 2018)]. This section focuses on recent studies revealing how non-opioid neuropeptides

influence stress, stress-induced changes in pain responses, and pain-induced changes in stress responses.

Acute stress is necessary for the survival of organisms and is known to alter nociception by reducing pain sensation, a phenomenon known as stress-induced analgesia (SIA) (Butler and Finn, 2009). One paradigm commonly used to induce acute stress in rodents is exposure to warm or cold water, which rodents prefer to avoid. Both forms of this stress induce analgesia, albeit through different mechanisms, with warm water swim SIA involving activation of opioid receptors, whilst cold water swim SIA requiring activation of *N*-methyl-D-aspartate receptors (NMDARs) (Marek et al., 1992). Indeed, icv injection of NPFF decreases warm but not cold water swim SIA, reinforcing the view that NPFF actions oppose opioid-mediated behaviors (Li et al., 2012) (for further details see Section 4 – Relation of non-opioid neuropeptide systems to opioid signaling). In rats exposed to water avoidance stress, blocking CRF_1 in the anterolateral part of the BNST (alBNST) decreased an anxiety-like phenotype and mechanical pain thresholds (Tran et al., 2014). In the CeA, both sustained inhibition of CRF-expressing neurons, as well as ablation of CRF-expressing neurons projecting to the *locus coeruleus* (LC), restored forced swim-induced SIA and increased mechanical pain thresholds in a mouse model of neuropathic pain (Andreoli et al., 2017). Consistent with this, in another model of acute stress, CRF knockdown in CeA rescued decreased visceral and somatic pain thresholds after water avoidance stress or colonic distension (Johnson et al., 2015).

OT and AVP also affect anxiety levels through modulation of amygdalar networks. Evoked endogenous OT release in the amygdala was sufficient to increase firing of CeL neurons (Knobloch et al., 2012), and AVP infusion enhanced neuronal activation in the CeA and BLA (Hernández et al., 2016) to produce a strong anxiety or anxiolysis, respectively (Knobloch et al., 2012).

While acute stress is crucial for survival, chronic stress comprises a series of maladaptive changes, resulting from overstimulation of the HPA axis, that culminate in decreased quality-of-life and increased propensity for developing stress-related disorders, such as generalized anxiety disorder (GAD), major depressive disorder (MDD), and post-traumatic stress disorder

(PTSD). These disorders themselves influence pain thresholds and several pain syndromes affect stress responses. One example of the latter is irritable bowel syndrome, a painful disorder characterized by abdominal pain, altered defecation and stress-induced changes in intestinal motility (Nozu and Okumura, 2015). Both central and peripheral CRF receptors, particularly CRF_1, have been investigated as potential therapeutic targets for treating this disorder, due not only to their anti-nociceptive actions, but to their effects on alleviation of anxiety symptoms (Nozu and Okumura, 2015; Taché, 2015). Because of the prominent role of CRF in initiating the stress response, CRF_1 has been investigated as a potential target for the treatment of stress-related conditions. In a rat model of monoarthritis, blocking CRF_1 in the LC alleviated pain-induced anxiety-like behaviors, but not pain itself (Borges et al., 2015). In the CeA, disruption of NMDAR GluN1 subunit expression in CRF-positive neurons enhanced acquisition and retention of auditory fear conditioning (Gafford et al., 2014). In this same structure, in a predator scent stress (PSS) model of PTSD, blocking CRF_1 abolished a hyperalgesic phenotype (Itoga et al., 2016). Together, this evidence suggests CRF receptors are highly relevant targets for the treatment of stress-related disorders, including pain-induced stress conditions and stress-induced pain syndromes.

NPS has also been the subject of considerable research examining its anxiolytic properties *per se* and in the context of painful conditions. In the early 2000s, NPS was first described as a neuropeptide that could increase wakefulness and suppress anxiety-like behaviors (Xu et al., 2004). More recently, it has been shown that icv administration of NPS dose-dependently produced panicolytic effects (Pulga et al., 2012), and that intranasal delivery of NPS reduced anxiety-like behaviors (Ionescu et al., 2012), and decreased pain sensation and anxiety levels in a rat model of arthritis (Medina et al., 2014). In a CCI model, NPS mRNA and peptide content were reduced in the amygdala, and these data are concomitant with an anxiety-like phenotype which could be reversed by icv administration of exogenous NPS (Zhang et al., 2014). Moreover, administration of NPS into the medial amygdala (MeA) produced anxiolysis (Grund and Neumann, 2018), and injection into the basolateral amygdala (BLA), alleviated stress responses in the PSS model of PTSD (Hagit et al., 2018).

In other recent studies, GAL_1 activation was shown to be involved in the decreased motivation associated with chronic pain (Schwartz et al., 2014). Notably, such decreased motivation is a common feature of depression, and alterations in the galaninergic system have been reported in rat models of depressive-like behavior (Wang et al., 2016), and in patients with major depressive disorder (Barde et al., 2016), thus linking the galanin/galanin receptor system to depression and pain interactions. Both GAL_1 and GAL_3 are likely to be involved in this comorbidity (add refs, esp. GAL_3).

Overall, experimental evidence supports the involvement of various non-opioid neuropeptide systems in multiple aspects of stress-related disorders. In addition, several of these neuropeptide-receptor systems may be excellent targets for new therapies for treatment of stress-related disorders and comorbid pain syndromes.

3.2 Feeding and drinking

The idea that food-seeking behavior and/or water balance/drinking share a common thread with pain is a new concept. In a recent study, food-deprived mice had decreased nocifensive responses to inflammatory pain, through NPY signaling from arcuate nucleus (ARC) agouti-related peptide (AgRP)-expressing neurons to NPY Y1 receptors in the PBN, in a process that did not require the co-transmitters, GABA and AgRP (Alhadeff et al., 2018). Indeed, other neuropeptide systems that are known to play a role in nociception, are also involved in food-seeking and drinking behavior. Neurotensin (NTS is a well-known anorectic peptide (Boules et al., 2013), and a population of NTS-containing lateral hypothalamus neurons was recently identified as being able to drive drinking independently of palatability, with delayed suppression of feeding (Kurt et al., 2018; Woodworth et al., 2017). Additionally, SST-expressing neurons of the tuberal nucleus that impinge on the BNST and PVN promote food-seeking behavior (Luo et al., 2018), in line with earlier findings supporting a role for SST and SST-expressing neurons in feeding as well as drinking (Stengel et al., 2015). Lastly, intra-amygdalar injection of RFRP-3, an endogenous ligand for NPFFR2, dose-dependently decreased food intake in rats (Kovács et al., 2014).

The aforementioned neuropeptide systems and brain areas/circuits have also been shown to influence nociceptive transmission. Whether similar neurons and mechanisms are involved in both nociception and feeding/drinking remains to be clarified, and the physiological or pathological conditions required to initiate interplay between these behaviors need to be established.

3.3 Addiction – reward and motivation

Addiction and chronic pain interact on two separate levels. Firstly, chronic pain is accompanied by changes in brain reward circuitry, resulting in both reward deficiency and anti-reward behavior, which exacerbate pain intensity and chronicity (Borsook et al., 2016). Secondly, the continuous use of opioid drugs that activate reward pathways (see also Section 4 – Relation of non-opioid neuropeptide systems to opioid signaling) to treat long-term pain, promotes the establishment of drug abuse disorders. Thus, knowledge of how emerging therapies affect reward and motivation *per se* and under chronic pain conditions is highly relevant.

Indeed, some neuropeptide systems that play a role in nociception have been linked to reward-seeking behaviors. It was recently shown that injections of morphine systemically and locally into the ventral tegmental area (VTA) increased release of SP in the VTA (Sandweiss et al., 2018). In turn, intra-VTA administration of SP or morphine increased dopamine (DA) release in the NAc via NK_1 activation, suggesting SP- and morphine-mediated mechanisms for facilitating DA release within the NAc share common pathways (Sandweiss et al., 2018). Additionally, genetic ablation of NK_1 in the VTA prevented expression of morphine-induced conditioned place preference (CPP). Similarly, icv administration of NPS also decreased morphine-induced CPP (Li et al., 2009b). In contrast, injection of orexin-A into the dentate gyrus facilitated acquisition, expression, and reinstatement of morphine-induced CPP (Guo et al., 2016).

CRF has also been a major focus of similar studies that examined its effects on pain and reward-seeking behaviors. One such study demonstrated that CCI-induced neuropathic pain

facilitated the expression of morphine-induced CPP through sustained activation of medial prefrontal cortex (mPFC) CRF-expressing neurons projecting to the NAc, and involved activation of CRF_1 (Kai et al., 2018). Chemogenetic inhibition of mPFC CRF neurons and optogenetic activation of mPFC-NAc CRF neurons prevented the expression of morphine-induced CPP in CCI mice, whereas optogenetic activation of this pathway in sham mice recapitulated the effects of CCI on morphine-induced CPP (Kai et al., 2018). Interestingly, none of these chemo- or optogenetic manipulations resulted in changes in pain thresholds, suggesting this pathway is specifically involved in reward-seeking behavior. Increased CRF and CRF_1 mRNA in the CeA is associated with decreased thermal pain thresholds in nicotine-dependent rats, which is reversed by systemic and local blockade of CRF_1 (Baiamonte et al., 2014). Systemic CRF_1 blockade also alleviated hyperalgesia in ethanol-dependent rats (Edwards et al., 2012).

Several non-opioid neuropeptides that influence reward-seeking in preclinical models of pain and addiction have been discussed in recent reviews, including SP (Muñoz and Coveñas, 2014; Sandweiss and Vanderah, 2015), NPY (Thorsell and Mathé, 2017), orexin (Tsujino and Sakurai, 2013), and CRF (Zorrilla et al., 2014). This topic is highly prominent within the fields of pain and addiction research, and future studies should consider the interactions between pain and reward circuitry as key to the expression of nociception as well as conditioned behaviors.

3.4 Sleep and wakefulness

Interactions between sleep and pain have been the focus of several studies over many years [see (Lautenbacher et al., 2006) for a review]. More recently, in a large human cohort study, it was revealed that several key features of sleep, including efficiency, and the frequency and severity of insomnia, were associated with pain sensitivity (Sivertsen et al., 2015). Moreover, these investigators found a synergistic effect regarding reduced pain thresholds in patients reporting both insomnia and chronic pain (Sivertsen et al., 2015). Indeed, understanding the bidirectional relationship between sleep and pain is crucial. Despite this, the

role individual neuropeptide systems play in coordinating sleep and pain remains largely unstudied.

Thus, administration of the NPSR antagonist [D-Cys(^{t}Bu)^{5}]NPS decreased wakefulness and increased time spent in non-rapid eye movement (REM) sleep, without affecting REM sleep (Oishi et al., 2014). Additionally, icv administration of NPS attenuated an REM sleep deprivation-induced anxiety-like phenotype (Xie et al., 2018). These studies provide important insights into how the NPS/NPSR system affects both sleep and sleep-related behavior changes, but their relation to nociception was outside the scope of these investigations. Nevertheless, demonstrating that the NPS/NPSR and other systems, such as orexin [see (Nevárez and de Lecea, 2018) for a review] and neuropeptide B (Dvorakova, 2018) and their cognate receptors, influence the sleep/wake cycle, supports the idea that specific activation/inhibition of these systems could produce alleviation of comorbid sleep and pain disorders.

4. Relation of non-opioid neuropeptide systems to opioid signaling

Opiate alkaloids isolated from the opium poppy *Papaver somniferum* have been used by humans for thousands of years. In 1975, the first report emerged of the presence in pig brain of two forms of enkephalin, an endogenous opioid, with potent agonist activity at opioid receptors (Hughes et al., 1975). This supported the idea that there was a ligand-receptor system that could be exploited for the purpose of controlling pain thresholds.

Opioid peptides are important effectors of nociceptive signaling that act via μ-, δ-, and κ-opioid receptors (MOR, DOR, and KOR, respectively). Notably, morphine, an agonist for all three ORs, is the “gold standard” against which all other analgesics are compared, yet even though it is a highly potent painkiller, its use is accompanied by deleterious side-effects that limit its long-term use. These range from constipation, nausea and vomiting to addiction, respiratory depression and even death (Schuckit, 2016). As such, a goal of preclinical research is to understand if and how emerging neuropeptide candidates for therapeutic development affect opioid signaling.

Indeed, evidence for interactions between opioid and non-opioid neuropeptide systems has been obtained in studies of the molecular, cellular, and/or behavioral components of the nociceptive network. A notable group of non-opioid neuropeptides with opioid-modulating properties is the RF-amide family of peptides. NPFF opposes opioid-induced changes in several behaviors, decreasing reward-seeking, locomotor activity, feeding and drinking, intestinal motility and nociception, when co-administered in supraspinal structures [see (Moulédous et al., 2010) for a review], despite having low affinity for opioid receptors (Yang et al., 2008). Other members of the RF-amide peptide family, including RFRP-3, 26RFa, PrRP-20, and Kp-10 have been shown to elicit NPFF receptor (NPFFR)-dependent hyperalgesia in the tail immersion test, with the latter two peptides partly reversing morphine analgesia via the same receptors (Elhabazi et al., 2013). Additionally, subcutaneous injection of an NPFFR antagonist potentiates the analgesic effects of morphine, and ameliorates naltrexone-precipitated signs of withdrawal in morphine-dependent mice (Elhabazi et al., 2012), suggesting NPFFR blockade ameliorates the side-effects of long-term use of opioid analgesics.

Other non-opioid neuropeptide systems interact with opioid peptide signaling. For example, the SST_4 receptor forms a heterodimeric complex with the DOR in the cortex, striatum and spinal cord, and simultaneous activation of both receptors leads to decreased cAMP and PKA activation in a cooperative manner (Somvanshi and Kumar, 2014). At the behavioral level, co-administration of orexin-A and morphine into the medial preoptic area produced potentiated analgesia, suggesting a synergy between OX_1R and opioid receptors (Emam et al., 2016). Similarly, central activation of the ghrelin receptor, GHSR1a, produced DOR- and KOR-dependent analgesia, and icv administration of morphine and GHSR1a agonist GHRP-2 produced synergistic analgesia (Zeng et al., 2014). In contrast, another study reported that ghrelin and GHSR1a agonists attenuate analgesia after i.p. injection of morphine (Zeng et al., 2013), indicating complex signaling phenomena underlie the interaction between opioid and ghrelin systems.

Furthermore, pharmacological and behavioral evidence suggests a possible crosstalk between the oxytocinergic and endogenous opioidergic signaling systems to produce OT-mediated analgesia. For example, after icv co-administration of naloxone and OT, the anti-hyperalgesic effect of OT was blocked/occluded (Russo et al., 2012). Fourth ventricle co-administration of opioid antagonists (naloxone, naloxonazine, nor-binaltorphimine and naltrindole) and OT demonstrate that OT may be involved in the supraspinal modulation of inflammatory pain through MOR and KOR, but not DOR. (Erfanparast et al., 2018; Russo et al., 2012).

Nevertheless, activation of some non-opioid neuropeptide systems produces opioid-independent analgesia. For example, icv administration of NPS produced analgesia even after co-administration of the OR antagonist naloxone (Li et al., 2009a). Furthermore, when initially tested for its anti-nociceptive properties, orexin-A produced thermal analgesia even after i.p. injection of naloxone (Bingham et al., 2001).

Interestingly, heteromerization of GAL_1 with MOR is reported to determine pharmacodynamic differences between opioid-like compounds, such as morphine and methadone, consistent with the less addictive opioid profile of methadone (Cai et al., 2019). Therefore, a novel strategy for analgesia could be the co-administration of GAL_1 agonists with opioids to produce a decrease in the effective analgesic doses of opioids, while counteracting their euphorigenic effects (Cai et al., 2019).

Regardless of any lack of demonstrated interaction of some non-opioid neuropeptide systems with opioid systems, studying the relationship of OR signaling and the analgesic, anxiolytic, addictive and other properties of all new therapies is of the utmost importance, as it allows identification of cross-talk between these systems, furthering progress in the identification and development of potential targets for improved pain therapy.

5. Interactions between non-opioid neuropeptide systems

As mentioned, although opioid drugs are potent painkillers, their use is accompanied by a plethora of undesired side-effects that limits their long-term use. Thus, there is an increased

interest in the discovery of other molecules that produce analgesia in a clinical setting, with reduced side-effects. In this regard, researchers have examined how non-opioid neuropeptides, which share signaling pathways with ORs, work in tandem to fine-tune nociceptive responses. Understanding how interplay between systems modulates pain sensation has become key for the development of therapeutic strategies.

It has been postulated that galanin receptor subtypes can form heteromers with each other and with other GPCRs, such as NPY Y_1 and Y_2 (Fuxe et al., 2012), thus expanding their signaling diversity. Indeed, the Y_1-mediated increase in food intake was reduced by icv co-administration of galanin (Parrado et al., 2007), whereas the mixed GALR agonist, GAL(1-15), increased binding affinity of radiolabeled agonists for Y_2 but not Y_1 (Díaz-Cabiale et al., 2010).

In the spinal cord, SP and CGRP, together with the classical neurotransmitter, glutamate, help regulate nocifensive responses in the tonic phase of the formalin test (Rogoz et al., 2014). Glutamate and SP, and glutamate and CGRP, released from DRG primary afferent neurons, help mediate cold and heat sensation, respectively (Rogoz et al., 2014), suggesting interactions between individual neuropeptides and classical neurotransmitter systems are involved in maintaining normal pain thresholds. Additionally, in inflammatory pain conditions, SP release from primary afferents onto layer I neurons of the dorsal horn is decreased by intrathecal injection of [Leu^{31},Pro^{34}]-NPY, via activation of Y_1 receptors (Taylor et al., 2014). On the other hand, CGRP expression in the spinal cord and DRG, usually associated with increased pain sensation, was increased in a mouse model of NPFFR2 overexpression, or after administration of a NPFFR2 agonist (Lin et al., 2017a), reflecting actions of RF-amide family peptides beyond modulating opioid receptor activity.

In the dorsolateral BNST (dlBNST), CRF-induced CPA is attenuated by co-administration of NPY in a Y_1 and Y_5 receptor-dependent manner (Ide et al., 2013). Similarly, ghrelin has been shown to depolarize AgRP/NPY neurons in the ARC by activation of its cognate receptor GHSR1a (Chen et al., 2017), and, as mentioned (Section 3.2 – Feeding and drinking), NPY signaling from the ARC to the PBN mediates hunger-elicited pain hyposensitivity (Alhadeff et

al., 2018). The former data may in part explain the latter findings, as ghrelin is released into the bloodstream to induce hunger (Sato et al., 2012).

Interactions between different neuropeptide systems are of interest for understanding pain biology, as well as other related behaviors. In the PVN, which is densely innervated by pericoerulear NPS-containing fibers, silencing of PVN OT-positive neurons blocks anxiolytic actions of icv administered NPS (Grund et al., 2017), and these neurons have also been shown to play a role in nociception (Eliava et al., 2016). Also, activation of NPFFR2 in the PVN increased serum corticosteroids in a CRFR-dependent manner, leading to cell activation, and increasing anxiety-like behaviors (Lin et al., 2017b). Additionally, in a model of PTSD, the anxiolytic effects of NPS administration into the BLA were dependent upon activation of NPY Y_1 receptor (Hagit et al., 2018).

From a general biological viewpoint, neural circuits are interconnected to ensure homeostasis and survival and no single manipulation of any particular central receptor system results in an isolated effect. Therefore, gaining insight into how different signaling components are linked and function together is of the utmost importance.

6. Interspecies differences and sexual dimorphism of non-opioid neuropeptide systems

Despite the development of numerous molecules targeting candidate non-opioid neuropeptide systems for the management of pain (Pérez de Vega et al., 2018), few reach the clinical trial stage and even fewer prove useful in the clinical setting. Two major issues hinder the transition of candidate drugs to viable pharmacological treatments.

Firstly, preclinical studies for ethical reasons usually resort to the use of non-human mammals to explore how manipulations of neuropeptide systems influence nociception, to measure pain behaviors or estimate nociceptive thresholds in intact organisms. The difficulty is then determining how different species, especially humans, react to the same manipulations. Thus, reports often emerge of findings that differ from previous studies, and these differences are attributed to ‘species differences’.

In a review of evidence concerning the effects of NTS receptor agonists on a variety of behaviors including pain, Boules and colleagues (2013) observed that “evidence suggests the analgesic efficacy of NTS analogues varies with their selectivity for NTS1 and NTS2, the pain model, and, probably, animal species”. This is a valid, evidence-based point, and is likely true for other non-opioid neuropeptide systems. For example, one study reported that pharmacological activation of NPFFR2 or inhibition of NPFFR1 produced analgesia in Sprague-Dawley (SD) rats (Lameh et al., 2010), while another study using Kunming mice reported no changes in nociception after activation or blockade of these receptors (Fang et al., 2011). Additionally, other members of the RF-amide peptide family, such as RFRP-3, Kp-10, PrRP-20, and 26 RFa, have been shown to induce NPFFR-mediated hyperalgesia in C57Bl6/N mice in the tail-immersion test (Elhabazi et al., 2013). While these studies employed different compounds and routes of administration (i.e., Lameh and colleagues tested i.p. delivery of non-peptidomimetic analogues that cross the blood-brain barrier (BBB), whereas Fang and colleagues, and Elhabazi and colleagues, administered peptidergic compounds icv), it is noteworthy that the expression profile of NPFFR1 and NPFFR2 varies among rodent species (Gouardères et al., 2004), which may partly explain the observed differences.

Moreover, in a model of pristane-induced arthritis, intraplantar administration of the SST analogue, octreotide, produced mechanical analgesia, and decreased C-fiber firing in DA, but not DA.1U rats (Yao et al., 2016); and these strains previously displayed different levels of pain sensitivity (Guo et al., 2015). The major genetic difference between these strains is the presence of different alleles for the major histocompatibility complex (MHC) (Stevenson et al., 1997), and yet they present clearly distinct responses to nociceptive stimulation. As such, it is predictable that more evolutionarily distinct species will display more major differences.

Another aspect that limits the validation of therapeutic targets suitable for use in the clinical setting is that most preclinical studies use male and not female subjects. Differences in nociception between the sexes are well documented, and of great interest, as the underlying mechanisms are still poorly understood (Mogil and Bailey, 2010). For example, migraine affects more women than men (Bigal and Lipton, 2009), but little is known about this

phenomenon. Additionally, the variability of pain thresholds in females during the oestrus cycle, which leads to changes in circulating hormone levels, adds a layer of complexity and difficulty to study design. Notwithstanding, there are reports that document differences and similarities between males and females when a neuropeptide system is activated and/or inhibited.

For example, male and female $VIP^{-/-}$ mice display increased microglial activation in the dorsal horn of the spinal cord and decreased bilateral paw withdrawal thresholds following unilateral spared nerve injury (SNI) (Gallo et al., 2017). Additionally, these mice develop bilateral sensitization after hindpaw incision, which persists for longer than unilateral sensitization observed in $VIP^{+/+}$ mice (Gallo et al., 2017). This evidence suggests VIP plays a role in lateralization and chronification of pain and exemplifies similar responses of males and females to identical manipulations.

In contrast, analysis of nocifensive behaviors in the formalin test revealed differences between male and female $NTS1^{-/-}$ mice in their dose-response relationships after morphine administration (Roussy et al., 2010), suggesting there is sexual dimorphism in the functional interaction of the neurotensinergic and opioidergic systems. In the tonic phase of the formalin test, SP release in layer III/IV and V/VI neurons of the dorsal horn of the spinal cord, measured as NK_1 internalization, was higher in female than male rats (Nazarian et al., 2014). In the same study, ovariectomy reduced SP release, which was reinstated by administration of estradiol in ovariectomized rats, and gonadectomized male and female rats had similar levels of SP release after formalin injection (Nazarian et al., 2014). Furthermore, injection of the SST analogue, octreotide, in the ventrolateral orbital cortex inhibited the tail-flick reflex and formalin-induced nocifensive behaviors in female, but not male rats (Qu et al., 2015). This supports the idea that males and females respond differently to pain, and specifically following manipulations of non-opioid neuropeptide systems.

Indeed, while some studies report that OT can exert its analgesic action in both females (Eliava et al., 2016), and males (González-Hernández et al., 2019; Juif et al., 2013; Juif and Poisbeau, 2013), others report a male-specific action of these peptides (Chow et al., 2018). In

contrast, human data suggest a female-specific analgesia induced by OT (Tracy et al., 2017) and AVP (Colloca et al., 2016).

Moreover, the expression of other behaviors that can affect pain thresholds, such as anxiety, can differ between males and females. For example, the maternal separation (MS) model of anxiety was not associated with changes in anxiety-like behaviors in male mice (Tan et al., 2017), while it produced changes in anxiety-like behaviors in the same strain of female mice (Pierce et al., 2014). Additionally, females subject to MS displayed vaginal hypersensitivity (Pierce et al., 2014), a clear example of how anxiety and pain are connected and are differentially modulated in males and females.

These lines of evidence highlight the need for preclinical studies to consider the use of different species, albeit while the need to replace animals with simpler models remains an imperative. Furthermore, expanding the scope of studies to include females will allow research to more easily identify biased and non-biased targets for pain management.

7. Development of pharmacological tools

The ultimate goal of experimental investigations into the biology of non-opioid neuropeptide signaling is to develop new therapeutic options for short- and long-term pain management. These treatments should preferably dampen nociceptive signaling and the expression of comorbid conditions, be safe for clinical use (reduced toxicity), have limited side-effects, and be suitable for simple administration, with a reduced frequency of administration required to achieve therapeutic concentrations, reflecting good pharmacokinetic and pharmacodynamic profiles.

In this regard, studies of non-opioid neuropeptide systems have led to the development of specific ligands and small molecule agonists/antagonists, some of which can cross the BBB. Recently, Elhabazi and colleagues (2017) demonstrated in rats that oral administration of RF313, a NPFFR antagonist first identified in 2015 (Bihel et al., 2015), potentiated morphine analgesia, whilst attenuating opioid-induced hyperalgesia (OIH) and tolerance. Demeule and co-workers (2014) combined the brain-penetrant properties of Angiopep-2 (An2) with NTS to

develop the conjugate ANG2002, which they administered peripherally to produce analgesia in models of inflammatory, neuropathic, and bone cancer pain. Additionally, like NTS, this compound proved to be more potent than morphine at equimolar doses. Another study of the signaling properties of NK_1 revealed that NK_1 internalization into endosomes is required for sustained activation of dorsal horn lamina I neurons, and expression of allodynia and nocifensive behaviors in inflammatory pain conditions (Jensen et al., 2017). In this study, the authors reported that conjugation of the NK_1 antagonist, spantide I (Span), with cholesterol (Chol) dampened endosomal NK_1 signaling and produced analgesia in mice. Furthermore, Span-Chol was stable in human cerebrospinal fluid (CSF). In a separate study, the same group investigated the ability of the conjugate, $CGRP_{8-37}$-Chol, to limit CGRPR signaling in endosomes, and reported that intrathecal injection of this hybrid antagonist alleviated mechanical allodynia in capsaicin-, formalin-, and CFA- models of inflammatory pain (Yarwood et al., 2017).

CGRP monoclonal antibodies and CGRPR antagonists have been particularly successful in the treatment of various headache syndromes (Iyengar et al., 2016). CGRP is a known modulator of trigeminal pain, a key component of migraine, and antibodies against the peptide or its receptor are likely to act at this peripheral level, since their high molecular weight hinders BBB penetration (Edvinsson et al., 2018; Holland et al., 2018; Iyengar et al., 2016).

Efforts have also been made to combine the analgesic properties of opioids with those of other neuropeptides. The opioid-NTS hybrid peptide PK20, as well as its metabolite PK20M, has been shown to produce thermal analgesia when administered both centrally and peripherally (Kleczkowska et al., 2013, 2010). Other studies assessed the analgesic properties of OR agonist/NK_1 antagonist compounds in the CCI model of neuropathic pain after intrathecal administration (Guillemyn et al., 2015; Starnowska et al., 2017). Yamamoto and colleagues first described TY032, a DOR and MOR receptor agonist and NK_1 antagonist (Yamamoto et al., 2011) and later used it to produce analgesia in a neuropathic pain model, without inducing CPP (Sandweiss et al., 2018). The latter observation is relevant to modern drug development when considering the use of opioid/non-opioid neuropeptide hybrids, as

currently used opioids have addictive properties and produce CPP in preclinical animal models. In line with this, the CRF_1 antagonist, E2508, was shown to alleviate visceral pain and reduce restraint stress-induced defecation without altering basal bowel patterns (Taguchi et al., 2017).

Thus, the value of understanding how new compounds affect both pain and related behaviors is not to be underestimated. As research in the field progresses, the focus is gradually shifting from a 'nociception-centric' to a more comprehensive perspective, with pain at the center of a network of intertwined behaviors and comorbid disorders.

Finally, the reader is referred to reviews on recent progress in the development of new treatments targeting non-opioid neuropeptide systems (Pérez de Vega et al., 2018), particularly SP (Hallberg and Sandstrom, 2018; Muñoz and Coveñas, 2014) and CRF (Zorrilla and Koob, 2010), as well as studies of novel ligands for the bradykinin receptor 2 (BK_2) (Deekonda et al., 2015; Lee et al., 2014, 2015).

8. Conclusions

As only a small number of peptide receptors are currently targeted for therapeutic purposes in general and a high percentage of FDA-approved drugs target opioid receptors, further research is urgently required.

Historically, class-A peptide GPCRs have been studied and pharmacologically targeted, as if they were small molecule-activated GPCRs (i.e. monoamine receptors). As a result, only 94 of the 440 approved drugs that target class A GPCRs, target peptide GPCRs (21%) and nearly half of these drugs target opioid receptors (43% of peptide-GPCR targeting drugs; This, together with the fact that the majority of peptide GPCRs remain without selective drugs for their activation and/or inhibition, highlights the need for further research and innovation in this field, and specifically in relation to non-opioid drugs to treat acute and chronic pain.

Acknowledgements

Research conducted in the authors' laboratories reviewed in this article was supported by the National Health and Medical Research Council (NHMRC) of Australia (ALG), CNRS # (ML), CNRS and/or ANR #). JC was supported by PhD scholarships from the University of Bordeaux (France) (*Initiative d'Excellence* - IdEx), and The University of Melbourne (Australia) (MIRS).

Author contributions

ALG, ML and JC conceived the topic and scope of the review. JC, ML and ALG drafted and edited the manuscript, and the schematic figures and table. AC and DK contributed a review of OT and AVP systems in pain and emotional control and edited the manuscript. SM edited the figures and edited the manuscript. All authors approved the final article.

Competing interests: The authors declare no competing interests.

References

Alhadeff, A.L., Su, Z., Hernandez, E., Klima, M.L., Phillips, S.Z., Holland, R.A., Guo, C., Hantman, A.W., De Jonghe, B.C., Betley, J.N., 2018. A Neural Circuit for the Suppression of Pain by a Competing Need State. Cell 173, 140-152.e15. https://doi.org/10.1016/j.cell.2018.02.057

Andreoli, M., Marketkar, T., Dimitrov, E., 2017. Contribution of amygdala CRF neurons to chronic pain. Exp. Neurol. 298, 1–12. https://doi.org/10.1016/j.expneurol.2017.08.010

Baiamonte, B.A., Valenza, M., Roltsch, E.A., Whitaker, A.M., Baynes, B.B., Sabino, V., Gilpin, N.W., 2014. Nicotine dependence produces hyperalgesia: Role of corticotropin-releasing factor-1 receptors (CRF1Rs) in the central amygdala (CeA). Neuropharmacology 77, 217–223. https://doi.org/10.1016/j.neuropharm.2013.09.025

Barde, S., Rüegg, J., Prud, J., Ekström, T.J., Palkovits, M., Turecki, G., 2016. Alterations in the neuropeptide galanin system in major depressive disorder involve levels of transcripts , methylation , and peptide. Proc. Natl. Acad. Sci. 113, E8472–E8481. https://doi.org/10.1073/pnas.1617824113

Bigal, M.E., Lipton, R.B., 2009. The epidemiology, burden, and comorbidities of migraine. Neurol. Clin. 27, 321–334. https://doi.org/10.1016/j.ncl.2008.11.011

Bihel, F., Humbert, J.-P., Schneider, E., Bertin, I., Wagner, P., Schmitt, M., Laboureyras, E., Petit-Demoulière, B., Schneider, E., Mollereau, C., Simonnet, G., Simonin, F., Bourguignon, J.-J., 2015. Development of a peptidomimetic antagonist of neuropeptide FF receptors for the prevention of opioid-induced hyperalgesia. ACS Chem. Neurosci. 6, 438–445. https://doi.org/10.1021/cn500219h

Bingham, S., Davey, P.T., Babbs, A.J., Irving, E.A., Sammons, M.J., Wyles, M., Jeffrey, P., Cutler, L., Riba, I., Johns, A., Porter, R.A., Upton, N., Hunter, A.J., Parsons, A.A., 2001. Orexin-A, an hypothalamic peptide with analgesic properties. Pain 92, 81–90. https://doi.org/10.1016/S0304-3959(00)00470-X

Borges, G.P., Mico, J.A., Neto, F.L., Berrocoso, E., 2015. Corticotropin-releasing factor mediates pain-induced anxiety through the ERK1/2 signaling cascade in locus coeruleus neurons. Int. J. Neuropsychopharmacol. 18, 1–6. https://doi.org/10.1093/ijnp/pyv019

Borsook, D., Linnman, C., Faria, V., Strassman, A.M., Becerra, L., Elman, I., 2016. Reward deficiency and anti-reward in pain chronification. Neurosci. Biobehav. Rev. 68, 282–297. https://doi.org/10.1016/j.neubiorev.2016.05.033

Boules, M., Li, Z., Smith, K., Fredrickson, P., Richelson, E., 2013. Diverse roles of neurotensin agonists in the central nervous system. Front. Endocrinol. 4, 1–16. https://doi.org/10.3389/fendo.2013.00036

Burbach, J.P.H., Luckman, S.M., Murphy, D., Gainer, H., 2001. Gene regulation in the magnocellular hypothalamo-neurohypophysial system. Physiol. Rev. 81, 1197–1267. https://doi.org/10.1152/physrev.2001.81.3.1197

Butler, R.K., Finn, D.P., 2009. Stress-induced analgesia. Prog. Neurobiol. 88, 184–202. https://doi.org/10.1016/j.pneurobio.2009.04.003

Cai, N., Quiroz, C., Bonaventura, J., Bonifazi, A., Cole, T.O., Purks, J., Billing, A.S., Massey, E., Wagner, M., Wish, E.D., Guitart, X., Rea, W., Lam, S., Moreno, E., Casadó-Anguera, V., Greenblatt, A.D., Jacobson, A.E., Rice, K.C., Casadó, V., Newman, A.H., Winkelman, J.W., Michaelides, M., Weintraub, E., Volkow, N.D., Belcher, A.M., Ferré, S., 2019. Opioid–galanin receptor heteromers mediate the dopaminergic effects of

opioids. J. Clin. Invest. 129, 2730–2744. https://doi.org/10.1172/JCI126912

Campos, C.A., Bowen, A.J., Roman, C.W., Palmiter, R.D., 2018. Encoding of danger by parabrachial CGRP neurons. Nature 555, 617–620. https://doi.org/10.1038/nature25511

Chen, S.R., Chen, H., Zhou, J.J., Pradhan, G., Sun, Y., Pan, H.L., Li, D.P., 2017. Ghrelin receptors mediate ghrelin-induced excitation of agouti-related protein/neuropeptide Y but not pro-opiomelanocortin neurons. J. Neurochem. 142, 512–520. https://doi.org/10.1111/jnc.14080

Chiba, T., Oka, Y., Kambe, T., Koizumi, N., Abe, K., Kawakami, K., Utsunomiya, I., Taguchi, K., 2016. Paclitaxel-induced peripheral neuropathy increases substance P release in rat spinal cord. Eur. J. Pharmacol. 770, 46–51. https://doi.org/10.1016/j.ejphar.2015.11.055

Chow, L.H., Chen, Y.H., Lai, C.F., Lin, T.Y., Chen, Y.J., Kao, J.H., Yi-Kung, E., 2018. Sex difference of angiotensin IV–, LVV-Hemorphin 7–, and oxytocin-induced antiallodynia at the spinal level in mice with neuropathic pain. Anesth. Analg. 126, 2093–2101. https://doi.org/10.1213/ANE.0000000000002795

Cichon, J., Blanck, T.J.J., Gan, W.B., Yang, G., 2017. Activation of cortical somatostatin interneurons prevents the development of neuropathic pain. Nat. Neurosci. 20, 1122–1132. https://doi.org/10.1038/nn.4595

Colloca, L., Pine, D.S., Ernst, M., Miller, F.G., Grillon, C., 2016. Vasopressin boosts placebo analgesic effects in women: a randomized trial. Biol. Psychiatry 79, 794–802. https://doi.org/10.1016/j.biopsych.2015.07.019

Deekonda, S., Rankin, D., Davis, P., Lai, J., Porreca, F., Hruby, V.J., 2015. Design, synthesis and biological evaluation of multifunctional ligands targeting opioid and bradykinin 2 receptors. Bioorganic Med. Chem. Lett. 25, 4148–4152. https://doi.org/10.1016/j.bmcl.2015.08.014

Demeule, M., Beaudet, N., Régina, A., Besserer-Offroy, É., Murza, A., Tétreault, P., Belleville, K., Ché, C., Larocque, A., Thiot, C., Béliveau, R., Longpré, J.M., Marsault, É., Leduc, R., Lachowicz, J.E., Gonias, S.L., Castaigne, J.P., Sarret, P., 2014. Conjugation of a brain-penetrant peptide with neurotensin provides antinociceptive properties. J. Clin. Invest. 124, 1199–1213. https://doi.org/10.1172/JCI70647

Devader, C., Moreno, S., Roulot, M., Deval, E., Dix, T., Morales, C.R., Mazella, J., 2016. Increased brain neurotensin and NTSR2 lead to weak nociception in NTSR3/sortilin knockout mice. Front. Neurosci. 10, 1–8. https://doi.org/10.3389/fnins.2016.00542

Díaz-Cabiale, Z., Parrado, C., Narváez, M., Millón, C., Puigcerver, A., Fuxe, K., Narváez, J.A., 2010. Regulatory Peptides The Galanin N-terminal fragment (1 – 15) interacts with neuropeptide Y in central cardiovascular control: Involvement of the NPY Y2 receptor subtype. Regul. Pept. 163, 130–136. https://doi.org/10.1016/j.regpep.2010.04.014

Duan, B., Cheng, L., Bourane, S., Britz, O., Padilla, C., Garcia-Campmany, L., Krashes, M., Knowlton, W., Velasquez, T., Ren, X., Ross, S.E., Lowell, B.B., Wang, Y., Goulding, M., Ma, Q., 2014. Identification of spinal circuits transmitting and gating mechanical pain. Cell 159, 1417–1432. https://doi.org/10.1016/j.cell.2014.11.003

Duan, H., Zhang, Y., Zhang, X., Xu, H., Shu, J., Xu, S., 2015. Antinociceptive roles of galanin receptor 1 in nucleus accumbens of rats in a model of neuropathic pain. J. Neurosci. Res. 93, 1542–1551. https://doi.org/10.1002/jnr.23611

Dvorakova, M.C., 2018. Distribution and function of neuropeptides W/B signaling system. Front. Physiol. 9, 1–13. https://doi.org/10.3389/fphys.2018.00981

Edvinsson, L., Haanes, K.A., Warfvinge, K., Krause, Di.N., 2018. CGRP as the target of new

migraine therapies - Successful translation from bench to clinic. Nat. Rev. Neurol. 14, 338–350. https://doi.org/10.1038/s41582-018-0003-1

Edwards, S., Vendruscolo, L.F., Schlosburg, J.E., Misra, K.K., Wee, S., Park, P.E., Schulteis, G., Koob, G.F., 2012. Development of mechanical hypersensitivity in rats during heroin and ethanol dependence: Alleviation by CRF1receptor antagonism. Neuropharmacology 62, 1142–1151. https://doi.org/10.1016/j.neuropharm.2011.11.006

Elhabazi, K., Humbert, J.-P., Bertin, I., Quillet, R., Utard, V., Scmitt, M., Bourguignon, J.-J., Laboureyras, E., Ben Boujema, M., Simonnet, G., Ancel, C., Simonneaux, V., Beltramo, M., Bucher, B., Sorg, T., Meziane, H., Schneider, E., Petit-Demoulière, B., Ilien, B., Bihel, F., Simonin, F., 2017. RF313, an orally bioavailable neuropeptide FF receptor antagonist, opposes effects of RF-amide-related peptide-3 and opioid-induced hyperalgesia in rodents. Neuropharmacology 118, 188–198. https://doi.org/10.1016/j.neuropharm.2017.03.012

Elhabazi, K., Humbert, J.P., Bertin, I., Schmitt, M., Bihel, F., Bourguignon, J.J., Bucher, B., Becker, J.A.J., Sorg, T., Meziane, H., Petit-Demoulière, B., Ilien, B., Simonin, F., 2013. Endogenous mammalian RF-amide peptides, including PrRP, kisspeptin and 26RFa, modulate nociception and morphine analgesia via NPFF receptors. Neuropharmacology 75, 164–171. https://doi.org/10.1016/j.neuropharm.2013.07.012

Elhabazi, K., Trigo, J.M., Mollereau, C., Moulédous, L., Zajac, J., Bihel, F., 2012. Involvement of neuropeptide FF receptors in neuroadaptive responses to acute and chronic opiate. Br. J. Pharmacol. 165, 424–435. https://doi.org/10.1111/j.1476-5381.2011.01563.x

Eliava, M., Melchior, M., Knobloch-Bollmann, H.S., Wahis, J., da Silva Gouveia, M., Tang, Y., Ciobanu, A.C., Triana del Rio, R., Roth, L.C., Althammer, F., Chavant, V., Goumon, Y., Gruber, T., Petit-Demoulière, N., Busnelli, M., Chini, B., Tan, L.L., Mitre, M., Froemke, R.C., Chao, M. V., Giese, G., Sprengel, R., Kuner, R., Poisbeau, P., Seeburg, P.H., Stoop, R., Charlet, A., Grinevich, V., 2016. A New Population of Parvocellular Oxytocin Neurons Controlling Magnocellular Neuron Activity and Inflammatory Pain Processing. Neuron 89, 1291–1304. https://doi.org/10.1016/j.neuron.2016.01.041

Emam, A.H., Hajesfandiari, N., Shahidi, S., Komaki, A., Ganji, M., Sarihi, A., 2016. Modulation of nociception by medial pre-optic area orexin a receptors and its relation with morphine in male rats. Brain Res. Bull. 127, 141–147. https://doi.org/10.1016/j.brainresbull.2016.09.009

Erami, E., Azhdari-Zarmehri, H., Ghasemi-Dashkhasan, E., Esmaeili, M.H., Semnanian, S., 2012. Intra-paragigantocellularis lateralis injection of orexin-A has an antinociceptive effect on hot plate and formalin tests in rat. Brain Res. 1478, 16–23. https://doi.org/10.1016/j.brainres.2012.08.013

Erfanparast, A., Tamaddonfard, E., Seyedin, S., 2018. Involvement of central opiate receptors in modulation of centrally administered oxytocin-induced antinociception. Iran. J. Basic Med. Sci. 21, 1275–1280. https://doi.org/10.22038/ijbms.2018.26302.6449

Fan, H., Zhang, T., Sun, K., Song, S., Cao, S., Zhang, H. long, Shen, W., 2015. Corticotropin-releasing factor mediates bone cancer induced pain through neuronal activation in rat spinal cord. Tumor Biol. 36, 9559–9565. https://doi.org/10.1007/s13277-015-3670-1

Fang, Q., Jiang, T., Li, N., Han, Z., Wang, R., 2011. Central administration of neuropeptide FF and related peptides attenuate systemic morphine analgesia in mice. Protein Pept. Lett. 18, 403–409.

Fischer, M.J.M., Schmidt, J., Koulchitsky, S., Klussmann, S., Vater, A., Messlinger, K., 2018.

Effect of a calcitonin gene-related peptide-binding L-RNA aptamer on neuronal activity in the rat spinal trigeminal nucleus. J. Headache Pain 19, 3. https://doi.org/10.1186/s10194-018-0832-8

Fuxe, K., Borroto-escuela, D.O., Romero-fernandez, W., Tarakanov, A.O., Calvo, F., Garriga, P., Tena, M., Narvaez, M., Millón, C., Parrado, C., 2012. On the existence and function of galanin receptor heteromers in the central nervous system. Front. Endocrinol. 3, 1–12. https://doi.org/10.3389/fendo.2012.00127

Gafford, G., Jasnow, A.M., Ressler, K.J., 2014. Grin1 receptor deletion within CRF neurons enhances fear memory. PLoS One 9. https://doi.org/10.1371/journal.pone.0111009

Gajjar, S., Patel, B.M., 2017. Neuromedin: An insight into its types, receptors and therapeutic opportunities. Pharmacol. Reports 69, 438–447. https://doi.org/10.1016/j.pharep.2017.01.009

Gallo, A., Leerink, M., Michot, B., Ahmed, E., Forget, P., Mouraux, A., Hermans, E., Deumens, R., 2017. Bilateral tactile hypersensitivity and neuroimmune responses after spared nerve injury in mice lacking vasoactive intestinal peptide. Exp. Neurol. 293, 62–73. https://doi.org/10.1016/j.expneurol.2017.03.019

Gimpl, G., Fahrenholz, F., 2001. The oxytocin receptor system: structure, function, and regulation. Physiol. Rev. 81, 629–683. https://doi.org/10.1152/physrev.2001.81.2.629

González-Hernández, A., Espinosa De Los Monteros-Zuñiga, A., Martínez-Lorenzana, G., Condés-Lara, M., 2019. Recurrent antinociception induced by intrathecal or peripheral oxytocin in a neuropathic pain rat model. Exp. Brain Res. 237, 2995–3010. https://doi.org/10.1007/s00221-019-05651-7

González-Hernández, A., Manzano-García, A., Martínez-Lorenzana, G., Tello-García, I.A., Carranza, M., Arámburo, C., Condés-Lara, M., 2017. Peripheral oxytocin receptors inhibit the nociceptive input signal to spinal dorsal horn wide-dynamic-range neurons. Pain 158, 2117–2128. https://doi.org/10.1097/j.pain.0000000000001024

Gouardères, C., Faura, C.C., Zajac, J.-M., 2004. Rodent strain differences in the NPFF 1 and NPFF 2 receptor distribution and density in the central nervous system 1014, 61–70. https://doi.org/10.1016/j.brainres.2004.04.005

Greco, M.C., Capuano, A., Navarra, P., Tringali, G., 2016. Lacosamide inhibits calcitonin gene-related peptide production and release at trigeminal level in the rat. Eur. J. Pain (United Kingdom) 20, 959–966. https://doi.org/10.1002/ejp.820

Greco, R., Mangione, A.S., Siani, F., Blandini, F., Vairetti, M., Nappi, G., Sandrini, G., Buzzi, M.G., Tassorelli, C., 2014. Effects of CGRP receptor antagonism in nitroglycerin-induced hyperalgesia. Cephalalgia 34, 616–623. https://doi.org/10.1177/0333102413517776

Greenwood-Van Meerveld, B., Mohammadi, E., Tyler, K., Pietra, C., Bee, L.A., Dickenson, A., 2014. Synergistic Effect of 5-Hydroxytryptamine 3 and Neurokinin 1 Receptor Antagonism in Rodent Models of Somatic and Visceral Pain. J. Pharmacol. Exp. Ther. 351, 146–152. https://doi.org/10.1124/jpet.114.216028

Grund, T., Goyon, S., Li, Y., Eliava, M., Liu, H., Charlet, A., Grinevich, V., Neumann, I.D., 2017. Neuropeptide S Activates Paraventricular Oxytocin Neurons to Induce Anxiolysis. J. Neurosci. 37, 12214–12225. https://doi.org/10.1523/JNEUROSCI.2161-17.2017

Grund, T., Neumann, I.D., 2018. Neuropeptide S Induces Acute Anxiolysis by Phospholipase C-Dependent Signaling within the Medial Amygdala. Neuropsychopharmacology 43, 1156–1163. https://doi.org/10.1038/npp.2017.169

Guillemyn, K., Kleczkowska, P., Lesniak, A., Dyniewicz, J., Van Der Poorten, O., Van Den Eynde, I., Keresztes, A., Varga, E., Lai, J., Porreca, F., Chung, N.N., Lemieux, C., Mika, J., Rojewska, E., Makuch, W., Van Duppen, J., Przewlocka, B., Vanden Broeck, J., Lipkowski, A.W., Schiller, P.W., Tourwé, D., Ballet, S., 2015. Synthesis and biological evaluation of compact, conformationally constrained bifunctional opioid agonist - Neurokinin-1 antagonist peptidomimetics. Eur. J. Med. Chem. 92, 64–77. https://doi.org/10.1016/j.ejmech.2014.12.033

Guo, S.J., Cui, Y., Huang, Z.Z., Liu, H., Zhang, X.Q., Jiang, J.X., Xin, W.J., 2016. Orexin A-mediated AKT signaling in the dentate gyrus contributes to the acquisition, expression and reinstatement of morphine-induced conditioned place preference. Addict. Biol. 21, 547–559. https://doi.org/10.1111/adb.12236

Guo, Y., Yao, F.R., Cao, D.Y., Li, L., Wang, H.S., Xie, W., Zhao, Y., 2015. The major histocompatibility complex genes impact pain response in DA and DA.1U rats. Physiol. Behav. 147, 30–37. https://doi.org/10.1016/j.physbeh.2015.04.009

Hagit, C., Ella, V., Kaplan, Z., Joseph, Z., Aleksander, M.A., 2018. Neuropeptide S in the basolateral amygdala mediates an adaptive behavioral stress response in a rat model of posttraumatic stress disorder by increasing the expression of BDNF and the neuropeptide YY1 receptor. Eur. Neuropsychopharmacol. 28, 159–170. https://doi.org/10.1016/j.euroneuro.2017.11.006

Hallberg, M., Sandstrom, A., 2018. From the Anti-Nociceptive Substance P Metabolite Substance P (1-7) to Small Peptidomimetics. Curr. Protein Pept. Sci. 19, 1038–1048. https://doi.org/10.2174/1389203719666180508122019

Hansen, R.R., Vacca, V., Pitcher, T., Clark, A.K., Malcangio, M., 2016. Role of extracellular calcitonin gene-related peptide in spinal cord mechanisms of cancer-induced bone pain. Pain 157, 666–676. https://doi.org/10.1097/j.pain.0000000000000416

Hardt, J., Jacobsen, C., Goldberg, J., Nickel, R., Buchwald, D., 2008. Prevalence of chronic pain in a representative sample in the United States. Pain Med. 9, 803–812. https://doi.org/10.1111/j.1526-4637.2008.00425.x

Hernández, V.S., Hernández, O.R., Perez de la Mora, M., Gómora, M.J., Fuxe, K., Eiden, L.E., Zhang, L., 2016. Hypothalamic vasopressinergic projections innervate central amygdala GABAergic neurons: implications for anxiety and stress coping. Front. Neural Circuits 10, 1–19. https://doi.org/10.3389/fncir.2016.00092

Holland, P.R., Saengjaroentham, C., Vila-Pueyo, M., 2018. The role of the brainstem in migraine: Potential brainstem effects of CGRP and CGRP receptor activation in animal models. Cephalalgia 0, 1–13. https://doi.org/10.1177/0333102418756863

Hughes, J., Smith, T.W., Kosterlitz, H.W., Fothergill, L.A., Morgan, B.A., Morris, H.R., 1975. Identification of two related pentapeptides from the brain with potent opiate agonist activity. Nature 258, 577–80.

Iadarola, M.J., Sapio, M.R., Wang, X., Carrero, H., Virata-Theimer, M.L., Sarnovsky, R., Mannes, A.J., FitzGerald, D.J., 2017. Analgesia by deletion of spinal neurokinin 1 receptor expressing neurons using a bioengineered substance P-Pseudomonas exotoxin conjugate. Mol. Pain 13, 1–14. https://doi.org/10.1177/1744806917727657

Ide, S., Hara, T., Ohno, A., Tamano, R., Koseki, K., Naka, T., Maruyama, C., Kaneda, K., Yoshioka, M., Minami, M., 2013. Opposing roles of corticotropin-releasing factor and neuropeptide Y within the dorsolateral bed nucleus of the stria terminalis in the negative affective component of pain in rats. J Neurosci 33, 5881–5894. https://doi.org/10.1523/JNEUROSCI.4278-12.2013

Ionescu, I.A., Dine, J., Yen, Y.C., Buell, D.R., Herrmann, L., Holsboer, F., Eder, M., Landgraf, R., Schmidt, U., 2012. Intranasally administered neuropeptide S (NPS) exerts anxiolytic effects following internalization into NPS receptor-expressing neurons. Neuropsychopharmacology 37, 1323–1337. https://doi.org/10.1038/npp.2011.317

Itoga, C.A., Roltsch Hellard, E.A., Whitaker, A.M., Lu, Y.L., Schreiber, A.L., Baynes, B.B., Baiamonte, B.A., Richardson, H.N., Gilpin, N.W., 2016. Traumatic Stress Promotes Hyperalgesia via Corticotropin-Releasing Factor-1 Receptor (CRFR1) Signaling in Central Amygdala. Neuropsychopharmacology 41, 2463–2472. https://doi.org/10.1038/npp.2016.44

Iyengar, S., Ossipov, M.H., Johnson, K.W., 2016. The role of CGRP in peripheral and central pain mechanisms including migraine. Pain 158, 543–559. https://doi.org/10.1097/j.pain.0000000000000831

Jensen, D.D., Lieu, T.M., Halls, M.L., Veldhuis, N.A., Imlach, W.L., Mai, Q.N., Poole, D.P., Quach, T., Aurelio, L., Conner, J., Herenbrink, C.K., Barlow, N., Simpson, J.S., Scanlon, M.J., Graham, B., McCluskey, A., Robinson, P.J., Escriou, V., Nassini, R., Materazzi, S., Geppetti, P., Hicks, G.A., Christie, M.J., Porter, C.J.H., Canals, M., Bunnett, N.W., 2017. Neurokinin 1 receptor signaling in endosomes mediates sustained nociception and is a viable therapeutic target for prolonged pain relief. Sci. Transl. Med. 9, 1–15. https://doi.org/10.1126/scitranslmed.aal3447

Johnson, A.C., Tran, L., Greenwood-Van Meerveld, B., 2015. Knockdown of corticotropin-releasing factor in the central amygdala reverses persistent viscerosomatic hyperalgesia. Transl. Psychiatry 5, e517. https://doi.org/10.1038/tp.2015.16

Juif, P.-E., Breton, J.-D., Rajalu, M., Charlet, A., Goumon, Y., Poisbeau, P., 2013. Long-lasting spinal oxytocin analgesia is ensured by the stimulation of allopregnanolone synthesis which potentiates GABAA receptor-mediated synaptic inhibition. J. Neurosci. 33, 16617–16626. https://doi.org/10.1523/JNEUROSCI.3084-12.2013

Juif, P.-E., Poisbeau, P., 2013. Neurohormonal effects of oxytocin and vasopressin receptor agonists on spinal pain processing in male rats. Pain 154, 1449–1456. https://doi.org/10.1016/j.pain.2013.05.003

Kai, Y., Li, Y., Sun, T., Yin, W., Mao, Y., Li, Jie, Xie, W., Chen, S., Wang, L., Li, Juan, Zhang, Z., Tao, W., 2018. A medial prefrontal cortex-nucleus acumens corticotropin-releasing factor circuitry for neuropathic pain-increased susceptibility to opioid reward. Transl. Psychiatry 8. https://doi.org/10.1038/s41398-018-0152-4

Kaneko, T., Kaneda, K., Ohno, A., Takahashi, D., Hara, T., Amano, T., Ide, S., Yoshioka, M., Minami, M., 2016. Activation of adenylate cyclase-cyclic AMP-protein kinase A signaling by corticotropin-releasing factor within the dorsolateral bed nucleus of the stria terminalis is involved in pain-induced aversion. Eur. J. Neurosci. 44, 2914–2924. https://doi.org/10.1111/ejn.13419

Kang, S.J., Kwak, C., Lee, J., Sim, S.E., Shim, J., Choi, T., Collingridge, G.L., Zhuo, M., Kaang, B.K., 2015. Bidirectional modulation of hyperalgesia via the specific control of excitatory and inhibitory neuronal activity in the ACC. Mol. Brain 8, 1–11. https://doi.org/10.1186/s13041-015-0170-6

Kleczkowska, P., Bojnik, E., LeAniak, A., Kosson, P., Van Den Eynde, I., Ballet, S., Benyhe, S., Tourwe, D., Lipkowski, A.W., 2013. Identification of Dmt-D-Lys-Phe-Phe-OH as a highly antinociceptive tetrapeptide metabolite of the opioid-neurotensin hybrid peptide PK20. Pharmacol. Reports 65, 836–846. https://doi.org/10.1016/S1734-1140(13)71064-8

Kleczkowska, P., Kosson, P., Ballet, S., Van den Eynde, I., Tsuda, Y., Tourwé, D., Lipkowski,

A.W., 2010. PK20, a new opioid-neurotensin hybrid peptide that exhibits central and peripheral antinociceptive effects. Mol. Pain 6, 86. https://doi.org/10.1186/1744-8069-6-86

Knobloch, H.S., Charlet, A., Hoffmann, L.C., Eliava, M., Khrulev, S., Cetin, A.H., Osten, P., Schwarz, M.K., Seeburg, P.H., Stoop, R., Grinevich, V., 2012. Evoked axonal oxytocin release in the central amygdala attenuates fear response. Neuron 73, 553–566. https://doi.org/10.1016/j.neuron.2011.11.030

Knobloch, H.S., Grinevich, V., Dabrowska, J., 2014. Evolution of oxytocin pathways in the brain of vertebrates. Front. Behav. Neurosci. 8, 1–13. https://doi.org/10.3389/fnbeh.2014.00031

Kormos, V., Gaszner, B., 2013. Role of neuropeptides in anxiety, stress, and depression: From animals to humans. Neuropeptides 47, 401–419. https://doi.org/10.1016/j.npep.2013.10.014

Kovács, A., László, K., Gálosi, R., Ollmann, T., Péczely, L., Zagoracz, O., Bencze, N., Lénárd, L., 2014. Intraamygdaloid microinjection of RFamide-related peptide-3 decreases food intake in rats. Brain Res. Bull. 107, 61–68. https://doi.org/10.1016/j.brainresbull.2014.07.002

Kurt, G., Woodworth, H.L., Fowler, S., Bugescu, R., Leinninger, G.M., 2018. Activation of lateral hypothalamic area neurotensin-expressing neurons promotes drinking. Neuropharmacology. https://doi.org/10.1016/j.neuropharm.2018.09.038

Lameh, J., Bertozzi, F., Kelly, N., Jacobi, P.M., Nguyen, D., Bajpai, A., Gaubert, G., Olsson, R., Gardell, L.R., 2010. Neuropeptide FF receptors have opposing modulatory effects on nociception. J. Pharmacol. Exp. Ther. 334, 244–254. https://doi.org/10.1124/jpet.109.164384.al.

Lariviere, W.R., Melzack, R., 2000. The role of corticotropin-releasing factor in pain and analgesia. Pain 84, 1–12. https://doi.org/10.1016/S0304-3959(99)00193-1

Lautenbacher, S., Kundermann, B., Krieg, J.C., 2006. Sleep deprivation and pain perception. Sleep Med. Rev. 10, 357–369. https://doi.org/10.1016/j.smrv.2005.08.001

Lee, Y.S., Hall, S.M., Ramos-Colon, C., Remesic, M., Lebaron, L., Nguyen, A., Rankin, D., Porreca, F., Lai, J., Hruby, V.J., 2015. Modification of amphipathic non-opioid dynorphin A analogues for rat brain bradykinin receptors. Bioorganic Med. Chem. Lett. 25, 30–33. https://doi.org/10.1016/j.bmcl.2014.11.026

Lee, Y.S., Rankin, D., Hall, S.M., Ramos-Colon, C., Ortiz, J.J., Kupp, R., Porreca, F., Lai, J., Hruby, V.J., 2014. Structure-activity relationships of non-opioid [des-Arg7]-dynorphin A analogues for bradykinin receptors. Bioorganic Med. Chem. Lett. 24, 4976–4979. https://doi.org/10.1016/j.bmcl.2014.09.033

Li, N., Han, Z., Fang, Q., Wang, Z., Tang, H., Ren, H., Wang, R., 2012. Neuropeptide FF and related peptides attenuates warm- , but not cold-water swim stress-induced analgesia in mice. Behav. Brain Res. 233, 428–433. https://doi.org/10.1016/j.bbr.2012.05.035

Li, S., Huo, M., Wu, X., Huang, Y., Wang, L., Zhang, X., 2017. Involvement of galanin and galanin receptor 1 in nociceptive modulation in the central nucleus of amygdala in normal and neuropathic rats. Sci. Rep. 1–10. https://doi.org/10.1038/s41598-017-13944-6

Li, W., Chang, M., Peng, Y.L., Gao, Y.H., Zhang, J. nan, Han, R.W., Wang, R., 2009a. Neuropeptide S produces antinociceptive effects at the supraspinal level in mice. Regul. Pept. 156, 90–95. https://doi.org/10.1016/j.regpep.2009.03.013

Li, W., Gao, Y.H., Chang, M., Peng, Y.L., Yao, J., Han, R.W., Wang, R., 2009b. Neuropeptide S inhibits the acquisition and the expression of conditioned place preference to morphine in mice. Peptides 30, 234–240. https://doi.org/10.1016/j.peptides.2008.10.004

Li, X., Guo, R., Sun, Y., Li, H., Ma, D., Zhang, C., Guan, Y., Li, J., Wang, Y., 2018. Botulinum toxin type A and gabapentin attenuate postoperative pain and NK1 receptor internalization in rats. Neurochem. Int. 116, 52–62. https://doi.org/10.1016/j.neuint.2018.03.010

Lin, Y., Liu, H., Day, Y., Chang, C., Hsu, P., Chen, J., 2017a. Activation of NPFFR2 leads to hyperalgesia through the spinal inflammatory mediator CGRP in mice. Exp. Neurol. 291, 62–73. https://doi.org/10.1016/j.expneurol.2017.02.003

Lin, Y., Yu, Y., Hong, W., Yeh, T., Chen, T., Chen, J., 2017b. NPFFR2 activates the HPA axis and induces anxiogenic effects in rodents. Int. J. Mol. Sci. 18, 1–13. https://doi.org/10.3390/ijms18081810

Luo, S.X., Huang, J., Li, Q., Mohammad, H., Lee, C.Y., Krishna, K., Kok, A.M.Y., Tan, Y.L., Lim, J.Y., Li, H., Yeow, L.Y., Sun, J., He, M., Grandjean, J., Sajikumar, S., Han, W., Fu, Y., 2018. Regulation of feeding by somatostatin neurons in the tuberal nucleus. Science 361, 76–81. https://doi.org/10.1126/science.aar4983

Lynds, R., Lyu, C., Lyu, G.W., Shi, X.Q., Rosén, A., Mustafa, K., Shi, T.J.S., 2017. Neuronal plasticity of trigeminal ganglia in mice following nerve injury. J. Pain Res. 10, 349–357. https://doi.org/10.2147/JPR.S120092

Magnussen, C., Hung, S.P., Ribeiro-da-Silva, A., 2015. Novel expression pattern of neuropeptide Y immunoreactivity in the peripheral nervous system in a rat model of neuropathic pain. Mol. Pain 11, 1–12. https://doi.org/10.1186/s12990-015-0029-y

Malet, M., Leiguarda, C., Gastón, G., McCarthy, C., Brumovsky, P., 2017. Spinal activation of the NPY Y1 receptor reduces mechanical and cold allodynia in rats with chronic constriction injury. Peptides 92, 38–45. https://doi.org/10.1016/j.peptides.2017.04.005

Marek, P., Mogil, J.S., Sternberg, W.F., Panocka, I., Liebeskind, J.C., 1992. N-methyl-d-aspartic acid (NMDA) receptor antagonist MK-801 blocks non-opioid stress-induced analgesia. II. Comparison across three swim-stress paradigms in selectively bred mice. Brain Res. 578, 197–203. https://doi.org/10.1016/0006-8993(92)90248-8

McDonald, T., Liang, H.A., Sanoja, R., Gotter, A.L., Kuduk, S.D., Coleman, P.J., Smith, K.M., Winrow, C.J., Renger, J.J., 2016. Pharmacological evaluation of orexin receptor antagonists in preclinical animal models of pain. J. Neurogenet. 30, 32–41. https://doi.org/10.3109/01677063.2016.1171862

Medina, G., Ji, G., Grégoire, S., Neugebauer, V., 2014. Nasal application of neuropeptide S inhibits arthritis pain-related behaviors through an action in the amygdala. Mol. Pain 10, 1–13. https://doi.org/10.1186/1744-8069-10-32

Mogil, J.S., Bailey, A.L., 2010. Sex and gender differences in pain and analgesia, in: Progress in Brain Research. Elsevier B.V., pp. 140–157. https://doi.org/10.1016/B978-0-444-53630-3.00009-9

Moreno-López, Y., Martínez-Lorenzana, G., Condés-Lara, M., Rojas-Piloni, G., 2013. Identification of oxytocin receptor in the dorsal horn and nociceptive dorsal root ganglion neurons. Neuropeptides 47, 117–123. https://doi.org/10.1016/j.npep.2012.09.008

Moulédous, L., Mollereau, C., Zajac, J., 2010. Opioid-modulating properties of the neuropeptide FF system. BioFactors 36, 423–429. https://doi.org/10.1002/biof.116

Muñoz, M., Coveñas, R., 2014. Involvement of substance P and the NK-1 receptor in human pathology. Amino Acids 46, 1727–1750. https://doi.org/10.1007/s00726-014-1736-9

Nakamura, Y., Izumi, H., Shimizu, T., Hisaoka-Nakashima, K., Morioka, N., Nakata, Y., 2013. Volume Transmission of Substance P in Striatum Induced by Intraplantar Formalin Injection Attenuates Nociceptive Responses via Activation of the Neurokinin 1 Receptor. J. Pharmacol. Sci. 121, 257–271. https://doi.org/10.1103/PhysRevB.50.12766

Nazarian, A., Tenayuca, J.M., Almasarweh, F., Armendariz, A., Are, D., 2014. Sex differences in formalin-evoked primary afferent release of substance P. Eur. J. Pain (United Kingdom) 18, 39–46. https://doi.org/10.1002/j.1532-2149.2013.00346.x

Nevárez, N., de Lecea, L., 2018. Recent advances in understanding the roles of hypocretin/orexin in arousal, affect, and motivation. F1000Research 7, 1421. https://doi.org/10.12688/f1000research.15097.1

Nicholson, B., Verma, S., 2004. Comorbidities in chronic neuropathic pain. Pain Med. 5 Suppl 1, S9–S27. https://doi.org/10.1111/j.1526-4637.2004.04019.x

Nozu, T., Okumura, T., 2015. Corticotropin-releasing factor receptor type 1 and type 2 interaction in irritable bowel syndrome. J. Gastroenterol. 50, 819–830. https://doi.org/10.1007/s00535-015-1086-8

Oishi, M., Kushikata, T., Niwa, H., Yakoshi, C., Ogasawara, C., Calo, G., Guerrini, R., Hirota, K., 2014. Endogenous neuropeptide S tone influences sleep-wake rhythm in rats. Neurosci. Lett. 581, 94–97. https://doi.org/10.1016/j.neulet.2014.08.031

Park, H.J., Moon, D.E., 2010. Pharmacologic management of chronic pain. Korean J. Pain 23, 99–108. https://doi.org/10.3344/kjp.2010.23.2.99

Parrado, C., Díaz-Cabiale, Z., García-Coronel, M., Agnati, L.F., Coveñas, R., Fuxe, K., Narváez, J., 2007. Region specific galanin receptor/neuropeptide Y Y1 receptor interactions in the tel- and diencephalon of the rat . Relevance for food consumption. Neuropharmacology 52, 684–692. https://doi.org/10.1016/j.neuropharm.2006.09.010

Peng, Y.L., Zhang, J.N., Chang, M., Li, W., Han, R.W., Wang, R., 2010. Effects of central neuropeptide S in the mouse formalin test. Peptides 31, 1878–1883. https://doi.org/10.1016/j.peptides.2010.06.027

Pérez de Vega, M.J., Ferrer-Montiel, A., González-Muñiz, R., 2018. Recent progress in non-opioid analgesic peptides. Arch. Biochem. Biophys. 660, 36–52. https://doi.org/10.1016/J.ABB.2018.10.011

Pierce, A.N., Ryals, J.M., Wang, R., Christianson, J.A., 2014. Vaginal hypersensitivity and hypothalamic-pituitary-adrenal axis dysfunction as a result of neonatal maternal separation in female mice. Neuroscience 263, 216–230. https://doi.org/10.1016/j.neuroscience.2014.01.022

Pulga, A., Ruzza, C., Rizzi, A., Guerrini, R., Calo, G., 2012. Anxiolytic- and panicolytic-like effects of Neuropeptide S in the mouse elevated T-maze. Eur. J. Neurosci. 36, 3531–3537. https://doi.org/10.1111/j.1460-9568.2012.08265.x

Qu, C.L., Dang, Y.H., Tang, J.S., 2015. Administration of somatostatin analog octreotide in the ventrolateral orbital cortex produces sex-related antinociceptive effects on acute and formalin-induced nociceptive behavior in rats. Neurochem. Int. 87, 77–84. https://doi.org/10.1016/j.neuint.2015.06.002

Reid, K.J., Harker, J., Bala, M.M., Truyers, C., Kellen, E., Bekkering, G.E., Kleijnen, J., 2011. Epidemiology of chronic non-cancer pain in Europe: narrative review of prevalence, pain treatments and pain impact. Curr. Med. Res. Opin. 27, 449–462.

https://doi.org/10.1185/03007995.2010.545813

Rogoz, K., Andersen, H.H., Lagerstrom, M.C., Kullander, K., 2014. Multimodal Use of Calcitonin Gene-Related Peptide and Substance P in Itch and Acute Pain Uncovered by the Elimination of Vesicular Glutamate Transporter 2 from Transient Receptor Potential Cation Channel Subfamily V Member 1 Neurons. J. Neurosci. 34, 14055–14068. https://doi.org/10.1038/nature16073

Roussy, G., Beaudry, H., Lafrance, M., Belleville, K., Beaudet, N., Wada, K., Gendron, L., Sarret, P., 2010. Altered morphine-induced analgesia in neurotensin type 1 receptor null mice. Neuroscience 170, 1286–1294. https://doi.org/10.1016/j.neuroscience.2010.08.016

Russo, R., D'Agostino, G., Mattace Raso, G., Avagliano, C., Cristiano, C., Meli, R., Calignano, A., 2012. Central administration of oxytocin reduces hyperalgesia in mice: implication for cannabinoid and opioid systems. Peptides 38, 81–88. https://doi.org/10.1016/j.peptides.2012.08.005

Sandweiss, A., Vanderah, T., 2015. The pharmacology of neurokinin receptors in addiction: prospects for therapy. Subst. Abuse Rehabil. 93. https://doi.org/10.2147/SAR.S70350

Sandweiss, A.J., McIntosh, M.I., Moutal, A., Davidson-Knapp, R., Hu, J., Giri, A.K., Yamamoto, T., Hruby, V.J., Khanna, R., Largent-Milnes, T.M., Vanderah, T.W., 2018. Genetic and pharmacological antagonism of NK1 receptor prevents opiate abuse potential. Mol. Psychiatry 23, 1745–1755. https://doi.org/10.1038/mp.2017.102

Santos, F.M., Silva, J.T., Rocha, I.R.C., Martins, D.O., Chacur, M., 2018. Non-pharmacological treatment affects neuropeptide expression in neuropathic pain model. Brain Res. 1687, 60–65. https://doi.org/10.1016/j.brainres.2018.02.034

Sargin, D., 2018. The role of the orexin system in stress response. Neuropharmacology 1–11. https://doi.org/10.1016/j.neuropharm.2018.09.034

Sato, T., Nakamura, Y., Shiimura, Y., Ohgusu, H., Kangawa, K., Kojima, M., 2012. Structure, regulation and function of ghrelin. J. Biochem. 151, 119–128. https://doi.org/10.1093/jb/mvr134

Schuckit, M.A., 2016. Treatment of Opioid-Use Disorders. N. Engl. J. Med. 375, 357–368. https://doi.org/10.1056/NEJMra1604339

Schuelert, N., Just, S., Kuelzer, R., Corradini, L., Gorham, L.C.J., Doods, H., 2015. The somatostatin receptor 4 agonist J-2156 reduces mechanosensitivity of peripheral nerve afferents and spinal neurons in an inflammatory pain model. Eur. J. Pharmacol. 746, 274–281. https://doi.org/10.1016/j.ejphar.2014.11.003

Schwartz, N., Temkin, P., Jurado, S., Lim, B.K., Heifets, B.D., Polepalli, J.S., Malenka, R.C., 2014. Decreased motivation during chronic pain requires long-term depression in the nucleus accumbens. Science 345, 535–542. https://doi.org/10.1126/science.1253994

Shinohara, K., Watabe, A.M., Nagase, M., Okutsu, Y., Takahashi, Y., Kurihara, H., Kato, F., 2017. Essential role of endogenous calcitonin gene-related peptide in pain-associated plasticity in the central amygdala. Eur. J. Neurosci. 46, 2149–2160. https://doi.org/10.1111/ejn.13662

Sivertsen, B., Lallukka, T., Petrie, K.J., Steingrimsdottir, O.A., Stubhaug, A., Nielsen, C.S., 2015. Sleep and pain sensitivity in adults. Pain 156, 1433–1439. https://doi.org/10.1097/j.pain.0000000000000131

Smith, B.H., Torrance, N., 2012. Epidemiology of neuropathic pain and its impact on quality of life. Curr. Pain Headache Rep. 16, 191–198. https://doi.org/10.1007/s11916-012-

0256-0

Somvanshi, R.K., Kumar, U., 2014. δ-Opioid receptor and somatostatin receptor-4 heterodimerization: Possible implications in modulation of pain associated signaling. PLoS One 9, 24–27. https://doi.org/10.1371/journal.pone.0085193

Starnowska, J., Costante, R., Guillemyn, K., Popiolek-Barczyk, K., Chung, N.N., Lemieux, C., Keresztes, A., Van Duppen, J., Mollica, A., Streicher, J., Vanden Broeck, J., Schiller, P.W., Tourwé, D., Mika, J., Ballet, S., Przewlocka, B., 2017. Analgesic Properties of Opioid/NK1 Multitarget Ligands with Distinct in Vitro Profiles in Naive and Chronic Constriction Injury Mice. ACS Chem. Neurosci. 8, 2315–2324. https://doi.org/10.1021/acschemneuro.7b00226

Stengel, A., Karasawa, H., Taché, Y., 2015. The role of brain somatostatin receptor 2 in the regulation of feeding and drinking behavior. Horm. Behav. 73, 15–22. https://doi.org/10.1016/j.yhbeh.2015.05.009

Stevenson, S., Li, X.Q., Davy, D.T., Klein, L., Goldberg, V.M., 1997. Critical biological determinants of incorporation of non-vascularized cortical bone grafts. Quantification of a complex process and structure. J. Bone Jt. Surg. - Ser. A 79, 1–16. https://doi.org/10.2106/00004623-199701000-00001

Taché, Y., 2015. Corticotrophin-releasing factor 1 activation in the central amygdale and visceral hyperalgesia. Neurogastroenterol. Motil. 27, 1–6. https://doi.org/10.1111/nmo.12495

Taguchi, R., Shikata, K., Furuya, Y., Hirakawa, T., Ino, M., Shin, K., Shibata, H., 2017. Selective corticotropin-releasing factor 1 receptor antagonist E2508 reduces restraint stress-induced defecation and visceral pain in rat models. Psychoneuroendocrinology 75, 110–115. https://doi.org/10.1016/j.psyneuen.2016.10.025

Tan, S., Ho, H.S., Song, A.Y., Low, J., Je, H.S., 2017. Maternal Separation Does Not Produce a Significant Behavioral Change in Mice. Exp. Neurobiol. 26, 390. https://doi.org/10.5607/en.2017.26.6.390

Taylor, B.K., Fu, W., Kuphal, K.E., Stiller, C.O., Winter, M.K., Chen, W., Corder, G.F., Urban, J.H., McCarson, K.E., Marvizon, J.C., 2014. Inflammation enhances Y1 receptor signaling, neuropeptide Y-mediated inhibition of hyperalgesia, and substance P release from primary afferent neurons. Neuroscience 256, 178–194. https://doi.org/10.1016/j.neuroscience.2013.10.054

Thorsell, A., Mathé, A.A., 2017. Neuropeptide Y in alcohol addiction and affective disorders. Front. Endocrinol. 8. https://doi.org/10.3389/fendo.2017.00178

Tracy, L.M., Labuschagne, I., Georgiou-Karistianis, N., Gibson, S.J., Giummarra, M.J., 2017. Sex-specific effects of intranasal oxytocin on thermal pain perception: A randomised, double-blind, placebo-controlled cross-over study. Psychoneuroendocrinology 83, 101–110. https://doi.org/10.1016/j.psyneuen.2017.05.028

Tran, L., Schulkin, J., Greenwood-Van Meerveld, B., 2014. Importance of CRF receptor-mediated mechanisms of the bed nucleus of the stria terminalis in the processing of anxiety and pain. Neuropsychopharmacology 39, 2633–2645. https://doi.org/10.1038/npp.2014.117

Tsujino, N., Sakurai, T., 2013. Role of orexin in modulating arousal, feeding, and motivation. Front. Behav. Neurosci. 7, 1–14. https://doi.org/10.3389/fnbeh.2013.00028

Vollesen, A.L., Benemei, S., Cortese, F., Labastida-Ramírez, A., Marchese, F., Pellesi, L., Romoli, M., Ashina, M., Lampl, C., 2018. Migraine and cluster headache – the common link. J. Headache Pain 19, 89. https://doi.org/10.1186/s10194-018-0909-4

Wang, P., Li, H., Barde, S., Zhang, M., Sun, J., Wang, T., Zhang, P., Luo, H., 2016. Depression-like behavior in rat: Involvement of galanin receptor subtype 1 in the ventral periaqueductal gray. Proc. Natl. Acad. Sci. 113, E4726–E4735. https://doi.org/10.1073/pnas.1609198113

Woodworth, H.L., Beekly, B.G., Batchelor, H.M., Bugescu, R., Perez-Bonilla, P., Schroeder, L.E., Leinninger, G.M., 2017. Lateral Hypothalamic Neurotensin Neurons Orchestrate Dual Weight Loss Behaviors via Distinct Mechanisms. Cell Rep. 21, 3116–3128. https://doi.org/10.1016/j.celrep.2017.11.068

Wrobel, L., Schorscher-petcu, A., Dupré, A., Yoshida, M., Nishimori, K., Tribollet, E., 2011. Neuroscience Letters Distribution and identity of neurons expressing the oxytocin receptor in the mouse spinal cord. Neurosci. Lett. 495, 49–54. https://doi.org/10.1016/j.neulet.2011.03.033

Xie, J.-F., Shao, Y.-F., Wang, H.-L., Wang, C., Cui, G.-F., Kong, X.-P., Wang, L.-X., Chen, Y.-N., Cong, C.-Y., Chen, H.-L., Hou, Y.-P., 2018. Neuropeptide S Counteracts Paradoxical Sleep Deprivation-Induced Anxiety-Like Behavior and Sleep Disturbances. Front. Cell. Neurosci. 12, 1–15. https://doi.org/10.3389/fncel.2018.00064

Xu, Y., Reinscheid, R.K., Huitron-Resendiz, S., Clark, S.D., Wang, Z., Lin, S.H., Brucher, F.A., Zeng, J., Ly, N.K., Henriksen, S.J., de Lecea, L., Civelli, O., 2004. Neuropeptide S: a neuropeptide promoting arousal and anxiolytic-like effects. Neuron 43, 487–497. https://doi.org/10.1016/j.neuron.2004.08.005

Yamamoto, T., Nair, P., Largent-Milnes, T.M., Jacobsen, N.E., Davis, P., Ma, S.W., Yamamura, H.I., Vanderah, T.W., Porreca, F., Lai, J., Hruby, V.J., 2011. Discovery of a potent and efficacious peptide derivative for δ/μ opioid agonist/neurokinin 1 antagonist activity with a 2′,6′- Dimethyl- l -tyrosine: In vitro, in vivo, and NMR-based structural studies. J. Med. Chem. 54, 2029–2038. https://doi.org/10.1021/jm101023r

Yang, H.T., Tao, T., Iadarola, M.J., 2008. Modulatory role of neuropeptide FF system in nociception and opiate analgesia. Neuropeptides 42, 1–18. https://doi.org/10.1016/j.npep.2007.06.004

Yang, Y., Zhang, Y., Hai, X., Li, Y., Qian, R., Li, J., Lian, S., 2015. Involvements of galanin and its receptors in antinociception in nucleus accumbens of rats with inflammatory pain. Neurosci. Res. 97, 20–25. https://doi.org/10.1016/j.neures.2015.03.006

Yao, F.R., Wang, H.S., Guo, Y., Zhao, Y., 2016. The local effect of octreotide on mechanical pain sensitivity is more sensitive in DA rats than DA.1U rats. Clin. Exp. Pharmacol. Physiol. 43, 213–220. https://doi.org/10.1111/1440-1681.12519

Yarwood, R.E., Imlach, W.L., Lieu, T., Veldhuis, N.A., Jensen, D.D., Klein Herenbrink, C., Aurelio, L., Cai, Z., Christie, M.J., Poole, D.P., Porter, C.J.H., McLean, P., Hicks, G.A., Geppetti, P., Halls, M.L., Canals, M., Bunnett, N.W., 2017. Endosomal signaling of the receptor for calcitonin gene-related peptide mediates pain transmission. Proc. Natl. Acad. Sci. 114, 201706656. https://doi.org/10.1073/pnas.1706656114

Zeng, P., Chen, J.X., Yang, B., Zhi, X., Guo, F.X., Sun, M.L., Wang, J.L., Wei, J., 2013. Attenuation of systemic morphine-induced analgesia by central administration of ghrelin and related peptides in mice. Peptides 50, 42–49. https://doi.org/10.1016/j.peptides.2013.09.017

Zeng, P., Li, S., Zheng, Y.H., Liu, F.Y., Wang, J.L., Zhang, D.L., Wei, J., 2014. Ghrelin receptor agonist, GHRP-2, produces antinociceptive effects at the supraspinal level via the opioid receptor in mice. Peptides 55, 103–109. https://doi.org/10.1016/j.peptides.2014.02.013

Zhang, M., Fu, F., Yu, L., 2017. Antinociception induced by galanin in anterior cingulate cortex in rats with acute inflammation. Neurosci. Lett. 638, 156–161. https://doi.org/10.1016/j.neulet.2016.12.034

Zhang, S., Jin, X., You, Z., Wang, S., Lim, G., Yang, J., McCabe, M., Li, N., Marota, J., Chen, L., Mao, J., 2014. Persistent nociception induces anxiety-like behavior in rodents: Role of endogenous neuropeptide S. Pain 155, 1504–1515. https://doi.org/10.1016/j.pain.2014.04.026

Zhang, Y., Gao, Y., Li, C., Dong, W., Dong, Y., Li, M., Liu, Y., Xu, S., 2019a. Galanin Receptor 1 Plays an Antinociceptive Effect via Inhibiting PKA Activation in the Nucleus Accumbens of Rats With Neuropathic Pain. Physiol. Res. 8408, 511–518.

Zhang, Y., Gao, Y., Li, C., Dong, W., Li, M., Liu, Y., Dong, Y., 2019b. Galanin plays a role in antinociception via binding to galanin receptors in the nucleus accumbens of rats with neuropathic pain. Neurosci. Lett. 706, 93–98. https://doi.org/10.1016/j.neulet.2019.05.016

Zhou, C.H., Li, X., Zhu, Y.Z., Huang, H., Li, J., Liu, L., Hu, Q., Ma, T.F., Shao, Y., Wu, Y.Q., 2014. Ghrelin alleviates neuropathic pain through GHSR-1a-mediated suppression of the p38 MAPK/NF-κB pathway in a rat chronic constriction injury model. Reg. Anesth. Pain Med. 39, 137–148. https://doi.org/10.1097/AAP.0000000000000050

Zorrilla, E.P., Koob, G.F., 2010. Progress in corticotropin-releasing factor-1 antagonist development. Drug Discov. Today 15, 371–383. https://doi.org/10.1016/j.drudis.2010.02.011

Zorrilla, E.P., Logrip, M.L., Koob, G.F., 2014. Corticotropin releasing factor: A key role in the neurobiology of addiction. Front. Neuroendocrinol. 35, 234–244. https://doi.org/10.1016/j.yfrne.2014.01.001

Damien Kerspern

L'astrocyte un nouvel acteur dans la modulation ocytocinergique : du réseau au comportement

Résumé

L'ocytocine est un neuropeptide capable de réguler de nombreux comportement sociaux et émotionnels via la modulation de circuit neuronaux de différentes structures cérébrales. De récentes études ont mis en avant la capacité de ce neuropeptide à moduler le circuit de l'amygdale et ses comportements associés, comme la peur, l'anxiété ou encore la douleur. La libération de ce peptide dans le système nerveux central est réalisée de manière synaptique mais aussi, et c'est le cas pour l'amygdale, via une transmission microvolumique. La majorité des synapses est entourée par des astrocytes, formant la synapse tripartite et faisant des astrocytes des acteurs indispensables pour la modulation de l'activité neuronale. Lors de ce travail de thèse, nous avons pu mettre en évidence qu'au sein de l'amygdale, la libération d'ocytocine induit une réponse astrocytaire à même de moduler les circuits neuronaux inhibiteurs et in fine les comportements amygdale-dépendant. Ainsi, ce travail renforce le rôle indispensable des astrocytes dans la modulation synaptique, au travers la démonstration de leur sensibilité à un neuropeptide, l'ocytocine.

Mots-clés : Ocytocine, Douleur, Anxiété, Confort, Astrocytes, Amygdale.

Résumé en anglais

The oxytocin is a neuropeptide involved in the modulation of several social and emotional behavior by modulating neural circuitry in different brain structures. Recent studies have highlighted the ability of this neuropeptide to modulate the amygdala circuit and its associated behavior, such as fear, anxiety, and pain. The release of this peptide in the central nervous system is carried out not only synaptically but also, and this is the case for the amygdala, via microvolumic transmission. Most synapses are surrounded by astrocytes, forming the tripartite synapse and making astrocytes essential players for the modulation of neuronal activity. During this thesis work, we were able to demonstrate that within the amygdala, the release of oxytocin induces an astrocytic response capable of modulating inhibitory neural circuits and ultimately amygdala-dependent behavior. Thus, this work reinforces the essential role of astrocytes in synaptic modulation, through the demonstration of their sensitivity to a neuropeptide, the oxytocin.

Key words: Oxytocin, Pain, Anxiety, Comfort, Astrocytes, Amygdala.